Correlating mammalian chromosome structure and function

Jenny Anne Croft

PhD

University of Edinburgh

1998

Man can climb to the highest summits, but he cannot dwell there long

George Bernard Shaw (1856-1950)

To my family

Declaration

I declare that this thesis has been composed by myself and all of the work is my own unless otherwise stated.

Jenny Anne Croft

March 1998

Abstract

The euchromatin of mammalian chromosomes is broadly divided into two types with opposing characteristics:

- G-bands are revealed by Giemsa staining. These bands are generally late replicating, AT-rich, low in gene density and appear to have a "closed" chromatin structure.
- R-bands are revealed by reverse Giemsa staining. These bands are generally early replicating, GC-rich, high in gene density and appear to have a more "open" chromatin structure.

These two band types are intercalated throughout the mammalian genome making comparative studies of their behaviour difficult. However, in the human genome, chromosome 18 predominantly displays the features of G-bands and chromosome 19 generally displays the features of R-bands. These chromosomes were shown to be comparable in DNA content and size at metaphase and are, thus, ideal to investigate further the apparent links between chromosome structure and function.

Some models of chromosome structure suggest differences in the higher order packaging of the different band types of metaphase chromosomes. Any differences should be reflected in the overall structure of chromosomes 18 and 19. Combining fluorescence *in situ* hybridisation and biochemical extraction of metaphase chromosomes, I detected no significant differences in their structure.

In contrast, the two chromosomes demonstrated different structural characteristics in the interphase nucleus. I found that chromosome 18 occupies a relatively condensed territory, close to the periphery of the nucleus, while chromosome 19 occupies a considerably larger territory, more centrally located. My studies of different cell types and on cells at different stages of the cell cycle suggest that these characteristics generally apply in human cells, but not in a somatic cell hybrid background. Analysis of nuclei with a reciprocal 18:19 translocation showed that the translocated segments were orientated towards the positions occupied by their structurally normal homologues. The size but not the positioning of an interphase territory appears to be dependent on transcriptional activity.

Furthermore, differences in the way that chromosomes 18 and 19 associate with the interphase nuclear matrix were found. Following salt extraction of nuclei, chromosome 19

remained firmly attached to the residual matrix, while chromosome 18 was released into the DNA loops.

Models of interphase territory organisation have been suggested where genes are preferentially localised to the outer surface of a territory. Using CpG-islands as gene markers, I found no evidence for this in metaphase and interphase chromosomes.

Histone modifications and histone variants allow chromatin structure to be modulated. The acetylation of the core histones is the most studied of such modifications and data in this thesis confirms that acetylation is a dynamic process. Analysis using an antibody to acetylated histone H4 and treatment of cells with inhibitors of deacetylation established that turnover of acetylation is greater in the gene-rich R-bands than in the gene-poor G-bands. Surprisingly, levels of acetylation are very low in the most highly transcribed regions of the human genome, the rRNA encoding regions. An alternative mechanism of chromatin remodelling may be involved in the organisation of these regions.

Only one third of the mass of a human chromosome is DNA, one third is made up of histones and the remainder consists of the relatively uncharacterised non-histone proteins. Human metaphase chromosomes were isolated and injected into mice, in an attempt to raise monoclonal antibodies to novel chromosomal proteins. Eight new antibodies were produced to nuclear components, none of which, however, localised to metaphase chromosomes.

The data presented in this thesis support the concept that the mammalian nucleus is a highly structured and compartmentalised organelle. This view is developed by demonstrating that each chromosome has a characteristic territory shape and position, relative to the nuclear periphery. This configuration appears to be determined by the functional properties of the chromatin types within a specific chromosome, and may be conferred by interactions with different nuclear structures mediated by histone and non-histone proteins. These findings have implications for how the organisation of the nucleus is orchestrated and suggest that chromosome structure and function are closely correlated.

Acknowledgements

As I approach the summit of this particular mountain, I should like to thank some of the numerous people who have helped me to climb.

Firstly, thanks to Wendy Bickmore for leading from the front and teaching me to appreciate and begin to comprehend the wonders of genetics. Paul Perry has been a good friend without whose computer and microscope wisdom most of this thesis would have been impossible (and he makes great bread!). Peter Teague has patiently and diligently dredged through my data to make some kind of sense of it. And Norman Davidson and Douglas Stuart in photography have helped visualise my data to enable others to make some kind of sense of it.

Thanks to my lab colleagues old and new, especially Kathy O, Shelagh (shoes) Boyle, Beth (the American) Sullivan, Muriel (young man) Lee, Jeff (bright shirts and bright ideas) Craig, Joanna (curtains) Bridger, Nicola (party) Mahy, Heidi (Alice in Wonderland) Sutherland, Richard (the mutant with two fish) Axton, Recky Thakra and, not forgetting, DJ (SpiceWorld) Kleinjan.

A mention to Sarah Danes for helping me through some bad times, sharing with me lots of good times and for introducing me to Munros (and Greg). Also to my fellow Munro baggers Jan (not bland) Lawen, Paul (star) Kersey, Tim (the Irish one) Reid, Isobel (beer belly) Ferguson, Chris (good things come in small packages) Watt, Nick (tea boy) Spedding, Will (Bridge champion) Ivory and Katherine (sheep rustler) Falconer. And for hours of fun, to everyone in the Edinburgh University Hillwalking Club, the Edinburgh Open Orchestra and the Hathern Dancing (and mad walkers) Group!

A big thanks to Catherine Spanswick for going through the whole experience with me at a distance, sharing many an adventure with me and remaining to be a very dear friend. To Greg, my best "amigo", who has stood by me through lots of thick and not so much thin! To my Nana for her cheery letters and "sausage money", and to my brother, Stuart, for his abuse and brilliance at "Boggle". To my extended family of Daisy, Toby, Nelly, Millie..... And last, but most certainly not least, to my Mum and Dad for their unfailing love and support in everything I do.

Now, which way down?

Abbreviations

2-D	two-dimensional
3-D	three-dimensional
A	adenine (purine)
AD	Actinomycin D
AMPS	ammonium persulphate
AT	adenine and thymine
ATP	adenosine triphosphate
bp	base pair of DNA
BrdU	5-bromo-2'-deoxyuridine
BSA	bovine serum albumin
C	cytosine (pyrimidine)
C-band	centromeric band
C-terminal	carboxy terminal
CAC	chromatin assembly complex
CAPS	3-[cyclohexylamino]-1-propanesulfonic acid
CBP	CREB-binding protein
CCD	charged couple device camera
cDNA	complementary DNA
C.elegans	*Caenorhabditis elegans*
CENP	centromere protein
CHO	Chinese Hamster Ovary
CLiP	centromere linking protein
CpG	cytosine and guanine
CREB	cAMP response element-binding
CREST	calcinosis, Raynaud's phenomenon, esophageal dysmotility, sclerodactyly, telangiectasia
DAPI	4, 6-diamidino-2-phenylindole
dATP	deoxyadenosine triphosphate
dCTP	deoxycytidine triphosphate
dGTP	deoxygaunosine triphosphate
dH_2O	distilled water
D.melanogaster	*Drosophila melanogaster*
dig	digoxigenin

DMEM	Dulbecco's modified Eagle's medium
DMSO	dimethyl sulphoxide
DNA	deoxyribose nucleic acid
DNAse	deoxyribonuclease
dNTP	deoxynucleoside triphosphate
dTTP	deoxythymidine triphosphate
dUTP	deoxyuridine triphosphate
EDTA	ethylenediaminetetra-acetic acid, disodium salt
EtOH	ethanol
FACS	fluorescence activated chromosome/cell sorting
FCS	foetal calf serum
FISH	fluorescence *in situ* hybridisation
FITC	fluoroscein isothiocyanate fluorochrome
g	gravities
G	guanine (purine)
G-band	longitudinal chromosome pattern produced by Giemsa staining
G1-phase	growth phase 1 of the cell cycle (pre-replication)
G2-phase	growth phase 2 of the cell cycle (post-replication)
GC	guanine and cytosine
GFP	green fluorescent protein
H	histone protein, also heavy isochore
HAT	hypoxanthine, aminopterin and thymidine, also histone acetyltransferase
HCl	hydrochloric acid
HD	histone deacetylase
HEPES	N-[2-hydroxyethyl]piperazine-N'-[2-ethanesulphonic acid]
HMG	high mobility group
hnRNA	heterogeneous nuclear RNA
hnRNP	heterogeneous nuclear RNP
HPRT	hypoxanthine phosphoribosyl transferase
HTF	*HpaII* tiny fragment (100-600bp)
INCENP	inner centromere protein
Kb	kilobase pairs of DNA
KCl	potassium chloride
KCM	potassium chromosome medium (120mM KCl, 20mM NaCl,

	10mM Tris-HCl pH8.0, 0.5mM EDTA, 0.1% Triton X-100)
KDa	kilo Daltons (molecular weight/10^3)
L	light isochore
LAP	lamin-associated protein
LBR	lamin B receptor
LINE	long interspersed repeat element
LIS	lithium diiodosalicylate
lys	lysine amino acid
M	molar
Mb	megabase pairs of DNA
MeCP	methyl-C binding protein
mRNA	messenger RNA
MOPS	3-[N-morpholino]propanesulfonic acid
NaB	sodium butyrate
NaCl	sodium chloride
NOR	nucleolar organising region
N-terminal	amino terminal
OD	optical density
p	chromosome short arm
PAGE	polyacrylamide gel electrophoresis
PBS	phosphate buffered solution
PEG	polyethylene glycol
PEV	position effect variegation
P/CAF	p300/CBP-associated factor
PcG	Polycomb group
PCNA	proliferating cell nuclear antigen
PCR	polymerase chain reaction
PI	propidium iodide fluorochrome
PML	promyelocytic leukemia
PMSF	phenylmethylsulphoxide
pol	polymerase
q	chromosome long arm
R-band	longitudinal chromosome pattern produced by reverse Giemsa staining
R'-band	mundane R-band

rDNA	rRNA encoding DNA
RNA	ribose nucleic acid
RNAse	ribonuclease
RNP	ribonucleoprotein
RNase	ribonuclease
rRNA	ribosomal RNA
S	Svedberg unit (sedimentation coefficient)
S-phase	synthesis phase of the cell cycle (replication)
SAR	scaffold attached region
ScII	scaffold protein II
S.cerevisiae	*Saccharomyces cerevisiae*
SDS	sodium dodecyl sulphate
SINE	short interspersed repeat element
S.maculata	*Salamandra maculata*
SMC	structural maintenance of chromosomes
S.pombe	*Schizosaccharomyces pombe*
SSC	standard saline citrate (1x: 150mM NaCl, 15mM tri-sodium citrate, pH7.4)
SSCM	4xSSC, 5% Marvel dried skimmed milk
ST	Student's T-test
T	thymidine (pyrimidine)
T-band	telomeric band (extreme form of R-band)
TBE	Tris, boric acid, EDTA buffer (90mM Tris-HCl, 90mM boric acid, 2mM EDTA pH8.0)
TBS	Tris buffered saline (50mM Tris-HCl, 150mM NaCl, pH7.5)
TBST	1xTBS, 0.1% Tween20
TE	Tris, EDTA buffer (10mM Tris, 1mM EDTA, pH8.0)
TEMED	N,N,N',N'-tetramethylethylenediamine
topo	topoisomerase
TR	Texas Red fluorochrome
trxG	trithorax group
Tris	2-amino-2-(hydroxymethyl)-1,3-propandiol
TSA	Trichostatin A
UV	ultraviolet
Xa	active X chromosome

Xi	inactive X chromosome
X.laevis	*Xenopus laevis*

Contents

1. Introduction

1.1 The structure of human metaphase chromosomes

Broadly, the chromosome has two basic functions:

1. Efficient packaging of DNA into the interphase nucleus to allow for transcription, replication and repair.
2. Highly condensed packaging at cell division ensuring disjunction of two identical sets of DNA. The highest degree of compaction is achieved at metaphase of mitosis and meiosis.

The present understanding of chromosome structure is based on several levels of organisation. At the first level, the DNA double helix wraps twice around a core histone protein octamer to form "nucleosomes" (Figure 1.1). The first electron microscope observations of chromatin fibres at low salt concentrations revealed nucleosomes as "beads on a string of DNA" (Miller & Bakken, 1972). The octamer consists of two each of the histone proteins H2A, H2B, H3 and H4. The nucleosome has been crystallised and is now well defined at 2.8Å resolution (Luger *et al.*, 1997).

The nucleosome was originally considered to merely prevent any process requiring DNA as the template, for example, transcription and replication. This has been revised to incorporate a more specific and dynamic role with selective interactions of the core histone proteins between themselves, DNA and other proteins (Pruss *et al.*, 1995; Czarnota & Ottensmeyer, 1996). Different types of nucleosome, making use of histone variants, appear to be involved with specialised functions, for example, at the centromere (Wolffe, 1995a). The core histones are subject to a number of post-translational modifications (Section 1.4.1.2).

At the second level of packaging, nucleosomes are organised into the "condensed fibre" mediated by the linker histone protein H1 and its variants (Figure 1.1) (Section 1.4.1.1). The helical "solenoid" model for packaging at this level was postulated by Finch and Klug in 1976, and has become well established (Bartolome *et al.*, 1994). Various other models have arisen, including that of a zigzagged ribbon (Woodcock *et al.*, 1993). Despite years of study, no single model has been substantiated. It is becoming more apparent that the condensed fibre is an irregular structure with some degree of helical coiling and zigzagging,

but more work using minimally destructive techniques is required (Horowitz *et al.*, 1994; van Holde & Zlatanova, 1995; Bednar *et al.*, 1995).

The final levels of packaging are much debated, but the radial "scaffold/ loop" model has predominated over the years (Figure 1.1) (Laemmli *et al.*, 1978; Marsden & Laemmli, 1979; Rattner & Lin, 1985; Boy de la Tour & Laemmli, 1988; Manuelidis & Chen, 1990; Bickmore & Oghene, 1996). In this model the condensed fibre is formed into loops of 50-200 Kb, attached at their base to a non-histone protein scaffold (Jackson *et al.*, 1990; Filipski *et al.*, 1990). Ultimately, the chromosome is compacted to form the chromatid of a metaphase chromosome. Longitudinal contraction is considered to occur through helical coiling of the central scaffold and lateral contraction by the twisting and coiling of the radial loops towards the scaffold (Boy de la Tour & Laemmli, 1988; Saitoh & Laemmli, 1994b).

The scaffold can be visualised microscopically following silver staining of hypotonically swollen chromosomes (Howell & Hsu, 1979) or as a residual fibrous framework surrounded by a cloud of DNA loops following histone extraction of metaphase chromosomes (Paulson & Laemmli, 1977; Earnshaw & Laemmli, 1983; Paulson, 1989; Bickmore & Oghene, 1996). This structure was upheld by the demonstration of fixed and symmetrical positions of genes on sister chromatids of non-extracted metaphase chromosomes (Baumgartner *et al.*, 1991). Further support for this model was received from the observations of the loops of the giant meiotic interphase lampbrush chromosomes of newt cells (Callan, 1982). Three-dimensional reconstruction of unfixed, unstained chromosomes revealed neither a dense nor hollow core within a chromatid (Harauz *et al.*, 1987). It is probable that the "scaffold" is a non-contiguous aggregate of discrete anchoring complexes and not a solid central rod (Earnshaw, 1988; Hock *et al.*, 1996). However, models exist which have no anchoring of DNA loops to a chromosome axis, the solenoid fibre instead twists and coils to form a randomly folded "chromonema" fibre (Belmont *et al.*, 1989; Belmont & Bruce, 1994; Robinett *et al.*, 1996).

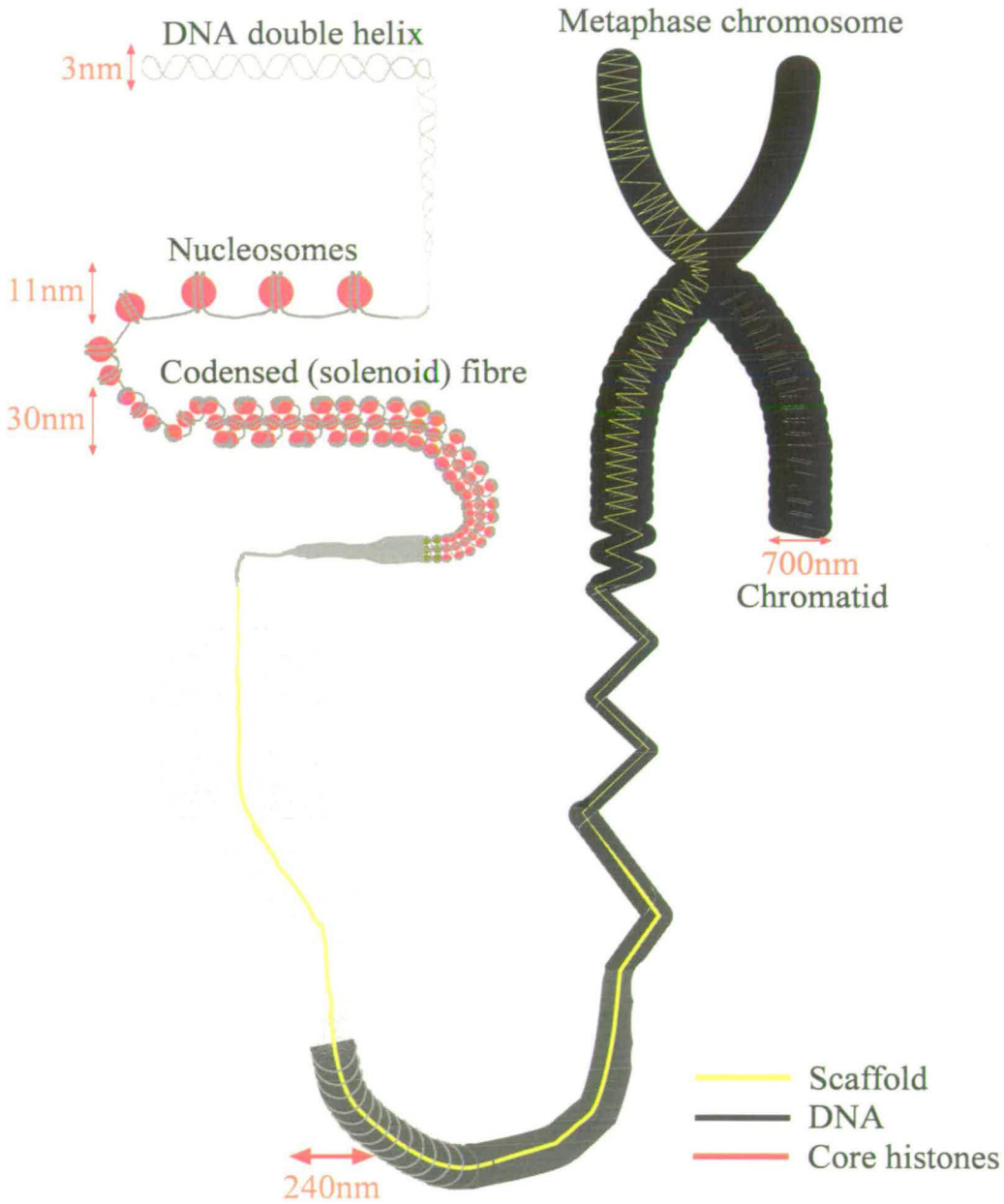

Figure 1.1 A model for the packaging of DNA into a metaphase chromosome Adapted from Craig (1995). The DNA double helix wraps twice around the histone octamer to form nucleosomes (6x compaction). These are then organised into the condensed (solenoid) fibre (40x). This is formed into loops attached at their base to the scaffold (~680x). The scaffold folds to form the metaphase chromatid (>10000x).

1.2 Human chromosome banding techniques

Over the years a number of different staining and labelling techniques have been developed that result in reproducible longitudinal patterns on chromosomes from a wide range of species. The mechanisms involved in producing these patterns are not fully understood, but there is an apparent interdependence between base composition, transcription, replication, recombination, repair and structure. It seems that bands reflect a basic level of chromosome organisation. Described here are the most widely used human chromosome banding techniques, whilst Section 1.3 discusses the striking functional differences that occur between the reciprocal band types.

1.2.1 C-banding and heterochromatin

Constitutive heterochromatin is traditionally defined as the portion of a chromosome that remains condensed throughout the cell cycle. It consists of highly repetitive DNA and in the human genome is found at the centromeres of every chromosome, on the long arm of the Y and at the pericentric regions of chromosomes 1, 9 and 16 (Miklos & John, 1979). These sites are genetically inert. Amounts of constitutive heterochromatin present at each site vary between individuals with no phenotypic consequences, and no active genes have been mapped to there in mammals as yet (Craig & Bickmore, 1993). However, there are genes which reside in the heterochromatic regions of *D.melanogaster* and only function correctly when in such an environment (Review: Gatti & Pimpinelli, 1992). Centromeric (C) banding results from denaturation of the DNA with alkali followed by renaturation with hot saline then staining with Giemsa (Figure 1.2) (Arrighi & Hsu, 1971; Sumner, 1990). C-bands are usually equated with constitutive heterochromatin although not all organisms show complete correspondence. Comings *et al.* (1973) showed that there was extraction of non-C-band DNA and retention of C-band DNA during the technique. Burkholder & Weaver (1977) showed that C-band DNA was protected against DNAse by the presence of non-histone proteins and it is likely that there is a tight association between DNA and protein in these regions.

1.2.2 G-banding, Q-banding and meiotic chromomeres

Quinacrine (Q) mustard was the first fluorochrome noted to produce a differential staining pattern along the length of both human and plant chromosome euchromatin and led to the

full karyotype analysis of the human complement (Figure 1.2) (Caspersson *et al.*, 1968 & 1970). The bright Q-bands are generally considered to be AT-rich, although the exact relationship with base composition is complex (Sumner, 1990).

If Giemsa or Leishmean's stains are preceded by treatment with hot saline (Sumner & Evans, 1971) or trypsin (Seabright, 1971), a reproducible pattern of light and dark bands along the length of the chromosomes is observed, termed G-banding (Figure 1.2). The bright Q-positive bands are also dark G-positive bands. However, Q-banding also reveals additional patterns in constitutive heterochromatin and hence the two are not strictly equivalent.

There is, as yet, no satisfactory hypothesis to explain the mechanism of G-banding. The observation that positive G-bands correspond to the bead-like structures of stained, untreated meiotic pachytene (stage of prophase I) chromosomes, called "chromomeres", suggests that these regions have an intrinsically different chromatin organisation (Okada & Comings, 1974; Ambros & Sumner, 1987).

1.2.3 R- and T-banding

Reverse (R) banding is produced when chromosome spreads are incubated in hot phosphate buffer before staining with Giemsa, producing a banding pattern complimentary to G-banding (positive R-bands correspond to negative G-bands and *vice versa*) (Figure 1.2) (Dutrillaux & Lejeune, 1971). The basis of R-banding seems to be the preferential denaturation of AT-rich DNA followed by intercalation of Giemsa at the under-denatured GC-rich regions. R-banding can also be achieved using a number of GC-specific fluorochromes (Section 1.3.1.1). Acridine orange stains single-stranded DNA red and double stranded DNA green. This stain has also been used to produce R-banding, further supporting the hypothesis of preferential DNA denaturation since negative R-bands appear red and positive R-bands appear green (Sumner, 1990).

Telomeric (T) banding is essentially the same as R-banding but the heat treatment is more severe or prolonged (Dutrillaux, 1978). A subset of R-bands are stained by this approach, greater than half of which are telomeric in location in humans, hence the name. The process of T-banding is thought to denature all but the most GC-rich parts of the genome. R-bands that are not T-bands will be referred to as mundane R-bands (R' bands) (Holmquist, 1992).

1.2.4 Replication banding

The incorporation of thymidine analogues during defined stages of S-phase can be used to study the relationship between timing of replication and chromosome banding. Both tritiated thymidine (Ganner & Evans, 1971) and 5-bromo-2'-deoxyuridine (BrdU) (Dutrillaux *et al.*, 1976; Somssich *et al.*, 1981; Vogel *et al.*, 1989; Fetni *et al.*, 1996; Bourgeois *et al.*, 1996; Review: Drouin & Holmquist, 1994) (Figure 1.2) have been used to label cells. Incorporation of analogues can be detected at the subsequent metaphase, most directly by immunofluorescence (Vogel *et al.*, 1989) or scanning ion analytic microscopy (Bourgeois *et al.*, 1996). Such experiments have revealed that R-bands replicate early and G-bands replicate late (Figure 1.2). In addition, different subsets of bands replicate at different times (Camargo & Cervenka, 1982). However, a recent high resolution study showed that the boundaries between G- and R-bands are defined by a gradient of replication timing rather than a sharp distinction (Strehl *et al.*, 1997). It has been shown that genes within a band (Goldman *et al.*, 1984; Hatton *et al.*, 1988), whole bands (Adolph *et al.*, 1992) and whole chromosomes (Riggs & Pfiefer, 1992; Hansen *et al.*, 1996) can have different replication times dependent upon cell type and developmental stage (Reviews: Holmquist, 1987; Villarreal, 1991).

1.2.5 Standardised nomenclature

Standardised karyotypes and ideograms for human chromosome banding have long been defined by the International System of Cytogenetic Nomenclature (ISCN, 1985). More elongated chromosomes show more bands and ISCN (1985) illustrates human karyotypes with approximately 400, 550 and 850 band resolution. Higher resolution ideograms have been published with approximately 1250 bands achieved by R-banding (Drouin & Richer, 1988) and 2000 bands attained by G-banding (Yunis, 1981). Positive bands show a range of staining intensities and both G-bands (Francke, 1994) and R-bands (Holmquist, 1992) have been sub-classified. A comparison of each of the different banding methods is depicted in Figure 1.2 for human chromosome 9.

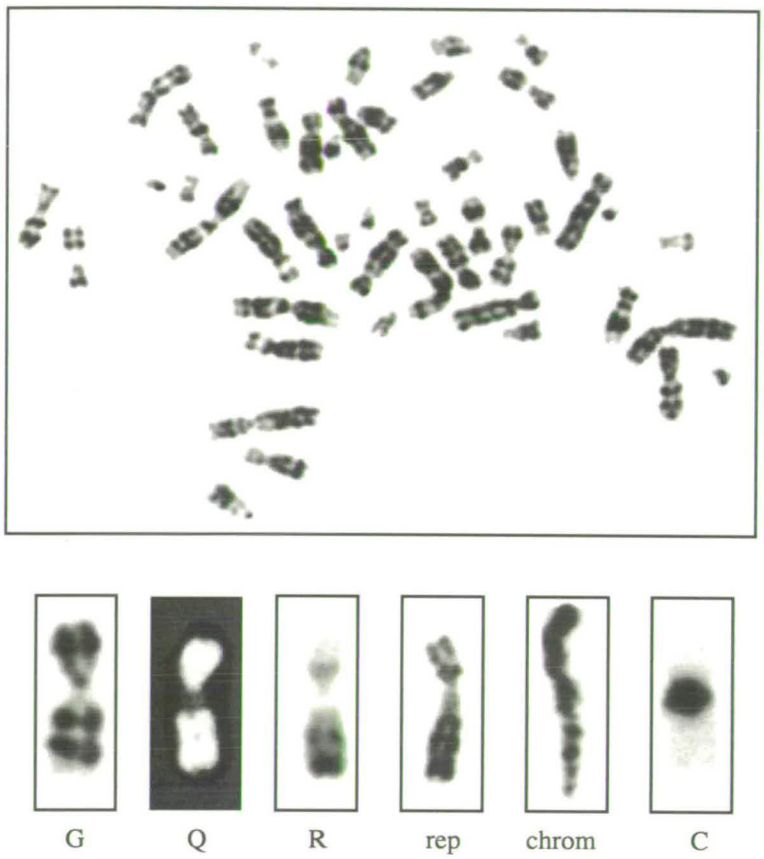

Figure 1.2 Banded human chromosomes
Taken from Bickmore & Sumner (1990). (**Top**) G-banded human metaphase chromosome spread. (**Bottom**) Examples of banded human chromosome 9. **G**- G-banding **Q**- Q-banding **R**- R-banding **rep**- replication banding, with early replicating regions staining dark **chrom**- meiotic pachytene chromomeres **C**- C-banding

1.3 Properties of the human chromosome bands

The bands of human chromosomes (Section 1.2) have a spectrum of associated functional properties (Table 1.1) (Reviews: Bickmore & Sumner, 1989; Craig & Bickmore, 1993; Gardiner, 1995; Bickmore & Craig, 1997).

Table 1.1 A summary of some of the properties of human chromosome bands
There is an apparent interdependence between the mechanisms of chromosome banding and processes of transcription, replication, recombination, repair and chromatin structure.

Band type	G	R	T
Relationship		Negative G-bands	Subset of R-bands
Some properties	Late replicating	Early replicating	Very early replicating
	Correspond to meiotic chromomeres	Correspond to meiotic inter-chromomeres	Not investigated
	Relatively AT-rich	Relatively GC-rich	Very GC-rich
	May contain more triplex DNA	May contain more Z-DNA	May contain more Z-DNA
	LINE-rich	SINE-rich	Very SINE-rich
	Early condensing	Late condensing	Latest condensing
	Low frequency of mitotic and meiotic chiasmata and breakpoints	High frequency of mitotic and meiotic chiasmata and breakpoints	Highest frequency of mitotic and meiotic chiasmata and breakpoints
	Low gene density	High gene density	Highest gene density
	Low CpG-island density	Higher CpG-island density	Highest CpG-island density
	Low levels of histone acetylation	High levels of histone acetylation	Not investigated

1.3.1 Base composition

In general, G-bands are AT-rich, R-bands are GC-rich and T-bands are the GC-richest portions of the human genome. The evidence for this is outlined below.

1.3.1.1 Base-specific fluorochromes and antibodies

There are a number of molecules which show variations in their degree of fluorescence dependent upon the base composition of the bound DNA. AT-specific fluorochromes reveal a G-band pattern, while the GC-specific fluorochromes give R-bands (Review: Sumner, 1990). Interestingly, it has been argued that base composition alone cannot account for the banding patterns observed with some fluorochromes. For example, significant fluorescence of daunomycin, which gives a G-banding pattern, will only occur when bound to DNA of <35% GC content (Comings & Drets, 1976). This figure is lower than the GC-poorest G-bands. Since Holmquist *et al.* (1982) found only a 3.2% average difference in base composition between G- and R-bands, it seems that this is not sufficient to account for daunomycin banding.

Antibodies to specific bases can be used to band denatured chromosomes. Anti-A and anti-T-bind preferentially to G-bands, and anti-C and anti-G bind preferentially to R-bands (Review: Sumner, 1990). Furthermore, Magaud *et al.* (1985) used an antibody to double-stranded DNA with stretches of polyG and polyC to identify R-bands.

The restriction enzyme *HaeIII* has a restriction site of GGCC and will, therefore, cut most frequently within the GC-richest parts of the genome. Fluorescence *in situ* hybridisation (FISH) with small *HaeIII* fragments from human genomic DNA reveals a strong signal on all GC-rich R-bands with a significantly weaker signal on GC-poor G-bands (Craig & Bickmore, 1994).

1.3.1.2 Isochores

On average the mammalian genome is 40% GC, but density gradient centrifugation reveals base distribution to be rather heterogeneous. Bernardi *et al.* (1985) divided non-satellite DNA segments of >200Kb into five arbitrary "isochores". The heavy isochores (H1, H2 and H3) are GC-rich and in humans represent approximately 62% of the total genome, while the

light isochores (L1 and L2) are GC-poor. The GC content of exons, introns and 3rd codon position of several genes was found to correlate well with the associated isochore (Bernardi, 1989; Mouchiroud *et al.*, 1991).

FISH with the individual isochores was used to determine their gross distribution along metaphase chromosomes (Saccone *et al.*, 1993). The L1 and L2 isochores picked out G-bands while R-bands were predominantly hybridised by the H1, H2 and H3 isochores. The H3 isochore alone labelled T-bands, in addition to the rDNA repeat regions. On a finer scale, a study of sequences from the GenBank data base showed that a major proportion of GC-rich genes were located in T-bands, while GC-poor genes were restricted to G-bands and R'-bands (Ikemura & Wada, 1991). Genes linked by <100Kb were found to have a similar GC content (Ikemura *et al.*, 1990), although within a length of sequence GC content could vary by up to 10%. GC content of sequences within a chromosome band can vary widely and adjacent G- and R-bands can contain sequences with similar base composition (Gardiner *et al.*, 1990; Pilia *et al.*, 1993). A close study of 8Mb of DNA in an X chromosome terminal R'-band, revealed that a single band can contain a composite of DNA from different isochores, but that the region of highest GC content corresponded to the region of highest gene density (DeSario *et al.*, 1996).

1.3.2 DNA distribution and unusual DNA conformations

The comparability between G-bands and meiotic chromomeres (Section 1.2.2) argues for a difference in packaging between G- and R-bands at mitosis. Indeed, chromosomes can be banded by Giemsa with no pre-treatments (Sumner, 1990) and G-bands have been observed on fixed, unstained mitotic chromosomes using phase microscopy and UV illumination at the maximum absorption for DNA (McKay, 1973). Using atomic force microscopy it was more recently shown that fixed, unstained, mitotic chromosomes display a longitudinal variation in thickness corresponding to a G-band pattern (Musio *et al.*, 1994). These observations may be a consequence of different quantities of DNA being packaged into the opposing band types. Alternatively, they may be the result of the differential distribution of proteins involved in chromatin packaging and modelling (Saitoh & Laemmli, 1994a & b).

Several conformational variations of DNA from the traditional B-form helix exist. One such variation is the left-handed Z-form helix which can be formed from alternating purine-pyrimidine sequences (Rich *et al.*, 1984). Antibodies to this form of DNA have been found

to identify primate R-bands (Viegas-Pequignot *et al.*, 1983). Triplex DNA forms when two pyrimidine strands share a common purine strand and antibodies to this type of DNA have been shown to identify mouse and human G-bands (Burkholder *et al.*, 1988). Whether these forms of DNA are present in unfixed or native chromosomes (Hill & Strollar, 1983), and what the function of such DNA could be, is still unknown.

1.3.3 Interspersed repeat elements

There are two major types of repeated sequences in the mammalian genome: satellites and interspersed repeats (Review: Singer, 1982). Satellites are long tandem repeats of short sequences (<200bp), reaching several Kb-Mb in total length. In humans, all centromeres are associated with α-satellite (Review: Willard, 1991), while β-satellite (Waye & Willard, 1989; Greig & Willard, 1992) and satellites I-IV (Miklos & John, 1979) are located at the non-centric C-banded regions on chromosomes 1, 9, 16 and Y (Section 1.2.1), and the short arms of the acrocentric chromosomes.

Interspersed elements are families of related sequences scattered at a high frequency throughout the genome and are considered to move by retrotransposition (Reviews: Singer, 1982; Weiner *et al.*, 1986). Short Interspersed Elements (SINEs) are <500bp long and are reiterated 10^5-10^6 times in the human genome. Long Interspersed Elements (LINEs) are several Kb long but occur in the order of 10^4-10^6 times. The *Alu* family of SINEs, are ~300bp in length and are present <910,000x, occupying almost 10% of the human genome. The full length *L1* LINE is 6.4Kb, although frequent truncation, attributed to incomplete reverse transcription, results in smaller fragments. Full and truncated sequences are reiterated <200,000x and ~100,000x respectively, together accounting for 7% of the human genome (Sun *et al.*, 1984; Hwu *et al.*, 1986). The two families differ in their base composition: *Alu* elements are 56% GC and *L1* elements are 42% GC (overall the whole human genome is approximately 40% GC) (Craig, 1995).

FISH studies in humans and mice, have revealed *Alu* elements to be concentrated in R-bands, the brightest regions corresponding to T-bands. Reciprocally, but less clear cut, *L1* elements show a predominance of hybridisation to G-bands, plus a sub-set of R-bands (Manuelidis & Ward, 1984; Korenberg & Ryowski, 1988; Moyzis *et al.*, 1989; Baldini & Ward, 1991; Boyle *et al.*, 1990). In accordance, *Alu* elements occur in the most GC-rich

isochores while *L1* elements are found most commonly in the GC-poor isochores (Soriano *et al.*, 1983). Digesting with the rare cutter restriction enzyme, *NotI* (CG|GGCCGC) results in digestion more frequently within R-bands than in G-bands (Section 1.3.7.4) allowing size fragmentation of the genome. *Alu* elements were shown to be enriched in smaller *NotI* fragments and depleted in longer ones. For *L1* elements the reverse was the case (Chen & Manuelidis, 1989; Sainz *et al.*, 1992). This reciprocal distribution is not absolute, since large-scale sequencing has revealed that SINEs are distributed relatively evenly in all band types (Chen *et al.*, 1989; Edwards *et al.*, 1990; Reviewed in Bickmore & Craig, 1997). One suggestion to reconcile this is that only elements that have retrotransposed recently are sufficiently close in sequence to the progenitor copy to hybridise to probes based on consensus sequence (Yoshiura *et al.*, 1994). The more recent retrotransposition events must, therefore, have occurred into R-bands and, indeed, retrotransposition in several species has been demonstrated to occur preferentially within transcriptionally active regions (Natsoulis *et al.*, 1989; Scherdin *et* al., 1990; Capel *et al.*, 1993). Distribution of elements may be directed by timing retrotransposition with replication of the different band types.

1.3.4 Condensation

The process of condensation of DNA from interphase to metaphase occurs at different rates in different regions. Drouin *et al.* (1991) demonstrated that G-bands condense early and R-bands condense late. This was revealed by the fact that R-sub-bands fuse more readily than G-sub-bands as the number of overall visible bands reduces from prophase to metaphase (Reviewed in: Bickmore & Craig, 1997). Similarly, it was shown that late replicating regions condense earlier in prophase than early replicating regions (Kuroiwa, 1971). The exact process of fusing is unclear and it has been argued that it is due to chromatin reorganisation and not merely contraction (Messier *et al.*, 1989). However, condensation is reversible and Claussen *et al.* (1994) stretched chromosomes up to five times the usual metaphase length to reveal prophase sub-bands.

Condensation can be inhibited by a variety of agents including the DNA intercalating dyes DAPI and ethidium bromide (Rocchi *et al.*, 1979), and the base analogue and methyltransferase inhibitor 5-azacytidine (Schmid *et al.*, 1984). Depleting ScII (Hirano & Mitchison, 1994) (Section 1.4.7), topoisomerase II (topo II) (Adachi *et al.*, 1991) (Section 1.4.6), or sequestering scaffold attachment sequences (SARs) (Strick & Laemmli, 1995) (Section 1.5.1) in *Xenopus laevis* egg extracts interferes with normal chromosome

condensation. Thus, it seems likely that the interaction of DNA with the chromosome scaffold is an integral part of the condensation process. Condensation, controlled by topo II, may play a role in sister chromatin decatenation and segregation (Holm, 1994).

1.3.5 Recombination, mutation and repair

Studies of the distribution of mitotic chiasmata in cells from patients with Blooms Syndrome have revealed hot-spots of recombination. Blooms Syndrome patients have an increased risk of developing cancer due to a high rate of mitotic crossing-over leading to rearrangements, amplifications and regions of homozygosity (Review: Rothstein & Gangloff, 1995). The causal mutation is in a gene encoding a DNA helicase considered to be involved in recombination repair (Ellis *et al.*, 1995), supported by the cytogenetic phenotype of increased chromatid exchange and chromosome breakage. Mapped chiasmata occur most frequently in R-bands (Kuhn *et al.*, 1985). There are indications that hot-spots occur at the same points in normal human mitotic cells which recombine at much lower frequencies. Blood cells subjected to X-irradiation show breakpoints and chiasmata which map most frequently to R-bands, and especially T-bands (Holmberg & Jonasson, 1973; Barrios *et al.*, 1989). Furthermore, breakpoints and rearrangements associated with cancer cells also cluster in R-bands, particularly T-bands (Trent *et al.*, 1989; Mitelman *et al.*, 1997). This may be influenced by selection in tumour cells for mutations in proto-oncogenes and tumour suppressor genes. Translocation breakpoints and inversions in mice (Ashley, 1988) and DNAse I-induced breakpoints in Chinese hamster ovary cells also prevail in R-bands (Folle *et al.*, 1997). In accordance, recombination frequency is highest in the GC-rich isochores and lowest in the GC-poor isochores (Eyre-Walker, 1993).

Studies of meiotic recombination, comparing physical and genetic maps, have resulted in the conclusion that the highest frequency of meiotic chiasmata occurs in T-bands, followed by R'-bands, G-bands and finally C-bands (Fang & Jagiello, 1988; Povey *et al.*, 1992; Chumakov *et al.*, 1992; Holmquist, 1992). In humans and mice, irrespective of band-type there is a high rate of recombination at telomeres and a low rate across centromeres (Laurie & Hulten, 1985; Nachman & Churchill, 1996).

Studies in organisms, as diverse as yeast and maize, have linked hot spots of recombination with regions of high gene density (Shenkar *et al.*, 1991; Goldway *et al.*, 1993; Civardi *et al.*, 1994; Wu & Litchen, 1994). Mutations that derepress transcriptional silencing at the

mating-type loci of *Schizosaccharomyces pombe* also relieve recombinational constraints (Thon *et al.*, 1994) and increased transcription in hamster cells enhances recombination (Nickoloff, 1992). Thus, susceptibility to recombination may purely be a consequence of an active, open chromatin structure, a feature of mammalian R-bands. However, in *Caenorhabditis elegans* meiotic recombination occurs in gene-poor regions (Barnes *et al.*, 1995) and mutants have been reported which alter the pattern but not the overall frequency of recombination (Zetka & Rose, 1995).

Fixed mutations at the molecular level have been shown to differ along regions of the mammalian genome. GC-rich genes show fewer base substitutions than AT-rich genes (Wolfe *et al.*, 1989). Levels of repair are loosely correlated with regions of highest gene activity in bacteria and humans alike (Downes *et al.*, 1993). This is logical, since a high mutation rate in regions containing many genes would be more deleterious than in gene-poor regions.

1.3.6 Methylation and sensitivity to digestion

DNAse I and II, micrococcal nuclease and most restriction endonucleases preferentially digest within R- and T-bands of intact chromosomes (Review: Sumner, 1990). C-bands are most resistant to digestion (Burkholder & Weaver, 1977). The precise banding patterns observed following nuclease treatment are dependable on various factors, including: duration of digestion, base content and length of recognition site, banding protocol, size of enzyme molecule and the ability of digested DNA to diffuse away from the chromosome. For example, studies using restriction endonucleases with AT-rich recognition sites have shown a preferential digestion in G-bands (Sumner *et al.*, 1990), R-bands (Ludena *et al.*, 1991; Tagarro *et al.*, 1992) and no particular band type (Ferrero *et al.*, 1993).

The most predominantly methylated nucleotide in the human genome is cytosine of the dinucleotide CpG. Antibodies to methyl-C have revealed R-bands and most strongly, T-bands and heterochromatic regions by immunofluorescence (Miller *et al.*, 1974; Barbin *et al.*, 1994). Methylation is involved in the control of gene expression, with high methylation of inactive genes and under-methylation of active genes, but this relationship is not clear cut (Reviews: Bird, 1992; Eden & Cedar, 1994; Bird *et al.*, 1995; Martienssen & Richards, 1995; Razin & Shemer, 1995) (Section 1.4.5). Methylation does have a clear role in genomic imprinting, where a gene is expressed dependent upon whether it has been

inherited paternally or maternally (Reviews: Efstratiadis, 1994; John & Surani, 1996). There is also support for the primary purpose of methylation being the neutralising of transposable elements, proviruses and other potentially harmful sequences (Yoder *et al.*, 1997). Roles in replication control have been recently suggested (Rein *et al.*, 1997).

The restriction enzyme *MspI* cuts naked DNA at C|CGG regardless of methylation status, however, it shows a strong bias for cutting non-methylated sites in chromatin. Methylation appears to be a general inhibitor of digestion in a chromatin context (Antequera *et al.*, 1989). When chromatin is treated with 5-azacytidine, which inhibits CpG methylation, nuclease accessibility is increased (Jablonka *et al.*, 1985; Sentis *et al.*, 1993), and heterochromatin and G-bands appear under-condensed (Viegas-Pequignot & Dutrillaux, 1976; Schmid *et al.*, 1984).

1.3.7 Gene distribution

There are a number of different approaches that have been taken to assess the distribution of genes across the human karyotype. Genes are most abundant in T-bands, while G-bands, and especially C-bands, have a dearth of genes.

1.3.7.1 Evidence from cDNA and RNA hybridisation

Yunis *et al.* (1977) isolated total human polyadenylated (polyA) mRNA from a lymphocyte cell line and made tritiated cDNA which was then hybridised to fixed chromosome spreads and autoradiographed. At a resolution of 300 bands, approximately 80% of signal localised to R-bands. Further to this, hybridisation of radiolabelled polyA RNA and heterogeneous nuclear RNA (hnRNA) revealed over 70% of the signal from each to emanate from R-bands (Yunis & Tsai, 1978). There is likely to be a bias with the samples of RNA used since genes transcribe at different levels within different cells.

1.3.7.2 Evidence from correlation with nuclease sensitivity mapping

Active or potentially active genes are preferentially digested with DNAse I due to the specific conformation of chromatin in these regions (Weintraub & Groudine, 1976; Reviews: Gross & Garrard, 1987; Elgin, 1988). This selective sensitivity is maintained in fixed mitotic chromosomes (Gazit *et* al., 1982). *In situ* nick translation of fixed

chromosome spreads using radioactively labelled bases and autoradiography has shown that DNAse I sensitive segments correspond generally to R-bands (Kerem *et al.*, 1984; Sumner *et al.*, 1993). However, there will be a collection of inactive genes, mainly tissue-specific, that will not be detected by this method.

1.3.7.3 Evidence from isochore studies

Mouchiroud *et al.* (1991) calculated that the gene density of the GC-richest 3% of the genome (H3 isochore) is about eight times higher than that of the GC-rich H1 and H2 isochores, which make up 31% of the genome, and about sixteen times more than the AT-rich L1 and L2 isochores, which make up the remainder of the genome. This data supports the fact that the GC-richest T-bands are more gene-rich than the GC-rich R-bands, which are more gene-rich than the GC-poor G-bands (Review: Gardiner, 1996).

1.3.7.4 CpG-islands as gene markers

Approximately 98% of the human genome possesses the dinucleotide CpG at a lower frequency than that expected by comparison with GpC frequency. Depletion of CpG is proposed to be due to the high rate of mutability of methyl-C to T followed by partner strand change from G to A (Selker & Stevens, 1985; Yebra & Bhagwat, 1995; Review: Bestor & Coxon, 1993). The remaining minor fraction of DNA has CpG at the expected frequency and cytosine is almost always non-methylated. This fraction is distributed throughout the genome in regions of 1-2 Kb in length called CpG-islands (Bird *et al.*, 1985; Bird, 1987). There are about 45,000 islands in the haploid human genome (Antequera & Bird, 1993).

Almost 60% of human genes have a CpG-island at the 5' end, including all housekeeping genes and widely expressed genes, and approximately 40% of tissue-specific genes or genes with limited expression so far studied (Larsen *et al.*, 1992). CpG-islands are useful landmarks for identifying genes in the genome. Although approximately 60% of tissue-specific genes are not represented, there is no significant difference between the distribution of genes with and without islands (Larsen *et al.*, 1992; Craig, 1995). CpG-islands have an open chromatin structure with nucleosome free regions, low levels of H1 (Section 1.4.1.1) and highly acetylated H3 and H4 (Section 1.4.1.2). It seems likely that these are sites of interaction between transcription factors and promoters (Tazi & Bird, 1990).

The restriction site of *HpaII* (C|CGG) is methylation sensitive and 25% of genomic *HpaII* sites are within CpG-islands (Bickmore & Bird, 1992). Unmethylated and accessible *HpaII* sites have been shown to cluster in R-bands which suggested that CpG-islands would preferentially be localised to these bands (Sentis *et al.*, 1993). CpG-islands may be isolated as the discrete small fractions (100-600bp) generated by cleavage with *HpaII* (Bird *et al.*, 1985). Craig and Bickmore (1994) biotinylated such fragments and used FISH to detect hybridisation to fixed human chromosome spreads. A strong correlation with R-bands, the strongest signal mainly being in the T-bands was revealed (Figure 1.3).

Cleavage of human genomic DNA with the methylation-sensitive restriction enzymes; *BssHII* (G|CGCGC), *EagI* (C|GGCCG) and *SacII* (CCGC|GG), in combination cuts CpG-islands but leaves inter-island DNA intact. FISH with the fraction separated using pulse-field gel electrophoresis, where inter-island distances were <100 Kb reflected the CpG-island profile, indicating that the majority of islands are within 100 Kb of each other (Craig & Bickmore, 1994; Review: Cross & Bird, 1995) (Figure 1.3).

The distribution of CpG-islands on rodent chromosomes also equates to the early replicating R-bands (Cross *et al.*, 1997a). Additionally, in chickens CpG-islands are concentrated to the microchromosomes (McQueen *et al.*, 1996), which constitute 25% of genomic DNA and replicate earlier than the macrochromosomes (Schmid *et al.*, 1989).

Complete *NotI* restriction maps have been constructed for the long arms of chromosome 21 (Ichikawa *et al.*, 1993) and chromosome 11 (Hosoda *et al.*, 1997). *NotI* (GC|GGCCGC) cuts almost exclusively within CpG-islands. Approximately 30% of islands in the human genome possess this site (Bickmore & Bird, 1992). *NotI* sites were most frequently located in R- and T-bands and the average spacing was less than in G-bands.

1.3.7.5 Evidence from mapped genes

Although the number of genes being mapped in the human genome is increasing almost exponentially, there is no database to assess the band locations. Discrepancies between banding resolution and mapping techniques would make results difficult to interpret. Using a resolution of 400 bands, Craig (1995) made an assessment of the location of 1771 genes, approximately 2% of the estimated total of 80,000 human genes (Antequera & Bird, 1993). He concluded that, based on relative proportion of euchromatin, T-bands contained over

twice the expected gene density, while G-bands possessed less than half of the number of expected genes (Table 1.2). A tendency for expressed sequence tags (ESTs) to cluster in R-bands was recently eluded to as evidence that genes cluster in these regions (Schuler *et al.*, 1996).

Table 1.2 Gene distribution across the human chromosome bands
Adapted from Craig (1995). 400 band resolution. 1771 mapped genes taken from listings in the Human Genome Data Base, Baltimore and from scanning the literature. Expected gene densities were estimated by assuming an even distributed of genes across euchromatin.

Band type	G	R	T
Proportion of euchromatin	45.5%	54.4%	20.2%
Proportion of genes	20.0%	80.0%	45.6%
Observed/expected gene density	0.44	1.47	2.26

It is interesting that in mice, genes appear to show considerably less variation in number across the chromosomes than in humans (Cross *et al.*, 1997a). It is considered that the human genome is more representative of an ancestral mammal and more closely linked in organisation to the genomes of cows, pigs and cats, than that of mice (O'Brien *et al.*, 1988). The genomes of rodents have become rearranged such that at the cytological level, large blocks that are gene-rich and gene-poor are not visible, as revealed by FISH with CpG-island fragments (Cross *et al.*, 1997a). However, this organisation does appear to be maintained on a finer scale, possibly indicating a functional constraint on maintaining such compartments.

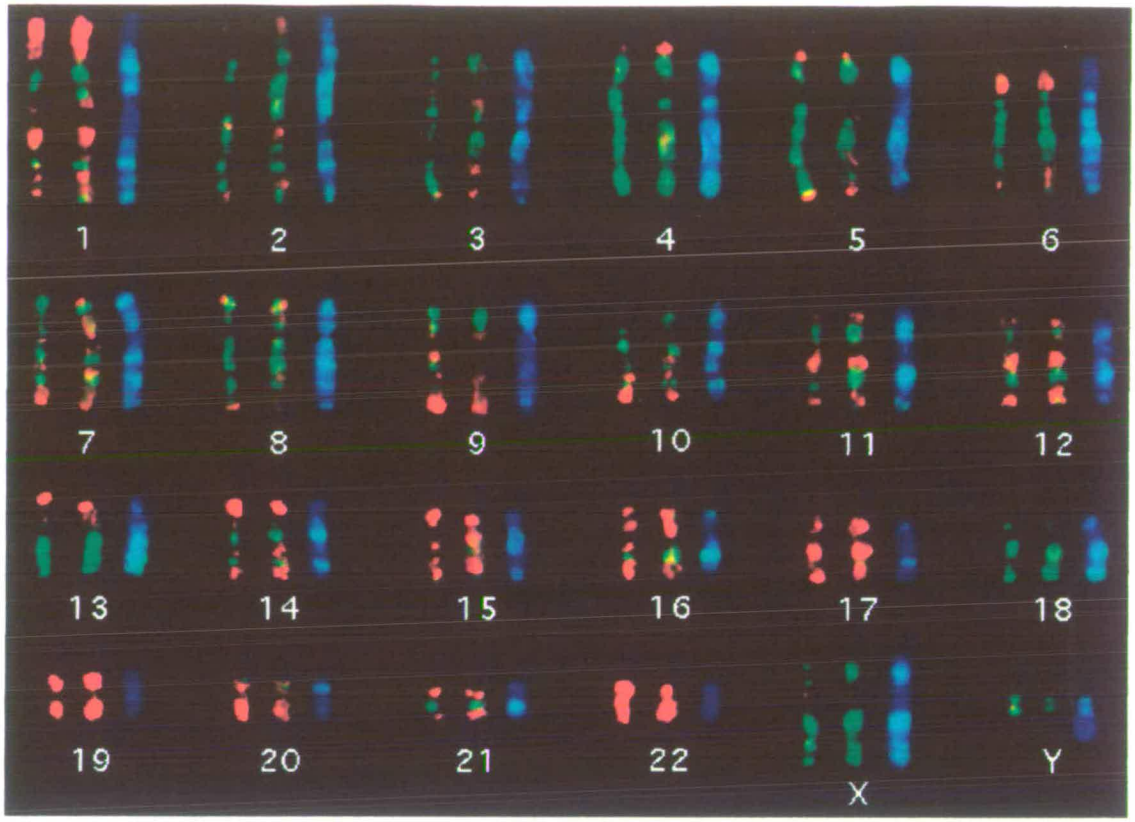

Figure 1.3 The clustering of CpG-islands throughout the human genome
Taken from Craig & Bickmore (1994). BrdU incorporation detected with anti-BrdU-FITC reveals late replicating regions in green. (**Left**) Biotin labelled *HpaII* fragments, selected to represent CpG-islands, and detected with avidin-TR (red). (**Middle**) Biotin labelled inter-island fragments <100 Kb, selected to represent regions of the genome where CpG-islands are high in density, and detected with avidin-TR (red). (**Right**) DAPI (blue) stained chromosomes.

1.4 Chromosomal proteins

The previous section discussed the pattern of attributes of chromosome bands. Each of the properties and processes described require interactions between DNA and an array of different proteins, acting at the various levels of chromosome packaging. This section discusses some of the key proteins involved.

1.4.1 Histone modifications and variants

Histones were originally considered to be metabolically inert components of chromatin, but the discovery of histone acetylation, methylation, ribosylation, ubiquitination and phosphorylation has altered that view. Both core and linker histones are subject to a different array of modifications and variant substitutions (Reviews: Bradbury, 1992; Wolffe, 1995a & b).

1.4.1.1 Linker histone modifications and variants

Variations in the degree of packaging of the condensed fibre may be achieved by substitution of alternative forms or differing amounts of H1 (Huang & Cole, 1984; Sun *et al.*, 1989; Brown *et al.*, 1996). H1 is considered to have a general role in chromatin condensation (Thoma *et al.*, 1979; Huang & Cole, 1984; Kamakaka & Thomas, 1990; Shen *et al.*, 1995), although it is not essential for mitotic chromosome formation (Ohsumi *et al.*, 1993; Shen *et al.*, 1995). It has recently been proposed that linker histone variants have a subtle and specific role in transcriptional regulation (Dimitrov & Wolffe, 1996; Shen & Gorovsky, 1996; Steinbach *et al.*, 1997; Review: Wolffe *et al.*, 1997a).

Phosphorylation of H1 creates an interesting paradox. Increased phosphorylation of all H1 variants increases throughout the cell cycle, peaking at mitosis (Talasz *et al.*, 1996), suggesting a correlation with increased condensation. In contrast, phosphorylation has been shown to loosen links between H1 and DNA, and to be associated with transcription and replication competent chromatin (Lu *et al.*, 1994 & 1995; Halmer & Gruss, 1996; Chadee *et al.*, 1997). It has been proposed that H1 phosphorylation is a first step mechanism, promoting transient decondensation and allowing access of proteins for transcription, replication and condensation (Roth & Allis, 1992; Lu *et al.*, 1994 & 1995), although condensation can occur without H1 phosphorylation (Guo *et al.*, 1995).

1.4.1.2 Core histone modifications and variants

The tight association of the core histones in the nucleosome is due to their globular C-terminal domains. Sites of ubiquitination on H2A and H2B are located here, but there is no evidence that ubiquitination results in the degradation of labelled histones. This modification appears most commonly on H2A and H2B of transcriptionally active chromatin (Nickel *et* al., 1989) and is present throughout the cell cycle until prophase, when it is lost until metaphase (Matsui *et al.*, 1979; Mueller *et al.*, 1985). The modification is required for transition from S-phase to G2 but apparently must be removed for metaphase chromosomes to condense (Review: Bradbury, 1992). Ubiquitinated H2A colocalises with replication complex proteins at interphase (Vassilev *et al.*, 1995).

The flexible N-terminal domains of core histones are the most highly conserved and possess the sites for most modifications. The most studied of these modifications is acetylation which will be discussed below. Little is known about the processes of phosphorylation and ribosylation. Ribosylation preferentially occurs on acetylated histones (Golderer & Grobner, 1991) suggesting possible links with transcriptional regulation. Phosphorylation has been shown to be promoted by factors that enhance levels of transcription (Mahadevan *et al.*, 1991), however, this modification has also been associated with heterochromatin and spreads along chromosomes coincident with condensation at the onset of mitosis (Hendzel *et al.*, 1997).

The number of known core histone variants is continually increasing. The transcription factor complex, TFIID contains a structure closely resembling that of the heterodimer of H3 and H4 (Hoffmann *et al.*, 1996; Xie *et al.*, 1996). It is tempting to envisage that DNA may wrap around parts of TFIID in a similar manner to the nucleosome and create a conformational change permissive for transcriptional initiation. Another such variant is that of the centromere-specific H3-like protein, CENP-A (Section 1.5.2).

1.4.1.3 Core histone acetylation

Acetylation occurs in the absence of histone synthesis and is a reversible process (Review: Loidl, 1994). The sites of acetylation are a defined set of lysine (lys) residues which are modified in a general order in most organisms (Turner & Fellows, 1989; Turner & O'Neill, 1995). Experiments with antibodies raised to the different isoforms of acetylated H4

suggest that each mediates a different effect on chromatin structure. In *Drosophila melanogaster* centric heterochromatin, H4 is hypoacetylated at lys5, 8 and 16, but shows high levels of lys12 acetylation (Turner *et al.*, 1992). H4 acetylated at lys16 is found in the most acetylated forms and is located at numerous sites along the hyperactive X chromosome of male but on no other chromosome in males or females (Turner *et al.*, 1992). This has been directly linked to dosage compensation allowing an increase in transcription of genes on the X chromosome in males to equalise X-linked gene expression to that of females (Section 1.4.8). Conversely, in female mammals the single inactive X chromosome (Xi) has low levels of H4 acetylation correlated with a general decrease in X-linked gene expression allowing for dosage compensation (Jeppesen & Turner, 1993; Belyaev *et al.*, 1996; Boggs *et al.*, 1996). However, three regions on Xi showed persistence of acetylated H4. Two of these regions are known to contain genes which are expressed on Xi and this supports the suggestion that H4 acetylation defines regions of transcriptional activity (Jeppesen & Turner, 1993). However, Keohane *et al.* (1996) demonstrated that deacetylation of Xi followed reduced gene expression and transition to late replication, and suggested that hypoacetylation is necessary for the maintenance but not the initiation of X-inactivation.

Levels of H4 acetylation are not uniform along metaphase chromosome. There is relatively high acetylation at regions corresponding to R-bands while, in contrast, heterochromatic regions are underacetylated (Jeppesen *et al.*, 1992). This appears to be maintained at interphase, as demonstrated by FISH with chromatin fragments fractionated by their general level of acetylation (Breneman *et al.*, 1996). Reflecting this colocalisation with gene-rich chromatin, interphase CpG island chromatin fractions have highly acetylated core histones (Tazi & Bird, 1990). In plants also, it has been shown that high levels of acetylation mirror the distribution of genes along chromosomes (Houben *et al.*, 1996; Idei *et al.*, 1996; Houben *et al.*, 1997).

Is core histone acetylation associated with genes generally, or only those which are transcriptionally active? Is the modification a passive marker or actively required for transcription? Probing of specific genes in chromatin fractionated by levels of lys acetylation suggested a correlation between high core histone acetylation and transcription (Hebbes *et al.*, 1988). However, immunofluorescence revealed that the transcriptionally active puffs of *D.melanogaster* polytene chromosomes were not associated with levels of H4 acetylation higher than that of the remaining euchromatin (Turner *et al.*, 1990). In addition,

the chicken β globin gene was shown to be endowed with highly acetylated forms of H4 even when not active (Hebbes *et al.*, 1992, 1994). Studies with a large number of genes in human cells support the hypothesis that states of H4 acetylation are connected with transcriptional potential rather than transcriptional activity directly (O'Neill & Turner, 1995).

In accordance, substitution experiments in *Saccharomyces cerevisiae* define a role for H4 acetylation in the regulation of transcriptional silencing. Substitution of lys16 with neutral amino acids, mimicking acetylation, results in derepression at the mating-type loci and telomeres. Substitution with a positively charged amino acid show no such affect, suggesting that it is conservation of the positive charge at this position that correlates with repression (Review: Thompson *et al.*, 1993). Interestingly, acetylation of H3 and H4 may have different affects. While deletions of the H4 N-terminus results in general derepression, deletions of the N-terminus of H3 results in hyperactivity of some genes. (Mann & Grunstein, 1992) and swapping the N-terminus of H3 onto H4 shows a more severe derepression than the deletion of the H4 N-terminus alone (Ling *et al.*, 1996). The silent mating-type loci and telomeres of yeast correspond to regions of hypoacetylation of the core histones (Braunstein *et al.*, 1996). Additionally, hypoacetylation is essential for gene repression in centromeric heterochromatin and for proper chromosome function (Ekwall *et al.*, 1997).

Lee *et al.* (1993) demonstrated a positive role for acetylated H4 and the other core histones in the binding of the transcription factor, TFIIIA to chromatin *in vitro*. Removal of the N-terminal tails from the core histones also facilitated this interaction. In separate studies, both acetylation and removal of the N-terminal of H4 aided binding of the transcription factor GAL4 (Vettese-Daley *et al.*, 1994 & 1996). This facilitation of transcription was independent of, but inhibited by, linker histone binding (Ura *et al.*, 1997). There is a modest reduction in wrapping of DNA around the core histone octamer as a result of acetylation and this could hold the key to the mechanism of derepression and transcriptional promotion (Review: Garcia-Ramirez *et al.*, 1995). However, it is also possible that histone acetylation creates or eliminates binding sites for particular activator or repressor proteins, aside from any changes in general chromatin structure.

Treatment of cells with the inhibitors of histone deacetylase activity, sodium butyrate (Riggs *et al.*, 1977; Vidali *et al.*, 1978) and Trichostatin A (Yoshida *et al.*, 1990), cause a generalised increase in transcription. In addition, silent, virally transduced genes can be reactivated by treatment with Trichostatin A (Chen *et al.*, 1997). However, van Lint (1996) showed an altered activity in only 8 of 340 human genes examined after treatment with Trichostatin A. In complete contrast, treatment has been shown to actually inhibit transcription of specific genes. For example, steroid-dependent activation of chicken egg white genes was blocked by treatment with sodium butyrate (McKnight *et al.*, 1980). Recent studies in *S.cerevisiae* suggest that an alternative region in each of the core histones, distinct from those containing the sites for acetylation, are responsible for basal transcriptional repression (Lenfant *et al.*, 1996). It is likely that acetylation plays a subtle, possibly indirect and gene-specific, role in transcriptional regulation.

1.4.1.4 Acetyltransferases, deacetylases and acetylated histone binding proteins

The most direct link between acetylation and transcriptional activity has arisen from the cloning of several histone acetyltransferases and deacetylases (Reviews: Grunstein, 1997; Wade *et al.*, 1997; Wolffe *et al.*, 1997b). Histone acetylatransferases (HATs) are characterised into two types: A and B. Cytoplasmic acetylation for chromatin assembly involves the B-type HATs (see below). It was a nuclear, A-type HAT that was purified and cloned in *Tetrahymena* (Brownell *et al.*, 1996), and found to have homology to the *S.cerevisiae* transcriptional coactivator, GCN5 (Georgakopoulos & Thireos, 1992). The HAT domains of each protein are complementary (Wang *et al.*, 1997). Gcn5p has the capacity to acetylate H3 and H4 at specific residues most commonly modified for transcription (Kuo *et al.*, 1996) however, *in vivo* Gcn5p is required to be part of a complex for HAT activity (Candau *et al.*, 1997). Similar enzymatic activities have since been established for the human GCN5 homologue, P/CAF (p300/CBP-associated factor) (Yang *et al.*, 1996b), a factor which interacts with the coactivator complex p300/CBP (CBP: CREB-binding protein; CREB: cAMP response element-binding protein), which also has intrinsic HAT activity (Bannister & Kuozarides, 1996; Ogryzko *et al.*, 1996). p300/CBP interacts with a variety of sequence-specific transcription factors via several activators, including CREB (Figure 1.4). Interestingly, P/CAF competes with the adenovirus transcription factor, E1A, for association with p300/CBP. The E1A-p300/CBP complex also has HAT activity and it could be that E1A directs this activity to alternative targets resulting in inappropriate gene expression and transformation (Yang *et al.*, 1996b). Further to this, a component of

TFIID has been shown to have HAT activity in humans, flies and yeast, alike (Mizzen *et al.*, 1996) (Figure 1.4). Interestingly, a putative HAT encoded by the *D.melanogaster males-absent on the first (mof)* is considered to be involved in dosage compensation, since mutations in this gene are lethal and lead to hypoacetylation of the male X chromosome (Hilfiker *et al.*, 1997) (Sections 1.4.1.3 & 1.4.8). There is little significant sequence identity or structural similarity with any of the above mentioned HATs, emphasising the diversity of such Gcn5p-like proteins (Neuwald & Landsman, 1997).

Histone deacetylases (HDs) are also linked directly to transcriptional control, but not explicitly to repression. An affinity matrix containing trapoxin, a deacetylase inhibitor, was used to isolate the human HD, HDAC1 (Taunton *et al.*, 1996). This protein is homologous to *S.cerevisiae* RPD3, mutations in which disrupt both the activation and repression of specific genes (Vidal & Gaber, 1991). In addition, a second human HD, HDAC2, binds to YY1, a DNA-binding protein that can act as both a repressor or activator (Yang *et al.*, 1996a). A complex picture is being built to explain the gene-specificity of HD-mediated repression (Reviews: Grunstein, 1997; Pazin & Kadonaga, 1997). It remains to be determined whether deacetylation actually causes repression. That the effects of HD mutations interfere with both activation and repression, suggests that it is not simply a matter of deacetylation passively corresponding to repression. The binding of other repressor proteins appear to be modulated by histone acetylation (Edmondson *et al.*, 1996).

Chromatin is assembled during replication using H4 acetylated at lys5 and 12 but hypoacetylated H3 in mammals (Sobel *et al.*, 1995; Turner & O'Neill, 1995). The B-type HATs are responsible for this H4 acetylation (Review: Brownell & Allis, 1996). The chromatin assembly complex (CAC) is made up of H3, acetylated H4 and CAF-1 (chromatin assembly factor-1). Many chromatin assembly factors construct nucleosomes in the absence of replication and do not discriminate between newly synthesised histones and histones isolated from chromosomes (Review: Kaufman & Botchan, 1994). However, CAF-1 possesses both of these specificities. This protein has three sub-units, one of which is p48 (Verrault *et al.*, 1996), a polypeptide shared with yeast B-type HAT (Parthun *et al.*, 1996) and human HDAC1 (Taunten *et al.*, 1996), and which is involved in the high affinity interaction of these complexes with H4. This link between p48 and both HAT and HD activity has led to the model in which deacetylation, following assembly, may be required to release CAF-1 and allow subsequent maturation of chromatin (Review: Roth & Allis, 1996).

Is the specific acetylation of H4 essential for chromatin assembly? The N-termini of H3 or H4 can be deleted without preventing nucleosome assembly in yeast (Kayne *et al.*, 1988; Megee *et al.*, 1995; Ling *et al.*, 1996) and *X.laevis* egg extracts (Freeman *et al.*, 1996), but deletion of both simultaneously does block assembly, suggesting a degree of redundancy. CAF-1 is also needed for reassembly of chromatin after DNA repair (Gaillard *et al.*, 1996), and indeed the presence of lys residues at the H4 N-terminus appears to be necessary for maintaining genome integrity and progress through the cell cycle (Megee *et al.*, 1995; Review: Turner, 1995).

1.4.2 The Polycomb- and trithorax-group proteins

The homeotic genes of *D.melanogaster* provide a model for the study of maintenance of gene expression states through development. Two classes of chromatin maintenance proteins have proved to be important: Polycomb group (PcG) repressors and trithorax group (trxG) activators (Review: Simon, 1995).

Over a dozen PcG proteins are known and although diverse, some share certain motifs. The chromodomain of the Polycomb protein is also found in the constitutive heterochromatin associated protein HP1 (Paro & Hogness, 1991; Messmer *et al.*, 1992; Suso Platero *et al.*, 1995), as well as a number of other heterochromatin associated proteins in a variety of species, and is essential for chromosomal localisation and repressive activity (Singh *et al.*, 1991; Pearce *et al.*, 1992; Saunders *et al.*, 1993; Review: Lohe & Hilliker, 1995). Protein-protein interaction is probably the function of the chromodomain (Ball *et al.*, 1997). This has led to the belief that PcG proteins exert their affects via formation of large complexes, which vary in composition from site to site (Pelegri & Lehmann, 1994; Muller *et al.*, 1995; Strutt & Paro, 1997). Once associated with chromatin, how does the PcG complex cause repression? Support is gathering for a model involving the formation of heterochromatin-like structures, where the cooperating PcG proteins wrap the locus into an inaccessible configuration which can extend along chromatin in a manner similar to that of position effect variegation (PEV) (Paro, 1993; Henikoff, 1996; Strutt *et al.*, 1997; Review: Pirrotta, 1997) (Section 9.4.1). Disruption of the PcG complex results in local decondensation of polytene chromosomes at expected sites (Rastelli *et al.*, 1993). However, it has recently been shown that PcG binding blocks DNA polymerase II activation, but does not simply exclude all proteins since T7 RNA polymerase finds access to transcribe the region (McCall & Bender, 1996).

It is the role of the trxG proteins to counteract PcG-induced repression. These proteins are heterogeneous in sequence, structure, site of action and mechanism and there is no evidence that they form a complex (Reviews: Orlando & Paro, 1995; Pirrotta, 1995). The trxG proteins work to facilitate the binding of activators to promoter regions by creating an open chromatin configuration. A much studied example is the *D.melanogaster* GAGA protein, encoded by the *trithorax-like* gene, which acts in conjunction with the ATP-dependent chromatin remodelling protein NURF (Tsukiyama *et al.*, 1994; Review: Granok *et al.*, 1995) (Section 1.4.3).

There are equivalents of PcG and trxG proteins in other eukaryotes (Singh *et al.*, 1991; Pearce *et al.*, 1992; Muller *et al.*, 1995; Goodrich *et al.*, 1997; Reviews: Lohe & Hilliker, 1995; Gould, 1997; Schumacher & Magnuson, 1997). The mouse *Bmi1* gene shares striking homology to the *D.melanogaster* PcG protein Posterior sex combs (Brunk *et al.*, 1991; van Lohuizen *et al.*, 1991). Bmi1 has recently been shown to be part of a multimeric complex with other PcG-like proteins which colocalise in speckles in interphase nuclei. Mutations in Bmi1 which destroy complex formation also disrupt embryonic development (Alkema *et al.*, 1997). Bmi1 coimmunoprecipitates with HPH1, a human homologue of the *D.melanogaster* PcG protein Polyhomeotic (Alkema *et al.*, 1997; Gunster *et al.*, 1997), and RING1, a human RING-finger containing protein (Satijn *et al.*, 1997). The RING-finger has been implicated in DNA- and protein-protein interactions (Review: Freemont, 1993) and RING1 can act as a transcriptional repressor. This data suggests that BMI1, RING1 and HPH1 are all components of a mammalian PcG complex.

1.4.3 ATP-dependent chromatin remodelling complexes

Evidence points to a competition model for transcriptional activity, where transcriptional activators work to counteract multiprotein repression complexes (Elgin, 1996; Kingston *et al.*, 1996). Such activators include the SWI/SNF multisubunit complex consisting of approaching a dozen components (Reviews: Peterson & Tamkun, 1995; Peterson, 1996). The SWI/SNF complex interacts directly with DNA in an ATP-dependent manner. Models have been constructed in which this binding displaces H2A-H2B from the core nucleosome creating access for transcription factors such as GAL4 in *S.cerevisiae* (Cote *et al.*, 1994; Owen-Hughes *et al.*, 1996). The SWI and SNF proteins are also an integral part of the RNA polymerase II holoenzyme in *S.cerevisiae* (Wilson *et al.*, 1996). In this capacity the SWI/SNF complex is probably used to facilitate binding of the transcription initiation

complex. Homologues of the SWI/SNF complex have been identified in both *D.melanogaster* and humans but recent studies have shown that the story is far from simple. Functionally distinct SWI/SNF-like complexes exist, made up of different combinations of subunits and involved in chromatin remodelling at different gene loci (Cairns *et al.*, 1996; Wang *et al.*, 1996; Review: Peterson, 1996).

NURF (nucleosome remodelling factor) was purified by Tsukiyama & Wu (1995) from *D.melanogaster* and is also a multi-subunit ATP-dependent chromatin remodelling complex. NURF is distinct from SWI/SNF but interestingly, one of the sub-units of NURF is ISWI, the imitation SWI gene (Tsukiyama *et* al., 1995). The interaction between NURF and the nucleosomes is impaired by removal of the N-termini of the core histones (Georgel *et al.*, 1997). Therefore, while the substrate recognised by SWI/SNF is DNA (Laurent *et al.*, 1993), NURF requires a DNA-histone complex.

It is likely that there are a great number of other protein complexes involved in modulating access to DNA within chromatin (Review: Krude & Elgin, 1996).

1.4.4 High mobility group (HMG) proteins

There are three families of HMG proteins all characterised by being of low molecular weight, highly charged and abundant. All were originally identified by their association with chromatin, but between families there is little sequence and motif homology (Review: Bustin *et al.*, 1990).

HMG-14 and -17 bind specifically to the core nucleosomes (Alfonso *et al.*, 1994) and are preferentially localised to regions of the genome which are actively being transcribed (Postnikov *et al.*, 1991; Review: Bustin *et al.*, 1990). Both proteins increase the efficiency of initiation of transcription (Paranjape *et al.*, 1995; Trieschmann *et al.*, 1997 and, at least for HMG-14, this is achieved by disruption of H1-dependent chromatin compaction (Ding *et al.*, 1997). Abundance, wide distribution and evolutionary conservation suggest an important role for these proteins, however, an open chromatin structure and normal growth is maintained in the absence of both proteins in a chicken cell line (Li *et al.*, 1997).

The DNA binding domain common to HMG-1 and -2 gave rise to the term "HMG-box", a motif since found in a diversity of other proteins (Reviews: Grosschedl *et al.*, 1994; Bianchi

& Lilley, 1995). There are two sub-families of HMG-box proteins. HMG-1 and -2 and the nucleolar transcription factor, UBF are members of the sub-family characterised by proteins that are present in all cell types, have multiple HMG-boxes and have a low sequence binding specificity. Proteins that have a restricted distribution, one HMG-box and bind to specific sequences make up the other sub-family, and include the mammalian male sex determining factor, SRY and enhancer binding factors LEF-1 and TCF-1. All of these proteins share the common capacity to bend DNA and a binding affinity for distorted DNA structures (Suda *et al.*, 1996). They have been assigned architectural roles, moulding and bending DNA. HMG-1 and -2 are involved in: recombination (van Gent *et al.*, 1997), chromatin assembly (Review: Travers, 1994), transcriptional activation by stabilising promoter complexes (Shykind *et al.*, 1995; Zappavigna *et al.*, 1996) and transcriptional repression by replacing H1 as a linker (Ner & Travers, 1994; Ura *et al.*, 1996). No differences in HMG-1 and -2 abundance in transcribed versus non-transcribed chromatin has been identified by immunoprecipitation of chicken chromosomes (Postnikov *et al.*, 1991), and HMG-1 has been shown to not be stably associated with chromatin *in vivo* (Falciola *et al.*, 1997). However, HMG-1 has been localised to *D.melanogaster* polytene chromosome puffs, again suggesting a link with transcriptional activity (Ghidelli *et al.*, 1997). Some mitotic banding has also been reported for HMG-2 (Smith *et al.*, 1978). The functions of HMG-1 and -2 remain poorly understood.

HMG-I and -Y differ by the presence or absence of an 11 amino acid sequence but the functional difference between the two forms is not yet known (Friedmann *et al.*, 1993). Both forms of the protein bind specifically to AT-rich sequences *in vivo* and *in vitro* (Struass & Varshavsky, 1984; Reeves & Nissen, 1990; Reeves & Wolffe, 1996), including AT-rich SARs (Saitoh & Laemmli, 1994a). HMG-I (Y) is a structural component of chromatin required for normal enhancer function by facilitating protein-DNA and protein-protein interactions promoted by DNA bending, as demonstrated with the human interferon-β gene promoter (Thanos *et al.*, 1993; Falvo *et al.*, 1995; Yie *et al.*, 1997) and T-cell receptor α-chain promoter (Bagga & Emerson, 1997). Displacement of H1 by HMG-I (Y) correlates with derepression (Zhao *et al.*, 1993). Disney *et al.* (1989) and Saitoh and Laemmli (1994a) have both shown by immunolocalisation that HMG-I (Y) is concentrated in C- and G-bands, consistent with a preference for AT-rich DNA. However, it is difficult to reconcile how this relates to its transcription promoting abilities. In contrast, HMG-I has been localised to the transcriptionally active puffs of *D.melanogaster* polytene

chromosomes (Ghidelli *et al.*, 1997). A general architectural role may be accompanied by a requirement for its DNA binding abilities at genes to promote transcription, perhaps particularly within AT-rich repressed regions.

1.4.5 Methylated-DNA binding proteins

The requirement for cytosine methylation during development has been highlighted by the lethality of methyltransferase gene disruption in mice (Li *et al.*, 1992). The correlation between transcriptional repression and cytosine methylation has long been established (Section 1.3.6). To cause gene inactivation, methyl-CpGs must be close to a gene promoter (Murray & Grosveld, 1987), which must, in turn, be controlled by methylation sensitive transcription factors (Tate & Bird, 1993). The degree of repression is proportional to the density of methylation and depends upon promoter strength (Boyes & Bird, 1992). There is some confusion as to the exact mode of repression. CpG-islands have been shown to confer a permissive environment for expression of a globin transgene, which depends to a degree on the site of integration (Shewchuk & Hardison, 1997). Expression of the same transgene was previously shown to be directly linked to chromatin accessibility, but not methylation status (Garrick *et al.*, 1996). One report has suggested that methylation does not alter bulk chromatin structure since no decrease in DNAse accessibility of a methylated, under-expressed, transgene was observed. However, there was increased resistance to the methylation-insensitive restriction enzyme *MspI* (CCGG) (Weng *et al.*, 1995).

Repression by methylation is accompanied by a more stable chromatin structure which is generally resistant to nucleases (Keshet *et al.*, 1986) (Section 1.3.6). There is considerable debate as to how this change in structure arises. H1 is involved in chromatin condensation (Thoma *et al.*, 1976; Huang & Cole, 1984; Kamakaka & Thomas, 1990; Shen *et al.*, 1995) and reduction of nucleosome mobility (Ura *et al.*, 1995), and has been shown in several studies to bind preferentially to methylated DNA (Ball *et al.*, 1983; Levine *et al.*, 1993; McArthur & Thomas, 1996). Other studies refute this observation (Bird *et al.*, 1995; Campoy *et al.*, 1995), although lower levels of H1 have been confirmed at methylation-free CpG-islands than in methylated chromatin (Tazi & Bird, 1990). Alternatives point to the increasing number of methylated DNA binding proteins.

The ubiquitously expressed, vertebrate methylated DNA binding protein 1 (MDBP-1), is associated with specific DNA sequences which contain methyl-C (Supakar *et al.*, 1988). A

second protein, MDBP-2 has been found to be an H1 variant and binds in a non-sequence specific manner to methyl-CpG containing DNA (Jost & Hofsteenge, 1992). Methyl-C binding protein 1 (MeCP1), also a ubiquitously expressed, vertebrate protein, binds to DNA containing at least 12 methyl-CpGs and blocks transcription *in vivo* and *in vitro* (Meehan *et al.*, 1989; Boyes & Bird, 1991). It has recently been shown to share a motif with mammalian HRX protein which is related to *D.melanogaster* trithorax (Cross *et al.*, 1997b) (Section 1.4.2). MeCP2 is a very abundant vertebrate protein which, unlike MeCP1, requires only one methyl-CpG to bind (Lewis *et al.*, 1992; Meehan *et al.*, 1992). Immunofluorescence revealed this protein to be associated with heterochromatin in mice and rats with less bright and uniform signals throughout euchromatin. The association with heterochromatin is methyl-CpG dependent (Nan *et al.*, 1996). MeCP2 is essential for mouse development (Tate *et al.*, 1996) and has been shown to displace H1 and cause repression at methyl-CpG containing promoters (Nan *et al.*, 1997). It is considered to be a global repressor of transcription. Each of the different methylated DNA binding proteins are likely to act together in their specific and non-specific manners to aid tight transcriptional control in a complex genome (Bird, 1995; Bird *et al.*, 1995).

1.4.6 Topoisomerase II

Topoisomerase II (topo II) is the best characterised protein from the chromosome scaffold fraction (ScI) (Lewis and Laemmli, 1982; Review: Wang, 1996). Indeed, strong evidence for the existence of the scaffold was obtained from immunolocalisation studies of topo II in chickens (Earnshaw & Heck, 1985; Earnshaw *et al.*, 1985) and humans (Gasser *et al.*, 1986). Adachi *et al.*, (1989) showed that topo II preferentially bound to DNA sequences considered to be associated with the chromosome scaffold (Section 1.5.1).

Acting as a dimer, topo II is an enzyme that catalyses strand-passage reactions where one intact DNA double helix passes completely through another in an ATP-dependent manner (Reviews: Roca, 1995; Wang, 1996). It has been implicated in many aspects of chromosome function in eukaryotes, including: separation of newly replicated DNA (Yang *et al.*, 1987), pre-mitotic condensation (Uemura *et al.*, 1987; Adachi *et al.*, 1991; Hirano & Mitchison, 1993), derepression of chromatin for transcription (Varga-Weisz *et al.*, 1997) and separation of chromatids at anaphase (Holm *et al.*, 1985; Uemura *et al.*, 1987; Shamu & Murray, 1992; Ishida *et al.*, 1994; Gimenez-Abian *et al.*, 1995; Review: Holloway, 1995). The DNA decatenation ability of topo II has been linked to each of these roles. However,

recent studies have suggested that decatenation is not required for chromosome condensation and that topo II is required purely in its structural context for pre-mitotic condensation (Andreassen *et al.*, 1997).

The role of topo II as a loop anchoring protein of the chromosome scaffold has been challenged. Hirano and Mitchison (1993) showed that although essential for assembly and condensation of chromosomes in the *X.laevis* egg extracts, pre-formed chromosome morphology was maintained despite subsequent topo II depletion. Immunofluorescence revealed topo II to be uniformly distributed throughout the chromosomes and not restricted to the axis. This more general dispersal has been substantiated in histone depleted HeLa chromosomes (Boy de la Tour & Laemmli, 1988) and in *D.melanogaster* (Swedlow *et al.*, 1993). There are several possible explanations for these discrepancies. Alternative preparation and fixation protocols were used and may differentially affect chromosome structure and topo II localisation. In addition, it seems probable that various species of topo II exist, with differing functions and localisations at particular cell cycle stages. Different antibodies may recognise distinct topo II species-specific epitopes.

In mammalian cells two isoforms of topo II have been identified: α (170KDa) and β (180KDa). Differential immunofluorescence has revealed that it is topo II α that is located on the chromosomes. Topo II β shows a more diffuse localisation throughout the nucleoplasm at interphase and mitosis (Chaly *et al.*, 1996). A clear function for the β isoform has not been established. More detailed immunolocalisation studies have found that topo II α has a cell cycle stage dependent staining pattern (Swedlow *et al.*, 1993; Rattner *et al.*, 1996; Sumner, 1996; Cobb *et al.*, 1997; Meyer *et al.*, 1997). Non-proliferating cells lack detectable levels of topo II α (Heck & Earnshaw, 1986; Chaly *et al.*, 1996). In G1, staining is low in intensity and diffuse. Chromosomes are stained strongly at prophase, becoming more directed to the axis at late prophase. At metaphase staining is most concentrated at the centromeres. In addition, topo II α inhibitors disrupt centromere structure and chromatid separation (Rattner *et al.*, 1996). It seems likely that this enzyme plays several important roles in chromosome structure at various stages of the cell cycle (Review: Warburton & Earnshaw, 1997). This multitude of activity may be controlled by phosphorylation (Heck & Earnshaw, 1989; Taagepera *et al.*, 1993)

1.4.7 Structural maintenance of chromosomes (SMC) proteins

ScII, the second most abundant protein of the chromosome scaffold fraction, has been cloned and sequenced and immunolocalisation shows this protein to be located along the axis of metaphase chromosomes as seen for topo II (Saitoh *et al.*, 1994). ScII is structurally related to the SMC (structural maintenance of chromosomes) family of proteins (Reviews: Peterson, 1994; Hirano *et al.*, 1995; Saitoh *et al.*, 1995). This family consists of a rapidly expanding number of proteins all concerned with chromosome condensation and sister chromatid separation. The over-lap between condensation and cohesion may reflect the necessity of the former for the latter (Sumner, 1991; Holm, 1994). Members of the SMC family include: *S.cerevisiae* SMC1 and SMC2 (Strunnikov *et al.*, 1993 & 1995), *S.pombe* Cut3 and Cut14 (cell untimely torn) (Saka *et al.*, 1994), *X.laevis* XCAP-C and XCAP-E (*Xenopus* chromosome-associated polypeptides) (Hirano & Mitchison, 1994), *C.elegans* DPY-27 (involved in sex chromosome dosage compensation) (Chuang *et al.*, 1994) (Section 1.4.8), and *Mycoplasma hydorhinis* 115p (Notarnicola *et al.*, 1991). The importance of these proteins in establishing the condensed chromosome state has been pointed to by mutations in the yeast SMC genes which result in chromosome condensation and segregation anomalies. Immunodepletion of XCAP-C and XCAP-E in *X.laevis* egg extracts leads to a block in chromosome assembly, and disassembly of previously condensed chromosomes, suggesting a further role in maintenance of chromosome structure (Hirano & Mitchison, 1994).

All members of the SMC family share a common head-rod-tail structure. The head domain contains an NTP-binding domain, the rod domain is an extended central coiled coil and the tail domain is a conserved globular tail. The tail domain has some sequence homology to protein regions known to be involved in ATP binding and hydrolysis, however, the predicted folding of this region is analogous to DNA binding domains. The overall structure is reminiscent of mechanochemical motor proteins, for example kinesin. One model suggests that SMC proteins bind to the base of DNA loops on the chromosome scaffold with their tail and attach to the loop with their head, mechanochemically pulling the loop in towards the base (Reviews: Peterson, 1994; Hirano *et al.*, 1995; Saitoh *et al.*, 1995). Multiple SMC proteins occur in the cells of many organisms, each a member of a phylogenetic sub-group and these may physically interact to stabilise the condensed state (Review: Koshland & Strunnikov, 1996).

Topoisomerase I expression partly complements the cut3 mutation (Saka *et al.*, 1994). An association between XCAP-C, XCAP-E and topo II has also been implicated by work with condensins. XCAP-C and XCAP-E make up the 8S condensin, of unknown function, and along with three other sub-units the 13S condensin, required for chromosome assembly. One of these additional sub-units, XCAP-H, is a homologue of the *D.melanogaster barren* gene product, originally identified by a mutation that causes defects in sister chromatid separation. Barren has been shown to regulate topo II activity (Bhat *et al.*, 1996). Topo II is targeted to mitotic chromosomes independently of the 13S condensin (Hirano & Mitchison, 1997), but both are required for chromosome condensation and structure, and possibly interact once chromosomally associated. The 13S condensin has been shown to possess an ATP-dependent ability to supercoil DNA in the presence of topoisomerase (Kimura & Hirano, 1997). A novel protein in *S.cerevisiae* which interacts genetically with Smc1p has been identified independently by two groups. MCD1 (mitotic chromosome determinant) was identified by Guacci *et al.* (1997) and another allele of the same protein, termed SCC1 (sister chromatid cohesion) was discovered by Michaelis *et al.* (1997). Mutations in the MCD1/SCC1 gene result in defects in chromosome condensation and cohesion (Review: Heck, 1997).

Recently, an ATP-independent DNA renaturation promoting activity has been established for Cut3 and Cut14 as a complex (Sutani & Yanagida, 1997). This function may be mechanistically distinct from the function of these proteins during condensation. Smc1p and Smc2p have also been shown to possess an alternative function in recombination repair (Jessberger *et al.*, 1996).

1.4.8 Dosage compensation

Since mammalian females possess two X chromosomes and males have just one, it is necessary to balance gene expression from the X chromosome between the two sexes. Random inactivation of one of the female X chromosomes has been found to be the solution in mammals, while other mechanisms of dosage compensation are used in *D.melanogaster* and *C.elegans* (Reviews: Midgeon, 1994; Kelley & Kuroda, 1995; King *et al.*, 1995).

The human female inactive X chromosome (Xi) is associated with hypoacetylated H3 and H4 (Jeppesen & Turner, 1993; Belyaev *et al.*, 1996; Boggs *et al.*, 1996) (Section 1.4.1.3). This feature of X-inactivation is highly conserved in vertebrates suggesting that it plays a

key role (Wakefield *et al.*, 1997). Keohane *et al.* (1996) demonstrated that deacetylation of Xi follows silencing of X-linked genes and expression of the *XIST* (X inactive specific transcript) gene, and therefore, was necessary for the maintenance but not the initiation of X-inactivation. The *XIST* gene is expressed only on Xi (Borsani *et al.*, 1991; Brockdorff *et al.*, 1991; Brown *et al.*, 1991; Review: Rastan, 1994). This gene does not encode a protein but the RNA coats Xi, solely and entirely, at interphase (Brown *et al.*, 1992; Clemson *et al.*, 1996; Lee *et al.*, 1996), controlled possibly by altered RNA stability (Panning *et al.*, 1997; Sheardown *et al.*, 1997). *XIST* expression is required for initiation but not maintenance of inactivation (Brown & Willard, 1994). Xi shares features of heterochromatin other than hypoacetylation and gene silencing, namely, late replication (Camargo & Cervenka, 1982; Takagi *et al.*, 1982; Riggs & Pfiefer, 1992) and hypermethylation (Miller *et al.*, 1974; Bernardino *et al.*, 1996). Distinctive staining properties, associated with heterochromatinisation are also apparent at interphase and metaphase (Barr & Bertram, 1949; Kanda, 1973; Belmont *et al.*, 1986). Late replication is not necessary for inactivation (Yoshida *et al.*, 1993), while hypomethylation causes aberrant *XIST* expression and inappropriate inactivation of all X chromosomes (Beard *et al.*, 1995; Panning & Jaenisch, 1996).

In *D.melanogaster*, the male X chromosome becomes transcriptionally hyperactive to compensate for the female possessing double the number of X-linked genes (Arkhipova & Meselson, 1997; Reviews: Bashaw & Baker, 1996; Lucchesi, 1996). This is accompanied by hyperacetylation of H4 (Turner *et al.*, 1992; Bone *et al.*, 1994) and a bloated appearance of the chromosome. The *maleless* (*mle*) gene and the four *male-specific lethal* (*msl*) gene products are associated almost exclusively with the X chromosome in males, but not females (Kuroda *et al.*, 1991; Palmer *et al.*, 1993; Gorman *et al.*, 1995; Zhou *et al.*, 1995). Loss-of-function mutations result in death of homozygous males and lethality correlates with a failure to dosage compensate. The formation of a complex is suggested from the fact that X chromosome-specific association of any one protein relies on the presence of the others. Binding of the complex is necessary for hyperacetylation of H4 (Bone *et al.*, 1994; Bone & Kuroda, 1996). MLE has homology to DNA/RNA helicases, while MSL-1 contains characteristics common to transcriptional activators including HMG-1. MSL-3 contains two chromodomains, a motif considered to direct binding to chromatin via protein-protein interactions (Koonin *et al.*, 1995) (Section 1.4.2). Finally, MSL-2 is a RING-finger protein (Bashaw & Baker, 1995; Zhou *et al.*, 1995), a motif implicated in DNA-protein and protein-

protein interactions (Review: Freemont, 1993) (Section 1.4.2). MSL-2 has been implicated to be the key protein for complex localisation (Kelley *et al.*, 1995) but, MLE/MSL complex X chromosome-association is RNA-dependent (Richter *et* al., 1996). A possible candidate for such a role is *roX1* encoded RNA (Meller *et al.*, 1997). However, *roX1* mutant male flies still dosage compensate and the MLE/MSL complex localises to the X chromosome, suggesting possible redundancy. It is interesting to note the dependence upon RNAs as well as proteins in X-inactivation.

Yet another mechanism for dosage compensation occurs in the nematode, *C.elegans*. Hermaphrodites (XX) reduce transcription levels of both X chromosomes to achieve the same levels produced by males (XO). The DYP-27 protein becomes specifically localised to the X chromosomes of hermaphrodites, but is diffusely distributed in male cells. Mutation in the *dpy-27* gene results in elevated X chromosome transcript levels in XX animals and in *XO lethal-1* (*xol-1*) mutant XO embryos DPY-27 becomes localised to the X chromosome and the animals die from inappropriately low X chromosome transcript levels. DPY-27 is a member of the SMC family putatively involved in chromosome condensation (Chuang *et al.,* 1994) (Section 1.4.7) so it is possible that this protein reduces transcription by condensing chromatin along the two X chromosomes. Binding of DPY-27 is dependent upon expression of a number of other genes including DPY-26 and the SDC proteins, some of which also have X chromosome binding specificity (Chuang *et al.*, 1996; Lieb *et al.*, 1996).

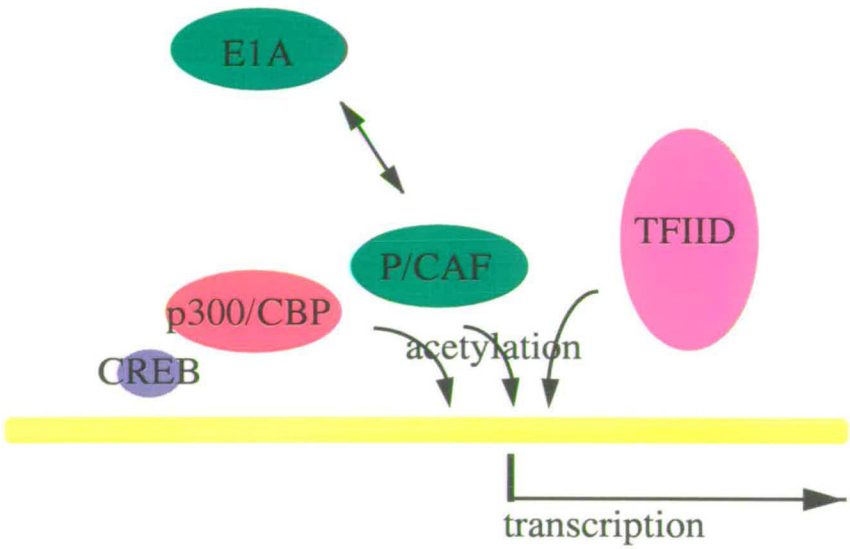

Figure 1.4 Histone acetylation at the promoter
Adapted from Yang *et al.* (1996b) and Wade *et al.* (1997). Activating transcription factors, for example CREB, recruit the coactivator/histone acetyltransferase complex p300/CBP-P/CAF which derepresses the nucleosome allowing access for TFIID and the remainder of the basal transcription complex. TFIID also has histone acetyltransferase activity. P/CAF competes with the adenovirus transcription factor, E1A, for association with p300/CBP. The E1A-p300/CBP complex also has HAT activity and it could be that E1A directs this activity to alternative targets resulting in inappropriate gene expression and transformation (Section 1.4.1.4).

1.5 Compartments of the metaphase chromosome

Section 1.1 outlined the structure of human metaphase chromosomes. In this section the functional compartments of metaphase chromosomes are discussed.

1.5.1 DNA sequences associated with the chromosome scaffold

The term "chromosome scaffold" is used in this thesis to describe the morphological framework remaining after histone extraction of metaphase chromosomes (Paulson & Laemmli, 1977; Earnshaw & Laemmli, 1983; Paulson, 1989), or the metaphase chromosome core traced immunologically with antibodies to topo II (Earnshaw & Heck, 1985; Earnshaw *et al.*, 1985; Gasser *et al.*, 1989) (Section 1.4.6) or ScII (Saitoh *et al.*, 1994) (Section 1.4.7).

FISH was used to visualise the types of sequences that bind to the morphological scaffold of salt extracted human metaphase chromosomes. Origins of replication correlated well with positions of attachment (Bickmore & Oghene, 1996). An inhibitor of topo II, epipodophyllotoxin, traps enzyme molecules covalently integrated into DNA. When topo II is denatured during DNA purification, a double strand break is left at sites of *in vivo* action. The same cutting sites have been identified in metaphase chromosomes and interphase nuclei (Razin *et al.*, 1993) and a correlation between these attached sequences and replication origins was apparent. Many of these sequences were also reminiscent of SARs (Iarovaia *et al.*, 1996) (Section 1.6.5).

Only a subset of AT-rich SARs identified from LIS extracted nuclear scaffolds (Section 1.6.5) have been shown to bind to chromosome scaffolds (Mirkovitch *et al.*, 1988). However, using AT-specific fluorochromes, Saitoh & Laemmli (1994a & b) traced what they considered to be a SAR-rich chromosome backbone ("AT-queue"). The importance of SARs in chromosome structure is supported by the fact that the assembly of condensed chromosomes in *X.laevis* egg extract is inhibited by the addition of a synthetic protein that binds to AT-rich DNA (Strick & Laemmli, 1995; Review: Swedlow & Hirano, 1996). There appears to be no enrichment of transcribed sequences amongst SARs (Mirkovitch *et al.*, 1984; Gasser *et al.*, 1989). Being AT-rich, SARs are likely to be more concentrated in G-bands and this has been shown to be the case (Jarman & Higgs, 1988; Saitoh & Laemmli, 1994a & b; Craig *et al.*, 1997).

The nucleoskeleton prepared by electoelution of nuclei is associated with the processes of transcription and replication (Cook, 1984; Jackson & Cook, 1985 & 1986; Jackson *et al.*, 1988 & 1996) (Section 1.6.5). Cook (1994 & 1995) has postulated that there are no permanent sequences of attachment to the chromosome scaffold, but that polymerases involved in transcription and replication at interphase aggregate and pull together attached sequences, thus condensing the chromosomes for mitosis. However, Craig *et al.* (1997) demonstrated that when attached and loop DNA from electroeluted metaphase chromosomes were hybridised by FISH to metaphase chromosomes, there was no preferential localisation to gene-rich regions (Section 1.6.5). This argues that the sites of attachment to the chromosome scaffold are determined by sequence and not function.

1.5.2 The centromere

The centromere is a highly specialised chromatin environment and harbours a unique array of proteins (Review: Pluta *et al.*, 1995). In mammals, the centromere forms at the primary chromosome constriction. α-satellite is found at all mammalian centromeres and is intimately associated with the mitotic scaffold (Bickmore & Oghene, 1996). Strissel *et al.* (1996) argued that loop sizes are smaller and SARs are more concentrated at centromeres compared with chromosome arms. However, in this study a similar degree of hybridisation appeared to be present at centromeres following FISH with non-SAR DNA suggesting that there was incomplete suppression of repeat sequences. In addition, Craig *et al.* (1997) did not find a concentration of SARs at centromeres. The apparently condensed chromatin packaging at centromeres may be accounted for by the resistance of kinetochore and other centrosomal components to extraction, thus sterically preventing DNA loop formation. Such chromatin packaging may be responsible for the physical appearance of this region in non-extracted chromosomes. It may also be related to its function, for instance, insulating the centromere from transcriptional activity and/or providing mechanical strength. That centromeres C-band highlights this underlying, condensed chromatin structure. In fission yeast, centromeres are heterochromatic and silence genes placed therein (Allshire *et al.*, 1994). Furthermore, it seems that the presence of heterochromatin is essential for centromere function in yeast (Allshire *et al.*, 1995), just as the primary constriction is necessary for mammalian centromere function (Voullaire *et al.*, 1993).

There is an abundance of both topo II and ScII at centromeres, in addition to CENPs (centromere proteins) and INCENPs (inner centromere proteins). CENP-A is a homologue

of H3 and appears to be incorporated specifically into centromeric nucleosomes (Sullivan *et al.*, 1994). CENP-B (Earnshaw *et al.*, 1987), binds specifically to α-satellite DNA (Haaf *et al.*, 1992) and lies beneath the kinetochore (Cooke *et al.*, 1990). It does not distinguish between an active and inactive centromere on a dicentric chromosome (Sullivan & Schwartz, 1995). The kinetochore coats centromeric DNA (Cooke *et al.*, 1993) and active components include CENPs C, E (Wood *et al.*, 1997) and F, and MCAK. The location and function of CENP-D is not known, but interestingly, this protein has high homology to RCC1 protein, a regulator for the onset of chromosome condensation (Bischoff *et al.*, 1990; Review: Dasso, 1993).

The INCENPs A and B were identified with a monoclonal antibody that was raised against the proteins of the chicken mitotic chromosome scaffold. Throughout mitosis these proteins, which are encoded by a single gene, are located between the centromeres of sister chromatids. At anaphase both proteins relocate to the spindle and the nascent cleavage furrow. Whether the INCENPs play a role in sister chromatid cohesion is unclear, but a role in formation of the cleavage furrow and in organisation of the cytoskeleton is likely (Cooke *et al.*, 1987; Mackay *et al.*, 1993; Eckley *et al.*, 1997). INCENPs were the first of a set of proteins, termed passenger proteins, that are associated with mitotic chromosomes, but relocate as mitosis progresses. It is possible that rather than having a direct role in chromosome structure or dynamics, they are merely using the chromosomes to help them move to the right part of the nucleus at which their function is required (Review: Earnshaw & Bernat, 1991).

CLiPs (chromatid linking proteins) contain epitopes which are recognised by the autoimmune sera found in CREST (calcinosis, Raynaud's phenomenon, esophageal dysmotility, sclerodactyly, telangiectasia) scelrodoma patients, from which many of the CENPs were also identified. These proteins localise between the chromatids of mitotic chromosomes (Rattner *et al.*, 1988). Although this localisation suggests a role in sister chromatid cohesion, no such function has been established. In *D.melanogaster*, specific proteins involved in this function have been identified (Kerrebrock *et al.*, 1995; Stratmann & Lehner, 1996).

1.5.3 The telomere

Human telomeres consist of tandem arrays of TTAGGG repeats bound to specific proteins. These structures act to protect chromosome ends from degradation, recombination and fusion, so preventing activation of DNA damage cell cycle check points (Review: Zakian, 1997). In normal human cells, telomeres shorten with successive generations probably due to loss of terminal sequences as a result of DNA polymerase-mediated replication (Harley *et al.*, 1990). In tumours and immortalised cells, this shortening is halted by the activation of telomerase, a reverse transcriptase capable of extending telomeric arrays (Counter *et al.*, 1992; Kim *et al.*, 1994; Blasco *et al.*, 1997). Telomere length is stably maintained in such cells suggesting the presence of a regulatory mechanism for limiting telomere elongation. This role in humans has been assigned to the telomeric-repeat binding protein (TRF1) (Chong *et al.*, 1995; van Steensel & de Lange, 1997). TRF1 does not affect the expression of telomerase and thus appears to act in *cis*. A second protein, TRF2, may also be involved (Broccoli *et al.*, 1997; Bilaud *et al.*, 1997). In *S.cerevisiae*, Rap1p is involved in telomere length regulation (Marcand *et al.*, 1997). Overexpression of TRF1 and Rap1p results in shorter telomere length suggesting that a negative feedback loop exists which can detect the quantity of protein at the telomere.

Telomeres are also characterised by an unusual chromatin configuration. The extreme ends of human telomeres are organised in a non-nucleosomal, nuclease-resistant chromatin (Tommerup *et al.*, 1994). A heterochromatin-like structure is present at yeast and *D.melanogaster* telomeres that can silence genes placed in the vicinity by a phenomenon known as position effect variegation (PEV) (Levis *et al.*, 1985; Aparicio *et al.*, 1991; Renauld *et al.*, 1993; Nimmo *et al.*, 1994; Cockell *et al.*, 1995).

1.5.4 The mitotic chromosome periphery

The surface of mitotic chromosomes is coated with a cocktail of proteins and RNAs, termed the perichromosomal layer (Reviews: Rattner, 1992; Hernandez-Verdun & Gautier, 1994). Identification of the constituents of the perichromosomal layer has been based mainly on antibodies cross-reacting with this compartment. Proteins identified include:

- Nuclear matrix proteins - The peripherin antigen raised against isolated nuclear matrices coats the periphery of mitotic chromosomes (Chaly *et al.*, 1984). This antigen has not been characterised further.

- Inner nuclear envelope proteins - One 70KDa member of the DNA-binding Ku proteins (Mimori *et al.*, 1986) is localised to the mitotic chromosome periphery. At interphase it is localised to the nuclear periphery and is considered to link DNA loops to the inner nuclear envelope (Higashiura *et al.*, 1992).
- Nucleolar proteins - A surprising number of nucleolar proteins relocate to the chromosome periphery in mitosis. For instance, fibrillarin is believed to be involved in early processing of rRNA in the nucleolus but is associated with the mitotic chromosome periphery (Ochs *et al.*, 1985; Jimanez-Garcia *et al.*, 1989; Yasuda & Maul, 1990). Ki-67, a nucleolar antigen and cell proliferation marker (Gerdes *et al.*, 1984; Verheijen *et al.*, 1989), is associated with satellite DNA in the nucleoplasm of early G1 cells (Bridger *et al.*, 1997). In late G1, S and G2 the protein becomes localised to the nucleoli and during mitosis it is found at the chromosome periphery. It is considered that this protein may organise chromatin, including rDNA and aid nucleogenesis.
- Ribonucleoproteins (RNPs) - The mitotic chromosome periphery is associated with a number of RNAs forming RNPs but these remain poorly characterised (Spector & Smith, 1986; Gautier *et al.*, 1992).

Little is known about how and why the perichromosomal layer forms, and different proteins may have alternative functions. These proteins may provide a protective blanket against cytoplasmic components when the nuclear membrane breaks down at mitosis. Alternatively, the chromosomes may act as a carrier, passive or active, ensuring that specific proteins and RNA are directed to the new nuclei. It is known that the chromosome surface acts as a template upon which the components of the new inner nuclear envelope assemble (Section 1.6.6). These surface proteins may help orchestrate this assembly and may be involved in compartmentalising the nucleus and setting up chromosome territories.

1.6 Compartments of the interphase nucleus

The interphase nucleus is a highly structured organelle and the processes involved in transcription and replication, which occur throughout interphase, appear to be compartmentalised. This segregation may be a result of, or a requirement for, efficient and controlled nuclear function.

1.6.1 Packaging of chromatin in the interphase nucleus

Chromatin compaction varies as cells move from G1. It is least condensed at S-phase, condensing again through G2 and reaching maximal condensation at metaphase (Gollin *et al.*, 1984; Robinett *et al.*, 1996). While in *S.cerevisiae* there may only be a 2-fold difference between the level of compaction at metaphase and S-phase (Umesono *et al.*, 1983), in mammals the estimated total decondensation is approximately 10-fold (Rattner & Lin, 1985; Lawrence *et al.*, 1990).

Interestingly, compaction appears to be less in R-band regions than in G-band regions, as assessed by measuring the two-dimensional (2-D) distances between probes separated by 0.1-1.5Mb and specifically localised in each of the band types (Yokota *et al.*, 1997). Transcriptionally active chromatin may be less condensed as a requirement for or as a direct consequence of transcription. Surprisingly, this has not been found to be the case for the active (Xa) and inactive (Xi) mammalian X chromosomes (Section 1.4.8). Three-dimensional (3-D) analysis has revealed that the two chromosomes occupy similar volumes in the interphase nucleus (Eils *et al.*, 1996). However, Xa has a more irregular, and thus larger, surface area when compared to Xi. The increased number of invaginations could allow access to transcription components from the interchromosomal channels (Section 1.6.3). The condensed appearance of G-band verses R-band regions in 2-D nuclei may be a result of a similar difference in shape between inactive and active regions, rather than a direct difference in volume. However, the Xa and Xi possess the same number of genes and X-inactivation acts to actively repress transcription. This repression is likely to be achieved by a distinct mechanism to the processes involved in chromatin structure at gene-poor G-bands.

1.6.2 Functional compartments

The most striking sub-division of the nucleus is the nucleolus (Reviews: Warner, 1990; Hernandez-Verdun, 1991; Scheer & Weisenberger, 1994). This structure is the site of rRNA synthesis and is the location of the rRNA-encoding sequences (rDNA) (except 5S RNA which is synthesised outside of the nucleolus). Nucleoli are readily visualised by light microscopy as single or multiple dense, non-membranous nuclear structures. The exact organisation, size and number of nucleoli depends upon ribosome biogenesis. By FISH, some rDNA sites have been shown not to be associated with the nucleoli and are considered to be inactive, lacking the proteins required for nucleolus formation (Wachtler *et al.*, 1986). A large number of proteins, generally involved in ribosome biogenesis, are preferentially located in nucleoli. These include: RNA polymerase I, nucleolin (Lapeyre *et al.*, 1987; Caizergues-Ferrer *et al.*, 1989) and fibrillarin (Ochs *et al.*, 1985).

A number of other nuclear bodies have been identified, each containing a specific array of proteins. These include:

- Coiled bodies - In the nuclei of many mammalian cell types, 2-6 coiled bodies are present. Often associated with the periphery of the nucleolus, these bodies contain proteins and RNAs important for RNA splicing, including all snRNPs (small nuclear ribonucleoproteins) (Fakan *et al.*, 1984; Carmo-Fonseca *et al.*, 1991a & b) and the nucleolar-associated protein, fibrillarin (Jimenez-Garcia *et al.*, 1994). Almost all of the relatively uncharacterised protein, p80-coilin, accumulates in the coiled bodies (Anrade *et al.*, 1991; Bohmann *et al.*, 1995a). Interestingly, one form of the Wilms' tumour suppressor gene (WT1) localises to coiled bodies in addition to the 20-50 speckles occupied by snRNPs throughout the nucleus (Larsson *et al.*, 1995; Review: Charlieu *et al.*, 1995) (see below). The role of WT1 in RNA splicing remains unknown. Coiled bodies are likely to be involved in the processing of RNA, possibly of nucleolar-specific transcripts. Other possible roles include assembly, storage and/or regeneration of snRNPs (Reviews: Lamond & Carmo-Fonseca, 1991; Bohmann *et al.*, 1995b; van Driel *et al.*, 1995).
- PML (promyelocytic leukaemia) bodies - Accumulations of PML protein form into dense fibrillar bodies in normal cells but show a general punctate distribution in cells of patients suffering from PML (Ascoli & Maul, 1991; Daniel *et al.*, 1993; Weis *et al.*, 1994). The function of the PML protein and PML bodies remains unknown. Neither

pre-mRNA nor splicing components localise to these structures (Stuurman *et al.*, 1992; Weis *et al.*, 1994).

- Gems - The protein encoded by a gene mutated in >98% of patients with spinal muscular atrophy termed SMN (survival of motor neurons) (Lefebvre *et al.*, 1995) is localised to 2-6 nuclear bodies, frequently found close to coiled bodies (Liu & Dreyfuss, 1996). SMN is associated with hnRNPs (heterogeneous nuclear RNPs), responsible for processing and transport of mRNAs (Review: Dreyfuss *et al.*, 1993), the nucleolar-specific protein fibrillarin and other novel proteins. More recently SMN has been shown to have an essential role in snRNP biogenesis (Fischer *et al.*, 1997; Liu *et al.*, 1997).

In addition to these relatively large nuclear bodies (0.1-1μm), components involved in the processes of transcription, splicing and replication have been shown to accumulate in foci, often referred to as speckles or interchromatin granules (Reviews: Haaf & Schmid, 1991; Spector, 1993; van Driel *et al.*, 1995). Fluorescent labelling of nascent transcripts, and immunolocalisation of RNA polymerase II and a variety of transcription factors and splicing components, in transcriptionally active nuclei, have revealed a generally dispersed distribution in addition to 20-50 speckles (Fu & Maniatis, 1990; Spector, 1990; Wansink *et al.*, 1993; Bregman *et al.*, 1996; Fay *et al.*, 1997; Grande *et al.*, 1997; Zeng *et al.*, 1997). In poorly transcribing cells, or cells blocked for transcription using chemicals or heat shock, the majority of nascent transcripts, RNA polymerase II and splicing components relocate to the speckles, giving more accentuated and enlarged foci (Zeng *et al.*, 1997). Only RNA polymerase II hyperphosphorylated at its C-terminal domain is located in speckles, while the hypophosphorylated enzyme is dispersed (Bregman *et al.*, 1995). By FISH, polyadenylated RNA was shown to concentrate with the speckles (Carter *et al.*, 1993). In addition, several unique pre-mRNAs have been localised there (Lawrence *et al.*, 1993; Xing *et al.*, 1993 & 1995). Speckle localisation has also been established for microinjected RNAs and transcipts produced from transfected DNA in an intron-dependent manner (Wang *et al.*, 1991; Huang & Spector, 1996).

Speckles are probably storage sites for transcription and splicing factors and the bulk of transcription and splicing occurs throughout the nucleus (Review: Singer & Green, 1997). Not all speckles recognised by antibodies against the splicing component SC-35 are associated with nascent transcripts. Indeed, there are many sites within the nucleus, other

than speckles, where nascent transcripts are located (Wansink *et al.*, 1993). Furthermore, Zhang *et al.* (1994) determined by FISH that sites of transcription of specific genes correlated with sites of splicing, but that these sites were located between speckles. This localisation was reminiscent of the perichromatin fibrils, previously described as sites of pre-mRNA processing (Review: Fakan, 1994). However, the sample size used by Zhang *et al.* (1994) was insufficient to draw any general conclusions. Recently, splicing factors fused to green fluorescent protein (GFP), which allows live cell observations, have been shown to leave speckles in peripheral extensions and accumulate at sites of newly activated genes (Misteli *et al.*, 1997).

Fluorescent labelling of nascent DNA and immunofluorescence to components of the replication machinery have shown that replication occurs in a specific spatial pattern. There are hundreds of small domains scattered throughout the nucleus in early S-phase and fewer, larger domains in late S-phase (Nakayasu & Berezney, 1989; Fox *et al.*, 1991; Kill *et al.*, 1991; O'Keefe *et al.*, 1992; Hutchison, 1995; Ferreira *et al.*, 1997).

1.6.3 The chromosome territory hypothesis

It is now also widely accepted that chromosomes occupy separate and distinct territories in the interphase nuclei of animal and plant species. This organisation was first described by Rabl in 1885, in cells of *Salamandra maculata*. The work of Boveri in 1909, using *Ascaris megalocephala*, further established this hypothesis of constant chromosome identity throughout the cell cycle. Electron microscopy (EM) studies failed to distinguish chromosomal territories (Wischnitzer, 1973) and so these theories were discarded by most at that time. Models describing non-territorial chromosome arrangements were favoured (Comings, 1968) until the recent techniques of UV-laser-micro-irradiation and FISH prompted a wide acceptance of the chromosome territory hypothesis (Reviews: Hiliker & Appels, 1989; Haaf & Schmid, 1991; Cremer *et al.*, 1993).

By micro-irradiating Chinese hamster nuclei with a UV-laser, small sub-nuclear areas could be marked by spiking DNA repair with tritiated thymidine. When such cells were followed through to the subsequent mitosis, autoradiography or antibodies to UV-damaged DNA showed damage to be restricted to a few chromosomes (Zorn *et al.*, 1979; Cremer *et al.*, 1982b; Hens *et al.*, 1983; Review: Cremer *et al.*, 1993). A correlation was found between the DNA content and frequency with which each chromosome was hit. Also, it is interesting

to note that homologous chromosomes were hardly ever damaged simultaneously. In contrast, in *D.melanogaster* homologous chromosomes are usually paired at interphase and have been shown to interact genetically (Tartoff & Henikoff, 1991). Using FISH, LaSalle & Lalande (1996) determined that the homologues of a human gene subject to imprinting were associated transiently during late S-phase. However, it seems that homologous pairing in human nuclei does not normally occur.

Irradiation experiments have also suggested that mammalian chromosomes too may have a "Rabl-conformation". This conformation, in which chromosomes are in a V-shape with telomeres close to each other at the nuclear periphery (Cremer *et al.*, 1982a), has been observed in *S.maculata* (Rabl, 1885), *D.melanogaster* polytene chromosomes (Hiraoka *et al.*, 1990; Marshall *et al.*, 1996) and in several plant species (Fussell, 1975; Rawlins *et al.*, 1991). Further analyses of mammalian centromeres and telomeres have revealed that their positioning during interphase is dynamic, with movement of centromeres from the periphery more internally as interphase progresses and telomeres generally randomly located throughout the nucleus (Manuelidis, 1985a; Bartholdi, 1991; Ferguson & Ward, 1992; Vourc'h *et al.*, 1993; Broccoli & Cooke, 1994; He & Brinkley, 1996). However, live cell observations of the chromosomal protein CENP-B fused to GFP, found that centromeres show little movement throughout interphase and are located with no peripheral or central bias (Shelby *et al.*, 1996). It seems likely that the different centromere arrangements are cell type-specific (Manuelidis, 1984).

Isotopic *in situ* hybridisation and FISH made it possible to visualise whole chromosomes and interphase territories were observed directly in rodent-human somatic hybrid cells (Manuelidis, 1985b; Schardin *et al.*, 1985) and later in human cells *per se* (Pinkel *et al.*, 1986; Lichter *et al.*, 1988; Popp *et al.*, 1990; Aquiles Sanchez *et al.*, 1997; Reviews: Manuelidis, 1990; Cremer *et al.*, 1993; Trask *et al.*, 1993). In addition, probes delineating chromosome segments indicate that within a territory each chromosome portion has a distinct domain (Rappold *et al.*, 1984; Lengauer *et al.*, 1991; Zink *et al.*, 1997). Robinett *et al.* (1996) integrated a vector containing the *Eschericia coli* lac operator region into Chinese Hamster Ovary (CHO). Using a GFP-lac repressor fusion protein they were able to follow the position of the site of integration in live analysis. These, and other recent studies using laser bleaching (Abney *et al.*, 1997) and fluorescently labelled topo II in *D.melanogaster* (Marshall *et al.*, 1997b), have shown the chromatin of the interphase nucleus to be relatively

immobile. This is consistent with chromosome territory confinement. All of this work has culminated in the formation of two models for the arrangement of chromosome territories:

1. The compartment and intercompartment model (Manuelidis, 1990; Cremer *et al.*, 1993; Zirbel *et al.*, 1993; Kurz *et al.*, 1996; Strouboulis & Wolffe, 1996; Dietzel *et al.*, 1998).
2. The random-walk/giant-loop model (van den Engh *et al.*, 1993; Sachs *et al.*, 1995; Yokota *et al.*, 1995).

Although not completely contrasting, these hypotheses are distinct. It is likely that the reality is a compromise between the two. In the first instance, each chromosome has a very strict territory around which a series of channels connect the chromosome with the remainder of the nucleus and, via the nuclear pores, the cytoplasm (Dietzel *et al.*, 1998; Reviews: Blobel, 1985; Manuelidis, 1990; Cremer *et al.*, 1993; Strouboulis & Wolffe, 1996) (Figure 1.5). RNA transcript tracks extending from the nuclear interior to the nuclear periphery (Lawrence *et al.*, 1989; Xing *et al.*, 1993) were presumed to be moving along such channels. Splicing proteins and a specific RNA transcript have been shown to be excluded from the interior of chromosomal territories (Zirbel *et al.*, 1993).

The second model proposes that interphase chromosomes consist of flexible chromatin loops of several Mb attached to a supple backbone which also shows characteristic random walk behaviour (van den Engh *et al.*, 1993; Sachs *et al.*, 1995; Yokota *et al.*, 1995). This arrangement would result in a degree of overlap between chromosomal domains and no strict interchromosomal channels would be maintained.

1.6.4 Does each chromosome have a specific location?

In metaphase spreads the acrocentric chromosomes are closer together than would be expected from a random distribution (Ferguson-Smith & Handmaker, 1961; Kaplan *et al.*, 1993) and the same particular rDNA containing chromosomes remain associated with one another through successive cell cycles (Bobrow & Heritage, 1980). This supports the idea that the distribution of chromosomes at metaphase reflects interphase chromosomal organisation.

A surprisingly precise arrangement of chromosomes is maintained on the mitotic spindle (Naegele *et al.*, 1995), supporting the notion that chromosomes are not distributed randomly with relation to one another. Some studies have suggested that mere physical size

determines the positioning of chromosomes, with small autosomes tending to be more centrally located on the metaphase plate than larger autosomes (Warburton *et al.*, 1973; Wollenberg *et al.*, 1982). There is also evidence, however, that size is not the major determinant and that early replicating, gene-rich chromosomes are more centrally located and late replicating, gene-poor chromosomes tend towards the periphery (Miller *et al.*, 1963; Hens *et al.*, 1982). Of course, it is well established that the inactive X chromosome, in the form of the Barr body, is positioned close to the nucleolus or at the periphery of the female interphase mammalian nucleus (Barr & Bertram, 1949; Dyer *et al.*, 1989). Could the genetic inactivity of a chromosome or chromosomal domain impose a peripheral situation for that region in the interphase nucleus? And conversely, are active regions more centrally located? Condensed blocks of heterochromatin can be seen in the nuclei of many eukaryotes and in some instances they appear to preferentially lie at the nuclear periphery (Rae & Francke, 1972; Mathog *et al.*, 1984; Review: Comings, 1980). Interestingly, it has been demonstrated that upon infection by herpes simplex virus the chromatin of human HeLa cells is forced to the nuclear periphery and rendered transcriptionally inactive, while non-encapsidated viral genomes are exclusively centrally located, the region of the nucleus active for viral genome replication and nucleocapsid formation (Puvion-Dutilleul & Bessse, 1994).

The fact that the human Y chromosome is significantly closer to the nucleolus than would be expected if randomly distributed, has been attributed to the association of the heterochromatic regions of the Y and the acrocentric chromosome short arms (Weipoltshammer *et al.*, 1996). However, although characteristic positions have been implied in mammalian nuclei, no chromosome has been shown to occupy a consistent address with respect to another (Review: Manuelidis, 1990). In plant nuclei, however, this concept has been firmly established, with specific arrangements of chromosomes indicated from the frequencies of particular spontaneous or radiation-induced chromosomal exchanges (Example: Sax, 1940; Reviews: Avivi & Feldman, 1980; Heslop-Harrison, 1990).

Probes for specific regions of human chromosomes were used for FISH to human central nervous system cells and analysed in 3-dimensions (3-D) by optical sectioning (Manuelidis & Borden, 1988). Probes for the heterochromatic regions of chromosomes 1 (1q12) and 9 (9q12), were always associated with the nuclear periphery or nucleolus. Meanwhile, a probe for the T-band, 1p36 was always found in the nuclear interior. This, and other FISH data (Lawrence *et al.*, 1988; Lawrence & Singer, 1991; Xing *et al.*, 1995), supports the

concept of a highly compartmentalised nucleus, with transcriptionally active chromatin more internally located, and transcriptionally inactive regions more peripherally located. Nonetheless, there is little consistent evidence that mammalian chromosomes regularly adopt defined positions within the nucleus that relate to their activity and, indeed some studies have suggested that positioning of chromosomes is random (Popp *et al.*, 1990; Aquiles Sanchez *et al.*, 1997).

1.6.5 The nuclear matrix

Nuclei can be extracted with salt to reveal a morphological framework, termed the "nuclear matrix", surrounded by loops of DNA (McCready *et al.*, 1979; Vogelstein *et al.*, 1980). The residual protein content of 2M salt extracted nuclei and metaphase chromosomes have been compared (Lewis *et al.*, 1984; Pieck *et al.*, 1985) and the predominant protein in both is topo II (Section 1.4.6). Nuclei show a more complex range of proteins, but there are also proteins which are present at the chromosome scaffold and not at the nuclear matrix, for example, ScII (Section 1.4.7). Many of the proteins of the nuclear matrix remain to be identified. Protein composition appears to differ between cell types, however, lamins are members of a common set of nuclear matrix proteins (Stuurman *et al.*, 1990; Hozak *et al.*, 1995) (Section 1.6.6).

There is evidence that the nuclear matrix is associated with nascent RNA and DNA (McCready *et al.*, 1980; Berezney & Buchholtz, 1981; Voglestein *et al.*, 1980; Jackson *et al.*, 1981 & 1984), transcriptionally active sequences (Ciejek *et al.*, 1983; Robinson *et al.*, 1983; Jackson & Cook, 1993); replication origins (Dijkwel *et al.*, 1986; Razin *et al.*, 1986 & 1993; Amati & Gasser, 1988; Sykes *et al.*, 1988), enhancers (Cockerill & Garrard, 1986; Jenuwein *et al.*, 1997), chromatin domain boundaries (Phi-Van & Stratling, 1988; Thompson *et al.*, 1994a; Kalos & Fournier, 1995), transcription factors (Sun *et al.*, 1994), histone acetyltransferase activity (Hendzel *et al.*, 1994) and histone deacetylase activity (Hendzel *et al.*, 1991).

Salt extraction was criticised by Mirkovitch *et al.* (1984) for causing sliding and randomising attachment sites. A less harsh protein extraction procedure was developed using the detergent-like molecule lithium diiodosalicylate (LIS). Thorough digestion of the extracted nuclei with restriction enzymes was followed by centrifugation, the insoluble "nuclear scaffold" attached DNA forming a pellet and the soluble loop DNA remaining in

the supernatant. Exonuclease III has also been used for the digestion of DNA from extracted nuclei (Gasser & Laemmli, 1986). Using these techniques SARs have been identified in many organisms (Review: Gasser *et al.*, 1989). These SARs are AT-rich sequences (>70% AT) of several hundred base pairs, containing homopolymer tracts of dA and dT, and often containing the topo II *in vitro* consensus sequence (GTNA/TAC/TATTNATNNA/G) (Review: Laemmli *et al.*, 1992). No preferential association of transcribed or replicated DNA with the LIS extracted nuclear scaffold was observed, however, SARs prepared following such extraction bind specifically to salt extracted nuclear matrices (Izaurralde *et al.*, 1988). Proteins localised to the nuclear scaffold include: topo II (Adachi *et al.*, 1989), H1 (Kas *et al.*, 1989), lamin B (Luderus *et al.*, 1992) (Section 1.6.6), HMGI/Y (Zhao *et al.*, 1993) (Section 1.4.4) and the nucleolar-specific protein, nucleolin (Dickinson & Kohwi-Shigematsu, 1995).

Jackson *et al.* (1990) found a large difference in loop sizes generated from the above techniques and argued that use of non-physiological conditions resulted in the artifactual attachments and associations (Cook, 1988; Jack & Eggert, 1992; Craig, 1995). A method was developed by Cook (1984) and Jackson *et al.* (1988) which involves encapsulating living cells in agarose beads, incubation in a physiological buffer, permeabilisation with a detergent, and restriction enzyme digestion. The cells and nuclei are protected from aggregation by the agarose, circumventing the use of hypertonic or hypotonic buffers and the need for chromatin stabilisers such as polyanions, Cu^{2+} and Ag^{+}. Electroelution is used to remove digested loop DNA from the agarose and the remaining residual framework in this instance is termed the "nucleoskeleton". Surprisingly, a similar set of sequences and processes have been assigned to nucleoskeletons as those of salt extracted nuclear matrices. Despite removal of most of the chromatin major cellular functions including transcription (Jackson & Cook, 1985; Jackson *et al.*, 1996; Review: Cook, 1989) and replication (Jackson & Cook, 1986; Reviews: Jackson, 1990 & 1991, Cook, 1991) can be initialised at the nucleoskeleton. Proteins shown to be associated with the nucleoskeleton include: RNA polymerase (Jackson & Cook, 1985), DNA polymerase (Jackson & Cook, 1986; Hozak *et al.*, 1993), proliferating cell nuclear antigen (PCNA) (Hozak *et al.*, 1993), lamins (Hozak *et al.*, 1995), and transcription factors (van Wijen *et al.*, 1993; Sun *et al.*, 1994).

Craig *et al.* (1997) have used FISH to examine the distribution along metaphase chromosomes of attached and loop DNA prepared from nuclei extracted with salt, LIS and

electroelution. It was found that DNA attached to the nuclear matrix or scaffold hybridised preferentially to the gene-poor G-bands. Conversely, DNA attached to the nucleoskeleton preferentially hybridises to the gene-rich R-bands. This study demonstrated that the differing sequence characteristics of DNA associated with the nuclear scaffold, matrix and nucleoskeleton are maintained across the genome. This is further discussed in Section 4.2.4.

1.6.6 The nuclear lamina and the inner nuclear membrane

The nuclear membrane consists of two concentric bilayers. The outer nuclear membrane shares its proteins and properties with the endoplasmic reticulum, of which, it is a continuation. The inner nuclear membrane is distinct and contains a unique set of proteins (Review: Gerace & Foisner, 1994), including lamin B receptor (LBR) (Worman *et al.*, 1988; Ye & Worman, 1994) and lamina-associated polypeptides (LAP) 1 (Martin *et al.*, 1995) and 2 (Furukawa *et al.*, 1995). Direct interaction occurs between each of these proteins and the nuclear lamina, a meshwork of intermediate filaments that lines the surface of the inner nuclear envelope and associates with interphase chromatin (Glass & Gerace, 1990; Belmont *et al.*, 1993; Taniura *et al.*, 1995; Review: Gerace & Burke, 1988). Disruption of the nuclear lamina results in the redistribution of replication components and blocks replication progression (Ellis *et al.*, 1997; Spann *et al.*, 1997).

Data from reconstituted liposomes and reassembly assays in sea urchin eggs suggests that LBR is a major chromatin docking protein (Pyrpasopoulou *et al.*, 1996; Collas *et al.*, 1996) and LBR interacts with chromodomain-containing human homologues of HP1 (Ye & Worman, 1996 & 1997) raising the possibility that this protein mediates interphase chromosome organisation via the heterochromatic, HP1-associated regions. LAP2 also binds chromatin but appears not to be a major docking protein. It was recently shown that LAP2 is involved in the regulation of lamina growth during the cell cycle (Yang *et al.*, 1997).

Use of an LBR-GFP fusion protein has allowed the dynamics of the inner nuclear membrane to be observed in living cells (Ellenberg *et al.*, 1997). It appears that during most of mitosis the entire nuclear membrane becomes an integral part of the endoplasmic reticulum. At telophase, a change in phosphorylation state would allow LBR (and possibly other inner membrane proteins) to bind chromatin. As each receptor becomes bound it will be immobilised and as new receptors are recruited the chromosomes are progressively coated

with the LBR-containing membrane and sealed off from the cytoplasm. The sites at which LBR specifically binds the chromosomes is likely to dictate where and how the chromosomes will be located in the nucleus (Chaudhary & Courvalin, 1993; Review: Marshall & Wilson, 1997).

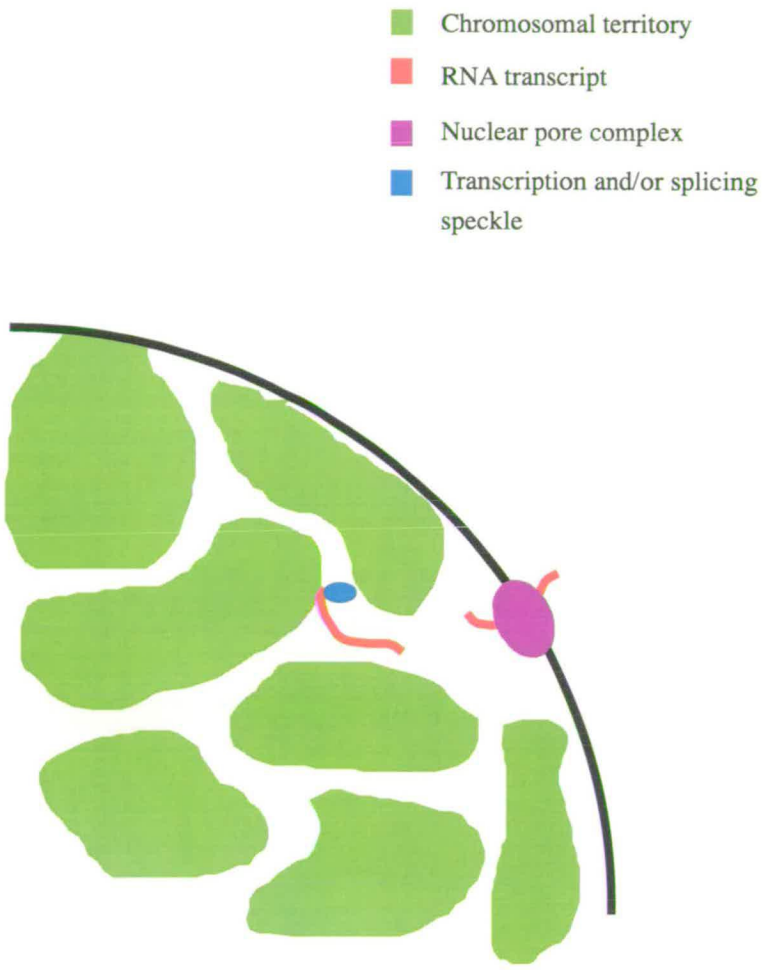

Figure 1.5 The organisation of chromosome territories in the interphase nucleus Adapted from Cremer *et al.*(1993). In this hypothesis chromosomes occupy a distinct and discrete territory in the interphase nucleus (compartment). Channels (intercompartment) run between territories, along which RNAs and proteins travel.

1.7 Proposed research: Utilising human chromosomes 18 and 19

The contrasting G- and R-band types (Sections 1.2 & 1.3) are intercalated throughout the mammalian genome, making comparative studies of their behaviour difficult. In the human genome, however, two chromosomes are unique in that they display the features of a particular band type in their entirety: chromosomes 18 and 19.

Chromosome 18 is next in line to chromosome 19 in cytogenetic idiograms based on the physical length of human metaphase chromosomes. Attempts to determine the relative DNA content of each of the human chromosomes have used analysis of fluorescent DNA stains with no base bias, by image or flow cytometry, and measurements of incorporated radioactive DNA precursors by autoradiography. Morton (1991) determined an average relative DNA content from a number of such experiments. Chromosomes 18 and 19 were estimated to posses 2.7% and 2.1% respectively, of total DNA in the human genome. Taking the total DNA content of the human genome to be 3200Mb, chromosome 18 was estimated to be 85Mb in size and chromosome 19 to be 67Mb. This gives a ratio for 19:18 of 0.79, and thus emphasises the comparability in size observed cytogenetically for these two chromosomes.

However, while being comparable in size these two chromosomes are completely contrasting in their structural and functional features. The majority of R-bands along chromosome 18 are R'-bands while on chromosome 19 T-bands dominate (Holmquist, 1992) (Figure 1.6). Chromosome 18 consists of mainly dark-staining G-bands, while there are no dark-staining G-bands and few small light-staining G-bands on chromosome 19. Thus, chromosome 18, as a whole, may reflect many of the features of G-bands and chromosome 19 may show many of the features designated to T-bands.

FISH with small fragments of human genomic DNA cut with *HaeIII* (GG|CC), chosen to represent the GC-richest parts of the genome, reveals signal on chromosome 19 to be considerable and much stronger than that on chromosome 18. FISH with small *Sau3A1* (GATC) fragments with no sequence bias gives a similar intensity of signal on both chromosomes (Craig & Bickmore, 1994) (Figure 1.6). Chromosome 18 is thus GC-poor next to GC-rich chromosome 19.

FISH with CpG-island fragments (Figure 1.6) and fragments with small inter-CpG-island distances (Figure 1.6), show little hybridisation signal on chromosome 18 and heavy labelling on chromosome 19 (Craig & Bickmore, 1994) (Section 1.3.7.4). From these results it would be expected that chromosome 18 has a lower gene density than chromosome 19. This appears to be the case. The Human Genome Database has a list of mapped genes allocated to each chromosome which is updated daily. At the end of October, 1997, 5801 assigned genes were recorded and of these, 290 were pseudogenes. Table 1.3 shows the allocation of genes for several chromosomes. It is striking that chromosome 18 has the fewest genes of any autosome (when including pseudogenes), while chromosome 19 has almost 3x the expected number of genes and almost 5x the observed:expected ratio of chromosome 18 (Table 1.3). The pattern of gene distribution between chromosomes has remained the same. In a survey published by Schuler *et al.* (1996), mapped random ESTs, which are argued to mark genes, were recorded. A significant deficit of ESTs (expressed sequence tags) were shown to be present on chromosome 18 (0.7x expected number), while an excess of ESTs were mapped to chromosome 19 (1.6x expected number).

Table 1.3 The allocation of genes to different human chromosomes
Data is taken from the Human Genome Database, Baltimore. 5511 total genes were assigned as of the end of October, 1997 (excluding pseudogenes). Estimates of the proportion of total genomic DNA content are taken from Morton (1991).

Chromosome	Gene allocation	Proportion of total genomic DNA content	Observed/expected gene density
1	556 (10.1%)	8.2%	1.2
2	318 (5.8%)	8.0%	0.7
11	368 (6.7%)	4.5%	1.5
13	77 (1.4%)	3.6%	0.4
18	82 (1.5%)	2.7%	0.6
19	335 (6.1%)	2.1%	2.9
21	89 (1.6%)	1.6%	1.0
22	117 (2.1%)	1.7%	1.2
X	376 (6.8%)	5.1%	1.3
Y	22 (0.4%)	1.9%	0.2

Interestingly, the three autosomes with the lowest gene load are the three most commonly found human trisomies. Trisomy of chromosome 18 occurs at a frequency of 1 in 6,600 live

births and results in Edwards' syndrome (Buyse, 1990). Individuals with this syndrome suffer developmental and mental retardation and are unlikely to live more than a few days. However, there are no recorded chromosome 19 trisomy live births. It has been suggested that trisomy for chromosome 19 is lethal, leading to early abortions which are not detectable, reflecting the very high gene load of this chromosome (Kuhn *et al.*, 1985).

After incorporation of BrdU into late replicating DNA, Craig and Bickmore (1994) used an antibody to BrdU conjugated with FITC (green fluorochrome) for visualisation of the late replicating regions of the genome (Figure 1.6). Chromosome 18 can be seen to be predominantly late replicating, while chromosome 19 is generally early replicating. Dutrillaux *et al.* (1976) divided replication into 18 arbitrary stages (1 being the earliest stage and 18 being the latest). The chromosome 18 G-bands replicated at stages 13 and 14, while the R-bands replicated at stages 7 and 8. By contrast, the chromosome 19 G-bands replicated at stages 10 and 11, while the R-bands replicated between stages 1-6.

As expected, chromosome 18 shows low levels of H4 acetylation along its entire length. Aside from the centromere, chromosome 19 has a predominance of highly acetylated H4 (Jeppesen *et al.*, 1992) (Figure 1.6).

Chromosomes 18 and 19 are comparable in size, but contrasting in their structural and functional features (Table 1.4). In their entirety, these chromosomes represent two extremes of chromosomal environment, that throughout the remainder of the human genome are intercalated and difficult to dissect apart. In this thesis I investigate whether human chromosomes 18 and 19 can be used as representations of the different band types and be utilised to explore the links between vertebrate chromosome structure and function further. At both metaphase and interphase, further differences between these two chromosomes are established and results extrapolated to elaborate on the relationship between the banding types which they each depict.

The areas in which comparisons between these two chromosomes were made, are as follows:

- Structure of traditionally fixed and salt extracted metaphase chromosomes.
- Dynamics of histone acetylation along the length of metaphase chromosomes.
- Position and shape of territories taken up in interphase nuclei.

- An attempt to identify potentially novel non-histone proteins and/or histone modifications by the raising of new monoclonal antibodies to metaphase chromosomes.

Table 1.4 A summary of the contrasting features of human chromosomes 18 and 19
Chromosomes 18 and 19 are comparable in size but contrasting in their structural and functional features.

Chromosome 18	**Chromosome 19**
85Mb (2.7% total genome)	67Mb (2.1% total genome)
No R-bands are T-bands	All R-bands are T-bands
Relatively GC-poor	Relatively GC-rich
Low CpG-island density	High CpG-island density
0.6x expected number of genes	2.9x expected number of genes
High number of trisomies (1 in 6,600 new borns)	No recorded trisomies
Generally late replicating	Generally early replicating
Low levels of H4 acetylation	High levels of H4 acetylation

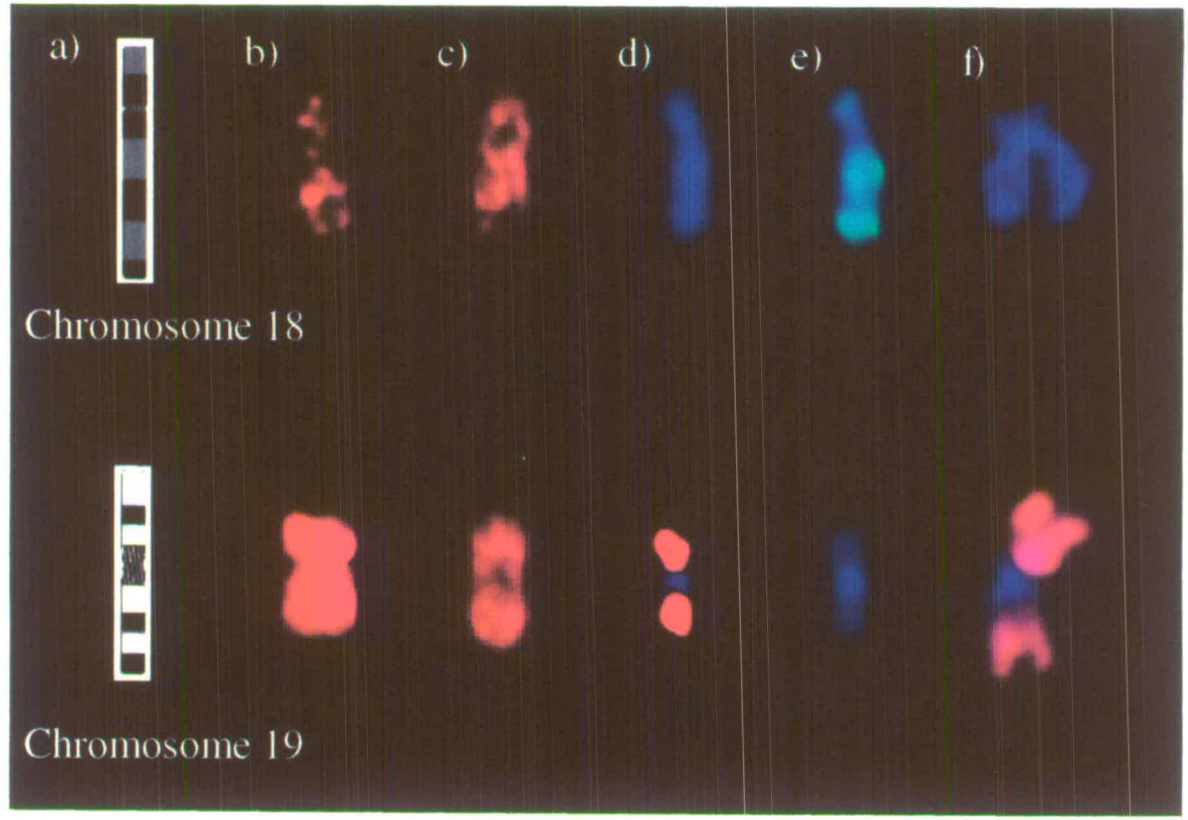

Figure 1.6 Some of the features of human chromosomes 18 and 19
(**a**) Ideogram of the chromosomes at 400 bands/genome resolution. Black- G-bands Grey- R'-bands White- T-bands (**b-d**) Taken from Craig (1995). FISH signal from hybridisation of 100-600bp DNA fragments (red) generated by digestion of human genomic DNA with: (**b**) *HaeIII* (GGCC), (**c**) *Sau3A1* (GATC) or, (**d**) *HpaII* (CCGG). In the latter of these panels, chromosomes were counterstained with DAPI (blue). (**e**) Taken from Craig & Bickmore (1994). Incorporation of BrdU into late replicating regions detected by immunofluorescence with anti-BrdU-FITC (green) on DAPI stained chromosomes (blue). (**f**) Immunofluorescence with an antibody raised to acetylated H4 (R41) (TR/red) on DAPI stained chromosomes (blue). Antibody provided by Prof. B.M. Turner, University of Birmingham.

2. Materials and methods

2.1 Mammalian cell culture

2.1.1 Cell counting and cell viability

Cells were counted using a haemocytometer (Weber Scientific International Ltd.) which has a chamber 0.1mm in height with an etched grid of $1mm^2$ subdivided into 400 squares. The total volume defined by the grid was $1x10^{-4}$ ml. To simultaneously test for cell viability, 250µl cells were mixed with an equal volume of nigrosine (0.45% diluted in phosphate buffered saline (PBS)) and 10µl were added to the haemocytometer chamber. Nigrosine stains only dead cells. To obtain cell concentrations per ml, the total number of cells over the grid was multiplied by $2x10^4$.

2.1.2 Thawing cells from storage in liquid nitrogen

Cells were stored in liquid nitrogen suspended in freezing medium (6% DMSO in foetal calf serum (FCS)). On removal to thaw, tubes were immediately incubated at 37°C in a beaker of water. Cells were diluted in medium, centrifuged at 400g for 5 minutes, resuspended in fresh medium and transferred to a tissue culture flask.

2.1.3 Culture of human and rodent-human hybrid cell lines

REN2 (49 XXXXY) and FATO (46 XY) are human lymphoblast cell lines. These cells were grown as suspension cultures in RPMI (Gibco BRL) supplemented with 10% FCS. Cells were split 1:3 in fresh medium every 2-3 days. Every 7 days the cells were spun at 250g for 5 minutes and resuspended in fresh medium at a concentration of $5x10^5$ cells/ml.

The following lines were grown as monolayer cells. The human mesothelioma cell line, JU77 and the mouse-human monochromosome hybrid cell line, PgMe-25 were grown in RPMI supplemented with 10% FCS. The two Chinese hamster-human monochromosome hybrid cell lines, GM11010 and GM10449A, and the human fibrosarcoma cell line, HT1080, were grown in DMEM (Gibco BRL) supplemented with 10% FCS. The mouse-human monochromosome hybrid cell line, A91neo was grown in RPMI supplemented with 10% FCS and 400µg/ml G418 Sulphate (Gibco BRL) to select for the resistance tagged

human chromosome 1. Finally, the myeloma cells, Sp2/0 were grown in RPMI supplemented with 10% myoclone FCS. The cells from each of these lines were allowed to grow to near confluence before splitting. Medium was poured off, the cells washed twice in PBS then covered in a thin layer of 10% trypsin in versene and placed at 37°C for 5 minutes. Gentle agitation dislodged the cells, medium was added and the cells were pelleted at 250g for 5 minutes.

All cells were incubated at 37°C with 5% CO_2. To promote the number of cells at metaphase, 2 hours prior to harvesting 0.1μg/ml of colcemid (Gibco BRL), a microtubule poison, was added.

2.1.4 Primary lymphocyte culture

Fresh peripheral blood from a normal male was taken and cultures were set up immediately. 0.8ml of blood were added to 9.2ml of RPMI supplemented with 10% FCS, and stimulated with the mitogen phytohaemagglutinin at a final concentration of 4μg/ml. Best results were obtained when blood was cultured in 20ml round-bottomed universals (Life Technologies). Cells were incubated at 37°C and 5% CO_2.

Cells were synchronised after 48 hours in culture. Methotrexate was added to a final concentration of 10^{-7}M. This prevents the formation of thymidine and thus blocks cells at the G1/S boundary, or within S phase if already entered. After 16 hours the medium was replaced with fresh medium warmed to 37°C. After a further 4.5 hours colcemid was added to a final concentration of 0.1μg/ml. The cells were harvested after a further 10 minutes.

2.1.5 Primary fibroblast culture

A normal male foetal lung primary fibroblast cell culture, GM01604A, was obtained from the National Institute of General Medical Sciences Human Genetic Mutant Cell Repository, New Jersey. The culture was grown and harvested by Dr. J.A. Fantes, MRC Human Genetics Unit, Edinburgh. The growth medium was RPMI supplemented with 15% FCS, 100μg/ml streptomycin and 100 units/ml penicillin. Cells were incubated at 37°C and 5% CO_2.

Fibroblast cultures arrested in G1 were obtained by growing to monolayer confluency then replacing with medium containing only 2% FCS. After 2-3 days, when no rounded mitotic cells could be seen, the cells were harvested (Tobey *et al.*, 1988). Medium was poured off and the cells washed twice in PBS. Cells were covered in a thin layer of 10% trypsin in versene and placed at 37°C for 5 minutes. Gentle agitation dislodged the cells, medium was added and the cells were pelleted at 250g for 5 minutes.

2.1.6 Harvesting and fixing metaphase spreads

After harvesting, cells were suspended in a mildly hypotonic solution, 0.075M KCl, at a concentration of $2x10^6$ cells/ml. The hypotonic solution was added dropwise while continually agitating the tube. The cell suspension was left at room temperature for 30 minutes before centrifuging at 400g for 5 minutes. Cells were then fixed with fresh 3:1 methanol:glacial acetic acid. 2ml of fix was added dropwise to the cells while the tube was agitated using a vortex. A further 8ml of fix were added and the tubes were placed on ice for a minimum of 10 minutes or stored at -20°C overnight. Cells were fixed twice more and stored indefinitely at -20°C.

2.2 Preparation of DNA

2.2.1 Treatment of cells for DNA extraction

Cells for extraction were washed in ice cold PBS. Human peripheral blood was centrifuged at 180g for 5 minutes and resuspended in an equivalent volume of ice cold red blood cell lysis buffer (154mM NH_4Cl, 10mM $KHCO_3$, 0.1mM EDTA). Tubes were left on ice for 10 minutes, centrifuged as before and washed in ice cold PBS.

Using 5ml Sarstedt tubes, cells were suspended in sufficient PBS such that the suspension was cloudy and viscous but relatively easy to manipulate ($2x10^7$-10^8 cells/ml). An equal volume of lysis buffer (100mM Tris-HCl pH7.5, 100mM NaCl, 10mM EDTA, 1% Sarkosyl) was added slowly then the tubes were inverted to mix over a period of 5 minutes. RNAse was added to a concentration of 100µg/ml and the lysate left at 37°C for 30 minutes. Proteinase K (Boehringer) was then added to a final concentration of 100µg/ml and the tubes incubated at 55°C for 4 hours, being inverted every 30 minutes for 3 minutes.

2.2.2 Phenol/chloroform extraction

DNA was extracted from the cell lysate with an equal volume of phenol (pre-heated to 60°C), followed by phenol:chloroform:octan-2-ol (25:24:1) and finally chloroform:octan-2-ol (24:1). Tubes were repeatedly inverted over a period of 10 minutes, left for 5 minutes on ice then centrifuged at 700g for 5 minutes. The aqueous layer was transferred to a new tube after each extraction step.

2.2.3 Dialysis

Dialysis tubing (Visking) was prepared by boiling for 10 minutes in a large volume of 2% $NaHCO_3$ in 1mM EDTA pH8.0, rinsing in dH_2O and storing submerged in 1mM EDTA pH8.0 at 4°C. Immediately prior to use, a length of tubing was boiled for 10 minutes in dH_2O. Extracted DNA was dialysed against 1000x volume of TE buffer (10mM Tris, 1mM EDTA, pH8.0) with 100mM NaCl at 4°C for 24 hours then against 1000x volume TE buffer only, at 4°C for 24 hours. DNA was stored at 4°C.

2.2.4 Ethanol precipitation

DNA was precipitated by adding 0.1x volume of 3M sodium acetate and 2.5x volume ethanol. Samples were incubated at -20°C for a minimum of 1 hour or overnight before centrifuging at 12000g for 15 minutes at 4°C. DNA pellets were washed twice in 80% ethanol, vacuum dried and suspended in the appropriate volume of TE buffer. Samples were stored at 4°C.

2.2.5 Measuring quality and quantity of DNA

DNA concentration was measured spectrophotometrically and/or by gel electrophoresis alongside DNA of known concentration (Section 2.3).

DNA was diluted 1:1000 in TE buffer and transferred to a quartz cuvette. The absorbence or optical density (OD) at 260nm (A_{260}) was measured. An OD of 1 corresponds to ~50µg/ml of DNA. To determine the purity of DNA the A_{280} was also measured. Pure DNA has an A_{260} /A_{280} of 1.8, values lower than this indicate contamination by proteins, RNA or phenol.

2.3 Electrophoresis of DNA

Horizontal agarose gels (0.5-1% in 1xTBE) were used to resolve molecules of 0.2 to 50Kb. The electrophoresis buffer was 1xTBE (90mM Tris-HCl, 90mM boric acid, 2mM EDTA pH8.0). To resolve small fragments (0.05 to 5Kb) horizontal 2% Nusieve gels were used.

To provide DNA samples with a density high enough to sink to the bottom of the wells, 1 volume of 6x loading buffer (15% Ficoll 400, 0.25% Bromophenol Blue, 0.25% xylene cyanol) was added to 5 volumes of DNA. The dyes included in this buffer provided convenient size markers whose electrophoretic mobility depended on gel concentration. Commercially available DNA size markers (ϕX174 DNA *HaeIII* digest and λ DNA *HindIII* digest) were diluted to 50ng/μl and 250-500ng loaded per well.

The DNA-intercalating fluorescent stain ethidium bromide (2,7-diamino-10-ethyl-9-phenyl-phenathridium bromide) was used to stain DNA gels. Gels were soaked in 0.25μg/ml of ethidium bromide with mild agitation for 30 minutes, then destained in dH_2O for a further 30 minutes. Stained DNA was visualised with UV light from a transilluminator. Gels were photographed using an Appligene (Oncor) television camera and images were printed instantly using a Mitsubishi video copy processor or with a Kodak MP-4 Land camera using Kodak Plus-X pan film with 1-3 minute exposure.

2.4 Polymerase chain reaction (PCR)

2.4.1 Human-specific *Alu* PCR

2.4.1.1 Choice of primers

The following primers were used for human-specific *Alu* PCR:

#153 5' GGGATTACAGGCGTGAGCCAC 3' (Breen *et al.*, 1992),
#154 5' TGCACTCCAGCCTGGGCAACA 3' (Breen *et al.*, 1992),
#451 5' GTGAGCCGAGATCGCGCCACTGCACT 3' (Alveiler & Porteous, 1992),
#SB30 5' ACAGAGCGAGACTCCGTCTC 3' (Ms. S. Boyle, MRC Human Genetics Unit, Edinburgh).

The positions of each of these are shown relative to the human *Alu* consensus sequence in Figure 3.9.

2.4.1.2 Preparation of the primers

All primers were synthesised at the MRC Human Genetics Unit, Edinburgh and stocks were provided in 1ml ammonium hydroxide. 350µl of stock were precipitated (Section 2.2.4) and resuspended in 200µl TE buffer. The concentration was determined (Section 2.2.5) and the oligo diluted to 250ng/µl.

2.4.1.3 Amplification method

This method was adapted from Arveiler & Porteous (1992). The following were mixed in a 500µl tube: 10µl 10xPCR buffer (Perkin Elmer Cetus); 10µl 25mM magnesium chloride (Perkin Elmer Cetus); 2µl dNTP mix (2mM each of dATP, dGTP, dCTP and dTTP (Promega)); 50ng template DNA; 25ng primer DNA; 2.5 units *Taq* polymerase (Perkin Elmer Cetus) and dH_2O to 100µl. The reaction was mixed, spun briefly and overlaid with 50µl mineral oil (Sigma) to prevent evaporation. Reactions were amplified using a thermal cycler (Perkin Elmer Cetus). The following cycling conditions were used: 94°C for 5 minutes pre-soak, denaturation at 94°C for 45 seconds, annealing at 60°C for 1 minute and extension at 72°C for 1 minute increasing by 6 seconds/cycle. After 40 cycles, reactions were frozen at -20°C. An aliquot of 10µl was analysed by electrophoresis. Products from each primer reaction were pooled, precipitated (Section 2.3.4) and the concentration was determined (Section 2.3.5). Products were labelled for FISH by nick translation (Section 2.5.1).

2.4.2 Linker PCR

2.4.2.1 Catch-linkered products and primers

Dr. S.H. Cross, University of Edinburgh, provided catch-linkered DNA from fractions of human chromosome 18 and 22 DNA purified using the methylated DNA binding column (Cross *et al.*, 1994) (Section 4.3). Chromosomes were sorted using fluorescence activated chromosome sorting (FACS) by Dr. N. Carter, Sanger Centre, Cambridge (Section 2.8.2), digested with *MseI* (T | TAA) and a sample of this DNA was catch-linkered. The remaining

DNA was purified through the column and fractions representing CpG-island and non-CpG-island DNA were also catch-linkered. The following catch linkers were used:

Chromosome 18

CH18-1 5'TACCGTTAAGCGTCAATCATGG3'

CH18-2 3' GGCAATTCGCAGTTACTACC5'

Chromosome 22

CH22-1 5'TAAGTACTGCACCAGCAAATCC3'

CH22-2 3' TCATGACGTGGTCGTTTAGG5'

The pairs of linkers were annealed together and ligated to the *MseI* digested DNA. CH18-2 and CH22-2 were used as primers for linker PCR.

2.4.2.2 Amplification method

The following were mixed in a 500µl tube: 5µl 10x tricine PCR buffer (20mM $MgCl_2$, 300mM tricine pH8.4, 100mM β-mercaptoethanol, 0.1% gelatin); 20µl dNTP mix (2mM each of dATP, dGTP, dCTP and dTTP (Promega)); 50ng template DNA; 25ng primer DNA; 2.5 units *Taq* polymerase (Perkin Elmer Cetus) and dH_2O to 50µl. The reaction was mixed, spun briefly and overlaid with 50µl mineral oil (Sigma). Reactions were amplified using a thermal cycler (Perkin Elmer Cetus). The following cycling conditions were used: 94°C for 7 minutes pre-soak, denaturation at 94°C for 30 seconds, annealing at 50°C for 45 seconds and extension at 72°C for 1 minute increasing by 1 second/cycle. After 35 cycles, reactions were frozen at -20°C. An aliquot of 10µl was analysed by electrophoresis.

2.4.2.3 Labelling products for FISH by PCR

Products were labelled for FISH by a second round of PCR incorporating biotin-16-dUTP or digoxigenin-11-dUTP. The following were mixed in a 500µl tube: 5µl 10x tricine PCR buffer (20mM $MgCl_2$, 300mM tricine pH8.4, 100mM β-mercaptoethanol, 0.1% gelatin); 5µl each of 2mM dATP, dGTP and dCTP (Promega); 2.5µl 0.5mM dTTP; 5µl 50nM biotin-16-dUTP (Boehringer) or 5µl 125nM digoxigenin-11-dUTP (Boehringer); 50ng template DNA; 25ng primer DNA; 2.5 units *Taq* polymerase (Perkin Elmer Cetus) and dH_2O to 50µl. Cycling conditions as in Section 2.4.2.2.

2.5 Non-isotopic DNA labelling

DNA was labelled using biotin-16-dUTP or digoxigenin-11-dUTP. These analogues were incorporated into DNA by PCR (Section 2.4.2) or nick translation. Following either method, unincorporated nucleotides were removed and efficiency of labelling was assessed as described in Section 2.5.3.

2.5.1 Nick translation

1.5µg of DNA were added to 4µl 10x nick translation salts (0.5M Tris-HCl-HCl pH7.5, 0.1M $MgSO_4$, 1mM DTT, 500µg/ml Bovine serum albumin (BSA)), 4µl each of 2mM dATP, dGTP and dCTP, 2µl of 0.5mM dTTP and 4µl 1mM biotin-16-dUTP or digoxigenin-11-dUTP. DNAse I (Gibco BRL) was diluted to a concentration of 20units/ml in dH_2O at 4°C and 2µl added to the reaction mixture to give a final concentration of 1unit/ml. After the addition of 1µl DNA polymerase I (Gibco BRL, 10units/µl), dH_2O was added to make the total volume of reaction mixture 40µl. The reaction was mixed thoroughly and allowed to proceed at 16°C for 90 minutes. The reaction was stopped by placing at -20°C.

A plasmid containing chromosome 1 centromeric heterochromatin (Cooke & Hindley, 1979) was labelled directly with a fluorochrome, by Mrs. P. Malloy, MRC Human Genetics Unit, Edinburgh. This was achieved by nick translation using the following concentrations: 500ng DNA, 2µl 10x nick translation salts (as above), 2.5µl each of 2mM dATP, dGTP and dCTP, 1.5µl of 0.5mM dTTP and 1µl 1mM dUTP conjugated to Spectrum Orange fluorochrome (Gibco BRL). DNAse I and DNA polymerase I were added and remaining procedures carried out as directed above.

2.5.2 Removal of unincorporated label

Sephadex G50 (Pharmacia) was swollen in an excess of dH_2O, washed several times in dH_2O, equilibrated in TE and autoclaved. Spin columns were made by inserting a small plug of sterile siliconised glass wool in a 1ml syringe, filling the syringe with Sephadex and centrifuging at 100g for 5 minutes. Reactions were made up to 100µl with TE buffer and centrifuged through the spin columns at 100g for 5 minutes, separating the unincorporated

nucleotides from the nick translated DNA fragments. Collected labelled DNA probes were stored at -20°C.

2.5.3 Quantifying label incorporation

Gridded nitrocellulose membranes were prepared by soaking briefly in dH_2O followed by 20xSSC (3M NaCl, 0.3M tri-sodium citrate, pH7.4) for 10 minutes then allowing to air dry. Labelled DNA probes were diluted to $1x10^{-2}$ and $1x10^{-3}$ and 1µl of each was spotted twice onto a gridded membrane. After the spots had dried, a further 1µl was added to one of each dilution. On the same membrane 20, 10, 2 and 1pg of appropriately labelled lambda DNA standards (Boehringer) were spotted. DNA was cross-linked onto the membrane by exposure to 30mJ of UV irradiation.

For detection, the membrane was immersed in buffer 1 (0.1M Tris-HCl pH7.5, 0.15M NaCl) for 5 minutes at room temperature then in 3% BSA in buffer 1 at 37°C for 30 minutes. 10µl streptavidin-alkaline phosphatase (Boehringer) and/or anti-digoxigenin-alkaline phosphatase (Boehringer) were added to 10ml of buffer 1 and placed in a sealed polythene bag with the membrane for 30 minutes at room temperature with continuous agitation. The membrane was washed twice for 15 minutes in buffer 1 then for 5 minutes in 0.1M Tris-HCl, pH9.5. The colour reaction was developed by incubation of the membrane, in a sealed polythene bag, with 5ml of 0.1M Tris-HCl, pH9.5 and 2 drops from bottles 1-3 from the alkaline phosphatase substrate kit IV (Vector). The substrates in this colour reaction are 5-bromo-4-chloro-3-indolyl phosphate and nitroblue tetrazolium, which produce a blue reaction product. A complete colour reaction was usually observed within an hour and an estimate of the concentration of DNA labelled probe was made by comparison with the lambda standards.

2.6 Fluorescence *in situ* hybridisation (FISH)

The technique of fluorescence *in situ* hybridisation (FISH) is used to determine the chromosomal origin of isolated DNA (Langer-Safer *et al.*, 1982). Methods used here were developed by Dr. J.A. Fantes, MRC Human Genetics Unit, Edinburgh (Fantes *et al.*, 1992).

2.6.1 Slide preparation

Glass slides were prepared by soaking in detergent solution and washing with dH_2O before storage in a dilute solution of HCl in ethanol. Immediately prior to slide making, slides were polished with muslin.

Methanol:acetic acid fixed cells (Section 2.1.5) were removed from storage at -20°C, left to warm to room temperature for 30 minutes and centrifuged at 400g for 5 minutes. Fresh fix was added to a volume of 0.5-2ml, depending on the number of fixed cells, and the cells resuspended. One drop of suspension from a narrow-mouthed pastette was dropped onto a horizontal slide from a height of about 30cm. The spread of cells on the slide was improved by coating the slides with a thin layer of moisture, usually by breathing. An air humidity of >50% also aided spreading. The slides were gently blown upon until the spread dried. Spreading was monitored by phase contrast microscopy. Slides were stored under vacuum for 2-6 days prior to hybridisation. When fixed material of more than 2 years old was to be used, slides were treated with pepsin prior to hybridisation (Section 2.6.2).

Cytocentrifuged slides (Section 2.10) were stored for up to 1 month prior to FISH. Fixation was reversed by immersing slides in 2:5 0.07M NaOH:EtOH for 3 minutes then washing in 2xSSC (300mM NaCl, 30mM tri-sodium citrate, pH7.4) before RNAse treatment and hybridisation as described in Section 2.6.3.

Slides of salt extracted chromosomes and nuclei (Section 2.9) were stored for up to 1 week prior to FISH. No RNAse treatment was required and thus the slides were dehydrated through an ethanol series and hybridisation was carried out as described in Section 2.6.3.

2.6.2 Pepsin treatment

Slides were dehydrated in acetone for 5 minutes then dried under vacuum. RNAse treatment was carried out as in Section 2.6.3. 43µl of 11M HCl was added to 50ml of dH_2O and pre-heated to 37°C. 125µl of 2% pepsin was then added and the slides were incubated for 5 minutes before washing in PBS with 50mM $MgCl_2$. Slides were dehydrated through an ethanol series and hybridisation was carried out as described in Section 2.6.3.

2.6.3 Hybridisation

Slides were mounted vertically in a metal slide rack and subsequent incubations carried out in 200ml glass troughs. Slides were first treated with 100µg/ml RNAse in 2xSSC for 1 hour at 37°C, washed briefly in 2xSSC and dehydrated through an ethanol series (2 minutes each in 70%, 90% and 100% ethanol). The slides were left to dry under vacuum for 10 minutes before being heated in a 70°C oven for 5 minutes and immediately denatured in 70% formamide, 2xSSC at 70°C for 2-3 min. After passing through 70% ethanol at 4°C and an ethanol series as above, slides were again vacuum dried.

Concurrent with slide preparation the probes were prepared. 150ng of labelled DNA (Section 2.5), usually suspended in TE was precipitated with 5µg salmon sperm DNA and human C_0t 1 DNA (the amount of which varied from 5 to 50µg, depending on the potential repeat content of the probe) (Gibco BRL). After the addition of two volumes of ethanol, probes were spun down under vacuum until they had precipitated, and resuspended in 10µl hybridisation mix (50% deionised formamide, 10% dextran sulphate, and 1% Tween20, in 2xSSC) at 4°C. Commercial probes were usually provided in or with hybridisation buffer and did not require addition of salmon sperm DNA or human C_0t 1 DNA. All probes were denatured at 70°C for 5 minutes and reannealed at 37°C for 15 minutes before spotting onto pre-cleaned coverslips. The denatured slides were carefully laid onto the appropriate coverslip and sealed with rubber solution (TipTop) before placing in a metal tray in a 37°C water bath overnight.

2.6.4 Washing and detection

Slides were washed in glass racks in 200ml troughs. After removal of the rubber cement, they were immersed in 50% formamide in 2xSSC at 45°C for 3 minutes, with gentle agitation to facilitate detachment of the coverslips. Slides were washed a further 3x in the same buffer then for 4x3 minutes in 2xSSC at 45°C and 4x3 minutes 0.1xSSC at 60°C before transferring to 4xSSC/0.1% Tween 20. Detection was carried out in a moist chamber pre-heated to 37°C. Biotin was detected with sequential layers of fluorochrome-conjugated avidin (Fluorescein (FITC) or Texas Red (TR) -avidin), biotinylated anti-avidin, and a further layer of fluorochrome-conjugated avidin. Digoxigenin was detected with sequential layers of FITC-conjugated anti-digoxigenin and FITC-conjugated anti-sheep. Detection

reagents were diluted in SSCM (4xSSC, 5% Marvel dried skimmed milk) to the appropriate concentration (Table 2.1). After incubation with 40µl SSCM for 5 minutes at room temperature, 40µl of the appropriate detection layer were applied to each slide and covered with a square of parafilm. Slides were incubated in the moist chamber at 37°C for 45 minutes, followed by 3 washes of 2 minutes in 4xSSC/0.1% Tween20 at 37°C.

All slides were mounted with 1µg/ml DAPI, or 0.2µg/ml Propidium Iodide (PI) in Vectashield (Vector). Coverslips were sealed with rubber solution (Pang) and slides were stored in the dark at 4°C.

2.6.5 Detecting bromodeoxyuridine incorporation

Bromodeoxyuridine (BrdU) at 1mM final concentration, was added to cells in culture 30 minutes-4 hours prior to harvesting, to allow determination of the late replicating regions of the genome. As an additional detection layer following FISH, FITC-conjugated anti-BrdU, diluted to the appropriate concentration in SSCM (Table 2.1), was applied to each slide and covered with a layer of parafilm. Slides were incubated in a moist chamber at 37°C for 1 hour, followed by 3 washes of 2 minutes in 4xSSC/0.1% Tween 20 at 37°C, before mounting.

Since the FITC-conjugated anti-BrdU antibody used here detects BrdU only in single stranded DNA, slides not undergoing FISH must be denatured. Slides were dipped in 2:5 0.07M NaOH:EtOH for 90 seconds, then washed in PBS/1% Marvel for 10 minutes. Anti-BrdU was applied as above. Slides were mounted and stored as in Section 2.6.4.

2.6.7 FISH on three-dimensional nuclei

This method for the maintenance of three-dimensional nuclei through the process of FISH was obtained from Dr. J.M. Bridger, University of Heidelberg.

HT1080 human fibrosarcoma cells were grown on microscope slides that had been previously dipped in EtOH and flamed, by placing each slide in a sterile petri dish and covering with medium containing approximately $5x10^5$ cells/ml. Slides were ready for FISH once the cells were approximately 70% confluent. Slides were washed 3x 5 minutes in PBS,

fixed in 4% paraformaldehyde for 20 minutes, washed for 3x 5 minutes in PBS and permeabilised in 0.5% saponin/ 0.5% Triton X-100 in PBS for 20 minutes. The slides were washed again for 3x 5 minutes before incubating in 20% glycerol in PBS for 30 minutes. All incubations were carried out at room temperature. Slides were then dipped into liquid nitrogen 5x until the slides were completely frozen then allowing the slides to thaw slowly to room temperature each time before re-freezing. Following this, slides were placed in 0.1M HCl in dH_2O for 5 minutes, rinsed in dH_2O then heated in a 70°C oven for 5 minutes, before denaturing in 70% formamide, 2xSSC for 3 minutes then 50% formamide, 2xSSC for 1 minute, both at 75°C. Slides were washed briefly in 2xSSC immediately before applying the probe. Probes were prepared, hybridised and detected as described in Sections 2.6.3 and 2.6.4.

Table 2.1 Antibodies and fluorochrome-conjugates used for FISH
CS - cell sorting grade

Antibody or fluorochrome-conjugate	Source	Stock concentration (mg/ml)	Dilution
FITC-avidin D CS	Vector	2.0	1:500
TR-avidin D CS	Vector	2.0	1:500
Biotinylated anti-avidin D	Vector	0.5	1:100
Anti-sheep-FITC	Vector	1.5	1:100
Anti-digoxigenin-FITC $F(ab')_2$	Boehringer	0.2	1:40
Anti-BrdU-FITC	Boehringer	0.1	1:10

2.7 Cell cycle fractionation

2.7.1 Cell cycle fractionation by elutriation

FATO cells (Section 2.1.3) were fractionated, according to size and density, using the JE-5.0 Elutriation System (Beckman) (Section 6.5). BrdU was added to the cell culture 45 minutes prior to harvesting (Section 2.6.5). $1x10^8$ cells were washed in PBS, suspended in 50ml of elutriation buffer (PBS, 1% FCS, 0.3mM EDTA, 0.1% glucose) then passed through a 40µm pore filter. $1x10^6$ cells were removed for FACS analysis (Section 2.14.2) and $2x10^6$ cells were fixed (Section 2.1.5). The remaining cells were fractionated from the

standard 5ml chamber, at 15°C, at increasing flow rates with a rotor speed of 2500rpm (Table 2.2).

For each fraction, 200ml were collected, the middle 100ml were kept and the remainder discarded. Between collection of fraction 1 and 2, a further 100ml were collected and discarded. This was to prevent contamination between fractions. From each fraction the cells were counted (Section 2.1.1), a sample set aside for analysis by flow cytometry (Section 2.7.2) and the remainder fixed for slide preparation (Section 2.6.1).

Table 2.2 Flow rates and estimated particle sizes of each elutriator fraction
Rotor speed was 2500rpm except where indicated.

Fraction	Flow rate (ml/minute)	Particle diameter (μm)
1	20	9
2	22.5	10
3	28	11
4	33	12
5	39	13
6	45	14
7	51	15
8	59	16
9	59 at 1500rpm	26

2.7.2 Flow cytometry of cells

The flow cytometer used for the fluorescence activated cell sorting (FACS) analysis of cell fractions was a FACScan (Becton Dickenson). The method of preparation of cells for analysis was adapted from Vindelov *et al.* (1983). A sample of cells from each fraction were suspended in FACS citrate buffer (250mM sucrose, 40mM tri-sodium citrate, 5% DMSO, pH7.6) at $1x10^6$cells/400μl. Cells were stored at this stage, at -20°C, until required for analysis. FACS stock solution (3.4mM tri-sodium citrate, 0.5mM Tris-HCl, 1.5mM spermine tetrahydrochloride, 0.1% Nonidet P40, pH7.6) was used to make up all subsequent FACS solutions. After thawing rapidly, 900μl of FACS solution A (3μg/ml trypsin) was added and the cells incubated for 10 minutes at room temperature, with gentle agitation. 750μl of FACS solution B (100μg/ml RNAse, 500μg/ml BSA) was added and the cells incubated for 30 minutes at room temperature, with gentle agitation. Finally, 750μl of ice

cold FACS solution C (2μg/ml PI, 5.7mM spermine tetrahydrochloride) was added and the cells stored on ice for 30 minutes or at 4°C for up to 1 week. Forward scatter (particle size) and fluorescence emission were recorded for 10000 events from each cell sample using software developed by Becton Dickinson.

2.8 Preparation of metaphase chromosomes

2.8.1 Isolation of metaphase chromosomes

This technique has been adapted by Dr. J.A. Fantes, MRC Human Genetics Unit, Edinburgh, from Sillar & Young (1981) (Fantes *et al.*, 1983). The REN2 or FATO human cell line (Section 2.1.3) was seeded at $4x10^5$ cells/ml and after 30 hours colcemid was added to a final concentration of 0.1μg/ml. Cells were harvested 16 hours later by centrifuging at 400g for 5 minutes and washed in fresh ice-cold complete medium to remove dead cells and debris. The pellet was resuspended in 0.075M KCl hypotonic solution ($5x10^6$cells/ml). After incubation for 20 minutes at 37°C the cells were placed on ice and 250μl removed to determine the mitotic index. 5mls of 3:1 methanol:acetic acid was added to the sample and allowed to stand on ice for 10 minutes. After centrifugation at 180g for 5 minutes the supernatant was removed and the pellet resuspended in a small volume of fixative. A slide was prepared from this (Section 2.6.1) and the number of divisions observed in approximately 100 cells. A mitotic index of >60% was expected and if this was achieved the cells in hypotonic solution were centrifuged at 180g for 5 minutes and resuspended in ice cold polyamine buffer (15mM Tris-HCl, 0.2mM spermine, 0.5mM spermidine, 2mM EDTA, 0.5mM EGTA, 80mM KCl, 20mM NaCl, 14mM β-mercaptoethanol, pH7.2) at 10^7 cells/ml. An estimate of the number of chromosomes and nuclei expected were calculated from the mitotic index.

The cells were centrifuged at 180g for 5 minutes and resuspended in ice cold polyamine buffer with 0.1% digitonin. The cellular membranes were disrupted by immediately vortexing the cells for 60 seconds. This was monitored by placing a drop of suspension on a slide previously spread with Hoechst 33258 and observing using a fluorescence microscope. Whole nuclei were removed by centrifugation at 180g for 10 minutes. The supernatant was kept and the pellet resuspended in polyamine buffer with 0.1% digitonin, vortexed for 5 seconds, centrifuged at 180g for 10 minutes. The supernatants were pooled and stored for

up to 4 weeks at 4°C or up to 6 months at -70°C with 15% glycerol. The pellets were pooled as a nuclear fraction and stored as with the chromosome fraction.

2.8.2 Flow cytometry of chromosomes

Pure preparations of chromosomes 18, 19 and X were sorted using fluorescence activated chromosome sorting (FACS) by Dr. D. Green, MRC Human Genetics Unit, Edinburgh and Dr. N. Carter, Sanger Centre, Cambridge. Metaphase chromosomes were prepared from the REN2 human cell line (Section 2.8.1) and stained with 0.5µg/ml Hoechst 33258 immediately prior to sorting. A sample of 0.75ml was loaded into a cooled syringe set to infuse at a rate of 0.4ml/hour. This resulted in a chromosome flow rate of 1000/second through a 50µm glass nozzle into a stream of PBS. A 1W 351-364nm wavelength laser beam was focused with crossed cylindrical lenses onto the liquid stream. The average peak fluorescence intensity of each chromosome measured on opposite sides of the stream and perpendicular to the laser beam was accumulated. Under computer control the appropriate sorting thresholds were set for the chromosome of interest and chromosomes fluorescing between these values were sorted by charged droplet deflection into a small quantity of polyamine buffer.

2.9 Salt extraction of chromosomes and nuclei

Metaphase chromosomes prepared from the REN2 cell line at a concentration of ~$1x10^8$/ml or nuclei prepared from the FATO cell line at a concentration of ~$1x10^7$/ml (Section 2.8.1), were applied to slides 12 hours in advance of salt extraction. 20µl was distributed in the centre of a slide and spread across the surface using the pipette tip. Slides were air dried horizontally.

Using isolation buffer (10mM Tris-HCl pH8.0, 10mM EDTA, 0.1% NP40 detergent, 20µg/ml PMSF, 0.1mM $CuSO_4$), the following salt extraction solutions were made: 0M, 0.5M, 1.0M, 1.2M, 1.8M NaCl. Each extraction solution was placed in a large trough permitting sufficient depth for the slides to be totally immersed.

Slides were lowered into each trough using a mesh platform, allowing the slides to be gently flooded with extraction solution. Chromosomes and nuclei showed best morphology when extracted sequentially: 30 minutes extraction in 0M NaCl solution and 15 minutes extraction

in all subsequent salt concentrations. Slides were fixed by immersing in 3:1 methanol:glacial acetic acid for 2x 15 minutes. Slides were air dried and stored at room temperature for FISH (Section 2.6).

2.10 Cytocentrifugation and immunofluorescence

Metaphase spreads for immunofluorescence cannot be fixed with methanol/acetic acid, as this process may destroy the antigenic epitope or even extract the proteins under investigation. Instead, spreads are produced by spinning cells onto slides by cytocentrifugation.

2.10.1 Cytocentrifugation

After harvesting, cells were suspended in 0.075M KCl, at a concentration of $2x10^6$ cells/ml. The cell suspension was left at room temperature for 30 minutes before placing on ice and diluting with ice cold hypotonic solution to a concentration of $2x10^5$cells/ml. 500µl of cell suspension was aliquoted into buckets (Cyto-Tek) loaded with slides and 1ml filter paper (Sakura). Buckets were spun at 400g for 10 minutes in the cytospin (Cyto-Tek). Slides were then washed in potassium chromosome medium (KCM) (120mM KCl, 20mM NaCl, 10mM Tris-HCl pH8.0, 0.5mM EDTA, 0.1% Triton X-100) for 10 minutes.

Buckets were washed in detergent overnight then rinsed in EtOH and allowed to air dry before re-using. Filters were discarded after use.

2.10.2 Immunofluorescence

Slides were not allowed to dry out and were agitated as little as possible. 40µl of primary antibody, diluted to the required concentration in KCM with 10% serum (Table 2.3), was applied to each slide and covered with a square of parafilm. Incubation was carried out in a moist chamber at room temperature for 2 hours. Slides were washed by immersion in KCM for 10 minutes in a 100ml glass trough. 40µl of secondary antibody, diluted in KCM with 10% of the appropriate serum (Table 2.3), was applied and again, covered with a square of parafilm. 30 minute incubation was carried out in a moist chamber before immersing the slides in KCM for 10 minutes. Slides were fixed in <4% paraformaldehyde, diluted in KCM for 15 minutes, before washing in dH_2O. Slides were then allowed to air dry and were either

mounted with 1μg/ml DAPI in Vectashield (Vector) and coverslips sealed with rubber solution, or stored in the dark at room temperature for FISH.

Table 2.3 Dilutions of primary and secondary antibodies used for immunoflourescence
N - not known

Antibody	Produced in	Source	Stock concentration (mg/ml)	Dilution
Anti-histone, pan	Mouse	Boehringer	0.2	1:100
Anti-acetylated H4 (R41)	Rabbit	Prof. B. Turner, Birmingham	N	1:100
Anti-mouse-FITC $F(ab')_2$	Sheep	Sigma	1.0	1:100
Anti-mouse-TR	Sheep	Vector	1.5	1:100
Anti-rabbit-FITC	Goat	Vector	1.5	1:100
Anti-rabbit-TR	Goat	Vector	1.5	1:100

2.11 Immunocytochemistry

This protocol was modified from Larsson *et al.*, 1995. 400μl of JU77 human mesothelioma cells (Section 2.1.3) at a concentration of $5x10^3$ cells/ml were seeded into each $1cm^2$ well of a chamber slide (Nunc). Slides were incubated at 37°C for 1 week or until chambers were ~75% confluent. Cells were rinsed in PBS at 4°C, fixed in methanol:acetone, 1:1 at -20°C for 10 minutes then rehydrated and stored immersed in PBS/0.02% sodium azide at 4°C for up to 1 week.

For staining, cells were pre-incubated for 45 minutes in blocking buffer (2% BSA, 0.1% sodium azide, 0.2% Tween20, 6.7% glycerol) at room temperature. Cells were incubated with primary antibody (100μl/chamber) for 1 hour at room temperature and washed with PBS/0.2% Tween20. Secondary antibodies conjugated with FITC or TR were used against mouse, rabbit or human IgG, $F(ab')_2$ (Table 2.4). After 30 minutes incubation with secondary antibody (100μl/chamber), slides were washed with PBS/0.2% Tween20. Primary and secondary antibodies were diluted, as appropriate, in blocking buffer (Table 2.4).

Table 2.4 Dilutions of primary and secondary antibodies used for immunocytochemistry
N - not known

Antibody	Produced in	Source	Stock concentration (mg/ml)	Dilution
Anti-α tubulin	Mouse	Sigma	N	1:500
Anti-Sp1	Rabbit	Santa Cruz	0.1	1:50
Anti-PCNA	Human	Dr C.J. Hutchison, Dundee	N	1:10
Anti-histone, pan	Mouse	Boehringer	0.2	1:100
Anti-Sm	Mouse	Dr. I. Mattaj, Heidelberg	N	1:100
Anti-U1A	Rabbit	Dr. I. Mattaj, Heidelberg	N	1:100
Anti-human-TR $F(ab')_2$	Goat	Jackson Laboratories	1.5	1:250
Anti-rabbit-TR $F(ab')_2$	Goat	Jackson Laboratories	1.5	1:250
Anti-mouse-FITC $F(ab')_2$	Sheep	Sigma	1.0	1:250

Chambers were disassembled to allow mounting. All slides were mounted with 1μg/ml DAPI in Vectashield (Vector), or incubated in 100μg/ml RNAse in 2xSSC for 1 hour at 37°C, rinsed in 2xSSC and mounted with 0.2μg/ml PI in Vectashield. Coverslips were sealed with rubber solution (Pang). Slides were stored in the dark at 4°C.

2.12 Monoclonal antibodies

Methods for monoclonal antibody production used here were modified from Kennet *et al.* (1978) and Yelton *et al.* (1978) and developed by Ms. A. Seawright, MRC Human Genetics Unit, Edinburgh.

2.12.1 Immunisation

Five Balb-C mice were immunised. Pre-immune serum was collected from each mouse. For the initial injection the antigens were prepared in TiterMax adjuvant. Subsequent injections did not include an adjuvant. Booster immunisations were carried out one month

following this and finally, four days prior to removal of the mouse spleen for fusion. For all immunisations, 200µl of antigen was injected subcutaneously in the abdomen.

2.12.1.1 Preparation of the adjuvant

TiterMax (Vaxcel) is a synthetic copolymer adjuvant in a microparticulate-stabilised water-in-oil emulsion. The stock tube was allowed to warm to room temperature and vortexed for 30 seconds to produce a homogenous suspension. 500µl of TiterMax was added to 500µl of aqueous antigen and vortexed for 1 minute. The emulsion looked like "whipped cream" and held together when a drop was submerged on a pipette tip into a beaker of water indicating that it was stable. 200µl of emulsion was injected into each mouse.

2.12.1.2 Preparation of the aqueous antigen

Metaphase chromosomes prepared from the REN2 human cell line (Section 2.1.3) were retrieved from storage at -70°C. Tubes were spun at 3500g for 5 minutes and the supernatant carefully removed using a thin tipped pastette. The pellets were pooled and made up to a final concentration of $1x10^9$ chromosomes/ml in polyamine buffer (excluding digitonin).

Nuclei for injection were obtained from the nuclear fraction attained during the preparation of metaphase chromosomes (Section 2.8.1). Tubes were retrieved from storage at -70°C, spun at 3500g for 5 minutes and the supernatant removed. The pellets were pooled and made up to a concentration of $1x10^9$ nuclei/ml in polyamine buffer (excluding digitonin).

FACS sorted chromosomes (Section 2.8.2) were retrieved from storage at -70°C, spun at 3500g for 5 minutes and the supernatant removed. The pellets were pooled and made up to $1x10^5$ chromosomes/ml in polyamine buffer (excluding digitonin).

2.12.2 Fusion

The spleen of one mouse was removed and placed in a 60mm petri dish in complete medium (RPMI, 10% myoclone FCS, 0.2 units/ml human insulin, 0.2mM pyruvate, 0.5mM oxaloacetate, 2mM $_L$-glutamine, 12.5mM MOPS buffer). The cells were removed from the spleen using two syringes with 26 gauge needles. Several holes were poked in the spleen

then medium was forced gently through the spleen with one syringe while the tissue was held in place by the other. Care was taken not to pull displaced cells back into the syringe. The cells were pelleted in a conical tube at 180g and the supernatant was removed. The pellet was tapped loose then suspended in 5ml of ice cold 0.17M NH_4Cl for 10 minutes. Ice cold RPMI was added and the cells were pelleted as before then resuspended in 10ml of ice cold RPMI.

Cells were counted and tested for viability (Section 2.1.1). 50% of spleen cells were suspended in freezing medium (Section 2.1.2) and stored in liquid nitrogen for fusion at a later date. The remaining spleen cells were mixed at a ratio of 1:5 with previously grown myeloma cells, Sp2/0 (Section 2.12.2.1) then spun at 250g for 5 minutes. The supernatant was removed, the pellet tapped loose then 0.5ml of freshly made 35% polyethylene glycol (Koch Light) was added and the tube gently swirled to resuspend the cells. The tube was spun at 90g for 5 minutes. After a further 3 minutes, 5ml of RPMI was added slowly over a period of 2 minutes. The tube was gently swirled over a period of 5 minutes to resuspend the cells then spun at 250g for 5 minutes. The supernatant was removed and 5ml of complete medium supplemented with 13.6mg/l hypoxanthine, 0.4mg/l aminopterin and 5mg/l thymidine (HAT) was added without disturbing the pellet. The pellet was left undisturbed for 7 minutes then the tube was gently swirled to resuspend the cells. HAT supplemented complete medium was added to make a total volume of 60ml and the cells were plated into 4x96 0.2ml well plates previously coated with macrophage feeder cells (Section 2.12.2.2). Cells retrieved from liquid nitrogen for fusion were plated into 2x96 0.2ml well plates. 4 drops from a 1ml graduated pastette were distributed into each well. On the following day, 2 drops of HAT supplemented complete medium were added.
On each occasion, cells from the spleen from one mouse and stored cells from a second mouse were fused and plated. 6x96 0.2ml plates were the maximum number being maintained. Plates would be incubated at 37°C in one of two separate incubators using one of two separately made bottles of complete medium.

2.12.2.1 Myeloma cells for fusion

2 weeks prior to fusion an ampoule of myeloma cells, Sp2/0 was retrieved from liquid nitrogen (Section 2.1.2) and cultured (Section 2.1.3) to attain $<1x10^8$ cells. To harvest the flasks, medium (RPMI, 10% myoclone FCS) was poured off and the cells washed twice in PBS. Cells were covered in a thin layer of 10% trypsin in versene and placed at 37°C for 5

minutes. Gentle agitation dislodged the cells, medium was added and the cells were pelleted at 400g for 5 minutes. Cells were resuspended in 20ml of serum-free RPMI and counted (Section 2.1.1).

2.12.2.2 Macrophage feeder cells

Mouse peritoneal macrophages were activated by intra-peritoneal injection of thioglycollate medium. After 4 days cells were collected by injection of 5ml of ice cold PBS into the peritoneal cavity. The body of the mouse was pummelled a few times before withdrawing the PBS and placing in a tube on ice. Any cells were pelleted at 750g for 10 minutes. After removal of the supernatant, the pellet was tapped loose and suspended in 5ml of ice cold 0.17M NH_4Cl for 10 minutes. The cells were pelleted as before, washed several times and resuspended in PBS. A sample was diluted 1:4 in methyl violet acetic acid for counting (Section 2.1.1). Cells were stored in liquid nitrogen in ampoules of $6x10^6$/ml in freezing medium (Section 2.1.2).

One ampoule of macrophages was retrieved from liquid nitrogen to coat 6x96 0.2ml well plates. On removal to thaw, tubes were immediately incubated at 37°C in a beaker of water. Cells were diluted in medium (RPMI, 10% FCS), centrifuged at 400g for 5 minutes then suspended into 80mls of medium. 2 drops from a 1ml graduated pastette were distributed into each well and the plates incubated at 37°C.

2.12.3 From fusion mixture to stable secreting hybrid

Every 2-3 days, supernatant was removed from each well with a pastette and replaced with fresh medium. A fresh pastette was used for each column of wells, producing minimal cross-contamination. After 7 days hybrid colonies were usually visible. Once a colony occupied between 50-75% of the well, supernatant was removed for testing using immunocytochemistry (Section 2.11).

Colonies which were positive antibody producers were subbed up into 2ml wells by scraping the surface of the 0.2ml well with a pastette and transferring the majority of dislodged cells. 1ml of fresh medium was added to each 2ml well. 4 drops of fresh medium were added to the 0.2ml well to maintain until the 2ml well colony had taken. Colonies

were continually tested and subbed into several 2ml wells on different plates, fed from different bottles of medium and placed in separate incubators.

Colonies of interest were eventually subbed into $25cm^2$ flasks (2 separate flasks for each hybridoma). Once confluent, a flask was split. 75% of the cells were suspended in freezing medium for storage in liquid nitrogen. The remaining cells were used to maintain the flask until 6 ampoules were stored and a successful subcloning had been carried out (Section 2.12.4).

2.12.4 Dilution subcloning

Cells were counted (Section 2.1.1) and a series of dilutions prepared until concentrations of 100 cells/ml and 50 cells/ml were reached in total volumes of 10ml. Half of a 96x0.2ml well plate was seeded with each cell concentration: 2 drops from a 1ml graduated pastette distributed into each well, plus 2 drops of fresh medium. Concentrations of 10 cells/well and 5 cells/well were, thus, achieved.

Colonies were fed and screened as before (Section 2.11). Any wells with more than one initial colony was disregarded. The best antibody producing colonies were selected for subbing (Section 2.12.3) and were maintained until 6 ampoules were stored in liquid nitrogen. Each hybridoma was subcloned twice.

Supernatants from interesting hybridomas were collected throughout, any cells were pelleted by centrifugation at 400g for 10 minutes and discarded. Supernatants were stored in aliquots at 4°C and -20°C.

2.13 Protein analysis

2.13.1 Preparation of nuclear and cytoplasmic proteins

This procedure was adapted from Lee *et al.* (1987). REN2 cells (Section 2.1.3) were harvested gently at 100g for 5 minutes and washed twice in PBS. Cells were counted (Section 2.1.1), washed in ice cold RSB hypotonic (10mM HEPES pH6.2, 10mM NaCl, 1.5mM $MgCl_2$, 100µg/ml PMSF, 1µg/ml aprotinin, 1µg/ml leupeptin, 1µg/ml pepstatin) then suspended in RSB hypotonic solution at $5x10^7$cells/ml and kept on ice. The cell suspension

was homogenised using a tight fitting Dounce homogeniser for up to 100 strokes. Cell fractionation was monitored by phase contrast microscopy. The homogenate was centrifuged in eppendorf tubes, at 400g for 10 minutes at 4°C. The supernatant was separated into further tubes and centrifuged as before. This supernatant was distributed into ampoules, glycerol added to 10% and stored at -70°C as the cytoplasmic fraction.

The pellets were resuspended in RSB hypotonic solution and centrifuged as before. These pellets were then pooled and resuspended in ice cold lysis buffer (50mM Tris-HCl pH8.0, 1.2M NaCl, 1% Triton X-100, 0.02% sodium azide, 100µg/ml PMSF, 1µg/ml aprotinin, 1µg/ml leupeptin, 1µg/ml pepstatin) at ~$1x10^8$nuclei/ml. The tubes were vortexed for 5 seconds then kept on ice for 15 minutes before being sonicated at 10 amplitude microns for 30 seconds. This fraction was distributed into ampoules, glycerol added to 10% and stored at -70°C as the nuclear fraction.

2.13.2 Sodium dodecyl sulphate - polyacrylamide gel electrophoresis of proteins (SDS-PAGE)

Polyacrylamide gels, 10.0x10.5cm and 0.75mm thick were poured using an SE245 Mighty Small Dual Gel Caster (Hoefer). 40% 29:1 acrylamide:bis (Bio-Rad) was diluted to the appropriate concentration (8-15%) with 375mM Tris-HCl pH8.8 and 0.1% sodium dodecyl sulphate (SDS) for the resolving gel. Polymerisation was initiated by adding ammonium persulphate (AMPS) to 0.1% and N,N,N',N'-tetramethylethylenediamine (TEMED) to 0.1%. Gels were poured immediately between a glass and an alumina plate, to a level 0.5cm below the teeth of an inserted comb, overlaid with 0.1% SDS and allowed to set for at least 30 minutes. The overlaid SDS was tipped off and a layer of stacking gel poured to the top of the comb. For the stacking gel, 40% 29:1 acrylamide:bis was diluted to 5% with 125mM Tris-HCl pH 6.8 and 0.1% SDS. Polymerisation was initiated by adding 0.1% AMPS and 0.1% TEMED. Stacking gels were allowed to set for at least 30 minutes. Combs were carefully removed and wells washed with dH_2O. Gel sandwiches were placed into an SE 260 Mighty Small Vertical Slab Unit (Hoefer) and Tris-HCl-glycine running buffer (25mM Tris-HCl, 250mM glycine, 0.1% SDS) was added.

Samples were diluted in loading buffer (50mM Tris-HCl pH6.8, 2% SDS, 0.1% bromophenol blue, 10% glycerol). 100mM dithiothreitol was added immediately prior to loading. Samples were run against Rainbow coloured protein molecular weight markers

(Amersham) (Table 2.5). Samples were heated in a hot block to 90°C for 4 minutes before loading. Gels were run at a constant 200V until the proteins had been separated by the required amount (monitored by positions of the Rainbow coloured protein markers).

Gels were either stained with Coomassie Blue (Section 2.13.3) or used to establish a Western blot (Section 2.13.4).

Table 2.5 Rainbow coloured protein molecular weight markers
(Amersham)

Protein	Molecular weight (KDa)	Colour	Low range	High range
Insulin chain A	2.35	blue	*	
Insulin chain B	3.4	blue	*	
Aprotinin	6.5	blue/black	*	
Lysozyme	14.3	magenta	*	*
Trypsin inhibitor	21.5	green	*	*
Carbonic anhydrase	30.0	orange	*	*
Ovalbumin	46.0	yellow	*	*
Bovine serum albumin	66.0	red		*
Phosphorylase β	97.4	brown		*
Myosin	220.0	blue		*

2.13.3 Coomassie staining

Gels were immersed in 5 volumes of Coomassie Blue staining solution (0.25% Coomassie Blue dye, 45% methanol, 10% glacial acetic acid) for a minimum of 2 hours with gentle agitation. The staining solution could be re-used. 45% methanol with 10% glacial acetic acid was used to soak the gel overnight to destain. Gels were rinsed several times more in destaining solution before photographing then drying.

For drying, gels were laid on Whatman 3MM paper and covered over with Saran wrap. This sandwich was placed in a gel dryer and the gel was allowed to dry under suction for 1 hour at 80°C.

2.13.4 Semi-dry blotting of proteins (Western blotting)

A MilliBlot graphite electrode system was used for semi-dry transfer (Millipore). The following three buffer system was used for most blots. An alternative system used for the transfer of strongly negatively charged proteins is described in Section 2.13.5.

Gels were marked for orientation by cutting away the top right corner, then immersed in cathode buffer (0.025M Tris-HCl, 0.04M glycine, 20% methanol, pH 9.4) and gently agitated for 30 minutes. Seven sheets of Whatman 3MM filter paper and one sheet of Immobilon-P PVDF transfer membrane (Millipore) were cut to the size of each gel. The transfer membrane was soaked sequentially in 70%, 90% and 100% methanol for 15 seconds, then in dH_2O for 15 seconds before equilibrating in anode buffer 2 (0.025M Tris-HCl, 20% methanol, pH10.4) for 5 minutes. 2 sheets of filter paper were soaked in anode buffer 1 (0.3M Tris-HCl, 20% methanol, pH10.4) then placed on the anode electrode plate. 1 sheet of filter paper was soaked in anode buffer 1 and placed on top of the other 2 sheets. The transfer membrane was placed on top of this (the top right corner was cut away to allow orientation), followed by the gel and the 4 remaining sheets of filter paper, pre-soaked in cathode buffer. Care was taken to avoid air bubbles between the layers and any trapped air was eased out by rolling a glass rod gently over the stack. The cathode electrode plate was assembled over the stack. A constant current was passed through the system calculated from the size of the gel being blotted: $2mA/cm^2$ for 90 minutes.

Transfer membranes were allowed to dry and were stored at room temperature for up to 1 week prior to protein detection. Lanes were marked on the membrane with indelible ink to allow future identification. Post-transfer gels were stained with Coomassie Blue (Section 2.13.3) to ensure that adequate transfer had occurred.

2.13.5 Semi-dry blotting of negatively charged proteins

For highly negatively charged proteins, for example, histones, it was necessary to use an alternative transfer system for semi-dry blotting. Gels, filter paper and transfer membrane (2 pieces for each gel) were prepared as in Section 2.13.4, except only one transfer buffer (10mM CAPS buffer, 10% methanol) was required, replacing cathode buffer and anode buffers, 1 and 2. Three pieces of filter paper were stacked on the anode electrode plate, followed by the first transfer membrane, the gel, the second transfer membrane and the 4

remaining sheets of filter paper. The cathode electrode plate was assembled over the stack and the blotting carried out as in Section 2.13.4. The highly negatively charged proteins transferred, generally to the upper transfer membrane, while in the previous three transfer buffer system, such proteins remained in the gel. This was probably because the basic charge of these proteins was neutralised by SDS and remained uncharged in the three transfer buffer system. As before, however, the majority of proteins transferred to the lower transfer membrane.

2.13.6 General protein staining

For general permanent staining of proteins on the transfer membrane amido black stain (0.1% amido black, 45% methanol, 10% acetic acid) was used. Dry membranes were not pre-soaked. Membranes were immersed in amido black stain for 1 hour with gentle agitation, washed in dH_2O then destained (45% methanol, 10% acetic acid) overnight. Amido black stain could be re-used.

For general transient staining of proteins Ponceau S solution (0.1% Ponceau S, 5% acetic acid, Sigma) was used. Dry membranes were pre-soaked in dH_2O. Membranes were immersed in Ponceau S solution for 10 minutes then rinsed in dH_2O. Presence of the appropriate protein bands were assessed before continuing with immunostaining of the membrane for specific proteins (Section 2.13.7). Ponceau S staining did not interfere with subsequent protein detection and was washed out of the membrane during immunostaining. Ponceau S solution could be re-used.

2.13.7 Immunostaining of specific proteins

For detecting specific proteins the Boehringer chemiluminescence system was used. Dry membranes were pre-soaked in methanol for 5 minutes, rinsed in dH_2O then washed briefly in Tris-HCl buffered saline (TBS) (50mM Tris-HCl, 150mM NaCl, pH7.5). Membranes were incubated in 1% blocking reagent in TBS, 125µl/cm^2 of membrane, for 1 hour at room temperature. Primary antibodies were diluted to the appropriate concentration in 0.5% blocking reagent in TBS (Table 2.6). Membranes were incubated in a sealed bag, with primary antibody at 125µl/cm^2 of membrane, for 12-60 hours at 4°C, with gentle agitation. A further 1 hour incubation at room temperature was occasionally carried out. Membranes were washed twice in an excess of TBS, or more stringently in TBST (1xTBS, 0.1%

Tween20), for 10 minutes at room temperature, with vigorous agitation. Horseradish peroxidase-labelled secondary reagent was diluted to 20U/ml in 0.5% blocking reagent in TBS. Membranes were incubated in a sealed bag, with secondary reagent at 125µl/cm^2 of membrane, for 1 hour at room temperature. Prior to detection, blots were washed in an excess of TBS or TBST for 4x15 minutes at room temperature, with vigorous agitation.

Excess buffer was drained from the washed blots and placed, sample side up, in a tray. Detection reagent was added to cover the blots for 1 minute. The detection reaction is based on the oxidation of a diacylohydrazide, luminol, in the presence of hydrogen peroxide and horseradish peroxidase. An intermediate reaction product is formed, which decays to the ground state by emitting light. Blots were then transferred to a piece of Saran Wrap and wrapped, ensuring that no air bubbles were trapped. The blot was exposed, sample side up, to Kodak X-Omat film for 10 seconds-1 hour.

Table 2.6 Dilutions of primary antibodies for detection of proteins on a Western blot
N - not known

Antibody	Source	Concentration (mg/ml)	Dilution
Anti-Sp1	Santa Cruz	0.1	1:100
Anti-α tubulin	Sigma	N	1:500
Anti-acetylated H4 (r41)	Prof. B. Turner, Birmingham	N	1:250
Anti-acetylated H4 (r41) pre-immune serum	Prof. B. Turner, Birmingham	N	1:250

2.14 Image capture and analysis

2.14.1 The Zeiss microscope with a charged couple device (CCD) camera

Slides were screened with a Zeiss Axioplan fluorescence microscope equipped with a triple band-pass filter set (Chroma) which allowed sequential visualisation of FITC (green), TR (red) and DAPI (blue) images using a computer-driven excitation filter wheel. As the polychroic filter and emission filter remained in place while acquiring the three images, image registration was perfect. Metaphase spreads were imaged using a cooled charged couple device (CCD) camera fitted with a KAF 1400 chip (Photometrics). Separate grey scale images of probe signal and counterstain were pseudocoloured and merged using an Apple Mackintosh Quadra 900 computer with SmartCapture software, developed by Digital Scientific. Background hybridisation was remove by normalisation and removal of the lowest-intensity pixels. Care was taken that this did not interfere with chromosome hybridisation signals. Images were stored on portable hard discs (SyQuest) and were printed using a Kodak ColourEase dye sublimation printer.

2.14.2 The confocal microscope

Slides were screened with a BioRad MRC600 confocal laser scanning microscope equipped with a dual filter set which allowed visualisation of both FITC (green) and PI (red) images, simultaneously. Nuclei were scanned and imaged using BioRad Som software. Images from 7 high resolution scans were averaged using a Kalman electronic filter and displayed side by side. These images could be pseudocoloured and merged. Images were stored and printed as above.

3. Tools from the human genome for exploring links between chromosome structure and function

3.1 Introduction

In order to study links between vertebrate chromosome structure and function, I chose to focus in particular upon the comparably sized, but behaviourally contrasting, human chromosomes 18 and 19. In addition, I used human chromosomes 1, 11 and 22 for a number of studies.

Chromosome 1 is the largest human chromosome and possesses adjacent cytological bands that represent the two most extreme and contrasting band types. The tip of the p-arm of this chromosome consists of several T-bands, which are highly GC-rich and very early replicating (Figure 3.1) (Sections 1.2 & 1.3). This region shows a high density of CpG-islands (Craig & Bickmore, 1994) and a high level of histone acetylation (Jeppesen *et al.*, 1992) (Section 1.6.1). Directly adjacent to this, and between it and the centromere, is a region that is dominated by GC-poor, late replicating and particularly dark staining G-bands (Francke, 1994). The R-bands present are R'-bands, which have less extreme features than T-bands (Figure 3.1) (Sections 1.2 & 1.3). Reflecting this, the region shows a low density of CpG islands and low levels of histone acetylation. These juxtaposing regions can be taken to represent the banding type which predominates in each: the tip of the chromosome having the general features of R-bands and the adjacent region reflecting G-band behaviours. Chromosome 1 possesses an unusually large region of pericentric heterochromatin at its q-arm (Figure 3.1).

Chromosome 11 is a metacentric chromosome, of middling size, containing a relatively even distribution of both of G- and R-bands (Figure 3.1). It has been allocated a generally high gene number (Table 1.3).

Human chromosomes 18 and 19 are comparable in DNA content, but contrasting in their structural and functional features (Section 1.7). Each one can be taken as a whole chromosome representation of the two extremes of band type. Chromosome 18 is GC-poor, has a low density of CpG islands, has one of the lowest number of gene assignments of any human autosome and replicates predominantly late in S phase. Very little hyperacetylated

histone H4 is detected on this chromosome. These are all of the features common to G-bands, and indeed, chromosome 18 consists mainly of G-bands, many of which are dark staining, and R'-bands (Figure 3.1) (Sections 1.2, 1.3 & 1.7). Chromosome 19, however, is GC-rich, has a very high density of CpG islands, has a disproportionately high number of gene assignments for its size and replicates generally early in S phase. A high level of hyperacetylated histone H4 has been detected along its length. The majority of R-bands are T-bands, and there are few, small G-bands on chromosome 19 (Figure 3.1) (Sections 1.2, 1.3 & 1.7). These chromosomes are, thus, ideal tools to study the links between mammalian chromosome structure and function.

Finally, chromosome 22, one of the smallest of the human chromosomes is an acrocentric chromosome (Figure 3.1). The centromere and p-arm of each acrocentric chromosome consists of many highly repeated sequences, including satellite sequences (Miklos & John, 1979) and clusters of genes that encode 18S, 5.8S and 28S ribosomal RNA (rRNA) (Henderson *et al.*, 1972; Schmickel *et al.*, 1985) (Section 7.3). The rRNA encoding genes are transcribed by RNA polymerase I (with the exception of the 5S rRNA genes which are situated at various, non-acrocentric regions of the genome and are transcribed by RNA polymerase III). These regions are of the most intensely transcribed in the human genome and 30-40 copies of each rRNA encoding array are present at each site (Warton *et al.*, 1988; Review: Sollner-Webb & Tower, 1986). As a handle to this unique chromosomal environment, chromosome 22 was chosen to study. The q-arm of this chromosome is CpG-island-rich, early replicating (Figure 1.3) and gene-rich (Table 1.3).

In order to study these chromosomes in human cells, hybridisation probes for the entire length of each specific chromosome were required for use in FISH (Section 2.6) (Reviews: van Ommen *et al.*, 1995; Heng *et al.*, 1997). For FISH, the DNA probe is labelled, usually with biotin or digoxigenin (dig). Chromosomes or nuclei are prepared on glass slides then, both the slides and DNA probe are denatured, added together and allowed to hybridise over night. After washing off non-specifically bound probe, hybridisation is detected using fluorescently-labelled avidin (a molecule with a high affinity for biotin) or anti-dig antibody. Whole chromosome probes are a complex mixture of DNA sequences complimentary to specific regions along the length of a single chromosome, which when used together in a single hybridisation reaction, "paint" the chromosome of interest. In addition, these paints will contain repeat sequences that are genome-wide and it is often necessary to suppress

hybridisation from these sequences. This is usually achieved by adding an excess of human C_0t 1 DNA to the probe mixture prior to denaturation. Human C_0t 1 DNA is prepared from the fraction of sheared and heat denatured total human DNA that has been re-annealed before $C_0t = 1$, where C_0= concentration (moles/litre) of single stranded DNA at time 0, and t= time after cooling commences (seconds). This fraction contains fragments that are high in copy number (>10^4 copies) and re-annealed early in the reaction (Review: Lewin, 1994). In the human genome, these sequences include α-satellite, LINEs and SINEs (Section 1.3.3).

There are several approaches that have been taken to make single chromosome painting probes:

- FISH probes have been prepared from DNA libraries cloned from FACS sorted chromosomes (Pinkel *et al.*, 1988; Lichter *et al.*, 1988; Fuscoe *et al.*, 1989). There is frequently a lack of hybridisation to portions of the target chromosome by such probes, possibly due to the absence of sequences in the cloned library that are inherently difficult to clone. Alternatively, the digestion of FACS sorted chromosomal DNA with a restriction enzyme and attachment of a catch-linker, allows linker PCR to produce labelled DNA for FISH. This will be further described in Section 3.3.2. A remaining problem is that FACS does not always produce entirely pure fractions of specific chromosomes, thus, careful monitoring of sorting is required.
- Labelling DNA from rodent-human monochromosome hybrid cell lines (Kievits *et al.*, 1990). A further development of this method, involves using human-specific *Alu* or L1 PCR to amplify the human DNA present in the hybrid (Nelson *et* al., 1989; Lichter *et al.*, 1990). In this instance, a non-uniform distribution of signal may be observed along the chromosomes, since each repeat element shows a bias of distribution towards a particular set of bands, *Alu* elements to R-bands and L1 elements to G-bands (Section 1.4.3).
- Degenerate oligo PCR (DOP-PCR) of FACS sorted chromosomes (Telenius *et al.*, 1992). To create apparently cleaner and region-specific probes, chromosomes prepared by microdissection have been used as the starting material for DOP-PCR (Guan *et al.*, 1994). However, microdissection is time consuming and requires specialised equipment. DOP-PCR has a high potential for amplification of contaminant DNA.

Commercial paints are available for most human chromosomes and this source was adequate for human chromosome 1 and 11 paints. A large amount of chromosome 18 and 19 specific paint was required and it was considered to be more efficient and economical to make paints

for these chromosomes than purchase them commercially. The strategy I decided to use in the first instance was a human specific *Alu*-PCR protocol to amplify human DNA from rodent-human hybrid cell lines containing either chromosome 18 or 19 as the only human material. Such hybrid cell lines are readily available and the PCR protocol is well established. The chromosome 22 paint used, was provided by Dr. S. Cross, University of Edinburgh. This paint was prepared from FACS sorted chromosomes which were digested and a catch-linker attached.

Rodent-human monochromosome hybrid cell lines were also collected for human chromosomes 1 and 22. These, along with the hybrid cell lines containing only human chromosome 18 or 19, were used as starting material for several experiments throughout this thesis. Characterisation of each of these hybrids is described in the following section.

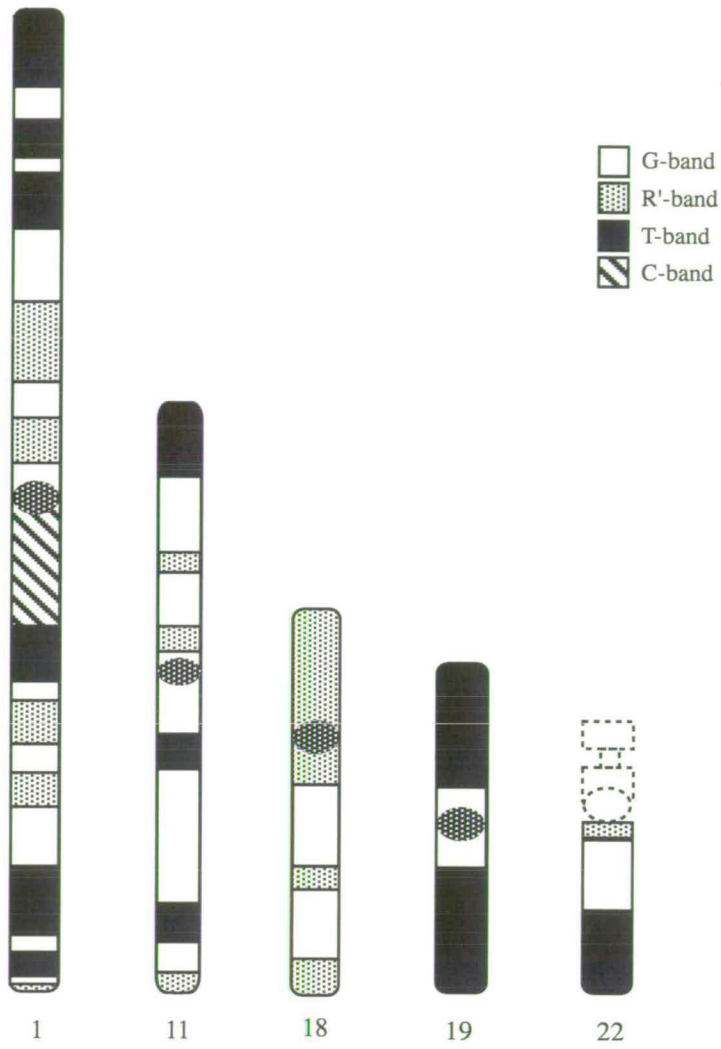

Figure 3.1 R-banding ideograms of human chromosomes 1, 11, 18, 19 and 22
Adapted from Holmquist(1992). Ideograms are of the 300 bands/genome resolution. Chromosome 18 consists of G-bands and R'-bands and in its entirety shows the features generally associated with G-bands. By contrast, the majority of R-bands are T-bands and there are few G-bands on chromosome 19. This chromosome shows the features generally associated with R-bands. These two extremes of environment are also represented by adjacent regions at the tip of the p-arm of chromosome 1. Chromosome 22 was the chromosome chosen to exemplify the human acrocentric chromosomes.

3.2 Rodent-human somatic hybrid cell lines

Rodent-human somatic hybrid cell lines were developed in the 1960s, following observations that cells in culture could be induced to fuse by chemical treatment, or addition of inactivated Sendai virus (Review: Witowski, 1986). When rodent-human cell fusions are made and subsequently cultured, there is a progressive loss of human genetic material, until often only a single or partial human chromosome are retained. Such hybrid cells have been selected and propagated, and a large number of repositories stocking a variety of lines exist.

Rodent-human monochromosome hybrid cell lines containing chromosomes 1, 18, 19 and 22 were obtained. These lines proved useful as starting material for several experiments. Hybrid cell lines are intrinsically unstable and it was, thus, important to characterise each before utilisation.

3.2.1 Selection and source of the hybrid cell lines

Chinese hamster-human monochromosome hybrid cell lines were obtained from the National Institute of General Medical Sciences, Human Genetic Mutant Cell Repository, New Jersey. GM11010 was stated to contain chromosome 18 as the only human component and GM10449A was stated to contain only human chromosome 19.

The A91neo hybrid cell line consists of mouse A9 cells carrying a single human chromosome 1 tagged with a dominant selectable marker (pSV2-neo) for resistance to G418 Sulphate (Koi *et al.*, 1989). Thus, it was possible to select for maintenance of the human chromosome, by growing cells in culture medium containing G418 Sulphate. This line was supplied by the National Institute of Environmental Health Sciences, North Carolina.

The mouse-human monochromosome 22 hybrid cell line, PgMe-25, was produced by fusing Pg19 mouse cells derived from a malignant melanoma with human leukocytes using an inactivated Sendai virus (Guerts van Kessel *et al.*, 1981). This line was stocked at the MRC Human Genetics Unit.

3.2.2 Confirming the human complement of the hybrid cell lines

To assess the human complement of the hybrid cell lines used in this study, total DNA was extracted from each (Section 2.3), biotin labelled by nick translation (Section 2.4) and hybridised to human metaphase spreads by FISH (Section 2.9). 10μg of C_0t 1 DNA was added for 150ng of DNA probe to suppress hybridisation of repeat sequences.

Figure 3.2 shows the hybridisation of total DNA from the GM11010 cell line to a representative human metaphase spread. The hybridisation signal is confined to a single chromosome (Figure 3.2a), which was confirmed to be chromosome 18 after analysis of the enhanced DAPI stain (Figure 3.2b). However, the hybridisation signal along the length of the chromosome was consistently weaker on the q-arm than on the p-arm. This suggests that some GM11010 cells lack part of the q-arm of human chromosome 18.

Figure 3.3 shows the hybridisation of total DNA from the GM10449A cell line to a representative human metaphase spread. The hybridisation signal is confined to a single chromosome (Figure 3.3a), confirmed as chromosome 19 by analysis of the enhanced DAPI stain (Figure 3.3b). GM10449A contains an intact chromosome 19 and this is the only human component in this cell line.

Figure 3.4 shows the hybridisation of total DNA from the PgMe-25 cell line to a representative human metaphase spread. It was necessary to add a large amount of human C_0t 1, for cross-hybridisation suppression, since this probe had a wealth of repeat sequences due to the repeat-rich p-arm of chromosome 22 (Section 1.4.3). 50μg of C_0t 1 DNA was added for 150ng of probe, plus the length of time for pre-annealing of the probe to this DNA was extended to 37°C for 30 minutes. Even with this suppression, FISH signals were present on several other regions of the genome, as well as covering the entirety of chromosome 22. In particular, the short arms of the other acrocentric chromosomes and a region close to the centromere of the X chromosome had probe bound. Repeats present on chromosome 22 may have homologies with sequences at these other regions, not represented in human C_0t1 and thus not competed out. Such middle repeat sequences may include β-satellite and satellites I-IV, or rRNA-encoding sequences (Section 1.4.3 & 7.3). Alternatively, mouse repeats may have homologies with sequences at these human regions.

Finally, it is possible that these human regions are represented in the hybrid cell line in addition to a complete chromosome 22.

Figure 3.5 shows the hybridisation of total DNA from the A91neo cell line to a representative human metaphase spread. It is apparent that this hybrid cell line contains the entire length of chromosome 1 as its only human component.

It was important to next assess the state of the human chromosomes in each of these cell lines, especially GM11010, which was suggested to lack part of the q-arm of human chromosome 18 in a proportion of hybrid cells (Figure 3.2), and PgMe-25, which potentially contained material originating from several human chromosomes other than chromosome 22 (Figure 3.4).

3.2.3 Assessing the integrity of the human component of the hybrid cell lines

Section 3.2.2 confirmed that the rodent-human hybrid cell lines GM11010, GM10449A and A91neo contained human chromosomes 18, 19 and 1 respectively, as their sole human component. However, Figure 3.2 indicated that part of the q-arm of human chromosome 18 was missing in a proportion of cells. Also, in addition to lighting up human chromosome 22, PgMe-25 DNA hybridised to other regions of the genome, probably through cross-hybridisation of highly repetitive sequence but possibly through contamination of human material other than chromosome 22 in the hybrid cell line (Figure 3.4). In order to assess the state of the human chromosome within the hybrid cell lines, total human genomic DNA was biotin labelled by nick translation and hybridised, by FISH to metaphase spreads from each of the four hybrid cell lines. Probes were pre-annealed with human C_0t1 DNA. For each hybrid cell line, approximately 50 metaphase spreads were analysed for the presence of the expected human chromosome and any additional human material was recorded.

Figure 3.6 shows hybridisation of total human genomic DNA to a metaphase spread from the hybrid cell line GM11010. Almost one fifth of metaphase spreads from this hybrid cell line were lacking the expected human chromosome 18 (Table 3.1). Of those that did have a human chromosome 18, 35% of spreads revealed part of the q-arm of the chromosome to be

missing, hence the weak signal along this region of chromosome 18 after FISH with DNA prepared from this hybrid cell line (Figure 3.2). No additional human material was found.

Hybridisation of total human genomic DNA to metaphase spreads of GM10449A revealed the hybrid to apparently contain an intact chromosome 19 as its only human component (Figure 3.7). This cell line was very stable and no spreads were observed where human chromosome 19 was not present, nor where extra human material was present (Table 3.1).

Table 3.1 The integrity of the human genetic material in the rodent-human hybrid cell lines
Approximately 50 metaphase spreads were analysed after FISH with total human genomic DNA, to the rodent-human hybrid cell lines GM11010, GM10449A, PgMe-25 and A91neo. These hybrid cell lines were supposed to contain human chromosomes 18, 19, 22 or 1, respectively, as their only human component. The extra human material present in the PgMe-25 line was of chromosome 22 origin, with 100% of spreads revealing an extra band of material integrated into a rodent chromosome and 10% possessing, in addition, an autonomous but small fragment of chromosome 22 (Figure 3.8c).

Cell line	GM11010	GM10449A	PgMe-25	A91neo
Number of chromosomes per spread	17-23	20-44	30-58	54-65
% spreads with human chromosome absent	17.1	0.0	19.0	3.2
% spreads with human chromosome incomplete	28.6	0.0	81.0	19.4
% spreads with complete expected human chromosome	54.3	100.0	0.0	77.4
% spreads with extra human component	0.0	0.0	100.0	0.0

Figure 3.8a shows hybridisation of total human genomic DNA to a metaphase spread of the human chromosome 22 containing hybrid, PgMe-25. Every spread contained an autonomous acrocentric human chromosome, presumed to be chromosome 22, but smaller than might be anticipated. In addition, all metaphase spreads observed contained an extra band of human material incorporated into one of the rodent chromosomes (Table 3.1). FISH using a chromosome 22 paint (Section 3.3.3) established that both the autonomous acrocentric chromosome and the extra band were of chromosome 22 origin (Figure 3.8c). Less than 10% of spreads possessed extra autonomous human material which was very

small and lacked any telling morphology. This, too was confirmed to be of chromosome 22 origin (Figure 3.8c).

Figure 3.9 shows hybridisation of total human genomic DNA to a metaphase spread from A91neo. Few cells in this hybrid line were lacking human chromosome 1, however, almost 20% of human chromosomes 1 present were missing part of the p-arm (Figure 3.9c & d).

The analyses of each of these hybrid cell lines was made early in their passage. Long passage of the cells was avoided and preparation of DNA, or other experimentation, was carried out during the first few weeks after retrieving the cells from liquid nitrogen. Frozen ampoules were replaced the first time the cells were split after reaching close to confluency.

In conclusion, the rodent-human monochromosome 19 hybrid cell line was the only line that contained a stable and complete human chromosome. The deficiencies of the other hybrids did not prevent these lines from being used, with careful consideration of the exact inadequacies of each.

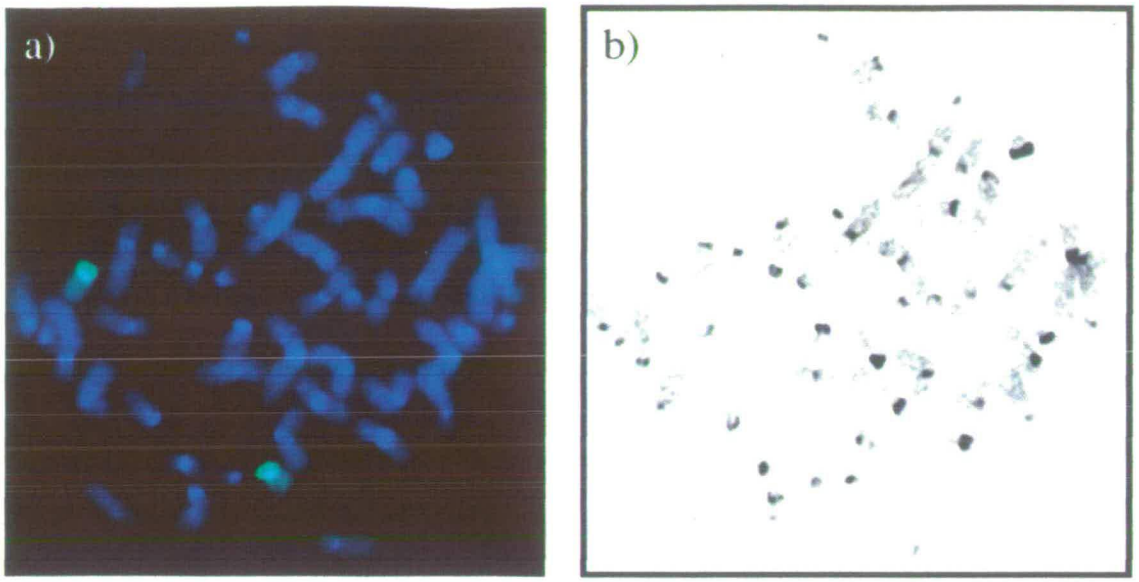

Figure 3.2 Identification of human material from the rodent-human hybrid cell line GM11010
Total DNA was extracted from GM11010, biotin labelled and hybridised to REN2 human metaphase spreads (49, XXXXY) by FISH. (**a**) The probe was detected using avidin-FITC (green). Chromosomes were counterstained with DAPI (blue). (**b**) Grey scale representation of the DAPI stained spread.

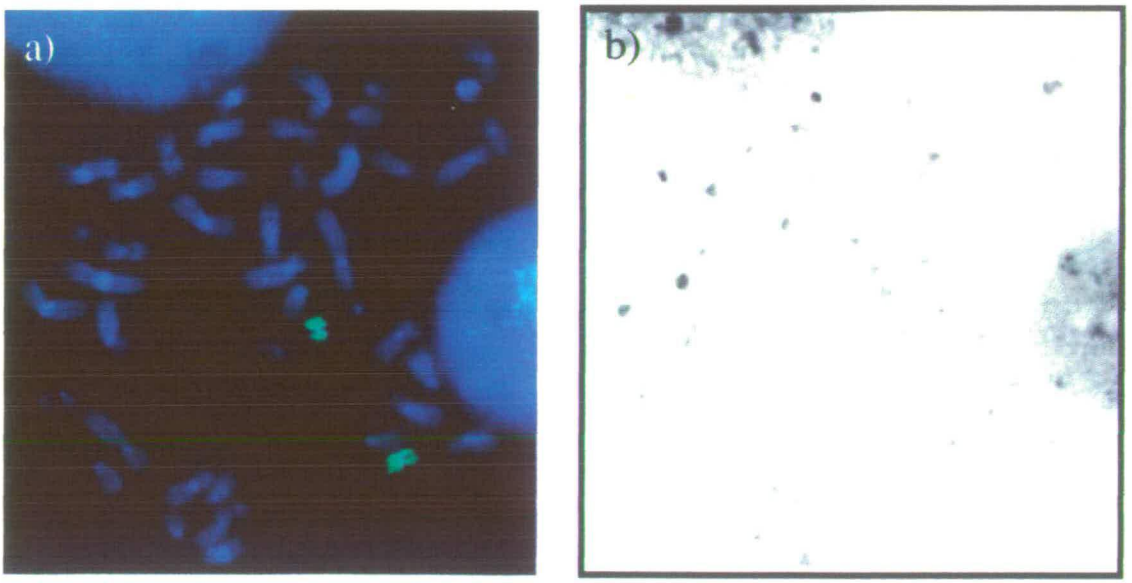

Figure 3.3 Identification of human material from the rodent-human hybrid cell line GM10449A
Total DNA was extracted from GM10449A, biotin labelled and hybridised to REN2 human metaphase spreads (49, XXXXY) by FISH. (**a**) The probe was detected using avidin-FITC (green). Chromosomes were counterstained with DAPI (blue). (**b**) Grey scale representation of the DAPI stained spread.

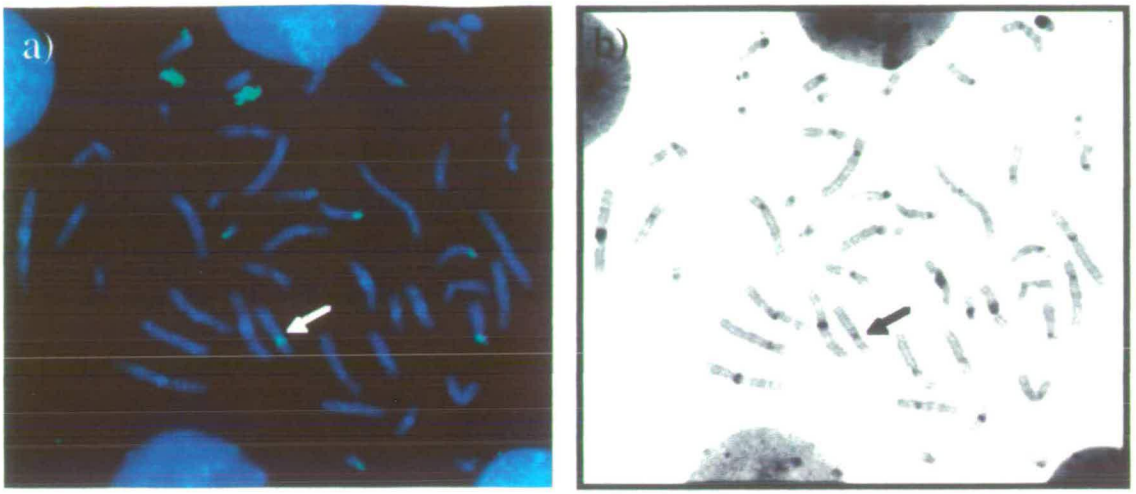

Figure 3.4 Identification of human material from the rodent-human hybrid cell line PgMe-25
Total DNA was extracted from PgMe-25, biotin labelled and hybridised to FATO human metaphase spreads (46, XY) by FISH. Arrow indicates the X chromosome. (**a**) The probe was detected using avidin-FITC (green). Chromosomes were counterstained with DAPI (blue). (**b**) Grey scale representation of the DAPI stained spread.

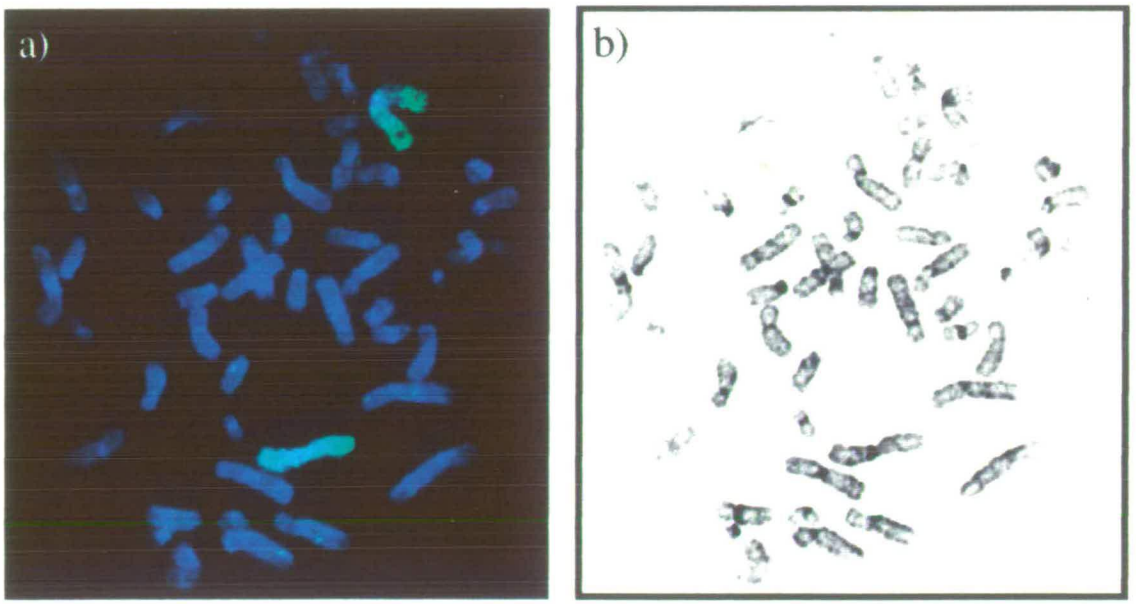

Figure 3.5 Identification of human material from the rodent-human hybrid cell line A91neo
Total DNA was extracted from A91neo, biotin labelled and hybridised to REN2 human metaphase spreads (49, XXXXY) by FISH. (**a**) The probe was detected using avidin-TR (red). Chromosomes were counterstained with DAPI (blue). (**b**) Grey scale representation of the DAPI stained spread.

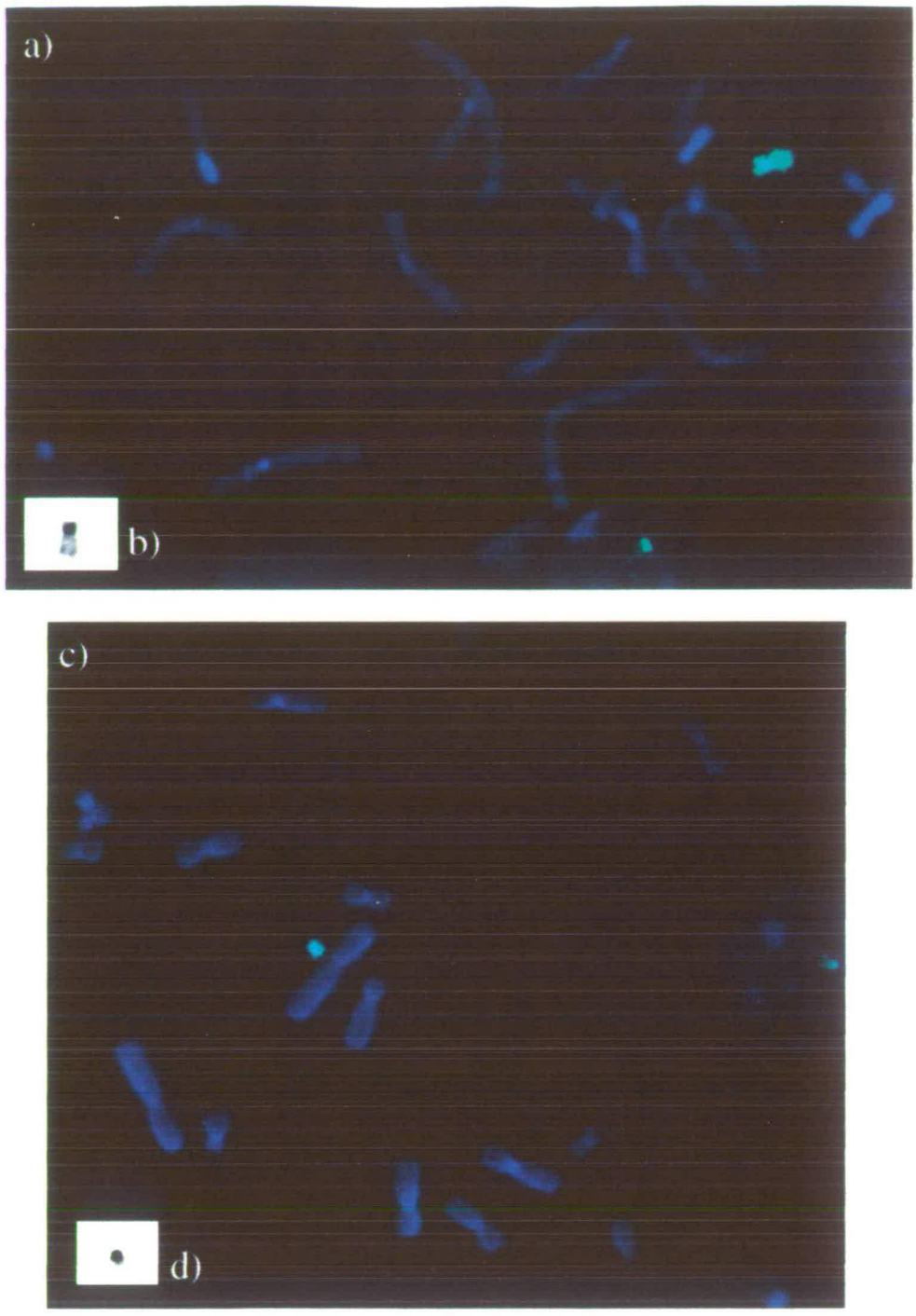

Figure 3.6 The integrity of the human material in the rodent-human hybrid cell line GM11010

Total genomic human DNA was labelled with biotin and hybridised to metaphase spreads from the hybrid cell line using FISH. (**a**) (**c**) The probe was detected using avidin-FITC (green). Chromosomes were counterstained with DAPI (blue). (**b**) (**d**) Grey scale representation of the DAPI stained human material. (**a**) (**b**) A spread with a complete chromosome 18 and no additional human material. (**c**) (**d**) A spread with an incomplete chromosome 18. A portion of the q-arm is apparently missing.

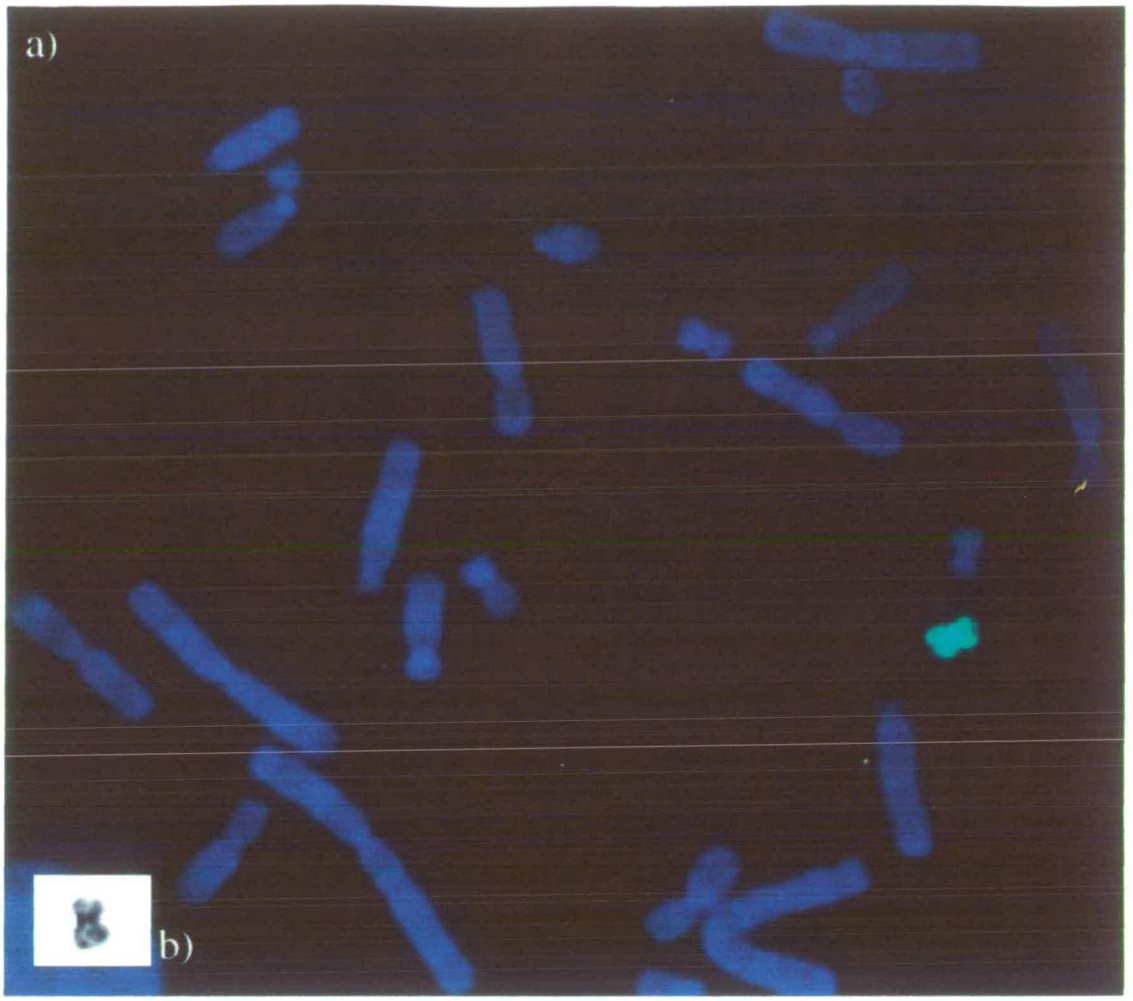

Figure 3.7 The integrity of the human material in the rodent-human hybrid cell line GM10449A

Total genomic human DNA was labelled with biotin and hybridised to metaphase spreads from the hybrid cell line using FISH. (**a**) The probe was detected using avidin-FITC (green). Chromosomes were counterstained with DAPI (blue). (**b**) Grey scale representation of the DAPI stained human material. Human chromosome 19 appears to be present in its entirety, as the only human material.

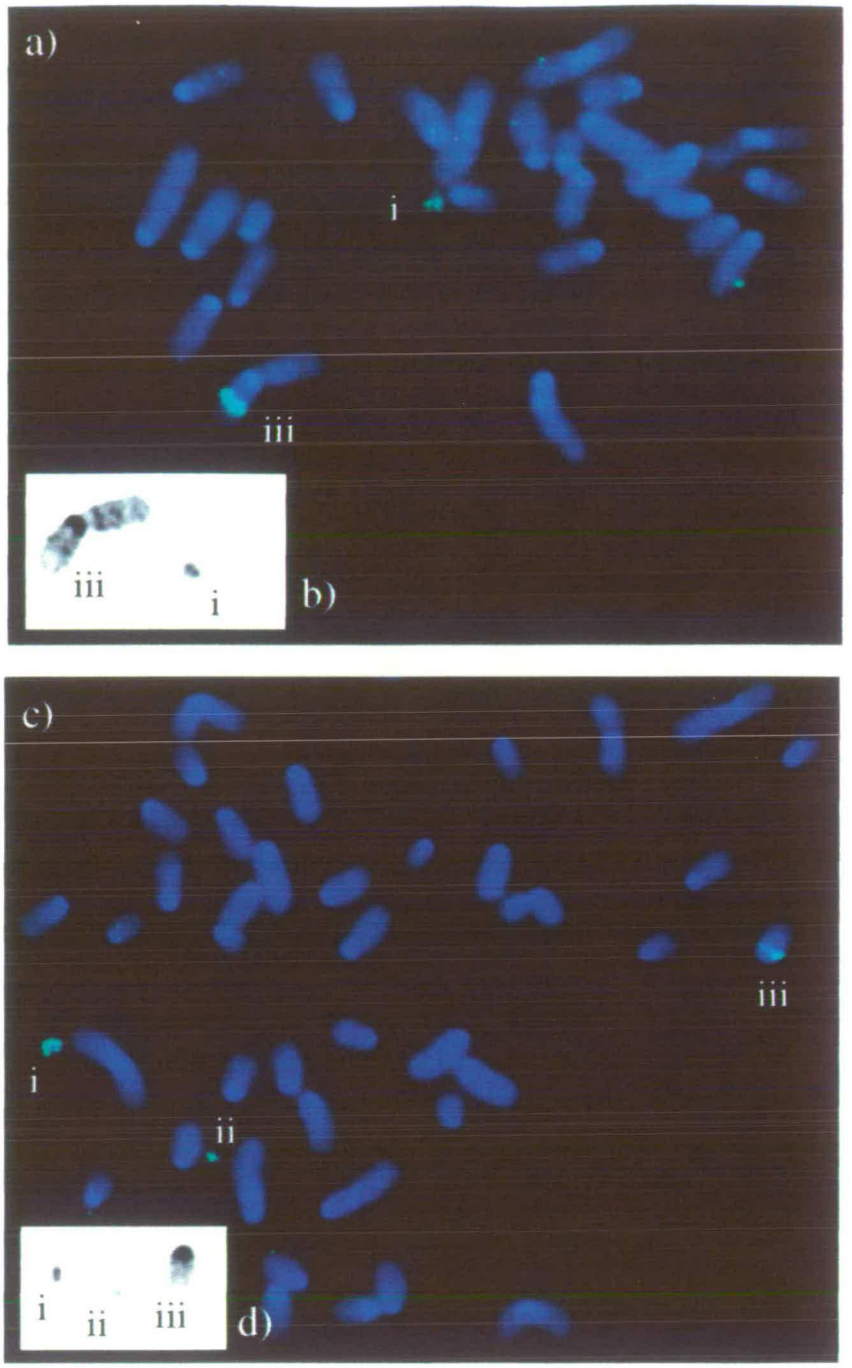

Figure 3.8 The integrity of the human material in the rodent-human hybrid cell line PgMe-25

(**a**) (**b**) Total genomic human DNA was labelled with biotin and hybridised to metaphase spreads from the hybrid cell line using FISH. (**c**) (**d**) Hybridisation of a biotin labelled chromosome 22 probe (Section 3.3.3) to a PgMe-25 spread. (**a**) (**c**) Probes were detected using avidin-FITC (green). Chromosomes were counterstained with DAPI (blue). (**b**) (**d**) Grey scale representation of the DAPI stained human material. (**i**) Apparently incomplete chromosome 22. (**ii**) Autonomous chromosome 22 material. (**iii**) Extra band of chromosome 22 material integrated into a rodent chromosome, present in all spreads observed.

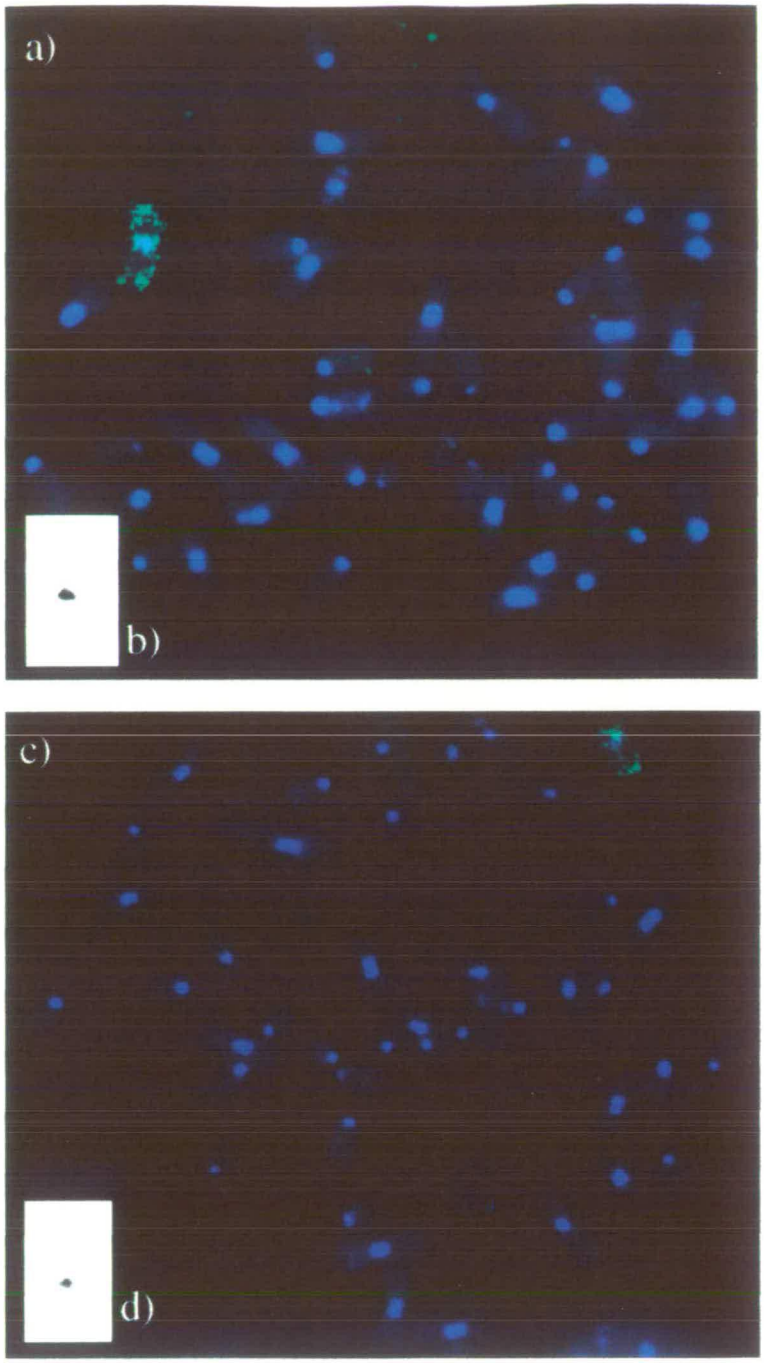

Figure 3.9 The integrity of the human material in the rodent-human hybrid cell line A91neo

Total genomic human DNA was labelled with biotin and hybridised to metaphase spreads from the hybrid cell line using FISH. (**a**) (**c**) The probe was detected using avidin-FITC (green). Chromosomes were counterstained with DAPI (blue). (**b**) (**d**) Grey scale representation of the DAPI stained human material. (**a**) (**b**) A spread with a complete chromosome 1 and no additional human material. (**c**) (**d**) A spread with an incomplete chromosome 1.

3.3 Human monochromosome paints

Labelling of total DNA from GM11010 resulted in a paint that was weak along the q-arm of human chromosome 18 compared to the remainder of the chromosome (Section 3.2.2 & Figure 3.2). This probe was not adequate for a useful human chromosome 18 paint. However, labelling of total DNA from the chromosome 19 hybrid produced a probe that, although covered chromosome 19 completely, often showed hybridisation to other regions of the human genome despite a high degree of C_0t 1 suppression (Section 3.2.2). Human-specific *Alu*-PCR is a good way of amplifying the human DNA specifically from hybrids, and so this approach was taken to try to prepare complete and consistent human chromosome 18 and 19 paints.

3.3.1 Human-specific *Alu*-PCR

The *Alu* family of short interspersed repeat elements (SINEs) constitutes at least 10% of the human genome. Each element is approximately 300bp in length and reiterated, in either orientation, between 500,000 and 1,000,000 times (Section 1.3.3). Rodent DNA also contains SINEs, dominated by a major family with sequence homology to the human *Alu* element. However, unlike the human *Alu* element, the rodent equivalent is only ~130bp long (Jelinek & Schmid, 1982). A portion of the consensus sequences of the human and Chinese hamster *Alu* elements is shown aligned in Figure 3.10. PCR using primers specific to the human *Alu* consensus sequence can be used to amplify human DNA specifically from a rodent-human cell hybrid (Nelson *et al.*, 1989). The primers are made in one orientation and, thus, inter-element amplification will only occur if two human *Alu* elements lie an appropriate distance apart, in opposite orientations.

The human specific *Alu* primers (#153, #154, #451 and #SB30), chosen to amplify human DNA from the hybrid cell lines, are shown in Figure 3.10 and described in Section 2.4.1.1. The cycling conditions for PCR are described in Section 2.4.1.3. Each primer was shown individually to amplify fragments of total human DNA but not Chinese hamster DNA (Figure 3.11a). To produce paints for chromosome 18 and 19, *Alu*-PCR using each of these human specific primers was used to amplify human DNA specifically from GM11010 and GM10449A, respectively (Figure 3.11b). The products of each primer reaction were pooled.

Approximately, 1.5μg of DNA were biotin labelled by nick translation (Section 2.5.1) and 150ng used as a probe for FISH onto human metaphase spreads.

The labelled *Alu*-PCR products from GM10449A produced a chromosome 19 paint which consistently gave strong FISH signal covering the entire length of the chromosome, except for at centromeric heterochromatin, as expected (Figure 3.12c). However, the same method using GM11010 DNA as the template did not produce a good paint for chromosome 18. As discussed in Section 3.2.3, GM11010 is very unstable and the chromosome 18 is lacking part of the q-arm in approximately 30% of cells, while the whole chromosome is absent from almost 20% of cells. The deficiencies of the hybrid cell line were exaggerated by Alu-PCR (Figure 3.12a). Since *Alu* elements dominate in R-bands, particularly T-bands, of which chromosome 18 has few (Korenberg & Rykowski, 1988; Baldini & Ward, 1991; Holmquist, 1992) (Section 1.4.3), *Alu*-PCR will amplify fragments from chromosome 18 far less efficiently than from chromosome 19, which is rich in T-bands. An alternative strategy adopted for the production of a complete monochromosome 18 paint is described in the next section.

3.3.2 Producing a complete human monochromosome 18 FISH paint

FACS was used to sort and collect chromosomes 18 by Dr. N. Carter, Sanger Centre Cambridge (Section 2.8.2). DNA from the collected chromosomes were digested with *MseI* (T|TAA) and catch-linkered (Section 2.4.2.1) by Dr. S. Cross, University of Edinburgh. The sequences of the catch-linkers used were as follows:

CH18-1 5'TACCGTTAAGCGTCAATCATGG3'
CH18-2 3' GGCAATTCGCAGTTACTACC5'

Using the CH18-2 sequence as a primer, the fragments were amplified by linker PCR using the cycling conditions described in Section 2.4.2.2. Fragments were labelled for FISH by incorporating dUTP conjugated with biotin or dig into the PCR reaction (Section 2.4.2.3). These fragments should be representative of the entire length of chromosome 18. Figure 3.13 shows an example of a human metaphase spread after hybridisation the catch-linkered chromosome 18 material. This probe paints the whole of chromosome 18.

3.3.3 FISH paints for other human chromosomes

A commercial FISH paint was used for chromosome 1 (Gibco BRL) which had been prepared from FACS sorted chromosomes which were digested, cloned (Fuscoe *et al.*, 1989) and directly labelled with Spectrum Orange fluorochrome. This probe had to be supplemented with a chromosome 1 centromeric heterochromatin probe since the repeat sequences present in this region were under-represented in the cloned library. This additional DNA probe was cloned by Cooke & Hindley (1979) and labelled directly by Mrs. P. Malloy, MRC Human Genetics Unit, Edinburgh, by incorporating dUTP conjugated to Spectrum Orange into a nick translation reaction (Section 2.5.1). Figure 3.14a shows a typical human metaphase spread hybridised with these two probes. Approximately half of the p-arm of chromosome 1 in every spread showed a weaker hybridisation signal than the remainder of the chromosome. This may be due to the absence of representative sequences in the cloned library.

Another FISH paint used was for human chromosome 11. An adequate probe was purchased commercially (Cambio) and Figure 3.15 shows hybridisation of this to a human metaphase spread. This paint was made by DOP-PCR of FACS sorted chromosomes (Telenius *et al.*, 1992) (Section 3.1) and covers the entire length of the chromosome.

A chromosome 22 FISH paint was obtained from Dr. S. Cross, University of Edinburgh. This paint was produced from FACS sorted chromosomes that were digested and catch-linkered. As before, *MseI* (T | TAA) was used for digestion and the catch-linker sequences were as follows:

CH22-1 5'TAAGTACTGCACCAGCAAATCC3'
CH22-2 3' TCATGACGTGGTCGTTTAGG5'

Using linker CH22-2 as a primer, fragments were amplified by PCR and labelled for FISH by incorporating dUTP conjugated with biotin into the PCR reaction (Section 2.4.2). Figure 3.16 shows a human metaphase spread hybridised with this FISH paint. Despite a high quantity of suppression, with 50μg of C_0t 1 DNA added for 150ng of probe and an extended period of re-annealing of 30 minutes at 37°C, signal appeared on all of the acrocentric chromosomes. This was expected due to the homology of the repeat sequences at these sites

(Section 3.2.2). However, the predominance of signal was on chromosome 22 and its entire length was illuminated.

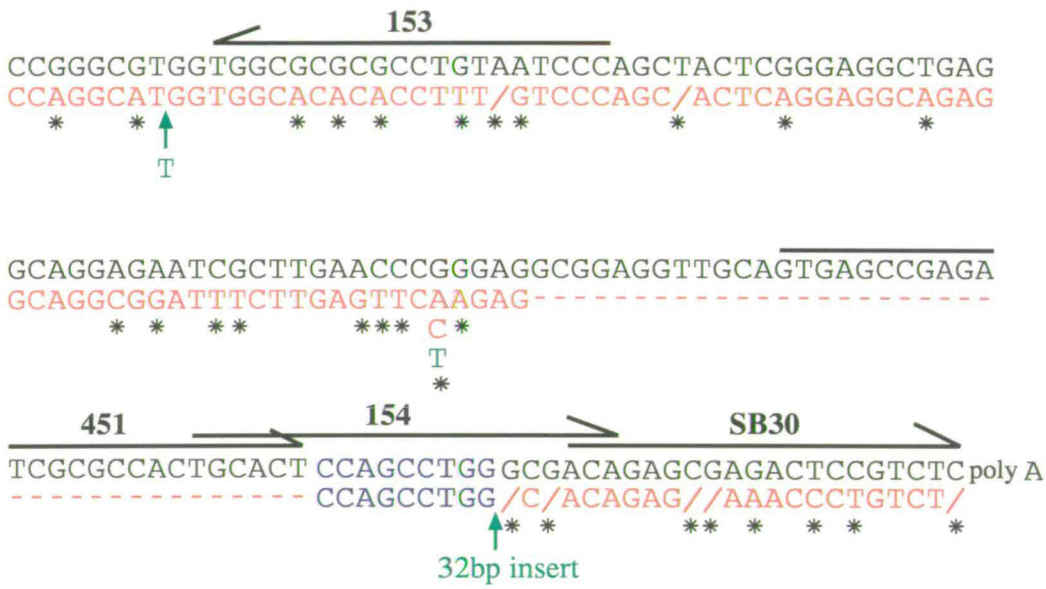

Figure 3.10 Human and Chinese hamster *Alu* consensus sequences
The human sequence is taken from Jurka & Milosavljevic(1991) (black). The Chinese hamster sequence is taken from Jelinek & Schmid(1982) (red). Only one strand of each is shown for clarity. The dashed line (-) indicates a portion of the human sequence not present in Chinese hamster *Alu* elements. The Chinese hamster has a 32bp insert not represented in the human sequence. The blue portion of sequence indicates a highly conserved 9bp region. The arrows indicate the position and direction of the human-specific *Alu*-PCR primers: #153 and #154 (Breen *et al.*, 1992), #451 (Alvieler & Porteous, 1992) and #SB30 (Ms. S. Boyle, MRC Human Genetics Unit, Edinburgh) (Section 2.4.1.1).

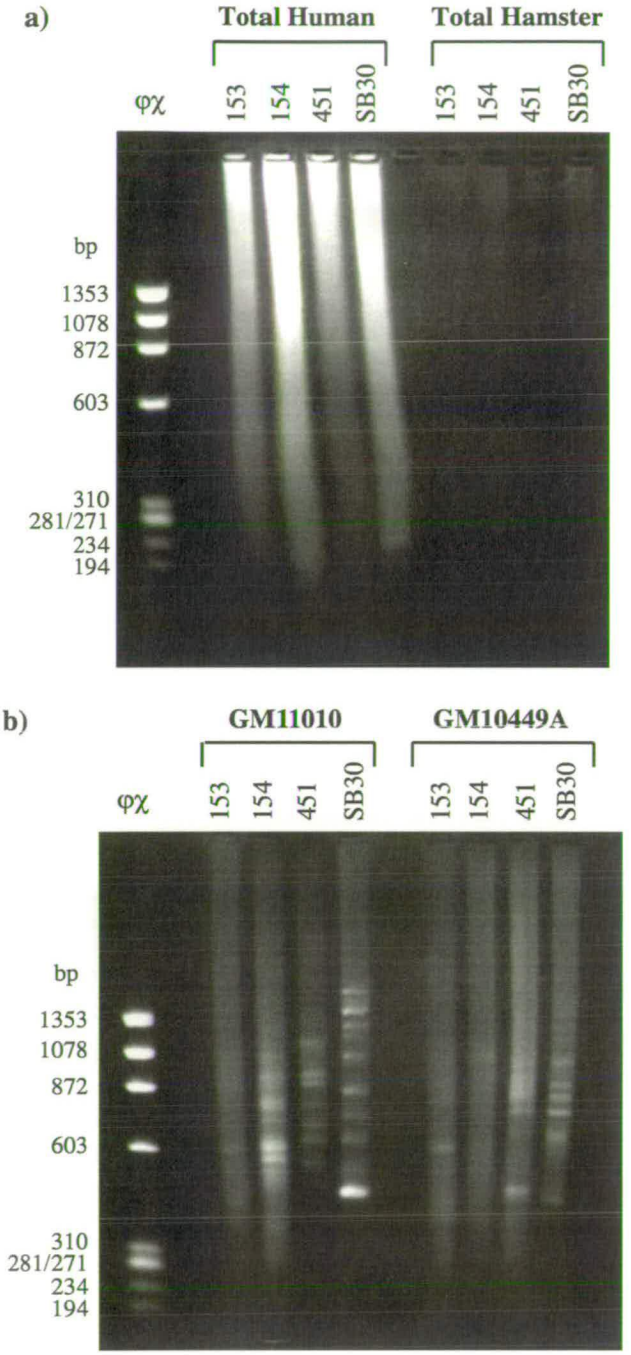

Figure 3.11 Confirming the specificity of human *Alu*-PCR primers
2% Nusieve agarose gel run in 1xTBE (Section 2.3). Total DNA was prepared from (**a**) human or Chinese hamster cell lines, or (**b**) the Chinese hamster-human monochromosome cell lines GM11010 (human chromosome 18) or GM10449A (human chromosome 19). 50ng of template DNA were amplified by *Alu*-PCR (Section 2.4.1) using each of the primers (#153, #154, #451 and #SB30) shown in Figure 3.10 and described in Section 2.4.1.1. 10µl product was loaded in each lane and stained with ethidium bromide. Each primer was confirmed as being human specific since amplified DNA was detected in all lanes except those where Chinese hamster DNA alone was the template.

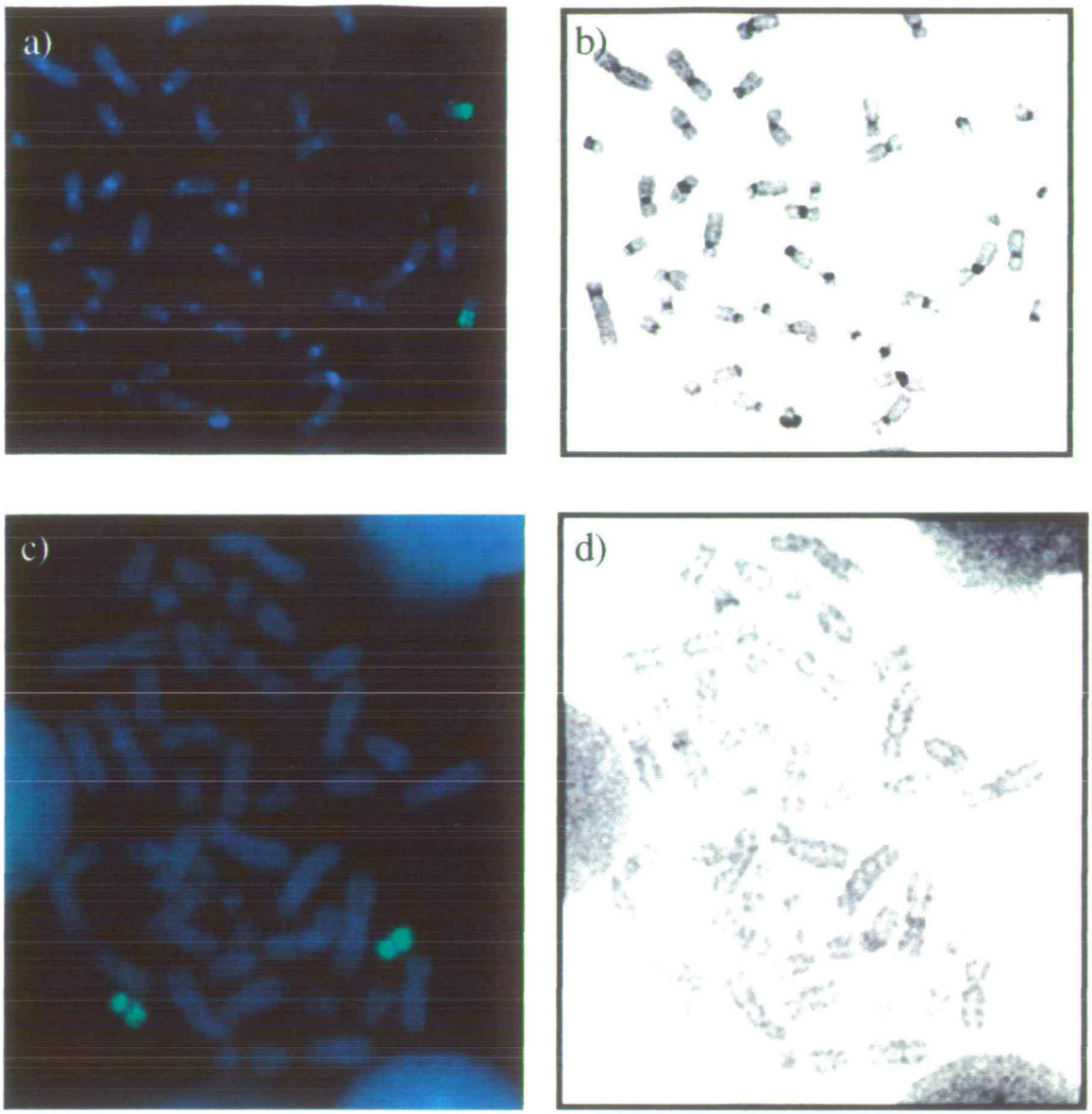

Figure 3.12 Painting human metaphase spreads by FISH with *Alu* PCR monochromosome probes

(**a**) (**c**) Fragments amplified by human-specific *Alu* PCR of DNA from the hybrid cell lines, GM11010 (a) and GM10449A (c), were biotin labelled and hybridised to REN2 human metaphase spreads (49, XXXXY) by FISH (Section 3.3.1). The probe was detected using avidin-FITC (green). Chromosomes were counterstained with DAPI (blue). (**c**) (**d**) Grey scale representation of the DAPI stained spreads. Note the partial coverage of the chromosome 18 probe but the complete coverage of the chromosome 19 probe.

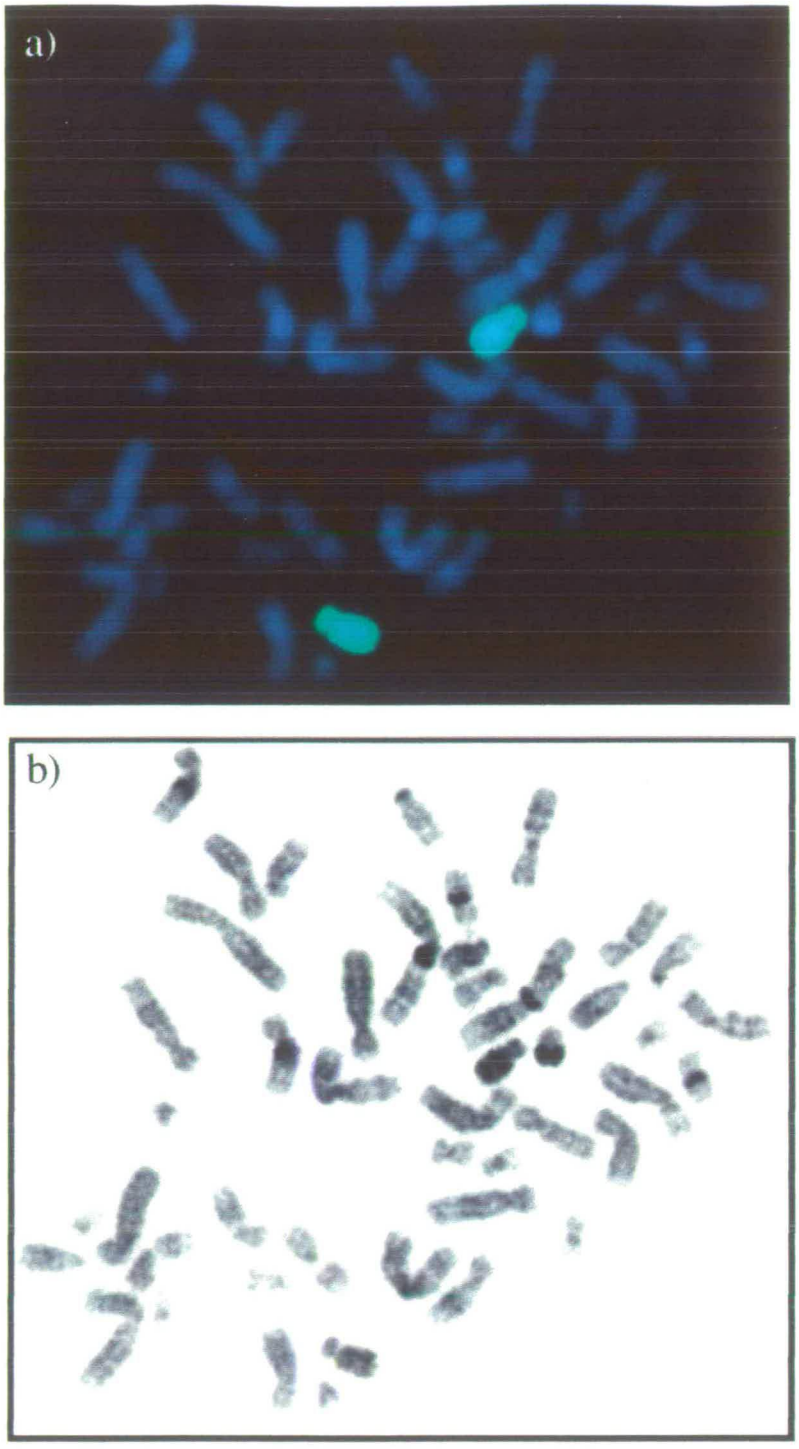

Figure 3.13 A complete human chromosome 18 FISH paint
(**a**) FACS sorted chromosomes 18 were digested, catch-linkered and labelled by incorporation of biotin-dUTP in a PCR reaction using one of the catch-linkers as a primer (Section 3.3.2). Provided by Dr. S. Cross, University of Edinburgh. The probe was hybridised to REN2 human metaphase spreads (49, XXXXY) by FISH and detected using avidin-FITC (green). Chromosomes were counterstained with DAPI (blue). (**b**) Grey scale representation of the DAPI stained spread.

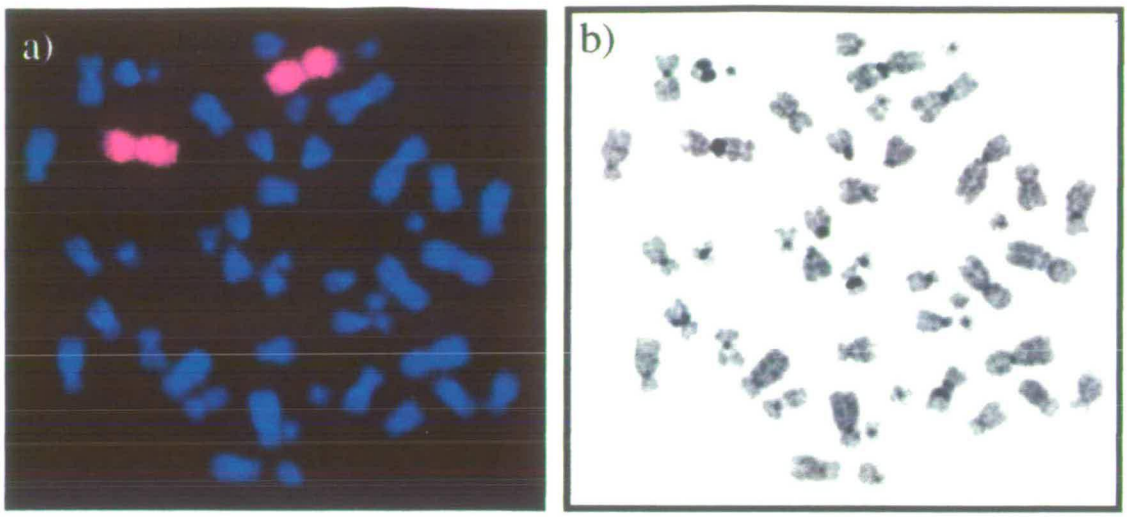

Figure 3.14 FISH paint for human chromosome 1
(**a**) Chromosome 1 paint directly labelled with Spectrum Orange (Gibco) and supplemented with a centric heterochromatin probe directly labelled with Spectrum Orange by Mrs. P. Malloy, MRC Human Genetics Unit, Edinburgh (Section 3.3.3). The probe was hybridised to FATO human metaphase spreads (46, XY) by FISH and chromosomes were counterstained with DAPI (blue). (**b**) Grey scale representation of the DAPI stained spread.

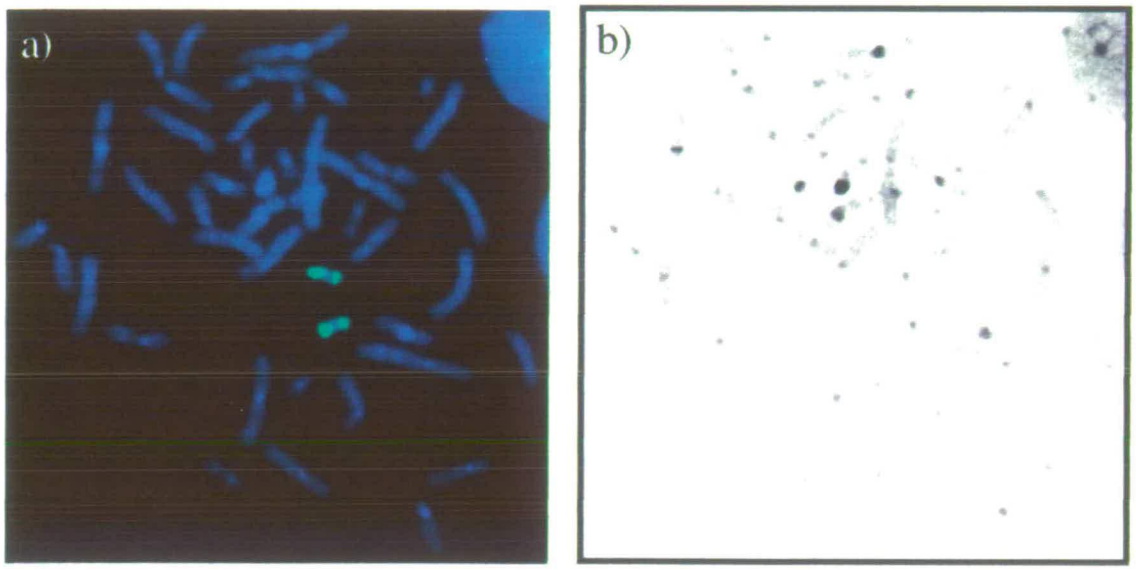

Figure 3.15 FISH paint for human chromosome 11
(**a**) Chromosome 11 FISH paint labelled with biotin (Cambio) and detected with avidin-FITC (green) (Section 3.3.3). The probe was hybridised to FATO human metaphase spreads (46, XY) by FISH and chromosomes were counterstained with DAPI (blue). (**b**) Grey scale representation of the DAPI stained spread.

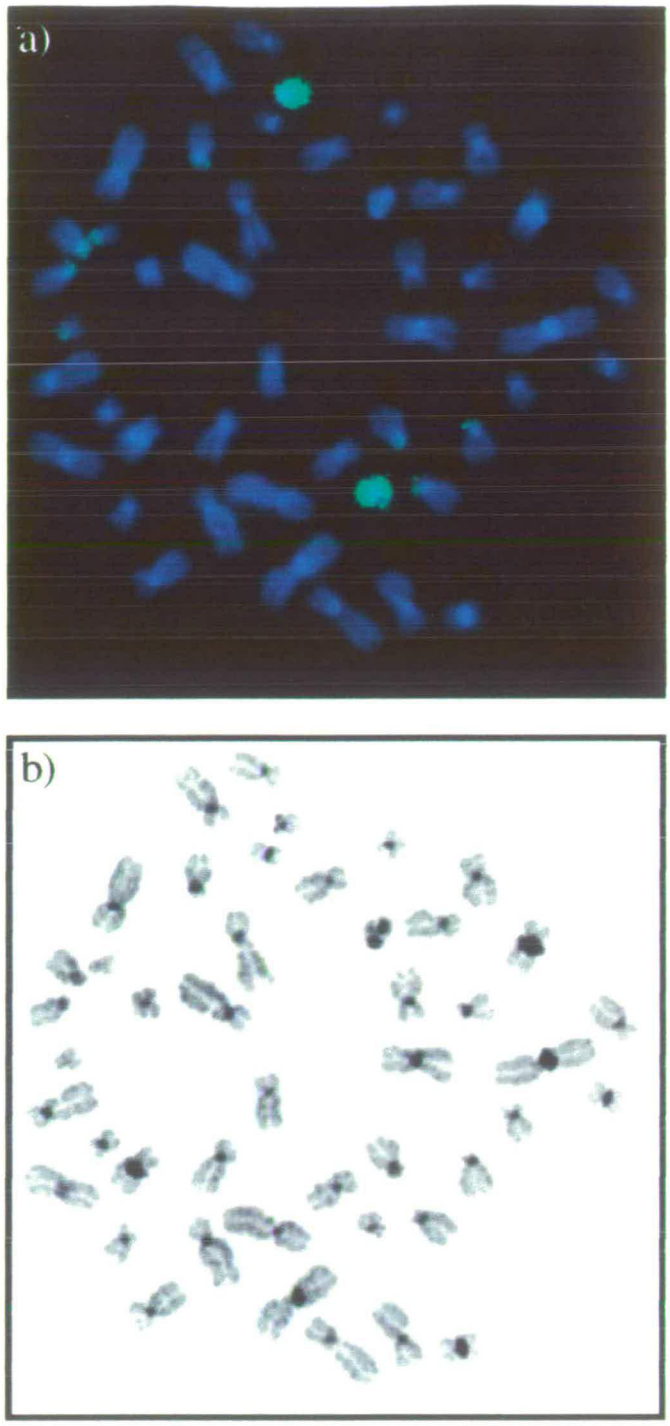

Figure 3.16 FISH paint for human chromosome 22
(**a**) FACS sorted chromosomes 22 were digested, catch-linkered and labelled by incorporation of biotin-dUTP in a PCR reaction using one of the catch-linkers as a primer (Section 3.3.3). Provided by Dr. S. Cross, University of Edinburgh. The probe was hybridised to FATO human metaphase spreads (46, XY) by FISH and chromosomes were counterstained with DAPI (blue). (**b**) Grey scale representation of the DAPI stained spread.

3.4 Comparing the physical size of human chromosomes 18 and 19 at metaphase

The sites at which DNA attaches to the chromosome scaffold and the nature of this scaffold are the cause of much controversy. Several types of DNA sequence have been implicated and, indeed, some or all of these may be true sites of attachment. Such sequences include origins of replication, sites of active transcription and/or AT-rich sequences (Section 1.6.1). Chromosomes 18 and 19 are completely contrasting in their functional features (Section 1.7 & 3.1). Does this influence the way the DNA of these two chromosomes are packaged for mitosis as dictated by the DNA scaffold attachment sequences?

In typical, 3:1 methanol:acetic acid fixed human chromosome spreads these two chromosomes appear to be of similar size. Estimates of DNA content associate chromosome 18 with 2.68% and chromosome 19 with 2.12% of total DNA in the human genome, giving a ratio for 19:18 of 0.79 (Morton, 1991) (Section 1.7), with chromosome 18 having on average 20% more DNA than chromosome 19. This data was collected from a number of analyses carried out using image or flow cytometry, and measurements of incorporated radioactive DNA precursors by autoradiography. Care was taken to avoid any base specific bias with the use of fluorochromes.

Chromosome condensation is a dynamic process which proceeds, through prophase to metaphase, at different rates along the length of each chromosome and probably does not result in the same ultimate level of compaction in all regions (Drouin *et al.*, 1991) (Section 1.4.5). Because of differences in compaction between the different stages of mitosis, it was necessary to compare chromosomes that were within the same spread. Mid-metaphase spreads from 3:1 methanol:acetic acid fixed primary male lymphocytes and a lymphoblast cell line, FATO were prepared (Section 2.1) and hybridised to the monochromosome paints for chromosomes 18 and 19 by FISH (Section 2.6). Using differentially labelled probes allowed simultaneous detection of the paints with distinct fluorochromes (Figure 3.17a & c). After identification of the chromosomes of interest from each spread, IPLab Spectrum software was used to measure the length, width and area, of each chromosome from images showing the chromosomes stained with the DNA stain DAPI (Figure 3.17b & d). Twenty five images were analysed and measurements averaged for the two homologues of each chromosome (Table 3.2). A previous study of 3:1 methanol:acetic acid fixed human male

lymphocyte spreads are also recorded in Table 3.2 (Van Dyke *et al.*, 1986). Despite the variability in mean length measured for the primary lymphocyte and cell line spreads, the ratio of chromosomes 19:18 remained approximately the same, at 0.9. The length differences between different cell types probably reflects the degree of condensation in response to colcemid treatment.

Table 3.2 The ratio of physical size of human chromosomes 18 and 19 at metaphase
The mean length or area taken up by the two homologues of the chromosomes of interest in each spread were measured and the ratio of chromosome 19 to chromosome 18 was calculated. In each case 25 mid-metaphase spreads were assessed. *- data taken from Van Dyke *et al.*, 1986 +/- standard error of mean
N- not calculated

Origin of spreads	Measurement	Mean value		19:18
		18	19	
Primary lymphocytes	Length (μm)	$5.3^{+/-0.2}$	$4.4^{+/-0.2}$	$0.85^{+/-0.02}$
Primary lymphocytes	Area (μm^2)	$79.8^{+/-2.8}$	$72.6^{+/-3.0}$	$0.92^{+/-0.04}$
Lymphoblast cell line	Length (μm)	$3.5^{+/-0.1}$	$3.2^{+/-0.1}$	$0.89^{+/-0.02}$
Lymphoblast cell line	Area (μm^2)	$53.7^{+/-2.0}$	$47.7^{+/-1.8}$	$0.90^{+/-0.02}$
*Primary lymphocytes	Length (μm)	$2.8^{+/-0.1}$	$2.6^{+/-0.1}$	$0.97^{+/-N}$

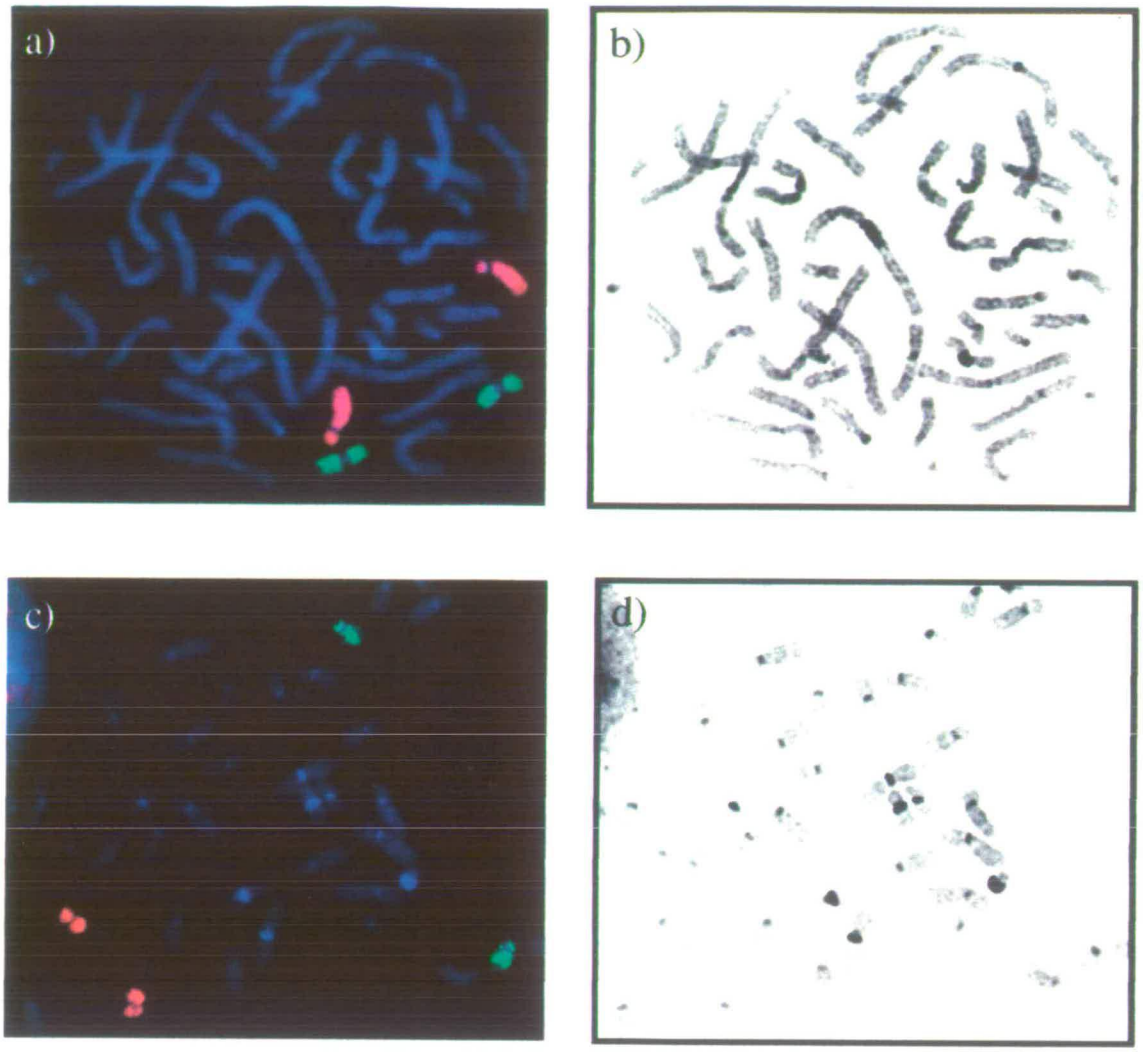

Figure 3.17 Identifying human chromosomes 18 and 19 in the same metaphase spread
(**a**) (**b**) All chromosomes counterstained with DAPI (blue). Typical metaphase spread from primary lymphocytes (46, XY) hybridised with chromosome 18 FISH paint, labelled with biotin and detected with avidin-TR (red), and chromosome 19 FISH paint, labelled with dig and detected with anti-dig-FITC (green). (**c**) (**d**) Representative metaphase spread from the FATO human lymphoblastoid cell line (46, XY) hybridised with chromosome 18 FISH paint, labelled with dig and detected with anti-dig-FITC (green), and chromosome 19 FISH paint, labelled with biotin and detected with avidin-TR (red). (**b**) (**d**) Grey scale representation of the DAPI stained spreads.

3.5 Summary

Human chromosome 18 has approximately 20% more DNA and is on average 10% larger than chromosome 19 in typical 3:1 methanol:acetic acid fixed metaphase spreads. It appears that the DNA of chromosome 18 may be more tightly packaged than that of chromosome 19, although these differences are not as large as might be expected considering the extreme reciprocal functional characteristics of these two chromosomes (Section 1.7). Using these data (Section 3.4) and the chromosome FISH paints produced (Section 3.3), more specific questions can now be asked about the packaging of these two chromosomes. This is approached in the next chapter by use of salt extraction to strip away proteins and so unravel the chromosomes.

4. Exploring higher order human metaphase chromosome packaging

4.1 Introduction

Salt can be used to extract proteins, including histones, and release chromosomal DNA into loops, tethered to a scaffold which runs along the chromosome axis. This chapter uses salt extraction of human chromosomes 18 and 19 to examine further their DNA packaging, determining sequences that might be involved in attachments to the chromosome scaffold. These experiments have implications upon the packaging of DNA for the entire human genome.

4.2 The scaffold attachments of human metaphase chromosomes

The chromosome scaffold (Section 1.5.1) is a morphological term used to describe the residual framework which remains following protein extraction of metaphase chromosomes (Paulson & Laemmli, 1977; Earnshaw & Laemmli, 1983; Paulson, 1989) with salt or polyanions. Various operational techniques have also been developed to determine the nature of the proteins and DNA associated with the scaffold. Scaffold attached regions (SARs) were identified from LIS extraction of nuclei. SARs are AT-rich and contain homoploymer tracts of dA and dT (Mirkovitch *et al.*, 1984; Gasser & Laemmli, 1986; Gasser *et al.*, 1989; Laemmli *et al.*, 1992). Electroelution of physiologically extracted, agarose embedded nuclei assigned sites of replication and transcription to the, so called, nucleoskeleton (Jackson & Cook, 1985 & 1986; Jackson, 1991; Jackson *et al.*, 1996). Finally, mapping the cutting sites of topo II, a long established scaffold protein (Section 1.4.6), on salt extracted nuclei and metaphase chromosomes has suggested that replication origins may play a key role in chromosome organisation (Razin *et al.*, 1993). This possibility is upheld by the visualisation some origins of replication, by FISH, at the core of salt extracted metaphase chromosomes (Bickmore & Oghene, 1996).

Three hypotheses of scaffold-loop metaphase chromosome folding now predominate (Figure 4.1) and will be discussed in turn. These are differentiated by the types of DNA attachments involved:

1. AT-rich SARs (Saitoh & Laemmli, 1994a & b).
2. Sites of transcription (Cook, 1994 & 1995).
3. Origins of replication (Razin *et al.*, 1986 & 1993; Bickmore & Oghene, 1996).

4.2.1 Chromosome bands and the AT-queue

The fluorescent dye, daunomycin, shows a greater fluorescence when bound to AT-rich DNA (>65% AT). It has been argued that this dye can be used to trace the path of AT-rich SARs in metaphase chromosomes (the AT-queue). The non-fluorescent dye, methyl green, also binds preferentially to AT-rich DNA and using this to quench the general fluorochrome YOYO-1, DNA excluded from the AT-queue can be delineated. Combining these staining protocols, Saitoh & Laemmli (1994a & b) produced a striking reciprocal pattern along the length of the metaphase chromosomes of the Indian muntjac. Daunomycin highlighted the G-bands and methyl green/YOYO-1 stained the R-bands. It was concluded from this that the AT-queue is more tightly coiled within G-bands, with consequently more DNA and possibly smaller loop sizes in these regions. The R-bands are likely to contain an unfolded AT-queue, with larger DNA loop sizes predicted (Figures 4.1 & 4.2).

The AT-queue was also identified immunologically by tracing topo II and HMG-I (Y) localisation (Saitoh & Laemmli, 1994a & b). Both of these proteins are concentrated within G-bands, consistent with a more tightly folded scaffold in these regions. Topo II has been previously shown to have a non-uniform distribution along chromosomes (Earnshaw & Heck, 1985) (Section 1.4.6). ScII has been demonstrated to colocalise with topo II, also showing a non-uniform distribution along chromosomes (Saitoh *et al.*, 1994). HMG-I (Y) is not considered as a structural protein and, indeed has been shown to be involved in transcriptional activation (Section 1.4.4). However, this protein has been previously shown to have a preference for AT-rich DNA (Struass & Varshavsky, 1984; Disney *et al.*, 1989; Reeves & Nissen, 1990; Reeves & Wolffe, 1996) and may be involved in promoting transcription in generally repressed regions.

At a finer resolution, Jarman & Higgs (1988) showed eight operational SARs to be located within the human β-globin locus, situated within a G-band, while none where found within the α-globin locus, situated in a T-band, supporting the bias distribution of SARs.

Originally determined in nuclei, the relationship between SARs present at interphase and at metaphase is unclear. Only a subset of SARs identified from LIS extracted nuclear scaffolds have been shown to bind to chromosome scaffolds (Mirkovitch *et al.*, 1988). Since chromosomes refold in exactly the same way each metaphase, it seems likely that there will be some consistency in sites of attachment throughout the cell cycle.

4.2.2 Polymerases as structural determinants of the chromosome

The model postulated by Cook (1994 & 1995) is in sharp contrast to that described above and proposes that RNA polymerases are the basis of metaphase chromosome structure, that is, DNA attachments are functionally determined. It is proposed that transcription factories, observed at interphase as discrete foci (Jackson *et al.*, 1993; Wansink *et al.*, 1993; Grande *et al.*, 1997) are immobile and attached to the nucleoskeleton (Jackson & Cook, 1985; Cook, 1989). During prophase these foci may aggregate, as the nucleoskeleton depolymerises, condensing each chromosome and being visible as chromomeres. One flaw in this model is that chromomeres actually correspond to gene-poor G-bands, not gene-rich R-bands (Section 1.4.2). The model also implies that loop size will vary between chromosome bands, with R-bands containing smaller loops since they are more transcriptionally active, and thus associated with more transcription factories, than G-bands (Figure 4.1).

4.2.3 Associations between the origins of replication and the chromosome scaffold

The precise nature and organisation of mammalian origins of replication is unclear (Reviews: Hand, 1978). It seems likely that origins are spaced fairly frequently throughout the genome, but at different stages of development and in different tissues, alternative sets of origins are initiated (Hamlin & Dijkwel, 1995). Fibre autoradiographic studies have shown that chromosomal DNA is replicated by two divergent replication forks sharing a common origin. These replicons are spaced 30-300Kb apart and clusters of 5-20 replicons are activated synchronously, possibly each representing a high resolution replication band (Holmquist, 1987) (Section 1.3.4).

A similarity between the size of loops and replicon frequency has been recognised at metaphase and interphase in many species (Buongiorno-Nardelli *et al.*, 1982) including humans (Marsden & Laemmli, 1979; Tomilin *et al.*, 1995). Additionally, where the frequency of replication origin usage in *X.laevis* becomes less, as cell cycle length shortens during embryogenesis (Blumenthal *et al.*, 1974), the size of nuclear DNA loops become smaller and metaphase chromosomes become larger and fatter, in accordance (Micheli *et al.*, 1993).

Attachments to the salt extracted nuclear matrix have been shown to map with putative origins of replication throughout the cell cycle (Berezney & Buchholtz, 1981; Dijkwel *et al.*,

both the salt extracted nuclear matrix (Vogelstien *et al.*, 1980; Berezney & Buchholtz, 1981) and to the physiologically extracted nucleoskeleton (Jackson & Cook, 1986; Jackson, 1990 & 1991; Cook, 1991). By FISH, origins of replication have been shown to associate with the scaffold of salt extracted human metaphase chromosomes (Bickmore & Oghene, 1996), and topo II cleavage sites correlate well with known origins of replication in *D.melanogaster* (Razin *et al.*, 1993). In *S.cerevisiae*, autonomously replicating sequence (ARS) elements have also been shown to associate with a chromosome scaffold (Amati & Gasser, 1988 & 1990). The remnants of replication origin clusters have been observed to persist at the chromosome scaffold throughout the cell cycle in a number of species (Meng & Berezney, 1991; Adachi & Laemmli, 1992; Diffley *et al.*, 1994; Sparvoli *et al.*, 1994). However, clustering of replication loci does not require an interaction with a predefined nuclear matrix (Cox & Laskey, 1991).

4.2.4 Different sites of scaffold attachment probed by different extraction protocols

In an attempt to resolve the discrepancies of the three hypotheses described above, Craig *et al.* (1997) took scaffold and loop DNA from nuclei and chromosomes extracted with salt, LIS or by electroelution. This DNA was labelled and hybridised to human metaphase chromosomes by FISH. Attached DNA from LIS extracted nuclei was shown to preferentially hybridise to G-bands confirming that SARs are, indeed, more frequent in these regions than in R-bands. Reciprocally, attached DNA from electroeluted nuclei preferentially hybridised to R-bands, consistent with transcriptionally active sequences being the predominant sites of attachment to the nucleoskeleton. Finally, attached DNA from salt extracted nuclei tended to localise to G-bands but to a lesser extent than was observed for LIS extracted nuclei.

Attached DNA from LIS extracted metaphase chromosomes, rather than from nuclei, hybridised preferentially to G-bands, as before. When attached DNA was collected from electroeluted metaphase chromosomes, there was no biased hybridisation. This suggests that transcriptional activity may only be involved in setting up attachments to a nuclear substructure at interphase. Similarly, a more even distribution resulted from hybridisation with attached DNA from salt extracted metaphase chromosomes. These data suggest that the attachments being analysed by electroelution and salt extraction are dynamic. Clearly, the nuclear scaffold, nuclear matrix and nucleoskeleton are not equivalent.

From this study, it seems likely that DNA attachments mediated by transcription may only be involved at interphase. DNA attachments to LIS extracted nuclei and chromosomes appear to be relatively consistent, suggesting that SARs may be permanent sites of attachment to a nuclear and chromosome scaffold. DNA attachments sampled by salt extraction of chromosomes show a relatively even distribution of attachment sites along the length of chromosomes. How does this compare with the morphological scaffold of salt extracted chromosomes?

4.2.5 The implications of the three scaffold-loop models of metaphase chromosome structure for human chromosomes 18 and 19

What differences in the structure of chromosomes 18 and 19 might be expected for each of the three models of scaffold-loop metaphase chromosome structure (Figure 4.1)? If the AT-rich SAR queue was the basis of packaging, then it might be expected that there would be more loop attachments in the AT-rich G-bands than the R-bands. Thus, AT-rich chromosome 18 would have more attachments along its length and smaller DNA loop sizes than GC-rich chromosome 19. If, on the other hand, as proposed by Cook (1994 & 1995) actively transcribed genes form the majority of scaffold attachment sites then gene-poor chromosome 18 would, by complete contrast, have fewer attachment sites and longer DNA loops than gene-rich chromosome 19. Finally, if origins of replication were the key binding sites then the relatively evenly spaced distribution of these would be reflected in regular attachments and roughly equal DNA loop sizes in these two chromosomes. Of course, it is possible that evenly spaced attachments may be defined by sequences other than replication origins, for example, boundary elements.

To assess each of these possibilities, metaphase chromosomes were extracted with increasing concentrations of salt, stripping proteins and releasing the DNA loops, leaving the scaffold attachments intact. The loop sizes of chromosomes 18 and 19 were then compared.

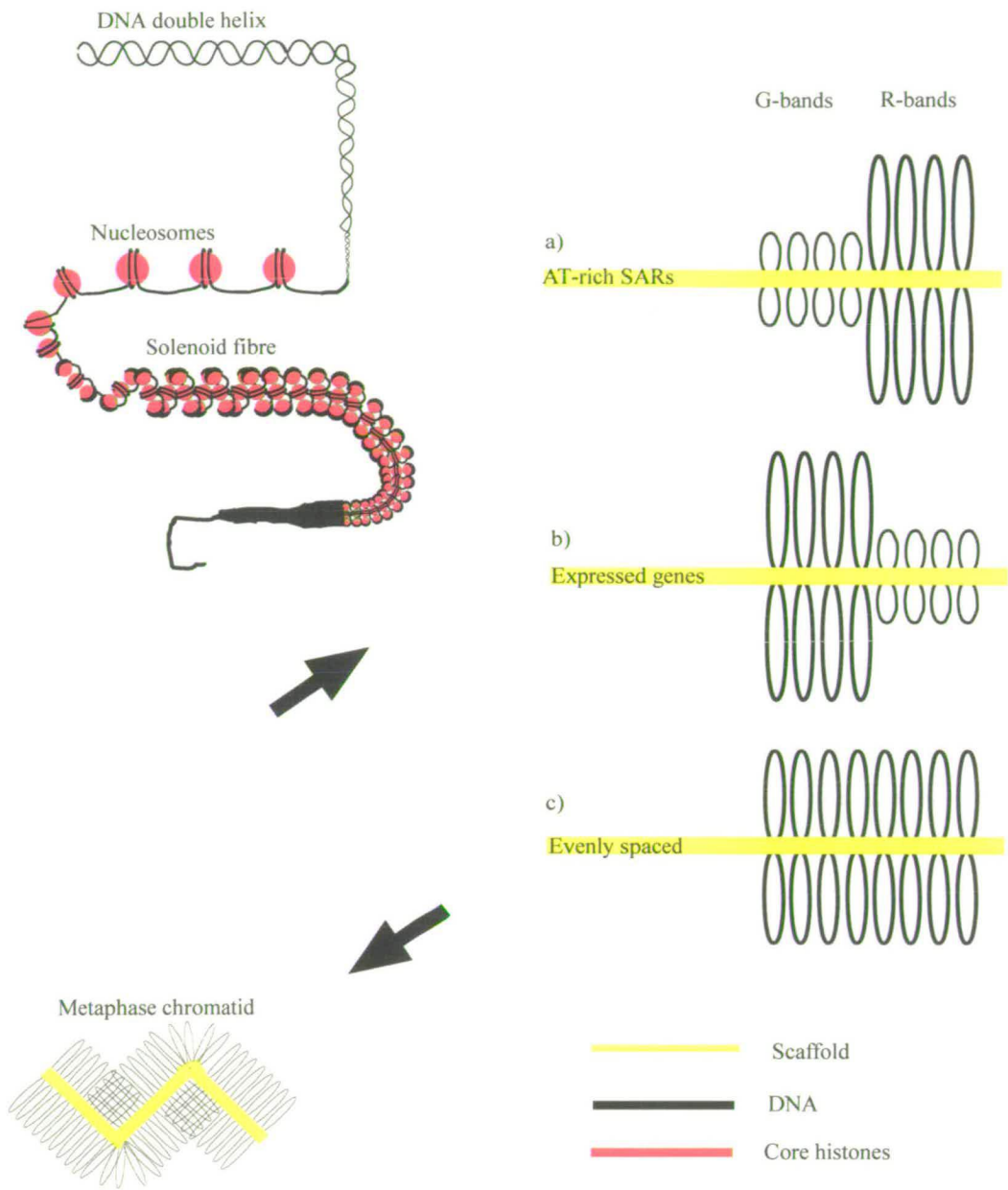

Figure 4.1 Three models of higher order packaging of human metaphase chromosomes (**a**) Binding of AT-rich SARs to a protein scaffold (Saitoh & Laemmli, 1994a & 1995b). (**b**) Binding of transcriptionally active regions to a scaffold by polymerases (Cook, 1994 & 1995). (**c**) Evenly spaced attachment to a scaffold at sites corresponding to, for example, replication origins (Razin *et al.*, 1986 & 1993; Bickmore & Oghene, 1996). Each model has implications for the looping of DNA in G-bands and R-bands.

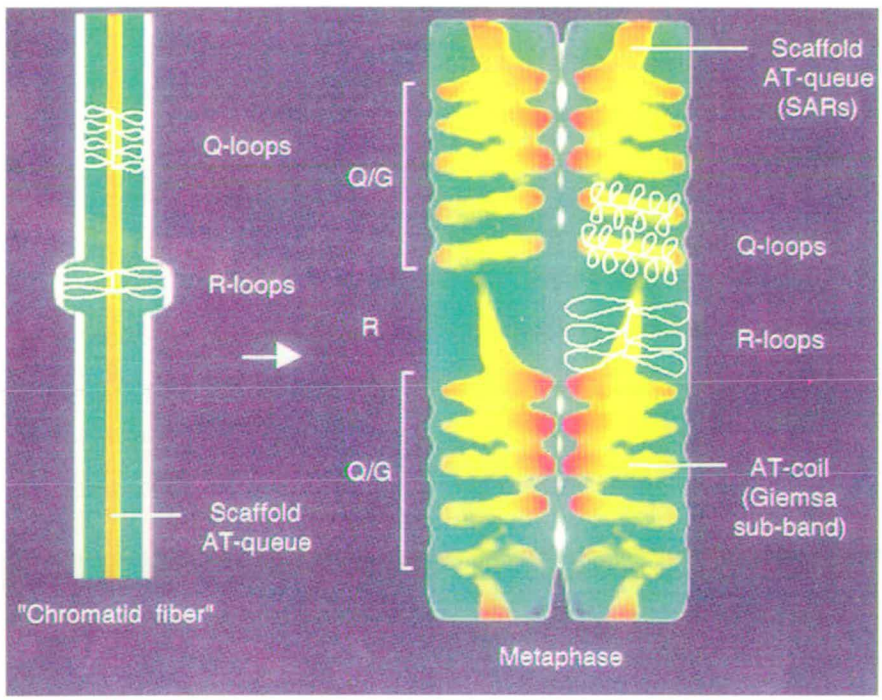

Figure 4.2 The AT-rich queue
Taken from Laemmli *et al.* (1994a & b) (**Left**) Hypothetical chromatid fibre which folds to form the more compact metaphase chromosome (**Right**). Daunomycin stains the AT-rich DNA queue (yellow), while AT-binding methyl green is used to quench the general fluorochrome YOYO so that it is excluded from the AT-queue (green). Loops are not directly observed but inferred. Q/G relates to G-bands, and R indicates R-bands. Loop sizes are considered to be smaller in G-bands than R-bands.

4.3 Salt extraction of human chromosomes 18 and 19

Metaphase chromosomes from the REN2 human lymphoblastoid cell line (49, XXXXY) were prepared in polyamine buffer (Section 2.8.1). To enrich for metaphase chromosomes, cells growing exponentially were treated with colcemid, a spindle depolymerising agent, up to 16 hours before harvesting. A mitotic index of >60% was required to be achieved. Cells were then swollen in hypotonic solution, pelleted and resuspended in polyamine buffer containing digitonin. Polyamines are basic molecules and their presence helps maintain the chromosomes in a condensed state during isolation (Wallace *et al.*, 1971). Digitonin pierces the cellular membrane, but not the nuclear membrane, and since cells undergoing mitosis have no nuclear membrane, metaphase chromosomes are released into the supernatant (Blumenthal *et al.*, 1979; Sillar & Young, 1981). Cells were spun, and the nuclear pellet and chromosome containing supernatant were stored with glycerol independently at -70°C. Chromosomes were later spread on slides and allowed to settle overnight. For extraction, slides were lowered gently into extraction buffer in the absence of salt and then sequentially into extraction buffers with increasing salt concentration (Section 2.9). The morphology of the chromosomes was more consistently maintained with sequential extraction than direct extraction in the desired salt concentration. It is apparent that metal ions occur naturally in chromosomes and are involved in stabilising the scaffold, thus, Cu^{2+} was included in the extraction buffer (Lewis & Laemmli, 1982). This method was adapted from Bickmore & Oghene (1996). Previous attempts to obtain mitotic cells from an adherent cell line grown on slides resulted in few spreads with insufficient separation of the individual chromosomes.

Different proteins are stripped from the chromosomes at different salt concentrations. The following salt concentrations were selected because they correlate with the specific loss of each of the core and linker histones (Wolffe, 1995):

- 0.5M - H1
- 1.0M - H2A and H2B
- 1.2M - H3 and H4
- 1.8M - All core and linker histones should be completely extracted

Following salt extraction chromosomes were fixed in 3:1 methanol:acetic acid, ensuring that the chromosomes would withstand the rigours of FISH. To identify chromosomes 18 and 19, FISH using the paints produced for each chromosome (Section 3.3) was carried out and extracted chromosomes were counterstained with DAPI (Figure 4.3). The general shape of

the chromosomes were maintained throughout these procedures. The primary centromeric constriction was obvious in all images, revealed as a bright region of DAPI staining. Chromosome 18 was clearly observed as acrocentric and chromosome 19 as metacentric. The sister chromatids of most of the chromosomes were separated, particularly at higher salt concentrations, often with a brightly staining axis along each. Sister chromatids showed a high degree of structural symmetry, arguing against artifactual DNA aggregation.

Twenty five chromosomes 18 and 19 with good morphology and obvious orientation, extracted at each salt concentration, were selected. Using IPLab Spectrum software, DAPI stained chromosome images were used to assess the maximum width, length and total area taken up by chromosomes at each salt concentration (Tables 4.1 & 4.2). The range of widths for both chromosomes at 1.8M NaCl extraction was 7-12μm. This is less than the dimensions (12-20μm) measured by electron microscopy of 2.0M NaCl extracted chromosomes (Paulson & Laemmli, 1977). DAPI staining is generally poor at discerning the outer limits of the halo where the relative concentration of DNA is low, thus explaining the underestimate of halo extent from DAPI stained images. Indeed, FISH signal was sometimes observed to extend beyond the DAPI staining. However, DAPI was the only fluorescent dye compatible with the fluorescence filter set used.

The range of lengths for both chromosomes at 0.0M NaCl was 4-5μm, which is approximately 40% longer than typical 3:1 methanol:acetic acid fixed lymphoblast chromosomes (Table 3.2). This suggests that some swelling of chromosomes occurs in extraction buffer, even in the absence of added salt. Such swelling has been previously described and is attributed to the chelation of divalent cations, for example Mg^{2+}, by EDTA present in the extraction buffer (Marsden & Laemmli, 1979; Bickmore & Oghene, 1996). Both chromosomes 18 and 19 maintain a ratio of 1:1, length:width from extraction in buffer without salt through to 1.8M NaCl. From the experiments in Section 3.4 it was calculated that the mean ratio of length:width for both chromosomes, from lymphoblastoid chromosomes fixed with 3:1 methanol:acetic acid, was 2:1. Therefore, it appears that this initial swelling occurs width-wise. Extraction with increasingly high salt causes the chromosomes to continue to expand equally both longitudinally and laterally, suggesting that the coiled scaffold gradually unwinds in addition to loops of DNA being released (Figures 1.1 & 4.1).

When mean width, length and area of the chromosomes at each salt concentration are shown graphically (Figure 4.4), it can be seen that they expanded to the same extent as salt

concentration increased. Indeed, the ratios of 19:18, for both width and area, remained at approximately 0.85, that is chromosome 18 was approximately 15% larger than chromosome 19, at every salt concentration (Table 4.2). An approximately 4-fold overall level of decondensation was achieved for each chromosome from 0.0M to 1.8M NaCl extraction (Table 4.2).

These experiments suggest that chromosome 18 has DNA loop sizes that are broadly the same as those of chromosome 19. The even spacing of sites of attachment, equally distributed along both chromosomes is the model best supported by these measurements (Section 4.1.3). This is also supported by Craig *et al.* (1997), who showed by FISH that attached DNA from salt extracted metaphase chromosomes hybridise relatively evenly along metaphase chromosomes. Exactly what constitutes such attachments remains to be established and it might be that a variety of different sequences are involved. Loop size was relatively even along the length of each chromatid and there was reasonable symmetry between chromatids of both chromosomes 18 and 19 (Figures 4.3 & 4.4). However, this does not eliminate the possibility that attachments have been randomised as suggested by Mirkovitch *et al.* (1984) (Section 1.6.5).

Cook's model (1994 & 1995), that regions of active transcription are the only permanent sites of attachment to the metaphase chromosome scaffold, is not supported by my results. There is no evidence from these experiments and those of Craig *et al.* (1997) to show that gene-rich regions have more attachments to the metaphase chromosome scaffold than gene-poor regions. If genes are not strongly associated with the scaffold, where are they positioned within the chromosome loop? Do they tend towards the outer region of loops where they might be most accessible to transcription machinery and involved in associations with a nuclear network outside of the chromosome?

Table 4.1 The width and length of metaphase chromosomes 18 and 19 extracted at increasing salt concentrations

Metaphase chromosomes from the REN2 human lymphoblastoid cell line were extracted with increasing concentrations of salt. FISH was used to identify chromosomes 18 and 19 and the width, length and area occupied by each of 25 chromosomes were measured using IPLab Spectrum software. +/- standard error of mean

Salt concentration	Mean width (μm)		Mean length (μm)		Mean length/width		Area of chromosome (μm^2)	
	18	19	18	19	18	19	18	19
0.0M	$4.63^{+/-0.11}$	$4.22^{+/-0.08}$	$4.75^{+/-0.11}$	$4.66^{+/-0.10}$	$1.03^{+/-0.04}$	$1.09^{+/-0.03}$	$379.5^{+/-14.5}$	$326.3^{+/-10.2}$
0.5M	$7.00^{+/-0.14}$	$5.75^{+/-0.13}$	$7.07^{+/-0.15}$	$6.10^{+/-0.11}$	$1.00^{+/-0.04}$	$1.06^{+/-0.03}$	$726.9^{+/-25.5}$	$574.7^{+/-17.7}$
1.0M	$9.08^{+/-0.20}$	$7.70^{+/-0.11}$	$9.20^{+/-0.14}$	$8.13^{+/-0.11}$	$1.01^{+/-0.04}$	$1.05^{+/-0.03}$	$1256.2^{+/-44.1}$	$985.1^{+/-21.4}$
1.2M	$9.96^{+/-0.15}$	$8.96^{+/-0.15}$	$9.41^{+/-0.17}$	$8.67^{+/-0.12}$	$0.93^{+/-0.05}$	$0.96^{+/-0.03}$	$1418.3^{+/-31.9}$	$1193.6^{+/-26.6}$
1.8M	$10.12^{+/-0.17}$	$8.80^{+/-0.19}$	$9.76^{+/-0.16}$	$8.91^{+/-0.18}$	$1.01^{+/-0.05}$	$0.96^{+/-0.05}$	$1459.5^{+/-33.1}$	$1266.1^{+/-45.9}$

Table 4.2 Comparing the DNA loops of salt extracted chromosomes 18 and 19

The ratio of mean width and area (Table 4.1) for chromosome 19:18 following extraction at increasing salt concentrations.

Salt concentration	19:18 area comparison	19:18 width comparison
0.0M	0.86	0.91
0.5M	0.79	0.82
1.0M	0.78	0.85
1.2M	0.84	0.91
1.8M	0.87	0.87
Mean value	0.83	0.87

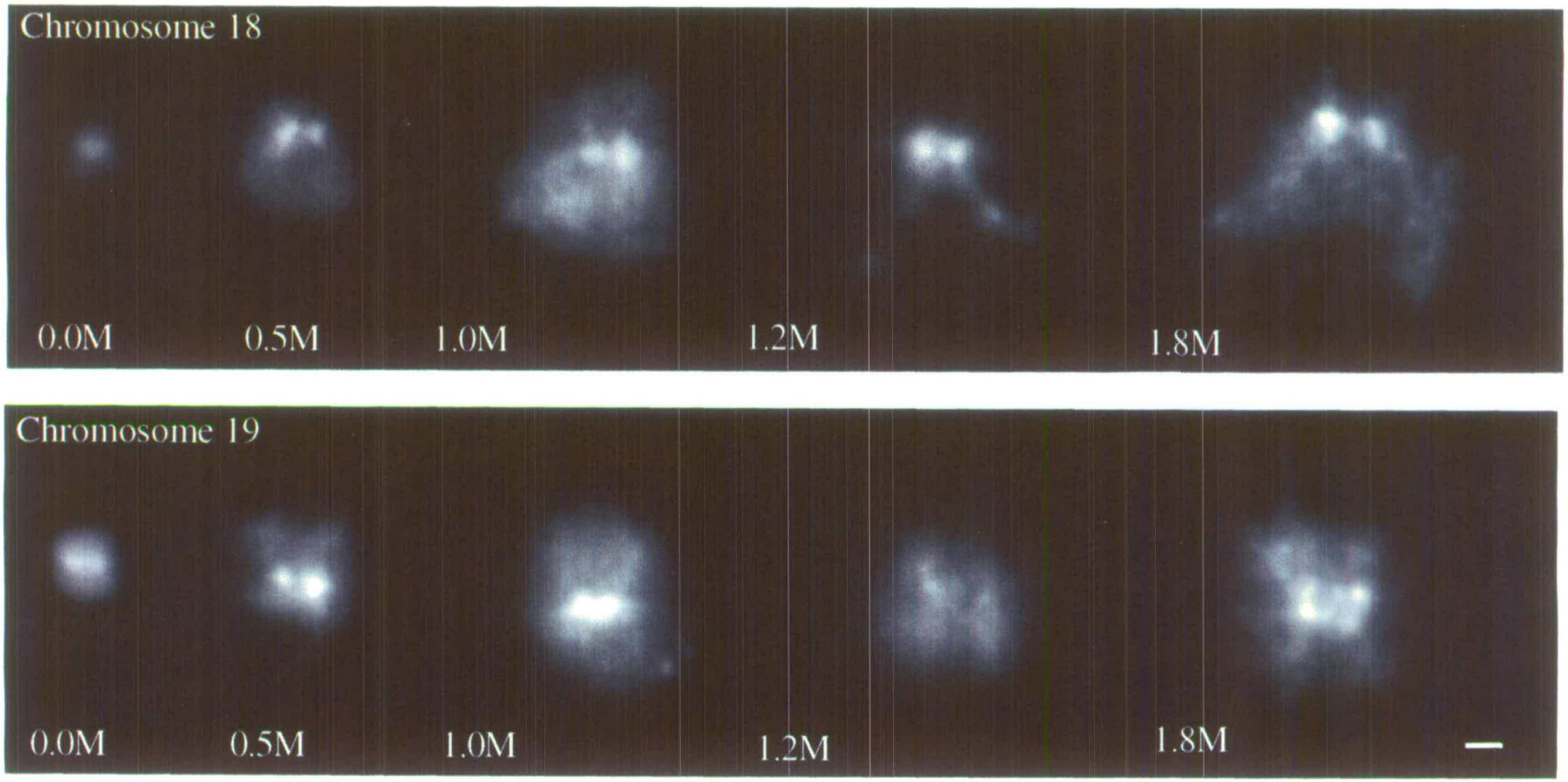

Figure 4.3 Salt extraction of human chromosomes 18 and 19
Grey scale images of DAPI stained chromosomes, representative for chromosomes 18 and 19, extracted at increasing salt concentrations. FISH with chromosome specific paints was used to identify the chromosomes. The centromeres are marked by bright regions of DAPI staining. The two sister chromatids of each chromosome can be observed. The two chromosomes do not change significantly in size with respect to one another as salt concentration increases. Bar = 1μm

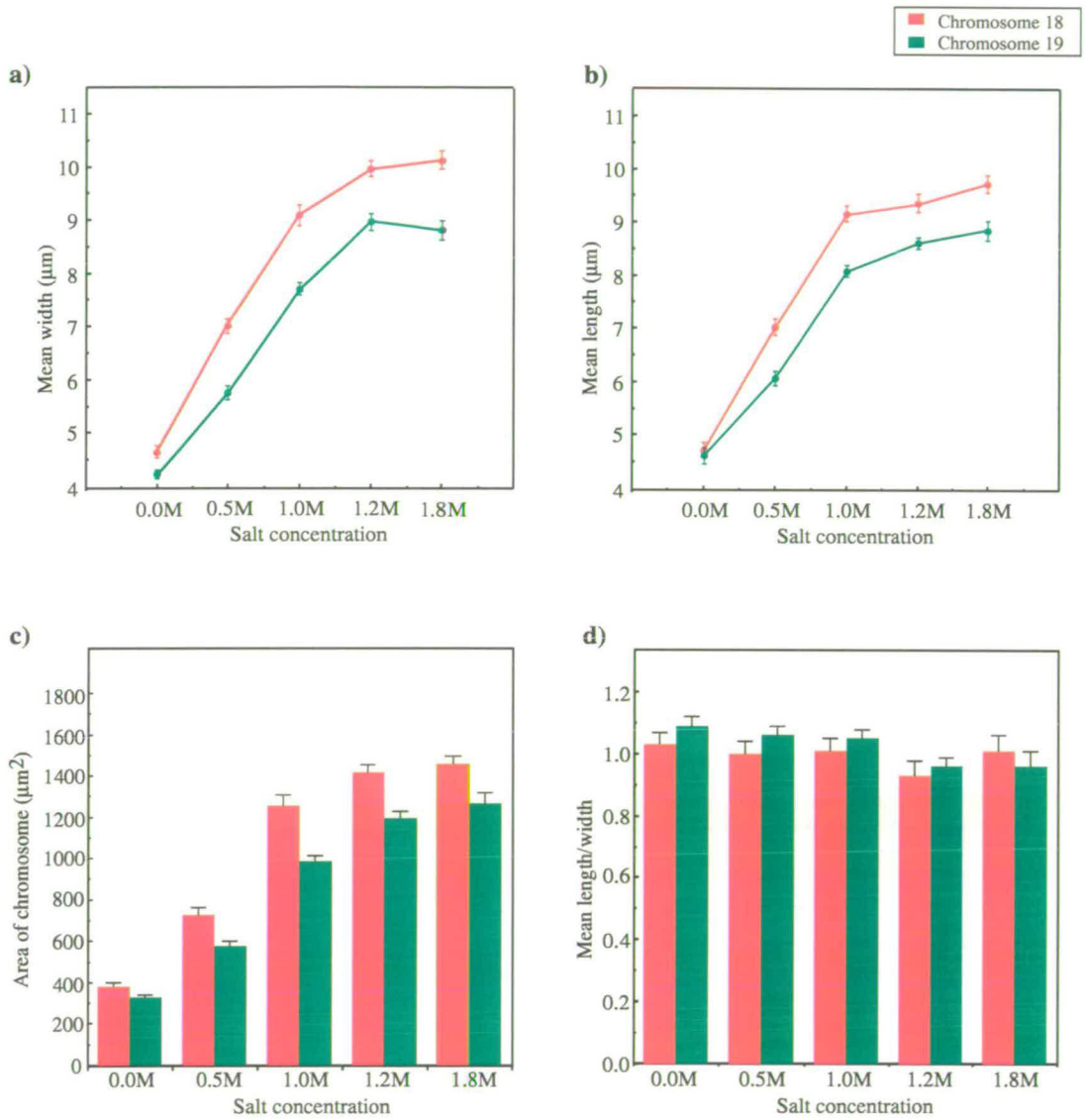

Figure 4.4 Comparisons between salt extracted human metaphase chromosomes 18 and 19

Graphs showing the parameters of human metaphase chromosomes 18 and 19 when extracted with increasing salt concentrations: (**a**) mean width (μm), (**b**) mean length (μm), (**c**) mean area (μm^2), and (**d**) mean length divided by width. FISH was used to identify chromosomes 18 and 19 and the width, length and area occupied by each of 25 chromosomes of each was measured using IPLab Spectrum software. +/– standard error of mean

4.4 The location of genes in salt extracted chromosome 18

The chromosome territory hypothesis of interphase nucleus organisation (Section 1.5.3) emphasises the importance of the periphery of each territory. Channels are considered to exist, which allow the movement of protein and RNA, but do not penetrate the confines of each territory area. RNA transcripts and splicing components are generally excluded from chromosome territories (Zirbel *et al.*, 1993). Further to this, Kurz *et al.* (1996) located coding and non-coding sequences in relation to chromosome territories. Their analysis of three coding sequences showed them to be positioned close to the periphery of the chromosome territories in which they reside, regardless of the activity of the genes which the sequences represented. The two non-coding sequences studied were localised either randomly or preferentially in the interior of the corresponding territory. The sample size in this experiment was very small and the authors suggest that further analysis of an increasing number of sequences are required. Genes located on the surface of a territory would be more readily in contact with transcription complexes and be able to recruit splicing factors from speckles (Section 1.5.2). The composition of proteins at the mitotic chromosome periphery may reflect this suggested distribution of genes (Section 1.6.5). The perichromosomal layer includes ribonuclear proteins, many of which remain uncharacterised (Spector & Smith, 1986; Gautier *et al.*, 1992), but may be remnants of splicing complexes. Also included are some nucleolar proteins, for example, fibrillarin, which is believed to be involved in early processing of rRNA in the nucleolus (Ochs *et al.*, 1985; Jimanez-Garcia *et al.*, 1989; Yasuda & Maul, 1990).

CpG-islands are ideal markers for human genes, with almost 60% of human genes having a CpG-island at the 5' end (Larsen *et al.*, 1992) (Section 1.3.7.4). Can CpG-islands be used collectively as gene markers to show exactly where genes are located within chromosomes? To test this, FISH probes were prepared from CpG-islands fractionated from individual chromosomes and hybridised to salt extracted mitotic chromosomes.

4.4.1 Preparing chromosome 18 CpG-island and non-CpG-island fragments for FISH

Cross *et al.* (1994) devised a methylated DNA binding column for the purification of CpG-island fragment libraries. By addition of linkers, these fragments could be amplified by PCR and labelled to be used as probes for FISH. Since chromosome 18 has so few CpG-islands and genes located along its length (Section 1.7 & Figure 1.3), this may be a

good chromosome on which to determine any pattern of CpG-island and, thus, gene distribution with respect to either the periphery or the interior of the chromosome. FISH using CpG- and non-CpG-island DNA fragments was performed upon salt extracted mitotic chromosomes and the distribution compared with the signal from whole chromosome 18 paint.

The chromosome 18 CpG-island fragment library was produced by Dr. S.H. Cross, University of Edinburgh. A preparation of chromosomes 18 were sorted by FACS (Dr. N. Carter, Sanger Centre, Cambridge) and digested with the restriction enzyme *MseI*. This enzyme has a cutting site of TTAA which cuts rarely within CpG-islands but frequently within bulk DNA and, thus, it leaves CpG-islands relatively in tact. The methyl-CpG binding domain (MBD) of the rat chromosomal protein, MeCP2 (Section 1.4.5) binds specifically to single symmetrically methylated CpG pairs (Cross *et al.*, 1994). MBD was attached to a column matrix, over which the chromosome 18 *MseI* fragments were passed. Methyl-CpG containing fragments were retained in the column while CpG-island fragments were contained in the fraction of fragments that bound weakly and were stripped from the column. The stripped fraction was then subjected to treatment with bacterial methyltransferase, to methylate all non-methylated CpGs. CpG-island containing fragments were then converted from weak binding to strong binding fragments and on a second run over the column those fragments which eluted at high salt were selected as a CpG-island library. The remaining fragments were kept as a non-CpG-island fraction. To confirm the identity of these fractions, a sample of fragments were cloned and tested for the presence of *BstU1* sites. This restriction enzyme recognises the sequence CGCG which occurs frequently within CpG-islands but rarely in bulk DNA (Cross *et al.*, 1994).

Catch-linkers CH18-1and CH18-2 (Section 3.3.2) were attached to the fragments of both the CpG- and non-CpG-island fractions. Using the CH18-2 sequence as a primer, the fragments were amplified by linker PCR using the cycling conditions described in Section 2.4.2.2. Fragments were labelled for FISH by incorporating dUTP conjugated with biotin or digoxigenin (dig) into the PCR reaction (Section 2.4.2.3). Prior to FISH, 200ng of probe were pre-hybridised with 20μg of human C_0t1 DNA to suppress highly repetitive sequences.

4.4.2 FISH with chromosome 18 CpG- and non-CpG-island fragments to extracted mitotic chromosomes

Figure 4.5a shows hybridisation of the chromosome 18 CpG-island probe to a typical 3:1 methanol:acetic acid fixed chromosome. When a whole human CpG-island probe is used to paint metaphase chromosomes, little or no hybridisation is observed along chromosome 18 (Craig & Bickmore, 1994) (Figure 1.3), due to the dominant hybridisation of this probe to regions of the genome with a high CpG-island density. However, hybridisation of CpG-islands from chromosome 18 alone resulted in a pattern of hybridisation that generally reflected its banding distribution, with the highest levels of hybridisation correlating with R-bands (compare Figure 4.5a & c with Figure 4.5e). This pattern of hybridisation was also revealed by FISH with the chromosome 18 CpG-island probe to salt extracted chromosomes (compare Figure 4.5b & d with Figure 4.5e). These data argue that this CpG-island probe truly reflects the distribution of genes along chromosome 18.

Metaphase chromosomes extracted with increasing salt concentrations (Section 4.3) were hybridised with differentially labelled chromosome 18 CpG-island probe and whole chromosome 18 paint (Section 3.3.2). Figure 4.6 shows a representative chromosome at each salt concentration. For each chromosome a graph of mean signal intensity laterally across the chromosome was drawn. To do this, the chromosome length was measured in pixels using IPLab Spectrum software. A line was then drawn manually width-wise, dividing the chromosome exactly in half length-wise. The parameters of the graph command were set such that it produced an average of the pixel intensities for each fluorochrome along the total length of the chromosome, for each pixel across its width.

The chromosomes were reasonably flat on the slide with the majority visible within one focal plane. The loops of DNA appear to spread across the surface of the slide resulting in a symmetry of loop sizes between sister chromatids and suggesting that loops above and below the chromosome axis have also spread horizontally (Also see: Bickmore & Oghene, 1996). If genes were preferentially located toward the periphery of the mitotic chromosome, that is, at the end of each loop, it might be expected that there would be a higher amount of signal from the CpG-island probe compared with that of the total chromosome paint at the extremes of the graphs. However, it is clear from Figure 4.6 that the distribution of CpG-island signal exactly mirrors that of total chromosome 18 paint.

As a reciprocal experiment, the non-CpG-island fraction was also hybridised to extracted mitotic chromosomes in conjunction with total chromosome 18 paint. Figure 4.7 shows a pattern of distribution very similar to that in Figure 4.6. It might have been expected that the signal from the non-CpG-island probe would drop away at the extremes of the graphs more sharply than the signal from the total chromosome paint.

It is difficult to prove that chromosomes prepared by salt extraction exactly preserve their intracellular structure. However, topo II is maintained along the chromosome axis and centromere proteins and the primary constriction appear to remain at the intracellular site of the chromosome (Personal communication: Dr. W.A. Bickmore). Analysing the distribution of CpG-island fragments on salt extracted chromosomes, I could detect no bias of signal either towards the chromosome axis or towards the outer edge of the loops. A similarly uniform distribution was observed with non-CpG-island fragments. From this it appears that there is no gross level of gene organisation laterally in metaphase chromosomes. These results argue against Cook's model (1994 & 1995) of transcription regions defining the sites of attachment and driving the condensation of the mitotic chromosome, since this would predict that CpG-islands would be located most frequently at the chromosome axis. The data in this section also demonstrate that genes are not preferentially located towards the outer edge of the metaphase chromosome, contradicting the conclusions of Kurz *et al.* (1996). However, the data set used in the latter study was small and, thus, may not be representative. The chromosome 18 CpG-island probe used in my investigations is likely to represent over half the number of coding genes present and indicates no bias of distribution of coding sequences towards the chromosome 18 periphery. Additionally, the experiments of Kurz *et al.* (1996) were carried out at interphase. It is possible that the decondensation of chromosomes following mitosis is accompanied by a reorganisation that results in coding sequences being brought preferentially to the surface of interphase chromosome territories. This will be further discussed in Section 7.5.

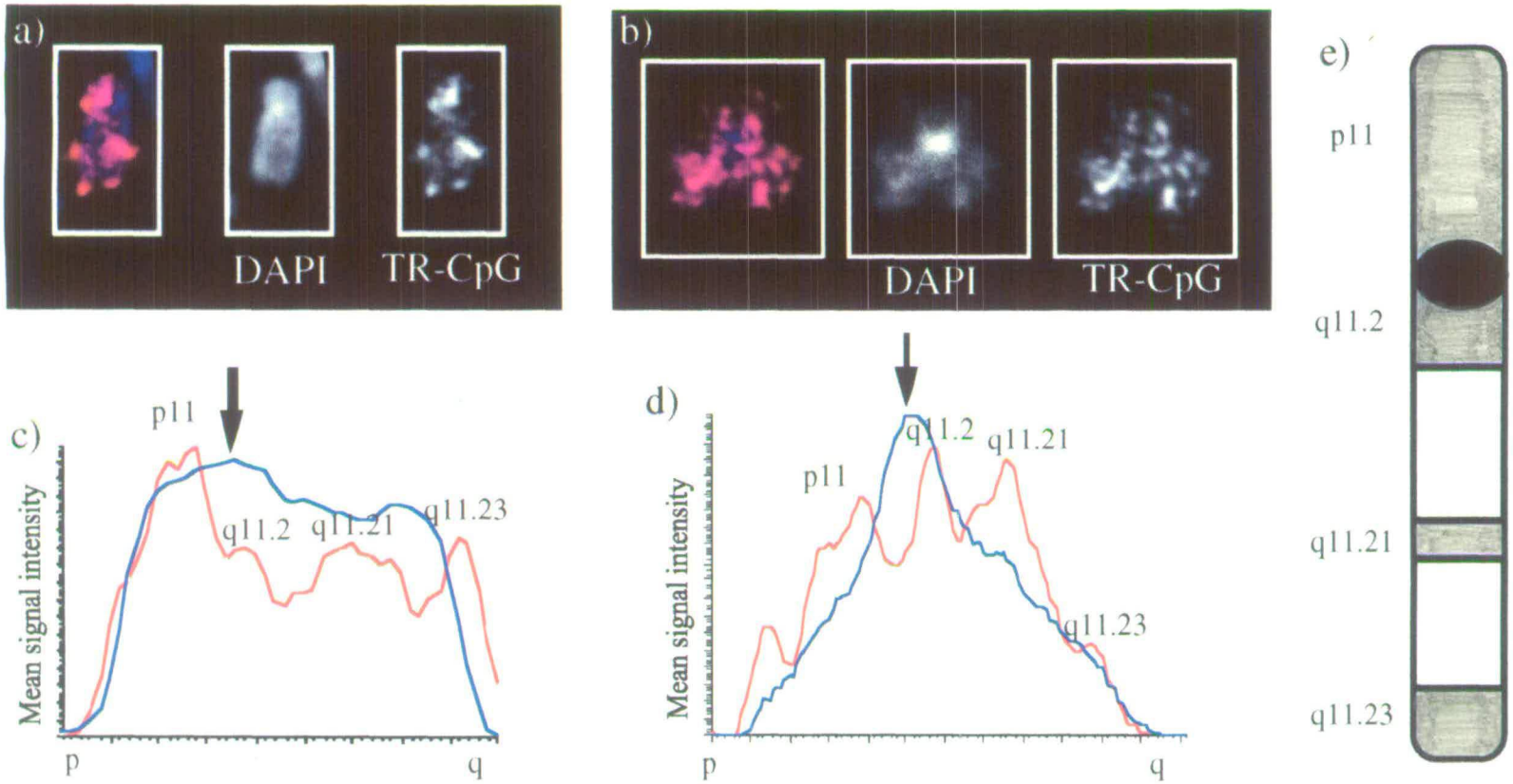

Figure 4.5 The distribution of CpG-island DNA along the length of chromosome 18
(**a**) (**b**) Hybridisation of chromosome 18 CpG-island fragments isolated using the methyl-CpG binding column (Cross *et al.*, 1994), labelled with biotin and detected with avidin-TR (red). Chromosomes counterstained with DAPI (blue). (**c**) (**d**) Graphs of average signal over the width of each chromosome, from the tip of the p-arm to the tip of the q-arm. The lines are the appropriate colour for the fluorochrome that they represent. (**a**) (**c**) Typical 3:1 methanol:acetic acid fixed chromosome 18. (**b**) (**d**) Chromosome 18 extracted with 1.2M salt. (**e**) Ideogram of chromosome 18 at 300 bands/genome resolution. Grey- R-bands White- G-bands Black- centromere

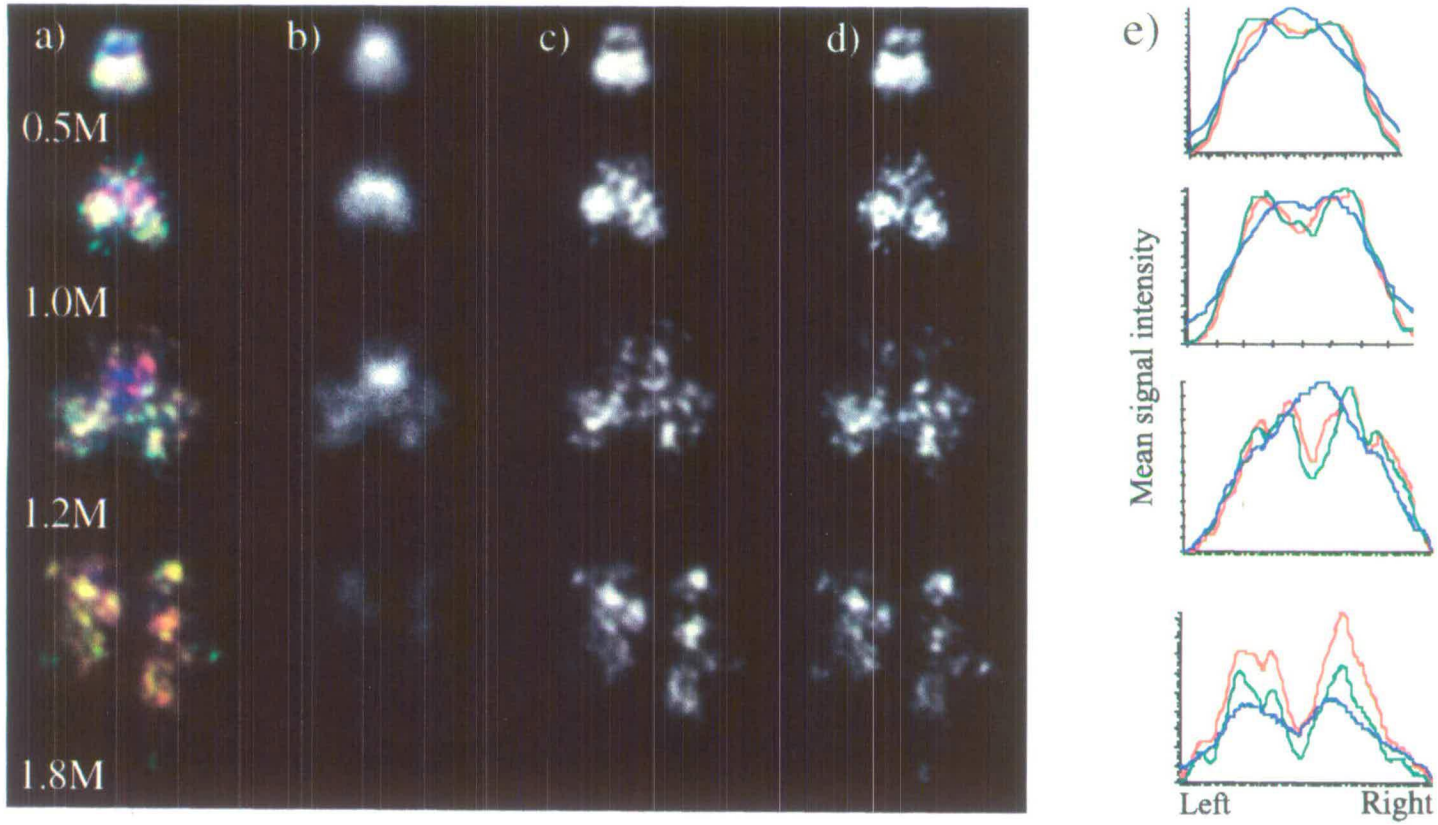

Figure 4.6 The distribution of CpG-island DNA laterally across salt extracted human chromosome 18
Chromosomes 18 extracted at increasing salt concentrations. (**a**) Co-hybridisation of chromosome 18 CpG-island fragments isolated using a methyl-CpG binding column (Cross *et al.*, 1994), labelled with biotin and detected with avidin-TR (red), and total chromosome 18 FISH paint, labelled with dig and detected with anti-dig-FITC (green). Chromosomes were counterstained with DAPI (blue). Grey scale representations of each fluorochrome are shown: (**b**) DAPI, (**c**) CpG-island DNA (TR), and (**d**) total human DNA (FITC). (**e**) Graphs of mean signal over the length, measured across the width of the each chromosome from left to right. The lines are the appropriate colour for the fluorochrome that they represent.

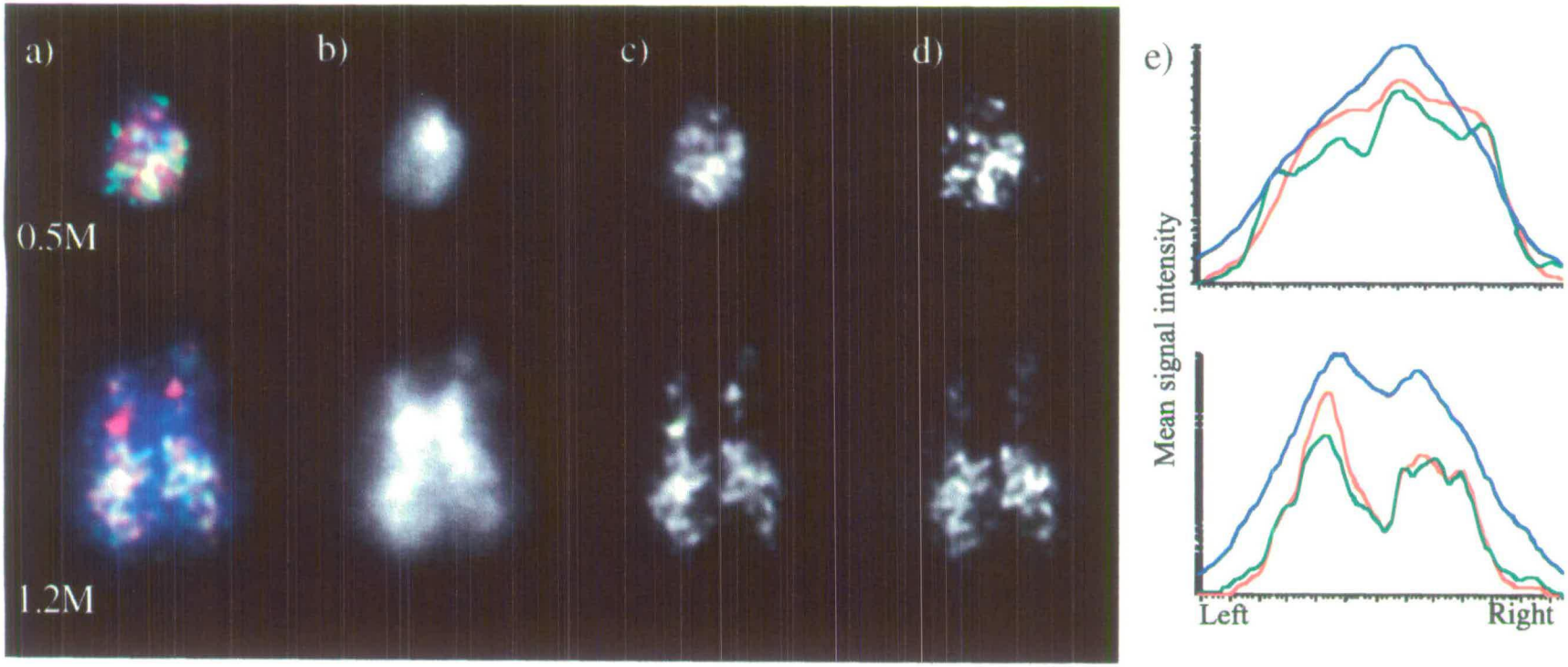

Figure 4.7 The distribution of non-CpG-island DNA laterally across salt extracted chromosome 18
Chromosome 18 extracted at increasing salt concentrations. (**a**) Co-hybridisation of chromosome 18 non-CpG-island fragments isolated using the methyl-CpG binding column (Cross *et al.*, 1994), labelled with biotin and detected with avidin-TR (red), and total chromosome 18 FISH paint, labelled with digoxigenin and detected with anti-digoxigenin-FITC (green). Chromosomes were counterstained with DAPI (blue). Grey scale representations of each fluorochrome are shown: (**b**) DAPI, (**c**) non-CpG-island DNA (TR), and (**d**) total human DNA (FITC). (**e**) Graphs of mean signal over the length of each chromosome, measured across the width of the chromosome from left to right. The lines are the appropriate colour for the fluorochrome that they represent.

4.5 Summary

The data presented in this chapter indicate that at metaphase, chromosomes 18 and 19 do not differ significantly in their structure and DNA packaging. In 3:1 methanol:acetic acid fixed spreads chromosome 18 was consistently found to be 10% larger than chromosome 19 (Section 3.4). When salt was used to strip away the proteins involved in chromatin folding, releasing a halo of DNA loops, chromosome 18 remained larger than chromosome 19 to a similar degree. This suggests that the loop sizes along the length of these two chromosomes are similar and that the loops are attached to the chromosome axis at positions that are relatively evenly spaced throughout the genome. These sites of attachments are not likely to be purely AT-rich SARs, nor transciptionally active regions, since these sites would be predicted to have completely contrasting distributions along these two chromosomes. In addition, genes, represented by CpG-islands, are neither predominantly distributed at the chromosome axis nor the surface of the chromosome loops. This conflicts with models that suggest that sites of transcription are the sites of attachment to the chromosome scaffold. It also suggests that genes are not exposed to the surface of metaphase chromosomes.

Although there is no striking difference in the higher order DNA packaging of human chromosomes 18 and 19 at metaphase that reflects the different gene densities of these two chromosomes, it has been previously demonstrated that there are contrasting differences at the level of the nucleosome (Section 1.7). Immunofluorescence to metaphase chromosomes has shown low levels of core histone H4 acetylation along the entire length of chromosome 18, while chromosome 19 has a predominance of highly acetylated H4 (Jepessen *et al.*, 1992) (Figure 1.6), consistent with acetylation being correlated with transcriptionally active chromatin. These immunofluorescence studies reveal the steady state of histone acetylation, but acetylation is a reversible process. Could human chromosomes 18 and 19 be used to investigate the dynamics of core histone acetylation? Chapter 5 approaches this question, attempting to build a more detailed picture of the differences and similarities between the chromatin of these two chromosomes.

5. Immunofluorescence studies of core histone acetylation along human metaphase chromosomes

5.1 Introduction

The previous chapter examined the DNA packaging of human chromosomes 18 and 19 at metaphase, showing no striking differences between the two chromosomes that reflect their contrasting functional features. This chapter steps back a structural level to that of the nucleosomes and core histones. The core histones are subject to a number of modifications, of which, acetylation is the most studied (Section 1.4.1). High levels of core histone acetylation in chromatin are correlated with potential transcriptional activity (Hebbes *et al.*, 1988, 1992 & 1994; Tazi & Bird, 1990; O'Neill & Turner, 1995), while hypoacetylation has been revealed at regions of transcriptional repression (Braunstein *et al.*, 1996; Ekwall *et al.*, 1997; Review: Thompson *et al.*, 1993).

The most direct link between acetylation and transcriptional activity has come from the cloning of the several histone acetyltransferases and deacetylases, many of which have been assigned activities as transcriptional co-activators (Brownell *et al.*, 1996; Yang *et al.*, 1996b; Taunton *et al.*, 1996; Reviews: Grunstein, 1997; Wade *et al.*, 1997). Acetylation facilitates the binding of transcription factors (Lee *et al.*, 1993; Vettese-Daley *et al.*, 1994 & 1996) and is considered, by most, to cause a reduction in the wrapping of DNA around the nucleosome, resulting in a more "open" chromatin structure (Review: Garcia-Ramirez *et al.*, 1995).

Antibodies raised to the different isoforms of acetylated H4 have been used, at the cytological level, to reveal patterns of distribution along metaphase chromosomes in several organisms. In general, the tri- and tetra-acetylated isoforms correlate with the most gene-rich regions of the genome (Jeppesen *et al.*, 1992; Turner *et al.*, 1992; Jeppesen & Turner, 1993; Houben *et al.*, 1996 & 1997; Idei *et al.*, 1996). Particularly striking is the link between hyperacetylation and the highly transcribed X-chromosome of *D.melanogaster* males (Turner *et al.*, 1992). Conversely, in humans the inactive X-chromosome (Xi) of females is hypoacetylated (Jeppesen *et al.*, 1992). Acetylation is clearly involved in sex chromosome dosage compensation, although not in its initiation (Keohane *et al.*, 1996). The study of human X-chromosomes segregated as micronuclei has shown Xi is also hypoacetylated at interphase (Surralles *et al.*, 1996), suggesting that acetylation patterns are generally maintained throughout the cell cycle. Since many transcription factors and polymerases appear to be displaced from mitotic chromosomes (Martinez-Balbas *et al.*, 1995; Segil *et al.*,

1996), it seems that heritable histone modifications, such as acetylation are likely to be a means of passing on information regarding the transcriptional status of a particular region (Jeppesen, 1997; Wade *et al.*, 1997). Breneman *et al.* (1996) fractionated chromatin derived from human interphase nuclei by their general levels of acetylation and hybridised these fragments to metaphase spreads by FISH. No competition of highly repetitive sequences was used resulting in some spurious hybridisation, but generally, regions of high acetylation hybridised to R-bands and hybridisation of fragments with low levels of acetylation corresponded to G-bands and heterochromatic regions.

Acetylation is reversible. Turnover of the acetylation of core histones continues throughout the cell cycle, with depletion of the more acetylated isoforms and a change in site usage, during mitosis (Turner, 1989). Two distinct populations of core histones have been shown to exist. By following incorporation of tritiated acetate, it was calculated that <15% of histones made up a minor population showing rapid acetylation and removal, while the remainder showed a less rapid turnover. No interconversion between the two populations appeared to occur. The turnover of acetylation for tetra-acetylated H4 was concluded to be greater than that of mono-acetylated H4 (Covault & Chalkley, 1980). How are these two populations of histones distributed throughout the genome? Is there a connection between acetylation turnover and transcriptional activity? What can be established about the turnover of acetylation along chromosomes 18 and 19?

To answer these questions, I made use of an antibody raised to acetylated H4 and observed differences in the pattern of binding along metaphase chromosomes following treatment of the cells with different inhibitors of deacetylation. By blocking deacetylation it is possible to compare the rates of the forward acetylation reaction only and, indeed, inhibitors of deacetylation have often been used to enhance patterns of immunofluorescence against acetylated histones. I used the changes in intensity of immunofluorescent signal at different chromosomal locations to establish a difference in acetylation turnover between G- and R-bands.

5.2 The dynamics of core histone acetylation

A rabbit polyclonal antibody (R41) raised to H4 acetylated at lysine 5 (lys5) was obtained from Prof. B. Turner, University of Birmingham. In mammals, lys16 is the position most commonly modified in mono-acetylated H4. Next to be acetylated is usually lys12 or lys8 and lastly, lys5 (Turner & Fellows, 1989), hence, the R41 antibody recognises

the most highly acetylated forms of H4. Immunofluorescence with this antibody to human metaphase chromosomes, has been previously shown to correlate strongly with R-bands (Jeppesen *et al.*, 1992) and to show little staining along the inactive X chromosome (Jeppesen & Turner, 1993).

Figure 5.1 shows a selection of human metaphase chromosomes following immunofluorescence with this antibody. Metaphase chromosomes for immunofluorescence cannot be fixed with typical 3:1 methanol:acetic acid, since this destroys or may even extract the antigenic epitope. Instead, metaphase spreads were attached to slides by cytocentrifugation (Section 2.10.1). Slides were incubated with R41 antibody for 2 hours at room temperature, followed by anti-rabbit antibody conjugated to Texas Red (TR) fluorochrome for 30 minutes (Section 2.10.2). They were fixed gently in 4% paraformaldehyde for 15 minutes before mounting with DAPI counterstain. Immunofluorescence with the pre-immune serum resulted in a general background and no staining of the chromosomes (results not shown). Figure 5.1 also shows chromosomes hybridised by FISH with *HpaII* tiny fragments, chosen to represent CpG-islands, which have also been shown to correlate strongly with R-bands (Craig & Bickmore, 1994). Strong R41 signal at R-bands was not unexpected, since R-bands are gene-rich (Section 1.3.7) and, thus more highly transcribed than G-bands. Particularly striking is that chromosome 18 shows very little R41 signal along its length and, thus, low levels of H4 acetylation while chromosome 19 shows a high degree of fluorescence, consistent with its high gene density and transcriptional activity (Figures 1.6 & 5.1).

This experiment demonstrates an overall state of acetylation of chromosomes in metaphase. To investigate the dynamics of acetylation, the patterns of fluorescence obtained along metaphase chromosomes using the R41 antibody were assessed following the treatment of cells with two different inhibitors of histone deacetylation:

- Sodium butyrate (NaB) - This has been known for a long time to result in increased histone acetylation (Riggs *et al.*, 1977; Vidali *et al.*, 1978) due to the non-competitive inhibition of histone deacetylase activity (Cousens *et al.*, 1979). The effective concentration is, however, rather high which causes subsidiary effects on other enzymes, in addition to altering both phosphorylation and methylation states of histones, other nuclear proteins and DNA (Boffa *et al.*, 1981 & 1994; Kruh, 1982; D'Anna *et al.*, 1983).
- Trichostatin A (TSA) - This is a very potent and specific inhibitor of histone deacetylation. It reversibly blocks the action of the histone deacetylase(s) by acting on the

enzymes themselves by a mechanism that is not fully understood (Yoshida *et al.*, 1990; Review: Yoshida *et al.*, 1995).

Both of these histone deacetylase inhibitors cause generalised increases in histone acetylation, with no distinction between the different lysine residues (Yoshida *et al.*, 1995). By assessing the increase of immunofluorescent signal at different regions along a metaphase chromosome, the turnover of acetylation in those regions can be compared. The degree of immunofluorescence signal obtained across a metaphase spread can sometimes vary and, thus, two regions on the same chromosome were chosen to study rather than comparing chromosomes 18 and 19 directly. An adjacent G- and R-band region on chromosome 1 were used for comparison. The tip of the p-arm of chromosome 1 consists of several T-bands and the region is generally early replicating, CpG-island-rich and shows a low level of steady state acetylation (Figure 5.1). Between this and the centromere, is a region that is dominated by particularly dark staining G-bands, is generally late replicating, poor in CpG-islands and shows a high level of steady state histone acetylation (Figure 5.1).

Cultures of the human REN2 lymphoblastoid cell line were treated prior to harvesting, as follows:

1. 4mM NaB for 2 hours
2. 10ng/ml TSA for 2 hours
3. No treatment

These treatments have been previously shown to be sufficient to perturb patterns of replication in human lymphoblastoid cells (Bickmore & Carothers, 1995). Cells were swollen in hypotonic and cytocentrifuged onto slides. Slides were incubated with R41 antibody for 2 hours at room temperature, followed by anti-rabbit-TR for 30 minutes (Section 2.10.2), then fixed in 4% paraformaldehyde for 15 minutes before mounting with DAPI counterstain. Figure 5.2 shows examples of immunofluorescence with R41 to chromosome 1 following each treatment. Following cytocentrifugation, sister chromatids of metaphase chromosomes are usually separated. The profiles of red and blue fluorescence intensity along the length of the p-arm are shown for the left chromatid of each representative chromosome. Visual patterns and profiles of immunofluorescence from sister chromatids were consistently similar. It is clear from the R41 (red) signal profile in Figure 5.2, that the distance from each peak to adjacent trough, is greater following treatment with NaB and greater still following treatment with TSA, than along untreated chromosomes. This is not paralleled by similar changes in DAPI (blue) fluorescence profile that might be attributed to

changes in chromosome condensation. Therefore, the data in Figure 5.2 suggests that the regions of highest acetylation on chromosome 1 become even more highly acetylated relative to the regions of lowest acetylation when deacetylation is inhibited.

In order to quantify this, a script was devised by Dr. P. Perry, MRC Human Genetics Unit, Edinburgh, using IPLab Spectrum software. The analysis performed by the script was as follows:

1. Manually a line was drawn along the length of the chromosome p-arm.
2. The line was divided into five segments of equal length (Figure 5.3a).
3. The total amount of red (R41) and blue (DAPI) fluorescent signal emanating from each segment was calculated by summing the intensity from each pixel within that segment (Table 5.1).

A direct comparison could now be made between segment 2, which was within the T-band dominated region of the p-arm (Figure 5.3a) and segment 4, which was within the dark G-band region. These two segments were chosen because they were entirely representative of the band type in which they resided. Both sister chromatids of 20 chromosomes for each treatment were analysed and the ratio of the total amount of red fluorescence for the selected segments was calculated (Table 5.1 & Figure 5.3b). The same analysis was made for the DAPI fluorescence. These measurements would act as an internal control for the possible effects of different degrees of chromatin compaction, since the chromosome length varied considerably between spreads (Table 5.1 & Figure 5.3c). Therefore, the R41 fluorescence was normalised by dividing by the DAPI fluorescence of the corresponding segment.

Segment 2 has a higher mean normalised total R41 fluorescence intensity than segment 4 in untreated chromosomes. In addition, the increase in intensity is greater for segment 2 than segment 4 after treatment with NaB and TSA. This difference is reflected in the increase in ratios of segment 2:4 following each treatment (Figure 5.3b). Using Student's T-test (ST), it was calculated that the increase in ratio was statistically significant (ST $p<0.0004$) between treated and untreated chromosomes. The increase in ratio between NaB and TSA treated chromosomes was also statistically significant (ST $p<0.0003$). From this it can be concluded that the rate of acetylation is faster in segment 2, than segment 4, implying that the rate of acetylation is faster in R-banded regions than G-banded regions.

The ratio of segment 2:4 DAPI fluorescence remains constant throughout (Figure 5.3c). This AT-specific fluorochrome gives a G-banding pattern of fluorescence reflected by the fact the

Table 5.1 The dynamics of histone acetylation along human chromosome 1

Cells were treated with one of two inhibitors of histone deacetylation, or subjected to no treatment, prior to harvesting. Immunofluorescence was carried out using an antibody to acetylated H4 (R41) on metaphase spreads counterstained with DAPI and images of 20 chromosomes 1, from slides following each treatment, were collected. One metaphase chromosome was analysed from the rodent-human somatic cell hybrid, A91neo (Figure 5.11c). Using a computer script devised by Dr. P. Perry, MRC Human Genetics Unit, Edinburgh, the p-arm of each chromosome was divided into five segments, of equal length (Figure 5.3) and the total amount of fluorescence in each segment was calculated for each segment. R41 fluorescence was normalised by dividing by the DAPI fluorescence for the corresponding segment. Segment 2 and 4 are representative of R- and G-band regions, respectively. +/- standard error of mean

Treatment	**Mean normalised total R41 fluorescence (pixels): segment 2**	**Mean normalised total R41 fluorescence (pixels): segment 4**	**Ratio of total R41 fluorescence (pixels): segment 2:4**	**Ratio of DAPI fluorescence (pixels): segment 2:4**
None	0.99	0.48	$1.5^{+/-0.02}$	$0.7^{+/-0.03}$
Sodium butyrate	1.07	0.41	$1.7^{+/-0.01}$	$0.7^{+/-0.03}$
Trichostatin A	1.42	0.49	$2.0^{+/-0.01}$	$0.7^{+/-0.03}$
Rodent-human somatic cell hybrid	1.01	0.42	1.6	0.8

ratio of segment 2:4 is approximately 0.5. The consistency of this figure confirms that the compaction of the chromosomes in each spread was approximately the same in these regions and was not affected by inhibition of deacetylation.

These data support the fact that there is a constant turnover of acetylation and that different regions of the genome show different rates of turnover. The gene-poor, G-bands show a rate of forward acetylation (and probably turnover) slower than the gene-rich, R-bands. Acetylation, in itself, may not be the only control of transcriptional activity of a gene, the rate at which an acetylation pattern is altered between different lysine residues and different nucleosomes may have consequences on gene activity. This is consistent with the findings of Covault & Chalkley (1980) who concluded that turnover of acetylation was greater for a minor population of highly acetylated species of H4. It is likely that this population of histones, which was estimated to be <15% of total histones, would be present in the most *Alu*-rich T-bands of the genome, which make up approximately 13% of the total genome (Holmquist, 1992). These experiments suggest that the turnover of histone acetylation along human chromosome 18 will generally be lower than along chromosome 19.

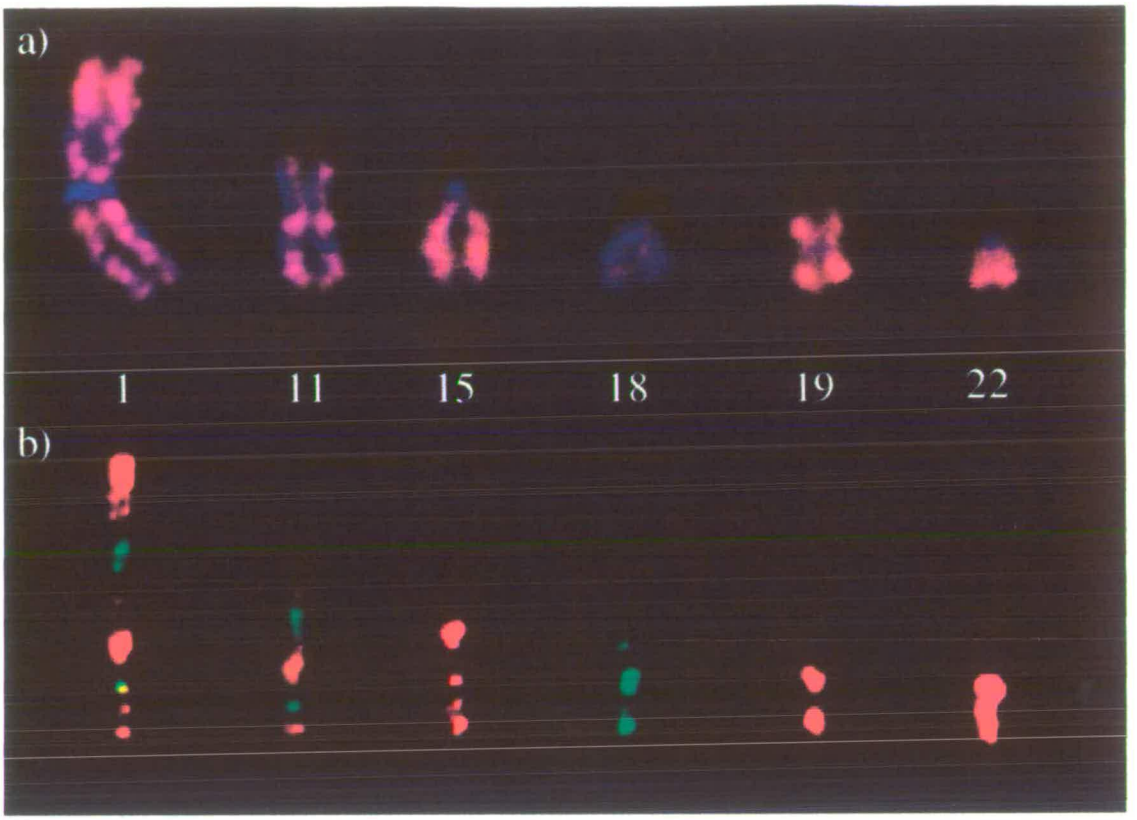

Figure 5.1 Immunofluorescence with R41 to human metaphase chromosomes
(**a**) Immunofluorescence with anti-acetylated H4 antibody (R41) detected with anti-rabbit-TR (red). Chromosomes were counterstained with DAPI (blue). (**b**) Adapted from Craig (1995). Chromosomes hybridised with small, biotin labelled *HpaII* fragments selected to represent CpG-islands and detected with avidin-TR (red). BrdU incorporation detected with anti-BrdU-FITC reveals late replicating regions in green.

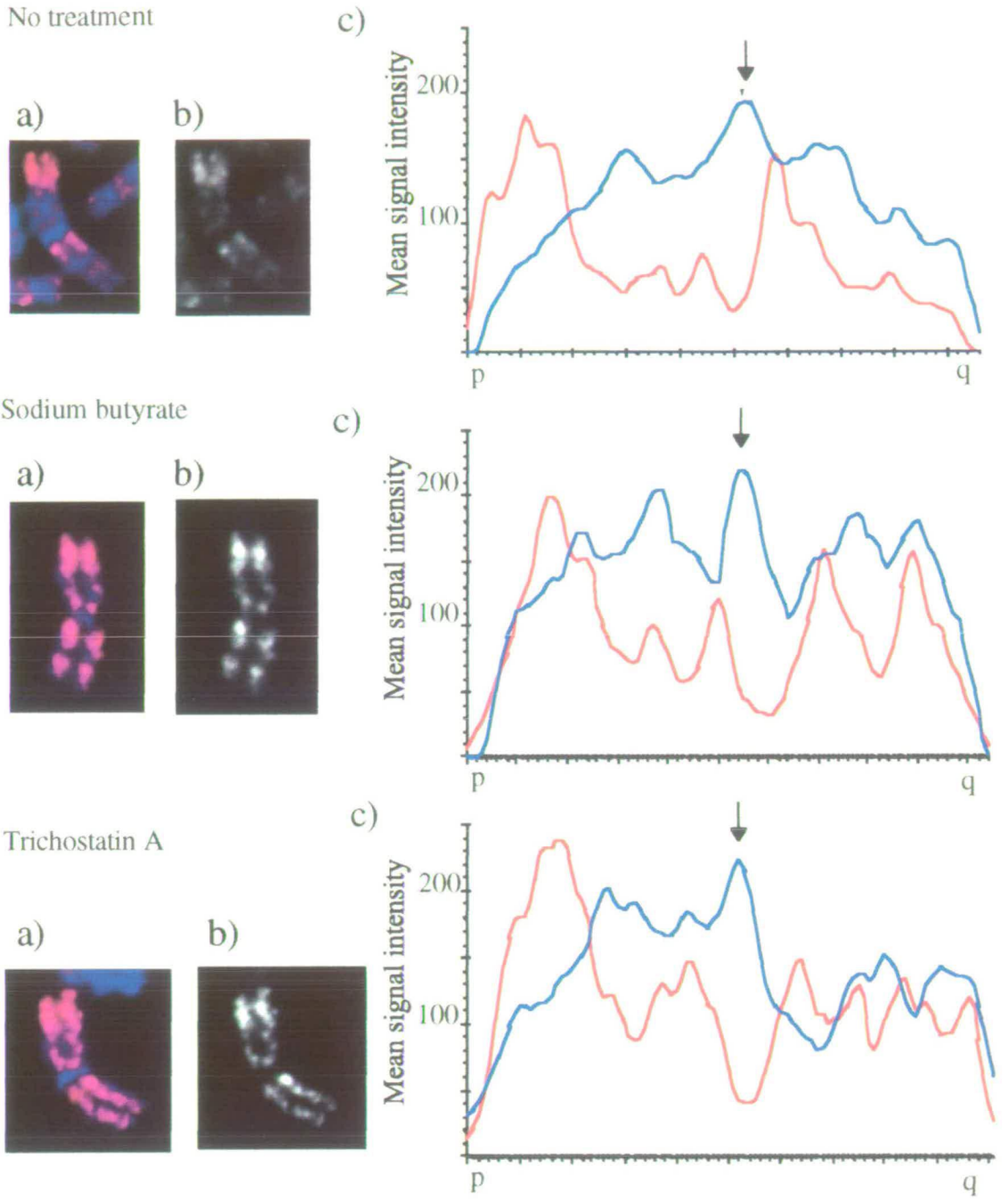

Figure 5.2 Immunofluorescence with R41 to human chromosome 1 following treatment with inhibitors of histone deacetylation

(**a**) Immunofluorescence with anti-acetylated H4 antibody (R41) detected with anti-rabbit-TR (red). Chromosomes counterstained with DAPI (blue). (**Top**) Chromosome 1 with no treatment. (**Middle**) Chromosome 1 following treatment with sodium butyrate. (**Bottom**) Chromosome 1 following treatment with Trichostatin A. (**b**) Grey scale representation of R41 (TR/red) signal. (**c**) Graphs of mean signal intensity over the width of the chromosome, measured along the length from the tip of the p-arm to the tip of the q-arm. Lines are the appropriate colour for the fluorochrome that they represent. Arrows indicate the position of the centromeres.

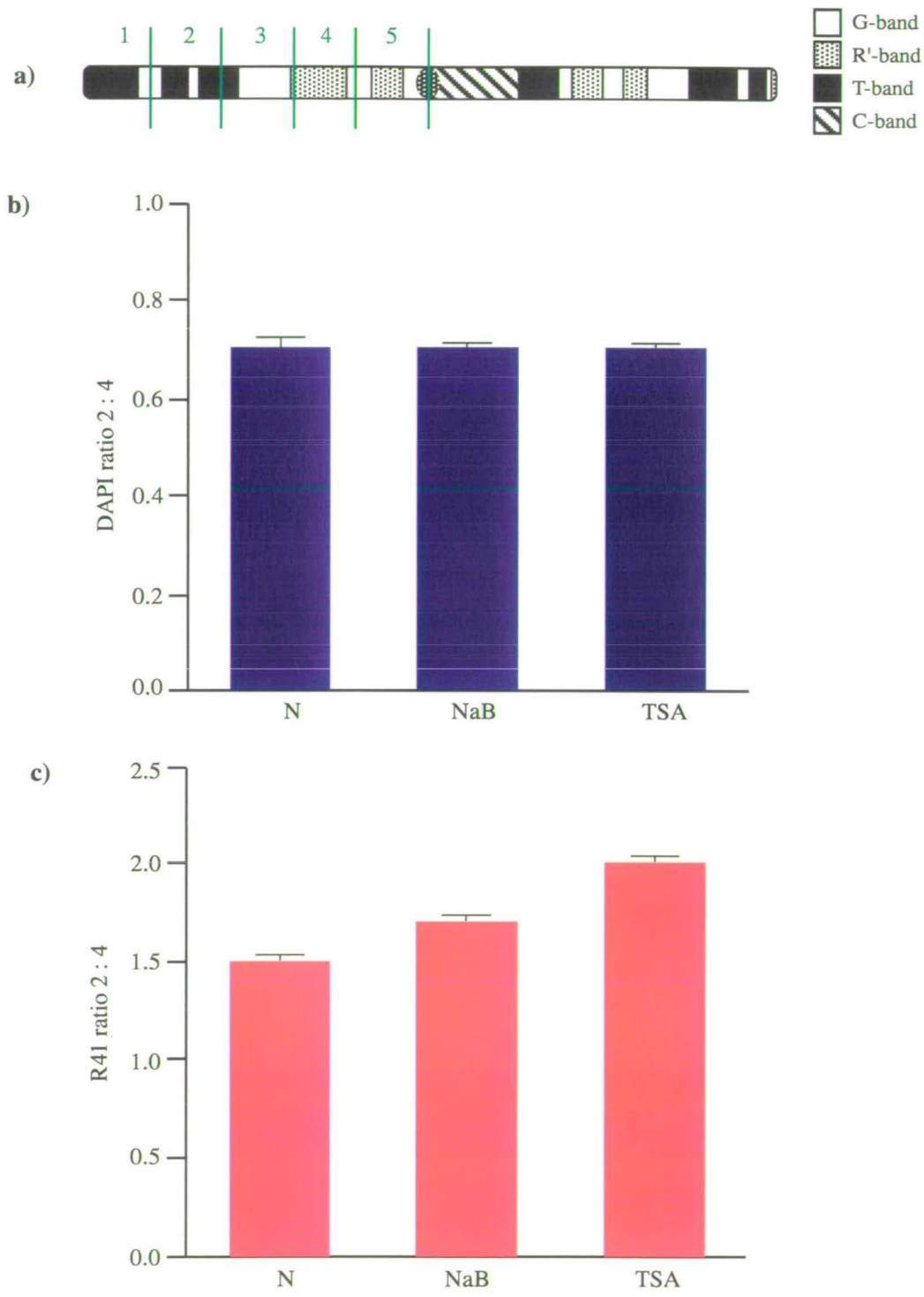

Figure 5.3 The dynamics of acetylation of H4 along the length of human chromosome 1 (**a**) An ideogram of chromosome 1 divided into the five equal segments along the p-arm used for analysis. (**b**) The ratio of segment 2:4 DAPI (blue) fluorescence. (**c**) The ratio of segment 2:4 R41 (TR/red) fluorescence. +/- standard error of the mean **N**- no treatment **NaB**- 4mM sodium butyrate added to cells for 2 hours prior to harvesting **TSA**- 10ng/ml Trichostatin A added to cells for 2 hours prior to harvesting

5.3 The chromatin environment of human rDNA

While analysing human metaphase spreads by immunofluorescence with R41 antibody, it was observed that the p-arms of each of the five acrocentric chromosomes showed little or no signal (Figure 5.4). This suggested that these regions were hypoacetylated, which is surprising, since they are one of the most highly transcribed regions of the human genome (Review: Sollner-Webb & Tower, 1986). This apparent hypoacetylation of rDNA was previously noted by Jeppesen (1997) but not adequately explained. The bulk of mammalian rDNA is hypomethylated and GC-rich, hence it fractionates with CpG-islands (Bird & Taggart, 1980; Cross *et al.*, 1994), and FISH with CpG-island fragments show strong hybridisation to the acrocentric p-arms (Craig & Bickmore, 1994) (Figures 1.3 & 5.4). Thus, like R-bands, rDNA is GC-rich and hypomethylated, but, unlike R-bands, it is hypoacetylated.

The centromere and p-arm of the acrocentric chromosomes (chromosomes 13, 14, 15, 21 and 22) can be broadly divided into four regions (Figure 5.5a) (Review: Choo, 1990), composed of various repetitive DNA sequences:

1. The most distal p-arm region is p13. On all acrocentrics this region constitutes β-satellite (Waye & Willlard, 1989; Greig & Willard, 1992), 724-satellite (Kurnit *et al.*, 1986) and a single copy sequence, designated ACR1 (Worton *et al.*, 1988).
2. The genes for the 28S, 18S and 5.8S ribosomal RNA (rDNA) are located within the stalk region, p12, often referred to as the nucleolar organising region (NOR) (Henderson *et al.*, 1972; Schmickel *et al.*, 1985). The 5S rDNA is situated at various non-acrocentric regions of the human genome. Each acrocentric chromosome possesses 30-40 copies of the 44Kb tandemly arranged ribosomal repeats, comprising of a 13Kb transcribed portion and an average 31Kb non-transcribed spacer (Figure 5.5b) (Worton *et al.*, 1988).
3. Adjacent to this region is a second variable region, p11, containing several types of repetitive DNA, but composed principally of satellites I, II, III and IV (Gosden *et al.*, 1975). All acrocentric chromosomes have satellite III DNA, while satellites I, II and IV are present at only a subset of the acrocentric chromosomes. Satellite I is a 42bp repeat and satellites II and III comprise of simple 5bp repeat units (Prosser *et al.*, 1986). Other sequences mapped to p11 include β-satellite (Waye & Willard, 1989; Greig & Willard, 1992) and 724-satellite (Kirnut *et al.*, 1986). Using FISH to extended chromatin fibres, these satellites appear to be arranged in contiguous blocks with little or no intervening DNA (Shiels *et al.*, 1997).

4. Finally, the primary constriction is universally considered to be the centromere of acrocentric chromosomes. It consists, as with all human centromeres, primarily of arrays of α-satellite DNA (Manuelidis, 1978; Mitchell *et al.*, 1985; Review: Singer, 1982).

The transcription of rDNA is catalysed by RNA polymerase I (pol I), differing from the remainder of the genome which relies upon RNA pol II (with the exception of the 5S rDNA which is transcribed by pol III). In order for a cell to produce its requisite of rRNA, the rDNA is required to be one of the most actively transcribed regions of the genome (Review: Sollner-Webb & Tower, 1986). Indeed, almost 80% of total cellular RNA is rRNA. This activity has been beautifully visualised by electron micrographic spreads of nucleolar chromatin which reveal "christmas-tree" structures as gradients of nascent transcripts emanate from the rDNA (Miller & Bakken, 1972). This high intensity of transcription is due to three factors:

1. The large number of pol I molecules simultaneously involved in transcription.
2. The high rate of elongation of pol I.
3. The high copy number of the template.

Figure 5.6 shows immunofluorescence with R41 simultaneously with FISH using CpG-island fragments for chromosome 22, fractionated using the methyl-CpG binding column (Cross *et al.*, 1994) (Section 4.3.1). Slides were incubated with the R41 antibody for 2 hours, at room temperature, followed by incubation with anti-rabbit-TR for 30 minutes. As before, slides were fixed with 4% paraformaldehyde for 15 minutes. For a reasonable FISH signal, incubation of slides in 2:5 0.07M NaOH:EtOH for 3 minutes immediately prior to FISH was used to reverse the paraformaldehyde fixation (Section 2.6.1). FISH was then carried out as previously described (Section 2.6). It is striking that the R41 signal drops away exactly at the point at which CpG-island hybridisation increases, at the transition from centromere to p-arm (Figure 5.6). In fact, it appears that levels of acetylation are even less than those present at the centromere. This is surprising since hypoacetylation is generally considered to be associated with transcriptional inactivity (Section 1.4.1.3).

At interphase the human acrocentric chromosomes aggregate at the nucleoli, non-membranous nuclear structures which are associated with rRNA synthesis (Reviews: Warner, 1990; Hernandez-Verdun, 1991; Scheer & Weisenberger, 1994) (Section 1.5.2). Figure 5.7 shows immunofluorescence with R41 and anti-histone, pan antibody (Boehringer) to human interphase nuclei. Cells from the JU77 human mesothelioma line were grown on slides and fixed with 1:1 methanol:acetone at 4°C. Slides were incubated with either

antibody for 1 hour at room temperature, followed by anti-rabbit-FITC for 30 minutes. Reduction in DAPI DNA staining is a marker for the nucleoli. Using IPLab Spectrum software, a graph of fluorescence intensity was measured along a line drawn through several nucleoli and it was demonstrated that R41 signal was reduced to a greater extent than the anti-histone, pan antibody signal and DAPI stain (Figure 5.7). This was consistently observed for 20 nuclei from each slide. Thus, it appears that nucleolar H4 is hypoacetylated, consistent with the observations of metaphase chromosomes, and supports the concept of acetylation as an inherited marker, maintained throughout the cell cycle. However, observations in three-dimensionally maintained nuclei and colocalisation of R41 and anti-histone, pan antibody are necessary to firm this conclusion.

The rDNA clusters are, so far, the only identified transcribed sequences on the p-arms of the human acrocentric chromosomes. The rDNA is in a unique chromatin environment, surrounded by repetitive sequences. It is possible that these repetitive sequences produce a chromatin structure that could not be penetrated by the R41 antibody. Alternatively, histones may not be present at all in these regions, with chromatin folding being organised by rDNA-specific core histone variants. To test this, immunofluorescence was performed on cytocentrifuged metaphase spreads of the REN2 human lymphoblastoid cell line, using an anti-histone, pan antibody which is described as recognising a common but uncharacterised histone epitope (Boehringer). Figure 5.8 shows three acrocentric chromosomes (13, 14 or 15), clearly showing fluorescent signal along the entire length of each. Graphs (Figure 5.8d) showing the mean intensity of signal over the width of one of the chromatids, show a relatively even intensity throughout the q-arm and even an increase in immunofluorescence at the p-arm. There is consistently a dip in fluorescence at the centromere. This is puzzling, since it has previously shown that immunofluorescence with an antibody to H3 peaks at the centromere (Personal communication: Dr. B.A. Sullivan). The anti-histone, pan antibody used here, is described as detecting an antigenic determinant which is present on all five histone proteins (H1, H2A, H2B, H3 and H4). Binding to Western blots of nuclear protein extracts (Section 2.13) failed to produce a signal in my experiments (data not shown), suggesting that the determinant may not be present in denatured histones.

The presence of anti-histone, pan antibody at the acrocentric p-arms establishes that antibody inaccessibility is apparently not the cause of the lack of R41 signal at these regions. It is still possible, however, that although most of the core histones are present, H4 may be lacking from these regions, although this seems unlikely, since there appears to even be an increase in the number of core histones present at the p-arms. It would be interesting to observe the

distribution of the core histones and each of their modified forms throughout the human genome, by immunofluorescence.

The presence of rDNA-specific core histone variants would not be an unusual concept. CENP-A is a centromere-specific H3 variant that has been suggested to be involved in setting up a distinct chromatin environment (Section 1.5.2). The nucleolus is associated with many specific proteins (Review: Hernandez-Verdun, 1991) (Section 1.6.2), including the transcription factor, UBF, which is necessary for rDNA transcription. This protein contains several HMG-box DNA-binding motifs (Leblanc *et al.*, 1993) (Section 1.4.4) and has been shown to bind to and bend DNA, juxtaposing two essential upstream transcriptional control elements of the rDNA (Bazett-Jones *et al.*, 1994). This UBF-DNA structure is termed an enhancesome and may disrupt or replace potential nucleosomes (Review: Wolffe, 1994a). The wrapping of DNA around enhancesomes is reminiscent of nucleosomes. Formation of an enhancesome appears to allow access of the pol I complex to rDNA for transcription.

Another possibility is that histone hyperacetylation is not required for pol I activity. The alterations in chromatin structure created by core histone acetylation may not be required for pol I, or may even act to repress activity. In addition, hypoacetylation may prevent pol II activity in the region, thus allowing pol I exclusive access. This is further discussed in Section 9.1.2.

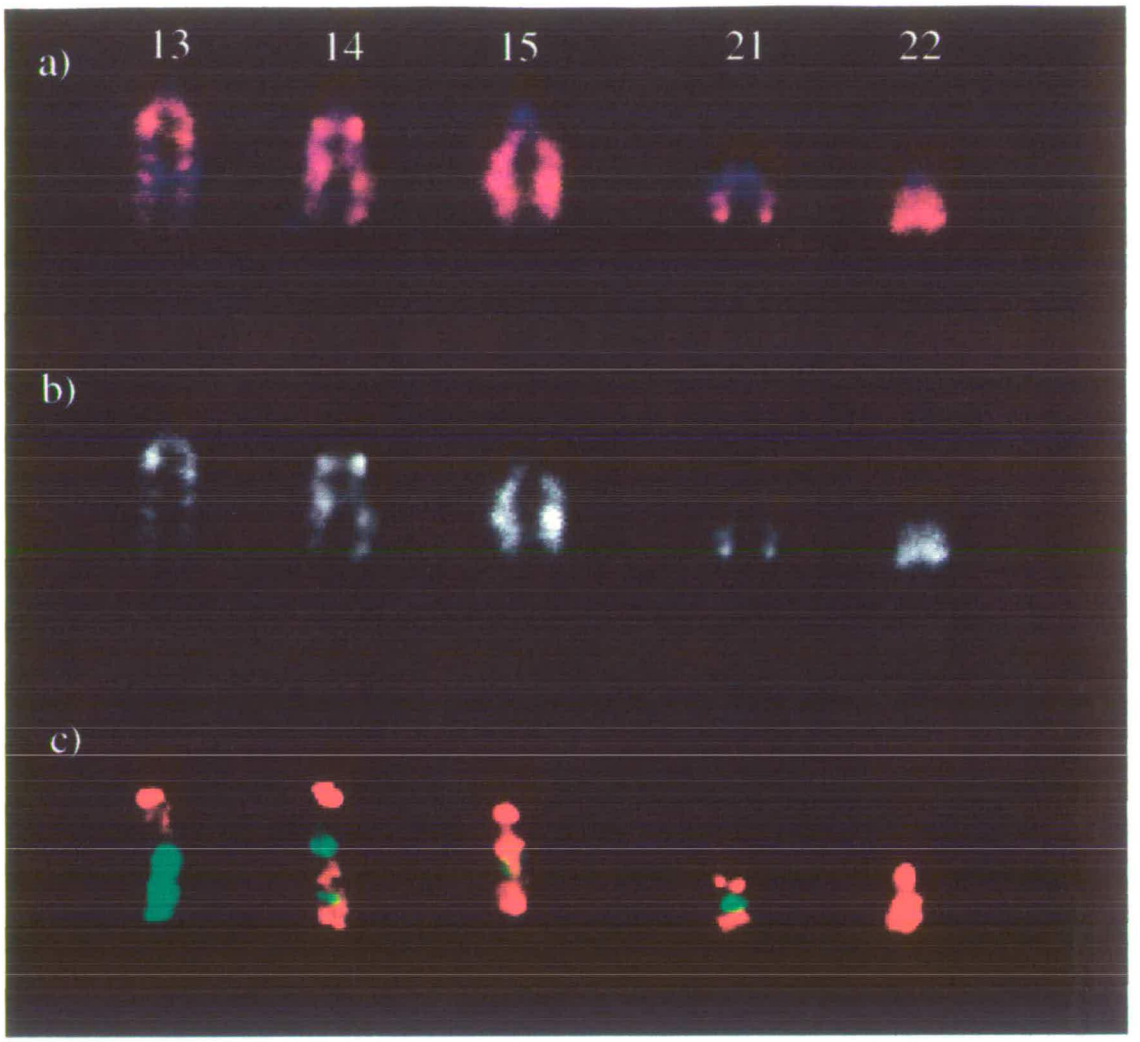

Figure 5.4 Immunofluorescence with R41 to the human acrocentric metaphase chromosomes

(**a**) Immunofluorescence with anti-acetylated H4 antibody (R41) detected with anti-rabbit-TR (red). Chromosomes were counterstained with DAPI (blue). (**b**) Grey scale representation of R41 (TR/red) image. (**c**) Adapted from Craig (1995). Chromosomes hybridised with small, biotin labelled *HpaII* fragments selected to represent CpG-islands and detected with avidin-TR (red). BrdU incorporation detected with anti-BrdU-FITC reveals late replicating regions in green.

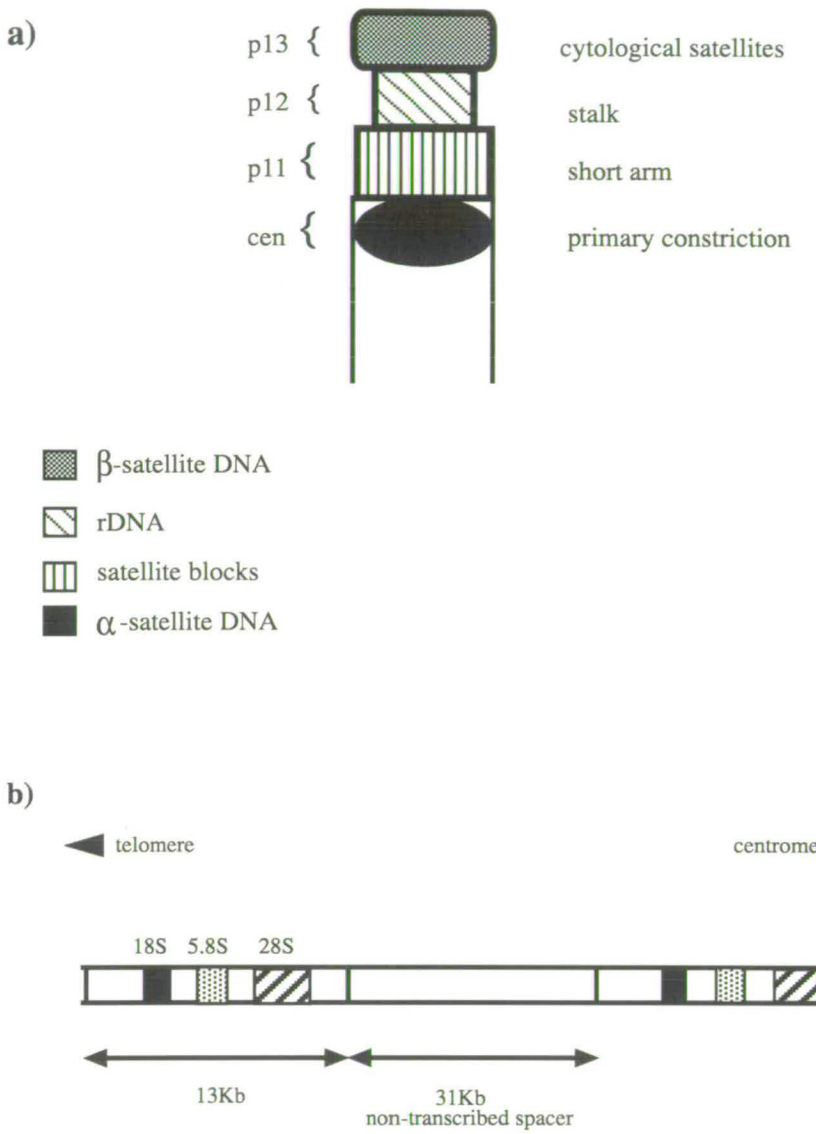

Figure 5.5 Schematic representation of the major repeats of the human acrocentric chromosome p-arms

(**a**) Taken from Sullivan(1995). The consensus organisation of the human acrocentric chromosome p-arms. (**b**) Adapted from Worton *et al.*(1985). The consensus organisation of the repeat unit of human ribosomal DNA.

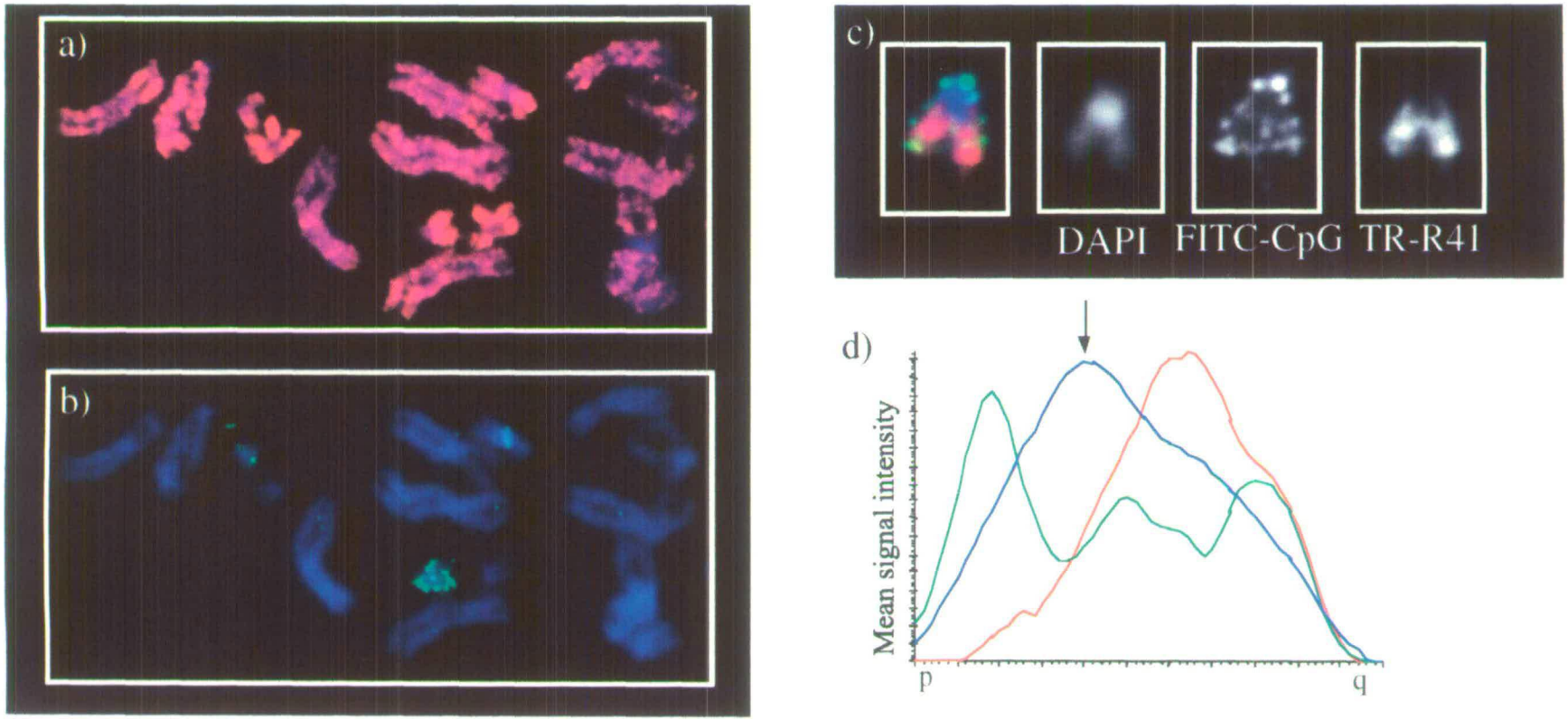

Figure 5.6 Immunofluorescence with R41 simultaneously with FISH of CpG-island DNA on human chromosome 22
Immunofluorescence to REN2 human metaphase spread (49, XXXXY) with anti-acetylated H4 antibody (R41) detected with anti-rabbit-TR (red) (**a**), followed by FISH with biotin labelled chromosome 22 CpG-islands, isolated using a methyl-CpG binding column, and detected with avidin-FITC (green) (**b**). Chromosomes were counterstained with DAPI (blue). (**c**) Greyscale representations of DAPI and signal fluorescence. Chromosome 22 from an alternative spread to that shown in (a). (**e**) Graph of mean signal intensity over the width of the chromosome, measured along the length from the tip of the p-arm to the tip of the q-arm. The lines are the appropriate colour for the fluorochrome that they represent.

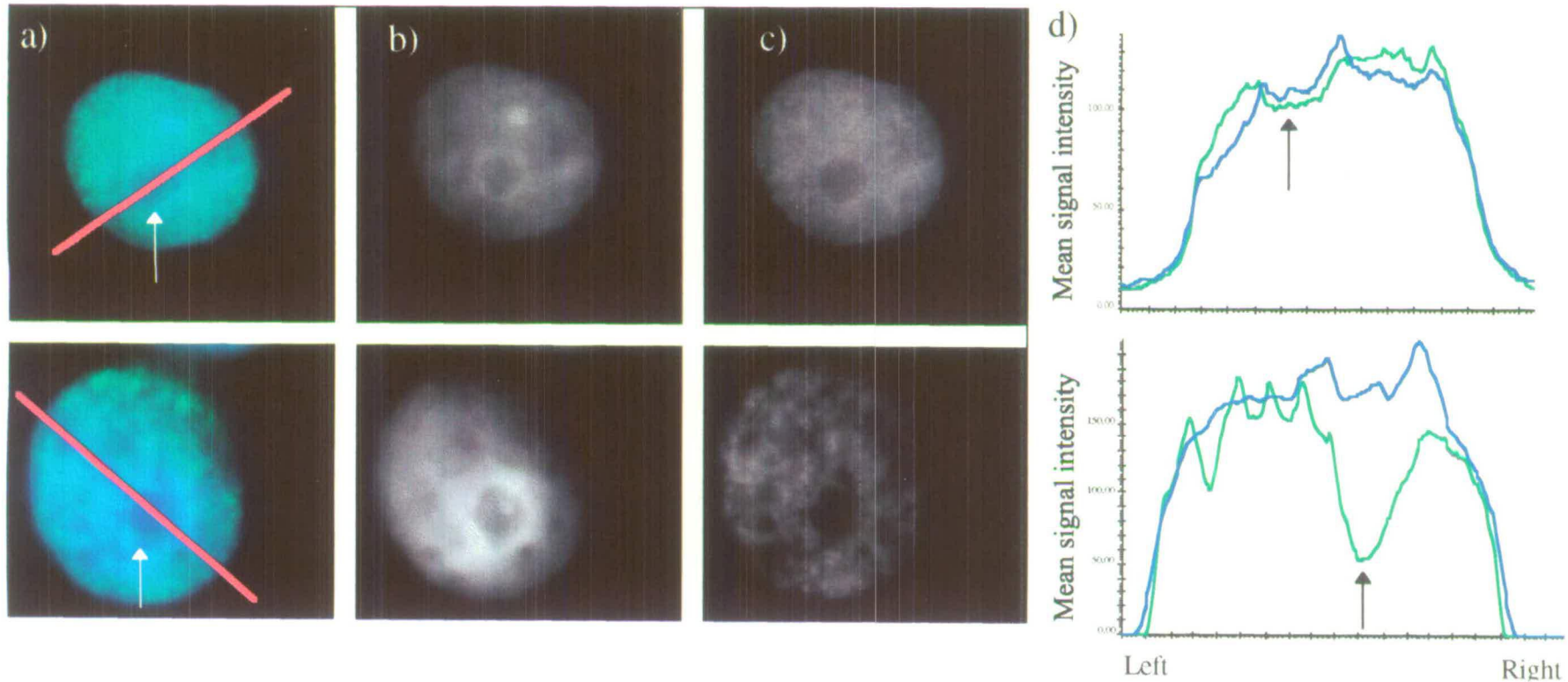

Figure 5.7 Immunofluorescence with R41 and anti-histone, pan antibody to human interphase nuclei
(**a**) Immunofluorescence with anti-histone, pan antibody detected with anti-mouse-FITC (green) (**Top**); and anti-acetylated H4 antibody (R41) detected with anti-rabbit-FITC (green) (**Bottom**). Nuclei were counterstained with DAPI (blue). Arrows indicate prominent nucleoli. (**b**) Grey scale representation of the DAPI image. Note the concentration of chromatin around the nucleoli. (**c**) Grey scale representation of the FITC (green) signal. (**d**) Graphs of mean signal intensity measured along the lines indicated in (a) from left to right. The lines are the appropriate colour for the fluorochrome that they represent . Arrows indicate prominent nucleoli from (a).

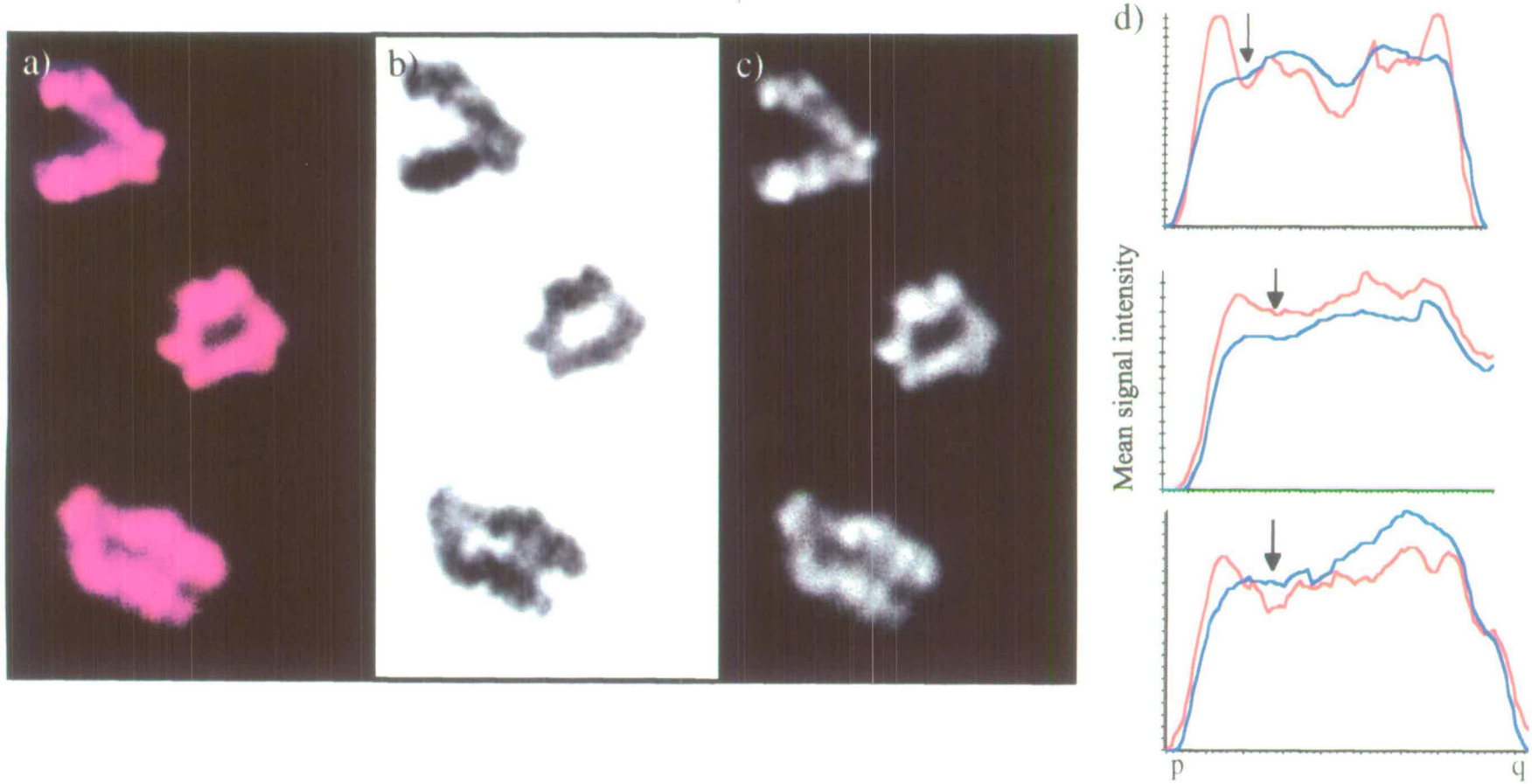

Figure 5.8 Immunofluorescence with an anti-histone pan antibody to human acrocentric metaphase chromosomes
(**a**) Selection of human acrocentric chromosomes (13,14 or 15) following immunofluorescence with a monoclonal anti-histone, pan antibody detected with anti-mouse-TR (red). Chromosomes were counterstained with DAPI (blue). (**b**) Grey scale representation of the DAPI stained chromosome. (**c**) Grey scale representation of anti-histone, pan antibody (TR/red) signal. (**d**) Graphs of mean signal intensity over width of the left chromatid of each chromosome, measured along the length from the tip of the p-arm to the tip of the q-arm. Arrow indicates centromere.

5.4 Histone acetylation of human chromosomes in a somatic cell hybrid background

Are the acetylation patterns of human metaphase chromosomes maintained in a somatic cell hybrid background, where normal transcription from human genes might be perturbed? Making use of the rodent-human somatic cell hybrids detailed in Section 3.2, I cytocentrifuged metaphase spreads of each onto slides for immunofluorescence with the R41 antibody (Section 2.10 & 5.2). FISH was performed simultaneously with total human DNA to aid identification of the human chromosome (Section 2.6 & 5.3).

Figure 5.9a shows a metaphase spread from the human chromosome 18 containing hybrid cell line, GM11010, following immunofluorescence with R41. The level of acetylation detected by R41 fluorescence on the human chromosome did not appear to be strikingly less than that on the Chinese hamster chromosomes, although the level of signal was more equivalent to the regions of least fluorescence on the hamster chromosomes. There was no distinct pattern of signal along the length of chromosome 18 (Figure 5.9c) and it was difficult to establish the exact location and acetylation level of the centromere, since many of the human chromosomes in this line had been previously shown to be incomplete (Section 3.2).

A metaphase spread from the human chromosome 19 containing hybrid cell line, GM10449A, is shown in Figure 5.10a after immunofluorescence with R41. It is clear that chromosome 19 maintains its high level of acetylation, with R41 signal as high as the highest levels on the Chinese hamster chromosomes along both chromosome 19 arms, but absent from the centromere (Figure 5.10c).

Figure 5.11a shows a metaphase spread from the human chromosome 1 containing hybrid cell line, A91neo, following immunofluorescence with R41 antibody. The pattern of R41 signal seen along chromosome 1 at metaphase in a human spread (Figure 5.2c) is maintained in the hybrid cell background, as shown by the graphs of mean signal intensity (Figure 5.11c & d). There is a high level of fluorescence at the tip of the p-arm, adjacent to a region of very low fluorescence. The difference between these two regions was assessed using the script described in Section 5.2. The ratio of segment 2:4 DAPI and R41 fluorescence was 0.8 and 1.6, respectively, comparable with the ratios calculated for normal human spreads (Table 5.1). The centromere shows the characteristic dip in fluorescence, demonstrating a lack of acetylated H4 in this region as seen in human cells.

A metaphase spread from the human chromosome 22 containing cell line, PgMe-25, is shown in Figure 5.12a following immunofluorescence with the R41. The level of fluorescence appears to be generally equivalent to that observed along most of the mouse chromosomes. A graph of signal intensity along the length of the chromosome (Figure 5.12c & d), although indicating a small dip at the centromere, shows a high level of R41 signal at the p-arm, in contrast to observations of chromosome 22 at metaphase in human spreads (Figures 5.4 & 5.6).

The general level of transcription from the human chromosomes in these hybrid cell lines is unknown, although the *neo* gene integrated for selection into human chromosome 1 of the A91neo cell line must be active. Transcription of some human genes is known to be normal in rodent cell backgrounds. The general patterns of H4 acetylated at lys5 along human chromosomes are maintained in a hybrid cell background. For example, the constitutive heterochromatin of the centromeres and the pericentric heterochromatin of chromosome 1 remains hypoacetylated, and chromosome 18 shows generally low levels of acetylation while chromosome 19 has generally high levels of acetylation. However, it appears that the mechanisms involved in reducing acetylation at the rDNA-containing chromosome 22 p-arm are not functional in a hybrid cell background. It has been previously established that human rDNA genes are transcriptionally inactive in a rodent hybrid cell background and that human acrocentric chromosomes do not associate with rodent nucleoli (Miller *et al.*, 1976; Miesfeld *et al.*, 1984; Kass *et al.*, 1987; Dante *et al.*, 1992). I also did not observe human chromosome 22 to be predominantly associated with the nucleolus in PgMe-25 nuclei (data not shown). The change in levels of human rDNA histone acetylation could be due to the absence or altered specificity of a particular deacetylase or protein which blocks acetylation, the presence or altered specificity of a specific acetyltransferase, or a different nuclear location. The requirement for nucleolar-specific histone deacetylases and/or acetyltransferases is supported by the finding of a nucleolar-specific histone deacetylase in maize (Lusser *et al.*, 1997).

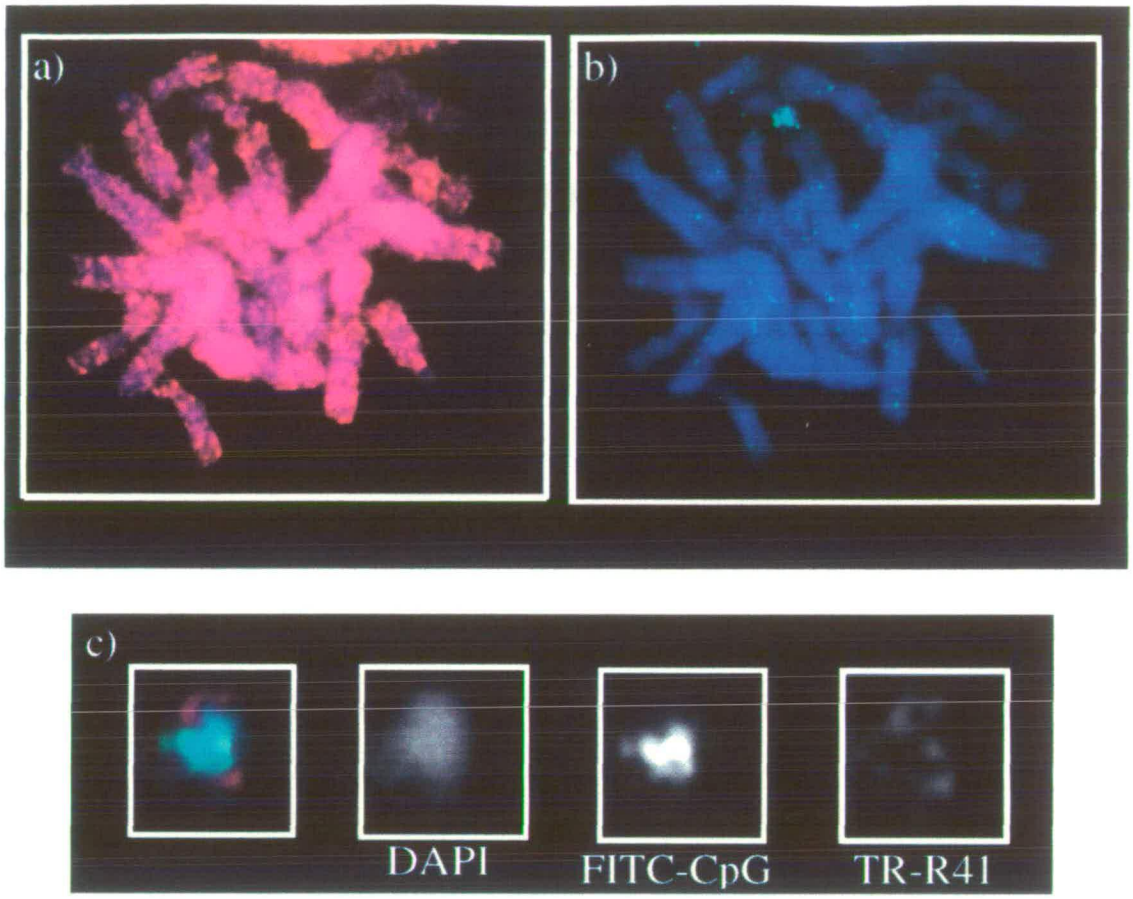

Figure 5.9 Immunofluorescence with R41 to metaphase spreads from the hybrid cell line, GM11010
Immunofluorescence to GM11010 metaphase spreads (human chromosome 18-containing hybrid cell line) with anti-acetylated H4 antibody (R41) detected with anti-rabbit-TR (red) (**a**), followed by FISH with biotin labelled whole human DNA, and detected with avidin-FITC (green) (**b**). Chromosomes were counterstained with DAPI (blue). (**c**) Greyscale representations of DAPI and signal fluorescence. Chromosome 18 from an alternative spread to that shown in (a).

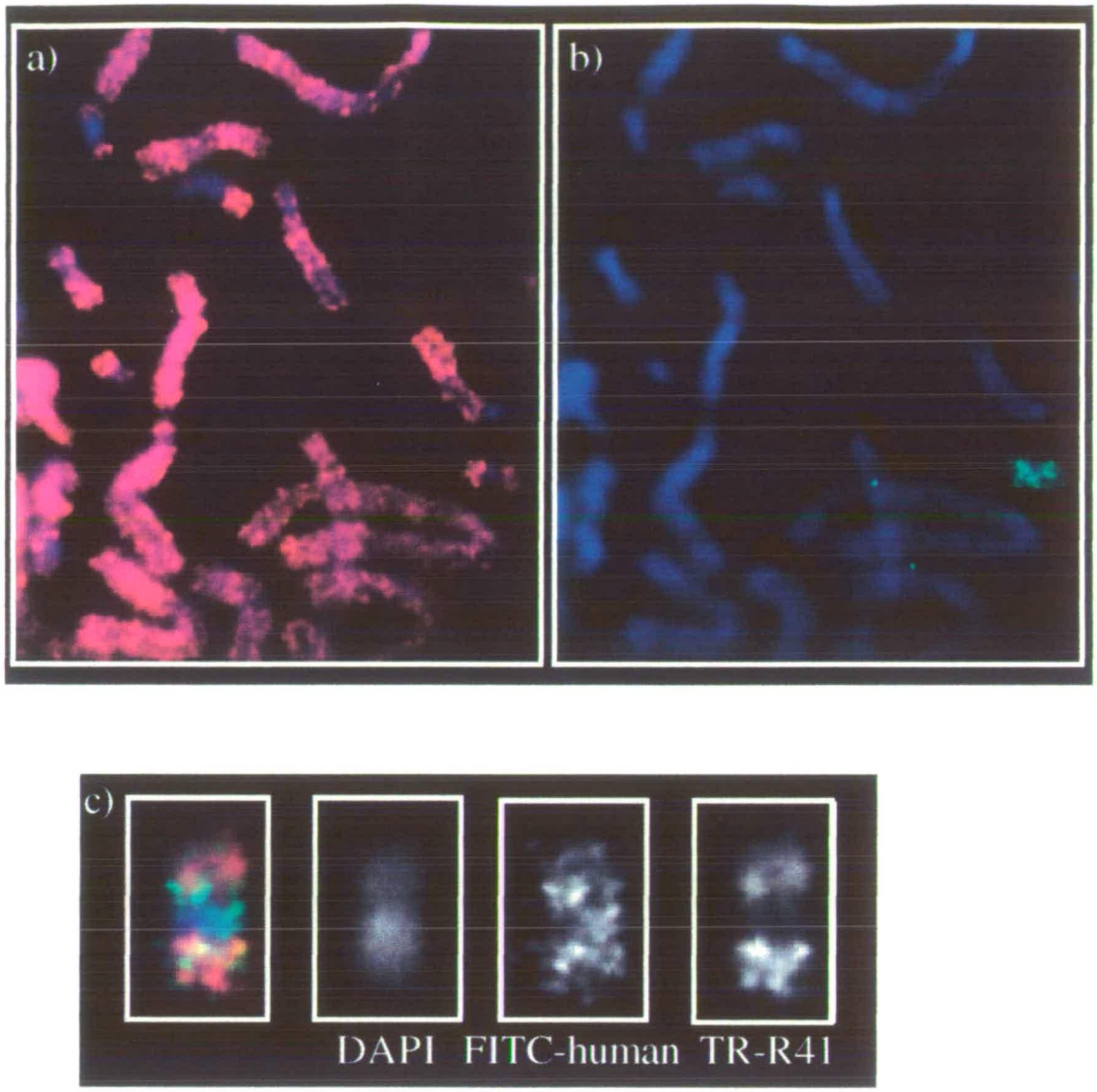

Figure 5.10 Immunofluorescence with R41 to metaphase spreads from the hybrid cell line, GM10449A

Immunofluorescence to GM10449A metaphase spreads (human chromosome 19-containing hybrid cell line) with anti-acetylated H4 antibody (R41) detected with anti-rabbit-TR (red) (**a**), followed by FISH with biotin labelled whole human DNA, and detected with avidin-FITC (green) (**b**). Chromosomes were counterstained with DAPI (blue). (**c**) Greyscale representations of DAPI and signal fluorescence. Chromosome 19 from an alternative spread to that shown in (a).

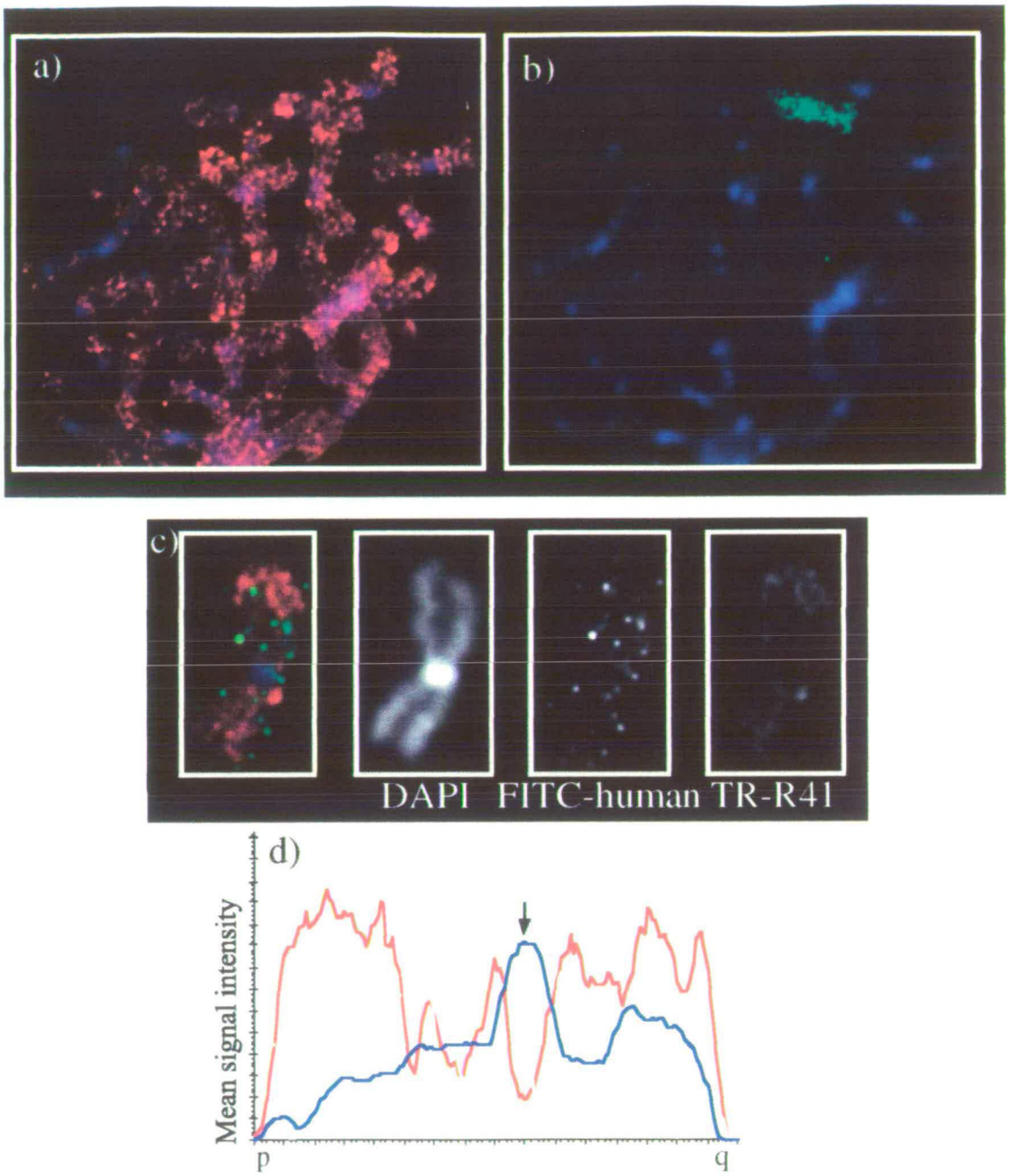

Figure 5.11 Immunofluorescence with R41 to metaphase spreads from the hybrid cell line, A91neo

Immunofluorescence to A91neo metaphase spreads (human chromosome 1-containing hybrid cell line) with anti-acetylated H4 antibody (R41) detected with anti-rabbit-TR (red) (**a**), followed by FISH with biotin labelled whole human DNA, and detected with avidin-FITC (green) (**b**). Chromosomes were counterstained with DAPI (blue). (**c**) Grey scale representations of DAPI and signal fluorescence. Chromosome 1 from an alternative spread to that shown in (a). (**d**) Graph of mean signal intensity over the width of the chromosome 1 shown in (c), measured along the length. The lines are the appropriate colour for the fluorochrome that they represent. Arrow indicates the centromere.

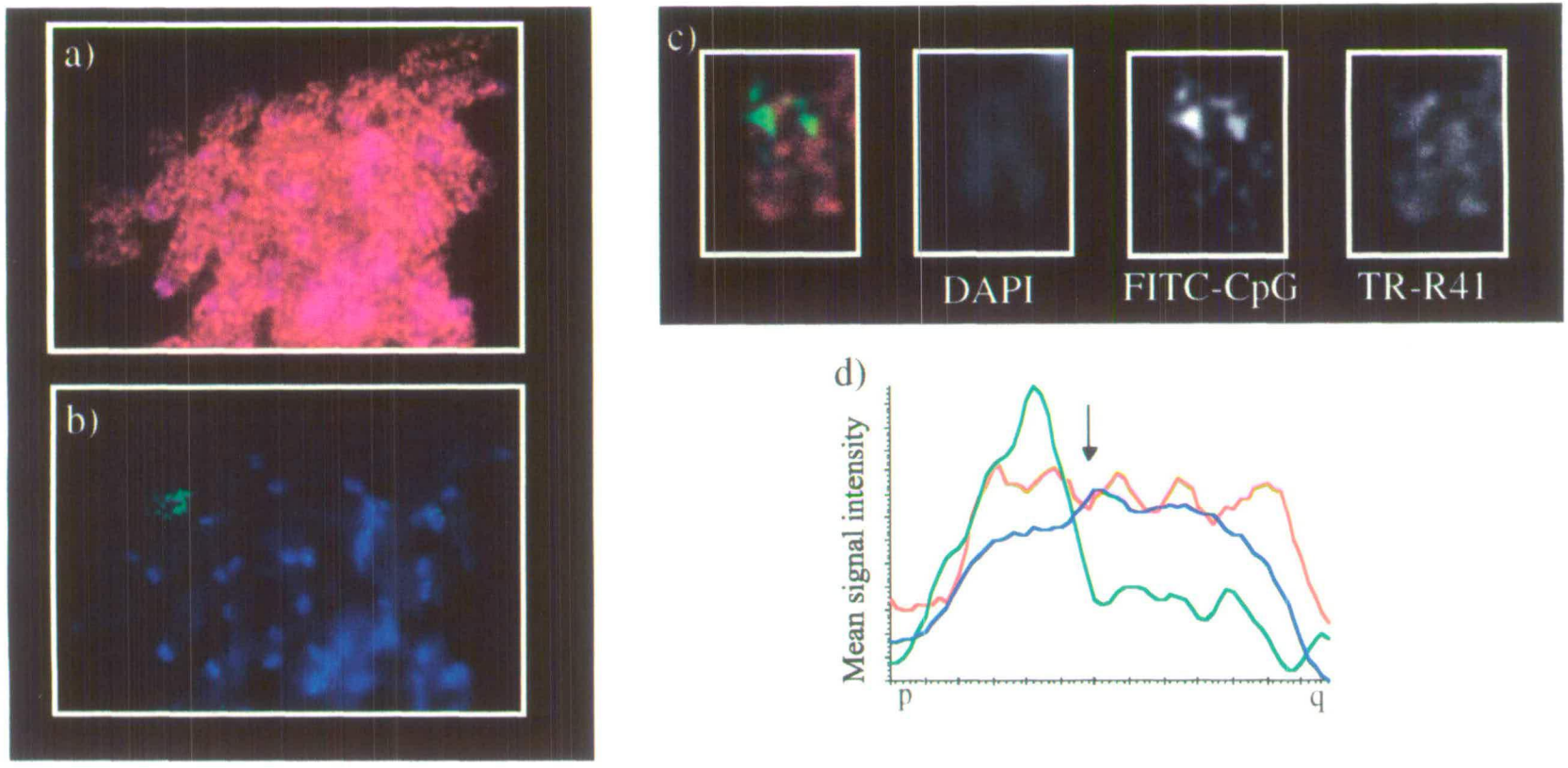

Figure 5.12 Immunofluorescence with R41 to metaphase spreads from the hybrid cell line, PgMe-25
Immunofluorescence to PgMe-25 metaphase spreads (human chromosome-22 containing hybrid cell line) with anti-acetylated H4 antibody (R41) detected with anti-rabbit-TR (red) (**a**), followed by FISH with biotin labelled whole human DNA, and detected with avidin-FITC (green) (**b**). Chromosomes were counterstained with DAPI (blue). (**c**) Grey scale representations of DAPI and signal fluorescence. Chromosome 22 taken from an alternative spread to that shown in (a). (**d**) Graph of mean signal intensity over the width of the chromosome 22 shown in (c), measured along the length. The lines are the appropriate colour for the fluorochrome that they represent. Arrow indicates the centromere.

5.4 Summary

Core histone acetylation acts as a marker for transcriptional activity of regions of the human genome. Immunofluorescence studies have shown the most highly acetylated regions correspond to the gene-rich, transcriptionally active, R-bands. Acetylation is not static, there is a turnover and steady state levels reflect the balance of acetyltransferase and deacetylase activities. Data presented in this chapter suggests that the rate of this turnover differs in different regions of the genome, with R-band regions showing a higher rate of acetylation than G-band regions. I predict that the <15% of histones which show a high turnover of acetylation (Covault & Chalkley, 1980) are located at the *Alu*-rich T-bands which make up approximately 13% of the human genome (Holmquist, 1992).

While acetylation has tended to correlate well with actively transcribed regions, the most highly transcribed regions of the human genome, the rDNA-containing regions are hypoacetylated. This apparent contradiction can be assigned several possible explanations. Although the rRNA genes that are being transcribed are hyperacetylated, these are interspersed with regions of under-transcribed, hypoacetylated DNA, not resolvable by the studies described here. Alternatively, the rDNA regions may possess an H4 variant which is required to alter chromatin structure and allow efficient pol I transcription. Finally, hypoacetylation may block pol II transcription while allowing, or even promoting pol I transcription. This is further discussed in Section 9.1.2. Clearly, the rDNA is a unique region which has implications on the absolute requirement of acetylated core histones for transcriptional activity.

The patterns of acetylated H4 distribution along human metaphase chromosomes are generally maintained in a hybrid cell background. The hypoacetylation of the rDNA-containing human chromosome 22 p-arm, however, is lost in a rodent cell background. This phenomenon needs to be confirmed for this and other human acrocentric chromosomes in hybrids and further studies may help to establish the mechanism and function of human rDNA hypoacetylation in normal human cells.

Chapter 4 concluded that the higher order levels of DNA packaging of the human chromosomes 18 and 19 is similar. This chapter has emphasised one of the differences between these two contrasting chromosomes at the chromatin level. Chromosome 18 has consistently low steady state levels of histone acetylation along its length, and is likely to have a generally low turnover of acetylation. Chromosome 19 is associated with high levels

of histone acetylation and will have a high level of acetylation turnover, reflecting its high density of R-bands and high transcriptional activity. Chapter 6 addresses the question of what happens to their DNA packaging in the interphase nucleus, when transcription takes place and when this and the other differences of behaviour between these chromosomes becomes manifest.

6. Interphase chromosome territories I: Functional compartmentalisation of the interphase nucleus

6.1 Introduction

The interphase chromosome territory hypothesis, in which each chromosome takes up a discrete and distinct region within an interphase nucleus, is now well established (Reviews: Hiliker & Appels, 1989; Manuelidis, 1990; Haaf & Schmid, 1991; Cremer *et al.*, 1993; Spector, 1993) (Section 1.6.3). Characteristic configurations and positions have been implied from isotopic *in situ* hybridisation and FISH studies of whole or partial human chromosomes in rodent-human hybrid cell lines (Manuelidis, 1985b; Scardin *et al.*, 1985) and later in human cells (Pinkel *et al.*, 1986; Lichter *et al.*, 1988; Popp *et al.*, 1990; Aquiles Sanchez *et al.*, 1997).

There is a precise arrangement of human chromosomes maintained on the mitotic spindle (Naegele *et al.*, 1995) and observations of chromosomes in metaphase spreads have suggested a non-random distribution. Some studies indicate that small autosomes tend to be more centrally located than larger autosomes (Warburton *et al.*, 1973; Wollenberg *et al.*, 1982), while other studies have shown early replicating, gene-rich chromosomes are more centrally located and late replicating, gene-poor chromosomes tend towards the periphery (Miller *et al.*, 1963; Hens *et al.*, 1982). It is well established that the inactive X-chromosome, in the form of the Barr body, is positioned close to the nucleolus or at the periphery of the female interphase mammalian nucleus (Barr & Bertram, 1949; Dyer *et al.*, 1989).

Probes for a variety of sequences from specific regions of human chromosomes have been used for FISH to show that transcriptionally inactive, heterochromatic regions are more peripherally located than active sequences (Lawrence *et al.*, 1988; Manuelidis & Borden, 1988; Lawrence & Singer, 1991; Xing *et al.*, 1995). Few previous studies have examined the shape and position of entire human chromosomes and none have related these territories to their functional characteristics. Popp *et al.* (1990) used a human chromosome 18-specific alphoid DNA probe to determine the positioning of this chromosome in 2-D and 3-D primary human amniotic fluid cells. They determined that although this chromosome was not located at the ends of these ellipsoid cells, it was significantly more often associated

with the nuclear envelope than might be expected from a random distribution. An X chromosome-specific alphoid DNA probe revealed a completely random distribution for the active X chromosome, while the inactive X chromosome was preferentially located centrally and attached to the nuclear envelope. Recently, Aquiles Sanchez *et al.* (1997) used paints to human chromosomes 2, 18, X and Y in neutrophils in 3-D. These cells consist of three or four lobes with specific appendages which can act as landmarks. However, this study implied that chromosome positioning was essentially random. Surprisingly, it was found in addition that chromosome 2 occupied a territory smaller than chromosome 18. The chromosome 2 paint used, however, clearly did not cover the entire metaphase chromosome evenly and so any estimates of territory size at interphase were flawed.

Therefore, there is little consistent evidence that mammalian chromosomes regularly adopt territory shapes in defined positions within the nucleus that relate to their activity. Given their functional differences, could chromosomes 18 and 19 occupy territories, specific in shape and position, that reflect the functional organisation of the interphase nucleus?

To answer this question, FISH was carried out with paints for human chromosomes 18 and 19, in addition to chromosome 1, 11 and 22 (Section 3.3) to 2-D, 3:1 methanol:acetic acid fixed interphase nuclei from a human lymphoblastoid cell line. The area and the position with relation to the nuclear periphery of the interphase chromosome territories were measured and compared. Further analysis of the chromosome 18 and 19 territories was then carried out on paraformaldehyde fixed 2-D nuclei, nuclei from different cell types and nuclei from distinct stages of the cell cycle. Finally, analysis of the location of these two chromosomes in 3-D interphase nuclei was attempted.

6.2 A rapid, two-dimensional approach to analysing the interphase territories of human chromosomes

To observe the interphase territories of a selection of human chromosomes FISH was carried out on slides prepared from the human lymphoblastoid cell line, FATO, using each of the whole chromosome paints described in Section 3.3. The interphase territories of chromosomes 18 and 19 were compared with each other and with those of chromosomes 1, 11 and 22.

The FATO lymphoblastoid cell line was chosen because it has a normal male karyotype (Figures 3.4, 3.14 - 3.16). Cells were harvested from an exponentially growing culture and fixed with 3:1 methanol:acetic acid (Section 2.1.5) resulting in a suspension of asynchronous nuclei (Table 6.1). Approximately 5% of cells were undergoing mitosis, as counted from slides made from this suspension and stained with DAPI. The thymidine analogue, bromodeoxyuridine (BrdU) was added 45 minutes prior to harvesting and detected with anti-BrdU-FITC (Section 2.6.5) allowing assessment of the number of nuclei undergoing replication (S-phase). The proportion of cells in the gap phases were estimated from FACS analysis (Section 2.7.2 & 6.5). Since most material was visible in a single optical plane, the nuclei could be considered to be essentially 2-D.

Table 6.1 Distribution of cell cycle stages in an exponentially growing culture of the FATO human lymphoblastoid cell line
Percentage of mitotic cells estimated by counting metaphase spreads present on a fixed slide (Section 2.1.5). BrdU was added 45 minutes prior to harvesting and detected with anti-BrdU-FITC (Section 2.6.5) allowing assessment of the number of nuclei undergoing replication (S-phase). Proportion of cells in the gap phases were estimated from FACS analysis (Section 2.7.2 & 6.5). S - synthesis phase (replication) G1, G2 - gap phases M - mitosis

Stage of cell cycle	% of nuclei in population
G1	51.6
S	17.8
G2	25.4
M	5.2

The advantages of analysing 3:1 methanol:acetic acid fixed 2-D nuclei are that they are easy to obtain from well established protocols, give good FISH signals, and large numbers of nuclei can be observed rapidly. Observations, however, are subjective and it was necessary to design two computer scripts for an objective analysis of the data.

6.2.1 Devising scripts for objective image analysis

To assess a large number of images, two scripts were designed to take a number of measurements in relation to the interphase nucleus and the territory occupied by each human chromosome of interest. Only interphase nuclei where the appropriate number of signals

were present and separate were selected. Experiments to be compared were carried out simultaneously and the exposure times for each image kept the same.

Both scripts were developed by Dr. Paul Perry, MRC Human Genetics Unit, Edinburgh using the Digital Scientific software, IPLab Spectrum. The steps involved in each script, are briefly described below. Script 1 was used for most analyses where the nuclei were approximately circular.

Script 1: Determining the size and position of a FISH signal within circular nuclei

The DAPI stained nucleus was automatically segmented from the background and the following measurements calculated for the segment (Figure 6.1):

- Area (pixels).
- Centroid co-ordinates.

To enhance the FISH signal, a mean intensity value was calculated for the background and subtracted from the image. A region of interest was drawn around the appropriate signal manually and the signal was automatically segmented from any remaining background. The following parameters were calculated for the signal segment (Figure 6.1):

- Area (pixels).
- Weighted centroid co-ordinates (this is the centre of the signal accounting for intensity).

The nuclear segment was converted to binary form. Using the co-ordinates of the signal weighted centroid as the centre, an appropriately sized segmentation disc was automatically adjusted by dilation and erosion until a single pixel with zero intensity was determined. This point was taken as the nearest edge of the nucleus to the signal. The distance from this point to the centroid of the signal, and the centroid of the nucleus to the centroid of the signal were calculated. The signal segment was converted to binary form, a chord was drawn automatically from the centroid of the segment to the nearest edge of the nucleus and the co-ordinates established for the first pixel with zero intensity. This was taken to be the edge of the signal nearest to the periphery of the nucleus and the distance between these two sets of co-ordinates were calculated. In this way, the following distances were recorded (Figure 6.1):

- The centre of the nucleus to the centre of the signal (pixels).

- The centre of the signal to the nearest edge of the nucleus (pixels).
- The edge of the signal to the nearest edge of the nucleus (pixels).

Fibroblast nuclei tend to be ellipsoid and, thus, measurements of distance for the signal from the centre or edge of the nucleus would be meaningless. Script 2 divided the nucleus according to total percentage area and the percentage of signal present in each segment was comparable whether the nucleus is circular or ellipsoid.

Script 2: Determining the distribution of FISH signal within ellipsoid nuclei

The DAPI stained nucleus was automatically segmented from the background and the area and centroid co-ordinates were calculated from the segment. The nucleus was divided into five concentric segments of equal area, from the periphery towards the centre of the nucleus. For each segment, the amount of FISH and DAPI fluorescence were calculated and represented as a percentage of the total (Figure 6.2).

Data for each experiment were stored as Microsoft Excel spreadsheets. All data analysis and statistics were carried out with help from Dr. P. Teague, MRC Human Genetics Unit, Edinburgh.

6.2.2 Assessing the representation of the chromosome 18 and 19 paints in interphase nuclei

Representing two opposing extremes of chromosomal environment, the most informative comparisons were those between chromosomes 18 and 19. However, the paints for these chromosomes were made in different ways and it was important to assess that the two probes represented the entire lengths of each chromosome. Observations at metaphase suggested that both chromosomes 18 and 19 were completely coated by their respective paints (Figure 3.17). A comparison was made between the areas taken up by the paints that I prepared (Section 3.3), commercially available probes for each chromosome and total DNA from the appropriate hybrid cell lines, following FISH to interphase nuclei. Also assessed was any difference in signal area due to the fluorochrome used. The fluorochromes used for these experiments were either FITC (green) or TR (red).

The specific chromosome 18 paint that I prepared consisted of FACS sorted chromosomes 18 which were digested and catch-linker sequences attached (Section 2.4.2 & 3.3.2). Amplification by PCR using one of the linkers as a primer and incorporating biotin-dUTP, allowed DNA to be labelled for use as a FISH probe. It is possible that many fragments of the digested chromosome are an inappropriate size for PCR and this could create patches with a dearth of hybridisation. The specific chromosome 19 paint that I prepared, was produced by a human specific *Alu* PCR protocol used to amplify the human component of the rodent-human monochromosome 19 hybrid cell line, GM10449A (Section 2.4.1 & 3.3.1). This strategy was expected to result in a concentration of probe representing R-bands, since such regions are *Alu*-rich and similarly could have resulted in a paint that was lacking in particular regions of the chromosome. Probes were labelled with biotin or digoxigenin and 10μg of human C_0t1 DNA were added for 150ng of probe to suppress hybridisation to highly repetitive sequences (Section 3.1).

The commercial paints (Oncor) were produced by combined human-specific *Alu* and L1 PCR to amplify human DNA from a human monochromosome-rodent hybrid cell line (Lichter *et al.*, 1990) (Section 3.1). Probes were provided in hybridisation buffer premixed with "blocking" DNA for repeat suppression and previously labelled with digoxigenin.

For the total paints, DNA was extracted (Section 2.3) from cells of the GM11010 (human chromosome 18) (Section 3.2) and GM10449A (human chromosome 19) (Section 3.2) hybrid lines. These DNAs were labelled with biotin by nick translation (Section 2.4). 10μg of human C_0t1 DNA were added for 150ng of probe to suppress binding to repeat sequences.

All paints were hybridised to FATO human interphase nuclei (Figures 6.3 & 6.4).

Figure 6.3a shows FISH signal from the catch-linkered chromosome 18 paint, labelled separately with biotin and digoxigenin and detected simultaneously with both FITC and TR fluorochromes, respectively. Using Script 1 (Section 6.2.1) the signals from each fluorochrome in 50 nuclei were assessed for the percentage of the total nuclear area covered by each probe (Table 6.2). Using a Student's T-test (ST), the signal area revealed by the red fluorochrome (TR) was calculated to be significantly (ST $p<0.0003$) larger than that shown by the green fluorochrome (FITC). The mean difference was 15%. This was expected since the cooled CCD camera is sensitive in the red part of the spectrum (>600nm). A BG38 filter

was placed in front of the camera to reduce far red emission (>680nm) which reduces a potentially greater problem. The green emission spectrum is confined (510-550nm) and less background signal is detected, hence, a more clearly defined signal area is established.

Table 6.2 Area comparisons between different chromosome paints and fluorochromes Biotin and dig labelled catch-linkered chromosome 18 paints were hybridised simultaneously by FISH to FATO human lymphoblastoid nuclei and detected with anti-dig-FITC and avidin-TR (Figure 6.3). 50 randomly selected nuclei were assessed. This was repeated with the chromosome 19 inter-*Alu* PCR paint (Figure 6.4). For the commercial (Oncor) and total hybrid DNA paints, 50 randomly selected and independent nuclei were assessed for each chromosome. The area of each signal was divided by the total nuclear area, determined using Script 1 (Section 6.2.1).

Chromosome paint	**% of total nuclear area**	
	FITC	TR
18 catch-linkered	$5.3^{+/-0.2}$	$6.1^{+/-0.2}$
19 inter-*Alu* PCR	$6.8^{+/-0.3}$	$7.6^{+/-0.1}$
18 commercial	$4.7^{+/-0.1}$	–
19 commercial	$6.2^{+/-0.2}$	–
18 total hybrid DNA	–	$5.7^{+/-0.1}$
19 total hybrid DNA	–	$7.9^{+/-0.1}$

Figure 6.4a shows FISH signal from the inter-*Alu* PCR chromosome 19 paint, labelled with biotin and digoxigenin and detected simultaneously with each fluorochrome. As before, using Script 1 (Section 5.2.1), the two signals in each fluorochrome from 50 nuclei were assessed for the percentage of the total nuclear area that was revealed by each probe (Table 6.2). As anticipated the signal area revealed by TR was, again, significantly larger than that shown by FITC (ST $p<0.0004$). The mean difference was 12%. Clearly, it was important to take this into consideration when assessing the signal domains in future experiments. Ideally domains to be compared should be detected with the same fluorochrome.

Figure 6.3 also shows FISH signal from the commercial (Figure 6.3b) and total hybrid DNA (Figure 6.3c) chromosome 18 paints. Using Script 1 (Section 5.2.1), the two signals for each paint from 50 nuclei were assessed for the percentage of the total nuclear area (Table 6.2). The commercial paint consistently took up a smaller area (approximately 10%) than the catch-linkered paint detected with the same fluorochrome (ST $p<0.016$). The mean area for the total hybrid DNA paint was slightly, though not significantly (ST $p<0.150$) smaller

than for the catch-linkered paint detected with the same fluorochrome, which was not unexpected, since it has previously been shown that the GM11010 hybrid cell line contains an incomplete human chromosome 18 (Section 3.2). These data suggest that the catch-linkered chromosome 18 paint (Section 3.3.2) reveals a domain for chromosome 18 that can be considered to be representative of the entire chromosome.

Figure 6.4 shows a similar analysis for the commercial (Figure 6.4b) and total hybrid DNA (Figure 6.4c) chromosome 19 paints. The commercial paint consistently took up an approximately 10% smaller area than the inter-*Alu* PCR paint detected with the same fluorochrome (ST $p<0.023$). The area taken up by the total hybrid DNA paint, when compared to the inter-*Alu* PCR paint detected with the same fluorochrome, was not significantly different (ST $p<0.340$). These data argue that the inter-*Alu* PCR chromosome 19 paint (Section 3.3.2) reveals a domain for chromosome 19 that can also be considered to be representative of the entire chromosome.

6.2.3 The areas of territories occupied by human chromosomes in the interphase nucleus

Each of the FISH paints described in Section 3.3 were used to assess the territories of these chromosomes in 2-D 3:1 methanol:acetic acid fixed human lymphoblastoid FATO interphase nuclei. The chromosome 1 paint was directly labelled with Spectrum Orange fluorochrome (Figures 3.14 & 6.5a) and was supplemented with a pericentric heterochromatin probe also labelled with Spectrum Orange (Section 3.3.3). Biotin labelled probes for chromosomes 11 (Figures 3.15 & 6.5b), 18 (Figures 3.13 & 6.6a), 19 (Figures 3.12 & 6.6b) and 22 (Figures 3.16 & 6.5c) were detected with avidin-FITC (Section 2.6). Using Script 1 (Section 6.2.1), the percentage of the total nuclear area for each of the two signals in 50 randomly selected nuclei were recorded for each chromosome of interest (Table 6.3). The percentage of total DNA content of the human genome contributed to by each chromosome (Morton, 1991), was used to estimate the expected percentage volume occupied in a 3-D nucleus. It was assumed that the 3-D nucleus contained each chromosome territory with no overlaps and no interchromosomal gaps. The estimated volumes were used to calculate an expected percentage of total nuclear area likely to be observed in 2-D nuclei (Dr. A. Carothers, MRC Human Genetics Unit, Edinburgh).

Table 6.3 The areas of human chromosome territories in human lymphoblastoid nuclei

Biotin labelled paints for chromosomes 11, 22, 18 and 19 were hybridised by FISH to FATO human lymphoblastoid nuclei and detected with avidin-FITC (Figures 6.5 & 6.6). Chromosome 1 paint was directly labelled with Spectrum Orange (Figure 6.5a). Observed % of total nuclear area was calculated from the two signals for each chromosome in 50 randomly selected nuclei. The area occupied by each signal was divided by the total nuclear area, determined using Script 1 (Section 6.2.2). The expected % of total nuclear area was estimated from the % DNA content of total genome contributed by each chromosome (Morton, 1991). +/- standard error of mean

Chromosome	Observed % of total nuclear area	Expected % of total nuclear area	Observed/ expected
1	$8.3^{+/-0.2}$	11.9	0.7
11	$7.4^{+/-0.2}$	8.1	0.9
18	$5.3^{+/-0.1}$	5.8	0.9
19	$6.8^{+/-0.3}$	4.9	1.4
22	$5.2^{+/-0.1}$	4.3	1.2

Figure 6.7 shows histograms comparing the distribution of standardised territory areas for each chromosome tested. The territory sizes for all of the described chromosomes show a normal distribution. In general, the mean interphase area decreases with chromosome size (1>11>18>22). However, chromosome 19 is the exception. Interestingly, with almost three times as many genes allocated as might be predicted from its DNA content, this chromosome takes up an area 40% larger that expected (Tables 1.4 & 6.3) (Figures 6.6b & 6.7). In contrast, chromosome 18, with almost half the number of allocated genes as expected but approximately the same DNA content as chromosome 19, is 10% smaller than the estimated area (Tables 1.4 & 5.3) (Figures 6.6a & 6.7). Chromosome 11 has approximately 50% more genes associated with it than estimated from its DNA content (Table 1.4) and has the same observed:expected area ratio as chromosome 18 (Table 6.3). This suggests that chromosome 19 is highly under-condensed, rather than chromosome 18 being over-condensed at interphase. This transcriptionally active chromosome may have a very "open" configuration to allow access to the transcription machinery.

The analysis of variance for territory areas occupied by chromosomes 18 between nuclei was calculated to be 0.010, while within nuclei the figure for homologues was 0.007. This difference was not significant ($p<0.079$). Interestingly, the analysis of variance for territory areas occupied by chromosome 19 between nuclei was 0.040, in contrast, within nuclei the

figure was 0.016. This difference was relatively significant ($p<0.001$) and implies that the areas occupied within a particular nucleus were more similar than when compared to the areas in other nuclei. Larger territories are possibly more prone to variation in visualised area due to differences in strength of hybridisation and degree of detection across slides. Alternatively, it could be that chromosome 19 shows different levels of compaction in between nuclei, suggesting that it is more dynamic throughout the cell cycle than chromosome 18.

Chromosome 1 had a surprisingly small mean territory area, at only twice that estimated from its DNA content (Tables 1.4 & 6.3) (Figures 6.5a & 6.7). It is possible that the large region of centromeric heterochromatin present on this chromosome (Figure 3.1) is highly compacted and has had a strong influence on the overall area. Also, the chromosome 1 paint used for FISH was previously shown to hybridise weakly at the tip of the p-arm (Figure 3.14) which will result in an under-representation of the interphase territory area. Human chromosomes 9 and 16 also possess regions of centric heterochromatin and it would be of interest to determine the compaction of these interphase chromosome territories.

Chromosome 22, has 20% more genes allocated to it than estimated from its DNA content and is a highly transcriptionally active chromosome as a result of the rDNA located on the p-arm (Section 5.3). This is reflected in the fact that it has a 20% larger area than estimated (Tables 1.4 & 6.3) (Figure 6.5c & 6.7). It also seems possible that there is a current under-representation of genes on chromosome 22 in the literature (Table 1.4) since there is a high density of CpG-islands along the length of this chromosome (Craig & Bickmore, 1994) (Figure 1.3). The influence of the rDNA regions on the interphase territory area of the other acrocentric chromosomes may also prove interesting.

Are there equally striking differences in the position of the territories of these chromosomes in the interphase nucleus? Can the position within the interphase nucleus of each of the chromosomes studied so far tell something more about the distribution of transcription within the nucleus?

6.2.4 The position of human chromosomes within the interphase nucleus

Aside from the differences in overall chromatin compaction, could there be differences in relative position within the nucleus between human chromosomes 18 and 19? The late-

replicating, gene-poor chromosome 18 may be positioned predominantly centrally where DNAse resistant, inactive chromatin is considered by some to reside (Hutchison & Weintraub, 1985; De Graaf *et al.*, 1990; Krystosek & Puck, 1990; Park & De Boni, 1996). Alternatively, chromosome 18 may show a preference for the periphery of the nucleus, with more actively transcribed chromosome 19, more centrally located, a concept suggested by the localisation pre-mRNA splicing components (Reviews: Lawrence *et al.*, 1993; Spector, 1993), polyadenylated RNA (Carter *et al.*, 1993) and active and inactive gene sequences (Lawrence *et al.*, 1988; Lawrence & Singer, 1991; Xing *et al.*, 1995). Other studies, however, have shown no bias in the distribution of nascent transcripts (Review: Fakan & Puvion, 1980), RNA polymerase II and a variety of transcription factors (Wansink *et al.*, 1993; Zeng *et al.*, 1997; Grande *et al.*, 1997) suggesting that there is no compartmentalisation within the nucleus that relates to transcription.

Script 1 (Section 6.2.1) measured several parameters that could be used to assess the position of chromosome specific FISH signals within each nucleus. The following distances (pixels) were calculated:

- The edge of the signal to the nearest edge of the nucleus standardised by dividing by the square root of the nuclear area (edge to edge).
- The centre of the signal to the edge of the nucleus standardised by dividing by the square root of the nuclear area (centre to edge).

These data for each chromosome are recorded in Table 6.4 and displayed in Figure 6.8. Both sets of distance measurements resulted in a similar pattern of territory distribution, suggesting that the size of a territory does not significantly influence these measurements. For example, the edge to edge distance for chromosome 1 places this chromosome generally at the periphery of the nucleus. Since this chromosome takes up one of the larger territory areas in the interphase nucleus, it has an increased likelihood of being observed juxtaposing the nuclear periphery than smaller territories. However, the centre to edge distance is also small, indicating that this chromosome territory is placed more peripherally not simply due to its large size. When the edge to edge distances are subtracted from the centre to edge distances similar values are obtained for each chromosome territory, although as expected, larger territories gave slightly larger differences (Table 6.4).

Table 6.4 The position of human chromosome territories in human lymphoblastoid nuclei

Biotin labelled probes for chromosomes 11, 22, 18 and 19 were hybridised by FISH to FATO human lymphoblastoid nuclei and detected with avidin-FITC (Figures 6.5 & 6.6). Chromosome 1 probe was directly labelled with Spectrum Orange (Figure 6.5a). The distances calculated for each signal in 50 randomly selected nuclei were divided by the √nuclear area (estimate of nuclear radius), determined using Script 1 (Section 6.2.1) and measured in pixels. +/- standard error of mean

Chromosome	Mean standardised edge to edge distance (a)	Mean standardised centre to edge distance (b)	Mean (a) - (b)
1	$0.04^{+/-0.006}$	$0.17^{+/-0.007}$	$0.13^{+/-0.003}$
11	$0.18^{+/-0.006}$	$0.32^{+/-0.006}$	$0.14^{+/-0.004}$
18	$0.08^{+/-0.009}$	$0.18^{+/-0.010}$	$0.10^{+/-0.004}$
19	$0.18^{+/-0.007}$	$0.34^{+/-0.006}$	$0.16^{+/-0.004}$
22	$0.16^{+/-0.009}$	$0.27^{+/-0.009}$	$0.11^{+/-0.003}$

In contrast to chromosome 1, chromosome 11 was rarely observed at the nuclear periphery (Figure 6.5b) and relatively large edge to edge and centre to edge distances were calculated (Table 6.4). Chromosome 18 was found to be peripherally located, while chromosome 19 was significantly more centrally positioned (ST $p<0.0001$). Chromosome 22 adopted a more intermediate position being more central then chromosomes 1 and 18, and more peripheral than chromosomes 11 and 19 (Figure 6.8).

A concentric circle drawn for the outer most 20% of the radius of a 2-D circle would produce a ring representing 36% of the total area. This area would extrapolate to being representative of 21.6% of the total volume of a 3-D sphere. If a territory were randomly positioned within a 3-D nucleus and the nucleus was flattened with no skew to 2-D, then it would be present in the outer 36% of the nuclear area with a probability of 21.6%. Based upon this mathematical model, a randomly located territory would have a centre to edge distance of approximately 0.41 (Dr. A. Carothers, MRC Human Genetics Unit, Edinburgh). All of the centre to edge measurements in Table 6.4 place the chromosome territories tested more peripheral in the nucleus than a randomly placed territory. However, nuclei are not likely to flatten evenly and with no skew as assumed by this model (see Section 6.4.3). In addition, the measurements in Table 6.4 were standardised relative to a broad estimate of the nuclear radius given by the square root of the nuclear area. This approximation may account for the apparent lack of chromosome territories in the centre of the nucleus and suggesting

that they do not give a true estimate for the position of a chromosome territory within the 3-D nucleus. Nonetheless, these measurements give estimates of the positions of chromosomes relative to one another along the radius of the nucleus.

The data presented in this section supports the concept of transcriptionally inactive chromatin being positioned towards the periphery of the nucleus, reserving the centre of the nucleus for transcriptionally active chromatin. Thus, the gene-poor chromosome 18 is peripherally located while the gene-rich chromosomes 11 and 19 are more centrally located. Chromosome 1, despite having a reasonable gene load, may be located at the nuclear periphery due to the influence of its large region of centric heterochromatin. However, the positioning of this chromosome may be evidence that this model is indeed incorrect. The positioning of chromosome 22, with its highly transcriptionally active rDNA, will be influenced by the positioning of the other acrocentric chromosomes and will determine the positioning of the nucleoli.

Positioning human chromosomes relative to one another in the interphase nucleus, and relating this positioning to the characteristics of each chromosome, may considerably improve our understanding of interphase nucleus organisation. Are these territory attributes an artefact of fixation with 3:1 methanol:acetic acid fixed nuclei or can they be reproduced in nuclei fixed by an alternative protocol?

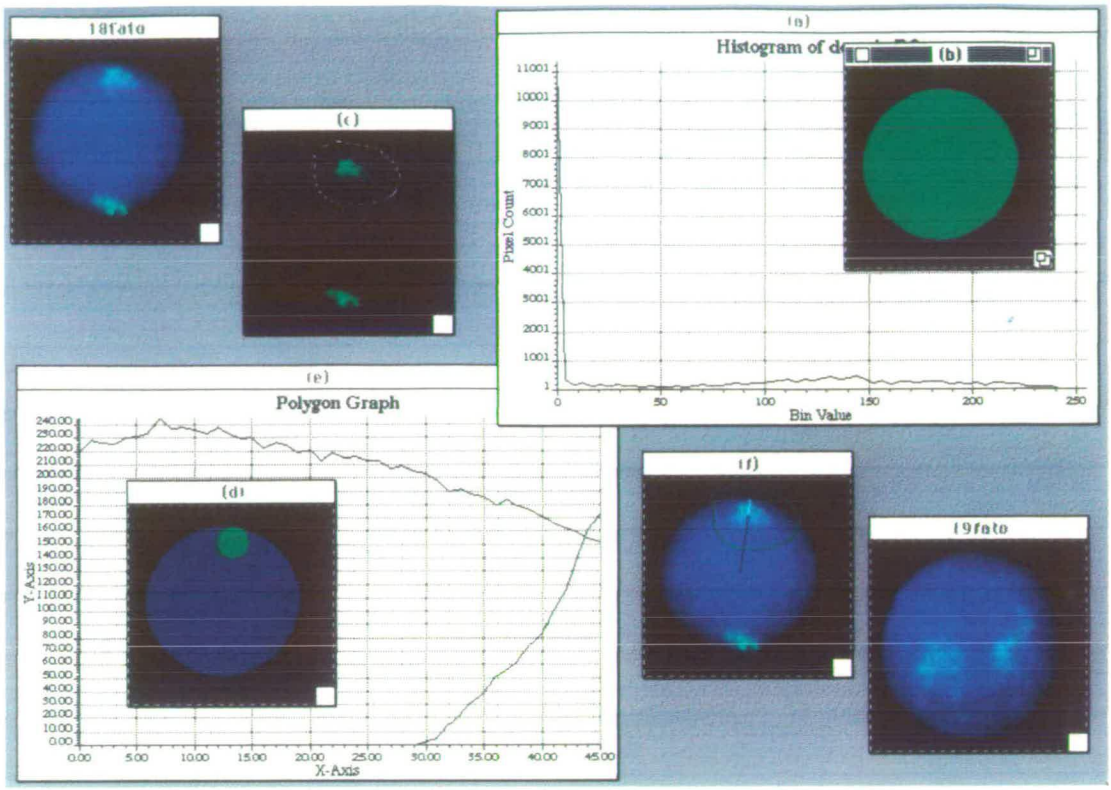

Figure 6.1 Script 1: Determining the size and position of a FISH signal within circular nuclei

Chromosome 18 and 19 FISH paints labelled with biotin and detected with avidin-FITC (green). Nuclei were counterstained with DAPI (blue). (**a**) (**b**) The DAPI stained nucleus was automatically segmented from the background. The area and weighted centroid were calculated. (**c**) A region of interest around the signal was manually selected. The area and weighted centroid were calculated. (**d**) The nuclear segment was converted to binary form. Using the co-ordinates of the signal weighted centroid as the centre, an appropriately sized segmentation disc was automatically adjusted by dilation and erosion until a single pixel with zero intensity was determined. This point was taken as the nearest edge of the nucleus to the signal. (**e**) The distance from this point to the centroid of the signal, and the centroid of the nucleus to the centroid of the signal were calculated. (**f**) The signal segment was converted to binary form, a chord was drawn automatically from the centroid of the segment to the nearest edge of the nucleus and the co-ordinates established for the first pixel with zero intensity. This was taken to be the edge of the signal nearest to the periphery of the nucleus and the distance between these two sets of co-ordinates were calculated.

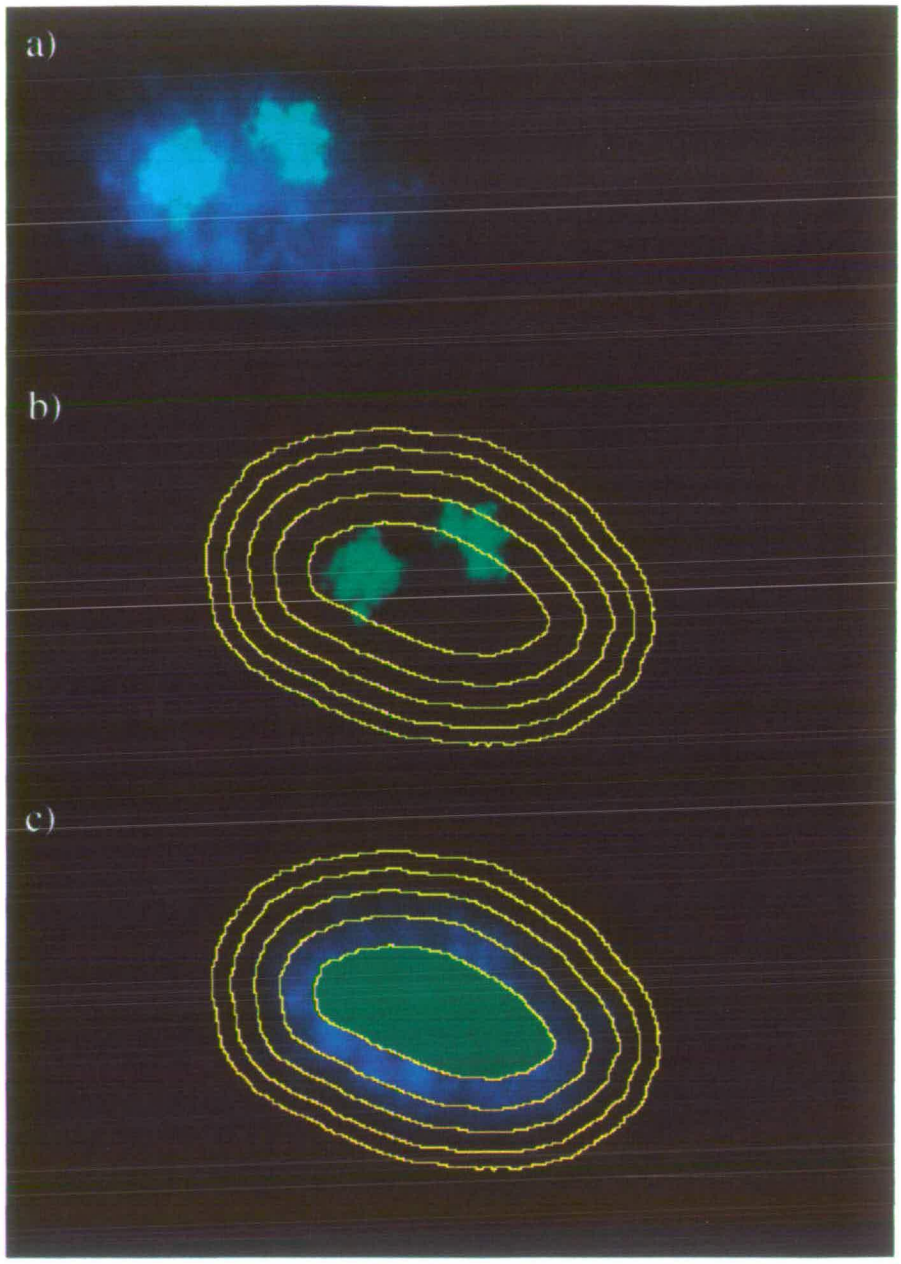

Figure 6.2 Script 2: Determining the distribution of FISH signal within ellipsoid nuclei

(**a**) Chromosome 19 FISH paint labelled with biotin and detected with avidin-FITC (green). Nucleus counterstained with DAPI (blue). The nucleus was automatically segmented from the background and the area and centroid co-ordinates were calculated. The area was divided equally by area into five segments using concentric circles, from the periphery towards the centre of the nucleus. For each segment, the amount of FISH (**b**) and DAPI (**c**) fluorescence were calculated and represented as a percentage of the total.

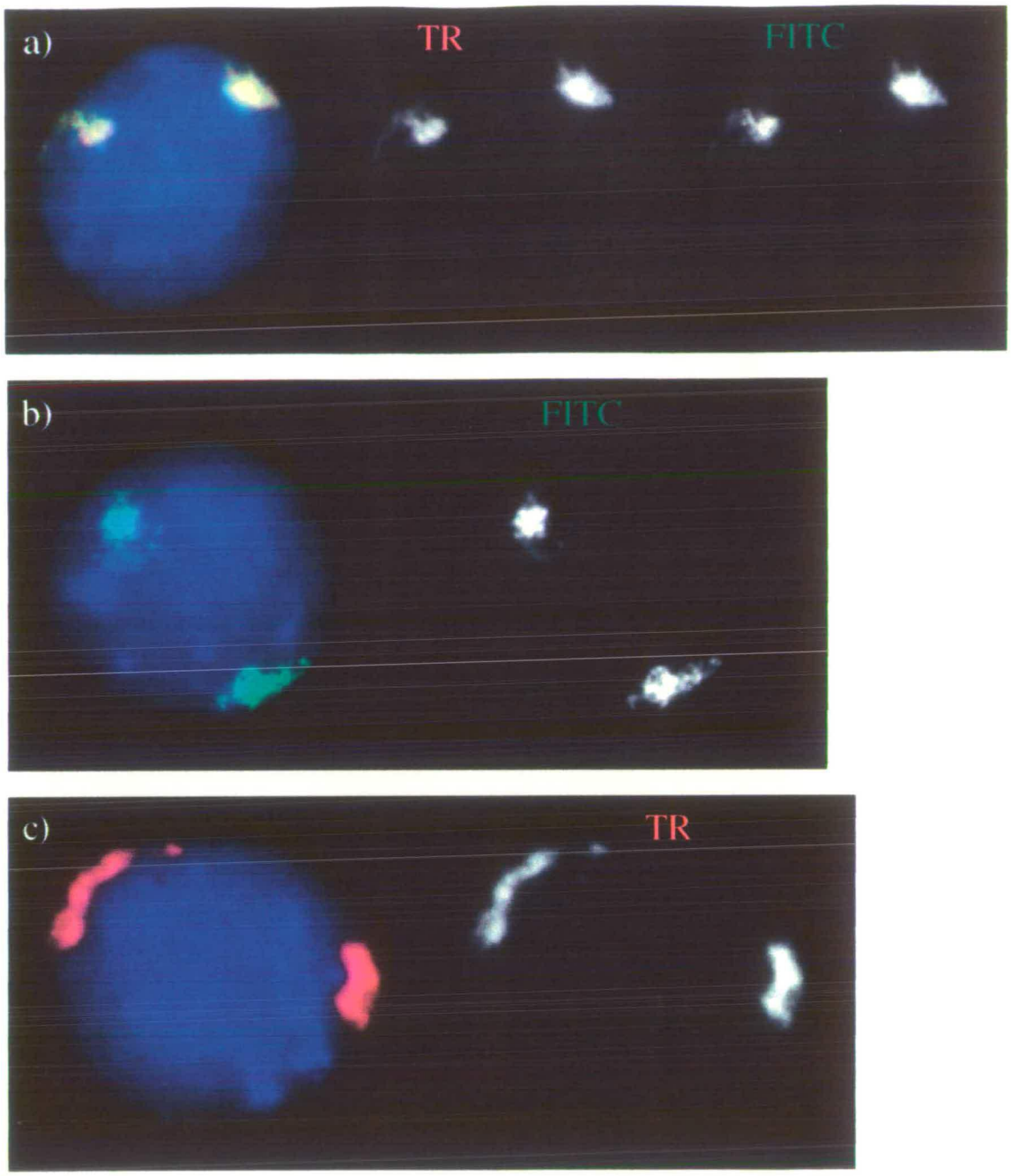

Figure 6.3 The coverage of chromosome 18 FISH paints
(**a**) Catch-linkered chromosome 18 FISH paint (Section 3.3.2) labelled with biotin and dig separately and detected simultaneously with avidin-TR (red) and avidin-FITC (green). (**b**) Commercial chromosome 18 FISH labelled with dig (Oncor) and detected with anti-dig-FITC (green). (**c**) Total DNA from the human chromosome 18-containing rodent hybrid cell line GM11010, labelled with biotin and detected with avidin-FITC (green) (Section 3.2). All nuclei were counterstained with DAPI (blue). (**Middle**) (**Right**) Grey scale representations of the FISH signals.

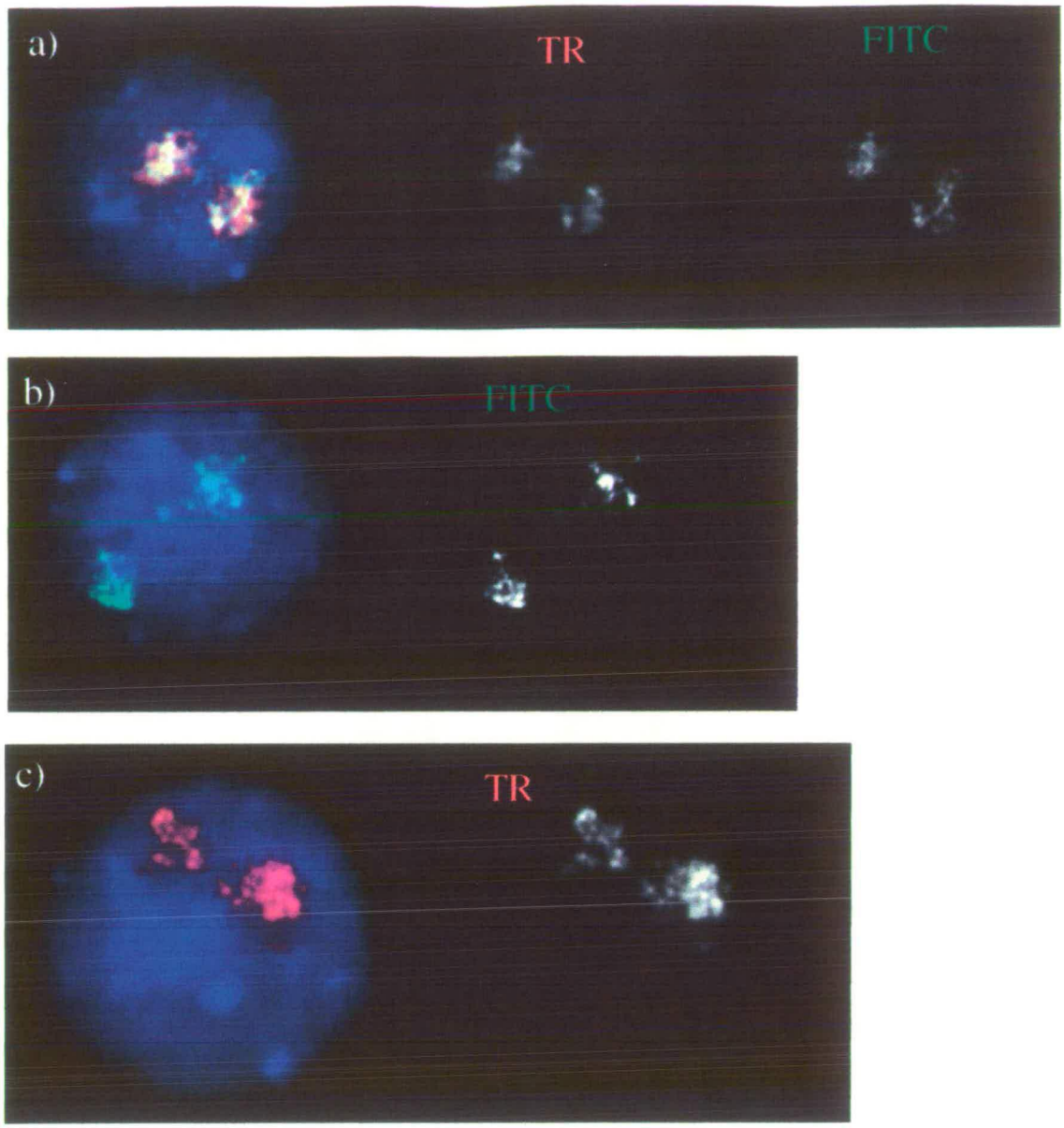

Figure 6.4 The coverage of chromosome 19 FISH paints
(**a**) Inter-*Alu* PCR chromosome 19 FISH paint (Section 3.3.1) labelled with biotin and dig separately and detected simultaneously with avidin-TR (red) and avidin-FITC (green). (**b**) Commercial chromosome 19 FISH labelled with dig (Oncor) and detected with anti-dig-FITC (green). (**c**) Total DNA from the human chromosome 19-containing rodent hybrid cell line GM10449A, labelled with biotin and detected with avidin-FITC (green) (Section 3.2). All nuclei were counterstained with DAPI (blue). (**Middle**) (**Right**) Grey scale representations of the FISH signals.

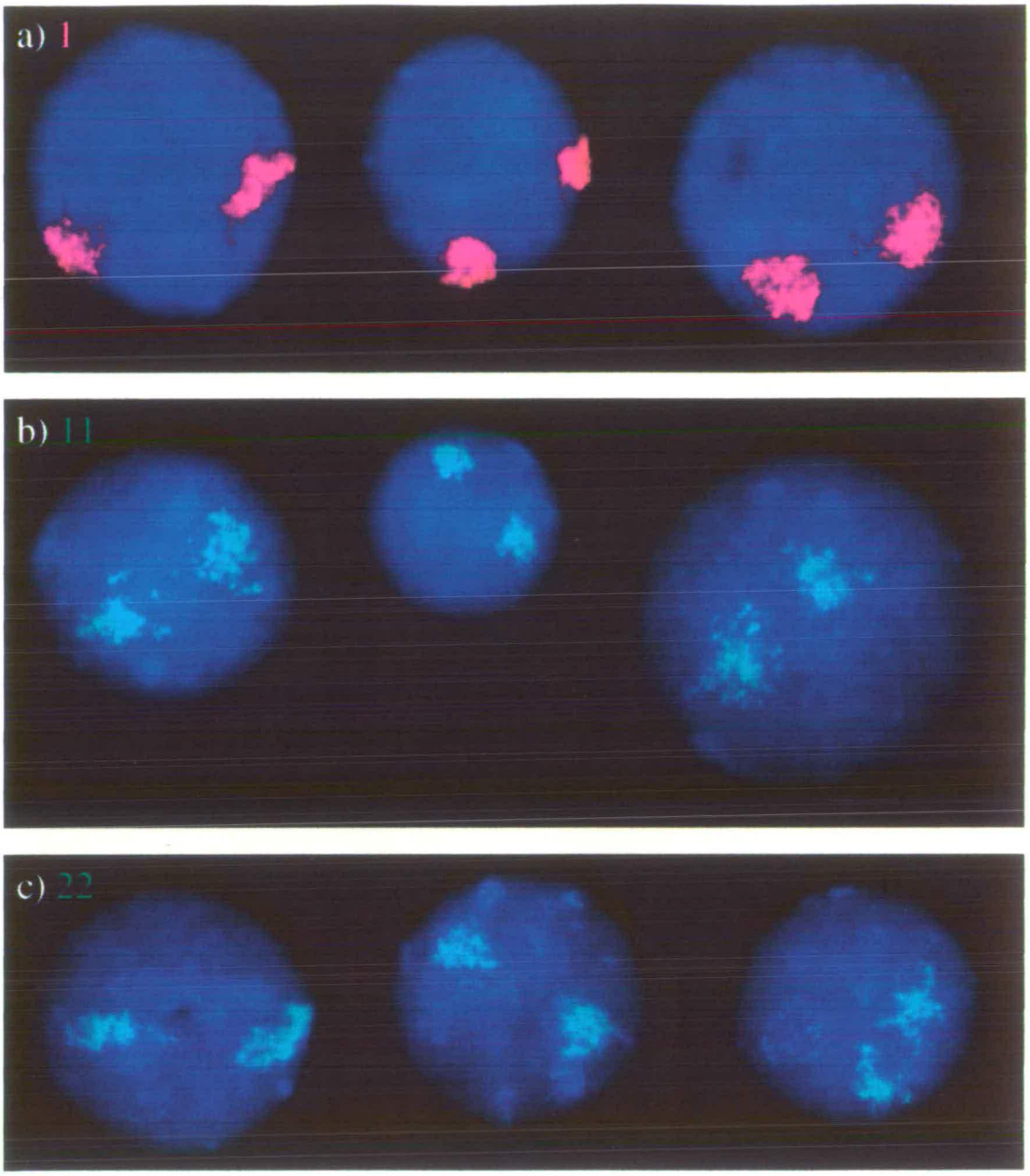

Figure 6.5 The interphase territories of human chromosomes 1, 11 and 22 in lymphoblastoid nuclei
Representative interphase nuclei from the FATO human lymphoblastoid cell line (46, XY) hybridised with chromosome paints by FISH. Nuclei were counterstained with DAPI (blue). (**a**) Chromosome 1 paint directly labelled with Spectrum Orange (Gibco) and supplemented with a centric heterochromatin probe directly labelled with Spectrum Orange (Section 3.3.3). (**b**) Chromosome 11 paint labelled with biotin (Cambio) and detected with avidin-FITC (green). (**c**) Chromosome 22 paint (Section 3.3.3) labelled with biotin and detected with avidin-FITC (green).

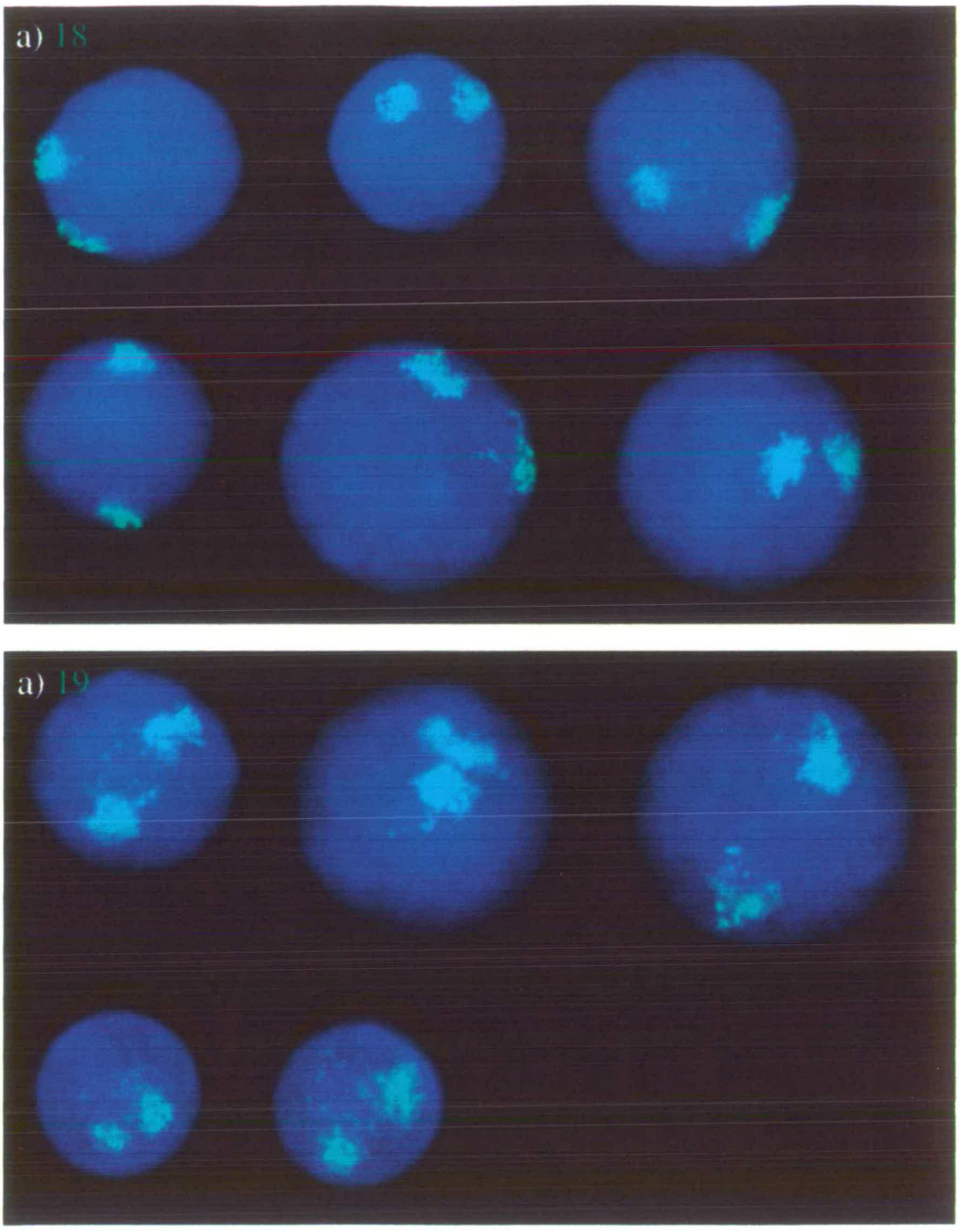

Figure 6.6 The interphase territories of human chromosomes 18 and 19 in lymphoblastoid nuclei
Representative interphase nuclei from the FATO human lymphoblastoid cell line (46, XY) hybridised with chromosome paints by FISH. Nuclei were counterstained with DAPI (blue). Paints labelled with biotin and detected with avidin-FITC (green). (**a**) Catch-linkered chromosome 18 paint (Section 3.3.2), and (**b**) inter-*Alu* PCR chromosome 19 paint (Section 3.3.1).

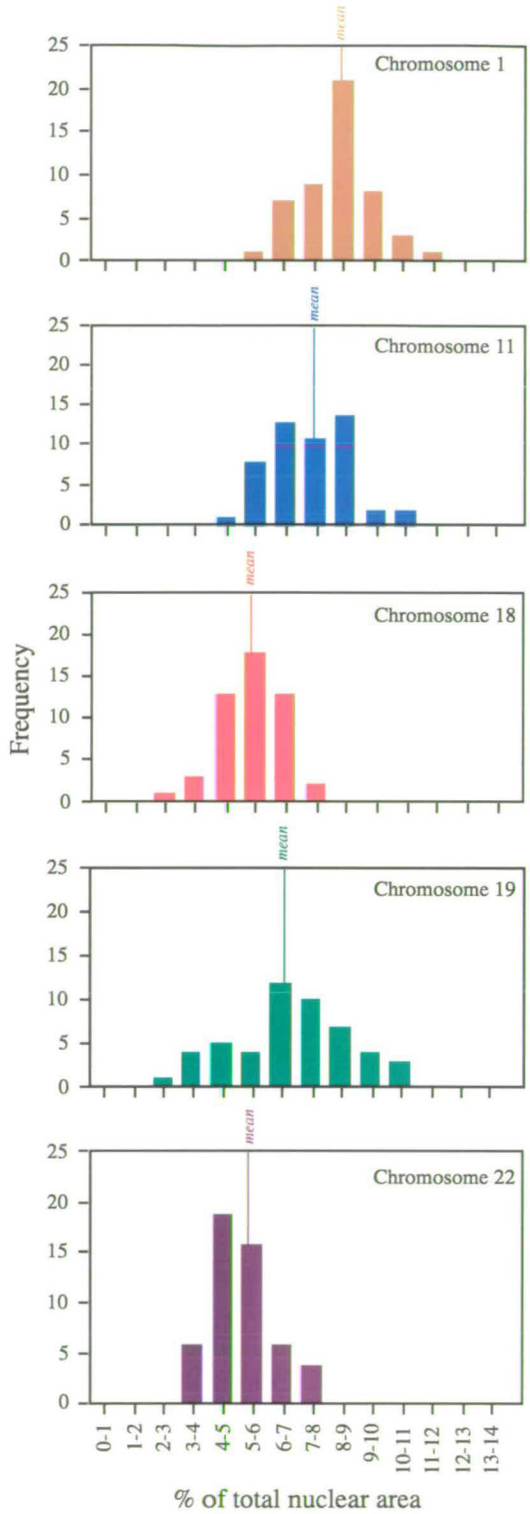

Figure 6.7 Histograms comparing the areas of human chromosome territories in lymphoblastoid nuclei

Using Script 1 (Section 6.2.1) measurements were taken from both homologues in 50 randomly selected FATO human lymphoblastoid nuclei (46,XY) fixed with 3:1 methanol:acetic acid and hybridised with the appropriate human chromosome paint (Section 6.2.3 & Figures 6.5 & 6.6). FISH signal area given as a percentage of the total nuclear area.

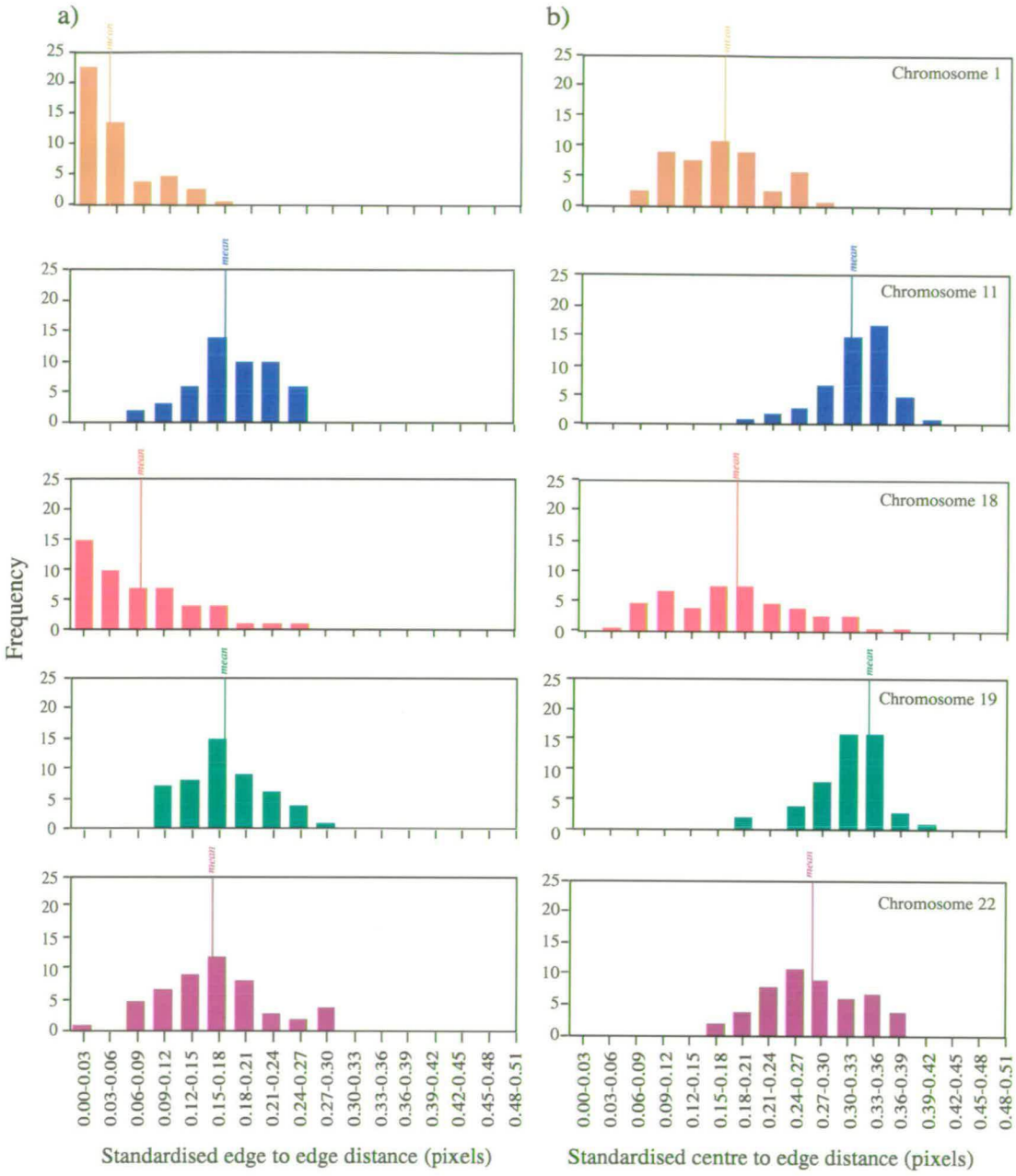

Figure 6.8 Histograms comparing the positions occupied by human chromosome territories in lymphoblastoid nuclei

Using Script 1 (Section 6.2.1) measurements were taken from both signals in 50 randomly selected FATO human lymphoblastoid (46,XY) nuclei fixed with 3:1 methanol:acetic acid and hybridised with the appropriate human chromosome paint (Section 6.2.3 & Figures 6.5 & 6.6). (**a**) Edge of the signal to the nearest edge of the nucleus. (**b**) Centre of the signal to the nearest edge of the nucleus. Distances standardised by dividing by the √nuclear area (estimate of nuclear radius).

6.3 The effects of nuclear fixation on interphase chromosome territories

To produce 2-D nuclei for FISH, 3:1 methanol:acetic acid is usually used to fix the cells (Section 2.6.1). This procedure causes the cells to dehydrate and proteins to precipitate. How and to what extent proteins are denatured is unknown (Pearse, 1968). However, comparisons with paraformaldehyde fixed, 3-D nuclei have suggested that any structural changes induced by this fixation are not significant (Manuelidis, 1985, Popp *et al.*, 1990; Lawrence & Singer, 1991; Hofers *et al.*, 1993; Robinett *et al.*, 1996). However, this has not been stringently tested and it was decided to use an alternative method of fixation to prepare slides for FISH and to assess any differences between the two methods.

Cells from the FATO human cell line were harvested and swollen in hypotonic solution then cytocentrifuged onto slides (Section 2.10.1). Slides were incubated in potassium chromosome medium (KCM) to wash away cytoplasmic debris, and then fixed in 4% paraformaldehyde for 15 minutes. FISH was performed using the standard protocol (Section 2.6) following reverse fixation in 2:5 0.07M NaOH:EtOH for 5 minutes. Paraformaldehyde does not cause dehydration, it fixes nuclei by crosslinking proteins in a number of complex reactions which can involve several different functional groups (Pearse, 1968). A recent study demonstrated that paraformaldehyde fixation resulted in a reduced level of histone displacement than typical 3:1 methanol:acetic acid fixation (Hendzel & Bazett-Jones, 1997).

Figure 6.9 shows a representative selection of nuclei fixed with paraformaldehyde and showing the territories of chromosomes 18 and 19 as revealed by FISH. The nuclei appeared slightly more distorted than typically 3:1 methanol:acetic acid fixed nuclei and there was more thickness maintained, making it difficult to capture images in a single focal plane. Using Script 1, measurements were taken from 50 randomly selected nuclei that possessed two clear territories (Tables 6.5 & 6.6).

The mean interphase territory area for both chromosome 18 and 19 were not significantly different between 3:1 methanol:acetic acid and 4% paraformaldehyde fixed nuclei (Table 6.5). The interphase territory of chromosome 18 was significantly smaller than that for chromosome 19 in paraformaldehyde fixed nuclei (ST $p<0.0001$).

Table 6.5 The areas of human chromosome 18 and 19 territories in alternatively fixed nuclei

Avidin-FITC was used to detect biotin labelled FISH paints for chromosomes 18 and 19 hybridised to human lymphoblastoid nuclei fixed with 3:1 methanol:acetic acid (Figures 6.6a & b) or with 4% paraformaldehyde (Figure 6.9). The area of each signal was divided by the total nuclear area, determined using Script 1 (Section 6.2.1). +/- standard error of mean

Chromosome	% of total nuclear area in 3:1 methanol:acetic acid fixed nuclei	% of total nuclear area in 4% paraformaldehyde fixed nuclei
18	$5.3^{+/-0.1}$	$5.0^{+/-0.2}$
19	$6.8^{+/-0.3}$	$6.2^{+/-0.2}$
19:18	1.28	1.24

The distance measurements for the position of the chromosome 18 interphase territory were not significantly different between the two fixation protocols (Table 6.6). However, the distance measurements for the position of the chromosome 19 territory were significantly different between the two fixation protocols (Table 6.6). This may be due to the slight distortion of the paraformaldehyde nuclei making estimates of nuclear radius made from the total nuclear area unreliable. Nonetheless, chromosome 18 is still positioned closer to the edge of the nucleus than chromosome 19, with $p<0.087$ for edge to edge distance and $p<0.010$ for centre to edge distance, using a Student's T test.

Table 6.6 The positions of human chromosome 18 and 19 territories in alternatively fixed nuclei

Avidin-FITC was used to detect biotin labelled FISH paints for chromosomes 18 and 19 hybridised to human lymphoblastoid nuclei fixed with 3:1 methanol:acetic acid (Figures 6.6a & b) or with 4% paraformaldehyde (Figure 6.9). The distances calculated for each signal were divided by the $\sqrt{}$nuclear area (estimate of nuclear radius), determined using Script 1 (Section 6.2.1) and measured in pixels. +/- standard error of mean

Chromosome	Mean standardised edge to edge distance	Mean standardised centre to edge distance
3:1 methanol:acetic acid fixed		
18	$0.08^{+/-0.009}$	$0.18^{+/-0.010}$
19	$0.18^{+/-0.007}$	$0.34^{+/-0.006}$
4% paraformaldehyde fixed		
18	$0.09^{+/-0.010}$	$0.21^{+/-0.011}$
19	$0.12^{+/-0.010}$	$0.24^{+/-0.010}$

So far my analysis has focused on human lymphoblastoid cells. Are the contrasting areas and positions of the chromosome 18 and 19 interphase territories maintained in other cell types or are particular territorial organisations cell type-specific?

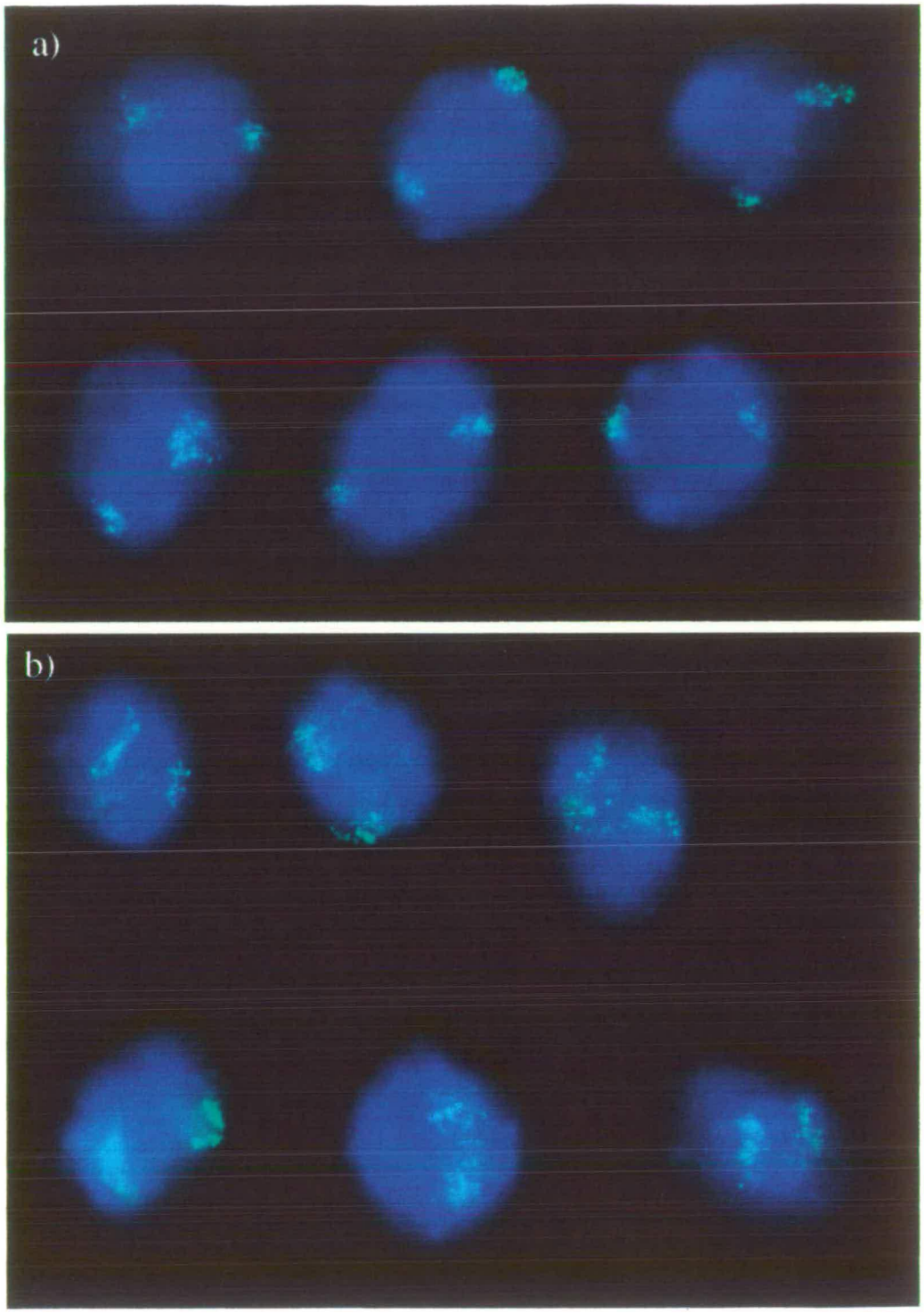

Figure 6.9 The interphase territories of human chromosome 18 and 19 in 4% paraformaldehyde fixed nuclei
Representative interphase nuclei from the FATO human lymphoblastoid cell line (46, XY). Nuclei were cytocentrifuged onto slides, fixed with 4% paraformaldehyde and hybridised by FISH with paints for: (**a**) chromosome 18 (Section 3.3.2), and (**b**) chromosome 19 (Section 3.2.1). Paints were labelled with biotin and detected with avidin-FITC (green). Nuclei were counterstained with DAPI (blue).

6.4 The territories of chromosomes 18 and 19 in interphase nuclei from different cell types

Approximately 25% of human genes are housekeeping and have widespread expression, while the remainder are tissue-restricted in their expression (Craig, 1995). However, there is no definite distinction between housekeeping and tissue-specific genes. Some housekeeping genes may be expressed at different levels or be differentially spliced in some tissues, and some tissue-specific genes may be expressed mainly in one tissue but at a low level in other tissues. If a different set of genes are expressed in the cells of one tissue type compared to that of another, is it necessary that the nucleus must be reorganised to allow this to occur?

In the first instance a human lymphoblastoid cell line was used for this study. The effects upon nuclear organisation of establishing a permanent growing cell line using Epstein-Barr virus are unknown (Neitzel, 1986). However, it has been shown that Herpes Simplex virus infection can cause a large re-organisation of endogenous chromatin in HeLa nuclei (Puvion-Dutilleul & Besse, 1994). Thus, it was important to compare the chromosome territory areas and positions established in lymphoblastoid nuclei with nuclei from primary lymphocytes. Nuclei from primary fibroblasts and fibrosarcoma cells were also analysed.

6.4.1 Selection of human cells of different tissue origin

Primary (1°) lymphocytes were collected from peripheral blood of a normal male, stimulated to divide with phytohaemagglutinin, cultured and fixed as described in Section 2.1.4. The karyotype was confirmed as normal after analysis of DAPI stained metaphase spreads (Figure 6.10).

1° fibroblasts were obtained from a normal male foetal lung biopsy and cultured and fixed as described in Section 2.1.5. This culture had been enriched for G1 nuclei.

An immortal cell line derived from a fibrosarcoma of a male patient, HT1080, was obtained from the European Collection of Animal Cell Cultures, Salisbury. This line was previously characterised to have 54% of cells with 46 chromosomes, however 80% of these cells had an extra C-group chromosome (6-12) and lacked a B-group chromosome (4 or 5). The remaining 46% of cells were lacking or had gained one or two chromosomes (Rasheed *et al.*,

1974). Polyploidy was not recorded. Since these were not gross abnormalities and rarely involved chromosomes 18 or 19 it was considered that this cell line would be adequate for analysis.

6.4.2 The areas occupied by human chromosome 18 and 19 territories in interphase nuclei from different cell types

As a proportion of total nuclear area the territories of both chromosomes 18 and 19 were found to be distinct within each cell type. While in 1° lymphocytes and lymphoblasts the chromosome 18 territories were similar to each other, the chromosome 19 territory was considerably larger in 1° lymphocytes than it was in lymphoblasts (Figure 6.10 & Table 6.7). Consequently, there is a larger ratio between the chromosome 18 and 19 territories in 1° lymphocytes, with chromosome 18 taking up less than half the area of chromosome 19. Chromosome 19 may be more transcriptionally active in 1° lymphocytes than lymphoblasts.

Table 6.7 The areas of human chromosome 18 and 19 territories in nuclei of different cell types
Avidin-FITC was used to detect biotin labelled FISH paints for chromosomes 18 and 19 hybridised to human nuclei from different cell types fixed with 3:1 methanol:acetic acid: primary lymphocytes (Figure 6.10), lymphoblasts (Figure 6.6), primary fibroblasts (Figure 6.11a) and fibrosarcoma cells (Figure 6.11b). The area of each signal was divided by the total nuclear area, determined using Script 1 (Section 6.2.1). +/- standard error of mean p-significance between the means for each chromosome in a particular cell type (Student's T test)

	% of total nuclear area		19:18	p
Cell type	Chromosome 18	Chromosome 19		
1° lymphocytes	$5.7^{+/-0.2}$	$9.2^{+/-0.3}$	1.61	0.0001
Lymphoblastoid cell line (FATO)	$5.3^{+/-0.2}$	$6.8^{+/-0.3}$	1.28	0.0002
1° fibroblasts	$4.7^{+/-0.3}$	$5.1^{+/-0.3}$	1.09	0.210
Fibrosarcoma cell line (HT1080)	$3.9^{+/-0.3}$	$6.7^{+/-0.3}$	1.72	0.0004

The territory areas of both chromosomes 18 and 19 were smaller in 1° fibroblasts and fibrosarcoma cells than 1° lymphocytes and lymphoblasts when measured as a percentage of total nuclear area (Figure 6.11 & Table 6.7). This may reflect a slightly different nuclear organisation resulting from the ellipsoid shape of the nuclei from former two cell lines.

Interestingly, in 1° fibroblasts the differences in territory area for chromosome 18 and 19 were not significant (ST $p<0.210$), while in fibrosarcoma cells chromosome 18 was almost one quarter the size of chromosome 19 (ST $p<0.0004$). This may reflect differences in the level of transcription of these chromosomes in the different cell types. A survey of the genes present upon these two chromosomes and the cell types in which they are likely to be active may prove useful. Clearly, alternative cell types offer different arrangements of chromosome territories which relate to their particular shape and transcriptional requirements. Nonetheless, the territory of chromosome 18 was consistently smaller than that of chromosome 19 (Figure 6.12 & Table 6.7).

6.4.3 The positions of human chromosomes 18 and 19 within the interphase nuclei of different cell types

The nuclei of both 1° fibroblasts and fibrosarcoma cells are ellipsoid in shape. Script 1, used for making position measurements based upon distances along an estimated radius, are invalid with this shape of nucleus, since there is no fixed radius. An alternative strategy was chosen to assess the relative positions of territories in the nuclei of such cells. The nucleus was divided into five concentric segments equal in area, from the periphery towards the centre of the nucleus (Section 6.1.2) (Figure 6.2) and the total amount of fluorescence from the FISH signal and DAPI counterstain was calculated in each segment. This method is equally valid for nuclei of all shapes. Several fibrosarcoma nuclei were shown to contain an extra chromosome 18 or 19. Images were collected of approximately 10 nuclei with trisomy 18 or 19 and these were separately analysed. The expected distribution of fluorescence was calculated using a mathematical model in which a sphere was collapsed with no skew into a circle and is based upon the relative volume of the sphere that each concentric segment of the circle would represent (Dr. A. Carothers, MRC Human Genetics Unit, Edinburgh). The observed total percentage DAPI and chromosome 18 or 19 signal fluorescence for each cell type was divided by the expected distribution (Table 6.8).

In all cell types the percentage of total DAPI fluorescence present in each segment followed the same pattern, with 30-40% more fluorescence at the nuclear periphery and <10% less fluorescence observed in the centre of the nucleus than expected (Table 6.8). An apparently higher density of DNA at the periphery of the nucleus compared to the centre suggests that the nuclei may have flattened by collapsing vertically pushing some of the nuclear volume to the edge. However, DAPI is an AT-specific fluorochrome and it may be that its

Table 6.8 The distributions of human chromosome 18 and 19 territories in nuclei of different cell types

Biotin labelled paints for chromosomes 18 and 19 were hybridised by FISH to human nuclei from different cell types and detected with avidin-FITC. Nuclei were counterstained with DAPI. Using Script 2 (Section 6.2.2) the percentage of total DAPI and FITC fluorescence was calculated within five concentric segments of equal area. The expected percentage fluorescence for each segment was estimated from a model in which a sphere is compressed with no skew (Dr. A. Caruthers, MRC Human Genetics Unit, Edinburgh). 1- outer most concentric segment 5- inner most concentric segment

Expected fluorescence distribution	Cell type	Primary lymphocytes		Lymphoblast cell line (FATO)		Primary fibroblasts		Fibrosarcoma cell line (HT1080)		Fibrosarcoma cell line (HT1080) with trisomies	
	Chromosome	18	19	18	19	18	19	18	19	18	19
	Number of nuclei analysed	50	47	49	50	50	49	50	50	10	8
	Observed/expected % FITC										
8.9	1	3.0	0.1	1.2	0.2	1.5	0.6	1.0	0.1	1.9	0.1
16.4	2	1.8	0.3	1.4	0.3	1.1	0.8	0.7	0.2	1.0	0.4
21.2	3	0.9	0.7	1.2	0.7	0.9	1.0	0.9	1.0	1.0	1.2
25.1	4	0.5	1.3	0.9	1.4	1.0	1.2	1.1	1.3	1.0	1.3
28.5	5	0.5	1.6	0.6	1.5	0.9	1.2	1.2	1.3	0.9	1.2
	Observed/expected % DAPI										
	1	1.3		1.4		1.3		1.3		1.3	
	2	1.0		1.1		1.0		1.0		1.0	
	3	1.0		1.0		1.0		1.0		1.0	
	4	1.0		0.9		1.0		1.0		1.0	
	5	0.9		1.0		1.0		1.0		0.9	

distribution is reflecting the distribution of AT-rich DNA. It would be interesting to assess the distribution of fluorescence from a number of different DNA fluorochromes to determine between these two possibilities. In addition, the way in which nuclei flatten following fixation with different protocols may be analysed using this Script.

In each cell type, the observed percentage of total chromosome 18 paint fluorescence was always more (1-3x) than expected in the outer most segment, while the inner most segment showed generally less fluorescence (0.5-1.2x) than expected (Table 6.8). Reciprocally, in each cell type, the distribution of chromosome 19 paint fluorescence was always less (0.1-0.6x) than expected in the outer most segment and more (1.2-1.6x) than expected in the inner most segment (Table 6.8). Figure 6.13 shows the ratio of mean chromosome 18 to chromosome 19 paint fluorescence for each segment in each cell type. It is clear from this data that in each cell type chromosome 18 territories are located more towards the periphery of the nucleus and chromosome 19 territories are located relatively more centrally (Table 6.8 & Figure 6.13). The opposing distribution of chromosomes 18 and 19 paint fluorescence is most striking in 1° lymphocytes and fibrosarcoma cells (Figure 6.13). Such differences in chromosome paint distribution between cell types may reflect slight differences in transcriptional activity and nuclear organisation.

6.4.4 The areas and positions of human chromosome 18 and 19 within a rodent-human hybrid nuclei

Are the properties that establish the contrasting territory size and position of chromosomes 18 and 19 in a human nucleus intrinsic to the chromosome or dependent upon the nuclear environment? This was tested by comparing the territories of these chromosomes in rodent-human monochromosome hybrid cell nuclei.

GM11010 is a Chinese hamster-human hybrid cell line containing chromosome 18 as its only human material, however, chromosome 18 is missing a portion of the q-arm in approximately 35% of cells (Section 3.2). GM10449A is a Chinese hamster-human hybrid cell line containing chromosome 19 as its only human material and chromosome 19 in this cell line is apparently intact (Section 3.2). Cells from each of these cell lines were harvested, swollen in hypotonic and fixed with 3:1 methanol:acetic acid (Section 2.1.6). Slides were prepared and hybridised with the appropriate chromosome paint by FISH. Using Script 1 (Section 6.2.1), measurements were taken for 50 randomly selected nuclei.

Figure 6.14a shows representative GM11010 nuclei hybridised with the chromosome 18 paint by FISH. Only one territory was observed in each nucleus indicating that only one human chromosome 18 is present in this hybrid line, consistent with the observations of metaphase spreads (Section 3.2). Any estimates of territory area would be invalid since part of the q-arm of this chromosome has been demonstrated to be missing in a substantial number of cells (Section 3.2). However, the mean chromosome territory area was calculated to be 3.0% of the total nuclear area, clearly an underestimate of the territory size of a complete chromosome (Tables 6.3 & 6.9). Surprisingly, the chromosome 18 territory was rarely observed juxtaposing the nuclear periphery. This was substantiated by measurements of edge to edge and centre to edge distance which were much larger than observed in normal human lymphoblasts (Table 6.4) and, indeed, not significantly smaller than for chromosome 19 in its respective rodent-human hybrid cell line (Table 6.9).

Table 6.9 The areas and positions of human chromosome 18 and 19 territories in rodent-human hybrid nuclei

Avidin-FITC was used to detect biotin labelled FISH paints for chromosomes 18 and 19 hybridised to the appropriate rodent-human monochromosome hybrid cell nuclei: chromosome 18-containing GM11010 (Section 3.2) (Figure 6.14a) and chromosome 19-containing GM10449A (Section 3.2) (Figure 6.14b). Using Script 1 (Section 6.2.1), 50 randomly selected nuclei were analysed. The area of each signal was divided by the total nuclear area. The distances calculated for each signal were divided by the √nuclear area (estimate of nuclear radius), measured in pixels. +/- standard error of mean p- significance between the means for each chromosome (Student's T test)

Hybrid cell line	Chromosome	% of total nuclear area	Mean standardised edge to edge distance	Mean standardised centre to edge distance
GM11010	18	$3.0^{+/-0.26}$	$0.21^{+/-0.02}$	$0.31^{+/-0.02}$
GM10449A	19	$8.0^{+/-0.42}$	$0.24^{+/-0.01}$	$0.38^{+/-0.01}$
p	19:18	0.000	0.280	0.001

Figure 6.14b shows representative GM10449A nuclei hybridised with chromosome 19 paint by FISH. As with the chromosome 18-containing hybrid cell line, one territory was observed in each nucleus consistent with the presence of one human chromosome 19 (Section 3.2). The mean territory area was calculated as being 8.0% of the total nuclear area, which is very similar to the percentage area observed in normal human lymphoblasts

(Tables 6.3 & 6.9). The edge to edge and centre to edge distances were also similar to those observed in normal human lymphocytes (Tables 6.4 & 6.9).

The sizes of territories occupied by chromosomes 18 and 19 remain very different from each other in a hybrid cell background (Table 6.9 & Figure 6.15a). Despite the underestimate of chromosome 18 territory size, it is so much smaller than the territory of chromosome 19 that the incompleteness of chromosome 18 in some nuclei alone cannot explain the difference. Histograms comparing the positioning of the chromosomes 18 and 19 within their respective hybrid nuclei are very similar (Figures 6.15b & c). There was no significant difference between either edge to edge mean distances (ST $p<0.280$) between the two chromosomes (Table 6.9). The centre to edge mean distances (ST $p<0.001$) were significantly different probably reflecting the difference in size between the two chromosome territories (Table 6.9). Interestingly, there is an apparently bimodal distribution of positioning for chromosome 18 evident from the histograms in Figures 6.15b & c, possibly representing the intact verses the deleted chromosome.

The transcriptional activity of chromosomes 18 and 19 in their respective hybrid lines is unknown. The degree of histone acetylation along the length of these chromosomes appears to be similar in normal and hybrid metaphase spreads (Section 5.4). Chromosome 18 is consistently hypoactylated along its entire length, consistent with transcriptional inactivity (Figure 5.9). On the other hand, chromosome 19 is consistently hyperacetylated along its entire length, indicating high transcriptional activity. (Figure 5.10) Thus, the nuclear territory area data conform with the apparent presumed transcriptional activities of the chromosomes in a hybrid cell background. Levels of histone acetylation only serve as a marker for potential transcriptional activity (Section 1.4.1.3) and, thus, true measurements of activity remain to be tested at the gene level. It would be interesting to know whether the timing of replication of these two chromosomes were maintained in a hybrid background (Section 1.2.4).

The positioning of the chromosome 18 and 19 territories are similar in their respective hybrid nuclei, with both chromosomes possessing a more central nuclear location. This data imply that the mechanisms involved in positioning chromosome 18 towards the periphery of the nucleus differ between Chinese hamster nuclei and human nuclei and possible mechanisms are discussed in Section 9.4. Manuelidis (1985) showed in nuclei of a

mouse-human hybrid with four human chromosomes (1,3,4 and X) that the human chromosomes had a reproducible position and shape. How these dispositions relate to those in normal human nuclei was not explored, however, this study does support the fact that mechanisms are in place in other mammalian nuclei for establishing a specific chromosome territory organisation, be there differences between species. An alternative explanation for the altered nuclear positioning of chromosome 18 is that the absence of part of the q-arm may be involved. It is possible that the portion of the chromosome that is missing includes an "organising" centre, that is, a sequence which binds particular proteins involved in directing this chromosome to the periphery of the nucleus. This explanation would be ruled out if after tagging the chromosome and introducing it into normal human lymphoblasts the chromosome repositioned to the nuclear periphery. Alternatively, hybridisation of a probe specific for the tip of the chromosome 18 q-arm, in addition to a chromosome 18 paint, would enable identification of and comparison between the intact and deleted chromosomes. The study of a human chromosome 18 and 19 translocation in Section 7.2 addresses these possibilities.

Up to this stage I have studied asynchronous cell populations. Do interphase chromosome territories alter in disposition throughout the cell cycle?

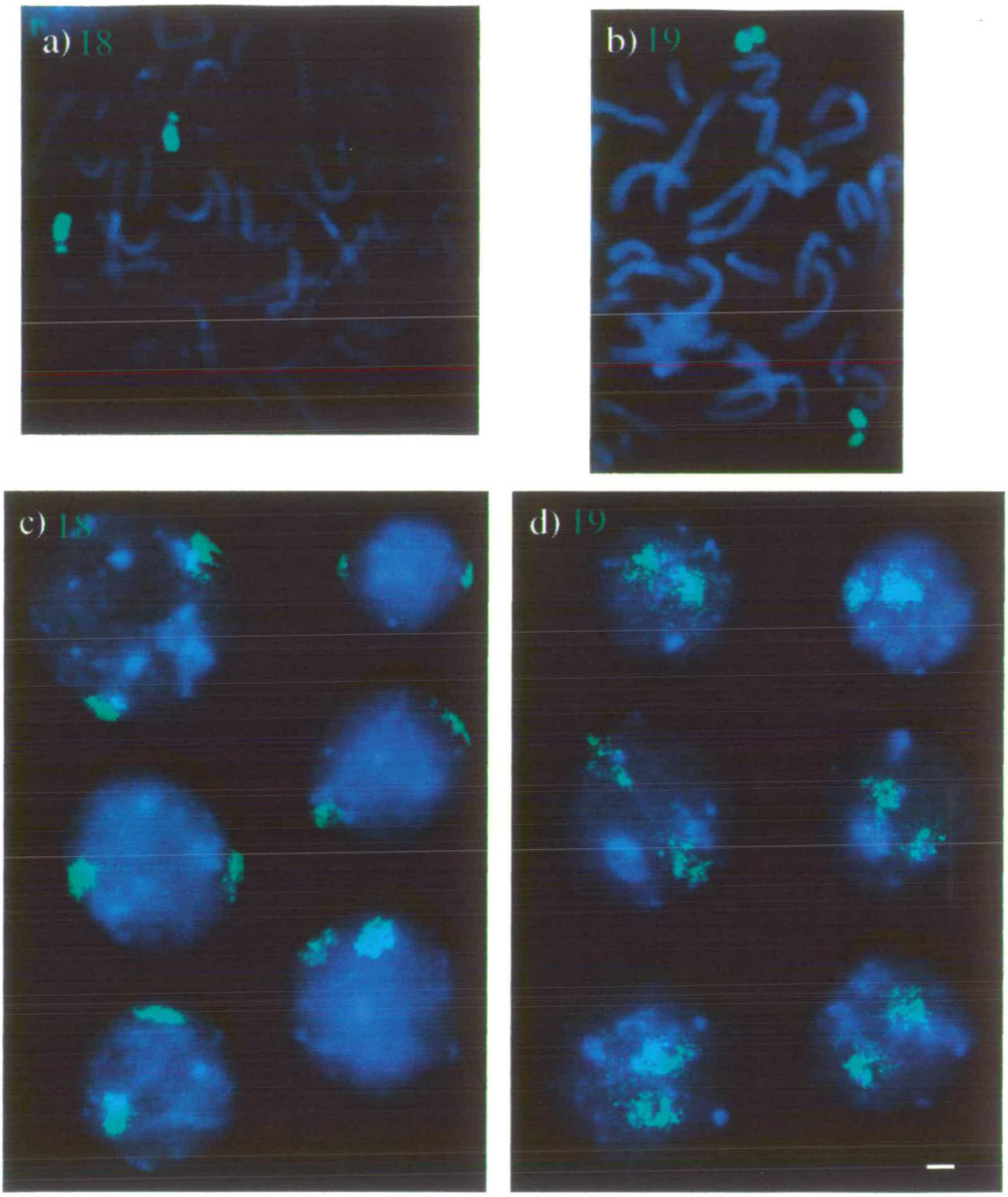

Figure 6.10 The interphase territories of human chromosomes 18 and 19 in 1° lymphocyte nuclei

Human 1° lymphocytes (46 XY) fixed with 3:1 methanol:acetic acid and hybridised with: (**a**) (**c**) human chromosome 18 paint (Section 3.3.2), and (**b**) (**d**) human chromosome 19 paint (Section 3.2.1). Both paints were labelled with biotin and detected with avidin-FITC (green). Nuclei and chromosomes were counterstained with DAPI (blue). (**a**) (**b**) Representative metaphase spreads. (**c**) (**d**) Selection of representative interphase nuclei. Bar=1μm

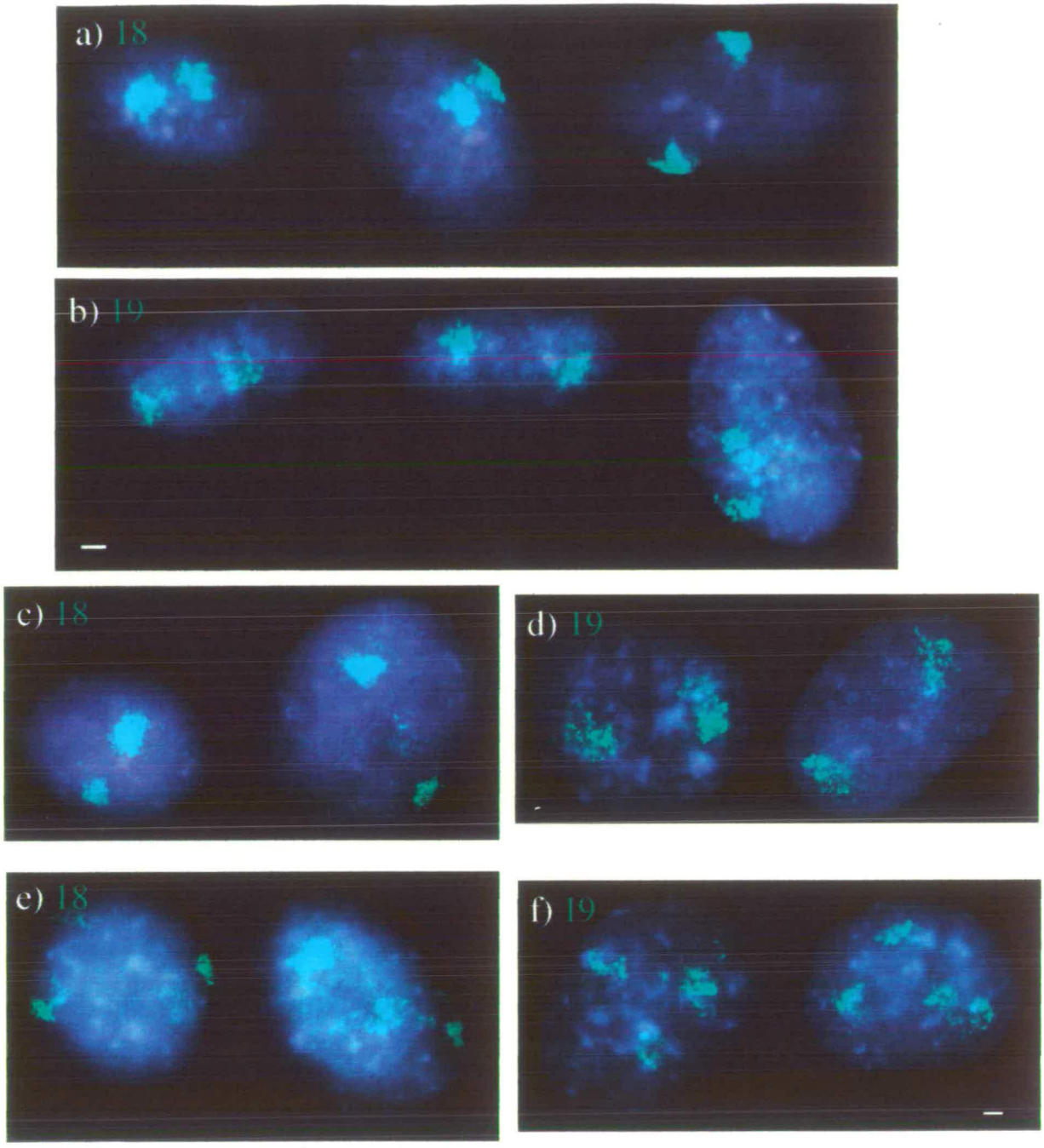

Figure 6.11 The interphase territories of human chromosomes 18 and 19 in 1° fibroblast and fibrosarcoma cell nuclei

(**a**) (**b**) Representative human 1° fibroblast nuclei (46, XY) fixed with 3:1 methanol:acetic acid. (**c**) (**d**) Representative human HT1080 fibrosarcoma cell nuclei (46, XY) fixed with 3:1 methanol:acetic acid. (**e**) (**f**) Examples of human HT1080 fibrosarcoma cell nuclei with trisomy for the chromosome 18 or 19, fixed with 3:1 methanol:acetic acid. Nuclei hybridised with: (**a**) (**c**) (**e**) human chromosome 18 paint (Section 3.3.2), and (**b**) (**d**) (**f**) human chromosome 19 paint (Section 3.2.1). All paints labelled with biotin and detected with avidin-FITC (green). Nuclei were counterstained with DAPI (blue). Bar=1μm

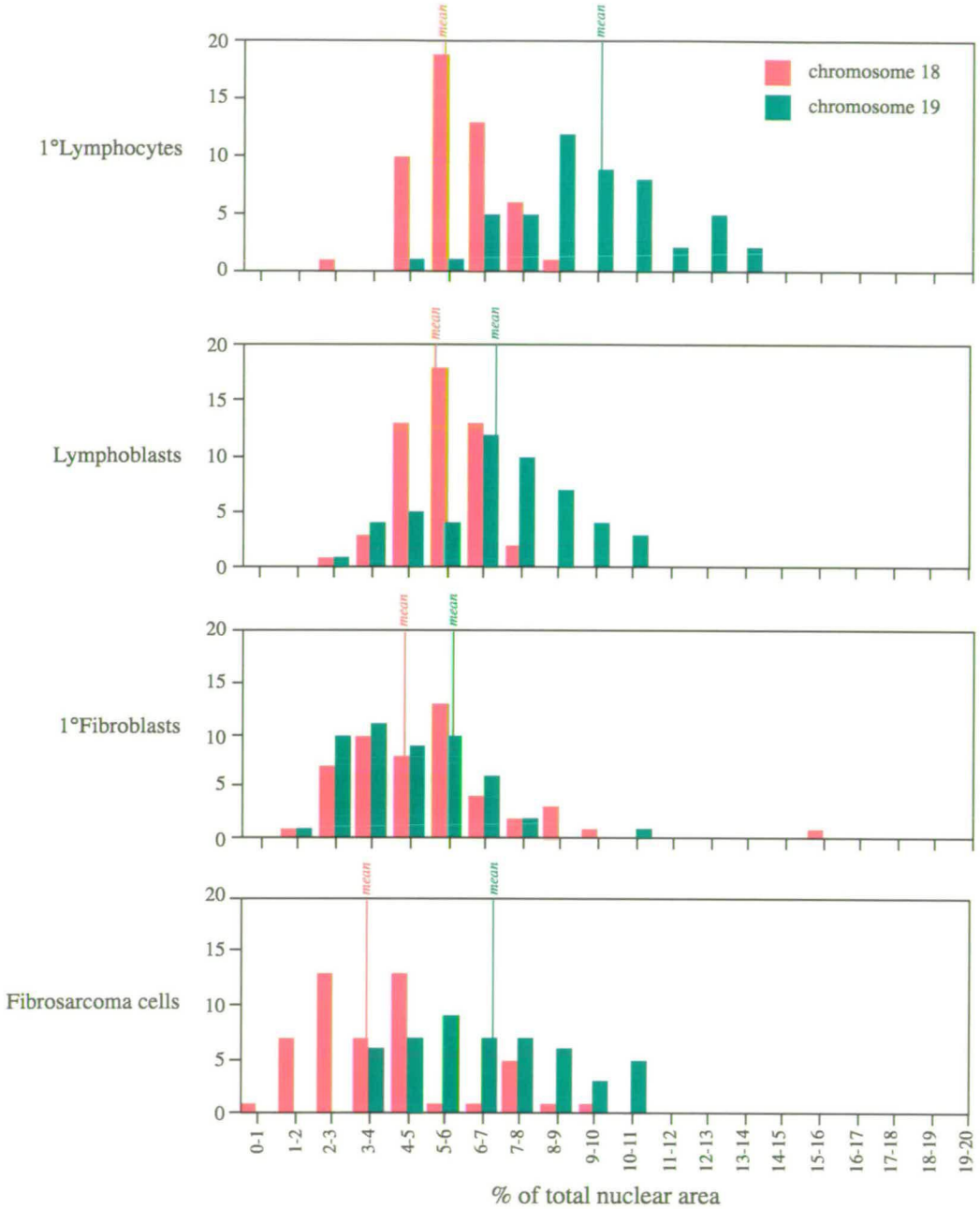

Figure 6.12 Histograms comparing the areas of human chromosome 18 and 19 territories in nuclei of differing cell types

Avidin-FITC was used to detect biotin labelled paints for human chromosomes 18 and 19 hybridised to human nuclei from different cell types fixed with 3:1 methanol:acetic acid: primary lymphocytes (Figure 6.10), lymphoblasts (Figure 6.6), primary fibroblasts (Figure 6.11a) and fibrosarcoma cells (Figure 6.11b). Using Script 1 (Section 6.2.1) measurements were taken from both homologues in 50 randomly selected nuclei. FISH signal area given as a percentage of the total nuclear area.

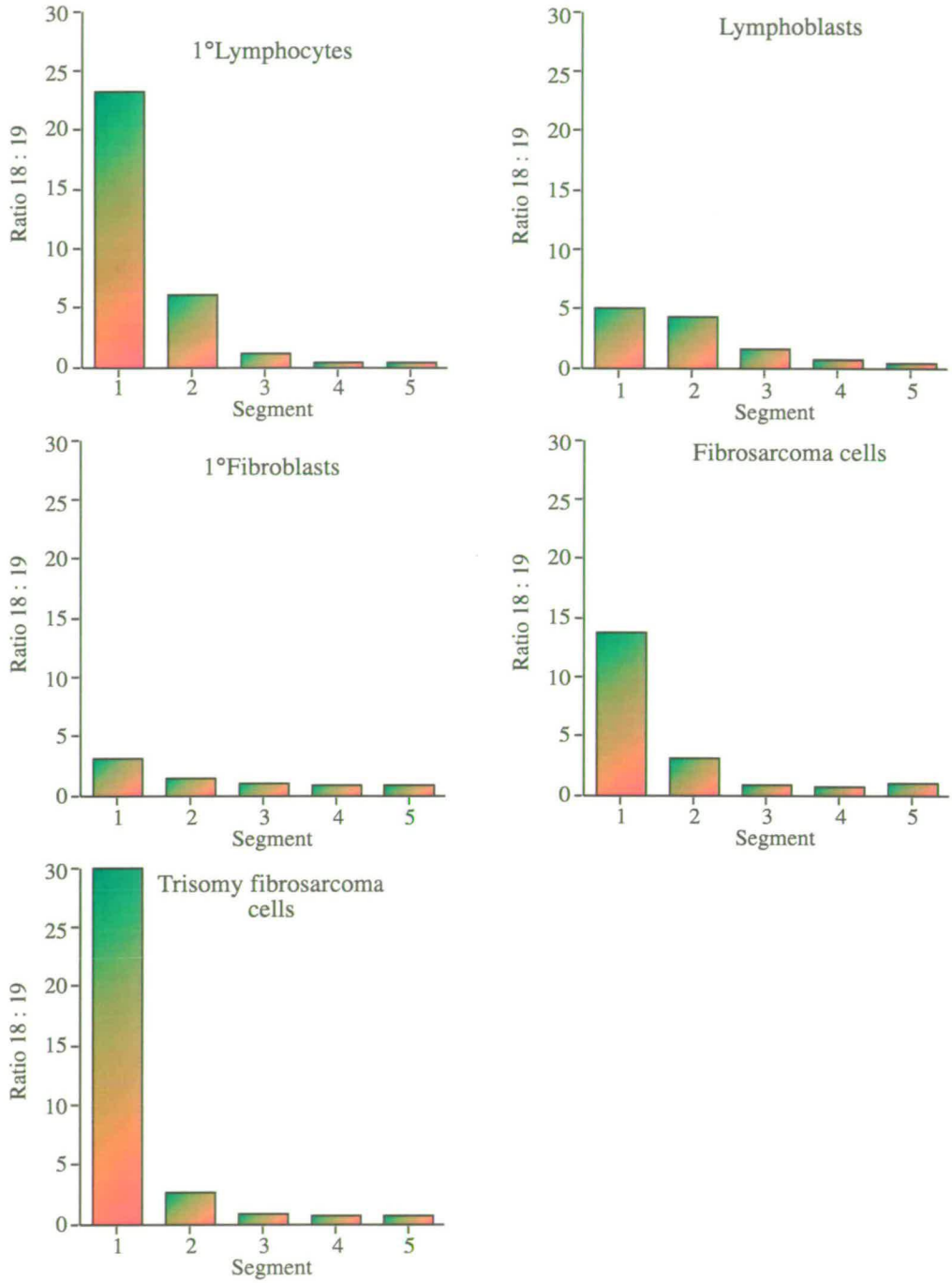

Figure 6.13 Histograms comparing the distribution of human chromosome 18 and 19 FISH paints within nuclei of different cell types

Avidin-FITC was used to detect biotin labelled paints for human chromosomes 18 and 19 hybridised to human nuclei from different cell types fixed with 3:1 methanol:acetic acid: primary lymphocytes (Figure 6.10), lymphoblasts (Figure 6.6), primary fibroblasts (Figure 6.11a) and fibrosarcoma cells (Figure 6.11b). Using Script 2 (Section 6.2.1) measurements were taken from ~50 randomly selected nuclei with two FISH signals for each cell type, or ~10 randomly selected fibrosarcoma nuclei with three FISH signals (Figure 6.11c & Table 6.8). The total fluorescence in each concentric segment was calculated as a percentage of the total nuclear fluorescence. The mean percentage chromosome 18 paint fluorescence was divided by the mean percentage chromosome 19 paint fluorescence for each concentric segment in each cell type.

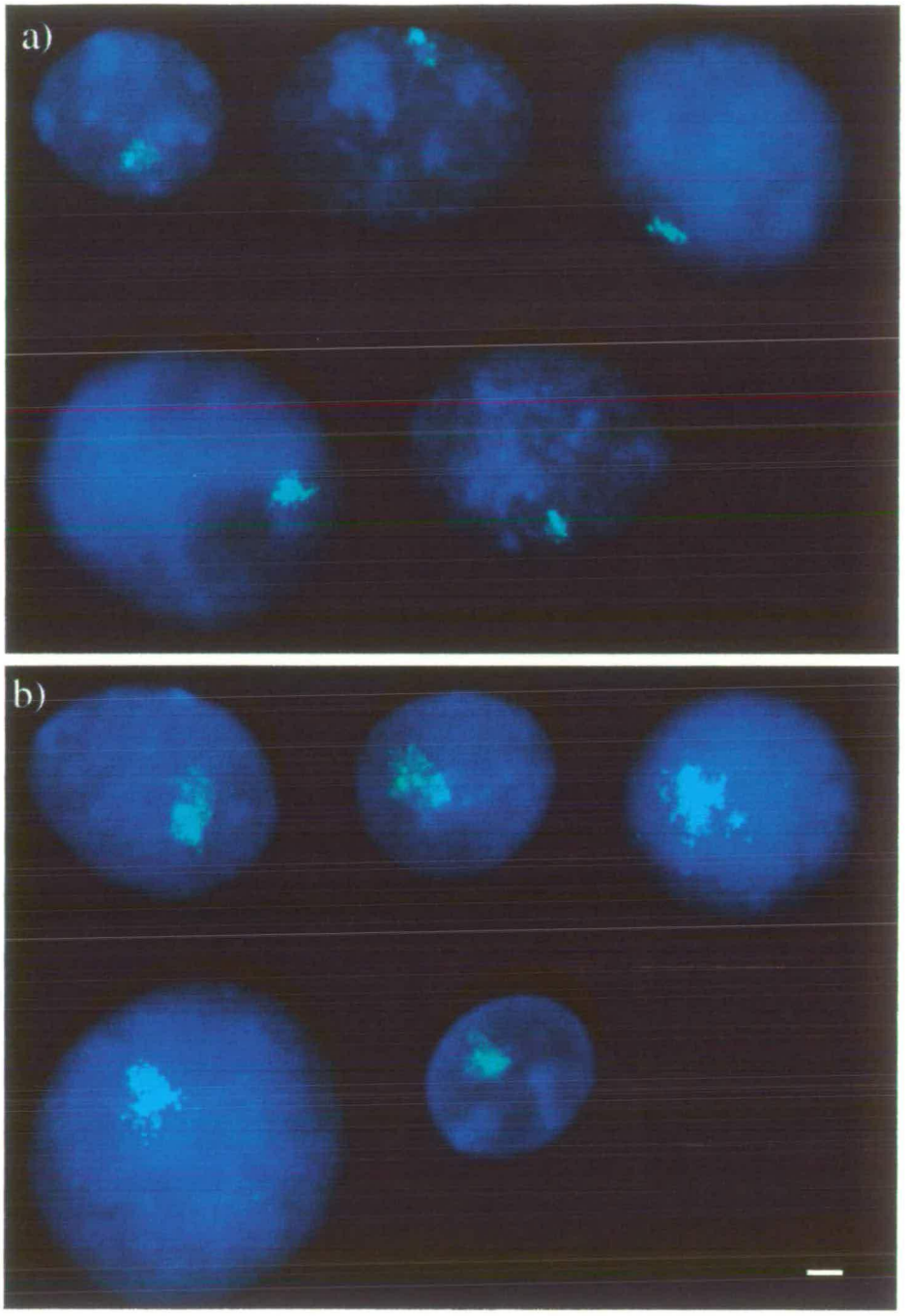

Figure 6.14 The interphase territories of human chromosomes 18 and 19 in rodent-human hybrid nuclei

(**a**) Representative interphase nuclei from the rodent-human chromosome 18-containing hybrid cell line, GM11010 (Section 3.2) hybridised with chromosome 18 paint (Section 3.3.2) labelled with biotin and detected with avidin-FITC (green). (**b**) Representative interphase nuclei from the rodent-human chromosome 19-containing hybrid cell line, GM10449A (Section 3.2) hybridised with chromosome 19 paint (Section 3.3.1) labelled with biotin and detected with avidin-FITC (green). All nuclei were counterstained with DAPI (blue). Bar=1μm

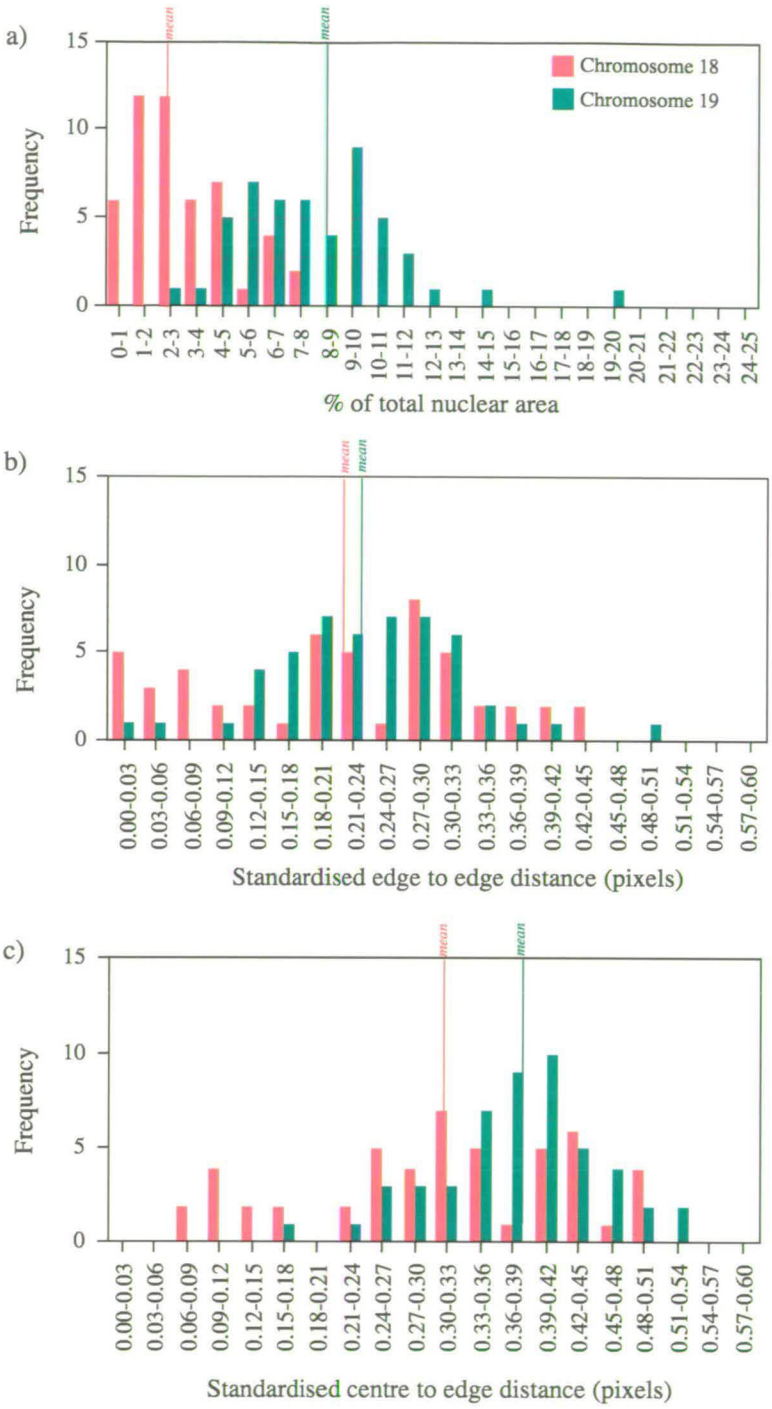

Figure 6.15 Histograms comparing the territories occupied by human chromosome 18 and 19 in rodent-human hybrid nuclei

Avidin-FITC was used to detect biotin labelled paints for chromosomes 18 and 19 hybridised to the appropriate rodent-human monochromosome hybrid cell nuclei fixed with 3:1 methanol:acetic acid: chromosome 18-containing GM11010 (Section 3.2) (Figure 6.14a) and chromosome 19-containing GM10449A (Section 3.2) (Figure 6.14b). Using Script 1 (Section 6.2.1) measurements were taken from the signals in 50 randomly selected nuclei. (**a**) FISH signal area given as a percentage of the total nuclear area. (**b**) Edge of signal to the nearest edge of the nucleus. (**c**) Centre of the signal to the nearest edge of the nucleus. Distances standardised by dividing by the √nuclear area (estimate of nuclear radius).

6.5 The interphase territories of human chromosomes 18 and 19 and different stages of the cell cycle

FISH using centromeric and telomeric probes has shown that chromosomes are not static throughout the cell cycle (Manuelidis, 1985a; Bartholdi *et al.*, 1991; Ferguson & Ward, 1992; Vourc'h *et al.*, 1993; He & Brinkley, 1996). It is possible that while the orientation of a chromosome territory changes as centromeres move from a peripheral to more central location, that the same relative organisation is maintained. However, it might be necessary that chromosomes alter their territory locations at particular stages of the cell cycle to be appropriately positioned for replication, for example, to take place at the correct time. During replication, it may also be necessary for chromatin to decondense, allowing access to the replication machinery. All nuclei analysed so far have been prepared from asynchronous cell cultures. For the case of human lymphoblasts, almost 50% of cells were at G1 in the cell cycle (Table 6.1), which is typical of an exponentially growing cell culture.

To look at chromosome territory dispositions throughout the cell cycle, a population of exponentially growing FATO human lymphoblasts were fractionated by centrifugal elutriation (Section 2.7.1). Cells were introduced into the centrifuge and an opposing flow rate of medium was set up such that the cells were maintained in an equilibrium. The flow rate was increased in a step-wise manner to force cells of a increasing size and density out of the chamber. In total, eight fractions of FATO cells were collected. From each fraction cell number was counted (Table 6.10) and an aliquot was analysed by fluorescence activated cell sorting (FACS). For FACS, nuclei were treated with RNAse and stained with propidium iodide (PI) (Section 2.7.2). PI is a stochiometric dye which stains both RNA and DNA. Fluorescence emission was assessed for each sample and plotted against frequency (Figure 6.16). Two peaks of fluorescence were observed in each sample, the second at twice fluorescence intensity of the first. The first peak corresponded to G1 cells and the second peak to G2 cells. Using software developed by Becton Dickenson, each peak was integrated to estimate the number of cells at each cell cycle stage (Table 6.10). Cells undergoing replication (S-phase) make up the trough between the G1 and G2 peaks.

The remainder of cells from each fraction were fixed with 3:1 methanol:acetic acid, slides were prepared and stained with DAPI. From these slides a random sample of 30 nuclei were imaged and using IPLab Spectrum software, the diameter and area of each nucleus was

Table 6.10 Analysis of the samples of lymphoblasts fractionated by elutriation

FATO human lymphocytes fractionated by centrifugal elutriation (Section 2.7.1). Samples from each fraction were fixed and slides made, images from which were used to calculate the mean size of 30 randomly selected nuclei. BrdU incorporated 45 minutes prior to cell harvesting and detection by imunofluorescence (Section 2.6.5) was used to assess the percentage of cells in S-phase. The number of cells present in each fraction were counted on a haemocytometre (Section 2.1.1). Proportions of cells in the gap phases were estimated from FACS analysis (Section 2.7.2 & 6.5).

Fraction	Mean nuclear area (μm^2)	Mean nuclear diametre	% of nuclei BrdU+ (S-phase)	Number of cells ($x10^5$)	% of nuclei in G1-phase (FACS analysis)	% of nuclei in G2-phase (FACS analysis)
1	$67.4^{+/-3.2}$	$9.4^{+/-0.20}$	12	1.0	81.3	18.7
2	$80.7^{+/-5.1}$	$11.1^{+/-0.23}$	10	2.1	90.0	10.0
3	$73.6^{+/-2.9}$	$10.8^{+/-0.14}$	16	5.0	76.5	23.5
4	$106.6^{+/-3.3}$	$11.9^{+/-0.12}$	28	5.4	73.2	26.8
5	$146.7^{+/-3.5}$	$13.7^{+/-0.16}$	54	1.3	55.7	44.3
6	$167.2^{+/-5.6}$	$15.4^{+/-0.11}$	58	1.9	31.8	68.2
7	$296.5^{+/-12.5}$	$19.1^{+/-0.25}$	38	1.1	28.6	71.4
8	$451.1^{+/-15.1}$	$22.4^{+/-0.28}$	20	0.6	20.4	79.6
Asynchronous	–	–	16	–	57.3	42.7

calculated (Table 6.10). Bromodeoxyuridine (BrdU) had been added to the cells 45 minutes prior to harvesting and elutriation. This thymidine analogue is incorporated into replicating DNA. Distribution of BrdU incorporation was detected in nuclei using an anti-BrdU-FITC antibody (Boehringer) (Section 2.6.6) (Figure 6.17). BrdU incorporation shows a specific spatial pattern of replication throughout S-phase of the cell cycle, with hundreds of small domains scattered throughout the nucleus in early S-phase and fewer, larger domains in late S-phase (Nakayasu & Berezney, 1989; O'Keefe *et al.*, 1992) (Figures 6.17 & 6.18). The percentage of nuclei revealing BrdU incorporation in each fraction was calculated from 200 nuclei from each slide (Table 6.10).

Using the data from Table 6.10, four fractions were chosen to represent each of the four major stages of the cell cycle: G1 (2), early S (5), late S (6) and G2 (8). FISH was carried out on these nuclei using the paints for chromosome 18 (Section 3.2.3) and chromosome 19 (Section 3.2.2) labelled with biotin and detected with avidin-TR (red). BrdU was simultaneously detected with anti-BrdU-FITC (green). Nuclei from each slide were assessed for size and pattern of BrdU incorporation. For each of the four cell cycle stages, images were collected for 50 nuclei that showed appropriate characteristics for that particular stage and using Script 1 (Section 2.1.2), the areas and positions of the chromosome 18 and 19 interphase territories were established.

6.5.1 The areas occupied by human chromosome 18 and 19 territories in interphase nuclei at different stages of the cell cycle

Figure 6.18 shows lymphoblast nuclei selected to represent each stage of the cell cycle following FISH with either human chromosome 18 or 19 paint and BrdU detection. Using Script 1, the signal areas for human chromosome 18 or 19 were collected from both signals in 50 randomly selected nuclei from each cell cycle stage (Table 6.11). The chromosome 18 interphase territory appeared to take up a larger area of G1 nuclei than nuclei from any other stage, although it remained significantly smaller than the chromosome 19 territory area at G1 (Figures 6.18 & 6.19). The chromosome 19 interphase territory takes up its largest nuclear area during early S-phase (Figures 6.18 & 6.19). Since chromosome 19 is replicated during early S-phase, the increase in territory size at this stage may reflect a more open chromatin configuration, required to allow access to replication machinery and/or an increase in the DNA content of this chromosome. Chromosome 18 replicates late in S-phase and would be anticipated to show its largest percentage area at this stage of the cell cycle if

protein accessibility were the key to determining territory size. There is no evidence that this is the case. However, this effect might be masked by the increase in nuclear size by late S-phase (Figure 6.17). By late S-phase the majority of chromatin has been duplicated and the nucleus is almost doubled in size. An increase in chromosome 18 territory area at this stage would not be as easily distinguished.

Chromosome 18 occupies a consistently significantly smaller territory than chromosome 19 throughout the cell cycle (Table 6.11), with $p<0.0001$ calculated at every stage using a Student's T-test. The difference between the areas of the two chromosome territories peaks in early S-phase due entirely to the increase in chromosome 19 territory size at this stage.

Table 6.11 The areas of human chromosome 18 and 19 territories in nuclei at different stages of the cell cycle
Avidin-TR was used to detect biotin labelled FISH paints for chromosomes 18 and 19 hybridised to human lymphoblastoid nuclei representing each of the stages of the cell cycle. Cell cycle stage determined from FACS analysis (Figure 6.21), nuclear size (Figure 6.22) and pattern of BrdU incorporation (Figure 6.23). The area of each signal was divided by the total nuclear area, determined using Script 1 (Section 6.2.1). +/- standard error of mean

	% of total nuclear area		19:18	p
Stage of cell cycle	chromosome 18	chromosome 19		
Asynchronous	$5.3^{+/-0.1}$	$6.8^{+/-0.3}$	1.28	0.0003
G1	$6.1^{+/-0.1}$	$7.3^{+/-0.2}$	1.20	0.0003
Early S	$5.5^{+/-0.2}$	$9.3^{+/-0.3}$	1.70	0.0001
Late S	$5.4^{+/-0.1}$	$7.7^{+/-0.2}$	1.43	0.0002
G2	$4.8^{+/-0.1}$	$6.6^{+/-0.2}$	1.40	0.0002

6.5.2 The positions of human chromosome 18 and 19 territories in interphase nuclei at different stages of the cell cycle

Chromosome 18 looks to be peripherally located throughout the cell, however, there is a tendency for the territory to be less peripheral as cells progress from G1 through to mitosis as assessed using Script 1 (Section 6.2.1) (Table 6.12 & Figures 6.18 & 6.20). Reciprocally, it can be seen that chromosome 19 remains more centrally located in the nucleus than chromosome 18 throughout the cell cycle. There is a tendency, in this instance, for the chromosome to move more peripherally as the cells progress from G1 through to mitosis.

The differences in territory position between chromosomes 18 and 19 remain significant, with $p<0.0003$ calculated at all stages using a Student's T-test.

Table 6.12 The positions of human chromosome 18 and 19 territories in nuclei at different stages of the cell cycle

Avidin-TR was used to detect biotin labelled FISH paints for chromosomes 18 and 19 hybridised to human lymphoblastoid nuclei representing each of the stages of the cell cycle. Cell cycle stage determined from FACS analysis (Figure 6.21), nuclear size (Figure 6.22) and pattern of BrdU incorporation (Figure 6.23). The distances calculated for each signal were divided by the √nuclear area (estimate of nuclear radius), determined using Script 1 (Section 6.2.1). +/- standard error of mean

Stage of cell cycle	**Mean standardised edge to edge distance**		**Mean standardised centre to edge distance**	
Chromosome	**18**	**19**	**18**	**19**
Asynchronous	$0.08^{+/-0.009}$	$0.18^{+/-0.007}$	$0.18^{+/-0.010}$	$0.34^{+/-0.006}$
G1	$0.08^{+/-0.008}$	$0.18^{+/-0.007}$	$0.19^{+/-0.009}$	$0.32^{+/-0.007}$
Early S	$0.11^{+/-0.010}$	$0.16^{+/-0.006}$	$0.22^{+/-0.011}$	$0.30^{+/-0.006}$
Late S	$0.12^{+/-0.011}$	$0.17^{+/-0.006}$	$0.23^{+/-0.011}$	$0.31^{+/-0.007}$
G2	$0.11^{+/-0.011}$	$0.16^{+/-0.008}$	$0.22^{+/-0.011}$	$0.30^{+/-0.007}$

The characteristic territory areas and positions of human chromosomes 18 and 19 appear to be set up at G1, immediately following mitosis, and maintained throughout the cell cycle. How closely do these 2-D observations relate to the organisation of these two chromosomes in nuclei in which 3-D has been preserved? The next step in confirming the relevance of this data so far is to compare these two contrasting chromosome territories in 3-D nuclei.

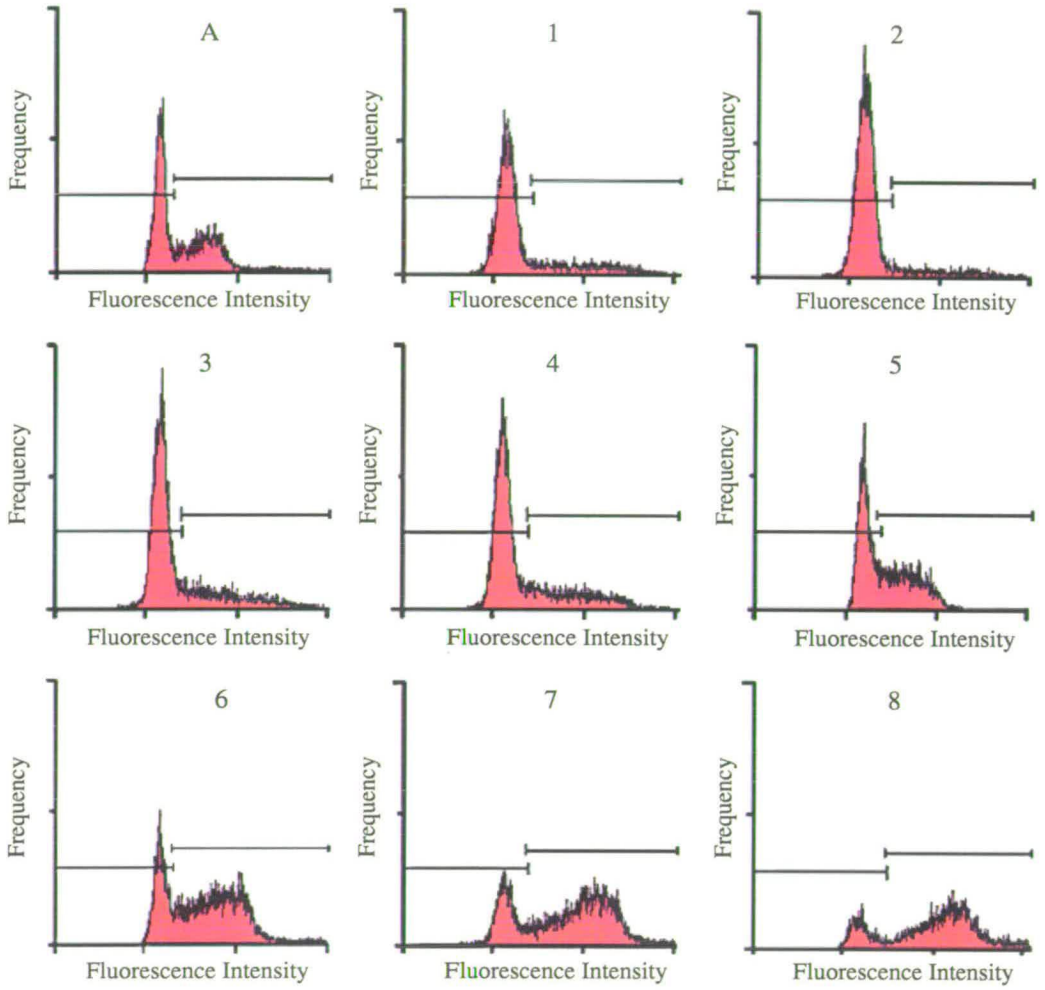

Figure 6.16 FACS analysis of human lymphoblasts fractionated by elutriation
FATO human lymphoblasts were fractionated by centrifugal elutriation (Section 2.7.1). A sample from each of the 8 fractions collected, in addition to a sample of asynchronous cells, were treated with RNAse and stained with PI. Fluorescence intensity was assessed by FACS analysis (Section 2.7.2). Two peaks of fluorescence were observed in each sample, the second at twice the degree of fluorescence of the first. The first peak corresponded to G1 nuclei and the second peak to G2 nuclei. Peaks were integrated under the lines indicated, to estimate the number of cells at each of these stages of the cell cycle (Table 6.10). **A** - asynchronous polulation

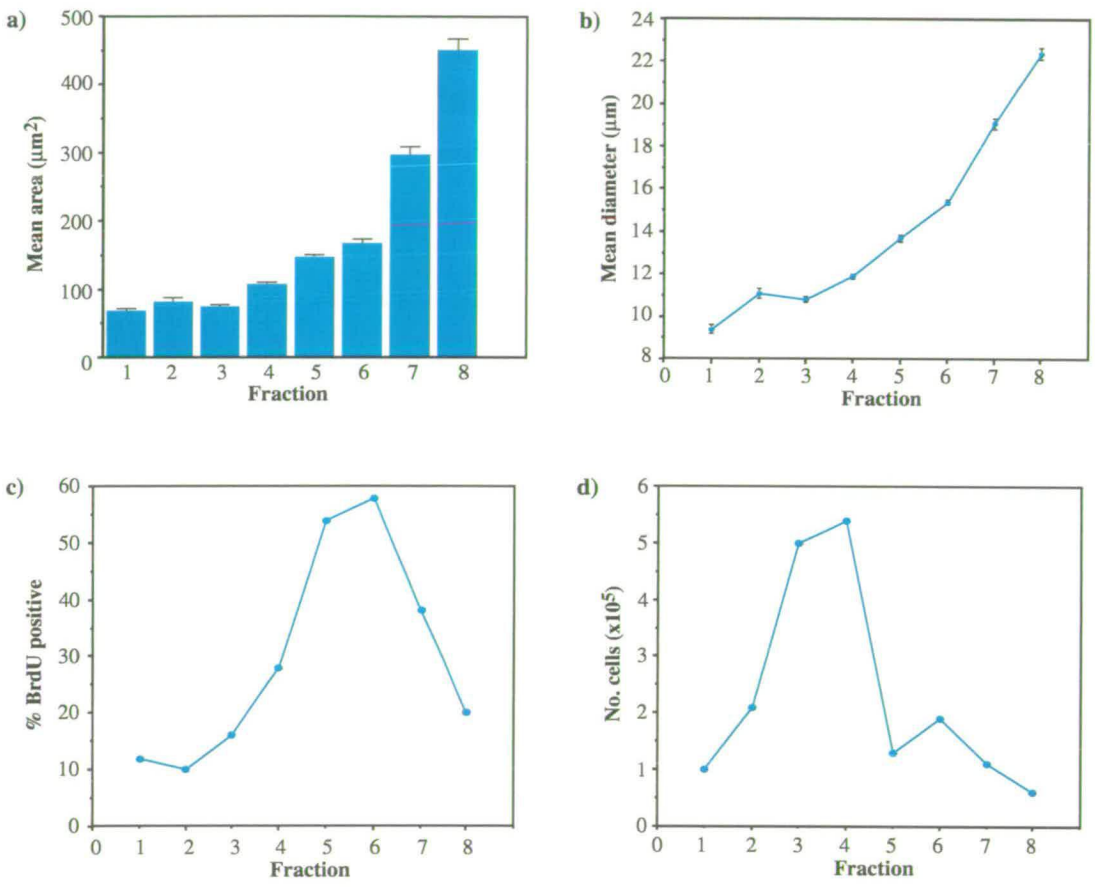

Figure 6.17 Comparing human lymphoblasts fractionated by elutriation
FATO human lymphoblasts were fractionated by centrifugal elutriation (Section 2.7.1). Slides were made from a fixed sample from each fraction stained with DAPI and used to calculate the mean (**a**) area (μm^2), and (**b**) diameter (μm), of 30 randomly selected nuclei. (**c**) Percentage of nuclei undergoing replication (S-phase). (**d**) Total number of cells present in each fraction. +/– standard error of mean

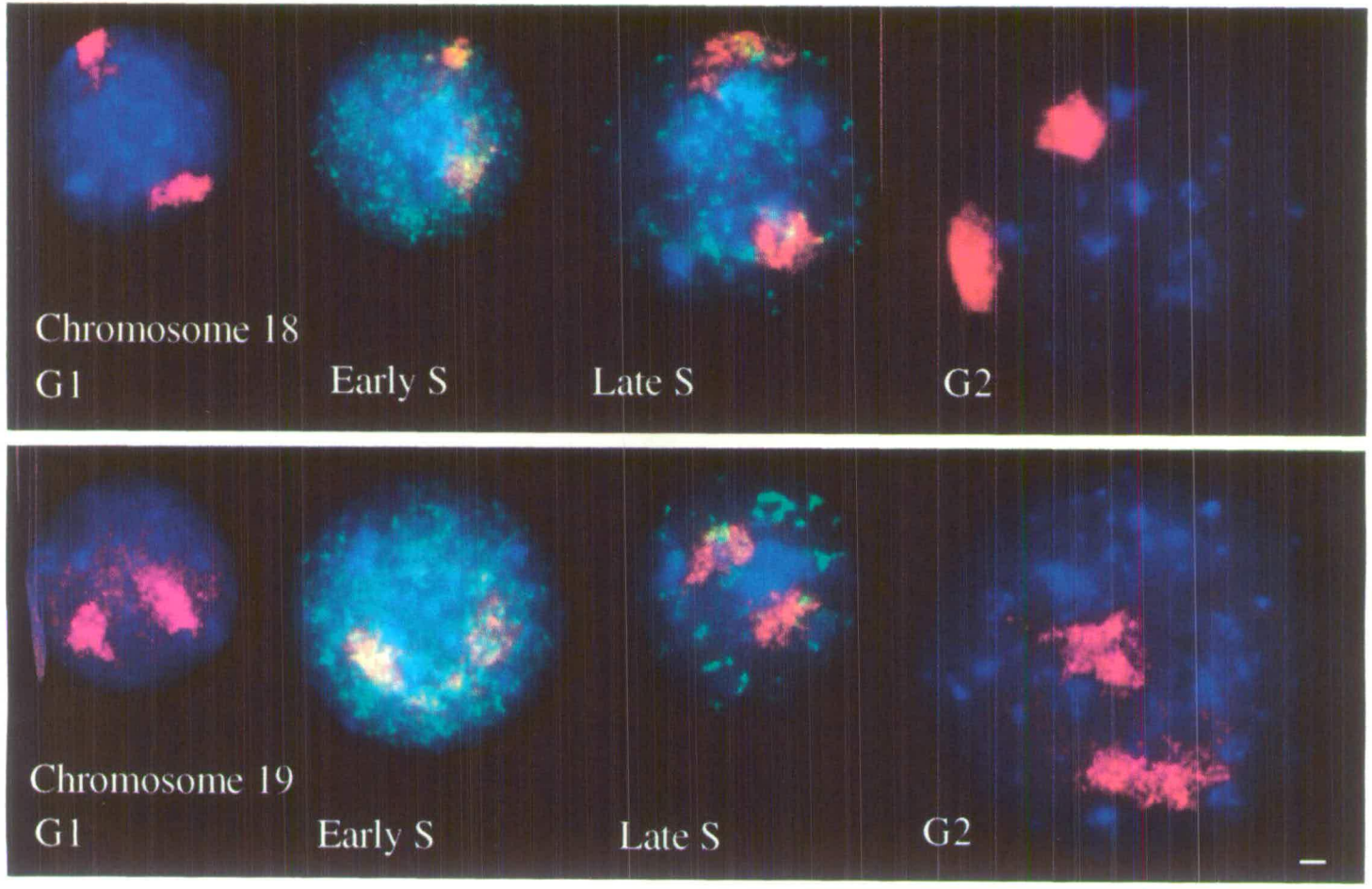

Figure 6.18 The territories of human chromosomes 18 and 19 in nuclei at different stages of the cell cycle
BrdU was incorporated into late replicating DNA for 45 minutes prior to cell harvesting and detected using anti-BrdU-FITC (green). Patterns of incorporation were used to help determine the cell cycle stage of a nucleus, with larger and fewer foci in late S-phase compared with early S-phase. Avidin-TR (red) was used to detect biotin labelled FISH paints for human chromosomes 18 and 19. All nuclei were counterstained with DAPI (blue). Bar=1μm

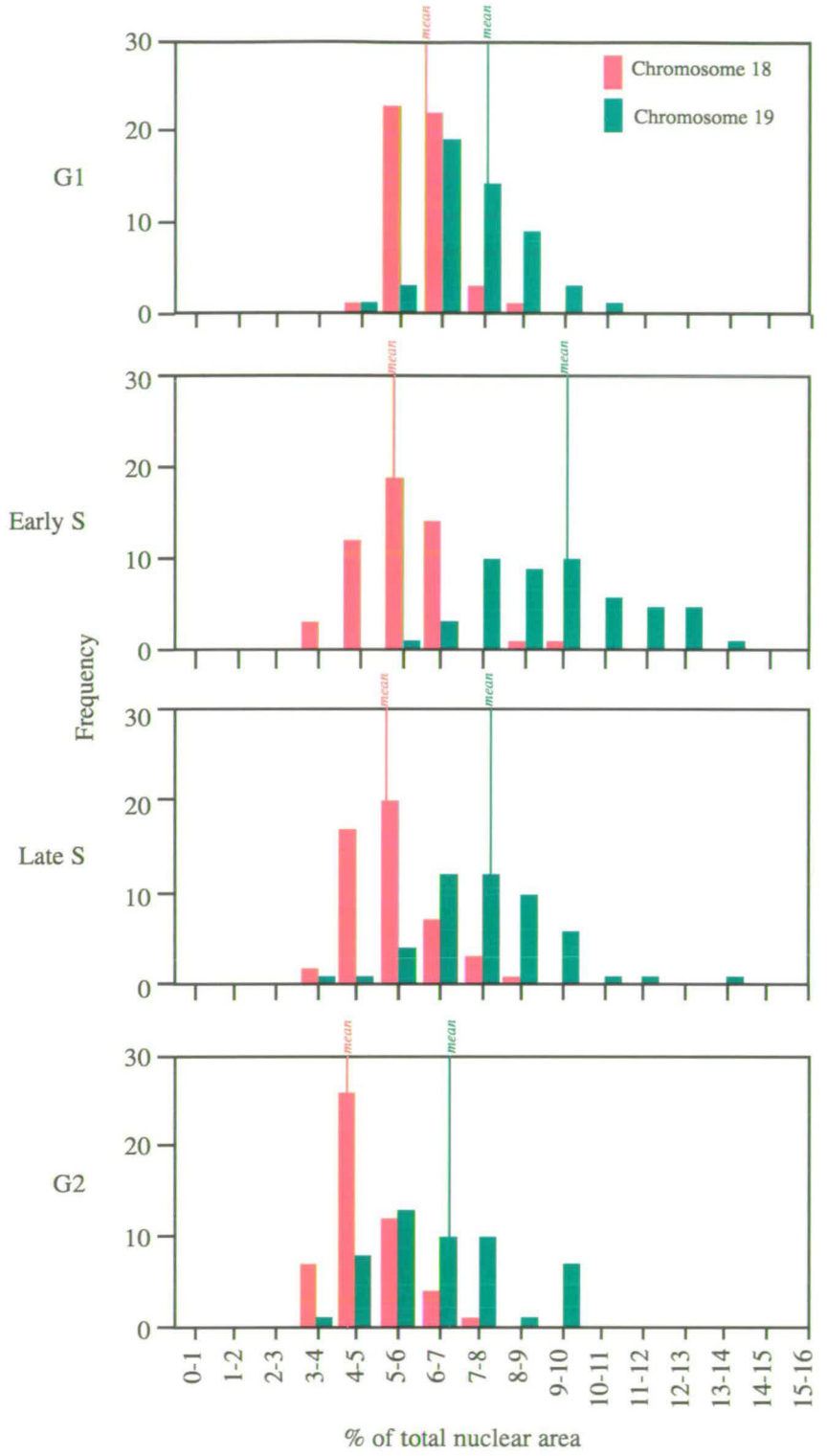

Figure 6.19 Histograms comparing the areas of human chromosome 18 and 19 territories in nuclei at different stages of the cell cycle

Using Script 1 (Section 6.2.1) measurements were taken from both signals in 50 randomly selected lymphoblastoid nuclei representative of each stage of the cell cycle fixed with 3:1 methanol:acetic acid and hybridised with human chromosome 18 or 19 paint. Cell cycle stage determined from FACS analysis (Figure 6.16), nuclear size (Figure 6.17) and pattern of BrdU incorporation (Figure 6.18). FISH signal area given as a percentage of the total nuclear area.

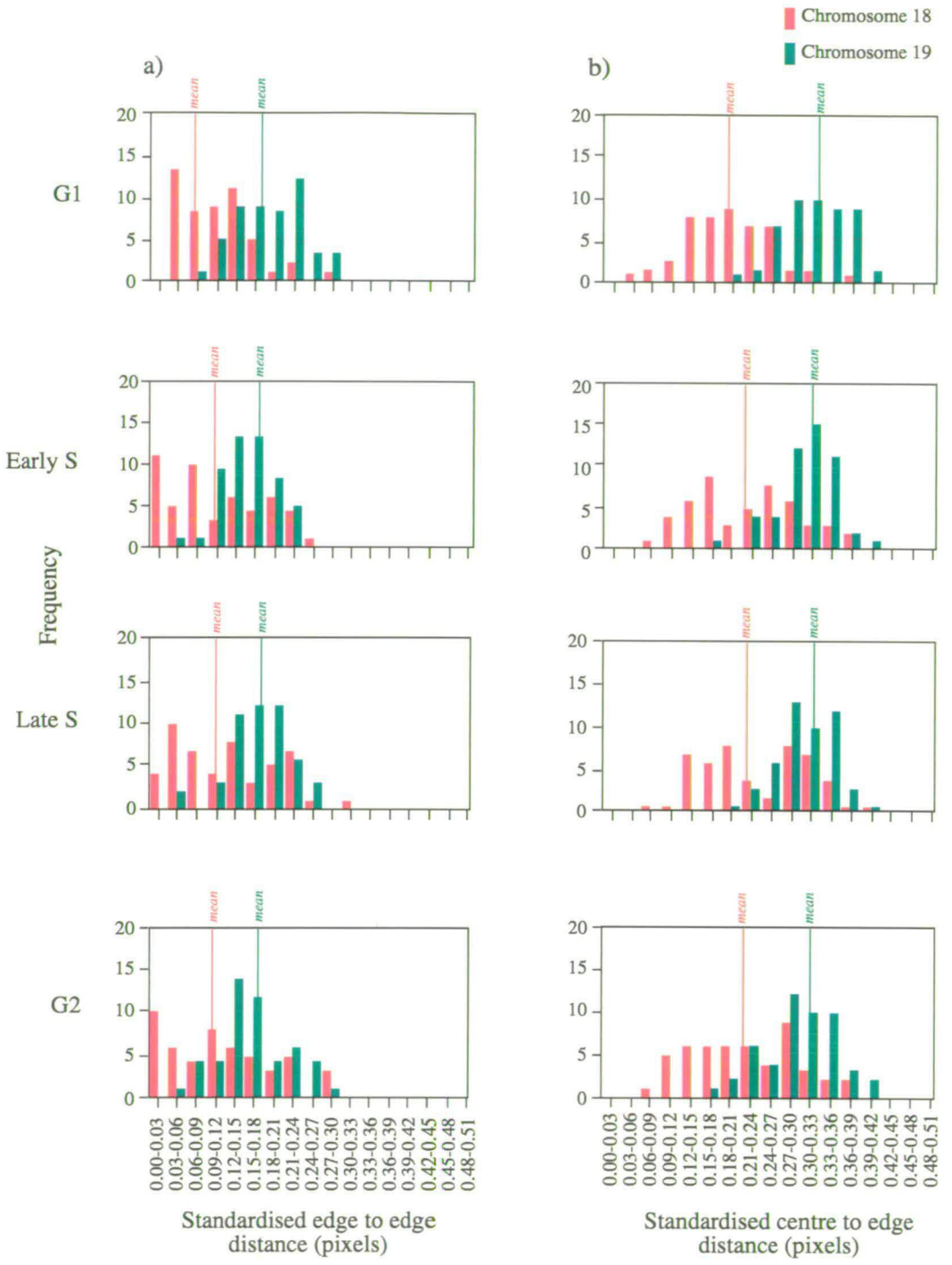

Figure 6.20 Histograms comparing the positions occupied by human chromosome 18 and 19 territories at different stages of the cell cycle

Using Script 1 (Section 6.2.1) measurements were taken from both signals in 50 randomly selected lymphoblastoid nuclei representing each of the stages of the cell cycle following FISH with a human chromosome 18 or 19 paint. Cell cycle stage determined from FACS analysis (Figure 6.16), nuclear size (Figure 6.17) and pattern of BrdU incorporation (Figure 6.18). (**a**) Edge of signal to the nearest edge of the nucleus. (**b**) Centre of the signal to the nearest edge of the nucleus. Distances standardised by dividing by the √nuclear area (estimate of nuclear radius).

6.6 The interphase territories of human chromosomes 18 and 19 by confocal sectioning of three-dimensional nuclei

It is difficult to imagine how a nucleus is compacted to form a 2-D structure. What forces cause the flattening of the nucleus: the physical dropping of the cellular suspension onto a slide, dehydration following evaporation of the methanol in the fixative or the squashing of a coverslip over the slide when mounting? It is probably a combination of all of these forces. Clearly, the contents of the nucleus are not homogenous and, thus, it is likely that a nucleus will not flatten evenly. To establish this, comparisons between the distribution of stochiometric DNA stains in 2-D and 3-D nuclei, denatured and not denatured and fixed with a variety of methods, may prove interesting. Measuring the degree of fluorescence in concentric segments of equal area (Script 2) showed that there is greater DAPI fluorescence in the centre of the nucleus than the periphery in several different cell types (Section 6.4.3). This suggests that nuclei may compact by collapsing in on themselves with relatively little skewing. The observations made with 2-D nuclei give a trend for the likely volume and position of the human chromosomes studied in normal, 3-D nuclei. Previous comparisons with paraformaldehyde fixed, 3-D preserved nuclei have suggested that any changes in nuclear organisation are not significant (Manuelidis, 1985, Popp *et al.*, 1990; Lawrence & Singer, 1991; Hofers *et al.*, 1993; Robinett *et al.*, 1996) and that projections of findings from 2-D to 3-D are valid. However, this has not been rigorously tested and, thus, analysis of 3-D preserved nuclei is necessary.

The protocol used here was developed by Dr. J.M. Bridger, University of Heidelberg (Section 2.6.7). Nuclei from the human fibrosarcoma cell line, HT1080 were grown on microscope slides until the cells were approximately 70% confluent. Slides were washed then fixed in 4% paraformaldehyde for 20 minutes. Triton X-100 detergent was used to permeabilise the cell membrane which was aided by a series of freeze and thaw steps. Slides were incubated in glycerol prior to this in order to help maintain nuclear morphology. Slides were placed in 0.1M HCl for 5 minutes to reverse fixation before FISH was carried out using the standard protocol (Section 2.6). The temperature of formamide denaturation, however, was performed at 75°C (5°C higher than the usual protocol). Nuclei were counterstained with the stochiometric DNA stain, PI (red). This procedure resulted in nuclei which had maintained a reasonable level of thickness. A typical ellipsoid fibrosarcoma cell nucleus was 4-5μm at the short diameter, 12-15μm at the long diameter and 7-12μm in the

vertical plane. Nuclei were imaged using a confocal microscope (Section 2.14.2) taking 1μm vertical sections (z-series).

Figure 6.21 shows a 3-D preserved fibrosarcoma cell nucleus following FISH with a chromosome 18 paint and confocal sectioning. During the sectioning of nuclei from this slide fluorescence from both the signal and counterstain faded rapidly. The reasons for this are unknown. This resulted in few sections being obtained and, thus, the nucleus represented here is incomplete. Nonetheless, it is apparent that both chromosome 18 territories are associated with the nuclear periphery throughout the z-series, at the side of the nucleus (Figure 6.21a). When a rotation of the nucleus was made about the x-axis, the territories also appeared to be in contact with the upper surface of the nucleus, which being the first section taken and, thus, having faded to a relatively small extent, probably is the boundary of the nuclear envelope (Figure 6.21b).

Figure 6.22 shows a 3-D preserved fibrosarcoma cell nucleus following FISH with a chromosome 19 paint and confocal sectioning. From this slide, nuclei produced between 7-12 sections at 1μm intervals with no significant degree of fading. As was seen previously with 2-D nuclei, chromosome 19 territories were less condensed than the chromosome 18 territories (Figure 6.22). The two chromosome 19 territories were not in contact with the periphery of the nucleus at any point through the z-series (Figure 6.22a). When a rotation of the nucleus was made about the x-axis, both territories appeared not to contact the nuclear envelope at either the upper or lower surface of the nucleus (Figure 6.22b). The regions of the nucleus with a dearth of PI staining correspond to the nucleoli. Both chromosome 19 territories seem to be juxtaposing the nucleoli.

It was difficult to obtain 3-D preserved nuclei with good FISH signals. The two examples shown here were selected from slides to represent the general trend observed for each chromosome of interest. Clearly, it is now necessary to improve this technique to obtain consistently good FISH signals and collect sections from a larger number of nuclei. There are several steps within the protocol that can be modified to enhance the FISH signals, these include, increased temperature of formamide denaturation, larger amount of probe, prolonged length of hybridisation and reduced stringency washes.

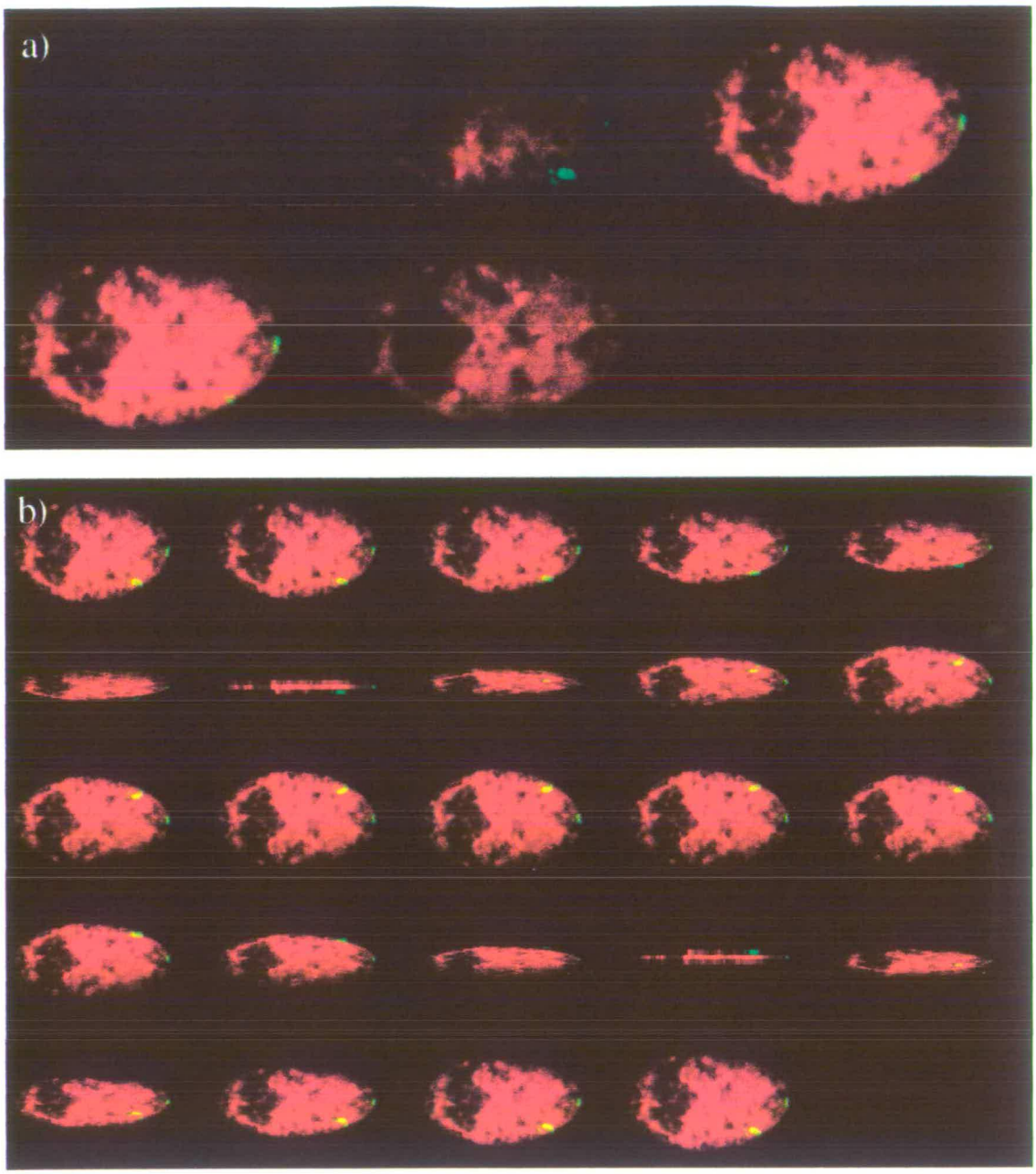

Figure 6.21 The territories of human chromosome 18 in a 3-D preserved nucleus
Avidin-FITC (green) was used to detect biotin labelled paint for human chromosome 18 following FISH to 3-D preserved nuclei (Section 6.6). Nuclei were counterstained with PI (red). (**a**) Z-series from upper to lower plane. 1μm intervals. (**b**) 360° rotation about the x-axis.

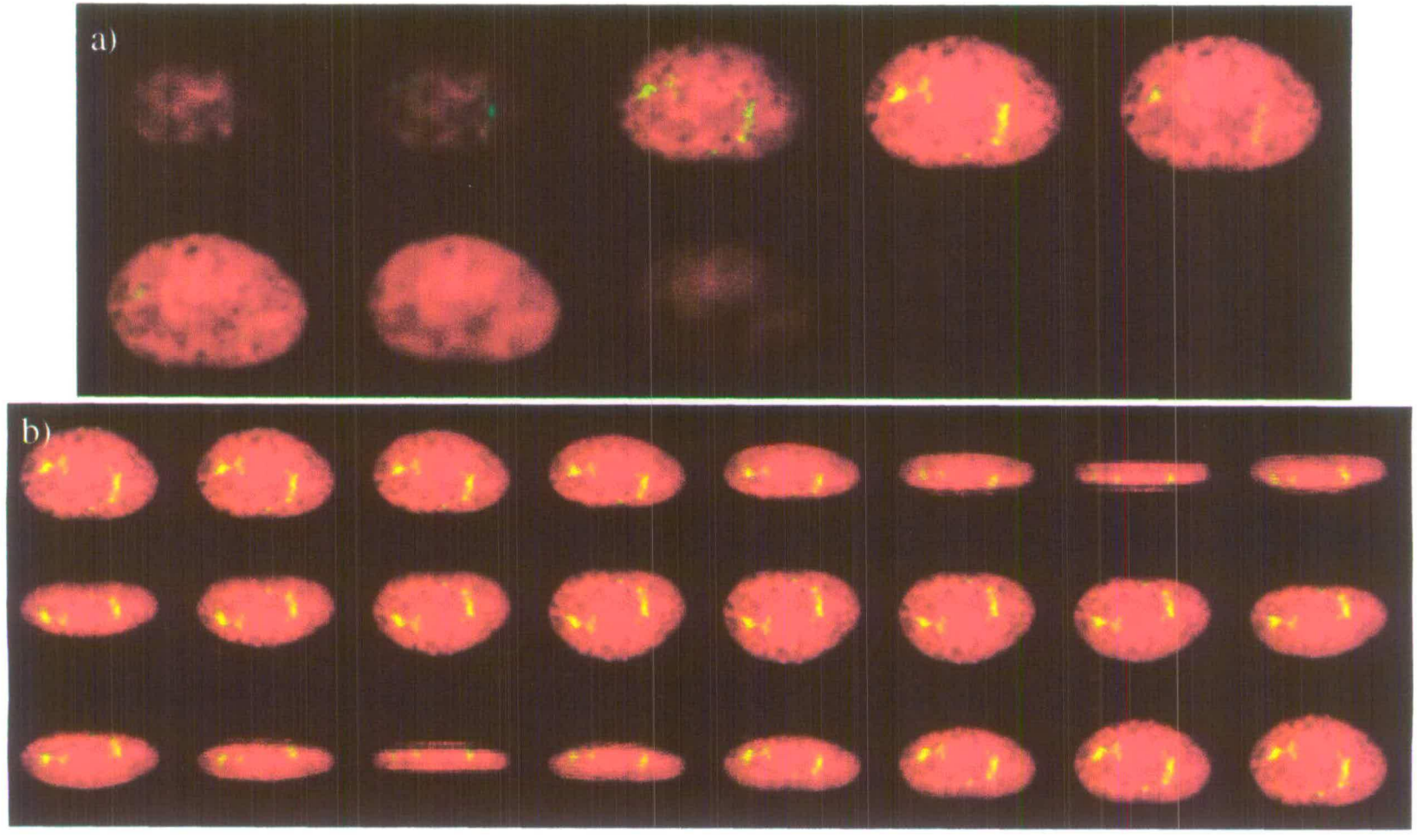

Figure 6.22 The territories of human chromosome 19 in a 3-D preserved nucleus
Avidin-FITC (green) was used to detect biotin labelled paint for human chromosome 19 following FISH to 3-D preserved nuclei (Section 6.6). Nuclei were counterstained with PI (red). (**a**) Z-series from upper to lower plane. 1μm intervals. (**b**) 360° rotation about the x-axis.

6.7 Summary

The data in this chapter support the concept of the nucleus as an organised and structured organelle. It has been demonstrated that chromosomes occupy distinct and discrete interphase territories and that these territories are probably defined by the functional behaviour of a chromosome and the organisation of functional compartments of the interphase nucleus.

Yokota *et al.* (1997) used FISH in 2-D human interphase nuclei with probes separated by 0.1-1.5Mb specifically from G- or R-band regions of the human genome and determined that the chromatin of G-bands was more condensed than that of R-bands. Human chromosome 18 consists mainly of dark-staining G-bands and R'-bands and in its entirety reflects many of the features of G-bands, being gene-poor, late replicating and hypoacetylated (Section 1.7 & 3.1). Conversely, chromosome 19 possesses few, small G-bands and its R-bands are T-bands and therefore, this chromosome is generally gene-rich, early replicating and hyperacteylated (Section 1.7 & 3.1). Chromosome 18 consistently occupied a significantly smaller territory area than chromosome 19 in 2-D nuclei fixed typically with 3:1 methanol:acetic acid (Section 6.2), as used by Yokota *et al.* (1997), and 4% paraformaldehyde fixed nuclei (Section 6.3). This difference was also maintained in different human cell types (Section 6.4) and throughout all stages of the cell cycle in lymphoblastoid nuclei (Section 6.5). Additionally, chromosome 1, with its large region of pericentric heterochromatin took up a smaller than expected area in interphase nuclei and conversely, transcriptionally active chromosomes 11 and 22 took up larger areas than expected based upon their DNA content (Section 6.2). These results and the study of Yokota *et al.* (1997) indicate that gene-poor, transcriptionally inactive chromatin remains condensed within the interphase nucleus and that gene-rich, transcriptionally active chromatin is more open, possibly allowing easier access to transcription complexes.

Surprisingly, despite the superficial appearance of the X chromosome in 2-D nuclei, evidence from 3-D studies have revealed that the mammalian active X chromosome (Xa) occupies a similar volume in the interphase nucleus to the inactive X chromosome (Xi) (Eils *et al.*, 1996). Xa was also shown to have a more irregular, and thus larger, surface area than Xi. The increased number of invaginations would allow access to transcription components. The condensed appearance of G-band verses R-band regions and chromosome 18 verses

chromosome 19 in 2-D nuclei may be a result of a similar difference in shape between inactive and active regions, rather than a direct difference in volume. Alternatively, X-inactivation may occur by a different mechanism to that involved at inactive autosomal regions that lack genes. While chromosomes 18 and 19 differ in gene content and transcriptional activity, Xa and Xi possess exactly the same gene density differing only in transcriptional activity. The 3-D studies presented in Section 6.6 are incomplete, but together with the results from 2-D nuclei (Figure 6.6), suggest that the volume and shape of chromosome 18 territories are very different to those of chromosome 19. Chromosome 18 territories probably occupy a smaller volume and/or are likely to show a smoother surface than chromosome 19 territories, which are likely to not only be larger but more dispersed.

The positioning of chromosome interphase territories also appears to be defined and distinct. There are conflicts in the literature as to where transcriptionally active verses inactive chromatin might be positioned in the interphase nucleus (Section 1.5.2). The comparisons made in this chapter between human chromosomes 18 and 19 suggest that transcriptionally inactive, late replicating chromatin shows a strong tendency to be located towards the nuclear periphery, with transcriptionally active, early replicating chromatin being more centrally located. Gene-poor, late replicating chromosome 18 was consistently and significantly observed closer to the periphery of the nucleus when compared with gene-rich, early replicating chromosome 19. This difference was revealed in 2-D 3:1 methanol:acetic acid fixed and paraformaldehyde fixed human lymphoblastoid nuclei (Sections 6.2 & 6.3). Contrasting territory positions were also maintained throughout the cell cycle (Section 6.5) and in nuclei of primary lymphocytes, primary fibroblasts and fibrosarcoma cells (Section 6.4). Human chromosome 1 was predominantly peripherally located which may be influenced by the positioning of its large region of pericentric heterochromatin. By comparison, transcriptionally active chromosomes 11 and 22 were more internally located (Section 6.2).

Transcriptional activity appears to play an important role in determining the positioning of chromosome territories in the interphase nucleus. How might this very specific chromosome territory organisation be orchestrated? The DNA sequence of a chromosome might determine its interphase territory disposition, either through the influence of the overall sequence composition, for example, GC- or AT-richness, or through specific "organising" blocks of sequence that may contain binding sites for specific nuclear proteins.

Alternatively, transcriptional activity *per se* or properties associated with transcriptionally active chromatin, for example, acetylation, may dictate chromosome territory dispositions. These possibilities are the focus of the next chapter.

7. Interphase chromosome territories II: Determinants of nuclear compartmentalisation

7.1 Introduction

Chapter 6 established that human chromosomes occupy discrete and distinct territories in the interphase nucleus. Gene-poor, late replicating human chromosome 18 occupies a condensed territory at the periphery of the nucleus while, in contrast, gene-rich, early replicating chromosome 19 produces a large and centrally located territory. In this chapter I try to address how the opposing dispositions of chromosome 18 and 19 territories arise: Are they intrinsic to some aspect of DNA sequence, are they an effect of transcriptional differences, or are they due to differences in chromatin structure? To begin to answer these questions, the behaviour of territories in nuclei from a reciprocal chromosome 18 and 19 translocation were studied. In addition, I analysed the effects of inhibiting transcription and histone deacetylation upon chromosome 18 and 19 territories in normal nuclei. Finally, the interaction of these chromosomes with the nuclear matrix was analysed.

7.2 The interphase territories of the derived chromosomes from a human chromosome 18 and 19 translocation

The physical proximity of different chromosomes in interphase nuclei can be inferred from the frequency of translocations seen between them (Qumsieyeh, 1995). In support of this, the most frequent chromosome rearrangements in humans are the Robertsonian translocations between the acrocentric chromosomes that are known to be physically close to each other in metaphase and interphase (Ferguson-Smith & Handmaker, 1961; Kaplan *et al.*, 1993), and the same particular rDNA-containing chromosomes remain associated with one another through successive cell cycles (Bobrow & Heritage, 1980). Translocations between chromosomes 18 and 19 appear to be very rare which might be due to the opposing physical proximities of the two chromosomes in the nucleus. In general, chromosome 18 is found as a partner in translocations with other chromosomes more than chromosome 19 (MRC Human Genetics Registry, Edinburgh). This bias might be driven by selection for the less deleterious effects of rearrangements involving gene-poor chromosomes as opposed to gene-rich chromosomes, such as chromosome 19.

It has been argued that lack of phenotypic abnormalities in individuals with balanced translocations is evidence that spatial arrangement of chromosome territories in the nucleus is not biologically important. This has been based upon the assumption that such translocations do not disrupt the normal nuclear localisation of chromosome territories (Qumsieyeh, 1995). Fixed primary lymphocytes were obtained from an individual with a balanced translocation between chromosomes 18 and 19 by Prof. P. Jacobs, Wessex Regional Genetics Laboratory, Salisbury (18;19)(p11;p13). The individual showed no clinical phenotype as a result of this translocation. The total amount of DNA exchanged was estimated to be 20Mb from chromosome 18 and 24Mb from chromosome 19. Slides were prepared from the 3:1 methanol:acetic acid fixed material and hybridised with the chromosome 18 and 19 paints, each labelled alternatively to allow simultaneous detection. Figure 7.1 shows a representative metaphase spread and examples of interphase nuclei from these slides. Script 1 (Section 6.2.1) was used to determine the positioning of both sets of normal and derived chromosomes from 50 randomly selected nuclei (Table 7.1).

Table 7.1 The interphase territory positions of the normal and derived human chromosomes 18 and 19 in t(18;19) nuclei
Nuclei from primary lymphocytes of an individual with a balanced translocation between chromosomes 18 and 19 hybridised with paints to human chromosomes 18 and 19. The distances calculated for each signal in 40 randomly selected nuclei were divided by the √total nuclear area (estimate of nuclear radius), determined using Script 1 (Section 6.2.1). +/- standard error of mean

Chromosome	Mean standardised edge to edge distance	Mean standardised centre to edge distance
18 normal	$0.06^{+/-0.013}$	$0.16^{+/-0.016}$
18 derived	$0.09^{+/-0.018}$	$0.21^{+/-0.021}$
19 normal	$0.18^{+/-0.011}$	$0.34^{+/-0.015}$
19 derived	$0.15^{+/-0.009}$	$0.29^{+/-0.010}$

Although the derived chromosome 18 tended to be less peripheral than the normal chromosome 18, this difference was not significant (ST $p<0.059$) (Table 7.1 & Figure 7.2). Also, the derived chromosome 19 tended to be less centrally located than the normal chromosome 19 but, again, this difference was not significant (ST $p<0.110$) (Table 7.1 & Figure 7.2). It is possible that the translocated portions of each derived chromosome has a small influence upon the positioning of the derived chromosomes. There was a striking difference in the orientation of the derived chromosomes and Figure 7.3 outlines the

analysis used to assess this. For each derived chromosome from the images of 60 randomly selected nuclei the translocated portion was determined to be either central or peripheral. If the majority of the translocated portion lay between the centre of the territory and the centre of the nucleus it was designated as being central. Reciprocally, if the majority lay between the centre of the territory and the nearest edge of the nucleus it was designated as being peripheral (Table 7.2). The translocated portion originating from chromosome 19 was centrally positioned in relation to the remainder of the derived chromosome 18 in almost 80% of nuclei. Reciprocally, the translocated portion originating from chromosome 18 was peripherally positioned in relation to the remainder of the derived chromosome 19 in almost 90% of nuclei. This suggests that <25Mb is sufficient to confer territory positioning and that this is influenced by DNA sequence differences between chromosomes, for example, base composition and/or interspersed repeat distribution. Alternatively, transcriptional activity, replication timing and/or levels of core histone acetylation may be involved. No live cells were available for this translocation, however, the following section perturbs transcription and histone deactetylation in normal nuclei to test some of these possibilities.

Table 7.2 The orientation of the derived chromosome territories in t(18;19) interphase nuclei

Nuclei from primary lymphocytes of an individual with a balanced translocation between chromosomes 18 and 19 hybridised with paints to human chromosomes 18 and 19. Orientation of the translocated portion with respect to the remainder of the derived chromosome determined as described in Section 7.2 and Figure 7.3 for 60 randomly selected nuclei.

Derived chromosome	Chromosome of origin of translocated portion	Translocated portion towards periphery of nucleus	Translocated portion towards centre of nucleus	Undetermined
18	19	15.0%	78.3%	7.7%
19	18	88.3%	7.7%	5.0%

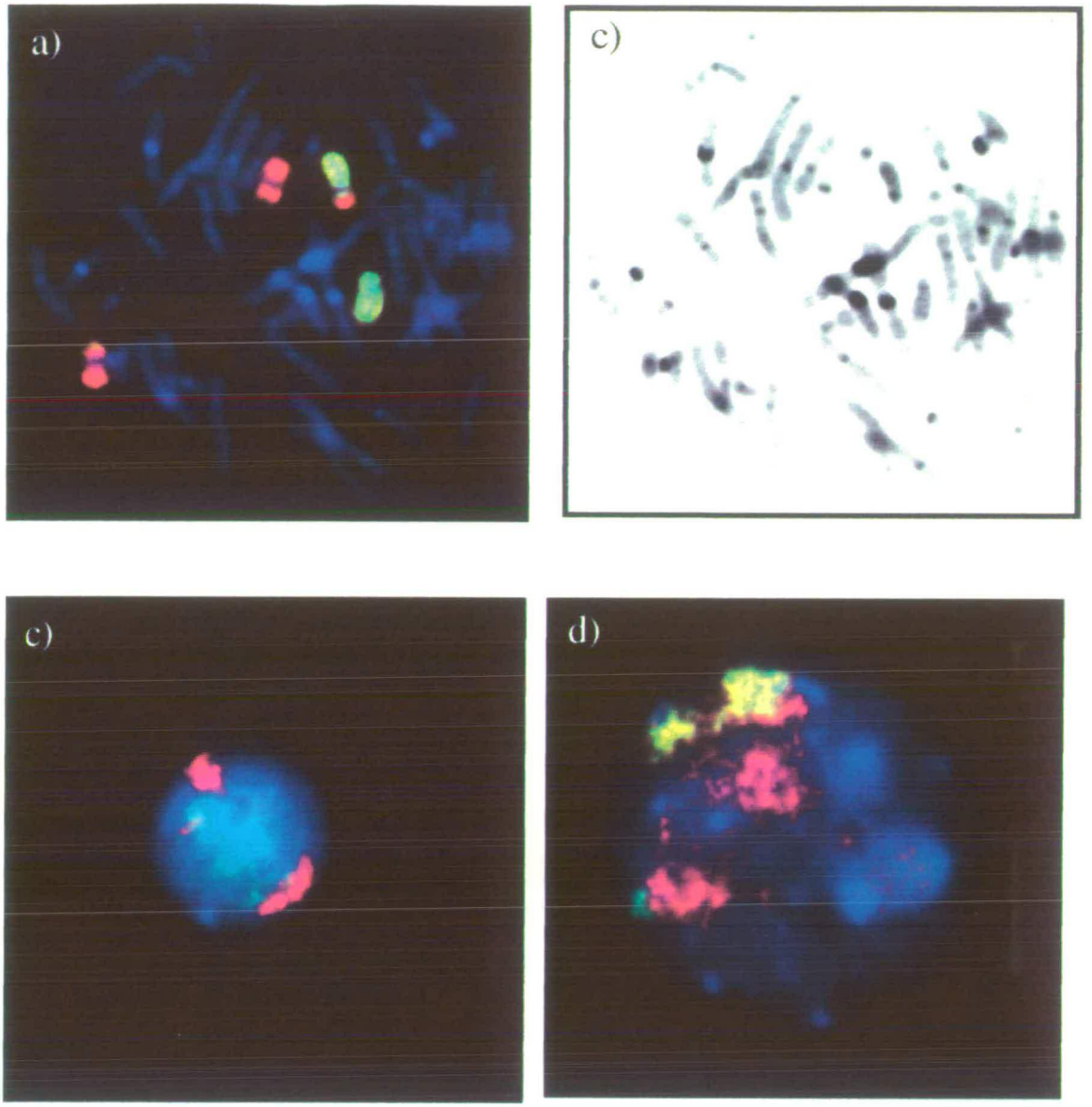

Figure 7.1 The interphase territories of normal and derived human chromosomes 18 and 19 in t(18;19) nuclei

(**a**) Metaphase spread from primary lymphocytes of an individual with a balanced translocation between chromosomes 18 and 19 hybridised simultaneously with paints for human chromosomes 18 (FITC/green) (Section 3.3.2) and 19 (TR/red) (Section 3.3.1). Chromosomes were counterstained with DAPI (blue). (**b**) Grey scale representation of DAPI stained metaphase spread. (**c**) Representative nucleus hybridised simultaneously with paints for human chromosome 18 (TR/red) and 19 (FITC/green). (**d**) Representative nucleus hybridised simultaneously with paints for human chromosome 18 (FITC/green) and 19 (TR/red). Nuclei were counterstained with DAPI (blue).

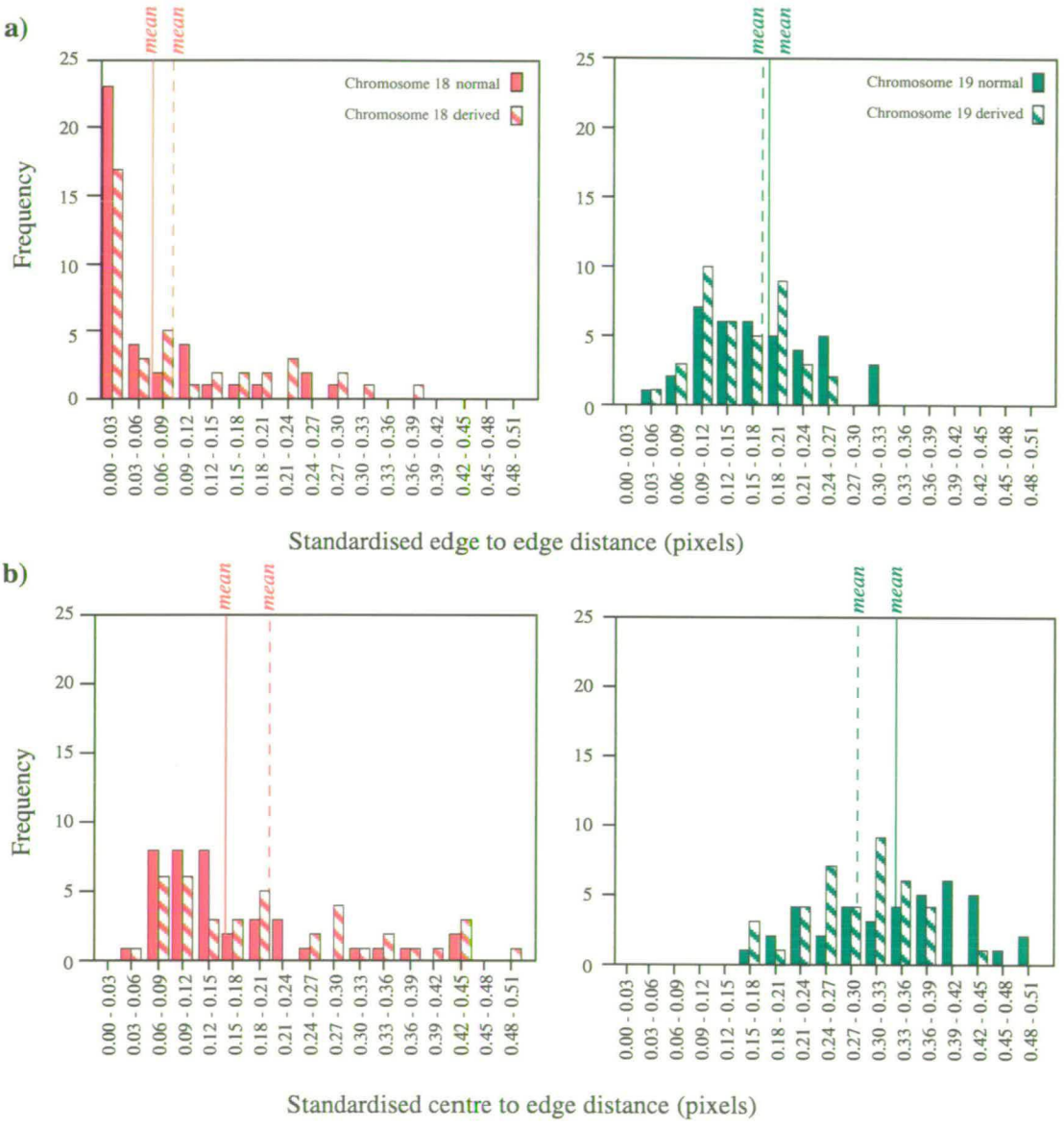

Figure 7.2 Histograms comparing interphase territory areas and positions of normal and derived human chromosomes 18 and 19 in t (18;19) nuclei

Using Script 1 (Section 6.2.1) measurements were taken from both signals in 50 randomly selected nuclei hybridised with paints for human chromosomes 18 or 19 by FISH. Paints were alternatively labelled to allow simultaneous hybridisation and detection with different fluorochromes. (**a**) Edge of the signal to the nearest edge of the nucleus. (**b**) Centre of the signal to the nearest edge of the nucleus. Distances standardised by dividing by the √nuclear area (estimate of nuclear radius).

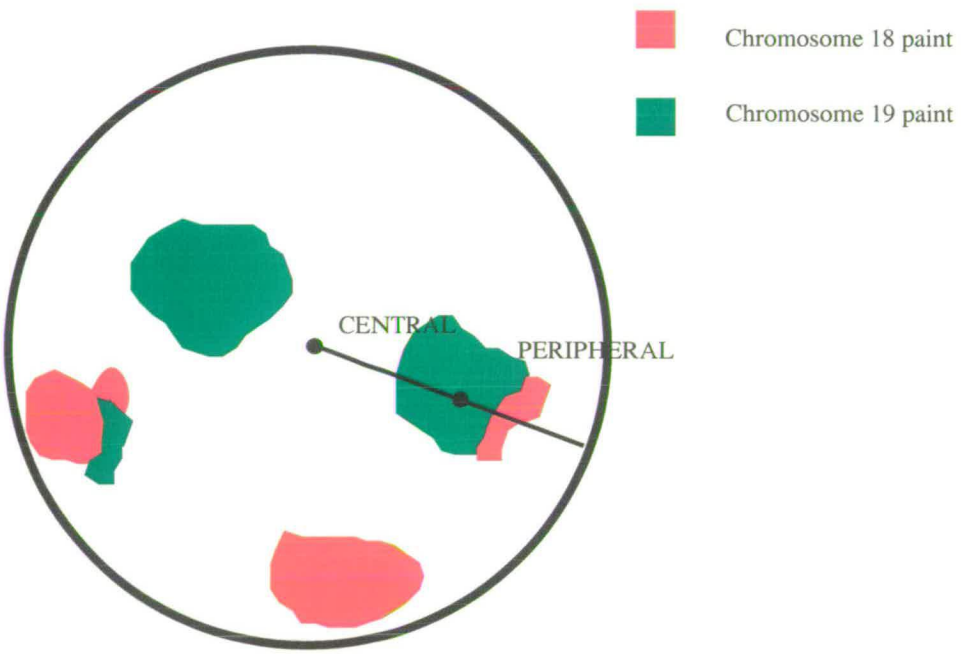

Figure 7.3 Analysing the orientation of derived translocation chromosome territories in interphase nuclei

Paints for human chromosomes 18 and 19 were alternatively labelled to allow simultaneous hybridisation and detection with different fluorochromes to t(18;19) nuclei. For each derived chromosome from the images of 60 randomly selected nuclei and the translocated portion was determined to be either central or peripheral. If the majority of the translocated portion lay between the centre of the territory and the centre of the nucleus it was designated as being central. Reciprocally, if the majority lay between the centre of the territory and the nearest edge of the nucleus it was designated as being peripheral.

7.3 The involvement of transcriptional activity in determining nuclear organisation

If chromosome 19 is maintained in an open configuration in interphase nuclei due to its high transcriptional activity then the territory may become more condensed if transcription was blocked. Additionally, the positioning of this chromosome at the centre of the nucleus may depend upon continued transcriptional activity. Epigenetic properties associated with potential transcriptional activity, for example, histone acetylation may also play a role in nuclear chromosome territory organisation.

7.3.1 The effects of blocking transcription with Actinomycin D (AD) upon nuclear organisation

One study has reported that treatment of human cells with chemicals which block transcription by RNA polymerase (pol) I and II causes chromosome territories to disperse and rDNA extends into "beaded strands" (Haaf & Ward, 1996). Blocking of pol I transcription alone does not cause disruption to chromosome territories, including the rDNA-containing nucleolus. In this section, the specific territories of chromosomes 18 and 19 in human nuclei are studied following a block in pol I and II transcription. Actinomycin D (AD) is considered to block transcription by binding tightly to DNA, preventing it from being an efficient template for RNA synthesis (Review: Stryer, 1981). AD concentrations of <0.1μg/ml inhibit pol I but not pol II, concentrations of >0.5μg/ml are required to have an affect upon pol II activity (Perry & Kelley, 1970).

AD was added to a culture of human FATO lymphoblasts at a concentration of 5μg/ml, 2 hours prior to harvesting. The concentration and duration of treatment was adapted from Carmo-Fonseca *et al.* (1992) and Pinol-Roma & Dreyfuss (1991). Most of the cells were fixed with 3:1 methanol:acetic acid for FISH, however, a sample of cells was cytocentrifuged onto slides for immunofluorescence with a monoclonal anti-Sm antibody that recognises U1, U2 and U4-6 snRNPs (Dr. I. Mattaj, EMBL, Heidelberg) (Lerner *et al.*, 1981) (Section 2.10.2 & Figure 8.11). It has been demonstrated that in transcriptionally active nuclei, nascent transcripts, RNA polymerase II and splicing components, including snRNPs, have a generally dispersed distribution in addition to 20-50 speckles of local concentration (Fu & Maniatis, 1990; Spector, 1990; Wansink *et al.*, 1993; Bregman *et al.*, 1996; Fay *et al.*, 1997; Grande *et al.*, 1997; Zeng *et al.*, 1997; Review: Spector, 1993). In

cells blocked for transcription, these speckles become more accentuated and enlarged (Spector *et al.*, 1983; Carmo-Fonseca *et al.*, 1992; Zeng *et al.*, 1997; Review: Spector, 1993). Slides were incubated with primary antibody for 1 hour at room temperature, followed by incubation with anti-mouse-FITC for 30 minutes and finally fixed with 4% paraformaldehyde. Figure 7.4 shows the immunolocalisation of anti-Sm antibody in nuclei from cells with and without treatment with AD. There was a noticeable, but not prominent, reorganisation of the speckles identified by this antibody, the speckles being larger and fewer following AD treatment. The 3:1 methanol:acetic acid fixed cells from the same culture were used to make slides and hybridised separately with the human chromosome 18 or 19 paints. The paints were labelled with biotin and detected with avidin-FITC (green) and nuclei were counterstained with DAPI (Figure 7.4). The continued presence of discrete chromosome territories contradicts the observations of Haaf & Ward (1996). However, α-amanitin and the adenosine analogue 5,6-dichloro-β-D-ribofuranosylbenzimidazole (DRB) were used to block pol II transcription in this instance, possibly accounting for the different affects upon nuclear organisation. Treatment of cells with DRB at a number of concentrations and durations did not result in a convincing alteration in anti-Sm antibody immunolocalisation and thus, was not used for this experiment. However, subsequent experiments using DRB, α-amanatin and AD have also not resulted in the break-down of interphase chromosome territories and confirms the results for the size and positioning of chromosome 18 and 19 territories recorded here (Presonal communication: Dr. J.M. Bridger). This is further discussed in Section 9.3.

Using Script 1 (Section 6.2.1), the areas and positions of chromosome 18 and 19 territories in nuclei following each treatment were assessed (Tables 7.3 & 7.4). The area occupied by the chromosome 18 territory following treatment with AD was not significantly different from that occupied by the chromosome in non-treated nuclei previously calculated (ST $p<0.280$). Interestingly, however, the chromosome 19 territory area was smaller than the area in non-treated nuclei although not highly significantly (ST $p<0.010$). As a result, chromosomes 18 and 19 occupied similar percentage areas in treated nuclei (Table 7.3 & Figure 7.5). There was no significant difference between the positioning of chromosome 18 and 19 territories within treated and non-treated nuclei (Table 7.4 & Figure 7.6).

Table 7.3 The effects of AD and TSA upon the interphase territory areas of human chromosomes 18 and 19

The FATO human lymphoblast cell line was treated with AD to block transcription or TSA to prevent histone deacetylation. Avidin-FITC was used to detect biotin labelled paints for chromosomes 18 and 19 hybridised to slides made from treated cells fixed with 3:1 methanol:acetic acid. Data for the nuclei from untreated cells are taken from Section 6.2.3. The area of each signal was divided by the total nuclear area, determined using Script 1 (Section 6.2.1). +/- standard error of mean p-significance of difference between chromosomes 18 and 19 (Student's T-test)

Treatment	% of total nuclear area		19:18	p
	Chromosome 18	Chromosome 19		
None	$5.3^{+/-0.1}$	$6.8^{+/-0.3}$	1.28	0.0002
AD	$5.4^{+/-0.2}$	$5.6^{+/-0.2}$	1.03	0.400
TSA	$4.9^{+/-0.1}$	$7.4^{+/-0.3}$	1.51	0.0001

Table 7.4 The effects of AD and TSA upon the interphase territory positions of human chromosomes 18 and 19

The FATO human lymphoblast cell line was treated with AD to block transcription or TSA to prevent deacetylation. Avidin-FITC was used to detect biotin labelled paints for chromosomes 18 and 19 hybridised to slides made from treated cells fixed with 3:1 methanol:acetic acid. Data for the nuclei from untreated cells are taken from Section 6.2.3. The distances calculated for each signal were divided by the √nuclear area (estimate of nuclear radius), determined using Script 1 (Section 6.2.1). +/- standard error of mean

Treatment	Mean standardised edge to edge distance		Mean standardised centre to edge distance	
	18	19	18	19
None	$0.08^{+/-0.009}$	$0.18^{+/-0.007}$	$0.18^{+/-0.010}$	$0.34^{+/-0.006}$
AD	$0.09^{+/-0.009}$	$0.17^{+/-0.007}$	$0.20^{+/-0.011}$	$0.30^{+/-0.008}$
TSA	$0.09^{+/-0.011}$	$0.19^{+/-0.006}$	$0.19^{+/-0.013}$	$0.31^{+/-0.006}$

7.3.2 The effects of blocking histone deacetylation with Trichostatin A (TSA) upon nuclear organisation

Hyperacetylation of core histones is associated with transcriptional potential while hypoacetylation has been established at regions of transcriptional repression (Sections 1.4.1.3 & 5.1). Consistent with this, human chromosome 18 has been shown to be hypoacetylated by lack of immunofluorescence with antibodies to hyperacetylated H4. Conversely, human chromosome 19 possesses hyperacetylated histones along its length (Jeppesen & Turner, 1993) (Figure 5.1). Being intimately linked to transcriptional potential,

alteration of acetylation levels may disrupt the disposition of the interphase territories of these chromosomes in interphase nuclei. Trichostatin A (TSA) is a very potent and specific inhibitor of histone deacetylation (Section 5.2). It reversibly blocks the action of the histone deacetylase(s) (Yoshida *et al.*, 1990; review: Yoshida *et al.*, 1995) causing generalised increases in histone acetylation.

TSA was added to a culture of FATO human lymphoblasts at a concentration of 10ng/ml for 2 hours. This treatment was previously shown to enhance levels of histone acetylation, with the most gene-rich regions of the genome, for example, chromosome 19, becoming more highly acetylated than the gene-poor regions, such as, chromosome 18 (Section 5.2). However, there was no direct proof that TSA had worked in this particular experiment. Cells were harvested, swollen in hypotonic solution and fixed with 3:1 methanol:acetic acid. Slides were hybridised separately with the human chromosome 18 or 19 paints by FISH. The paints were labelled with biotin and detected with avidin-FITC (green) and nuclei were counterstained with DAPI.

Using Script 1 (Section 6.2.1), the areas and positions of chromosome 18 and 19 territories in nuclei following each treatment were assessed (Tables 7.3 & 7.4). The mean chromosome 18 territory area was smaller than was observed in non-treated nuclei but this difference was not highly significant (ST $p<0.010$). The mean chromosome 19 territory was larger than was observed in non-treated nuclei but, again, this difference was not significant (ST $p<0.0003$) (Table 7.3 & Figure 7.5). However, these differences result in an exaggerated difference between the territory areas between the two chromosomes. There was no significant effect upon the positions of chromosomes 18 and 19 in treated nuclei (Table 7.4 & Figure 7.6).

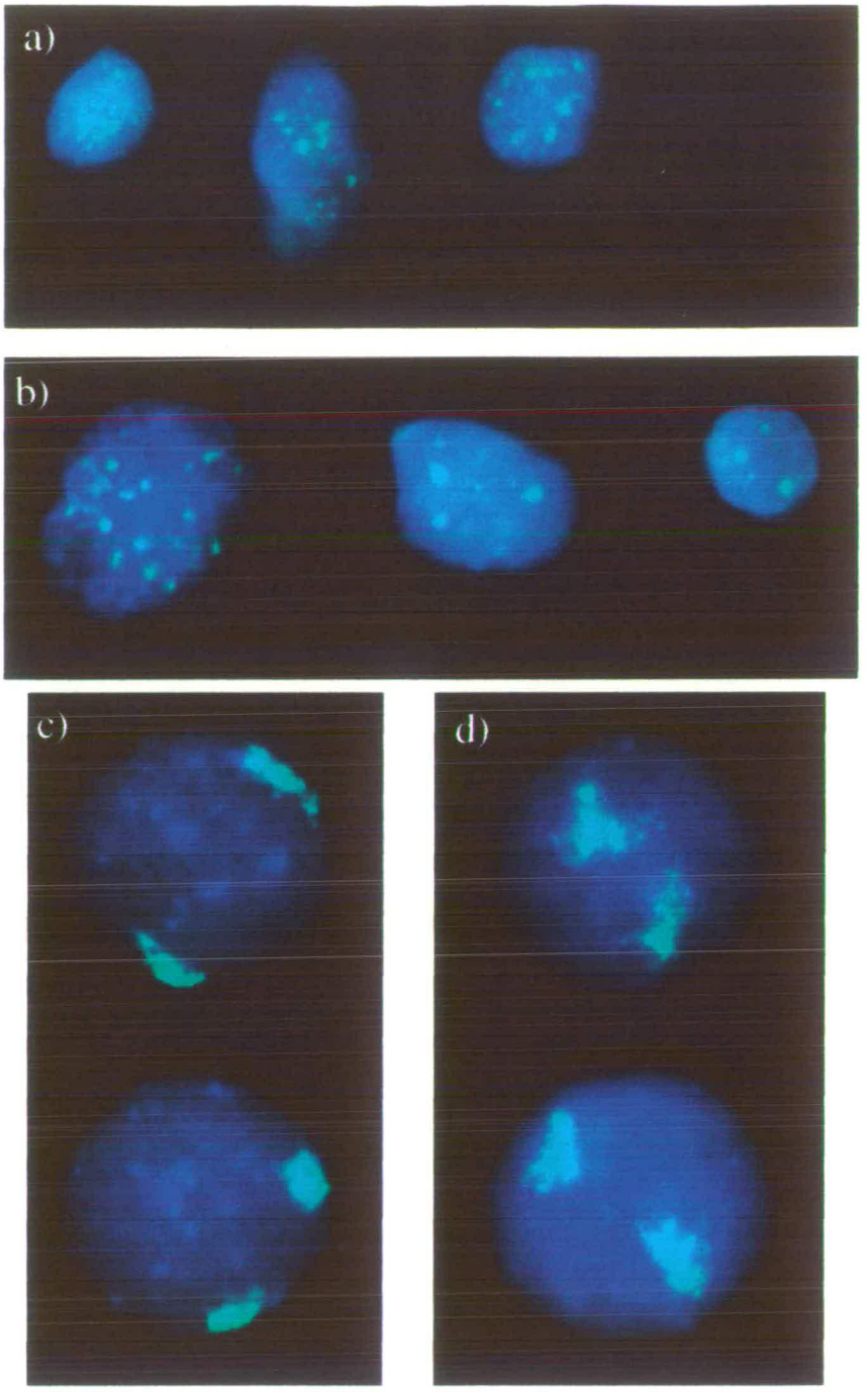

Figure 7.4 The effects of AD on nuclear organisation
(**a**) (**b**) Immunofluorescence with anti-Sm antibody detected with anti-mouse-FITC (green) on FATO human lymphoblasts. Nuclei were counterstained with DAPI (blue). (**a**) No treatment. (**b**) Cells treated with 5µg/ml AD for 2 hours to block transcription prior to harvesting. Note that the detected nuclear speckles are larger and fewer following AD treatment. (**c**) (**d**) Representative nuclei from FATO human lymphoblasts treated with AD hybridised with paints for human chromosomes (**c**) 18, and (**d**) 19, by FISH (Section 3.3). Paints were labelled with biotin and detected with avidin-FITC (green). Nuclei were counterstained with DAPI (blue).

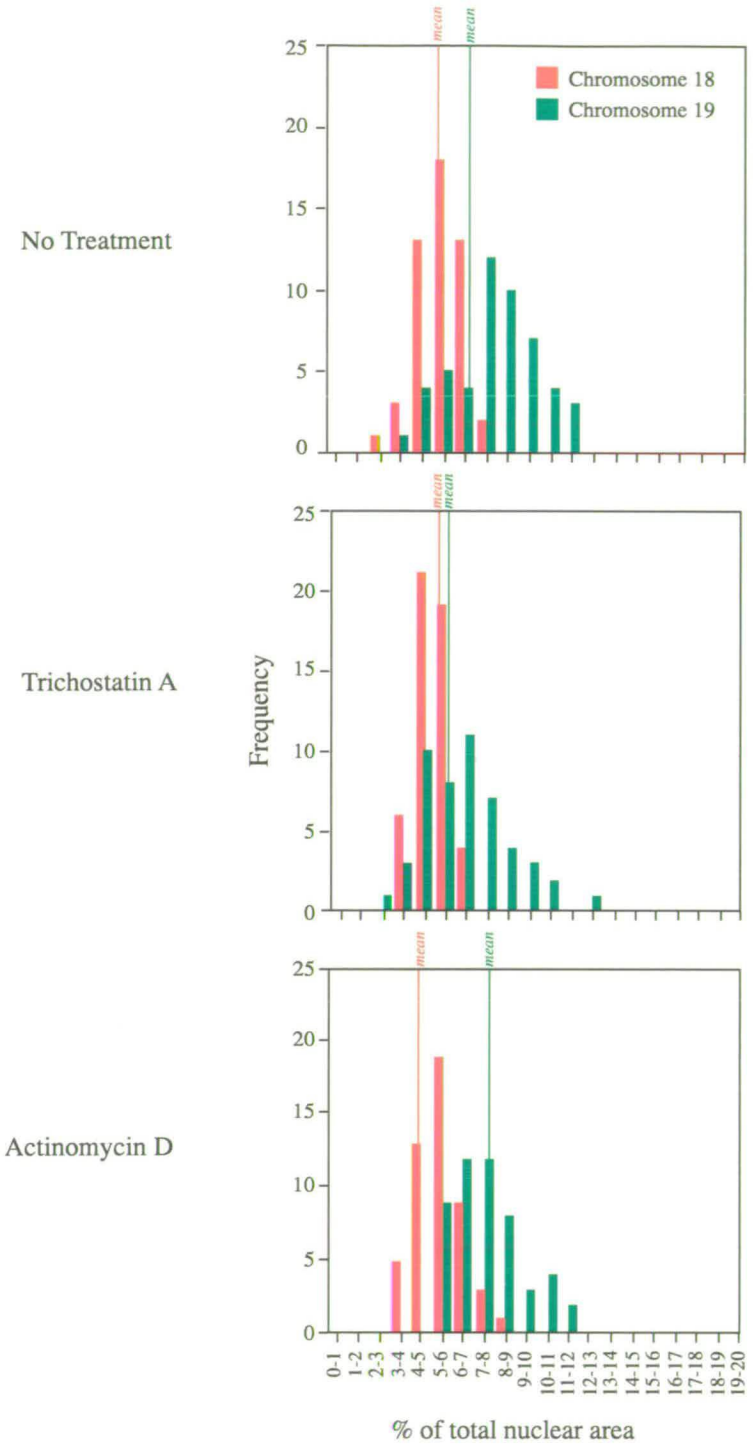

Figure 7.5 Histograms comparing the areas of human chromosome 18 and 19 territories in nuclei treated with AD and TSA

Cells were treated with 5g/ml AD (Section 7.3.1) or 10ng/ml TSA (Section 7.3.2) for 2 hours prior to harvesting. Using Script 1 (Section 6.2.1) measurements were taken from both signals in 50 randomly selected nuclei hybridised with paints for human chromosomes 18 or 19. Paints were labelled with biotin and detected with avidin-FITC. FISH signal area given as a percentage of the total nuclear area.

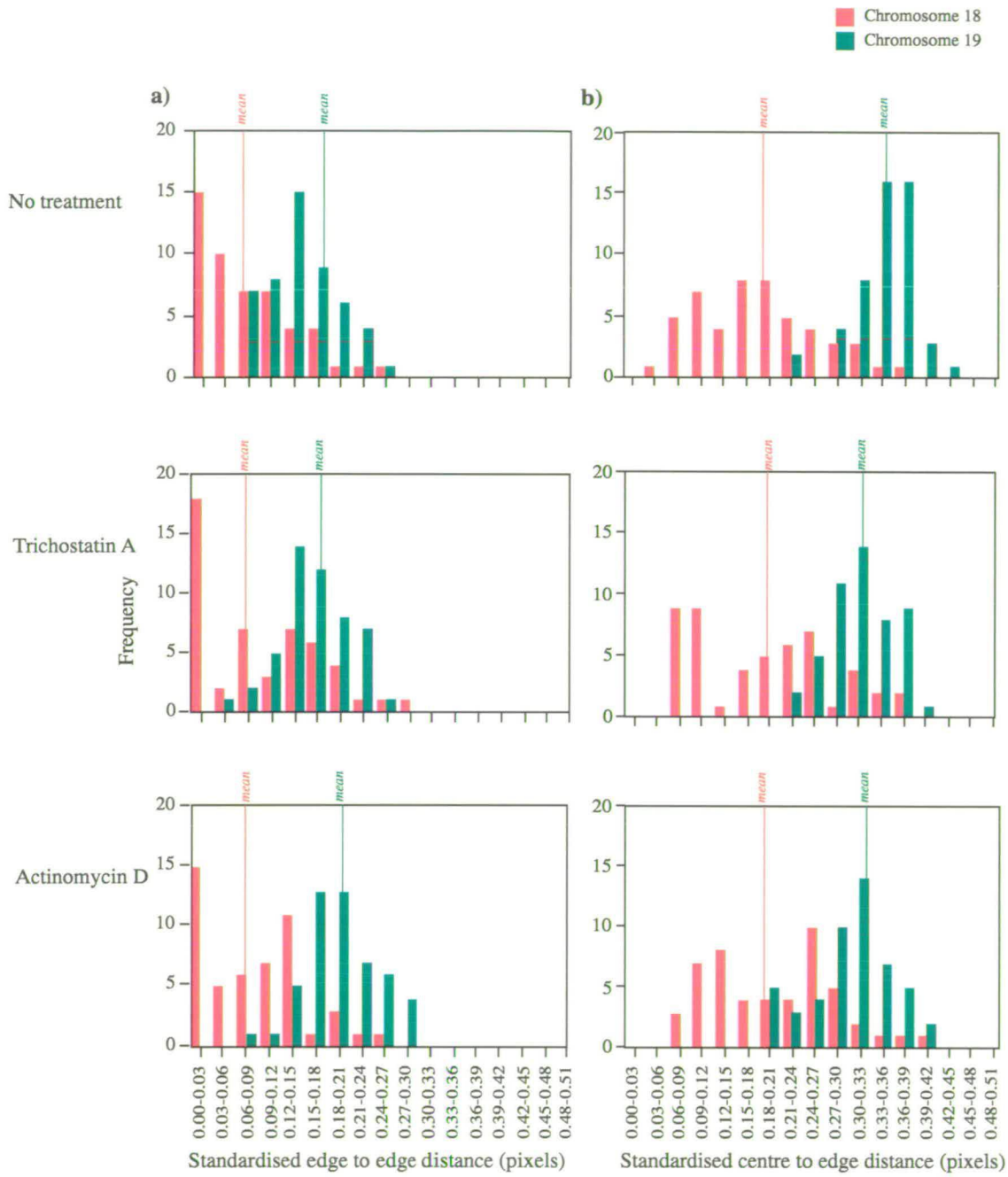

Figure 7.6 Histograms comparing the areas of human chromosome 18 and 19 territories in nuclei treated with AD and TSA

Cells were treated with 5µg/ml AD (Section 7.3.1) or 10ng/ml TSA (Section 7.3.2) for 2 hours prior to harvesting. Using Script 1 (Section 6.2.1) measurements were taken from both signals in 50 randomly selected nuclei hybridised with paints for human chromosomes 18 or 19. Paints were labelled with biotin and detected with avidin-FITC. (**a**) Edge of the signal to the nearest edge of the nucleus. (**b**) Centre of the signal to the nearest edge of the nucleus. Distances standardised by dividing by the √nuclear area (estimate of nuclear radius).

7.4 The involvement of the nuclear matrix in nuclear organisation

When nuclei are extracted with salt, DNA loops distend to form halos around a morphological framework, termed the "nuclear matrix" (McCready *et al.*, 1979; Vogelstein *et al.*, 1980). The residual protein content of the nuclear matrix includes topo II and proteins of the lamina, and a number of other proteins, many of which remain to be identified (Lewis *et al.*, 1984; Pieck *et al.*, 1985; Stuurman *et al.*, 1990; Hozak *et al.*, 1995). The types of DNA sequences shown to be associated with the nuclear matrix, principally in biochemical assays, include active genes (Ciejek *et al.*, 1983; Robinson *et al.*, 1983; Gerdes *et al.*, 1994), replication origins (Dijkwel *et al.*, 1986; Razin *et al.*, 1986 & 1993; Amati & Gasser, 1988; Sykes *et al.*, 1988), enhancers (Cockerill & Garrard, 1986; Jenuwein *et al.*, 1997) and chromatin domain boundaries (Phi-Van & Stratling, 1988; Thompson *et al.*, 1994a; Kalos & Fournier, 1995). Functionally the nuclear matrix has been shown to support the processes of transcription (Jackson *et al.*, 1981; Jackson & Cook, 1993; Sun *et al.*, 1994), replication (McCready *et al.*, 1980; Vogelstein *et al.*, 1980; Berezney & Buchholtz, 1981; Jackson *et al.*, 1984; Gerdes *et al.*, 1994) and histone acetyltation and deacetylation (Hendzel *et al.*, 1991; Hendzel *et al.*, 1994).

Salt extraction has been criticised as being a harsh treatment, destroying many of the sites of DNA attachment and creating artificial ones. Subsequently, other extraction techniques have been developed including the use of lithium diiodosalicylate (LIS) to produce a nuclear scaffold (Mirkovitch *et al.*, 1984) and the use of electroelution to produce a nucleoskeleton (Cook *et al.*, 1984; Jackson *et al.*, 1988) (Section 1.5.5). The DNA sequences involved at sites of attachment and the functions associated with each of these residual nuclear frameworks differ. While replication and transcription have been associated with both the nuclear matrix and the nucleoskeleton (Jackson & Cook, 1985 & 1986; Jackson *et al.*, 1996), these functions have not been shown to occur at the nuclear scaffold (Mirkovitch *et al.*, 1984; Gasser *et al.*, 1988). The AT-rich DNA sequences fractionating with the nuclear scaffold and termed "scaffold attachment sequences" (SARs) (Section 1.5.5) have been shown to associate with the nuclear matrix but not the nucleoskeleton (Izaurralde *et al.*, 1988). Each of these extraction procedures appear to "sample" different sets of DNA attachments to a residual nuclear framework (Craig *et al.*, 1997). The relationship between the nuclear matrix, nuclear scaffold, nucleoskeleton and the morphological nuclear matrix remains unclear. To further understand the DNA attachments made to the nuclear matrix

and their involvement in transcription and in maintaining the dispositions of chromosome territories, the position of human chromosomes 18 and 19 in salt extracted nuclei were analysed.

7.4.1 The areas and positions of human chromosomes 18 and 19 in nuclei extracted with salt

Nuclei were prepared from the FATO human lymphoblast cell line in polyamine buffer (Sections 2.8.1 & 4.2). For extraction, nuclei were spread on slides and allowed to settle overnight. Slides were then lowered gently into extraction buffer in the absence of salt and then sequentially into extraction buffers with increasing concentrations of salt (Section 2.9). Prior to FISH, slides were fixed in 3:1 methanol:acetic acid. The paints for human chromosomes 18 and 19 were alternatively labelled to allow simultaneous hybridisation and detection with different fluorochromes. The residual nucleus was stained with DAPI.

Table 7.5 The areas of human chromosomes 18 and 19 territories in nuclei extracted with salt
Nuclei from the FATO human lymphoblast cell line were treated with 5µg/ml AD for 2 hours to block transcription. Treated and non-treated nuclei were extracted with increasing concentrations of salt. Alternatively labelled paints for chromosomes 18 and 19 were hybridised simultaneously and detected with different fluorochromes. The area of each signal was divided by the total nuclear area, determined using Script 1 (Section 6.2.1) from 50 randomly selected nuclei in which no DNA halo was observed. +/- standard error of mean

	Salt concentration	% of total nuclear area		19:18
		Chromosome 18	Chromosome 19	
No treatment	0.0M	$5.6^{+/-0.1}$	$7.1^{+/-0.2}$	1.27
	0.5M	$7.8^{+/-0.1}$	$10.2^{+/-0.4}$	1.31
	1.0M	$8.9^{+/-0.1}$	$10.1^{+/-0.2}$	1.13
	1.2M	$8.9^{+/-0.2}$	$10.0^{+/-0.2}$	1.12
AD treatment	0.0M	$5.7^{+/-0.1}$	$7.2^{+/-0.3}$	1.26
	0.5M	$7.9^{+/-0.1}$	$7.8^{+/-0.2}$	0.99
	1.0M	$6.3^{+/-0.3}$	$8.1^{+/-0.3}$	1.29
	1.2M	$7.0^{+/-0.2}$	$6.9^{+/-0.1}$	0.99

Each slide contained both nuclei that possessed DNA halos and nuclei that had not been fully extracted or in which DNA loops did not fully distend. Slides extracted at higher salt

concentrations revealed an increased proportion of fully extracted nuclei, such that, at 0.5M NaCl, no nuclei were fully extracted, while at 1.8M NaCl, very few nuclei that had not been fully extracted were observed. Figure 7.7 shows representative nuclei in which most DNA remained confined within the nuclear envelope, hybridised simultaneously with the paints to human chromosome 18 and 19. The fluorochrome used to detect each signal was alternated. Using Script 1 (Section 6.2.1), position and area measurements for each signal were taken from 50 randomly selected nuclei (Tables 7.5 & 7.6).

Table 7.6 The positions of human chromosomes 18 and 19 territories in nuclei extracted with salt

Nuclei from the FATO human lymphoblast cell line were treated with 5μg/ml AD for 2 hours to block transcription. Treated and non-treated nuclei were extracted with increasing concentrations of salt. Alternatively labelled paints for chromosomes 18 and 19 were hybridised simultaneously and detected with different fluorochromes. The distances calculated for each signal were divided by the √nuclear area (estimate of nuclear radius), determined using Script 1 (Section 6.2.1) from 50 randomly selected nuclei in which no obvious DNA halo was observed. +/- standard error of mean

	Salt concentration	Mean standardised edge to edge distance		Mean standardised centre to edge distance	
		18	19	18	19
No treatment	0.0M	$0.07^{+/-0.008}$	$0.18^{+/-0.005}$	$0.17^{+/-0.006}$	$0.35^{+/-0.012}$
	0.5M	$0.07^{+/-0.006}$	$0.17^{+/-0.007}$	$0.19^{+/-0.008}$	$0.33^{+/-0.009}$
	1.0M	$0.05^{+/-0.009}$	$0.20^{+/-0.009}$	$0.19^{+/-0.008}$	$0.35^{+/-0.010}$
	1.2M	$0.10^{+/-0.008}$	$0.15^{+/-0.010}$	$0.15^{+/-0.010}$	$0.31^{+/-0011}$
AD treatment	0.0M	$0.08^{+/-0.004}$	$0.14^{+/-0.006}$	$0.18^{+/-0.007}$	$0.34^{+/-0.010}$
	0.5M	$0.04^{+/-0.006}$	$0.14^{+/-0.009}$	$0.16^{+/-0.009}$	$0.30^{+/-0010}$
	1.0M	$0.07^{+/-0.010}$	$0.16^{+/-0.014}$	$0.19^{+/-0.011}$	$0.31^{+/-0013}$
	1.2M	$0.04^{+/-0.010}$	$0.15^{+/-0.013}$	$0.14^{+/-0.015}$	$0.29^{+/-0.012}$

Both chromosomes 18 and 19 occupied a slightly larger territory area as a proportion of the total nuclear area (approximately 50% larger in both instances) in 0.5M NaCl extracted nuclei than was observed in non-extracted 3:1 methanol:acetic acid fixed nuclei (Tables 6.3 & 7.5). With increasing salt concentrations, while the chromosome 19 territory occupied a similar area, the chromosome 18 territory became less condensed (Table 7.5 & Figure 7.8). At 1.2M NaCl all of the core and linker histones should have been extracted in addition to other structural proteins (Wolffe, 1995). It appears that the condensed state of chromosome 18 may be mediated by proteins that are extractable by salt (>0.5M).

Measurements of edge to edge and centre to centre distances were unreliable, since often nuclei were quite distorted following salt extraction (Table 7.6). Nonetheless, chromosome 18 continued to occupy a territory that was consistently and significantly closer to the periphery of the nucleus than that of chromosome 19, at all salt concentrations (ST $p<0.0002$ at all salt concentrations) (Figure 7.9).

Table 7.7 The distribution of signal from paints for human chromosomes 18 and 19 in nuclei with a DNA halo following extraction with salt
Nuclei from the FATO human lymphoblast cell line were treated with 5μg/ml AD for 2 hours to block transcription. Treated and non-treated nuclei were extracted with increasing concentrations of salt. Alternatively labelled paints for chromosomes 18 and 19 were hybridised simultaneously and detected with different fluorochromes. Using IPLab Spectrum software, the total amount of fluorescence present in the DNA halo of 25 fully extracted nuclei was measured and calculated as a percentage of the total amount of fluorescence (Figure 7.11). +/- standard error of mean

	Salt concentration	Mean % of signal in DNA halo		
		18	19	DAPI
No treatment	1.0M	$42.0^{+/-2.0}$	$21.0^{+/-3.4}$	$34.7^{+/-1.6}$
	1.2M	$39.9^{+/-3.3}$	$22.6^{+/-2.4}$	$27.7^{+/-2.1}$
AD treatment	1.0M	$45.2^{+/-3.5}$	$23.0^{+/-3.4}$	$36.5^{+/-2.8}$
	1.2M	$39.2^{+/-2.9}$	$18.6^{+/-1.8}$	$30.1^{+/-2.7}$

Figure 7.10 shows representative nuclei that had been extracted with salt and from which loops of DNA were released hybridised simultaneously with the paints to human chromosome 18 and 19. Images were taken of 25 randomly selected nuclei that were extracted at 1.0M and 1.2M NaCl concentrations. At 1.8M NaCl nuclei were very distorted and morphology was often indiscernible (Figure 7.10c). It was instantly clear that in the majority of nuclei, the entirety of chromosome 18 was released into the DNA halo, while chromosome 19 remained within the residual nucleus. In a count of 200 nuclei at 1.2M NaCl, over 60% of chromosome 18 signals were considered as being in the DNA halo, while 20% of chromosomes 19 were localised to the DNA halo. To quantify this further, using IPLab Spectrum software, a line was drawn manually about the apparent residual nuclear matrix defined by bright DAPI fluorescence (Figure 7.11). The total amount of signal and DAPI fluorescence was measured within and outside of this defined region, that is, at the nuclear matrix and within the DNA halo respectively (Table 7.7). Approximately 30-35% of the DAPI signal was present in each DNA halo. On average 40% of chromosome 18

signal was in the DNA halo, while only 20% of chromosome 19 signal was located there. It appears that after extraction of soluble nuclear proteins with high salt chromosome 18 is free to migrate out of the nucleus. Chromosome 19 remains relatively tightly bound to the nuclear matrix. Is this attachment dependent upon continued transcription?

7.4.2 The areas and positions of human chromosomes 18 and 19 in nuclei treated with AD and extracted with salt

FATO human lymphoblastoid nuclei were treated with 5μg/ml of AD for 2 hours prior to harvesting (Section 7.3), extracted with salt at increasing concentrations and hybridised with paints for human chromosomes 18 and 19 by FISH. Using Script 1 (Section 6.2.1), position and area measurements for each signal were taken from 50 randomly selected nuclei in which DNA remained constrained within the confines of the nucleus (Tables 7.5 & 7.6).

The territory area of chromosome 18 was larger in 0.5M NaCl extracted nuclei than 3:1 methanol:acetic acid fixed nuclei (Tables 6.3 & 7.5), as observed with extracted non-treated nuclei (Section 7.4.1). However, this increased area was not observed at 1.0M NaCl extraction. This anomaly may be due to poor probe hybridisation and/or nuclear distortion but was not repeated due to lack of time. The territory area of chromosome 19 was smaller in salt extracted nuclei following treatment with AD than in untreated salt extracted nuclei, as seen in 3:1 methanol:acetic acid fixed nuclei before and after AD treatment (Tables 6.3 & 7.5).

Chromosome 18 territories remained predominantly peripheral while chromosome 19 territories were relatively central in the nucleus, with distance measurements broadly similar to those calculated for 3:1 methanol:acetic acid fixed nuclei and salt extracted nuclei not treated with AD (Tables 6.4 & 7.6). Thus, the positioning of the two chromosomes is maintained.

Nuclei that had been fully extracted by salt were also examined. Images were taken of 25 randomly selected nuclei that were fully extracted at 1.0M and 1.2M NaCl. As with cells that had not been treated with AD, in the majority of nuclei, chromosome 18 was present within the DNA halo, while chromosome 19 remained attached to the nucleus. The extent of the DNA halo was not increased when compared to nuclei without AD treatment. On average, 30-35% of DAPI fluorescence, 42% of chromosome 18 signal and 20% of

chromosome 19 signal was present in the DNA halo (Table 7.7), similar to non-treated nuclei. This suggests that the nuclear matrix attachments which chromosome 19 maintains are not dependent on active transcription. However, it is possible that AD acts to secure the possible nuclear matrix attachments of transcription complexes and the associated DNA. Attachment of sequences with transcriptional potential to the nuclear matrix may be mediated by a protein(s) distinct from the transcription complex itself.

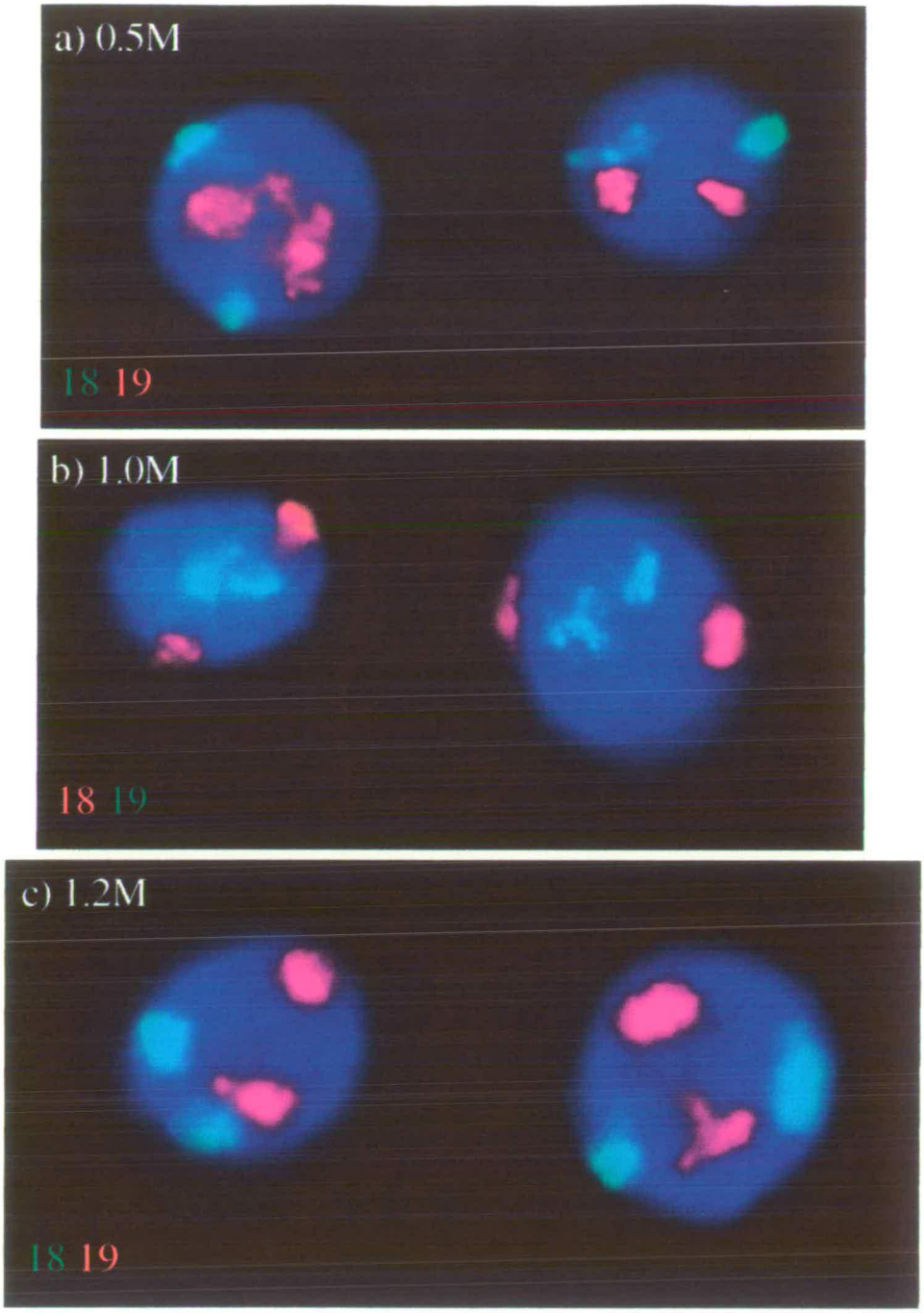

Figure 7.7 The interphase territories of human chromosomes 18 and 19 in nuclei with no DNA halo following extraction with salt
Representative nuclei from the FATO human lymphoblast cell line extracted with increasing concentrations of salt. Alternatively labelled paints for chromosomes 18 and 19 (Section 3.3) were hybridised simultaneously and detected with different fluorochromes. Nuclei counterstained with DAPI (blue). (**a**) (**c**) Chromosome 18 paint detected with FITC (green). Chromosome 19 paint detected with TR (red). (**b**) Chromosome 18 paint detected with TR (red). Chromosome 19 paint detected with FITC (green).

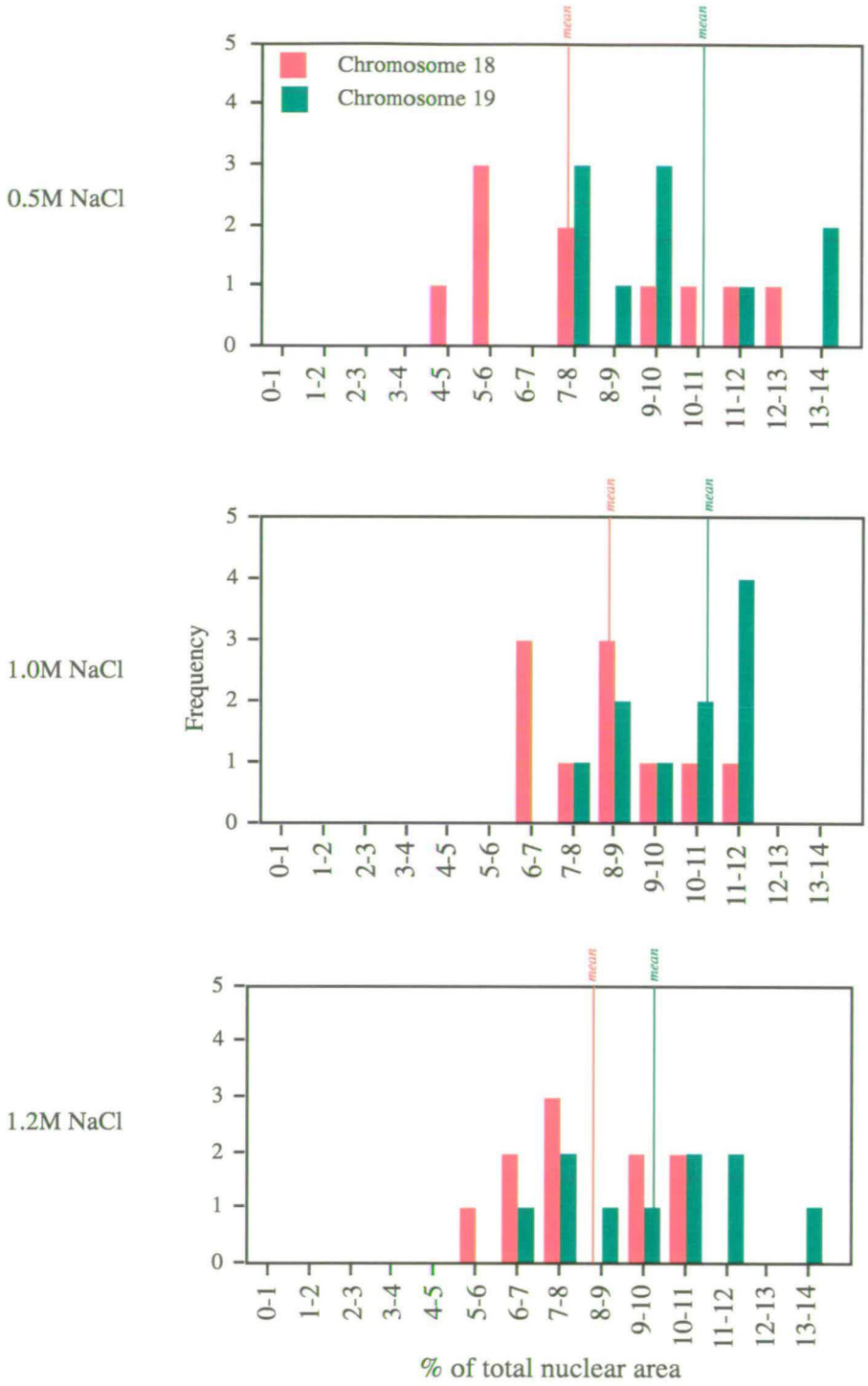

Figure 7.8 Histograms comparing the areas of human chromosomes 18 and 19 territories in nuclei extracted with salt

Slides were made from FATO human lymphoblast nuclei extracted with increasing concentrations of salt and hybridised simultaneously with alternatively labelled paints for human chromosomes 18 and 19 by FISH. Using Script 1 (Section 6.2.1) measurements were taken from both signals in 25 randomly selected nuclei, in which no DNA halo was observed. FISH signal area given as a percentage of the total nuclear area.

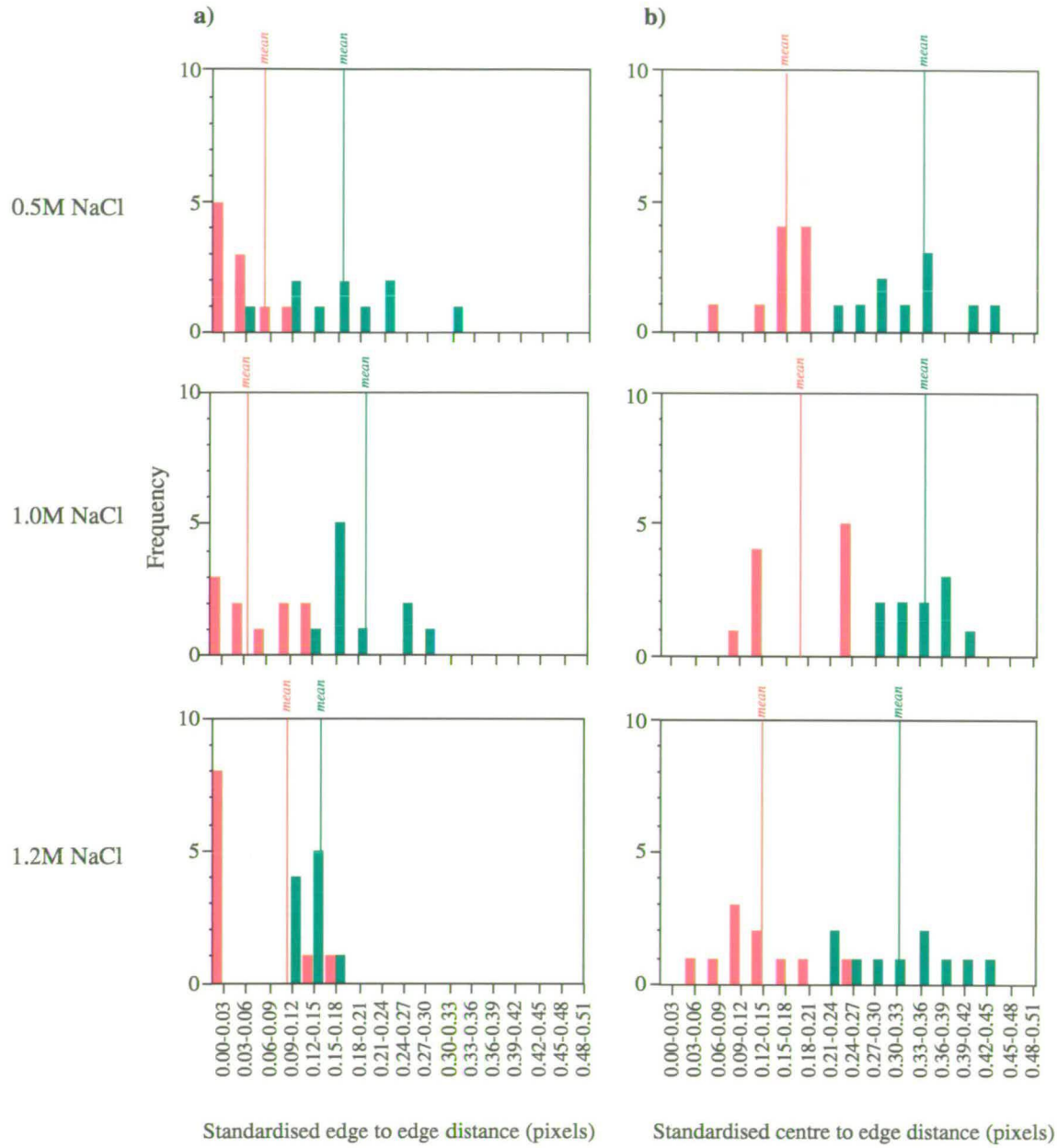

Figure 7.9 Histograms comparing the positions of human chromosomes 18 and 19 territories in nuclei extracted with salt

Slides were made from FATO human lymphoblast nuclei extracted with increasing concentrations of salt and hybridised simultaneously with alternatively labelled paints for human chromosomes 18 and 19 by FISH. Using Script 1 (Section 6.2.1) measurements were taken from both signals in 25 randomly selected nuclei, in which no DNA halo was observed. (**a**) Edge of the signal to the nearest edge of the nucleus. (**b**) Centre of the signal to the nearest edge of the nucleus. Distances standardised by dividing by the √nuclear area (estimate of nuclear radius).

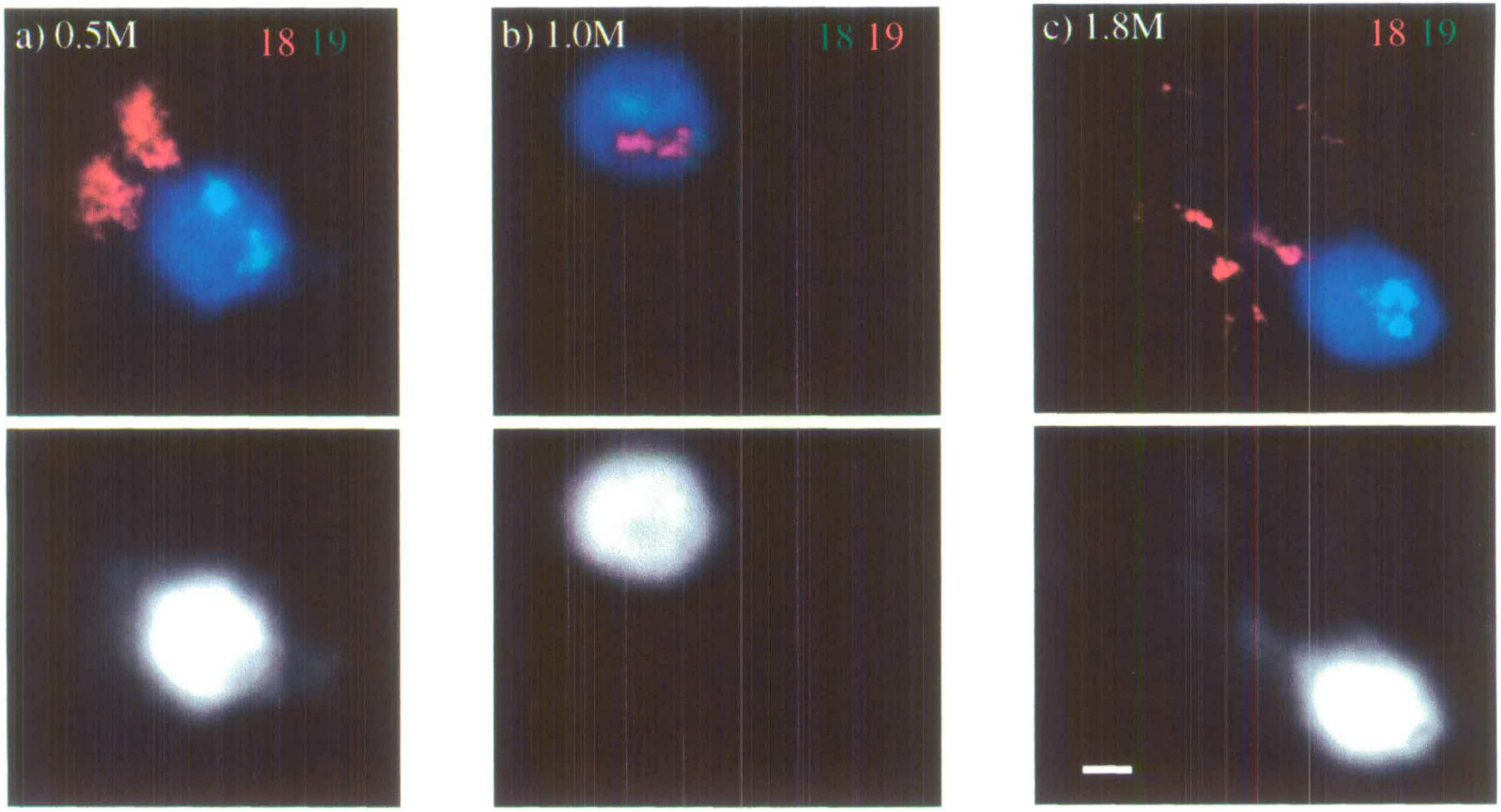

Figure 7.10 The territories of human chromosomes 18 and 19 in nuclei with a DNA halo following extraction with salt
Representative nuclei from the FATO human lymphoblastoid cell line extracted with increasing concentrations of salt. Alternatively labelled paints for chromosomes 18 and 19 (Section 3.3) were hybridised simultaneously and detected with different fluorochromes. Nuclei counterstained with DAPI (blue). (**a**) (**c**) Chromosome 18 paint detected with TR (red). Chromosome 19 paint detected with FITC (green). (**b**) Chromosome 18 paint detected with FITC (green). Chromosome 19 paint detected with TR (red). Bar= 1μm

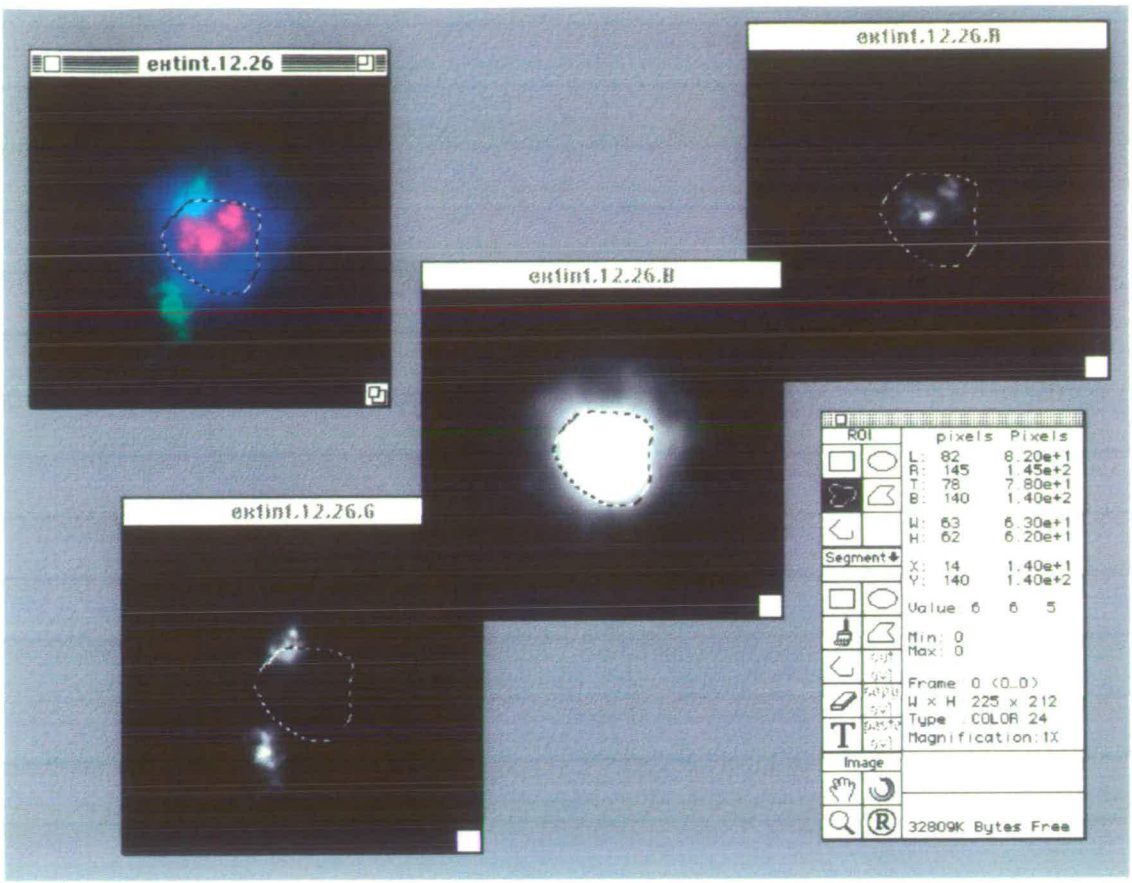

Figure 7.11 Analysing the distribution of paints for human chromosomes 18 and 19 in nuclei with a DNA halo following extraction with salt
Representative nuclei from the FATO human lymphoblastoid cell line extracted with increasing concentrations of salt. Alternatively labelled paints for chromosomes 18 and 19 (Section 3.3) were hybridised simultaneously and detected with different fluorochromes. Nuclei were counterstained with DAPI (blue). Using IPLab Spectrum software, a line was drawn manually about the apparent residual nuclear matrix defined by bright DAPI fluorescence. The total amount of signal and DAPI fluorescence was measured within and outside of this defined region, that is, at the nuclear matrix and within the DNA halo, respectively.

7.5 The location of genes in the interphase nuclear territory of human chromosome 18

The periphery of interphase chromosome territories have been associated with nascent transcripts and splicing components (Zirbel *et al.*, 1993). In addition, a sample of coding sequences have been demonstrated to lie preferentially to the edge of chromosome territories at interphase, while non-coding sequences were either randomly or preferentially located inside of territories (Kurz *et al.*, 1996). However, using CpG-islands as markers for genes, I demonstrated in Chapter 4 that there was no bias in distribution of genes laterally across salt extracted human chromosome 18 at metaphase. It is possible, however, that there is reorganisation as chromosomes decondense following mitosis, such that coding sequences are predominantly moved to the periphery of interphase chromosome territories. Therefore, I assayed whether CpG-islands locate to the outer surface of chromosome 18 interphase nuclear territories.

Nuclei extracted with salt (Section 7.4.1) were hybridised with differentially labelled chromosome 18 CpG-island probe (Section 4.3.1) and whole chromosome 18 paint (Section 3.2.3). Figure 7.12 shows nuclei extracted with 1.2M NaCl in which no DNA halo was observed. Figure 7.13 shows nuclei extracted with 1.2M NaCl from which DNA loops were distended. Where the red (TR) and green (FITC) fluorochromes colocalise, yellow signal is observed. Using IPLab Spectrum software, graphs measuring signal intensity were drawn along several axes at different angles through each chromosome territory (Figures 7.12 & 7.13). Consistently, there was no bias of signal distribution observed for either probe. If genes were preferentially located toward the periphery of the chromosome territory it might be expected that there would be a larger amount of signal from the CpG-island probe compared with that from the total chromosome paint at the extremes of the graphs.

Conversely, the non-CpG-island fraction from chromosome 18 was also hybridised to salt extracted nuclei in conjunction with total chromosome 18 paint. Figure 7.14 shows a pattern of distribution very similar to the territories in Figures 7.12 and 7.13. If genes were preferentially located toward the periphery of the chromosome territory it might have been expected that the signal from the non-CpG-island probe would drop away at the extremes of the graphs more sharply than the signal from the total chromosome paint.

These results argue against a predominant distribution of genes towards the periphery of chromosome territories at interphase and suggests that previously published studies have used an unrepresentative set of gene sequences. However, the apparently uniform distribution of genes across a chromosome territory may be the result of observations in 2-D made here, since there are likely to be genes on the upper and lower surfaces of the territory which may mask any peripheral signal bias. Since CpG-islands are 1-2Kb in length, spaced approximately every 300Kb (Craig & Bickmore, 1994), and loops have been estimated to be 50-200Kb (Section 1.1), although indirect, CpG-islands offer a reasonably good resolution to determine gene distribution within a chromosome at both interphase and metaphase. It would now be of interest to use the chromosome 18 CpG- and non-CpG-island paints in 3-D FISH analysis of nuclei (Section 6.6).

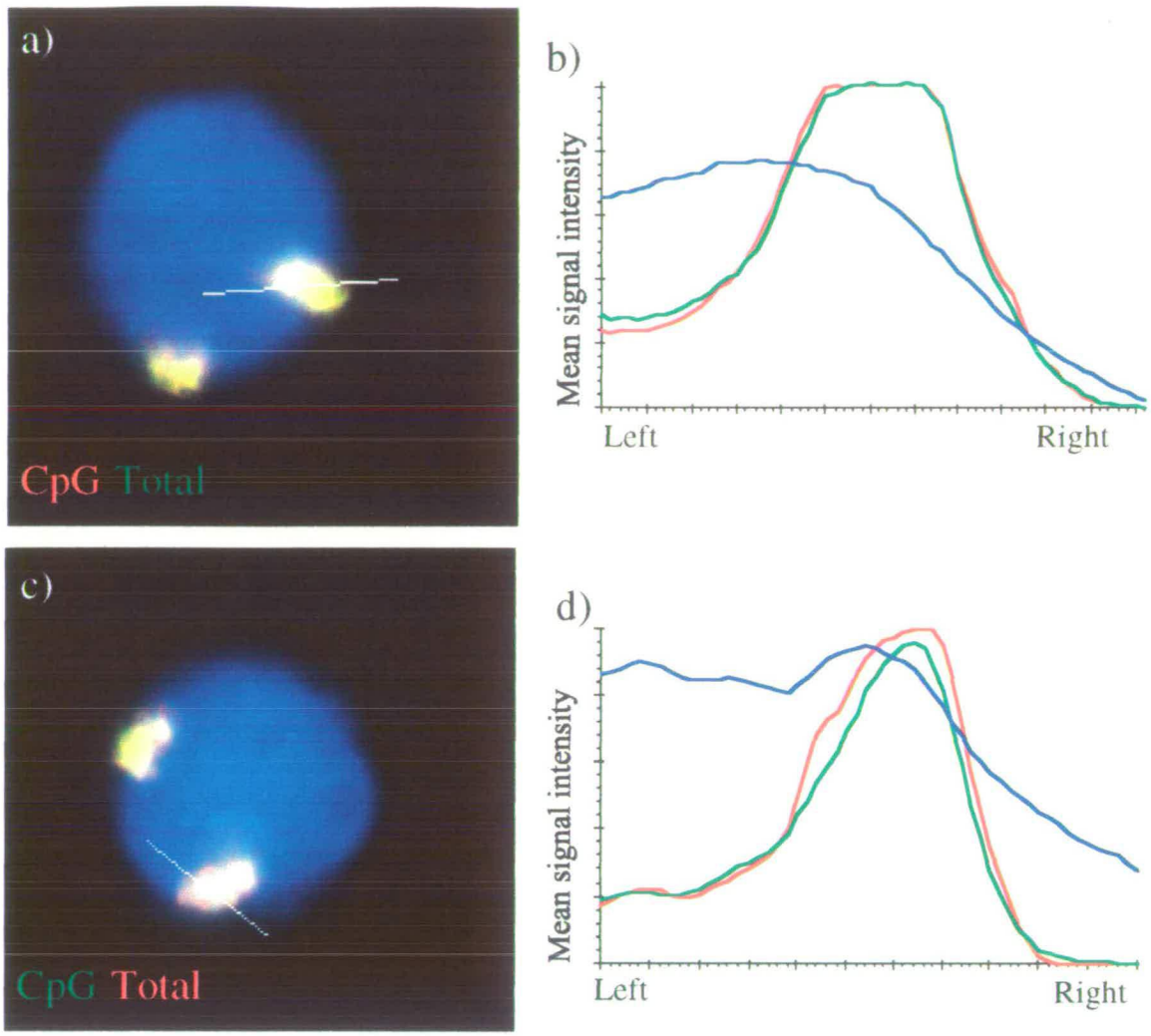

Figure 7.12 The distribution of CpG-islands in the interphase territory of human chromosome 18 in nuclei with no DNA halo following extraction with salt
Representative nuclei from the FATO human lymphoblast cell line extracted with 1.2M NaCl in which no obvious DNA halo was observed. Nuclei counterstained with DAPI (blue). Hybridisation of chromosome 18 CpG-island fragments isolated using the methyl-CpG binding column (Cross *et al.*, 1994) simultaneously with total chromosome 18 paint. (**a**) CpG-island probe detected with TR (red). Whole chromosome 18 paint detected with FITC (green). (**c**) CpG-island probe detected with FITC (green). Whole chromosome 18 paint detected with TR (red). (**b**) (**d**) Graph of mean signal intensity, across 1μm, along lines drawn in figures (a) and (c), respectively, from left to right. The graph lines are the appropriate colour for the fluorochrome that they represent.

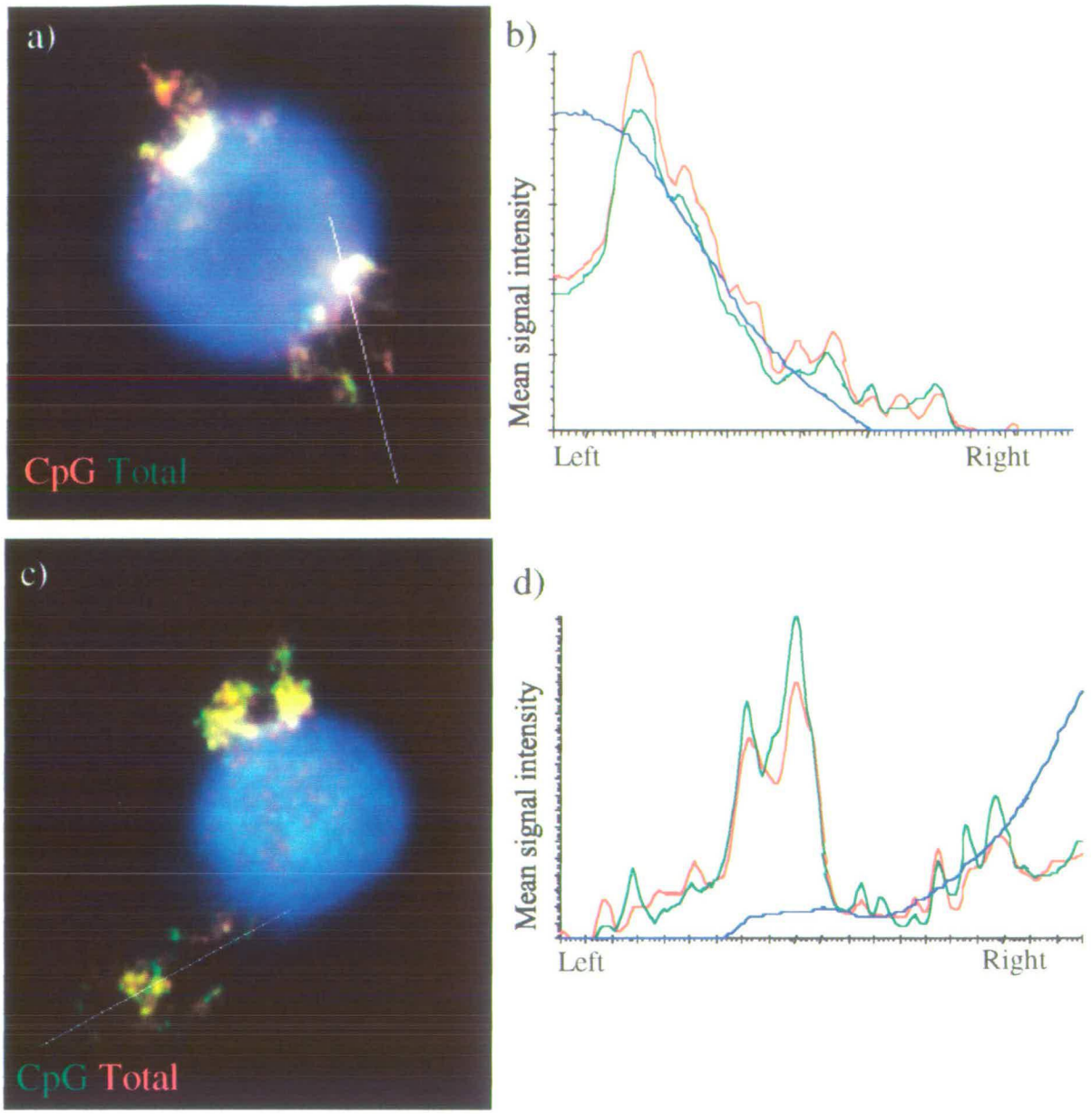

Figure 7.13 The distribution of CpG-islands in the interphase territory of human chromosome 18 in nuclei with a DNA halo following extraction with salt
Representative nuclei from the FATO human lymphoblast cell line extracted with 1.2M NaCl in which DNA halos were observed. Nuclei counterstained with DAPI (blue). Hybridisation of chromosome 18 CpG-island fragments isolated using the methyl-CpG binding column (Cross *et al.*, 1994) simultaneously with total chromosome 18 paint. (**a**) CpG-island probe detected with TR (red). Whole chromosome 18 paint detected with FITC (green). (**c**) CpG-island probe detected with FITC (green). Whole chromosome 18 paint detected with TR (red). (**b**) (**d**) Graph of mean signal intensity, across 1μm, along lines drawn in figures (a) and (c), respectively, from left to right. The graph lines are the appropriate colour for the fluorochrome that they represent.

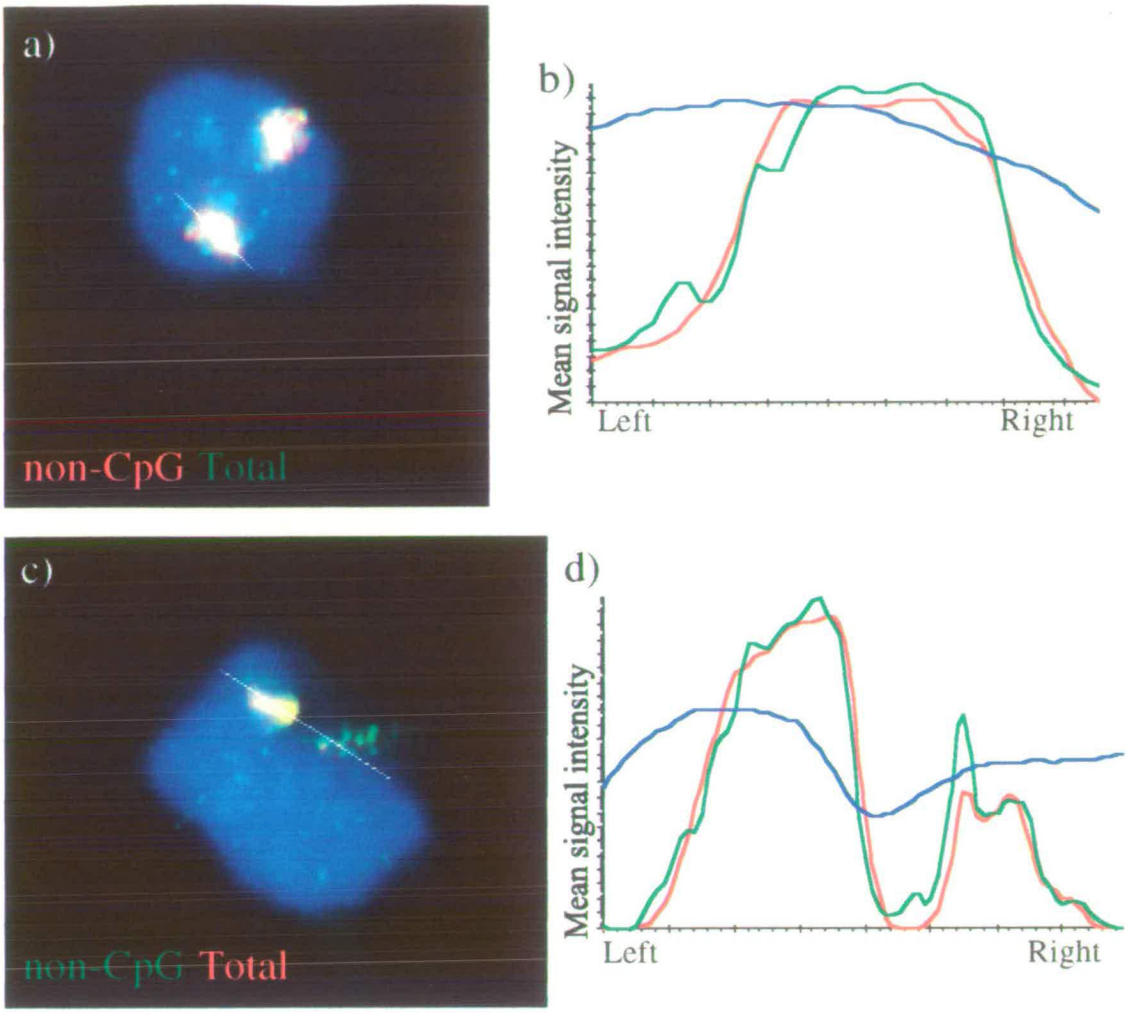

Figure 7.14 The distribution of non-CpG-islands in the interphase territory of human chromosome 18 in nuclei extracted with salt
Representative nuclei from the FATO human lymphoblast cell line extracted with 1.2M NaCl. Nuclei were counterstained with DAPI (blue). Hybridisation of chromosome 18 non-CpG-island fragments isolated using the methyl-CpG binding column (Cross *et al.*, 1994) simultaneously with total chromosome 18 paint. (**a**) Nucleus in which no obvious DNA halo was observed. non-CpG-island probe detected with TR (red). Whole chromosome 18 paint detected with FITC (green). (**c**) Nucleus with DNA halo. non-CpG-island probe detected with FITC (green). Whole chromosome 18 paint detected with TR (red). (**b**) (**d**) Graph of mean signal intensity, across 1μm, along lines drawn in figures (a) and (c), respectively, from left to right. The graph lines are the appropriate colour for the fluorochrome that they represent.

7.6 Summary

In this chapter, I addressed the factors involved in determining the size and position of interphase chromosome territories. The analysis of a reciprocal chromosome 18 and 19 translocation is consistent with DNA sequences on these chromosomes playing a role in the relative interphase territory dispositions of the two chromosomes (Section 7.2). Examination of other translocations between chromosome 18 and 19 or each of these chromosomes and the X chromosome, may prove informative. It would be necessary to establish cell lines from such translocations to allow analysis of treated and/or extracted nuclei or chromosomes. The influence of epigenetic features could then be studied, for instance, the levels of histone acetylation of a translocated portion may be altered by the remainder of the derived chromosome which may then effect its influence upon positioning. Cell lines with deletions in chromosome 18 may be obtained, to determine if a particular chromosomal sequence were important, or if the overall chromatin environment was the key for correct nuclear positioning.

Interestingly, AD treatment resulted in a significant decrease in the territory area of chromosome 19 when compared to that of chromosome 18. This suggests that transcriptional activity is instrumental in the organisation of chromosome territories in the nucleus. This data implies that chromosome 18 is not over-condensed in a normal human nucleus, but that chromosome 19 is actively decondensed, that is that the level of chromatin condensation observed for chromosome 18 is "default". Local decondensation may be the result of the presence of transcriptional complexes themselves or chromatin remodelling proteins such as *trithorax*-like proteins (Section 1.4.2). Alternatively, changes in chromatin configuration that accompany transcription, for example histone acetylation, may trigger the action of other, as yet unidentified, structural proteins. A previous study reported the dispersal of chromosome territories as a result of blocking transcription which was not observed here (Haaf & Ward, 1996). It would be worth repeating these experiments with other inhibitors of transcription and increasing the time of exposure to AD.

TSA acts to increase the total amount of acetylated histones in chromatin and it has been shown that more transcriptionally active regions become more highly acetylated relative to transcriptionally inactive regions (Section 5.2). There is an exaggerated difference between

the territory areas of chromosomes 18 and 19 following treatment with TSA which may indicate a role for histone acetylation in determining territory area.

Neither treatment with AD nor TSA altered the distinct positioning of the chromosome 18 and 19 territories. It is likely that the location of a particular territory is set up immediately following mitosis and physical constraints that exist thereafter throughout interphase, probably in the form of the nuclear matrix, prevent territory migration. Recent studies have marked and traced the chromatin of the interphase nucleus and demonstrated that it is relatively immobile, consistent with chromosome territory confinement (Abney *et al.*, 1997; Marshall *et al.*, 1997b) (Section 1.5.3). The data presented here suggest that chromosome territory positioning is a separate property to territory condensation.

The consistent localisation of chromosome 18 to the DNA halo of salt extracted nuclei suggests that this chromosome has fewer attachments to the matrix than chromosome 19, which remained confined to the residual nucleus. This supports models in which nuclear matrix attachments are mediated through transcriptionally active sequences. Surprisingly however, the use of AD to block transcription did not cause an increase in halo size, nor an increased localisation of chromosome 19 to the halo. Again, it would be worth repeating these experiments with other inhibitors of transcription and increasing the time of exposure to AD. Measurements of nuclei with no obvious DNA halo, showed that the chromosome 19 territory area had contracted when compared with salt extracted nuclei which had not been subjected to AD. This is consistent with observations in 3:1 methanol:acetic acid fixed nuclei which also showed reduced chromosome 19 territory size following AD treatment (Section 7.3). Therefore, it appears that active transcription may be necessary for a region to have an expanded territory size but not to be attached to the nuclear matrix.

The positioning of other chromosomes with regard to the DNA halo of extracted nuclei would be useful, particularly the positioning of probes specifically for G- and R-band regions of the genome.

Finally, the positioning of genes within a chromosome territory, as sampled by the distribution of a chromosome 18 CpG-island probe, revealed no bias of distribution towards the periphery of the interphase territory (Section 7.5). This argues against models in which transcriptional activity is limited to the interphase territory periphery (Zirbel *et al.*, 1993;

Kurz *et al.*, 1996; Reviews: Maneulidis, 1990; Cremer *et al.*, 1993; Strouboulis & Wolffe, 1996).

How are the contrasting sizes and positions of human chromosome 18 and 19 interphase territories established and maintained? Different proteins may be associated with each chromosome and the next chapter describes a method used to attempt to establish any such proteins.

8. Raising monoclonal antibodies against human metaphase chromosomes

8.1 Introduction

While one third of the mass of a human mitotic chromosome is DNA, one third is made up of the core and linker histones and the remaining one third consists of the relatively uncharacterised non-histone proteins (Earnshaw, 1988). In the previous chapters, it has been demonstrated that human chromosomes 18 and 19 are completely contrasting in their structural and functional features. These chromosomes differ in their DNA sequence, gene density, time of replication, histone content and chromatin packaging and territory positioning at interphase. Such characteristics are likely to be mediated through the non-histone chromosomal proteins.

Gels separating the proteins of isolated metaphase chromosomes, have revealed a complex series of bands, including histones and many non-histone proteins (Lewis *et al.*, 1984). Several approaches are being taken to identify non-histone chromosomal proteins. These include:

- Protein purification - This strategy has only been useful for abundant chromosomal proteins and was used for the identification of the two major scaffold proteins: ScII and topo II (Lewis & Laemmli, 1982). Human metaphase chromosomes were stabilised with polyanions, digested with microccocal nuclease, extracted with 2M NaCl and the scaffold components pelleted. Topo II and ScII were both purified from this scaffold pellet, representing 3-4% of total chromosomal proteins. Polyclonal antibodies raised to topo II have shown the protein localised to the scaffold of mitotic chromosomes (Earnshaw & Heck, 1985; Earnshaw *et al.*, 1985; Gasser *et al.*, 1986) (Section 1.4.6). ScII was only characterised more recently and is structurally related to the SMC family of proteins involved in chromosome condensation and sister chromatid separation (Saitoh *et al.*, 1994; Reviews: Peterson, 1994; Hirano *et al.*, 1995; Saitoh *et al.*, 1995) (Section 1.4.7).
- Genetic screens - These have mainly been carried out in the yeasts or *D.melanogaster*, since phenotypes can be easily and rapidly analysed, and many new chromosomal proteins have been isolated this way. For example, the search for suppressors of mating and sporolation defects in *S.cerevisiae* led to the identification of the Sir proteins (Rine *et al.*, 1979; Klar *et al.*, 1979). These proteins were further established to be involved in PEV following screens for mutants that caused derepression of marker genes affected by PEV at telomeres (Aparicio *et al.*, 1991) (Section 1.6.5).

- Homology based screens - A PCR probe encompassing the *D.melanogaster* chromodomain of HP1, the constitutive heterochromatin associated protein, was used to isolate homologues of HP1 in mouse and human (Singh *et al.*, 1991) (Section 1.4.2). The chromodomain has been found in a number of other heterochromatin associated proteins, including *D.melanogaster* Polycomb and other Polycomb group proteins (PcG) (Paro & Hognesss, 1991) (Section 1.4.2), and is essential for chromosomal localisation and repressive activity (Messmer *et al.*, 1992; Suso Platero *et al.*, 1995). The mouse proto-oncogene *bmi1* cDNA was used in a screen to search for a *D.melanogaster* homologue and the *Posterior sex combs* PcG gene was isolated. These proteins share homology with a number of functional domains, aside from a chromodomain which is absent from bmi1 (Brunk *et al.*, 1991; van Lohuizen *et al.*, 1991). This homology screening approach has established a growing group of heterochromatin associated proteins across a range of species, with homologies between different domains helping to establish the particular functions of each (Reviews: Lohe & Hilliker, 1995; Gould, 1997; Schumacher & Magnuson, 1997). There are limits to the diversity of chromosomal proteins likely to be found following solely this strategy.
- Cloning autoantigens - A large number of autoimmune sera to nuclear antigens have been identified (Review: Tan, 1982). The classic example of this approach was the use of autoantibodies from patients suffering from CREST scleroderma, containing anti-centromere antibodies, to isolate the CENPs (centromere proteins) (Moroi *et al.*, 1980; Earnshaw & Rothfield, 1985; Earnshaw *et al.*, 1987) (Section 1.6.9).

The characterisation of the antigens detected by novel monoclonal and polyclonal antibodies has defined a number of chromosomal proteins. Davis & Rao (1982) immunised rabbits with mitotic HeLa cell extracts and obtained an antiserum directed against mitotic chromosomes and prematurely condensed interphase chromosomes. However, such serum is polyclonal and will thus recognise a diversity of epitopes and antigens. First described by Kohler & Milstein (1975) mouse monoclonal antibodies allow the specificity of an antibody produced by a single spleen cell to be coupled with the tireless production of that antibody by a mouse myeloma cell. A variety of extracts have been used to immunise mice for the production of novel monoclonal antibodies which can then be used as reagents for the isolation and characterisation of the specific antigens and epitopes recognised. There are several examples of mitotic nuclear proteins which have been defined in this way.

Mice injected with purified HeLa nuclear non-histone chromatin proteins resulted in the production of a monoclonal antibody to the nuclear-mitotic apparatus (NuMA) protein

(Lyndersen & Pettijohn, 1980). This antigen is a constituent of the nuclear matrix at interphase but is concentrated at the spindle poles in mitosis. A chromatin containing fraction from rat liver cells was used to immunise mice and resulted in the production of a monoclonal antibody to another spindle apparatus protein, J17 (Newmeyer & Ohlsson-Wilhelm, 1985). Cooke *et al.* (1987) raised monoclonal antibodies to chicken chromosome mitotic scaffolds and identified the antigens termed INCENPs (inner centromere proteins). The INCENPs may play a role in sister chromatid cohesion, formation of the cleavage furrow or in organisation of the cytoskeleton (Cooke *et al.*, 1987; Mackay *et al.*, 1993 & 1997) (Section 1.5.2).

More recently, Adams & Hodge (1996) raised monoclonal antibodies by injection of metaphase chromosomes and chromatids from anaphase/telophase (prenuclei) of HeLa cells. One of these antibodies detects an epitope on metaphase chromosomes and chromatids that is not recognised once the chromatids are fully coalesced, immediately prior to decondensation and nuclear envelope formation. In canine epithelial cells, a monoclonal antibody termed LFM-1, has been raised to metaphase chromosomes and the antigen has been localised to chromosomes throughout mitosis, localise to the nucleus at G1 but excluded from the nucleus at G2 (Vega-Salas & Salas, 1996). Further analysis with this antibody suggests that this unknown, cell cycle regulated protein, localises to both the chromosomal surface and axis, both morphologically and biochemically.

By immunisation of mice with mitotic HeLa cell extract, two monoclonal antibodies, designated MPM-1 and MPM-2, were raised to phosphoproteins present along metaphase chromosomes and within the cytoplasm of mitotic cells (Davis *et al.*, 1983). MPM-2 has since been demonstrated to recognise a phosphoepitope present on a number of proteins phosphorylated immediately prior to mitosis, including microtubule organising centre proteins (Vandre *et al.*, 1984 & 1991), topoisomerase II (Taagepera *et al.*, 1993) and, most recently, the mitosis-promoting cdc25 phosphatase (Kuang *et al.*, 1994). MPM-1 also recognises a phospho-epitope present on microtubule organising proteins (Vandre *et al.*, 1984). Also from this screen MPM-12 predominantly stains mitotic cells and co-purifies with histone H1 kinase activity (Ganju *et al.*, 1992), and MPM-13 was shown to bind to the centrosome of interphase and metaphase cells (Rao *et al.*, 1989). No monoclonal antibody specific for metaphase chromosomes alone was established in this case.

The immunisation of mice with mitotic chromosomes and cell extracts from a variety of organisms, has raised antibodies to an array of different proteins, many of which are associated with mitotic chromosomes. Clearly, this is a useful way of identifying proteins involved in mitotic chromosome structure and function. Using this strategy, I wished to raise antibodies specifically to human chromosome 18 or 19, and thus identify new proteins or modifications involved in the structure and/or function of one or other of these chromosomes?

8.2 Synopsis for raising mouse monoclonal antibodies to human metaphase chromosomes

This scheme for the production of mouse monoclonal antibodies to human metaphase chromosomes is outlined in Figure 8.1.

8.2.1 Antigen preparation and immunisation

Metaphase chromosomes were prepared from the REN2 human cell line (49, XXXXY), as previously described (Section 2.8.1 & 4.2.6). Briefly, cells were treated with colcemid, harvested and swollen in hypotonic solution. A mitotic index of >60% was usually obtained. Cells were pelleted and resuspended in polyamine buffer containing digitonin. Polyamines help maintain chromosome structure, while digitonin pierces the cellular membrane but not the nuclear membrane, and since cells undergoing mitosis do not have a nuclear membrane, chromosomes are released into the supernatant. The suspension was spun and the nuclear pellet and supernatant were each stored with glycerol at -70°C.

All mice were injected initially with metaphase chromosomes prepared in an adjuvant, a non-specific stimulator of the immune system causing a local inflammatory response at the site of injection. Metaphase chromosomes were retrieved from storage, pelleted and pooled in polyamine buffer, excluding digitonin, to a final concentration of $1x10^9$ chromosomes/ml. 500µl of chromosome suspension were added to 500µl of adjuvant (Section 2.12.1.1) and 200µl were injected into each of five mice subcutaneously in the abdomen. This location enhances lymphocyte production in the spleen. Approximately $1x10^8$ chromosomes, then, were injected into each mouse. This was estimated to be approximately 25µg of protein (Table 8.1), comparable to quantities used in previous attempts to raise monoclonal antibodies (4-1000µg) (Example: Davis *et al.*, 1983).

Table 8.1 Estimated protein content of human metaphase chromosome antigens
Details of monoclonal antibody production outlined in Sections 2.12 and 8.2. If two thirds the mass of a chromosome is protein and 46 chromosomes consist of approximately 6pg DNA, then it can be estimated that 46 chromosomes contain 12pg of protein. From this, estimates of the protein content of each immunisation were calculated. PA- polyamine buffer

Immunisation	Mouse	Antigen	Estimated protein content (μg)
Initial	All	~$1x10^8$ total human metaphase chromosomes in 100μl PA + 100μl adjuvant	~25
Primary booster (one month following initial immunisation)	1	~$2x10^4$ FACS sorted human chromosomes 18 in 200μl PA	~0.005
	2	~$2x10^4$ FACS sorted human chromosomes 19 in 200μl PA	~0.005
	3	~$2x10^8$ total human metaphase chromosomes in 200μl PA	~50
	4	~$2x10^4$ FACS sorted human X chromosomes in 200μl PA	~0.005
	5	~$2x10^8$ human nuclei in 200μl PA	~2400
Secondary booster (four days prior to removal of spleen)	All	~$2x10^8$ total human metaphase chromosomes in 200μl PA	~50

One month later, the primary booster immunisation was carried out. No adjuvant was used on this occasion. Each mouse was injected with a different antigen, listed in Table 8.1. For the sorted chromosome injections, metaphase chromosomes were prepared as previously described (Section 2.8.1) and FACS sorted by Dr. D. Green, MRC Human Genetics Unit, Edinburgh, into pure preparations of chromosome 18, 19 and X (Section 2.8.2). To assess purity of the sort, 1-10μl of chromosome suspension from each preparation were used as a template for *Alu*-PCR (Section 2.4.1). Products were labelled by nick translation (Section 2.5.1) and hybridised to 3:1 methanol:acetic acid fixed normal human metaphase spreads by FISH (Section 2.6). Figure 8.2 shows the hybridisation signal following FISH with probes produced from example sorts, the majority of which appeared to be clean. Any contaminated sorts were discarded. FACS sorting is a laborious process and after pooling several clean sorts for each chromosome, only final concentrations of approximately $1x10^5$ chromosomes/ml were achieved. Total metaphase chromosomes were prepared as described for the initial immunisation. Nuclei were obtained from the nuclear fraction attained during the preparation of metaphase chromosomes (Section 2.8.1).

Why chose each of these different antigens? It was my original aim to raise antibodies to human chromosomes 18 and/or 19, to determine any proteins that may be differentially associated with either of these contrasting chromosomes. In addition, the cell line from which the metaphase chromosomes were prepared possesses three additional X chromosomes, all of which are inactive. It would be intriguing if antibodies could be raised that specifically recognised the inactive X chromosome. The protein content of the FACS sorted injections was very low (<0.005μg) so to improve my chances of raising an antibody to a chromosomal antigen, total metaphase chromosomes, and total nuclei were also used as stimulants.

Four days prior to removal of the mouse spleen, a final boost of 200μl of total metaphase chromosomes, at $1x10^9$ chromosomes/ml in polyamine buffer, excluding digitonin and with no adjuvant, was given.

8.2.2 Cell fusion

This method is described in detail in Section 2.12.2. Briefly, the mouse spleen was removed and punctured. Lymphocytes were displaced by pushing medium through the spleen and on each occasion half were stored at -70°C for fusion at a later date. The remaining lymphocytes were fused with Sp2/0 mouse myeloma cells to produce hybridomas. The cells were mixed at a concentration of 1:5 myeloma cells to spleen cells along with polyethylene glycol (PEG). PEG causes the disruption of the cell plasma membranes which, on occasions, results in the fusion of adjacent cells. In medium containing hypoxanthine, aminopterin and thymidine (HAT) the myeloma cells used will not grow. Aminopterin blocks *de novo* purine and pyrimidine synthesis and, while the myeloma cells are able to convert thymidine to pyrimidines using the salvage pathway, they have been modified to lack the enzyme, hypoxanthine phophoribosyl transferase (HPRT), required to convert hpoxanthine to purines. This enzyme is present in the lymphocytes, however, these cells have a limited life-span and thus, only hybridoma cells will grow over several days in HAT medium (Figure 8.1).

In total, 6x96 well plates were set up from each mouse spleen. Wells were previously coated with mouse macrophage feeder cells (Section 2.12.2.2) which act to ingest debris and dead cells. After 10 days most plates showed hybridoma colonies that occupied 50-75% of the well and the antibody containing supernatant was removed for screening (Section 8.2.3). The colonies obtained from each mouse spleen are recorded in Table 8.2.

Two mouse spleens produced the expected number of colonies. The reduced number of colonies produced from mouse 3 were due to bacterial contamination. The fusion of mouse 4 spleen cells was inefficient but the exact cause was unknown. Unfortunately, one mouse died prior to removal of the spleen.

Table 8.2 Number of hybridoma colonies produced from mice immunised with human metaphase chromosomes
Details of monoclonal antibody production outlined in Sections 2.12 and 8.2.

Mouse	Primary booster immunisation	Total number of colonies screened	Number of stable positive antibody producing colonies
1	Human chromosome 18	370	5
2	Human chromosome 19	20	0
3	Human X chromosome	35	0
4	Total human metaphase chromosomes	350	3
5	Human nuclei	Mouse died prior to spleen removal	0

8.2.3 Antibody screening by immunocytochemistry

Screening was carried by immunocytochemistry, selecting for antibody epitopes with nuclear localisation. The JU77 human mesothelioma cell line was used to seed the chambers of an appropriate number of 8-chamber slides (Section 2.11) since REN2 cells from which the antigens were prepared grow in suspension and not as an attached monolayer. Slides were incubated at 37°C until the surface of each chamber was approximately 50% covered with cells. Slides were then fixed with 1:1 methanol:acetone at -20°C for 10 minutes. This fixation was sufficiently stringent to adhere the cells firmly and allow storage of the slides for up to a week without deterioration, but did allow the binding of several test antibodies (Figure 8.3). Slides were pre-incubated with blocking buffer (2% BSA) before addition of the primary antibody for 1 hour at room temperature. After washing, slides were incubated with secondary antibody for a further 30 minutes at room temperature.

Along side each batch of hybridoma supernatants being tested, a number of controls were used. The appropriate control and secondary antibody dilutions were assessed using serial dilutions and are listed in Table 2.5. The controls were as follows:

1. Secondary antibody (anti-mouse $F(ab')_2$ fragments conjugated to FITC) alone. This resulted consistently in a general but low level background of signal and no specific pattern. $F(ab')_2$ fragments were used for specificity of binding. These fragments consist of the two antigen binding sites of an antibody without the tail region. The tail is responsible for the different functional activities of an antibody, for example, an ability to bind phagocytic cells and may instigate non-specific binding.
2. Anti-histone, pan antibody (Boehringer) detected with anti-mouse-FITC, colocalised with the DAPI fluorescence specifically within the cell nuclei (Figure 8.3a). Fluorescence was concentrated around but reduced in the nucleoli. The region surrounding the nucleoli often appears to be associated with heterochromatin (Personal communication: Dr. J.M. Bridger).
3. Anti-α-tubulin antibody (Sigma) detected with anti-mouse-FITC revealed a striking fibrous cytoplasmic pattern that was completely absent from the nucleus (Figure 8.3b). This distribution is typical of a cytoskeleton component (Blose *et al.*, 1984).

Each hybridoma supernatant was tested by immunofluorescence undiluted, in the first instance. For those supernatants showing nuclear localisation, hybridoma colonies were subbed into flasks and ampoules stored at -70°C. A series of hybridoma cell dilutions were set up to subclone until colonies were isolated that were stable in antibody production (Section 2.12.4). From all four mice from which hybridomas were obtained, 16 positive antibody producing colonies were identified during the initial screen. During hybridoma passage and subcloning several of these antibody patterns were lost until eventually 8 stable colonies were established. Ampoules of the stable colonies were stored at -70°C and collected supernatants were stored in aliquots at 4°C and -20°C. Antibodies were labelled with a number relating to the mouse from which they were obtained and the order in which the colonies were screened. The immunocytochemical patterns observed for the hybridoma supernatants were divided into three categories:

1. Nuclear speckles (Figure 8.4) - Any pattern with >200 local concentrations of fluorescence was termed nuclear speckles. Speckles were generally <0.5μm in diameter. Three of the supernatants: 1103, 1113 and 4225, revealed nuclear speckles that were evenly distributed throughout the nuclei but absent from nucleoli. The speckled pattern of 1103 showed varying degrees of intensity between nuclei, possibly due to cell cycle variation.
2. Nuclear spots (Figure 8.5) - Any pattern with <200 local concentrations of fluorescence was termed nuclear spots. Spots differed in size but were all <1μm in diameter.

Supernatant 1180 showed <50 punctuate spots, while 1320 and 4210 revealed 200>50 spots, in all instances evenly distributed throughout the nuclei.

3. Nucleolar staining (Figure 8.6) - A strong signal in the nucleolus was accompanied by <50 spots in the remainder of the nucleus for supernatants from 1213 and 4247.

In addition to the 8 antibodies produced here, two additional antibodies were donated by Dr. B. Lane, University of Dundee. These antibodies were obtained during a screen of hybridomas produced following immunisation with a keratin antigen. Both show a relatively uniform distribution in the nucleus with absence from the nucleolus (Figure 8.7), reminiscent of the anti-histone pan antibody (Figure 8.3).

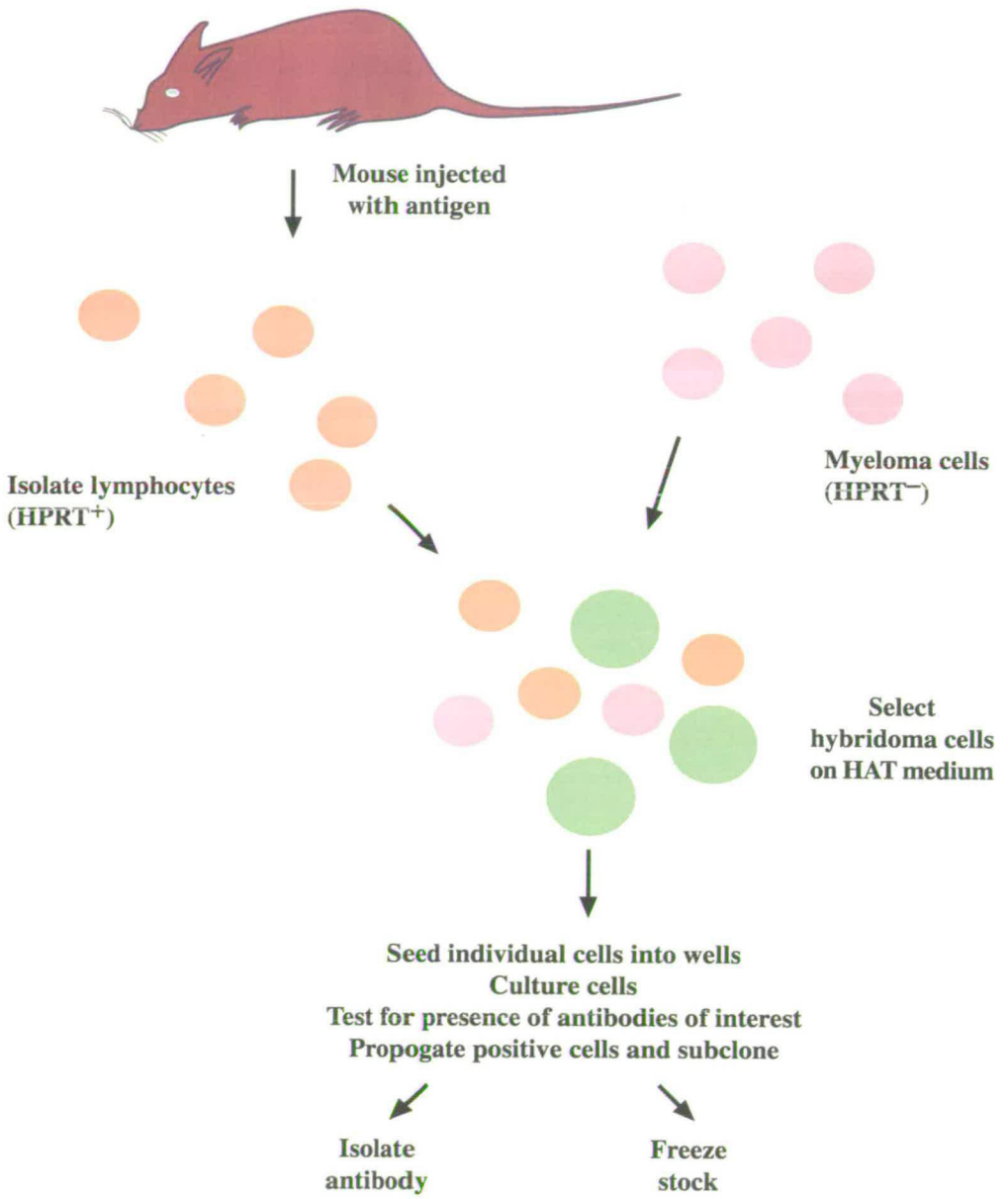

Figure 8.1 A scheme for the production of mouse monoclonal antibodies to human metaphase chromosomes

Details of monoclonal antibody production outlined in Sections 2.12 and 8.2. The spleen of mice immunised with human metaphase chromosomes were removed and punctured. Displaced lymphocytes were fused with Sp2/0 mouse myeloma cells to produce hybridomas using PEG. In HAT medium the myeloma cells used will not grow. Aminopterin blocks *de novo* purine and pyrimidine synthesis and, while the myeloma cells are able to convert thymidine to pyrimidines using the salvage pathway, they have been modified to lack the enzyme, HPRT, required to convert hpoxanthine to purines. This enzyme is present in the lymphocytes, however, these cells have a limited life-span and thus, only hybridoma cells, which are actively secreting antibodies into the supernatant, will grow over a reasonable period of time in HAT medium.

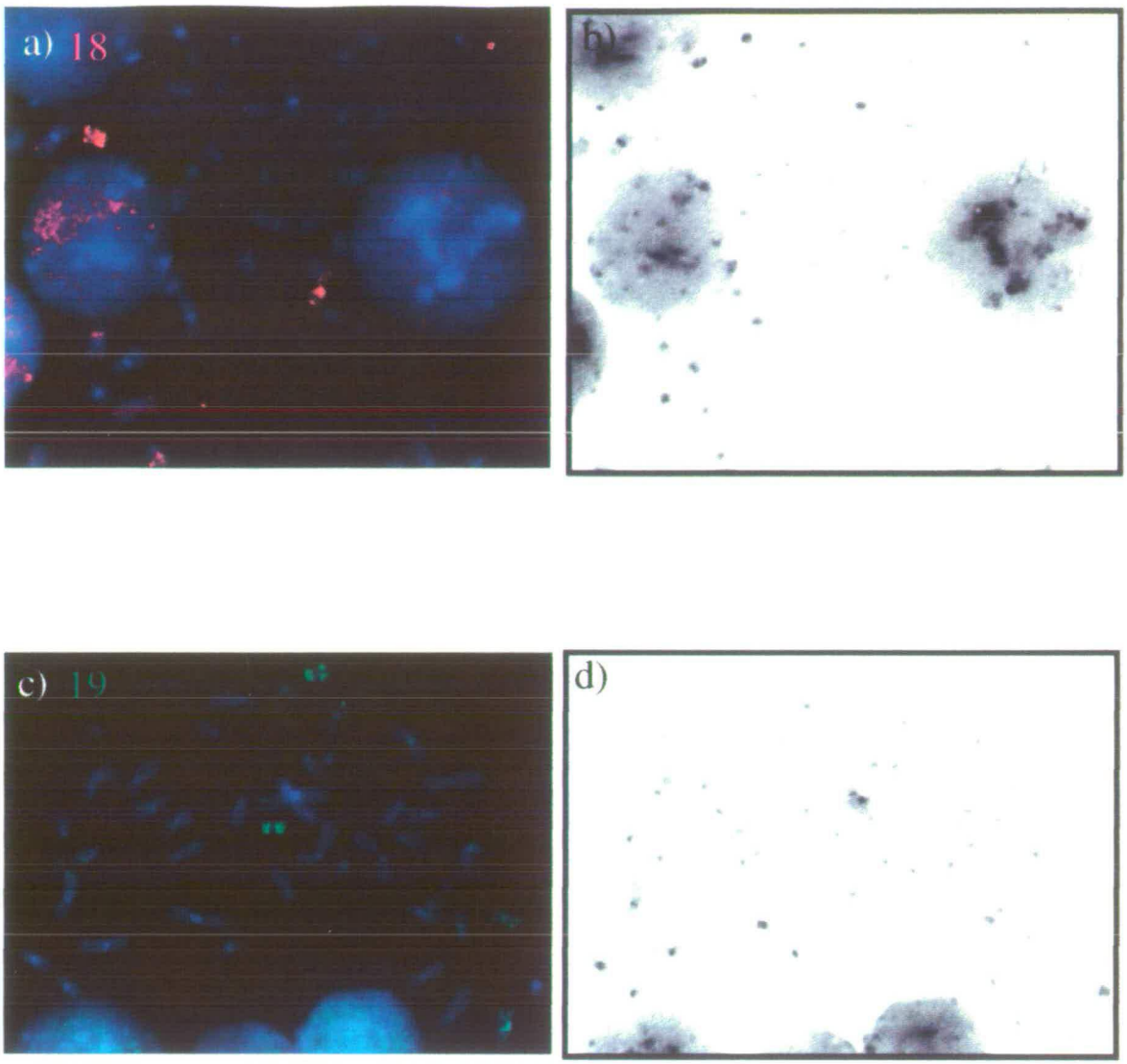

Figure 8.2 Testing for purity of FACS sorted chromosomes
Chromosomes 18 and 19 were FACS sorted by Dr. D. Green, MRC Human Genetics Unit, Edinburgh. To assess the purity of the sort, a sample of suspension was used for *Alu*-PCR, products biotin labelled by nick translation and hybidised by FISH to REN2 human metaphase spreads. Probes were detected with (**a**) avidin-TR (red), or (**c**) avidin-FITC (green), and chromosomes counterstained with DAPI (blue). FACS sorts: (**a**) chromosome 18, and (**c**) chromosome 19. (**b**) (**d**) Grey scale representations of DAPI images.

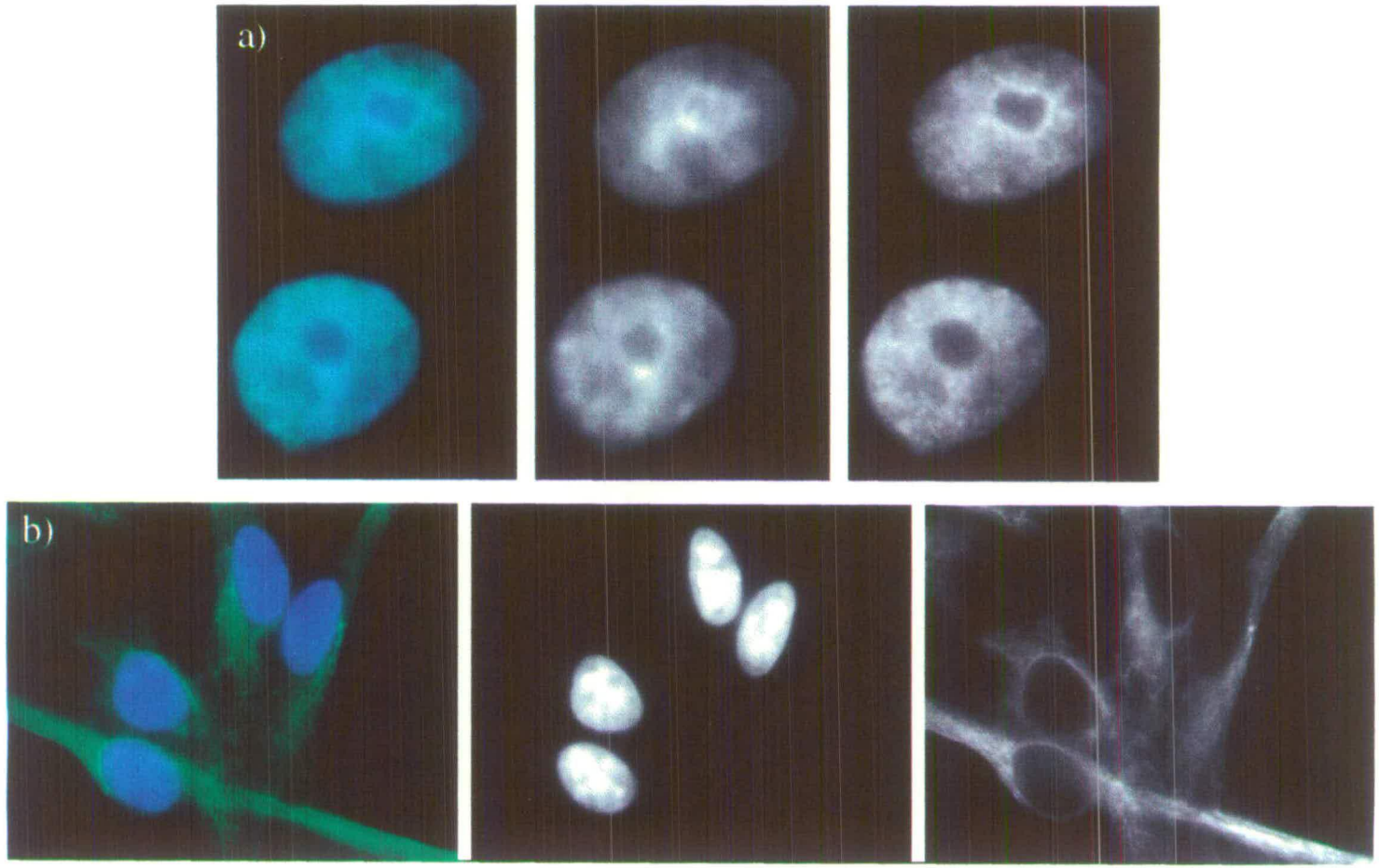

Figure 8.3 Immunocytochemistry with known antibodies
(**Left**) JU77 human mesothelioma cells bound with: (**a**) anti-histone pan, and (**b**) anti-α-tubulin. Both antibodies were detected with anti-mouse-FITC (green). Cells were counterstained with DAPI (blue). (**Middle**) Grey scale representation of the DAPI image. (**Right**) Grey scale representation of the antibody binding signal.

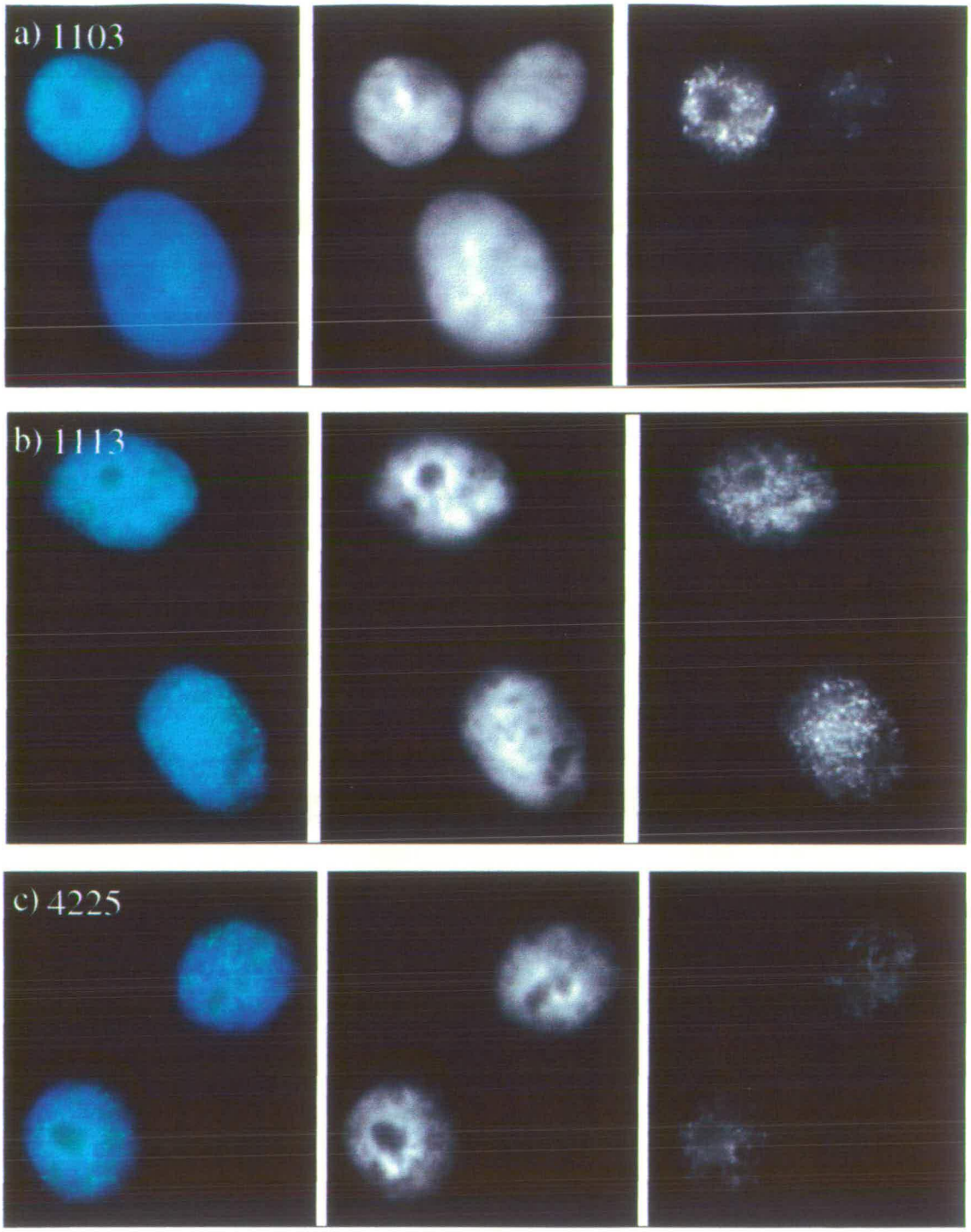

Figure 8.4 Hybridoma supernatants with speckled nuclear localisation
(**Left**) JU77 human mesothelioma cells bound with the following hybridoma supernatants established following immunisation with human metaphase chromosomes: (**a**) 1103; (**b**) 1113; and (**c**) 4225. All antibodies were detected with anti-mouse-FITC (green). Cells were counterstained with DAPI (blue). (**Middle**) Grey scale representation of the DAPI image. (**Right**) Grey scale representation of the antibody binding signal.

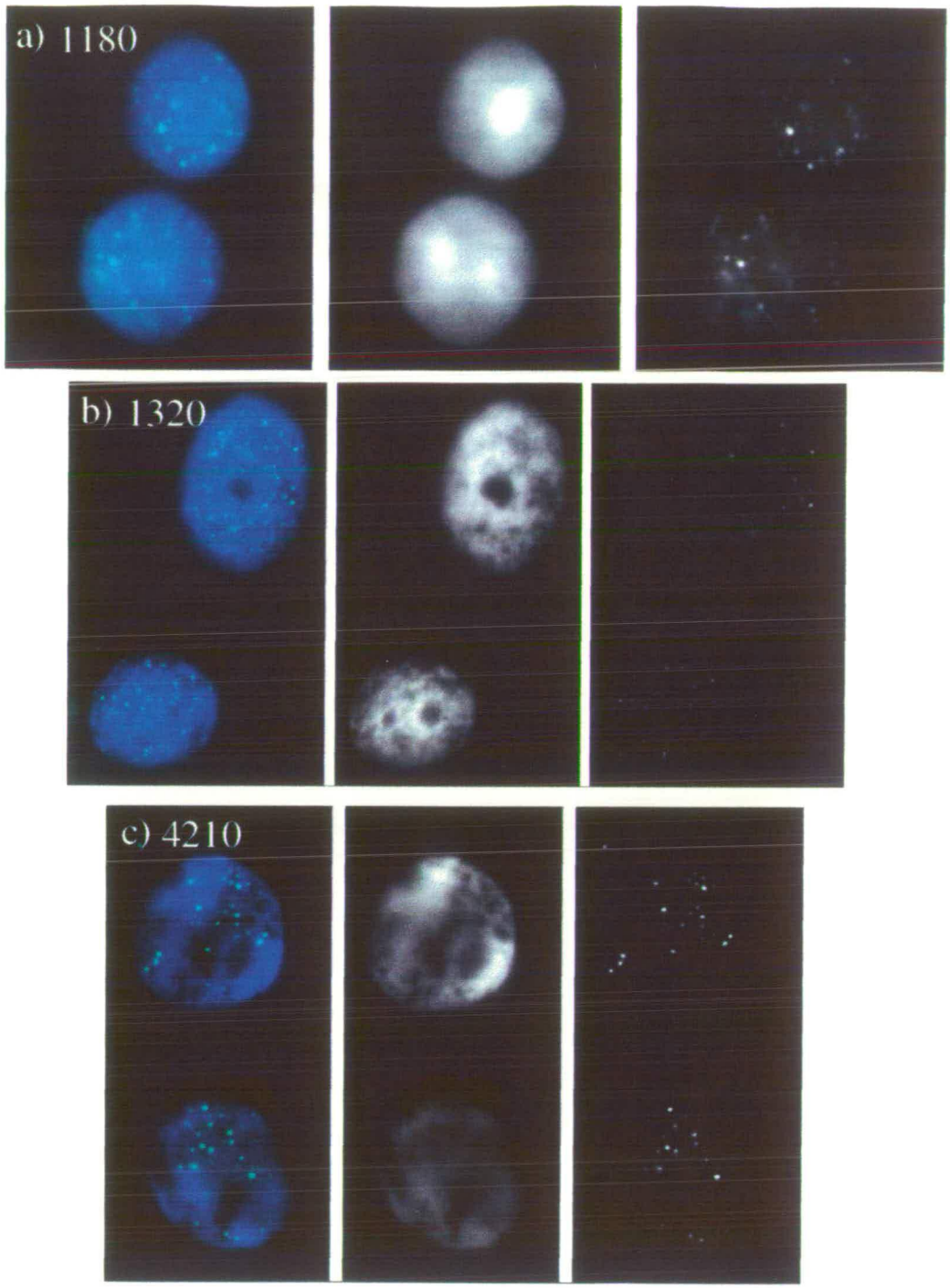

Figure 8.5 Hybridoma supernatants with spotted nuclear localisation
(**Left**) Ju77 human mesothelioma cells bound with the following hybridoma supernatants established following immunisation with human metaphase chromosomes: (**a**) 1180; (**b**) 1320; and (**c**) 4210. All antibodies were detected with anti-mouse-FITC (green). Cells were counterstained with DAPI (blue). (**Middle**) Grey scale representation of the DAPI image. (**Right**) Grey scale representation of the antibody binding signal.

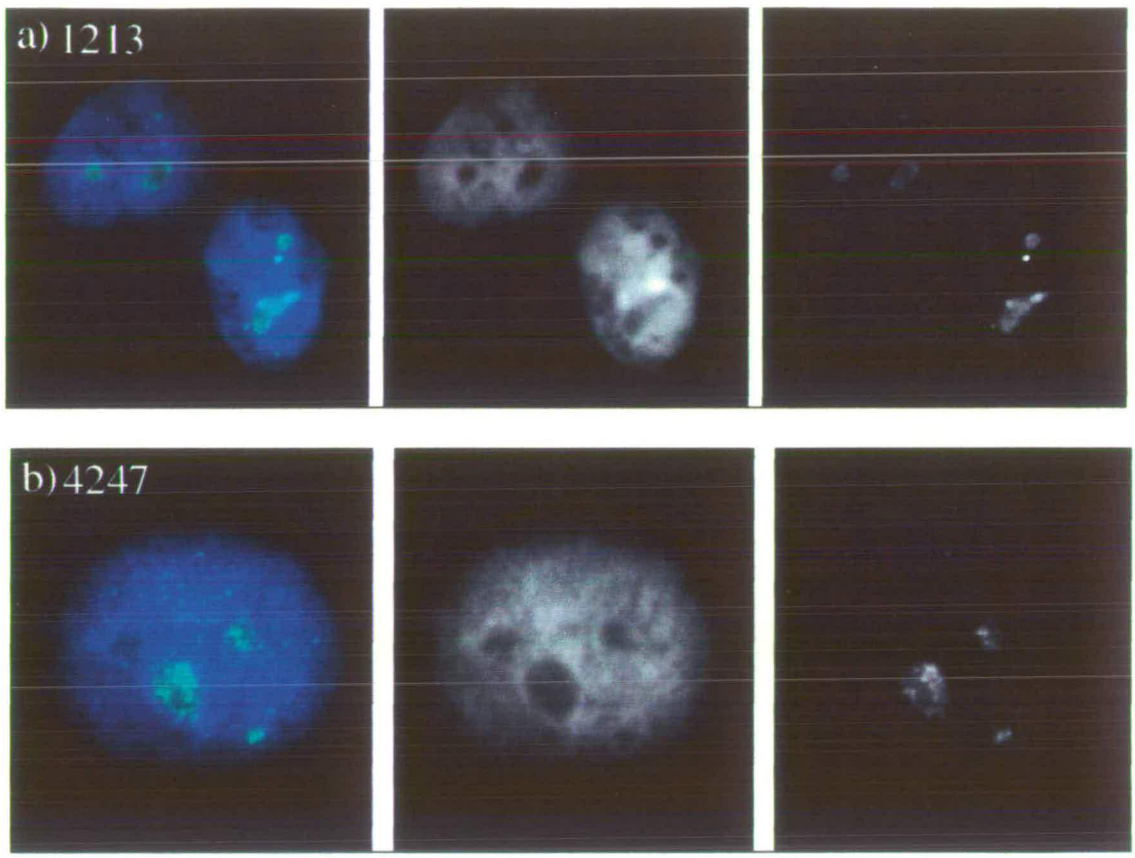

Figure 8.6 Hybridoma supernatants with nucleolar localisation
(**Left**) Ju77 human mesothelioma cells bound with the following hybridoma supernatants established following immunisation with human metaphase chromosomes: (**a**) 1213; and (**b**) 4247. All antibodies were detected with anti-mouse-FITC (green). Cells were counterstained with DAPI (blue). (**Middle**) Grey scale representation of the DAPI image. (**Right**) Grey scale representation of the antibody binding signal.

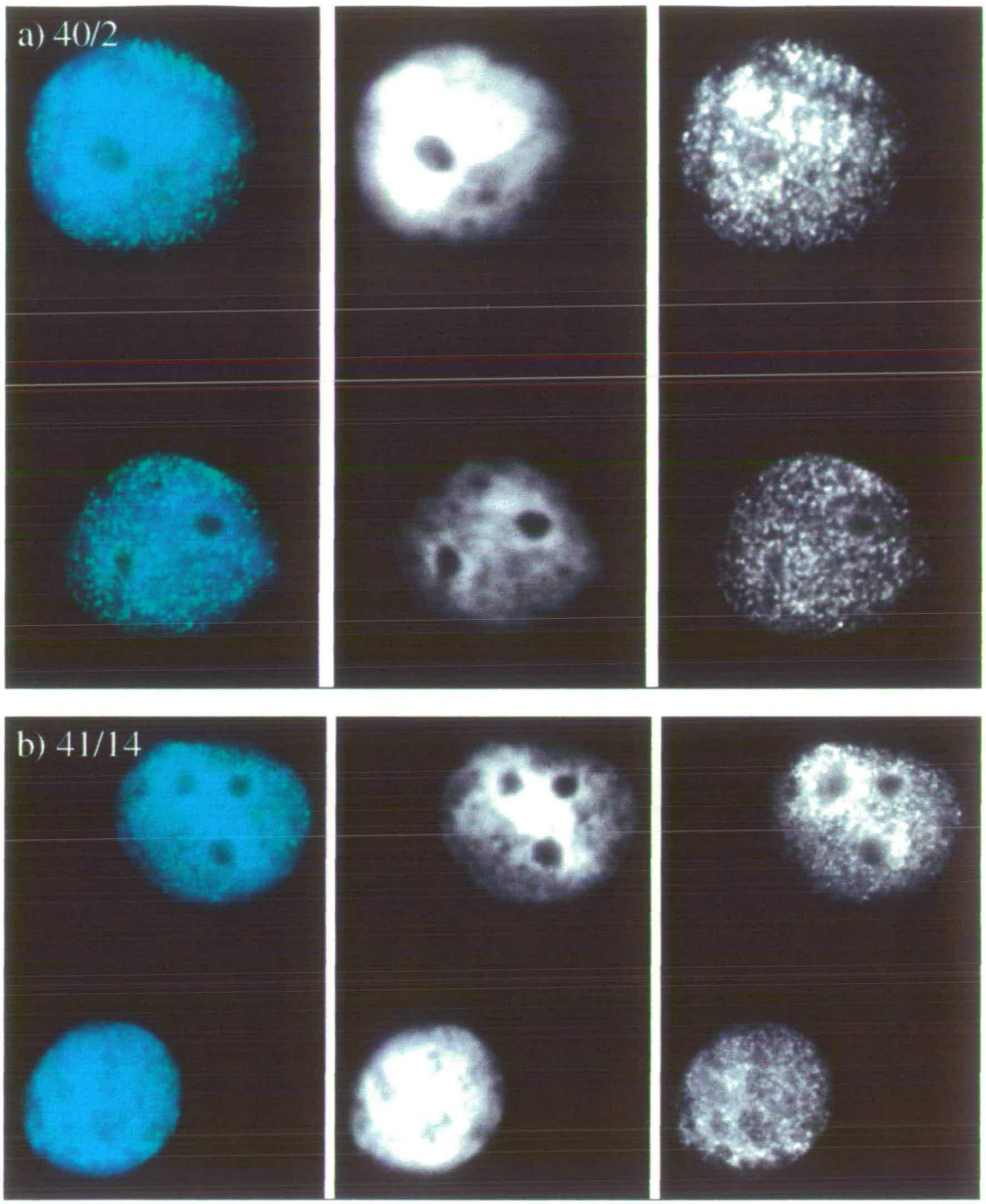

Figure 8.7 Hybridoma supernatants with general nuclear localisation
(**Left**) JU77 human mesothelioma cells bound with the following hybridoma supernatants donated by Dr. B. Lane, University of Dundee and established following immunisation with keratin: (**a**) 40/2; and (**b**) 41/14. All antibodies were detected with anti-mouse-FITC (green). Cells were counterstained with DAPI (blue). (**Middle**) Grey scale representation of the DAPI image. (**Right**) Grey scale representation of the antibody binding signal.

8.3 The distribution of antibody epitopes along human metaphase chromosomes

Cells in mitosis were not detectable with the chamber slides used for screening the hybridoma supernatants, since when cells begin to divide they generally round up and become detached from the slide surface. In order to detect any antibody binding to mitotic chromosomes, colcemid was added to REN2 human cells one hour prior to harvesting. Cells were cytocentrifuged unfixed onto slides (Section 2.10). Slides were incubated with primary antibody for 2 hours at room temperature, followed by incubation with anti-mouse-FITC. To try and maintain the antibody epitopes, slides were fixed, following antibody incubation, in 0.5-4% paraformaldehyde for 15 minutes at room temperature. This is one of the less stringent methods of fixation which acts by chemically cross-linking proteins (Pearse, 1968) (Section 6.3). A variety of alternative fixation methods were assessed, including 3:1 methanol:acetone, methanol alone and <4% formaldehyde.

Figure 8.8 shows the signal obtained with three of the hybridoma supernatants: 1103, 1113 and 4225. All three revealed a speckled pattern in interphase nuclei, as seen in JU77 mesothelioma cells (Figure 8.4), but no binding to metaphase chromosomes could be detected.

The two monoclonal antibodies, 40/2 and 41/14 gave speckled binding within interphase nuclei and, in addition, there was uniform staining along the length of metaphase chromosomes (Figure 8.9). Analysis of a number of spreads could not define any pattern of staining along the chromosome arms with respect to band types or regions of heterochromatin.

None of the remaining antibodies were found to bind to either nuclei or chromosomes prepared by cytocentrifugation. This may be due to an alteration in epitope shape or complete loss of epitope, caused by the treatment of the slides, both mechanical and chemical. Alternatively, there may be cell cycle changes to epitopes.

To what nuclear proteins do the epitopes recognised by each of the hybridoma supernatants belong? An indication may be determined by comparison with the patterns created by antibodies to known nuclear proteins.

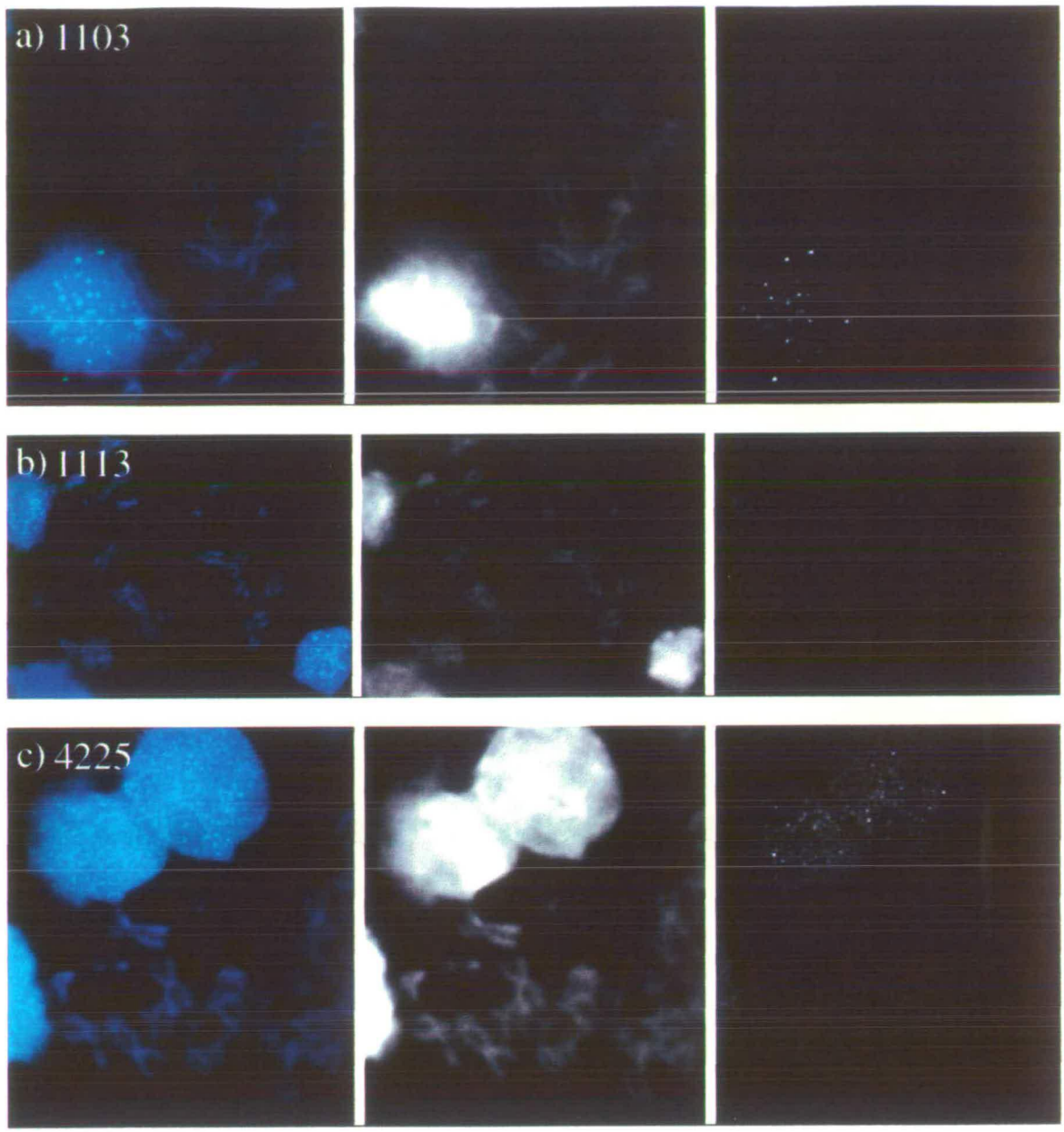

Figure 8.8 Immunocytochemistry with three hybridoma supernatants to metaphase spreads

Metaphase spreads of REN2 human lymphoblastoid (49, XXXXY) cells bound with 3 of the hybridoma supernatants established following immunisation with human metaphase chromosomes: (**a**) 1103; (**b**) 1113; and (**c**) 4225. (**Left**) Antibodies were detected with anti-mouse-FITC (green). Spreads were fixed with 4% paraformaldehyde following antibody incubation and counterstained with DAPI (blue). (**Middle**) Grey scale representation of DAPI image. (**Right**) Grey scale representation of the antibody signal.

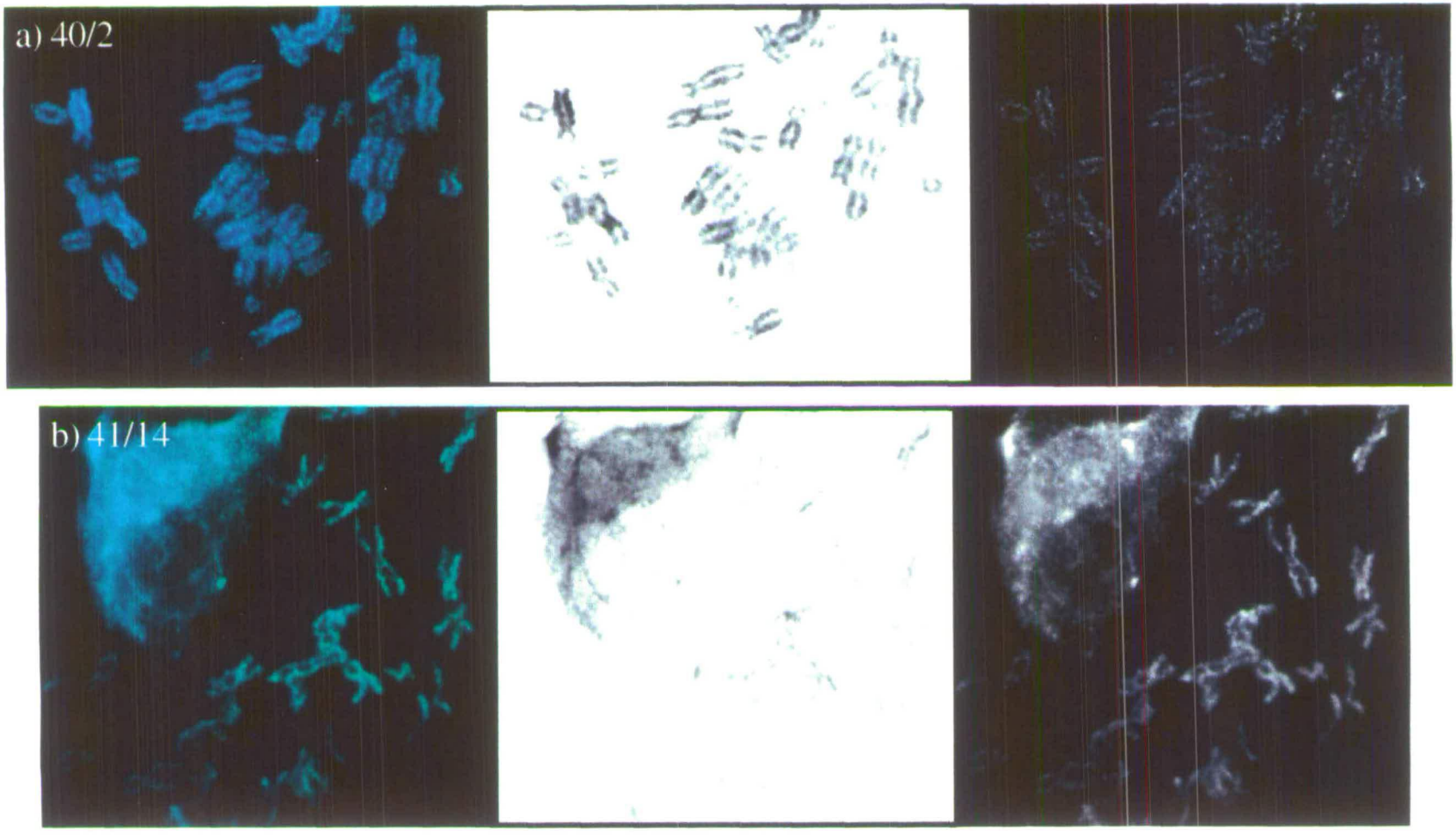

Figure 8.9 Immunocytochemistry with 40/2 and 41/14 hybridoma supernatants to metaphase spreads
Metaphase spreads of REN2 human lymphoblastoid (49, XXXXY) cells bound with (**a**) 40/2 and (**b**) 41/14, hybridoma supernatants donated by Dr. B. Lane, University of Dundee. (**Left**) Antibodies were detected with anti-mouse-FITC (green). Spreads were fixed with 4% paraformaldehyde following antibody incubation and counterstained with DAPI (blue). (**Middle**) Grey scale representation of DAPI image. (**Right**) Grey scale representation of the antibody signal .

8.4 The binding patterns of antibodies to known nuclear components

In order to gain an idea of the type of protein being recognised by each of the hybridoma supernatants, immunocytochemistry with antibodies to known nuclear proteins was carried out. Antibodies were selected to represent each of the major functions that occur in the nucleus:

- Transcription - The abundant transcription factor, Sp1 binds to the GC-box consensus sequence (GGGGCGGGG) (Letovsky & Dynan, 1989) which is present at numerous promoters and regulatory sequences. Figure 8.10a shows immunolocalisation of a mouse monoclonal antibody to Sp1 (Santa Cruz) detected with anti-mouse-FITC ($F(ab')_2$). This speckled pattern, which is dispersed throughout the nucleus, but absent from nucleoli, has also been seen with other transcription factors (Grande *et al.*, 1997) and RNA polymerase II (Zeng *et al.*, 1997).
- Replication - The proliferating cell nuclear antigen (PCNA) is an essential component of the DNA replication machinery. The PCNA antibody used here has been previously shown to coincide exactly with regions of biotin-dUTP incorporation, that is, sites of active replication (Hutchison, 1995). This is a human auto-immune antibody (Dr. C.J. Hutchison, University of Dundee) and was detected with anti-human-TR ($F(ab')_2$). A variety of immunolocalisation patterns were observed in different nuclei (Figure 8.10b) which correspond to the stages of the cell cycle (Kill *et al.*, 1991).
- RNA splicing - Two antibodies were obtained to components of the mRNA splicing complex (Dr. I. Mattaj, EMBL, Heidelberg) (Lerner *et al.*, 1981). Figure 3.11a shows human cells labelled with a monoclonal antibody directed against Sm proteins detected with anti-mouse-FITC $F(ab')_2$. These proteins are common to all snRNPs (Pettersson *et al.*, 1984) and show a speckled pattern of nuclear distribution in addition to a few bright, discrete foci termed coiled bodies (Fakan *et al.*, 1984; Carmo-Fonseca *et al.*, 1991a & b; Review: Spector, 1993) (Section 1.6.2). A more diffuse staining pattern was observed with a polyclonal antibody to the U1 snRNP specific protein, U1A (Scherly *et al.*, 1989), detected with anti-rabbit-TR $F(ab')_2$ (Figure 8.11b). This antibody is also known to highlight coiled bodies. Both antibodies were absent from the nucleoli. A rather more spotted pattern was shown to label with an antibody to the non-snRNP splicing component, SC-35 (Fu & Maniatis, 1990) and there was no accumulation of this protein within coiled bodies (Carmo-Fonesca *et al.*, 1991a). Speckled distribution and coiled body accumulation cannot be taken as the only indications of a component involved in mRNA splicing.

Attempts to perform colocalisation experiments with the hybridoma supernatants and these antibodies to known nuclear compartments were unsuccessful. Since the hybridoma supernatants originated from mouse, it was necessary to use antibodies produced in a different organism for colocalisation experiments. For colocalisation, slides were prepared as before (Section 8.2) and the known antibody, followed by the appropriate secondary antibody, were added as extra layers either before or after hybridisation with the hybridoma supernatant and its appropriate secondary antibody. Finally, slides were fixed with 4% paraformaldehyde. Unfortunately, patterns produced with an anti-Sp1 monoclonal antibody (Figure 8.10a) could not be reproduced with a rabbit polyclonal antibody (Santa Cruz). In addition, using the human anti-PCNA autoantibody (Figure 8.10b) and rabbit polyclonal anti-U1A antibody (Figure 8.11b), which alone produced defined patterns of distribution, in combination with the hybridoma supernatants, patterns were impossible to distinguish. The reasons for this were not clear and it would have been necessary to try a number of different known antibodies and colocalisation protocols. Each of the categories of nuclear patterns defined by the hybridoma supernatants described in Section 8.2 were, thus, superficially compared to the patterns of antibodies to known nuclear compartments defined above:

1. Nuclear speckles - The speckled patterns of 1103, 1113 and 4225 were all reminiscent of the transcription factor pattern as exemplified by Sp1 in Figure 8.10a.
2. Nuclear spots - This pattern may be observed because the antibody concentration in the tested supernatant was low. Similar patterns were revealed in titration experiments of the known antibodies at the lowest concentrations. Without co-localisation experiments it is impossible to tell whether the spots could be localised to coiled bodies (Figure 8.11) or other nuclear bodies (Review: Spector, 1993) but the number of spots in each nucleus suggest that this may be the case.
3. Nucleolar - The number of proteins located in the nucleoli is very large (Review: Hernandez-Verdun, 1991). Nucleolar accumulation of some proteins, such as RNA polymerase I, are a result of the high transcriptional activity in this region. Many, however, are directed to the nucleolus and are not present in other nuclear regions, for example, nucleolin (Lapeyre *et al.*, 1987) (Section 1.6.2). The nuclear speckles present along with the strong nucleolar staining of antibodies 1213 and 4225 suggests that these proteins are not solely nucleolar but are highly concentrated in the nucleolus.
4. General nuclear - The immunofluorescence patterns observed for 40/2 and 41/14 suggested that their corresponding proteins may be chromosomal since their distribution was similar to the anti-histone pan antibody (Figure 8.3a). This was confirmed by the observation of staining along the length of metaphase chromosomes (Section 8.3).

Clearly, these are merely conjectures and colocalisation experiments are essential. However, lack of time and priority for other experiments resulted in this approach being abandoned. To identify the antigens being recognised by the hybridoma supernatants, I performed Western blots with cytoplasmic and nuclear protein fractions.

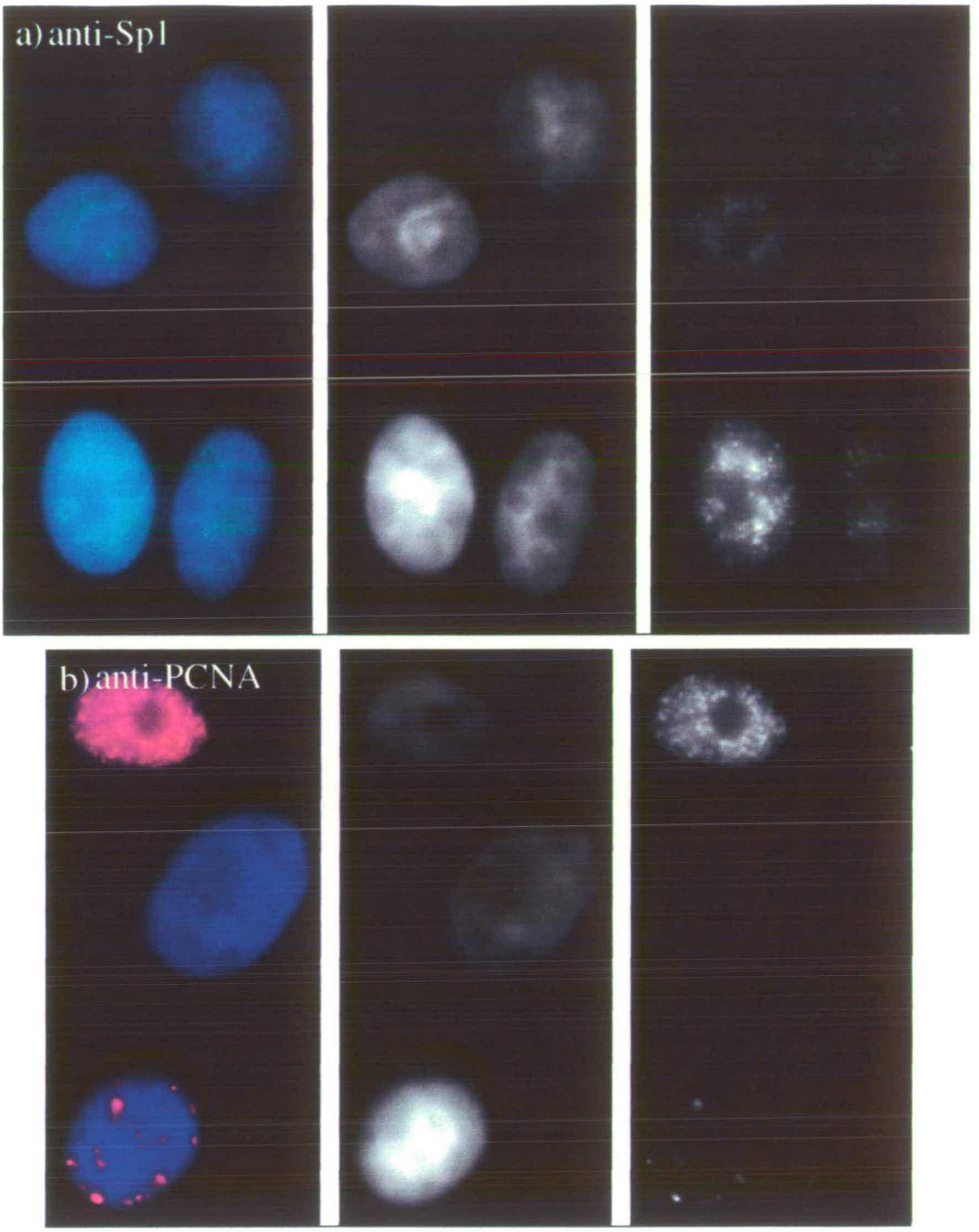

Figure 8.10 Immunocytochemistry with antibodies to components of transcription and replication complexes
Human mesothelioma cells, JU77 bound with: (**a**) anti-Sp1 (transcription factor); (**b**) anti-PCNA (member of the replication complex). (**Left**) Antibodies were detected with: (**a**) anti-mouse-FITC (green); (**b**) anti-human-TR (red). Cells were counterstained with DAPI (blue). (**Middle**) Grey scale representation of the DAPI image. (**Right**) Grey scale representation of the antibody binding signal. In (b) note the variable pattern that probably reflects different stages of the cell cycle: top nucleus in early S-phase, middle nucleus in gap phase and bottom nucleus in late S-phase.

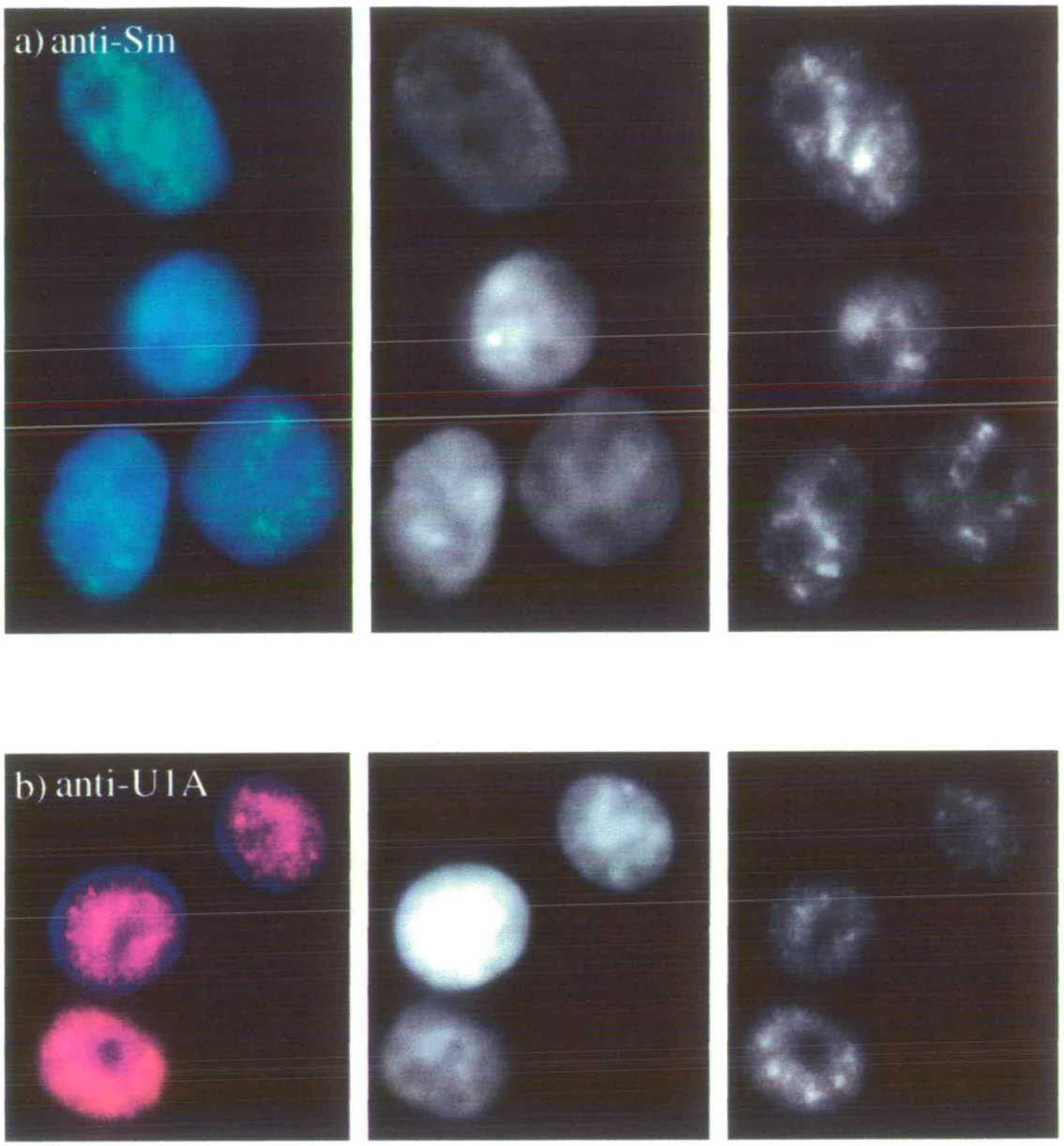

Figure 8.11 Immunocytochemistry with antibodies to mRNA splicing complex components
Human mesothelioma cells, JU77 bound with: (**a**) anti-Sm; (**b**) anti-U1A. (**Left**) Antibodies were detected with: (**a**) anti-mouse-FITC (green); (**b**) anti-rabbit-TR (red). Cells were counterstained with DAPI (blue). (**Middle**) Grey scale representation of the DAPI image. (**Right**) Grey scale representation of the antibody binding signal.

8.5 Analysis of the antigens recognised by the novel hybridoma supernatants by Western blotting

Denaturing polyacrylamide gels were run of nuclear and cytoplasmic fractions from human cells, transferred to membranes and incubated with each of the hybridoma supernatants to confirm their nuclear specificity and to determine the size and complexity of the antigens being recognised.

REN2 human cells were swollen in hypotonic solution and disrupted by homogenising (Section 2.13.1). The homogenate was centrifuged to separate the nuclear pellet from the supernatant, the cytoplasmic fraction. The nuclei were lysed using Triton X-100 detergent to produce the nuclear fraction. Each fraction was separated by denaturing polyacrylamide gel electrophoresis (PAGE) containing sodium dodecyl sulphate (SDS) (Section 2.1.2). Gels were stained with Coomassie blue to determine the protein concentration and complexity in each fraction (Figure 8.12a) (Section 2.13.3). Gels were next blotted by semi-dry transfer onto a PVDF transfer membrane using a graphite electrode system (Western blotting) (Section 2.13.4). Efficient transfer was assessed following reversible staining of the membrane with Ponceau S solution. Figure 8.12b shows a membrane permanently stained with amido black stain. Note that there were gaps in the nuclear fraction where proteins had clearly not transferred and that these appeared to correspond with abundant nuclear proteins (compare with Figure 8.12a).

Membranes were incubated with a number of control antibodies to test for fractionation and efficiency of transfer. Antibody binding was detected by chemiluminescence (Section 2.13.7). Figure 8.12c shows the result obtained for anti-Sp1 polyclonal antibody (Santa Cruz). This antibody should detect peptides of 106 and 95KDa in the nuclear fraction. Three bands of approximately 100, 75 and 40KDa were consistently detected in this fraction, suggesting that there was specific break down of one of the peptides. There was no Sp1 present in the cytoplasmic fraction. A polyclonal anti-α-tubulin antibody revealed a band of the appropriate size (55KDa) in the cytoplasmic fraction and, to a lesser extent, in the nuclear fraction (Figure 8.12d). The presence of tubulin in the nuclear fraction may represent cells accumulating mitotic spindle prior to nuclear membrane breakdown. Alternatively, there may be some contamination between the nuclear and cytoplasmic fractions.

One problem was the inability to detect histones with either a polyclonal anti-histone pan antibody or a polyclonal anti-acetylated H4 antibody (R41) (Prof. B. Turner, University of

Birmingham). Interestingly, the regions at which these antibodies would be located corresponded to the blank regions of amido black stained membranes (Figure 8.12b), suggesting that it was the transfer of these proteins that was failing. It was found that for highly negatively charged proteins, such as histones, it was necessary to use an alternative blotting buffer (Personal communication: Dr. K. Ekwall, MRC Human Genetics Unit, Edinburgh). CAPS was included in the transfer buffer (Section 2.13.5) which had an affect on the charge of these proteins causing them to move towards the cathode, in contrast to the majority of proteins. Figure 8.12e shows an amido black stained membrane following this type of transfer. The R41 antibody showed an extra band, when compared to the membrane following incubation with the corresponding rabbit pre-immune serum (Figure 8.12f), of the expected size for H4 (14KDa) (Figure 8.12g). No bands, however, were detected still with the anti-histone pan antibody. The reasons for this are unclear and this antibody is poorly characterised.

Despite numerous attempts with membranes blotted in both the standard manner and adapted for highly negatively charged proteins, and using less stringent washing and longer incubations, no bands for any of the hybridoma supernatants were detected by Western analysis. There are a number of reasons as to why this may have occurred:

- Poor protein transfer system.
- Degradation of the antibody binding epitope due to denaturation of the proteins by SDS treatment.
- Loss of specific protein modifications, for example, methylation, required for binding of the antibody to its epitope during processing.
- Instability of the protein or antibody.

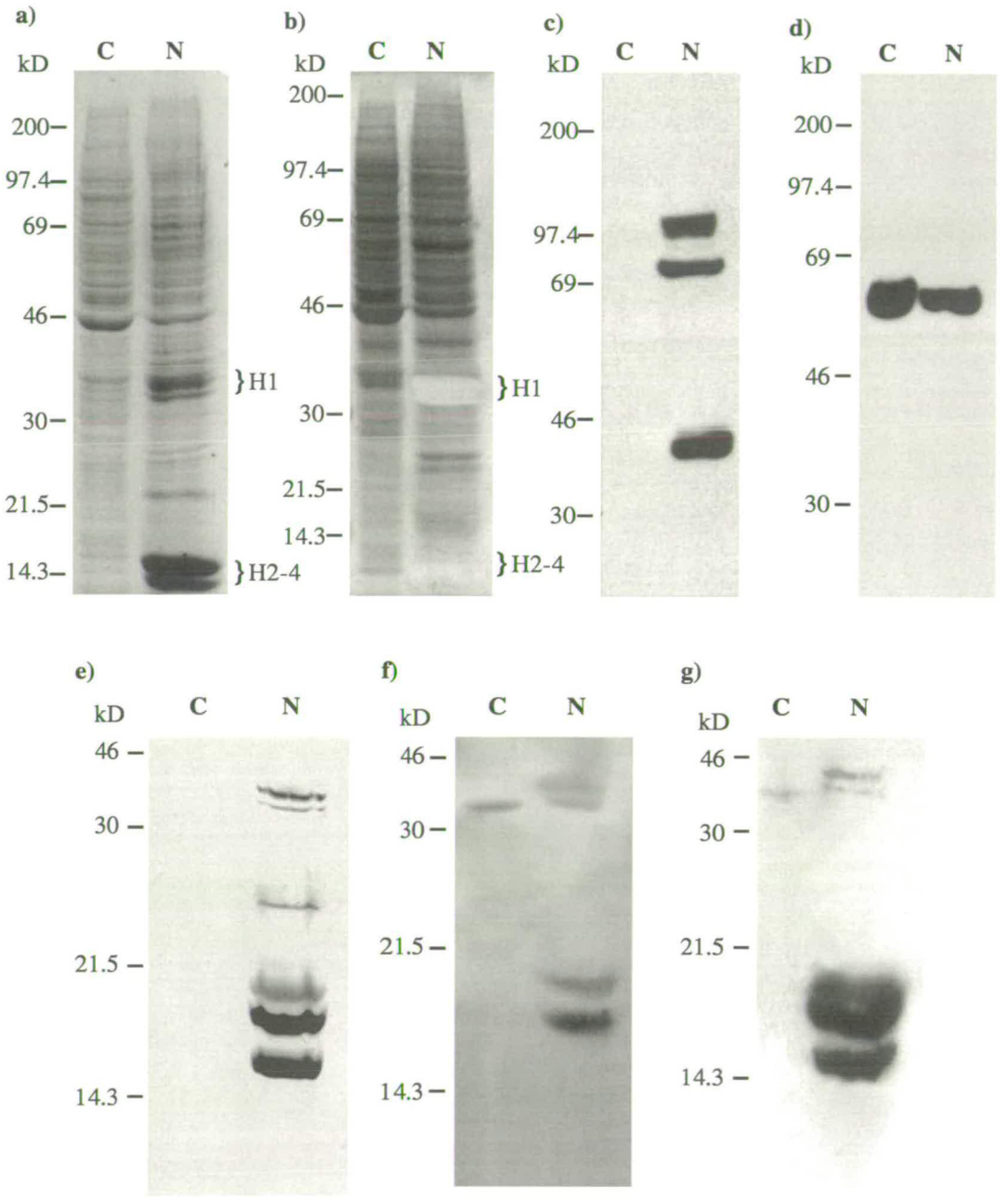

Figure 8.12 Incubation of control antibodies with Western blots of cytoplasmic and nuclear fractions

10% SDS-PAGE gels of nuclear (**N**) and cytoplasmic (**C**) protein fractions. Antibody binding was detected by chemiluminescence. (**a**) Example of a Coomassie stained gel. (**b**) Amido black stained membrane following semi-dry transfer of proteins from a gel, similar to that in (a), using standard methanol transfer buffers. (**c**) Incubation with anti-Sp1 rabbit polyclonal antibody. (**d**) Incubation with anti-α-tubulin rabbit polyclonal antibody. (**e**) Amido black stained membrane following semi-dry transfer of proteins from a gel, similar to that in (a), using CAPS transfer buffer for transfer of highly negatively charged proteins. (**f**) Incubation with R41 pre-immune serum. (**g**) Incubation with R41 anti-acteylated H4 antibody (Prof. B. Turner, University of Birmingham).

8.6 Discussion: The difficulties in producing hybridoma supernatants

In this chapter I have described a strategy for the production of new mouse monoclonal antibodies to human metaphase chromosomes. Following immunocytochemistry to both interphase nuclei and metaphase chromosome spreads it seemed likely that none of the new antibodies were directed to chromosomal proteins. A number of improvements in this strategy may have produced a greater selection of nuclear and, thus potentially chromosomal antibodies:

- Injection of mammalian chromosomes into a mammal is not likely to produce a large immune response. The New Zealand Black strain of mice is prone to spontaneous autoimmune disorders (Review: Howie & Heyler, 1968) and may have proved more useful (Personal communication: Prof. V. Van Heyningen).
- The total amount of protein injected into each mouse was extremely variable (0.005-2500μg) and, in most cases, small. From other such experiments in the literature, immunisation of a protein content of >500μg would have produced the required immune response.
- The screening procedure used may have resulted in discrimination of potentially useful antibodies. To sort through several hundred colonies it was necessary to select a screen that was rapid and easy to reproduce. It may be an advantage to screen using several methods simultaneously, for example, immunocytochemistry with alternative fixation of test cells, ELISA (enzyme-labelled immunosorbent assay) and Western blot incubation.

Hybridoma colonies are unstable and even after repeated subcloning it was difficult to maintain stable antibody producing colonies. The antibodies in storage were also unstable and often produced no or alternative staining patterns with immunocytochemistry a few days after being collected. This resulted in the loss of several antibodies producing interesting nuclear patterns. Eventually 8 reasonably stable antibodies were established. Added to these were two donated new mouse monoclonal antibodies (Dr. B. Lane, University of Dundee), which were shown by immunocytochemistry to localise to metaphase chromosomes.

The inability of all of these antibodies to detect bands on Western blots were likely to be due to loss of the antibody epitopes since the procedure involves the denaturing of native proteins. These antibodies were to be used to screen a human cDNA expression library to clone the gene(s) encoding the protein target of any of the antibodies of interest. Due to the

lack of time, inability to detect binding to Western blots and the general unpredictability in the behaviour of these antibodies, it seemed best to not pursue them further.

9. Discussion

In this thesis I have used selected human chromosomes, specifically 1, 18, 19, and 22 to examine the relationships between mitotic and interphase chromosome structure and function. My principal conclusions are that:

1. The higher order folding at mitosis of gene-rich and gene-poor regions of the human genome are the same.
2. Gene-rich regions not only have the highest steady state levels of hyperacetylated H4, but also show the highest turnover of acetylation.
3. In interphase, gene-rich regions are less condensed and more centrally located in the nucleus than gene-poor regions. Attachment of gene-rich regions to the nuclear matrix are different to those of gene-poor regions. Condensation but not nuclear position or matrix attachment is a function of transcription.

Human chromosomes 18 and 19 offer a unique system for studying chromosome structure and function. While G-bands and R-bands are generally intercalated throughout the mammalian genome, human chromosomes 18 and 19 are whole chromosome representations of these contrasting banding types. Chromosome 18 displays the features predominantly associated with G-bands: late replication, AT-richness, low gene density and low steady state levels of histone acetylation. By contrast, chromosome 19 generally displays the features of R-bands: early replication, GC-richness, high gene density and high levels and high turnover of acetylation (Section 1.7). These chromosomes were used throughout this thesis as tools to study the correlations between chromosome structure and function.

9.1 Core histone acetylation

Core histones are subject to a number of different modifications, including acetylation, methylation, ribosylation, ubiquitination and phosphorylation (Section 1.4.1.2). To date, acetylation is the most studied and understood (Section 1.4.1.3).

9.1.1 The dynamics of histone acetylation

In Chapter 5, I showed that gene-rich, R-band regions have not only the highest steady state levels of hyperacetylated H4, but also have the highest turnover of acetylation. It was demonstrated that treatment of cells with sodium butyrate and Trichostatin A (TSA), which

specifically block the action of histone deacetylase(s) (Section 5.2), visibly enhances the differences in acetylation levels between R- and G-bands on the same chromosome (human chromosome 1) (Figure 5.2). This implies that hypoacetylation in G-bands is less to do with increased deacetylation and more a reflection of lower acetyltransferase activity. Covault & Chalkley (1980) concluded that turnover of acetylation was highest in a minor population of highly acetylated species of H4 estimated to be <15% of total histones. It is likely that this population of histones would be present in the most *Alu*-rich T-bands of the genome, which make up approximately 13% of the total genome (Holmquist, 1992). Therefore, chromosome 19 would be expected to have a greater turnover of acetylation, and on blocking deacetylation, would have a greater increase in tri- and tetra-acetylated histones than chromosome 18.

Most transcription factors appear to be displaced from mitotic chromosomes (Martinez-Balbas *et al.*, 1995; Segil *et al.*, 1996). Core histone acetylation is a strong candidate for a method of passing on information regarding transcriptional potential of a particular region (Jeppesen, 1997; Wade *et al.*, 1997), since acetylation patterns are considered to be generally maintained throughout the cell cycle (Turner, 1989; Breneman *et al.*, 1996; Surralles *et al.*, 1996) (Section 5.1). However, recently a protein-dependent chromatin conformation has been demonstrated to mark genes scheduled for reactivation on mitotic chromosomes (Michelotti *et al.*, 1997) and how this might be linked to acetylation status has yet to be explored.

Acetylation has been demonstrated to facilitate the binding of transcription factors (Lee *et al.*, 1993; Vettese-Daley *et al.*, 1994 & 1996) and is widely considered to cause a reduction in the wrapping of DNA around the nucleosome, resulting in a more "open" chromatin structure (Review: Garcia-Ramirez *et al.*, 1995). In chapter 7, I showed that treatment of cells with TSA appeared to exaggerate the differences between the nuclear territory sizes of chromosomes 18 and 19. Chromosome 18 took up slightly smaller, and chromosome 19 occupied a considerably larger, proportion of the total nuclear area, when compared to untreated cells (Section 7.3.2). These data are in accord with the effects on mitotic chromosomes and suggest that acetylation acts directly to determine the degree of chromatin condensation at interphase, further establishing links between acetylation and transcriptional activity throughout the cell cycle.

9.1.2 Silencing at the rDNA

The highest levels of histone acetylation on human mitotic chromosomes correspond with the regions of highest density of genes transcribed by RNA polymerase II (pol II) (Figure 5.1). However, it was surprising that the rDNA-containing p-arms of the human acrocentric chromosomes were hypoacetylated, throughout the cell cycle, despite being of the most transcriptionally active regions of the human genome (Review: Sollner-Webb & Tower, 1986) (Figure 5.4). Hypoacetylation may be needed directly for RNA pol I activity and may even work to inhibit any RNA pol II activity in the rDNA. Recent findings in the organisation of rDNA in *S.cerevisiae* are particularly interesting (Review: Sherman & Pillus, 1997). The yeast has approximately 120 rRNA genes, each 9Kb in length, situated in a large tandem array on chromosome XII (Petes, 1979). Yeast maintains a stable genome despite the presence of repeated sequences and efficient homologous recombination. Successive amplification and deletion of the rDNA array could be deleterious to growth. Recombination rates between the rDNA repeats in *S.cerevisiae* is about 100x less frequent than meiotic exchange between unique sequences (Petes, 1979; Zamb & Petes, 1982). This recombinational repression has been shown to be dependent upon topoisomerases (Christman *et al.*, 1988; Cavalli *et al.*, 1996) and presence of the SIR2 protein (Gottleib & Esposito, 1989). Deletion and over-expression studies demonstrated that Sir2p, but none of the other known SIR proteins, were required to exert this recombinational repression (Fritze *et al.*, 1997). Using immunofluorescence, Sir2p was located to the nucleolus, in addition to an association with the chromosome telomeres (Gotta *et al.*, 1997). Recombination-initiating double strand breaks have been mapped to regions of increased accessibility (Wu & Litchen, 1994), suggesting that repression of exchange in rDNA is likely to be brought about by an alteration in chromatin structure and that this would be an effective way of controlling the frequency of recombination.

Is SIR2 also responsible for transcriptional regulation of rDNA? RNA pol II transcribed reporter constructs integrated into rDNA were shown to be silenced in a SIR2-dependent manner (Bryk *et al.*, 1997; Smith & Boeke, 1997). Potentially, SIR-2 repression may be responsible for blocking transcription from cryptic RNA pol II promoters that overlap with RNA pol I promoters in rDNA, indeed, episomal rDNA repeats can switch to being transcribed by RNA pol II (Conrad-Webb & Butow, 1995). The on/off switching of expression of RNA pol II-transcribed reporter constructs observed by Smith & Boeke (1997), led to a model suggesting that RNA pol II-gene expression alternates reciprocally

with the RNA pol I activity of the rRNA gene of insertion at any particular time. Using cross-linking techniques, active and inactive rRNA gene regions have been found in the same cell, with the ratio between them varying according to growth phase. Active regions were devoid of nucleosomes, randomly distributed along rDNA and no single locus was consistently active (Dammann *et al.*, 1993 & 1995). SIR2 may play a role in the regulation of the proportion of transcriptionally active and inactive rDNA units. For this, SIR2 would have to form a closed chromatin structure in only a subset of rDNA units. SIR2 may function by altering histone acetylation, an ability previously assigned to this protein at the telomeres and silent mating type loci (Braunstein *et al.*, 1993).

Associations between factors that are involved in transcriptional and recombinational repression and rDNA have not been established in other organisms. Indirect evidence, however, does exist in *D.melanogaster*, where it has been reported that the rDNA cluster on the X chromosome can act to sequester some component(s) of heterochromatin, thus acting as a position effect variegation (PEV) modifier (Spoffard & DeSalle: cited in Henikoff, 1990). This implies that the repressive protein complexes involved in PEV are required at the rDNA in addition. Indeed, transpositions that move the rDNA into euchromatin cause variegation of nucleolus formation (Hilliker & Appels, 1982). However, rDNA transposed via a P-element into euchromatin was demonstrated to be transcriptionally active and able to form nucleoli, although rDNA replication, effects upon surrounding euchromatin and rates of recombination within the rDNA were not assessed, but were noted to be possible reasons for the conserved localisation and organisation of rDNA (Karpen *et al.*, 1988).

It is clear that human rDNA does contain acetylated nucleosomes (Covault & Chalkley, 1980) and that two distinct chromatin structures coexist: one containing nucleosomes, representing the inactive genes, and one lacking a regular nucleosome organised repeat structure, representing the active genes (Conconi *et al.*, 1989). In rat, regions apparently lacking a regularly spaced nucleosomal pattern appear to be associated with acetylated core histones (Mutskov *et al.*, 1996). It has been noted in vertebrates, that changes in rate of rRNA synthesis are not accompanied by changes in the proportion of active verses inactive chromatin structures, as observed in *S.cerevisiae*. This has been assigned to the fact that gene activity is controlled at the level of transcription at available acetylated, non-nucleosomal genes by transcription factors, in vertebrates (Dammann *et al.*, 1993). These may include rDNA-specific transcription factors such as, TTF-1 (transcription

terminating factor 1) (Langst *et al.*, 1997). Interspersed acetylation may not be visible by immunofluorescence at the resolution studied here. However, it is still clear that, although the active rDNA may contain acetylated core histones, the environment surrounding each of these genes is hypoacetylated and must offer a challenge to the RNA pol II transcriptional machinery.

Methylation is also likely to have a role in rDNA transcriptional regulation (Reviews: Bird, 1993; Eden & Cedar, 1994; Martienssen & Richards, 1995; Razin & Shemer, 1995). It was recently shown that in rat, methylation within rDNA occurs mainly at the enhancer and promoter regions of inactive rRNA genes and that methylation of a particular promoter site correlated well with the transcriptional activity of that gene (Stancheva *et al.*, 1997).

In complete contrast to my results, immunofluorescence with antibodies to H4 acetylated at each of the four lysine residues revealed the NORs of both broad bean and barley to be hyperacetylated throughout the entire cell cycle (Houben *et al.*, 1996; Idei *et al.*, 1996). Labelling, on both mitotic chromosomes and in interphase nuclei, corresponded with localisation of rDNA (Hizume, 1992; Rawlins & Shaw, 1990) and silver staining, which highlights actively transcribing regions (Hizume, 1992). Recently, a histone deacetylase specific for the maize nucleolus was identified and its function appears to be regulated in a growth rate-dependent manner by phosphorylation (Lusser *et al.*, 1997). This suggests that acetylation does play a role in the transcriptional activity of rDNA in plants, but it seems likely to be a rather different role than that in vertebrates.

9.2 Sites of attachment to the chromosome scaffold and nuclear matrix

The chromosome scaffold (Sections 1.1 & 1.5.1) has been used as a morphological term throughout this thesis to describe the residual framework which remains following protein extraction of metaphase chromosomes (Paulson & Laemmli, 1977; Earnshaw & Laemmli, 1983; Paulson, 1989) with salt or polyanions. The metaphase chromosome axial core can also be traced immunologically with antibodies to topo II (Earnshaw & Heck, 1985; Earnshaw *et al.*, 1985; Gasser *et al.*, 1989) (Section 1.4.6) or ScII (Saitoh *et al.*, 1994) (Section 1.4.7). The nature of the DNA sequences and proteins involved in tethering DNA to the metaphase chromosome scaffold are much debated and various operational techniques, most based on extraction of interphase nuclei, have been developed from which

several models for scaffold-loop metaphase chromosome folding have been suggested. In Section 4.2, three predominating models and their possible effects upon the metaphase packaging of human chromosomes 18 and 19 were outlined (Figure 4.1).

AT-rich scaffold attached regions (SARs), which were originally defined from LIS extracted nuclei (Mirkovitch *et al.*, 1984; Gasser & Laemmli, 1986; Gasser *et al.*, 1989; Laemmli *et al.*, 1992), are predicted to be more concentrated in AT-rich G-bands than AT-poor R-bands. Craig *et al.* (1997) showed by FISH that attached DNA from LIS extracted nuclei and metaphase chromosomes hybridises preferentially to G-bands confirming that SARs are, indeed, most frequent in these regions. Thus, SARs would be more concentrated along chromosome 18 than 19 if they were involved in metaphase chromosome scaffold attachment, resulting in smaller DNA loop sizes (Saitoh & Laemmli, 1994a &b). In a second model, transcriptionally active sequences have been suggested to be permanent attachments to the chromosome scaffold (Cook, 1994 & 1995), with a concentration of attachments in gene-rich R-bands. Indeed, attached DNA from electroeluted nuclei preferentially hybridises to R-bands, consistent with transcriptionally active sequences being the predominant sites of attachment to the nucleoskeleton (Craig *et al.*, 1997). In this instance there would be a concentration of attachments along chromosome 19 compared to chromosome 18, resulting in smaller DNA loop sizes. However, attached DNA from electroeluted metaphase chromosomes showed no biased hybridisation (Craig *et al.*, 1997), suggesting that interphase nucleoskeleton attachments do not equate with metaphase chromosome scaffold attachments. In addition, FISH with a chromosome 18 CpG-island probe showed no preference for genes to be located along the axis of metaphase chromosomes (Section 4.4).

A third model, where metaphase chromosome scaffold attachments are relatively evenly spaced and where G- and R-bands have similar DNA loop sizes, was supported by analysis of salt extracted human chromosomes 18 and 19 (Section 4.2). These two chromosomes expanded to the same extent with increasing salt concentration. Craig *et al.* (1997) hybridised attached DNA from salt extracted metaphase chromosomes to human metaphase spreads by FISH and showed no bias in distribution. These data argue against the above models of scaffold-loop metaphase chromosome packaging.

To build upon these findings, probes that cover >200Kb at various points along chromosomes could be used for FISH to extracted chromosomes and their paths traced to determine the exact extent of individual loops. Paints that determine specific banded regions, including telomeres and centromeres, could also be used to light up these regions on extracted chromosomes and provide a means to directly compare loop sizes in different environments along the length of a chromosome. Bickmore & Oghene (1996) used this approach to show that origins of replication associate with the scaffold of salt extracted human metaphase chromosomes. There is increasing evidence that origins of replication may be involved in attachment to both the metaphase chromosome scaffold and the interphase nuclear structural framework. In *S.cerevisiae*, autonomously replicating sequence (ARS) elements have also been shown to associate with a chromosome scaffold (Amati & Gasser, 1988 & 1990). The salt extracted interphase nuclear matrix has also been associated with putative origin of replication sequences (Vogelstien *et al.*, 1980; Berezney & Buchholtz, 1981; Dijkwel *et al.*, 1986; Jackson & Cook, 1986; Razin *et al.*, 1986 & 1993; Sykes *et al.*, 1988; Jackson, 1990 & 1991; Cook, 1991; Razin *et al.*, 1993) (Section 4.2.3). The remnants of replication origin clusters have been observed to persist at the chromosome scaffold throughout the cell cycle in a number of species (Meng & Berezney, 1991; Adachi & Laemmli, 1992; Diffley *et al.*, 1994; Sparvoli *et al.*, 1994). Interestingly, a similarity between the size of DNA loops and number of replicons has been recognised in a wide range of species (Marsden & Laemmli, 1979; Buongiorno-Nardelli *et al.*, 1982; Micheli *et al.*, 1993; Tomilin *et al.*, 1995).

A library of operationally defined matrix attachment sequences, selected by their the ability to attach to isolated salt extracted interphase nuclear matrices, has been cloned from human chromosome 19 (Nikolaev *et al.*, 1996). Only 50% of sequenced clones were shown to be AT-rich (>75% AT). Thus, although the cytogenetically visualised AT-queue suggests more attachments within G-bands, there could additionally be less AT-rich attachment sequences that balance the number of attachments to an even spacing in G-bands and R-bands. Alternatively, there may be additional attachments to a structural framework which resides outside of the chromosome axial core. Nikolaev *et al.* (1996) went on to map several of their clones by FISH to human metaphase spreads and determined that they were spread evenly along chromosome 19, but too few clones were mapped to make a general statement as to the distribution of such sequences. It would be interesting to now map these clones to

salt extracted chromosomes and nuclei and determine if they are *bona fide* attachments sites, however, they are very small (<1Kb) making this difficult.

Salt extraction of interphase nuclei, similarly to metaphase chromosomes, resulted in the production of a residual nuclear matrix surrounded by loops of DNA (Section 7.4). I found that chromosome 18 was consistently localised to the DNA halo, while chromosome 19 remained associated with the residual matrix. It appears that after extraction of soluble nuclear proteins with high salt, chromosome 18 is free to migrate out of the nucleus. Chromosome 19 remains relatively tightly bound to the nuclear matrix. Craig *et al.* (1997) showed that attached DNA from salt extracted interphase nuclei tended to hybridise to G-band regions. These results suggest that chromosome 18 and other G-band-rich regions retain their attachments to a chromosome axial core scaffold but loose any attachments to a nuclear structural framework. This may be related to the strength of different attachments. The opposing locations of chromosomes 18 and 19 in salt extracted nuclei were not altered by blocking RNA pol I and II transcription with Actinomycin D (AD) (Section 7.4.2), suggesting that active transcription is not required for chromosome 19 to remain bound to the nuclear matrix. This dramatic difference in behaviour is in contrast to their similar higher order metaphase chromatin structure.

Taking all of this together, one conclusion might be that there are both permanent and temporary sites of attachment involved in chromosome architecture throughout the cell cycle (Razin & Gromova, 1995; Jackson, 1991; Craig *et al.*, 1997). The permanent sites are relatively evenly spaced along the length of chromosomes and may serve as anchors to an internal structure, maintaining chromosome morphology and identity. Exactly what sequences constitute such permanent attachments will remain a source of debate for some time. Are they defined by origins of replication, or some other evenly spaced sequence, such as boundary elements, or sequences of a specific nature, for example, rich in purines or pyrimidines? SARs are likely to be important sequences since they appear to be maintained throughout the cell cycle (Mirkovitch *et al.*, 1988; Craig *et al.*, 1997). These attachments may be anchored along the axial core of metaphase chromosomes in addition to other attachments within R-bands which serve to produce an even distribution. It is possible that the R-band attachments are temporary and are released at interphase to allow interaction of these gene-rich regions with a nuclear structural framework and associated transcriptional complexes. These and/or additional temporary attachments would be brought into play at

interphase, tethering chromosomes to an external nuclear structural framework and would be determined by regions actively being transcribed and/or replicated. In my studies I found that interphase attachments to the nuclear matrix do not require continued transcription (Section 7.5), suggesting that they are mediated by proteins other than RNA pol II.

9.3 The organisation of interphase chromosome territories

It is now also widely accepted that chromosomes occupy separate interphase nuclear territories. Models have been proposed by a number of groups in which genes are located at the periphery of interphase territories (Manuelidis, 1990; Cremer *et al.*, 1993; Zirbel *et al.*, 1993; Kurz *et al.*, 1996; Strouboulis & Wolffe, 1996). Zirbel *et al.* (1993) noted that a specific nascent transcript and general splicing components were situated outside of interphase territories and suggested the presence of channels connecting territories with nuclear pores (Blobel, 1985) (Figure 1.5). RNA transcript tracks extending from the nuclear interior to the nuclear periphery (Lawrence *et al.*, 1989; Xing *et al.*, 1993) are presumed to be moving along such channels. In an attempt to visualise these structures, mammalian cells were transfected with a recombinant vimentin gene containing a nuclear localisation signal. In these cells, vimentin was organised in large filamentous nuclear structures which remained outside of chromosomal domains and colocalised to RNA and protein previously shown to be outside of chromosomal domains (Bridger *et al.*, in press). In support of this Kurz *et al.* (1996) located active sequences to the territory periphery and showed an indifference for the location of inactive genes. However, experiments in this thesis have sampled the positioning of genes using chromosome 18 CpG- and non-CpG-island probes within metaphase chromosomes (Section 4.4) and interphase territories (Section 7.5) and have revealed no bias for the chromosome periphery at either of these cell cycle stages. The number of genes studied by both Zirbel *et al.* (1993) and Kurz *et al.* (1996) was very small and, thus, may not be representative. By contrast, CpG-islands represent almost 60% of genes (Larsen *et al.*, 1992).

It is possible that the apparently even distribution of genes that I observed across the chromosome 18 interphase territory was as a result of the flattening of nuclei into 2-D, with genes located on the upper and lower territory surfaces masking a peripheral bias. Alternatively, it may be that there is an alternative arrangement of genes within interphase territories. It was noted by Eils *et al.*, (1996) that the mammalian active X chromosome

(Xa) occupies a similar volume in the interphase nucleus to the inactive X chromosome (Xi) but that Xa has a more irregular, and thus larger, surface area than Xi. The increased number of invaginations was presumed to allow access to transcription components. The condensed appearance of G-band versus R-band regions (Yokota *et al.*, 1997) and chromosome 18 verses chromosome 19 in 2-D nuclei (Section 6.2) may be a result of a similar difference in shape between inactive and active regions on autosomes. The chromosome 19 territory was consistently visualised as a more "open" structure with gaps within the territory where no probe had hybridised (for example see Figure 6.6). It can be envisaged that channels run throughout the interphase domains of transcriptionally active regions, providing a means of transporting transcription and splicing complexes to, and RNA transcripts from genes.

Is continued transcriptional activity required for chromosome 19 to remain decondensed during interphase? It has been previously shown that blocking RNA pol II transcription results in the dispersal of interphase territories (Haaf & Ward, 1996). In Chapter 7, the territories of chromosomes 18 and 19 were analysed in human lymphoblastoid cells treated with AD to block transcription by RNA pol I and II. No dispersal of territories was observed (Section 7.3). Haaf & Ward (1996) used different inhibitors of transcription to AD. These experiments used cells cytocentrifuged onto slides and it is possible that the break-down of territories was associated with dead cells. Subsequent experiments using cells grown upon slides so that dead cells are washed off and treating DRB, α-amanatin and AD resulted in no dispersal of territories (Personal communication: Dr. J.M. Bridger). In my experiments chromosome 18 territories remained similar as a percentage of the total nuclear area when compared to non-treated nuclei. In contrast, chromosome 19 territories appeared to be more condensed following AD treatment. These results suggest that transcriptional activity may be instrumental in establishing territory size.

Brown *et al.* (1997) observed that Ikaros proteins, implicated in the organisation of genomic loci in B lymphocyte nuclei (Section 9.5.2), redistribute during the cell cycle. These proteins localise to 8-12 foci in G1 nuclei, disperse into bead-like structures during S-phase and rearrange into 16-24 foci in G2. These data support dynamic nuclear reorganisation during DNA replication and are in accord with my observations of changes in chromosome territory area at different cell cycle stages (Section 6.5.1). The chromosome 19 interphase territory takes up its largest nuclear area during early S-phase, the stage at which this

chromosome is replicated. Chromosome 18 replicates late in S-phase and might be expected to show its largest percentage area at this stage of the cell cycle. There was no evidence that this was the case. However, this effect might be masked by the increase in nuclear size by late S-phase. By late S-phase the majority of chromatin has been duplicated and the nucleus is almost doubled in size. An increase in chromosome 18 territory area at this stage would not be as easily distinguished. Decondensation of chromatin during S-phase may be required to allow access to replication machinery.

9.4 The positioning of interphase chromosome territories

The data in this thesis support the concept of the mammalian nucleus as a highly organised and compartmentalised organelle. It was established in Chapter 6 that human chromosomes occupy defined and distinct territories at interphase and that the positioning of these territories relate to the characteristics of the particular chromosome.

9.4.1 The location of transcription within the nucleus

Nascent transcripts, RNA polymerase II and a variety of transcription factors and splicing components have been shown to be concentrated in 20-50 speckles in the nucleus, which are probably sites of storage (Fu & Maniatis, 1990; Spector, 1990; Wansink *et al.*, 1993; Bregman *et al.*, 1996; Fay *et al.*, 1997; Grande *et al.*, 1997; Zeng *et al.*, 1997; Review: Singer & Green, 1997) (Section 1.6.2). A bias for speckles to be located more internally in the nucleus has been noted (Lawrence *et al.*, 1993). However, the majority of transcription is considered by most to take place throughout the nucleoplasm. Localisation of active and inactive gene sequences by FISH has suggested a preference for the centre of the nucleus for genes active in the particular cell type examined, while inactive genes were found close to the periphery of the nucleus or nucleolus (Manuelidis & Borden, 1988; Lawrence *et al.*, 1988; Lawrence & Singer, 1991; Xing *et al.*, 1995). By contrast, mapping of DNAse-sensitive sequences, considered to co-localise with transcriptionally active chromatin, have indicated a peripheral localisation for the majority of transcription (Hutchison & Weintraub, 1985; De Graaf *et al.*, 1990; Krystosek & Puck, 1990; Park & De Boni, 1996). This gives a completely contrasting model for the localisation of transcription within the nucleus from the evidence described above. The reason for this discrepancy remains to be determined but may be an experimental artefact, since DNA at the periphery of the nucleus is likely to be most easily accessed by DNAse.

Some studies have revealed that the bulk of replication at the periphery of the nucleus occurs during mid-S-phase (Nakayasu & Berezney, 1989; Kill *et* al., 1991; O'Keefe *et al.*, 1992), while others have reported that this chromatin replicates in late S-phase (Fox *et al.*, 1991; Hutchison, 1995; Ferreira *et al.*, 1997). These latter observations correlate with a peripheral localisation for transcriptionally inactive, and thus, late-replicating chromatin.

In support of the positioning of transcriptionally inactive chromatin at the periphery of the nucleus, gene-poor, late-replicating chromosome 18 was shown to located predominantly in this compartment (Section 6.2). Reciprocally, gene-rich, early replicating chromosome 19 was generally more centrally located in the nucleus. In addition, chromosome 1, with its large region of pericentric heterochromatin, also showed a bias for the nuclear periphery, while relatively gene-rich chromosomes 11 was more centrally positioned. A continuation of this study would be to compare the positioning of a gene-poor and gene-rich region from the same chromosome (for example, the adjacent G- and R-bands on the p-arm of chromosome 1). Using a total human CpG-island probe for FISH to nuclei has not revealed a bias in distribution (Personal communication: Dr. W.A. Bickmore). However, a whole chicken CpG-island probe did show a tendency to hybridise strongly in the centre than at the periphery of the nucleus (Personal communication: Ms. M. Gomez). In chickens, CpG-islands are strikingly concentrated to the microchromosomes (McQueen *et al.*, 1996), which constitute 25% of genomic DNA and replicate earlier than the macrochromosomes (Schmid *et al.*, 1989).

9.4.2 How is specific territory positioning orchestrated?

Positioning of interphase nuclear territories may be dependent upon a number of chromosome properties:

- Transcriptional activity
- Levels of core histone acetylation (Section 1.4.1.3)
- Presence of specific sequence motifs that bind particular proteins
- General base composition (Section 1.3.1)
- Distribution of interspersed repeats (Section 1.3.3)

Treatment of normal human nuclei with AD and TSA did not result in a change in the positioning of chromosomes 18 or 19 (Section 7.2). Therefore, it is likely that positioning

of chromosomes is independent of actual transcriptional activity or levels of core histone acetylation. Alternatively, once a chromosome is in a particular position, the constraints of the nuclear matrix may prevent any gross change. This is supported by the fact that chromatin of the interphase nucleus is relatively immobile (Robinett *et al.* 1996; Abney *et al.*, 1997; Marshall *et al.*, 1997b).

The shapes and orientations of territories may prove interesting in establishing a mechanism for positioning. Using telomere-specific probes, it has been established that chromosome 18 generally abuts the nuclear periphery along its length (Personal communication: Ms. S. Boyle). The telomeres were rarely found between the chromosome territory and the edge of the nucleus, suggesting that telomeres are not responsible for the peripheral nuclear positioning of this chromosome. In addition, Broccoli & Cooke (1994), showed that the targeting of telomeric sequences to an interstitial chromosome site did not alter the positioning of that site in the interphase nucleus. However, in *S.cerevisiae*, telomeres appear to play an important role in nuclear compartmentalisation (Section 9.5.2).

The study of a reciprocal translocation between chromosome 18 and 19 showed that sequence could apparently influence territory positioning (Section 7.2). The translocated p-arm sections (~20Mb) were orientated towards the positions occupied by their structurally normal homologues and, although not significantly, did influence the positioning of the entire territory with respect to the nuclear periphery. Unfortunately, no unfixed material has yet been obtained for this, or any other chromosome 18 and 19 translocations. A mouse translocation between syntenic chromosomes may be of use. The location of introduced yeast artificial chromosomes originating from human chromosome 18 or 19 might prove to be a means of determining the amount and type of sequence necessary to influence positioning. Since it appears that the physical proximity of different chromosomes in interphase nuclei can be inferred from the frequency of translocations seen between them (Ferguson-Smith & Handmaker, 1961; Kaplan *et al.*, 1993; Qumsieyeh, 1995), a comprehensive survey of naturally occurring human chromosome translocations would be interesting.

In a human-rodent hybrid background chromosome 18 did not show a bias for the nuclear periphery (Section 6.4.4). It may be that the sequences which influence human chromosome positioning are not recognised by the rodent positioning proteins. However, there was

evidence for a bimodal distribution of positions, with some territories being more peripheral and others being more central in the nucleus (Figure 6.15b & c). In the hybrid cell line (GM11010) used for these studies, chromosome 18 had been previously shown to be lacking part of the q-arm (Section 3.2). It is possible that within this deleted region specific sequences required for peripheral positioning are located. Initially this experiment should be repeated using an 18q-specific probe to determine the positioning of the complete and incomplete chromosomes. By tagging the chromosome 18 with a selectable marker, it may be possible to introduce the chromosome into normal human nuclei and assess its ability to reposition itself at the nuclear periphery. Analysis of human nuclei with different chromosome 18 deletions might prove informative. The observed bias orientation of the translocated tip of the chromosome 18 p-arm described above, argues that sequences on 18q are not solely responsible for directing the positioning of this chromosome. Interestingly, territory area (Section 6.4.4) and levels of acetylation (Section 5.4) for both chromosomes 18 and 19, appeared to remain similar to observations in normal human nuclei. However, replication timing appears to be altered, with chromosome 18 showing an earlier replication time in its hybrid background than expected (Personal communication: Dr. W.A. Bickmore).

What proteins may be involved in nuclear territory positioning? The inner nuclear membrane has been closely associated with peripheral chromatin and it seems that chromosomes contact the nuclear membrane at several points along their length (Mathog *et al.*, 1984; Glass & Gerace, 1990; Belmont *et al.*, 1993; Taniura *et al.*, 1995; Marshall *et al.*, 1996; Review: Gerace & Burke, 1988). The proteins of the inner nuclear membrane include the lamin B receptor (LBR) (Worman *et al.*, 1988; Ye & Worman, 1994). Recently, LBR has been shown to be a major chromatin docking protein (Pyrpasopoulou *et al.*, 1996; Collas *et al.*, 1996), which specifically interacts with chromodomain-containing human homologues of the HP1 protein (Ye & Worman, 1996 & 1997). Immunolocalisation of LBR to Chinese hamster chromosome spreads shows colocalisation with G-bands (Pyrpasopoulou *et al.*, 1996), possibly mediated by its interaction with HP1-like proteins. Based upon this observation, human chromosome 18 is likely to have more contacts with LBR and more contacts with the inner nuclear envelope and, thus, be positioned more peripherally than chromosome 19. This mechanism would also account for the peripheral bias of chromosome 1 which, with its large pericentric heterochromatin region, is likely to be associated with HP1-like proteins. Such a mechanism has been suggested to act in

D.melanogaster. The YA (young arrest) protein is an essential component of the nuclear lamina, which lines the inner nuclear membrane, and associates with chromatin, preferentially with the interbands of polytene chromosomes (Lopez *et al.*, 1997). YA-deficient eggs and embryos show abnormalities in chromosome condensation suggesting that YA may have a role in organising chromatin (Liu *et al.*, 1995). However, since YA mutant extracts are capable of decondensing chromatin and of supporting nucleus formation, it appears that this protein is primarily for the maintenance of nuclear organisation required during early development (Lopez *et al.*, 1997).

In human nuclei, Bridger *et al.* (1993) observed foci and fibres containing lamins A and C distributed throughout the nucleus at G1. As cells progressed towards S-phase these internal lamina structures disappeared. It was suggested that such structures preferentially polymerised to heterochromatin and migrated to the nuclear periphery during G1, moving heterochromatic regions with them. Human chromosome 18 shows its peripheral bias early in G1 and is likely not to rely solely on such a mechanism for its positioning (Section 6.5). Peripheral positioning of human chromosome 18 may be attained at the moment of nuclear envelope formation. The arrangement of chromosomes upon the metaphase plate appears to be very precise and ordered (Naegele *et al.*, 1995). Positioning may begin to be established as early as metaphase, anaphase or telophase and may be determined from FISH studies at these individual stages of mitosis.

Using the system devised by Robinett *et al.* (1996), in which a vector containing the *Escherichia coli* lac operator region is integrated into a specific region and a GFP-lac repressor fusion protein is used to follow the fate of that region in live analysis, it might be possible to tag chromosomes 18 and 19 specifically.

The Ki-67 protein is nucleolar for most of the cell cycle and coats mitotic chromosomes (Gerdes *et al.*, 1984; Verheijen *et al.*, 1989) (Section 1.5.4). In human early G1 nuclei, Ki-67 has been shown to be associated with satellite DNA, including that at centromeres, telomeres, heterochromatin and rDNA (Bridger *et al.*, 1997). This protein is not required for the existence of a functional nucleolus but is required for cell cycle progression. A possible explanation for the high affinity of Ki-67 with satellite DNA is that it directs these regions, particularly rDNA with which it remains associated throughout the entire of the cell cycle, to the nucleolus. Observations of chromosome territories in 3-D nuclei suggest that

for a particular territory there is an association with either the nuclear envelope or the nucleolus (Section 6.6) (Personal communication: Dr. J.M. Bridger, University of Heidelberg). Invaginations of the nuclear envelope have been observed to penetrate mammalian nuclei of many cell types (Fricker *et al.*, 1997), providing additional possible sites of chromatin attachment. It is plausible that there are several organising proteins with the affinity to bind to particular types of chromatin and to move this chromatin to specific regions of the nucleus. For a particular chromosome there may be a degree of competition between proteins destined for different locations and a compromise position is eventually reached by the end of G1. Human chromosome 18, for example, could be immediately associated with inner nuclear lamina proteins following mitosis due to LBR association. Ki-67 may bind to the centromeres and telomeres and attempt to pull this chromosome from the periphery of the nucleus. The LBR and inner nuclear membrane would be the stronger force in this instance. Human chromosome 19, on the other hand, probably has few associations with LBR and the influence of Ki-67 may pull this chromosome centrally, hence the observation of juxtaposition to the nucleolus in 3-D nuclei (Section 6.6) (Personal communication: Dr. J.M. Bridger). Since Ki-67 is only present in proliferating cells (Gerdes *et al.*, 1984; Verheijen *et al.*, 1989), observations of chromosome territory positions in resting cells might prove interesting. It is likely that many proteins involved in nuclear organising have yet to be identified (Section 9.5).

Human X chromosome inactivation as a mechanism of dosage compensation was introduced in Section 1.4.8. The *XIST* gene is expressed only on the inactive X chromosome (Xi) (Penny *et al.*, 1996; Komura *et al.*, 1997) and encodes an RNA which coats Xi, solely and entirely, at interphase (Brown *et al.*, 1992; Clemson *et al.*, 1996; Lee *et al.*, 1996). *XIST* expression is required for initiation but not maintenance of inactivation (Brown & Willard, 1994). Xi is associated with heterochromatic staining properties (Barr & Bertram, 1949; Kanda, 1973) and it is well established that this chromosome, in the form of the Barr body, is positioned close to the nucleolus or at the periphery of the female interphase mammalian nucleus (Barr & Bertram, 1949; Dyer *et al.*, 1989; Belmont *et al.*, 1986). Lee *et al.* (1996) introduced murine *Xist* sequences onto autosomes and induced dosage compensation in male cells. Interestingly, Xist RNA in transgenic male fibroblasts frequently occupied a peripheral nuclear position, thus resembling Xist RNA localisation in normal female fibroblasts. Whether Xist RNA directly influences the positioning of a chromosome has yet

to be established. It is possible that peripheral positioning is a requisite for inactivation of a chromosome.

9.5 The purpose of nuclear compartmentalisation

Mammals possess a highly complex genome, with 60-80,000 genes estimated to exist (Review: Bird, 1995). Spurious transcription from inappropriate genes and non-gene DNA could seriously effect the development and integrity of an organism, and it is therefore crucial for there to be accurate control of gene expression. Methods of controlling gene expression have been established throughout the entire process of protein production from transcription initiation and termination, mRNA processing and stability to translation. Mechanisms involved in the control of transcriptional initiation occur at all levels of chromosome structure. DNA methylation (Section 1.4.5), nucleosome positioning, and histone variants and modifications (Section 1.4.1) have all been demonstrated to play an important role in determining transcriptional activity. At the next level, chromatin remodelling protein complexes come into play, for example *Polycomb* and *trithorax* group proteins (Section 1.4.2). Nuclear compartmentalisation offers another level of transcriptional control at the highest level of chromatin packaging.

9.5.1 Silencing by proximity to heterochromatin in *cis*

There is an increasing awareness that the chromosomal and nuclear context of a gene can influence its activity. PEV occurs when a euchromatic gene is placed in the vicinity of heterochromatin, resulting in a variable but clonally inherited pattern of expression. This phenomenon is most generally considered to occur by the spreading of the heterochromatin associated repressive protein complexes, altering the structure of neighbouring euchromatin (Reviews: Karpen, 1994; Wallrath & Elgin, 1995). In *D.melanogaster* this spreading, which emanates from pericentric or telomeric heterochromatin, can cover as much as 2Mb. It has a gradient effect, with genes closest to the heterochromatin being most adversely affected. Extent of spreading appears to be controlled in a tissue-specific and developmental stage-specific manner (Lu *et al.*, 1996).

The yeasts, *S.cerevisiae* and *S.pombe*, possess two mating-type loci, encoding proteins involved in establishing alternative mating kinds. These genes are maintained transcriptionally silent, awaiting recombination with a permissive locus. The

chromodomain present in *D.melanogaster* Pc and HP1 is also shared by the *S.pombe* protein, Swi6, which is implicated in repression at the mating-type loci, probably by heterochromatin-like remodelling (Lorentz *et al.*, 1994). An increasing number of genes involved in repression of these loci are being established. In *S.cerevisiae*, mutations in several genes, including the SIR genes (silent information regulator) (Rine & Herskowitz, 1987; Review: Rivier & Rine, 1992), lead to de-repression of the mating-type loci. Two of the SIR proteins, Sir3p and Sir4p, have been shown to interact with H3 and H4, which would enable them to organise nucleosomes into a transcriptionally inactive conformation (Hecht *et al.*, 1995; Review: Grunstein *et al.*, 1995). Significantly, mutations at the N-termini of H3 and H4 cause de-repression at *S.cerevisiae* telomeres and the mating-type loci (Kayne *et al.*, 1988; Thompson *et al.*, 1994b).

S.pombe telomeres and centromeres, and *S.cerevisiae* centromeres have been shown to exert a PEV effect on genes placed in close proximity (Gottschling *et al.*, 1990; Renauld *et al.*, 1993; Allshire *et al.*, 1994; Nimmo *et al.*, 1994). Telomeric PEV in *S.cerevisiae* is accompanied by inaccessibility of DNA to the DNA-modifying protein, DAM methyltransferase (Gottschling, 1992). Mutations in several of the genes involved in silencing of the mating-type loci have also been shown to alleviate PEV (Aparicio *et al.*, 1991; Nimmo *et al.*, 1994; Allshire *et al.*, 1995). Mutations which de-repress centromeric regions in *S.pombe* resulting in increased chromosome loss, have led to the suggestion that heterochromatin may be a requirement for a fully functional centromere (Allshire *et al.*, 1995). Over-expression of Sir2p and Sir3p in *S.cerevisiae*, also results in chromosome loss, again, possibly due to defective centromere function (Holmes *et al.*, 1997). The SIR proteins have also been shown to be involved in DNA repair (Tsukamoto *et al.*, 1997). Clearly, silencing is not the only role of these proteins, their function is also essential for chromosome stability and integrity.

D.melanogaster HP1 is associated with constitutive heterochromatin and has dosage-dependent effects on PEV (Eissenberg *et al.*, 1992). The protein contains a chromodomain (Platero *et al.*, 1995), but has also been shown to bind directly to DNA (Sugimoto*et al.*, 1996). In embryos lacking functional HP1, abnormalities in chromosome morphology and segregation occur, consistent with a defect in chromosome condensation (Kellum & Alberts, 1995). At metaphase and anaphase, in addition to heterochromatin association, a considerable fraction of the protein is dispersed around the segregating

chromosomes, however, the purpose of this is unclear (Kellum *et al.*, 1995). Interestingly, *D.melanogaster* HP1 has been demonstrated to associated with the origin recognition complex (ORC) (Pak *et al.*, 1997). Various mutations in ORC subunits have been isolated that separate replication and silencing functions (Fox *et al.*, 1995) indicating that ORC may play a role in organising heterochromatin formation aside from its role in replication. Targeting Sir1p directly to the mating-type loci bypasses the requirement for ORC binding suggesting that ORC may act to recruit repressor proteins (Fox *et al.*, 1997). ORC may couple the end of replication with the onset of chromatin condensation and may regulate which regions will decondense at G1.

PEV in mammalian cells has been described at the centromere in a murine cell line (Butner & Lo, 1986). PEV-like phenotypes have also been observed in murine X-autosome translocations, due to the spreading of X-inactivation to the autosome segment (Russell & Montgomery, 1970). Transgenes have been recorded to be subject to PEV following insertion close to centromeres (Al-Shawi *et al.*, 1990; Robertson *et al.*, 1995; Dobie *et al.*, 1996; Festenstein *et al.*, 1996). Locus control regions (LCRs) are DNA sequences that direct high-level expression of a transgene independent of site of integration (Reviews: Epner *et al.*, 1992; Felsenfield, 1992). These regions have been isolated from several genes and are often associated with enhancers. LCRs are considered to act by ensuring an open chromatin configuration, increasing the probability of forming a stable transcriptional complex and thereby blocking the encroaching heterochromatin protein complexes (Grosveld *et al.*, 1987; Festenstein *et al.*, 1996). The exact mechanism of LCRs has yet to be elucidated.

There are now several naturally occurring murine and human mutations that are considered to be the result of position effects. Chromosomal rearrangements and deletions outwith a gene have been implicated in inappropriate repression or activation of that gene and the cause of the associated mutant phenotype. Such rearrangements can be up to several Kb from the gene in question, located either upstream or downstream and present in both somatic and germline cells (Reviews: Bedell *et al.*, 1996; Milot *et al.*, 1996). One such example in humans involves patients suffering from the eye disorder aniridia, usually associated with mutations in the PAX6 gene. Several pedigrees have been identified where no mutations have been found within the PAX6 gene but linked rearrangements have been located between 20 and 150Kb 3' of the gene (Fantes *et al.*, 1995; Danes, 1996). However,

lack of expression may be the result of the disruption of a long range regulatory element in these cases.

Interestingly, there are genes which reside in the heterochromatic regions of *D.melanogaster* and only function correctly when in such an environment (Review: Gatti & Pimpinelli, 1992). It is very possible that similar genes exist in other organisms.

9.5.2 Silencing by proximity to heterochromatin in *trans*

PEV apparently occurs in *trans* as well as in *cis* (Review: Marshall *et al.*, 1997a). In *D.melanogaster*, there is a dominant null mutation of the *brown* eye pigment gene (bw^D) caused by the insertion of a block of heterochromatin which misdirects this gene to associate with pericentric heterochromatin. Furthermore, as a result of homologous pairing, the wild-type allele localises to pericentric heterochromatin, providing an explanation for the variegated inactivation of this gene (Henikoff & Dreesen, 1989; Dreesen *et al.*, 1991; Dernburg *et al.*, 1996; Review: Henikoff, 1997). The silencing of bw^D and the association between the locus and pericentric heterochromatin is disrupted by *suppressors-of-PEV* mutations (Csink & Henikoff, 1996).

The telomeres of *S.cerevisiae* cluster at the periphery of the nucleus (Review: Gilson *et al.*, 1993) in association with the SIR3 and SIR4 products (Gotta *et al.*, 1996), which are required for telomeric silencing (Cockell *et al.*, 1995). Disruptions of SIR3 and SIR4 result in loss of telomere-nuclear membrane associations and cause derepression of telomeric and mating type silencing (Palladino *et al.*, 1993). When a reporter gene flanked by two silencer sequences was placed >200Kb from a telomere the gene was not silenced. Repression was restored by creation of a new telomere 10Kb from the gene or by overexpression of SIR3 and/or SIR4 (Maillet *et al.*, 1996). Sir3 and Sir4 are dispersed throughout the nucleus when overexpressed resulting in the conclusion that for efficient silencer function sequences require proximity to pools of SIR proteins achieved by proximity to telomeres or delocalisation of SIR proteins (Review: Marcand *et al.*, 1996). There is no evidence that human telomeres are heterochromatic and, indeed, they do not to occur in clusters but are dispersed randomly throughout the nucleus (Luderus *et al.*, 1996).

There is recent evidence showing the colocalisation of centromeric α-satellite DNA, HP1 and specific inactive but not active genes in mouse B lymphocyte nuclei (Brown *et al.*,

1997). Ikaros proteins also localise to these interphase heterochromatin domains and have been postulated to be "recruiters" of lymphoid-associated genes causing repression of specific genes essential to allow correct lymphocyte development. This creates a precedent for the role of nuclear positioning in the control of gene expression in mammals.

The periphery of the human nucleus may be a compartment associated with repression. Thus, the positioning of particular chromosomal domains to this region may be a requirement for, or a result of transcriptional repression. In accordance with this, transcriptionally inert chromosome 18 was predominantly observed at the periphery of the human nucleus, as was chromosome 1 with its large region of pericentric heterochromatin (Section 6.2.4). It may prove informative to assess the types of genes located on chromosomes 18 and 19. It might be expected that chromosome 18 mainly harbours genes which are cell type-specific or have limited developmental timing of expression and require strict transcriptional regulation.

9.5.3 Replication timing

Replication timing is closely linked to transcriptional activity (Goldman *et al.*, 1984; Hatton *et al.*, 1988; Reviews: Holmquist, 1987; Goldman, 1988; Villarreal, 1991) (Section 1.2.4). G-bands and chromosome 18 replicate late in S-phase while R-bands and chromosome 19 replicate early. The genes of the inactive X chromosome generally shift to become late replicating when compared to their active X chromosome alleles (Gartler *et al.*, 1992; Riggs & Pfiefer, 1992; Hansen *et al.*, 1996).

Chromosomal architecture has been shown to determine the sites of initiation of replication. When Chinese hamster ovary (CHO) cells were permeabilised with digitonin preserving the nuclear membrane, *X.laevis* egg extracts initiated replication at sites indistinguishable from normal CHO nuclei, however, CHO chromatin reconstructed *in vitro* extracts initiated replication at non-specific sites (Gilbert *et al.*, 1995; Wu & Gilbert, 1995; Lawlis *et al.*, 1996). Because of the physical differences between active early replicating and inactive late replicating genes, it is possible that by default replication begins at the most accessible sites. In addition, it has been suggested that when active genes are brought into contact with the nuclear matrix-associated transcription complexes, they are also brought into the proximity of replication complexes (Hassan & Cook, 1994). Hassan *et al.* (1994) found that both nascent RNA and DNA overlap, particularly early in S-phase, but also during mid and late

S-phase. This is surprising since, as previously noted, transcriptionally inactive chromatin is replicated during mid and late-S-phase. Wansink *et al.* (1994) showed that nascent RNA and DNA did not colocalise more than would be expected if the two were unrelated, concluding that transcription was temporarily halted in regions undergoing replication. The cause of these discrepancies is unclear.

Alternatively, origins of replication could be tagged with temporal information in the form of specific proteins or modifications. For example, hyperacetylation may mark a gene for early and hypoacetylation for late replication. However, this seems unlikely since deacetylation of the mammalian female inactive X chromosome occurs following a shift to late replication (Keohane *et al.*, 1994) (Section 1.4.8).

Finally, it might be the positioning of particular origins of replication within the nucleus that determine their timing of replication. Sites of replication have been demonstrated to be scattered throughout the nucleus during S-phase but with the bulk of replication at the periphery of the mammalian nucleus occurring during mid-S-phase (Nakayasu & Berezney, 1989; Kill *et* al., 1991; O'Keefe *et al.*, 1992). However, others have reported that chromatin at the periphery of the nucleus replicates in late S-phase (Fox *et* al., 1991; Hutchison, 1995). Ferreira *et al.* (1997) labelled a variety of mammalian cell types at defined stages of S-phase by pulse incorporation of halogenated deoxynucleotides and showed clear patterns in Chinese hamster fibroblasts in which late replicating DNA was peripherally located in the nucleus, proposing that late-replicating G-band regions were generally positioned there. Interestingly, this nuclear organisation was also determined in micronuclei which contain a variable chromosome number. In addition, this pattern of replication organisation was established in the presence of transcription and translation inhibitors, consistent with my observations of unaltered chromosome territory positioning in nuclei from cells treated with AD (Section 7.3) and suggesting that positioning is not an effect of active transcription.

9.5 New nuclear and chromosomal proteins

To study the nuclear positioning of different regions of genomic DNA it will be important to define further nuclear and chromosomal proteins.

To pursue biochemical approaches to the regulatory mechanisms involved in the assembly of chromatin and nuclei, *X.laevis* egg extracts have proved to be a valuable tool (Review: Almouzni & Wolffe, 1993). The manipulation of egg cell-free preparations through fractionation, depletion and supplementation has led to the identification of many new proteins and DNA sequences involved in chromosome structure. For example, the importance of SARs in chromosome structure was supported by the fact that the assembly of condensed chromosomes in *X.laevis* egg extracts was inhibited by the addition of proteins that bind to AT-rich DNA (Strick & Laemmli, 1995; Review: Swedlow & Hirano, 1996). The formation of nuclei *in vitro* is not restricted to *X.laevis* chromatin, and successful reconstitution has been obtained using human chromatin (Brown *et al.*, 1987).

Chapter 8 describes an attempt to use monoclonal antibody production to identify new chromosomal proteins. This approach was not successful and the reasons and suggested improvements for this strategy are discussed in Section 8.6.

A new and potentially very productive method of identifying new chromosomal and nuclear proteins involves the use of gene trap mutagenesis. When reporter constructs are transfected into cells in culture they potentially integrate randomly into each genome (Skarnes *et al.*, 1985). Tate *et al.* (personal communication), used a β-galactosidase reporter construct transfected into mouse embryonic stem cells. Screening for nuclear β-galactosidase enzyme activity by X-Gal staining was followed by further localisation of potentially interesting gene trap products, in nuclei and on metaphase chromosomes, by immunofluorescence with antibodies to β-galactosidase. Several novel chromosomal proteins, amongst other interesting nuclear proteins, have been identified and cloned and await further characterisation.

References

ABNEY, J.R., CUTLER, B., FILLBACH, M.L., AXELROD, D. & SCALETTAR, B.A. (1997). Chromatin dynamics in interphase nuclei and its implications for nuclear structure. *The Journal of Cell Biology* **137**, 1459-1468.

ADACHI, Y., KAS, E. & LAEMMLI, U.K. (1989). Preferential, co-operative binding of DNA topoisomerase II to scaffold-associated regions. *The EMBO Journal* **8**, 3997-4006.

ADACHI, Y., LUKE, M. & LAEMMLI, U.K. (1991). Chromosome assembly *in vitro*: Topoisomerase II is required for condensation. *Cell* **64**, 137-148.

ADACHI, Y. & LAEMMLI, U.K. (1992). Identification of nuclear pre-replicative centres poised for DNA synthesis in *Xenopus* egg extracts: Immunolocalisation study of replication protein A. *The Journal of Cell Biology* **119**, 1-15.

ADAMS, D.L. & HODGE, L.D. (1996). Postmetaphase nuclear formation: Loss of a chromosomal epitope coincident with apparent chromatid coalescence. *Chromosoma* **105**, 31-40.

ADOLPH, S., HAMEISTER, H. & SCHILDKRAUT, C.L. (1992). Molecular analysis of the aberrant replication banding pattern on chromosome 15 in murine T-cell lymphomas. *Chromosoma* **101**, 388-398.

ALFONSO, P.J., CRIPPA, M.P., HAYES, J.J. & BUSTIN, M. (1994). The footprint of chromosomal proteins HMG-14 and HMG-17 on chromatin subunits. *Journal of Molecular Biology* **236**, 189-198.

ALKEMA, M.J., BRONK, M., VERHOEVE, E., OTTE, A., VAN 'T VEER, L.J., BERNS, A. & VAN LOHUIZEN, M. (1997). Identification of Bmi1-interacting proteins as constituents of a multimeric mammalian *Polycomb* complex. *Genes and Development* **11**, 226-240.

ALLSHIRE, R.C., JAVERZAT, J.-P., REDHEAD, N.J. & CRANSTON, G. (1994). Position effect variegation at fission yeast centromeres. *Cell* **76**, 157-169.

ALLSHIRE, R.C., NIMMO, E.R., JAVERZAT, J.-P. & CRANSTON, G. (1995). Mutations de-repressing silent centromeric domains in fission yeast disrupt chromosome segregation. *Genes and Development* **9**, 218-233.

ALMOUZNI, G. & WOLFFE, A.P. (1993). Nuclear assembly, structure, and function: The use of *Xenopus in vitro* systems. *Experimental Cell Research* **205**, 1-15.

AL-SHAWI, R., KINNAIRD, J., BURKE, J. & BISHOP, J.O. (1990). Expression of a foreign gene in a line of transgenic mice is modulated by a chromosomal position effect. *Molecular and Cellular Biology* **10**, 1192-1198.

AMATI, B.B. & GASSER, S.M. (1988). Chromosomal ARS and CEN elements bind specifically to the yeast nuclear scaffold. *Cell* **54**, 967-978.

AMATI, B. & GASSER, S.M. (1990). *Drosophila* scaffold-attached regions bind nuclear scaffolds and can function as ARS elements in both budding and fission yeasts. *Molecular and Cellular Biology* **10**, 5442-5454.

AMBROS, P.F. & SUMNER, A.T. (1987). Correlation of pachytene chromomeres and metaphase bands of human chromosomes, and distinctive properties of telomeric regions. *Cytogenetic and Cell Genetics* **44**, 223-228.

ANDREASSEN, P.R., LACROIX, F.B. & MARGOLIS, R.L. (1997). Chromosomes with two intact axial cores are induced by G2 checkpoint override: Evidence that DNA decatenation is not required to template the chromosome structure. *The Journal of Cell Biology* **136**, 29-43.

ANRADE, L.E.C., CHAN, E.K.L., RASKA, I., PEEBLES, C.L., ROOS, G. & TAN, E.M. (1991). Human autoantibody to a novel protein of the nuclear coiled body: Immunological characterisation and cDNA cloning of p80-coilin. *Journal of Experimental Medicine* **173**, 1407-1419.

ANTEQUERA, F. & BIRD, A.P. (1993). Number of CpG-islands and genes in man and mouse. *Proceedings of the National Academy of Sciences U.S.A.* **90**, 11995-11998.

ANTEQUERA, F., MACLEOD, D. & BIRD, A.P. (1989). Specific protection of methylated CpGs in mammalian nuclei. *Cell* **58**, 509-517.

APARICIO, O.M., BILLINGTON, B.L. & GOTTSCHLING, D.E. (1991). Modifiers of position effect are shared between telomeric and silent mating-type loci in *S.cerevisiae*. *Cell* **66**, 1279-1287.

AQUILES SANCHEZ, J., KARNI, R.J. & WANGH, L.J. (1997). Fluorescent *in situ* hybridisation (FISH) analysis of the relationship between chromosome location and the nuclear morphology in human neutrophils. *Chromosoma* **106**, 168-177.

ARKHIPOVA, I., LI, J. & MESELSON, M. (1997). On the mode of gene-dosage compensation in *Drosophila*. *Genetics* **145**, 729-736.

ARRIGHI, F.E. & HSU, T.C. (1971). Localisation of heterochromatin in human chromosomes. *Cytogenetics* **10**, 81-86.

ARVEILIER, B. & PORTEOUS, D.J. (1992). Distribution of *Alu* and *L1* repeats in human YAC recombinants. *Mammalian Genome* **3**, 661-668.

ASCOLI, C.A. & MAUL, G.G. (1991). Identification of a novel nuclear domain. *The Journal of Cell Biology* **112**, 785-795.

ASHLEY, T. (1988). G-band position effects on meiotic synapsis and crossing over. *Genetics* **118**, 307-317.

AVIVI, L. & FELDMAN, M. (1980). Arrangement of chromosomes in the interphase nucleus of plants. *Human Genetics* **55**, 281-295.

BAGGA, R. & EMERSON, B.M. (1997). An HMG I/Y-containing repressor complex and supercoiled DNA topology are critical for long-range enhancer-dependent transcription *in vitro*. *Genes and Development* **11**, 629-639.

BALDINI, A. & WARD, D.C. (1991). *In situ* hybridisation banding of human chromosomes with *Alu*-PCR products: A simultaneous karyotype for gene mapping studies. *Genomics* **9**, 770-774.

BALL, D.J., GROSS, D.S. & GARRARD, W.T. (1983). 5-Methylcytosine is localised in nucleosomes that contain histone H1. *Proceedings of the National Academy of Sciences U.S.A.* **80**, 5490-5494.

BALL, L.J., MURZINA, N.V., BROADHURST, R.W., RAINE, A.R.C., ARCHER, S.J., STOTT, F.J., MURZIN, A.G., SINGH, P.B., DOMAILLE, P.J. & LAUE, E.D. (1997). Structure of the chromatin binding (chromo) domain from mouse modifier protein 1. *The EMBO Journal* **16**, 2473-2481.

BANNISTER, A.J. & KOUZARIDES, T. (1996). The CBP co-activator is a histone acetyltransferase. *Nature* **384**, 641-643.

BARBIN, A., MONTPELLIER, C., KOKALJ-VOKAC, N., GIBAUD, A., NIVELEAU, A., MALFOY, B., DUTRILLAUX, B. & BOURGEOIS, C.A. (1994). New sites of methylcytosine-rich DNA detected on metaphase chromosomes. *Human Genetics* **94**, 684-692.

BARNES, T.M., KOHARA, Y., COULSON, A. & HEKIMI, S. (1995). Meiotic recombination, noncoding DNA and genomic organisation in *Caenorhabditis elegans*. *Genetics* **141**, 159-179.

BARR, M.L. & BERTRAM, E.G. (1949). A morphological distinction between neurones of the male and female, and the behaviour of the nucleolar satellite during accelerated nucleoprotein synthesis. *Nature* **163**, 676-677.

BARRIOS, L., MIRO, R., CABALLIN, M.R., FUSTER, C., GUEDEA, F., SUBIAS, A. & EGOZCUE, J. (1989). Cytogenetic effects of radiotherapy: Breakpoint distribution in induced chromosome aberrations. *Cancer Genetics and Cytogenetics* **41**, 61-70.

BARTHOLDI, M.F. (1991). Nuclear distribution of centromeres during the cell cycle of human diploid fibroblasts. *Journal of Cell Science* **99**, 255-263.

BARTOLOME, S., BERMUDEZ, A. & DABAN, J. (1994). Internal structure of the 30nm chromatin fibre. *Journal of Cell Science* **107**, 2983-2992.

BASHAW, G.J. & BAKER, B.S. (1995). The *msl-2* dosage compensation gene of *Drosophila* encodes a putative DNA-binding protein whose expression is sex specifically regulated by *Sex-lethal*. *Development* **121**, 3245-3258.

BASHAW, G.J. & BAKER, B.S. (1996). Dosage compensation and chromatin structure in *Drosophila*. *Current Opinion in Genetics and Development* **6**, 496-501.

BAUMGARTNER, M., DUTRILLAUX, B., LEMIEUX, N., LILIENBAUM, A., PUALIN, D. & VIEGAS-PEQUIGNOT, E. (1991). Genes occupy a fixed and symmetrical position on sister chromatids. *Cell* **64**, 761-766.

BAZETT-JONES, D.P., LEBLANC, B., HERFORT, M. & MOSS, T. (1994). Short-range DNA looping by the *Xenopus* HMG-box transcription factor, xUBF. *Science* **264**, 1134-1137.

BEARD, C., LI, E. & JAENISCH, R. (1995). Loss of methylation activates *Xist* in somatic but not in embryonic cells. *Genes and Development* **9**, 2325-2334.

BEDELL, M.A., JENKINS, N.A. & COPELAND, N.C. (1996). Good genes in bad neighbourhoods. *Nature Genetics* **12**, 229-232.

BEDNAR, J., HOROWITZ, R.A., DUBOCHET, J. & WOODCOCK, C.L. (1995). Chromatin confirmation and salt-induced compaction: Three-dimensional structural information from cryoelectron microscopy. *The Journal of Cell Biology* **131**, 1365-1376.

BELMONT, A.S., BRAUNFELD, M.B., SEDAT, J.W. & AGARD, D.A. (1989). Large-scale chromatin structural domains within mitotic and interphase chromosomes *in vivo* and *in vitro*. *Chromosoma* **98**, 129-143.

BELMONT, A.S., BIGONE, F. & TS'O, P.O.P. (1986). The relative intranuclear positions of Barr bodies in XXX non-transformed human fibroblasts. *Experimental Cell Research* **165**, 165-179.

BELMONT, A.S. & BRUCE, K. (1994). Visualisation of G1 chromosomes: A folded, twisted, supercoiled chromonema model of interphase chromatid structure. *The Journal of Cell Biology* **127**, 287-302.

BELMONT, A.S., ZHAI, Y. & THILENIUS, A. (1993). Lamin B distribution and association with peripheral chromatin revealed by optical sectioning and electron microscopy tomography. *The Journal of Cell Biology* **123**, 1671-1685.

BELYAEV, N.D., KEOHANE, A.M. & TURNER, B.M. (1996). Differential underacetylation of histones H2A, H3 and H4 on the inactive X chromosome in human female cells. *Human Genetics* **97**, 573-578.

BEREZNEY, R. & BUCHHOLTZ, L.A. (1981). Dynamic association of replicating DNA fragments with the nuclear matrix of regenerating liver. *Experimental Cell Research* **132**, 1-13.

BERNARDI, G. (1989). The isochore organisation of the human genome. *Annual Review of Genetics* **23**, 637-661.

BERNARDI, G., OLOFSSON, B., FILIPSKI, J., ZERIAL, M., SALINAS, J., CUNY, G., MEUNIER-ROTIVAL, M. & RODIER, F. (1985). The mosaic genome of warm-blooded vertebrates. *Science* **228**, 953-958.

BERNARDINO, J., LAMOLIATTE, E., LOMBARD, M., NIVELEAU, A., MALFOY, B., DUTRILLAUX, B. & BOURGEOIS, C.A. (1996). DNA methylation of the X chromosomes of the human female: An *in situ* semi-quantitative analysis. *Chromosoma* **104**, 528-535.

BESTOR, T.H. & COXON, A. (1993). The pros and cons of DNA methylation. *Current Biology* **3**, 384-386.

BHAT, M.A., PHILIP, A.V., GLOVER, D.M. & BELLEN, H.J. (1996). Chromatid segregation at anaphase requires the *barren* product, a novel chromosome-associated protein that interacts with topisomerase II. *Cell* **87**, 1103-1114.

BIANCHI, M.E. & LILLEY, D.M. (1995). Applying a genetic cantilever. *Nature* **375**, 532.

BICKMORE, W.A. & BIRD, A.P. (1992). Use of restriction endonucleases to detect and isolate genes from mammalian cells. *Methods in Enzymology* **216**, 224-244.

BICKMORE, W. & CRAIG, J. (1997). *Chromosome bands: Patterns in the genome*. Texas: R.G. Landes Company.

BICKMORE, W.A. & OGHENE, K. (1996). Visualising the spatial relationships between defined DNA sequences and the axial region of extracted metaphase chromosomes. *Cell* **84**, 95-104.

BICKMORE, W.A. & SUMNER, A.T. (1989). Mammalian chromosome banding: An expression of genome organisation. *Trends in Genetics* **5**, 144-148.

BILAUD, T., BRUN, C., ANCELIN, K., KOERING, C.E., LAROCHE, T. & GILSON, E. (1997). Telomeric localisation of TRF2, a novel human telobox protein. *Nature Genetics* **17**, 256-239.

BIRD, A.P. (1987). CpG-islands as gene markers in the vertebrate nucleus. *Trends in Genetics* **3**, 342-347.

BIRD, A.P. (1992). The essentials of DNA methylation. *Cell* **70**, 5-8.

BIRD, A.P. (1994). Functions for DNA methylation in vertebrates. *Cold Spring Harbour Symposia on Quantitative Biology* **LVIII**, 281-285.

BIRD, A.P. (1995). Gene number, noise reduction and biological complexity. *Trends in Genetics* **11**, 94-100.

BIRD, A.P. & TAGGART, M.H. (1980). Variable patterns of total DNA and rDNA methylation in animals. *Nucleic Acids Research* **8**, 1485-1497.

BIRD, A.P., TAGGART, M.H., FROMMER, M., MILLER, O.J. & MACLEOD, D. (1985). A fraction of the mouse genome that is derived from islands of non-methylated, CpG-rich DNA. *Cell* **40**, 91-99.

BIRD, A., TATE, P., NAN, X., CAMPOY, J., MEEHAN, R., CROSS, S., TWEEDIE, S., CHARLTON, J. & MACLEOD, D. (1995). Studies of DNA methylation in animals. *Journal of Cell Science Supplement* **19**, 37-39.

BISCHOFF, F.R., MAIER, G., TILZ, G. & POSTINGL, H. (1990). A 47KDa human nuclear protein recognised by anti-kinetochore autoimmune sera is homologous with the protein encoded by *RCC1*, a gene implicated in onset of chromosome condensation. *Proceedings of the National Academy of Sciences U.S.A.* **87**, 8617-8621.

BLASCO, M.A., LEE, H.-W., HANDE, M.P., SAMPER, E., LANSDORP, P.M., DEPINHO, R.A. & GREIDER, C.W. (1997). Telomere shortening and tumour formation by mouse cells lacking telomerase RNA. *Cell* **91**, 25-34.

BLOBEL, G. (1985). Gene gating: A hypothesis. *Proceedings of the National Academy of Sciences U.S.A.* **82**, 8527-8529.

BLOSE, S.H., MELTZER, D.I. & FERAMISCO, J.R. (1984). 10nm filaments are induced to collapse in living cells microinjected with monoclonal and polyclonal antibodies against tubulin. *The Journal of Cell Biology* **98**, 847-858.

BLUMENTHAL, A.B., DIEDEN, J.D., KAPP, L.N. & SEDAT, J.W. (1979). Rapid isolation of metaphase chromosomes containing high molecular weight DNA. *The Journal of Cell Biology* **81**, 255-259.

BLUMENTHAL, A.B., KRIESTEIN, H.J. & HOGNESS, D.S. (1974). The units of DNA replication in *Drosophila melanogaster* chromosomes. *Cold Spring Harbour Symposia in Quantitative Biology* **XXXVIII**, 205-224.

BOBROW, M. & HERITAGE, J. (1980). Non-random segregation of nucleolar organising chromosomes at mitosis? *Nature* **288**, 79-81.

BOFFA, L.C., GRUSS, R.J. & ALLFREY, V.G. (1981). Manifold effects of sodium butyrate on nuclear function. *The Journal of Biological Chemistry* **256**, 9612-9621.

BOFFA, L.C., MARIANI, M.R. & PARKER, M.I. (1994). Selective hypermethylation of transcribed nucleosomal DNA by sodium butyrate. *Experimental Cell Research* **211**, 420-423.

BOGGS, B.A., CONNORS, B., SOBEL, R.E., CHINAULT, A.C. & ALLIS, C.D. (1996). Reduced levels of histone H3 acetylation on the inactive X chromosome in human females. *Chromosoma* **105**, 303-309.

BOHMANN, K., FERREIRA, J.A. & LAMOND, A.I. (1995a). Mutational analysis of p80 coilin indicates a functional interaction between coiled bodies and the nucleolus. *The Journal of Cell Biology* **131**, 817-831.

BOHMANN, K., FERREIRA, J.A. SNATAMA, N., WEIS, K. & LAMOND, A.I. (1995b). Molecular analysis of the coiled body. *Journal of Cell Science Supplement* **19**, 107-113.

BONE, J.R. & KURODA, M.I. (1996). Dosage compensation regulatory proteins and the evolution of sex chromosomes in *Drosophila*. *Genetics* **144**, 705-713.

BONE, J.R., LAVENDER, J., RICHMAN, R., PALMER, M.J. & TURNER, B.M. (1994). Acetylated histone H4 on the male X chromosome is associated with dosage compensation in *Drosophila*. *Genes and Development* **8**, 96-104.

BOURGEOIS, C.A., DENNEBOUY, R., GIBAUD, A., GERBAULT-SEUREAU, B., MALFOY, B., SLODZIAN, G., GALLE, P. & DUTRILLAUX, B. (1996). Scanning ion analytic microscopy for high-resolution detection of 5-bromo-2'-deoxyuridine incorporation in metaphase chromosomes. *Chromosome Research* **4**, 574-582.

BOVERI, T. (1909). Die blastomerenkerne von ascaris megalocephala und die theorie der chromosomenindividualitat. *Arch Zellforsch* **3**, 181-268.

BOY DE LA TOUR, E. & LAEMMLI, U.K. (1988). The metaphase scaffold is helically folded: Sister chromatids have predominantly opposite helical handedness. *Cell* **55**, 937-944.

BOYES, J. & BIRD, A. (1991). DNA methylation inhibits transcription indirectly via a methyl-CpG binding protein. *Cell* **64**, 1123-1134.

BOYES, J. & BIRD, A. (1992). Repression of genes by DNA methylation depends on CpG density and promoter strength: Evidence for involvement of a methyl-CpG binding protein. *The EMBO Journal* **11**, 327-333.

BOYLE, A.L., BALLARD, S.G. & WARD, D.C. (1990). Differential distribution of long and short interspersed element sequences in the mouse genome: Chromosome karyotyping by fluorescence *in situ* hybridisation. *Proceedings of the National Academy of Sciences U.S.A.* **87**, 7757-7761.

BRADBURY, E.M. (1992). Reversible histone modifications and the chromosome cell cycle. *BioEssays* **14**, 9-16.

BRAUNSTEIN, M., ROSE, A.B., HOLMES, C.D. & BRAOCH, J.R. (1993). Transcriptional silencing in yeast is associated with reduced nucleosome acetylation. *Genes and Development* **7**, 592-604.

BRAUNSTEIN, M., SOBEL, R.E., ALLIS, C.D., TURNER, B.M. & BROACH, J.R. (1996). Efficient transcriptional silencing in *Saccharomyces cerevisiae* requires a heterochromatin histone acetylation pattern. *Molecular and Cellular Biology* **16**, 4349-4356.

BREEN, M., ARVELIER, B. MURRAY, I., GOSDEN, J.R. & PORTEOUS, D.J. (1992). YAC mapping by FISH using *Alu*-PCR-generated probes. *Genomics* **13**, 726-730.

BREGMAN, D.B., DU, L., VAN DER ZEE, S. & WARREN, S.L. (1995). Transcription-dependent redistribution of the large subunit of RNA polymerase II to discrete nuclear domains. *The Journal of Cell Biology* **129**, 287-298.

BRENEMAN, J.W., YAU, P., TEPLITZ, R.L. & BRADBURY, E.M. (1993). A light microscopic study of linker histone distribution in rat metaphase chromosomes and interphase nuclei. *Experimental Cell Research* **206**, 16-26.

BRIDGER, J.M., HERRMANN, H., MUNKEL, C. & LICHTER, P. (in press). Identification of an interchromosomal compartment by polymerisation of nuclear-targeted vimentin. *Journal of Cell Science*

BRIDGER, J.M., KILL, I.R. & LICHTER, P. (1997). Association of Ki-67 with satellite DNA of the human genome in early G1 cells. *Chromosome Research* **5**, 1-12.

BRIDGER, J.M., KILL, I.R., O'FARRELL, M. & HUTCHISON, C.J. (1993). Internal lamin structures within G1 nuclei of human dermal fibroblasts. *Journal of Cell Science* **104**, 297-306.

BROCCOLI, D. & COOKE, H.J. (1994). Effect of telomeres on the interphase location of adjacent regions of the human X chromosome. *Experimental Cell Research* **212**, 308-313.

BROCCOLI, D., SMOGORZEWSAKA, A., CHONG, L. & DE LANGE, T. (1997). Human telomeres contain two distinct myb-related proteins, TRF1 and TRF2. *Nature Genetics* **17**, 231-235.

BROWN, C.J., HENDRICH, B.D., RUPERT, J.L., LAFRENIERE, R.G., XING, Y., LAWRENCE, J. & WILLARD, H.F. (1992). The human *Xist* gene: Analysis of a 17Kb inactive X-specific RNA that contains conserved repeats and is highly localised within the nucleus. *Cell* **71**, 527-542.

BROWN, C.J. & WILLARD, H.F. (1994). The human X-inactivation centre is not required for maintenance of X chromosome inactivation. *Nature* **368**, 154-156.

BROWN, D.B., BLAKE, E.J., WOLGEMUTH, D.J., GORDON, K. & RUDDLE, F.H. (1987). Chromatin decondensation and DNA synthesis in human sperm activated *in vitro* by using *Xenopus laevis* egg extracts. *The Journal of Experimental Zoology* **242**, 215-231.

BROWN, D.T., ALEXANDER, B.T. & SITTMAN, D.B. (1996). Differential effect of H1 variant over-expression on cell cycle progression and gene expression. *Nucleic Acids Research* **24**, 486-493.

BROWNELL, J.E. & ALLIS, C.D. (1996). Special HATs for special occasions: Linking histone acetylation to chromatin assembly and gene activation. *Current Opinion in Genes and Development* **6**, 176-184.

BROWNELL, J.E., ZHOU, J., RANALLI, T., KOBAYASHI, R., EDMONDSON, D.G., ROTH, S.Y. & ALLIS, C.D. (1996). Tetrahymena histone acetylatransferase A: A homologue to yeast Gcn5p linking histone acetylation to gene activation. *Cell* **84**, 843-851.

BROWN, K.E., GUEST, S.S., SMALE, S.T., HAHM, K., MERKENSCHLAGER, M. & FISHER, A.G. (1997). Association of transcriptionally silent genes with Ikaros complexes at centromeric heterochromatin. *Cell* **91**, 845-854.

BRUNK, B.P., MARTIN, E.C. & ALDER, P.N. (1991). *Drosophila* genes *Posterior sex combs* and *Suppressor two of zeste* encode proteins with homology to the murine *bmi-1* oncogene. *Nature* **353**, 351-353.

BRYK, M., BANERJEE, M., MURPHY, M., KNUDSEN, K.E. & GARFINKEL, D.J. (1997). Transcriptional silencing of Ty1 elements in the RDN1 locus of yeast. *Genes and Development* **11**, 255-269.

BUONGIORNO-NARDELLI, M., MICHELI, G., CARRI, M.T. & MARILLEY, M. (1982). A relationship between replicon size and supercoiled loop domains in the eukaryotic genome. *Nature* **298**, 100-102.

BURKHOLDER, G.D., LATIMER, L.J.P. & LEE, J.S. (1988). Immunofluorescent staining of mammalian nuclei and chromosomes with a monoclonal antibody to triplex DNA. *Chromosoma* **97**, 185-192.

BURKHOLDER, G.D. & WEAVER, M.G. (1977). DNA-protein interactions and chromosome banding. *Experimental Cell Research* **110**, 251-262.

BUSTIN, M., LEHN, D.A. & LANDSMAN, D. (1990). Structural features of HMG chromosomal proteins and their genes. *Biochemica et Biophysica Acta* **1049**, 231-243.

BUYSE, M.L. (1990). *Birth Defects Encyclopaedia.* Massachucetts: Blackwell Scientific Publications Ltd. pp381-388.

BUTNER, K. & LO, C.W. (1986). Modulation of *tk* expression in mouse pericentric heterochromatin. *Molecular and Cellular Biology* **6**, 4440-4449.

CAIRNS, B.R., LORCH, Y., LI, Y., ZHANG, M., LACOMIS, L., ERDJUMENT-BROMAGE, H., TEMPEST, P., DU, J., LAURENT, B. & KORNBERG, R.D. (1996). RSC, an essential, abundant chromatin-remodelling complex. *Cell* **87**, 1249-1260.

CAIZERGUES-FERRER, M., MARIOTTINI, P., CURIE, C., LAPEYRE, B., GAS, N., AMALRIC, F. & AMALDI, F. (1989). Nucleolin from *Xenopus laevis*: cDNA cloning and expression during development. *Genes and Development* **3**, 324-333.

CALLAN, H.G. (1982). Lampbrush chromosomes. *Proceedings of the Royal Society of London B* **214**, 417-448.

CAMARGO, M. & CERVENKA, J. (1982). Patterns of DNA replication of human chromosomes. II. Replication map and replication model. *American Journal of Human Genetics* **34**, 757-780.

CAMPOY, F.J., MEEHAN, R.R., MCKAY, S., NIXON, J. & BIRD, A. (1995). Binding of histone H1 to DNA is indifferent to methylation at CpG sequences. *The Journal of Biological Chemistry* **270**, 26473-26481.

CANDAU, R., ZHOU, J., ALLIS, D.C. & BERGER, S.L. (1997). Histone acetylatransferase activity and interaction with ADA2 are critical for GCN5 function *in vivo*. *The EMBO Journal* **16**, 555-565.

CAPEL, J., MONTERO, L.M., MARTINEZ-ZAPATER, J.M. & SALINAS, J. (1993). Non-random distribution of transposable elements in the nuclear genome of plants. *Nucleic Acids Research* **21**, 2369-2373.

CARMO-FONSECA, M., PEPPERKOK, R., CARVALHO, M.T. & LAMOND, A. (1992). Transcription-dependent colocalisation of the U1, U2, U4/6, and U5 snRNPs in coiled bodies. *The Journal of Cell Biology* **117**, 1-14.

CARMO-FONSECA, M., PEPPERKOK, R., SPROAT, B.S., ANSORGE, W., SWANSON, M.S. & LAMOND, A.I. (1991a). *In vivo* detection of snRNP-rich organelles in the nuclei of mammalian cells. *The EMBO Journal* **10**, 1863-1873.

CARMO-FONSECA, M., TOLLERVEY, D., PEPPERKOK, R., BARABINO, S.M.L., MERDES, A., BRUNNER, C., ZAMORE, P.D., GREEN, M.R., HURT, E. & LAMOND, A.I. (1991b). Mammalian

nuclei contain foci which are highly enriched in components of the pre-mRNA slicing machinery. *The EMBO Journal* **10**, 195-206.

CARTER, K.C., BOWMAN, D., CARRINGTON, W., FOGARTY, K., MCNEIL, J.A., FAY, F.S. & LAWRENCE, J.B. (1993). A three-dimensional view of precursor messenger RNA metabolism within the mammalian nucleus. *Science* **259**, 1330-1335.

CASPERSSON, T., FARBER, S., FOLEY, G.E., KUDYNOWSKI, J., MODEST, E.J., SIMONSSON, E., WAGH, U. & ZECH, L. (1968). Chemical differentiation along metaphase chromosomes. *Experimental Cell Research* **49**, 219-222.

CASPERSSON, T., ZECH, L. & JOHANSSON, C. (1970). Differential binding of alkylating fluorochromes in human chromosomes. *Experimental Cell Research* **60**, 315-319.

CAVALLI, G., BACHMANN, D. & THOMA, F. (1996). Inactivation of topoisomerases affects transcription-dependent chromatin transitions in rDNA but not in a gene transcribed by RNA polymerase II. *The EMBO Journal* **15**, 590-597.

CHADEE, D.N., ALLIS, C.D., WRIGHT, J.A. & DAVIE, J.R. (1997). Histone H1b phosphorylation is dependent upon ongoing transcription and replication in normal and *ras*-transformed mouse fibroblasts. *The Journal of Biological Chemistry* **272**, 8113-8116.

CHALY, N., BLADON, T., SETTERFIELD, G., LITTLE, J.E., KAPLAN, J.G. & BROWN, D.L. (1984). Changes in distribution of nuclear matrix antigens during the mitotic cell cycle. *The Journal of Cell Biology* **99**, 661-671.

CHALY, N., CHAN, J. & BROWN, D.L. (1996). Organisation of DNA topoisomerase II isotypes during the cell cycle of human lymphocytes and HeLa cells. *Chromosome Research* **4**, 457-466.

CHARLIEU, J.-P., LARSSON, S., MIYAGAWA, K., VAN HEYNINGEN, V. & HASTIE, N.D. (1995). Does the Wilms' tumour suppressor gene, WT1, play roles in both splicing and transcription? *Journal of Cell Science Supplement* **19**, 95-99.

CHAUDHARY, N. & COURVALIN, J.-C. (1993). Stepwise reassembly of the nuclear envelope at the end of mitosis. *The Journal of Cell Biology* **122**, 295-306.

CHEN, E.Y., LIAO, Y.-C., SMITH, D.H., BARRERA-SALDANA, H.A., GELINAS, R.E. & SEEBURG, P.H. (1989). The hormone growth locus: Nucleotide sequence, biology and evolution. *Genomics* **4**, 479-497.

CHEN, T.L. & MANUELIDIS, L. (1989). SINEs and LINEs cluster in distinct DNA fragments of Giemsa band size. *Chromosoma* **98**, 309-316.

CHEN, W.Y., BAILEY, E.C., MCCUNE, S.L., DONG, J.-Y. & TOWNES, T.M. (1997). Reactivation of silenced, virally transcribed genes by inhibitors of histone deacetylase. *Proceedings of the National Academy of Sciences U.S.A.* **94**, 5798-5803.

CHOO, K.H. (1990). Role of acrocentric cen-pter satellite DNA in Robertsonian translocation and chromosomal non-disjunction. *Molecular and Biological Medicine* **7**, 437-449.

CHONG, L., VAN STEENSEL, B., BROCCOLI, D., ERDJUMENT-BROMAGE, H., HANISH, J., TEMPST, P. & DE LANGE, T. (1995). A human telomeric protein. *Science* **270**, 1663-1667.

CHRISTMAN, M.F., DIETRICH, F.S. & FINK, G.R. (1988). Mitotic recombination in the rDNA of *S.cerevisiae* is suppressed by the combined action of DNA topoisomerase I and II. *Cell* **55**, 413-425.

CHUANG, P., ALBERTSON, D.G. & MEYER, B.J. (1994). DPY-27: A chromosome condensation protein homologue that regulate *C.elegans* dosage compensation through association with the X chromosome. *Cell* **79**, 459-474.

CHUANG, P.-T., LIEB, J.D. & MEYER, B.J. (1996). Sex-specific assembly of a dosage compensation complex on the nematode X chromosome. *Science* **274**, 1736-1739.

CHUMAKOV, I. *et al.* (1992). Continuum of overlapping clones spanning the entire human chromosome 21q. *Nature* **359**, 380-387.

CIEJEK, E.M., TSAI, M.-J. & O'MALLEY, B.W. (1983). Actively transcribed genes are associated with the nuclear matrix. *Nature* **306**, 607-609.

CIVARDI, L., XIA, Y., EDWARDS, K.J., SCHNABLE, P.S. & NIKOLAU, B.J. (1994). The relationship between genetic and physical distances in the cloned *α1-sh2* interval of the *Zea mays* L. genome. *Proceedings of the National Academy of Sciences U.S.A.* **91**, 8268-8272.

CLAUSSEN, U., MAZUR, A. & RUBSTOV, N. (1994). Chromosomes are highly elastic and can be stretched. *Cytogenetics and Cell Genetics* **66**, 120-125.

CLEMSON, C.M., MCNEIL, J.A., WILLARD, H.F. & LAWRENCE, J.B. (1996). XIST RNA paints the inactive X chromosome at interphase: Evidence for a novel RNA involved in nuclear/chromosome structure. *The Journal of Cell Biology* **132**, 259-275.

COBB, J., REDDY, R.K., PARK, C. & HANDEL, M.A. (1997). Analysis of expression and function of topoisomerase I and II during meiosis in male mice. *Molecular reproduction and Development* **46**, 489-498.

COCKELL, M., PALLADINO, F., LAROCHE, T., KYRION, G., LIU, C., LUSTIG, A.J. & GASSER, S.M. (1995). The carboxy termini of Sir4 and Rap1 affect Sir3 localisation: Evidence for a multicomponent complex required for yeast telomeric silencing. *The Journal of Cell Biology* **129**, 909-924.

COCKERILL, P.N. & GARRARD, W.T. (1986). Chromosomal loop anchorage of the kappa immunoglobulin gene occurs next to the enhancer in a region containing topoisomerase II sites. *Cell* **44**, 273-282.

COLLAS, P., COURVALIN, J.-C. & POCCIA, D. (1996). Targeting of membranes to sea urchin sperm chromatin is mediated by a lamin B receptor-like integral membrane protein. *The Journal of Cell Biology* **135**, 1715-1726.

COMINGS, D.E. (1968). The rationale for an ordered arrangement of chromatin in the interphase nucleus. *American Journal of Human Genetics* **20**, 440-460.

COMINGS, D.E. (1980). Arrangement of chromatin in the nucleus. *Human Genetics* **53**, 131-143.

COMINGS, D.E., AVELINO, E., OKADA, T.A. & WYANDT, H.E. (1973). The mechanism of C- and G-banding of chromosomes. *Experimental Cell Research* **77**, 469-493.

COMINGS, D.E. & DRETS, M.E. (1976). Mechanisms of chromosome banding. IX. Are variations in DNA base composition adequate to account for Quinacrine, Hoechst 33258 and daunomycin banding? *Chromosoma* **56**, 199-211.

CONCONI, A., WIDMER, R.M., KOLLER, T. & SOGO, J.M. (1989). Two different chromatin structures coexist in ribosomal RNA genes throughout the cell cycle. *Cell* **57**, 753-761.

CONRAD-WEBB, H. & BUTOW, R.A. (1995). A polymerase switch in the synthesis of rRNA in *Saccharomyces cerevisiae*. *Molecular and Cellular Biology* **15**, 2420-2428.

COOK, P.R. (1984). A general method for preparing intact nuclear DNA. *The EMBO Journal* **3**, 1837-1842.

COOK, P.R. (1988). The nucleoskeleton: Artefact, passive framework or active site? *Journal of Cell Science* **90**, 1-6.

COOK, P.R. (1989). The nucleoskeleton and the topology of transcription. *European Journal of Biochemistry* **185**, 487-501.

COOK, P.R. (1991). The nucleoskeleton and the topology of replication. *Cell* **66**, 627-635.

COOK, P.R. (1994). RNA polymerase: Structural determinant of the chromatin loop and the chromosome. *BioEssays* **16**, 425-430.

COOK, P.R. (1995). A chromomeric model for nuclear and chromosome structure. *Journal of Cell Science* **108**, 2927-2935.

COOKE, C.A., BAZETT-JONES, D.P., EARNSHAW, W.C. & RATTNER, J.B. (1993). Mapping DNA within the mammalian kinetochore. *The Journal of Cell Biology* **120**, 1083-1091.

COOKE, C.A., BERNAT, R.L. & EARNSHAW, W.C. (1990). CENP-B: A major human centromere protein located beneath the kinetochore. *The Journal of Cell Biology* **110**, 1475-1488.

COOKE, C.A., HECK, M.M.S. & EARNSHAW, W.C. (1987). The inner centromere protein (INCENP) antigens: Movement from inner centromere to midbody during mitosis. *The Journal of Cell Biology* **105**, 2053-2067.

COOKE, H.J. & HINDLEY, J. (1979). Cloning of human satellite III DNA: Different components are on different chromosomes. *Nucleic Acids Research* **6**, 3177-3197.

COTE, J., QUINN, J., WORKMAN, J.L. & PETERSON, C.L. (1994). Stimulation of GAL4 derivative binding to nucleosomal DNA by yeast SWI/SNF complex. *Science* **265**, 53-60.

COUNTER, C.M., AVILION, A.A., LEFEUVRE, C.E., STEWART, N.G., GREIDER, C.W., HARLEY, C.B. & BACCHETTI, S. (1992). Telomere shortening associated with chromosome instability is arrested in immortal cells which express telomerase activity. *The EMBO Journal* **11**, 1921-1929.

COUSENS, L.S., GALLWITZ, D. & ALBERTS, B.M. (1979). Different accessibilities in chromatin to histone acetylase. *The Journal of Biological Chemistry* **254**, 1716-1723.

COVAULT, J. & CHALKLEY, R. (1980). The identification of distinct populations of acetylated histone. *The Journal of Biological Chemistry* **255**, 9110-9116.

COX, L.S. & LASKEY, R.A. (1991). DNA replication occurs at discrete sites in pseudonuclei assembled from purified DNA *in vitro*. *Cell* **66**, 271-275.

CRAIG, J.M. (1995). The functional significance of mammalian chromosome banding. PhD thesis, University of Edinburgh.

CRAIG, J.M. & BICKMORE, W.A. (1993). Chromosome bands: Flavours to savour. *BioEssays* **15**, 349-354.

CRAIG, J.M. & BICKMORE, W.A. (1994). The distribution of CpG-islands in mammalian chromosomes. *Nature Genetics* **7**, 376-382.

CRAIG, J.M., BOYLE, S., PERRY, P. & BICKMORE, W.A. (1997). Scaffold attachments within the human genome. *Journal of Cell Science* **110**, 2673-2682.

CREMER, T., CREMER, C., BAUMANN, H., LUEDTKE, E.K., SPERLING, K., TEUBER, V. & ZORN, C. (1982a). Rabl's model of the interphase chromosome arrangement tested in Chinese hamster cells by premature chromosome condensation and laser-UV-microbeam experiments. *Human Genetics* **60**, 46-56.

CREMER, T., CREMER, C., SCHNEIDER, T., BAUMANN, H., HENS, L. & KIRSCH-VOLDERS. M. (1982b). Analysis of chromosome positions in the interphase nucleus of Chinese hamster cells by laser-UV-microirradiation experiments. *Human Genetics* **62**, 201-209.

CREMER, T., KURZ, A., ZIRBEL, R., DIETZEL, S., RINKE, B., SCHROCK, E., SPEICHER, M.R., MATHIEU, U., JAUCH, A., EMMERICH, P., SCHERTHAN, H., REID, T., CREMER, C. & LICHTER, P. (1993). Role of chromosome territories in the functional compartmentalisation of the cell nucleus. *Cold Spring Harbour Symposia on Quantitative Biology* **LVIII**, 777-792.

CROSS, S.H. & BIRD, A.P. (1995). CpG-islands and genes. *Current Opinion in Genetics and Development* **5**, 309-414.

CROSS, S.H., CHARLTON, J.A., NAN, X. & BIRD, A.P. (1994). Purification of CpG-islands using a methylated DNA binding column. *Nature Genetics* **6**, 236-244.

CROSS, S.H., LEE, M., CLARK, V.H., CRAIG, J.M., BIRD, A.P. & BICKMORE, W.A. (1997a). The chromosomal distribution of CpG-islands in the mouse: Evidence for genome scrambling in the rodent lineage. *Genomics* **40**, 454-461.

CROSS, S.H., MEEHAN, R.R., NAN, X. & BIRD, A. (1997b). A component of the transcriptional repressor MeCP1 shares a motif with DNA methyltransferase and HRX proteins. *Nature Genetics* **16**, 256-259.

CSINK, A.K. & HENIKOFF, S. (1996). Genetic modification of heterochromatic association and nuclear organisation in *Drosophila*. *Nature* **381**, 529-531.

CZARNOTA, G.J. & OTTENSMEYER, F.P. (1996). Structural states of the nucleosome. *The Journal of Biological Chemistry* **271**, 3677-3683.

DAMMANN, R., LUCCHINI, R., KOLLER, T. & SOGO, J.M. (1995). Chromatin structures and transcription of rDNA in yeast *Saccharomyces cerevisiae*. *Nucleic Acids Research* **10**, 2331-2338.

DAMMANN, R., LUCCHINI, R., KOLLER, T. & SOGO, J.M. (1995). Transcription in the yeast rRNA gene locus: Distribution of active gene copies and chromatin structure of their flaking regulatory sequences. *Molecular and Cellular Biology* **15**, 5294-5303.

D'ANNA, I.A., GURLEY, L.R. & TOBEY, R.A. (1983). Extent of histone modifications and H1° content during cell cycle progression in the presence of butyrate. *Experimental Cell Research* **147**, 407-417.

DANES, S. (1996). Molecular analysis of chromosome 11 rearrangements in human anaridia. PhD thesis, University of Edinburgh.

DANIEL, M.T., KOKEN, M., ROMAGNE, O., BARBEY, S., BAZARBACHI, A., STADLER, M., GUILLEMIN, M.C., DEGOS, L., CHOMIENNE, C. & DE THE, H. (1993). PML protein expression in haematopoietic and acute promyelocytic leukemia cells. *Blood* **82**, 1858-1867.

DANTE, R., PERCY, M.E., BADINI, A., MARKOVIC, V.D., MILLER, D.A., ROCCHI, M., NIVELEAU, A. & MILLER, O.J. (1992). Methylation of the 5' flanking sequences of the ribosomal DNA in human cell lines and in human-hamster hybrid cell line. *Journal of Cellular Biochemistry* **50**, 357-362.

DASSO, M. (1993). RCC1 in the cell cycle: The regulator of chromosome condensation takes on new roles. *Trends in Biochemical Sciences* **18**, 96-101.

DAVIS, F.M. & RAO, P.N. (1982). Antibodies specific for mitotic human chromosomes. *Experimental Cell Research* **137**, 381-386.

DAVIS, F.M., TSAO, T.Y., FOWLER, S.K. & RAO, P.N. (1983). Monoclonal antibodies to mitotic cells. *Proceedings of the National Academy of Sciences, U.S.A.* **80**, 2926-2930.

DEITZEL, S.,JAUCH, A., KIENLE, D., QU, G., HOLTGREVE-GREZ, H., EILS, R., MUNKEL, C., BITTNER, M., MELTZER, P.S., TRENT, J.M. & CREMER, T. (1998). Separate and variably shaped chromosome arm domains are disclosed by chromosome arm painting in human cell nuclei. *Chromosome Research* **6**, 25-33.

DE GRAAF, A., VAN HEMERT, F., LINNEMANS, W.A.M., BRAKENHOFF, G.J., DE JONG, L., VAN RENSWOUDE, J. & VAN DRIEL, R. (1990). Three-dimensional distribution of DNAse I-sensitive chromatin regions in interphase nuclei of embryonal carcinoma cells. *European Journal of Cell Biology* **52**, 135-141.

DERNBURG, A.F., BROMAN, K.W., FUNG, J.C., MARSHALL, W.F., PHILIPS, J., AGARD, D.A. & SEDAT, J.W. (1996). Perturbation of nuclear architecture by long-distance chromosome interactions. *Cell* **85**, 745-759.

DE SARIO, A., GEIGL, E.-M., PALMIERI, G., D'URSO, M. & BERNARDI, G. (1996). A compositional map of human chromosome band Xq28. *Proceedings of the National Academy of Sciences U.S.A.* **93**, 1298-1302.

DICKINSON, L.A. & KOHWI-SHIGEMATSU, T. (1995). Nucleolin is a matrix region DNA-binding protein that specifically recognises a region with high base-unpairing potential. *Molecular and Cellular Biology* **15**, 456-465.

DIFFLEY, J.F.X., COCKER, J.H., DOWELL, S.J. & ROWLEY, A. (1994). Two steps in the assembly of complexes at yeast replication complexes. *Cell* **78**, 303-316.

DIJKWEL, P.A., WNINK, P.W. & PODDIGHE, J. (1986). Permanent attachment of replication origins to the nuclear matrix in BHK-cells. *Nucleic Acids Research* **14**, 3241-3249.

DIMITROV, S. & WOLFFE, A.P. (1996). Remodelling somatic nuclei in *Xenopus laevis* egg extracts: Molecular mechanisms for selective release of histones H1 and H1° from chromatin and the acquisition of transcriptional competence. *The EMBO Journal* **15**, 5897-5906.

DING, H.-F., BUSTIN, M. & HANSEN, U. (1997). Alleviation of histone H1-mediated transcriptional repression and chromatin compaction by the acidic activation region in chromosomal protein HMG-14. *Molecular and Cellular Biology* **17**, 5843-5855.

DISNEY, J.E., JOHNSON, K.R., MAGNUSON, N.S., SYLVESTER, S.R. & REEVES, R. (1989). High-mobility group protein HMG-I localises to G/Q - and C-bands of human and mouse chromosomes. *The Journal of Cell Biology* **109**, 1975-1982.

DOBIE, K., LEE, M., FANTES, J.A., GRAHAM, E., CLARK, A.J., SPRINGBETT, A., LATHE, R. & MCCLENAGHAN, M. (1996). Variegated transgene expression in mouse mammary gland is determined by transgene integration locus. *Proceedings of the National Academy of Sciences U.S.A.* **93**, 6659-6664.

DOWNES, C.S., RYAN, A.J. & JOHNSON, R.T. (1993). Fine tuning of DNA repair in transcribed genes: Mechanisms, prevalence and consequences. *BioEssays* **15**, 209-216.

DREESEN, T.D., HENIKOFF, S., LOUGHNEY, K. (1991). A pairing-sensitive element that mediates *trans*-inactivation is associated with the *Drosophila brown* gene. *Genes and Development* **5**, 331-340.

DREYFUSS, G., MATUNIS, M.J., PINOL-ROMA, S. & BURD, C.G. (1993). hnRNP proteins and the biogenesis of mRNA. *Annual Review of Biochemistry* **62**, 289-321.

DROUIN, R. & HOLMQUIST, G.P. (1994). High-resolution replication bands compared with morphological G- and R-bands. *Advances in Human Genetics* **22**, 47-115.

DROUIN, R., LEMIEUX, N. & RICHER, C.L. (1991). Chromosome condensation from prophase to late metaphase: Relationship to chromosome bands and their replication time. *Cytogenetics and Cell Genetics* **57**, 91-99.

DROUIN, R. & RICHER, C.-L. (1988). High-resolution R-banding at the 1250-band level. II. Schematic representation and nomenclature of human RBG-banded chromosomes. *Genome* **32**, 425-439.

DUTRILLAUX, B. (1978). Nouveau systeme de marquage chromosomique: Les bandes T. *Chromosoma* **41**, 395-401.

DUTRILLAUX, B., COUTURIER, J., RICHER, C.-L. & VIEGAS-PEQUIGNOT, E. (1976). Sequence of DNA replication in 277 R- and Q-bands of human chromosomes using a BrdU treatment. *Chromosoma* **58**, 51-61.

DUTRILLAUX, B. & LEJEUNE, D (1971). Sur une nouvelle technique d'analysis du caryotype humain. *C. R. Acad. Sci. Paris Ser.* **272**, 2638-2640.

DYER, K.A., CANFIELD, T.K. & GARTLER, S.M. (1989). Molecular cytological differentiation of active from inactive X domains in interphase: Implications for X chromosome inactivation. *Cytogenetics and Cell Genetics* **50**, 116-120.

EARNSHAW, W.C. (1988). Mitotic chromosome structure. *BioEssays* **9**, 147-150.

EARNSHAW, W.C. & BERNAT, R.L. (1991). Chromosomal passengers: Toward an integrated view of mitosis. *Chromosoma* **100**, 139-146.

EARNSHAW, W.C. & HECK, M.M.S. (1985). Localisation of topoisomerase II in mitotic chromosomes. *The Journal of Cell Biology* **100**, 1716-1725.

EARNSHAW, W.C. & LAEMMLI, U.K. (1983). Architecture of metaphase chromosomes and chromosome scaffolds. *The Journal of Cell Biology* **96**, 84-93.

EARNSHAW, W.C., HALLIGAN, B., COOKE, C.A., HECK, M.M.S. &LIU, L.F. (1985). Topoisomerase II is a structural component of mitotic scaffolds. *The Journal of Cell Biology* **100**, 1706-1715.

EARNSHAW, W.C. & ROTHFIELD, N. (1985). Identification of a family of human centromere proteins using autoimmune sera from patients with scleroderma. *Chromosoma* **91**, 313-321.

EARNSHAW, W.C., SULLIVAN, K.F., MACHLIN, P.S., COOKE, C.A., KAISER, D.A., POLLARD, T.D., ROTHFIELD, N.F. & CLEVELAND, D.W. (1987). Molecular cloning of cDNA for CENP-B, the major human centromere autoantigen. *The Journal of Cell Biology* **104**, 817-829.

ECKLEY, D.M., AINSZTEIN, A.M., MACKAY, A.M., GOLDBERG, I.G. & ERNSHAW, W.C. (1997). Chromosomal proteins and cytokinesis: Patterns of cleavage furrow formation and inner centromere protein positioning in mitotic heterokaryons and mid-anaphase cells. *The Journal of Cell Biology* **136**, 1169-1183.

EDEN, S. & CEDAR, H. (1994). Role of DNA methylation in the regulation of transcription. *Current Opinion in Genetics and Development* **4**, 255-259.

EDMONDSON, D.G., SMITH, M.M. & ROTH, S.Y. (1996). Repression domain of the yeast global repressor *Tup1* interacts directly with histones H3 and H4. *Genes and Development* **10**, 1247-1259.

EDWARDS, A., VOSS, H., RICE, P., CIVITELLO, A., STEGEMANN, J., SCHWAGER, C., ZIMMERMANN, J., ERFLE, H., CASKEY, C.T. & ANGORGE, W. (1990). Automated DNA sequencing of the human HPRT locus. *Genomics* **6**, 593-608.

EFSTRADIADIS, A. (1994). Parental imprinting of autosomal mammalian genes. *Current Opinion in Genetics and Development* **4**, 265-280.

EILS, R., DIETZL, S., BERTIN, E., SCHORCK, E., SPEICHER, M.R., REID, T., ROBERT-NICOUD, M., CREMER, C. & CREMER, T. (1996). Three-dimensional reconstruction of painted human interphase chromosomes: Active and inactive X chromosome territories have similar volumes but differ in shape and surface structure. *The Journal of Cell Biology* **135**, 1427-1440.

EISSENBERG, J.C., MORRIS, G.D., REUTER, G. & HARTNETT, T. (1992). The heterochromatin-associated protein HP-1 is an essential protein in *Drosophila* with dosage-dependent effects on position-effect variegation. *Genetics* **131**, 345-352.

EKWALL, K., OLSSON, T., TURNER, B.M., CRANSTON, G. & ALLSHIRE, R.C. (1997). Transient inhibition of histone deacetylation alters the structural and functional imprint at fission yeast centromeres. *Cell* **91**, 1021-1032.

ELGIN, S.C.R. (1996). Heterochromatin and gene regulation in *Drosophila*. *Current Opinion in Genetics and Development* **6**, 193-202.

ELLENBERG, J., SIGGIA, E.D., MOREIRA, J.E., SMITH, C.L., PRESLEY, J.F., WORMAN, H.J. & LIPPINCOTT-SCHWARTZ, J. (1997). Nuclear membrane dynamics and reassmbley in living cells: Targeting of an inner nuclear membrane protein in interphase and mitosis. *The Journal of Cell Biology* **138**, 1193-1206.

ELLIS, D.J., JENKINS, H., WHITFIELD, W.G.F. & HUTCHISON, C.J. (1997). GST-lamin fusion proteins act as dominant negative mutants in *Xenopus* egg extract and reveal the function of the lamina in DNA replication. *Journal of Cell Science* **110**, 2507-2518.

ELLIS, N.A., GRODEN, J., YE, T.-Z., STRAUGHEN, J., LENNON, D.J., CIOCCI, S., PROYTCHEVA, M. & GERMAN, J. (1995). The Bloom's Syndrome gene product is homologous to RecQ helicases. *Cell* **83**, 655-666.

EPNER, E., KIM, C.G. & GROUDINE, M. (1992). What does the locus control region control? *Current Biology* **5**, 262-264.

EYRE-WALKER, A. (1993). Recombination and mammalian genome evolution. *Proceedings of the Royal Society of London B* **252**, 237-243.

FAKAN, S. (1994). Perichromatin fibrils are *in situ* forms of nascent transcripts. *Trends in Cell Biology* **4**, 86-90.

FAKAN, S., LESER, G. & MARTIN, T.E. (1984). Ultrastructural distribution of nuclear ribonucleoproteins as visualised by immunocytochemistry on thin sections. *The Journal of Cell Biology* **98**, 358-363.

FALCIOLA, L., SPADA, F., CALOGERO, S., LANGST, G., VOIT, R., GRUMMT, I. & BIANCHI, M.E. (1997). High mobility group 1 protein is not stably associated with the chromosomes of somatic cells. *The Journal of Cell Biology* **137**, 19-26.

FALVO, J.V., THANOS, D. & MANIATIS, T. (1995). Reversal of intrinsic DNA bends in the IFNβ gene enhancer by transcription factors and the architectural protein HMGI(Y). *Cell* **83**, 1101-1111.

FANG, J.S. & JAGIELLO, G.M. (1988). An analysis of the chromomere map and chiasmata characteristics of human diplotene spermatocytes. *Cytogenetics and Cell Genetics* **47**, 52-57.

FANTES, J.A., BICKMORE, W.A., FLETCHER, J.M., BALLESTA, F., HANSON, I.M. & VAN HEYNINGEN, V. (1992). Submicroscopic deletions at the WAGR locus, revealed by nonradioactive *in situ* hybridisation. *American Journal of Human Genetics* **51**, 1286-1294.

FANTES, J.A., GREEN, D.K. & COOKE, H.J. (1983). Purifying human Y chromosomes by flow cytometry and sorting. *Cytometry* **4**, 88-91.

FANTES, J., REDEKER, B., BREEN, M., BOYLE, S., BROWN, J., FLETCHER, J., JONES, S., BICKMORE, W., FUKUSHIMA, Y., MANNENS, M., DANES, S., VAN HEYNINGEN, V. & HANSON, I. (1995). Anaridia-associated cytogenetic rearrangements suggest that a position effect may cause the mutant phenotype. *Human Molecular Genetics* **4**, 415-422.

FAY, F.S., TANEJA, K.L., SHENOY, S., LIFSHITZ, L. & SINGER, R.H. (1997). Quantitative digital analysis of diffuse and concentrated nuclear distributions of nascent transcripts, SC35 and poly(A). *Experimental Cell Research* **231**, 27-37.

FELSENFIELD, G. (1992). Chromatin as an essential part of the transcriptional mechanism. *Nature* **355**, 219-224.

FERGUSON, M. & WARD, D.C. (1992). Cell cycle dependent chromosomal movement in pre-mitotic human T-lymphocyte nuclei. *Chromosoma* **101**, 557-565.

FERGUSON-SMITH, M.A. & HANDMAKER, S.D. (1961). Observations on the satellited human chromosomes. *The Lancet* **1**, 638-640.

FERRARO, M., PREDAZZI, V. & PRANTERA, G. (1993). In human chromosomes telomeric regions are enriched in CpGs relative to R-bands. *Chromosoma* **102**, 712-717.

FERREIRA, J., PAOLELLA, G., RAMOS, C. & LAMOND, A.I. (1997). Spatial organisation of large-scale chromatin domains in the nucleus: A magnified view of single chromosome territories. *The Journal of Cell Biology* **139**, 1597-1610.

FESTENSTEIN, R., TOLAINI, M., CORBELLA, P., MAMALAKI, C., PARRINGTON, J., FOX, M., MILIOU, A., JONES, M. & KIOUSSIS, D. (1996). Locus control region function and heterochromatin-induced position effect variegation. *Science* **271**, 1123-1125.

FETNI, R., DROUIN, R., RICHER, C.-L., LEMIEUX, N. (1996). Complementary replication R- and G-band patterns induced by cell blocking at the R-band/G-band transition, a possible regulatory checkpoint within the S phase of the cell cycle. *Cytogenetics and Cell Genetics* **75**, 172-179.

FILIPSKI, J., LEBLANC, J., YOUDALE, T., SIKORSKA, M. & WALKER, P.R. (1990). Periodicity of DNA folding in higher order chromatin structures. *The EMBO Journal* **9**, 1319-1327.

FINCH, J.T. & KLUG, A. (1976). Solenoidal model for superstructure in chromatin. *Proceedings of the National Academy of Sciences* **73**, 1897-1901.

FISCHER, U., LIU, Q. & DREYFUSS, G. (1997). The SMN-SIP1 complex has an essential role in spliceosomal snRNP biogenesis. *Cell* **90**, 1023-1029.

FOLLE, G.A., BOCCARDO, E. & OBE, G. (1997). Localisation of chromosome breakpoints induced by DNAse I in Chinese hamster ovary cells. *Chromosoma* **106**, 391-399.

FOX, C.A., EHRENHOFER-MURRAY, A.E., LOO, S. & RINE, J. (1997). The origin recognition complex, SIR1, and the S-phase requirement for silencing. *Science* **276**, 1547-1551.

FOX, C.A., LOO, S., DILLIN, A. & RINE, J. (1995). The origin recognition complex has essential functions in transcriptional silencing and chromosomal replication. *Genes and Development* **9**, 911-924.

FOX, M.H., ARNDT-JOVIN, D.J., JOVIN, T.M., BAUMANN, P.H. & ROBERT-NICOUD, M. (1991). Spatial and temporal distribution of DNA replication sites localised by immunofluorescence and confocal microscopy in mouse fibroblasts. *Journal of Cell Science* **99**, 247-253.

FRANCKE, U. (1994). Digitised and differentially shaded human chromosome ideograms for genomic applications. *Cytogenetics and Cell Genetics* **65**, 206-219.

FREEMAN, L., KURUMIZAKA, H. & WOLFFE, A.P. (1996). Functional domains for assembly of histones H3 and H4 into the chromatin of *Xenopus* embryos. *Proceedings of the National Academy of Sciences U.S.A.* **93**, 12780-12785.

FREEMONT, P.S. (1993). The RING finger: A novel protein sequence motif related to the zinc finger. *Annals of the New York Academy of Science* 174-192.

FRICKER, M., HOLLINSHEAD, M., WHITE, N. & VAUX, D. (1997). Interphase nuclei of many mammalian cell types contain deep, dynamic, tubular membrane-bound invaginations of the nuclear envelope. *The Journal of Cell Biology* **136**, 531-544.

FRIEDMANN, M., HOLTH, L.T., ZOGHBI, H.Y. & REEVES, R. (1993). Organisation, indelible-expression and chromosome localisation of the human HMG-I(Y) non-histone protein gene. *Nucleic Acids Research* **21**, 4259-4267.

FRITZE, C.E., VERSCHUEREN, K., STRICH, R. & ESPOSITO, R.E. (1997). Direct evidence for SIR2 modulation of chromatin structure in yeast rDNA. *The EMBO Journal* **16**, 6495-6509.

FU, X.-D. & MANIATIS, T. (1990). Factor required for mammalian spliceosome assembly is localised to discrete regions in the nucleus. *Nature* **343**, 437-441.

FURUKAWA, K., PANTE, N., AEBI, U. & GERACE, L. (1995). Cloning of a cDNA for lamin-associated polypeptide 2 (LAP2) and identification of regions that specify targeting to the nuclear envelope. *The EMBO Journal* **14**, 1626-1636.

FUSCOE, J.C., MCNICH, J.S., COLLINS, C.C. & VAN DILLA, M.A. (1989). Human chromosome-specific DNA libraries: Construction and purity analysis. *Cytogenetics and Cell Genetics* **50**, 211-215.

FUSSELL, C.P. (1975). The position of interphase chromosomes and late replicating DNA in centromere and telomere regions of *Allium cepa* L. *Chromosoma* **50**, 201-210.

GAILLARD, P.-H.L., MARTINI, E.M.-D., KAUFMAN, P.D., STILLMAN, B., MOUSTACCHI, E. & ALMOUZNI, G. (1996). Chromatin assembly coupled to DNA repair: A new role for chromatin assembly factor. *Cell* **86**, 887-896.

GANJU, R.K., PENKALA, J.E., WRIGHT, D.A., DAVIS, F.M. & RAO, P.N. (1992). MPM-12: A monoclonal antibody that predominantly stains mitotic cells and recognises a protein kinase. *European Journal of Cell Biology* **57**, 124-131.

GANNER, E. & EVANS, H.J. (1971). The relationship between patterns of DNA replication and of Quinacrine fluorescence in the human chromosome complement. *Chromosoma* **35**, 326-341.

GARCIA-RAMIREZ, M., ROCCHINI, C. & AUSIO, J. (1995). Modulation of chromatin folding by histone acetylation. *The Journal of Biological Chemistry* **270**, 17923-17928.

GARDINER, K. (1995). Human genome organisation. *Current Opinion in Genetics and Development* **5**, 315-322.

GARDINER, K. (1996). Base composition and gene distribution: Critical patterns in mammalian genome organisation. *Trends in Genetics* **12**, 519-524.

GARDINER, K., AISSANI, B. & BERNARDI, G. (1990). A compositional map of human chromosome 21. *The EMBO Journal* **9**, 1853-1858.

GARRICK, D., SUTHERLAND, H., ROBERTSON, G. & WHITELAW, E. (1996). Variegated expression of a globin transgene correlates with chromatin accessibility but not methylation status. *Nucleic Acids Research* **24**, 4902-4909.

GASSER, S.M., AMATI, B.B., CARDENAS, M.E. & HOFMANN, J.F.X. (1989). Studies on scaffold attachment sites and their relation to genome function. *International Review of Cytology* **119**, 57-96.

GASSER, S.M. & LAEMMLI, K.U. (1986). The organisation of chromatin loops: Characterisation of a scaffold attachment site. *The EMBO Journal* **5**, 511-518.

GASSER, S.M., LAROCHE, T., FALQUET, J., BOY DE LA TOUR, E. & LAEMMLI, U.K. (1986). Metaphase chromosome structure: Involvement of topoisomerase II. *Journal of Molecular Biology* **188**, 613-629.

GATTI, M. & PIMPINELLI, S. (1992). Functional elements in *Drosophila melanogaster* heterochromatin. *Annual review of Genetics* **26**, 239-275.

GAUTIER, T., DAUPHIN-VILLEMANT, C., ANDRE, C., MASSON, C., ARNOULT, J. & HERNANDEZ-VERDUN, D. (1992). Identification and characterisation of a new set of nucleolar ribonucleoproteins which line the chromosomes during mitosis. *Experimental Cell Research* **200**, 5-15.

GAZIT, B., CEDAR, H., LERER, I. & VOSS, R. (1982). Active genes are sensitive to deoxyribonuclease I during metaphase. *Science* **217**, 648-650.

GEORGAKOPOULOS, T. & THIREOS, G. (1992). Two distinct yeast transcriptional activators require the function of the GCN5 protein to promote normal levels of transcription. *The EMBO Journal* **11**, 4145-4152.

GEORGEL, P.T., TSUKIYAMA, T. & WU, C. (1997). Role of histone tails in nucleosome remodelling by *Drosophila* NURF. *The EMBO Journal* **16**, 4717-4726.

GERACE, L. & BURKE, B. (1988). Functional organisation of the nuclear envelope. *Annual Review of Cell Biology* **4**, 335-374.

GERACE, L. & FOISNER, R. (1994). Integral membrane proteins and dynamic organisation of the nuclear envelope. *Trends in Cell Biology* **4**, 127-131.

GERDES, J., LEMKE, H., BAISCH, H., WACKER, H.-H., SCHWAB, U. & STEIN, H. (1984). Cell cycle analysis of a cell proliferation-associated human nuclear antigen defined by the monoclonal antibody Ki-67. *The Journal of Immunology* **133**, 1710-1715.

GERDES, M.G., CARTER, K.C., MOEN, P.T.Jr. & LAWRENCE, J.B. (1994). Dynamic changes in the higher-level chromatin organisation of specific sequences revealed by *in situ* hybridisation to nuclear halos. *The Journal of Cell Biology* **126**, 289-304.

GEURTS VAN KESSEL, A.H.M., DEN BOER, W.C., VAN AGTHOVEN, A.J. & HAGEMEIJER, A. (1981). Decreased tumorgenisity of rodent cells after fusion with leukocytes from normal and leukaemic donors. *Somatic Cell Genetics* **7**, 645-656.

GHIDELLI, S., CLAUS, P., THIES, G. & WISNIEWSKI, J.R. (1997). High mobility group proteins cHMG1a, cHMG1b, and cHMGI are distinctly distributed in chromosomes and differentially expressed during ecdysone dependent cell differentiation. *Chromosoma* **105**, 369-379.

GILBERT, D.M., MIYAZAWA, H. & DEPAMPHILIS, M.L. (1995). Site-specific initiation of DNA replication in *Xenopus* egg extract requires nuclear structure. *Molecular and Cellular Biology* **15**, 2942-2954.

GILSON, E., LAROCHE, T. & GASSER, S. (1993). Telomeres and the functional architecture of the nucleus. *Trends in Cell Biology* **3**, 128-134.

GIMENEZ-ABIAN, J.F., CLARKE, D.J., MULLINGER, A.M., DOWNES, C.S. & JOHNSON, R.T. (1995). A post-prophase topoisomerase II-dependent chromatid core separation step in the formation of metaphase chromosomes. *The Journal of Cell Biology* **131**, 7-17.

GLASS, J.R. & GERACE, L. (1990). Lamins A and C bind and assemble at the surface of mitotic chromosomes. *The Journal of Cell Biology* **111**, 1047-1057.

GOLDERER, G. & GROBNER, P. (1991). ADP-ribosylation of core histones and their acetylated subspecies. *Biochemistry Journal* **277**, 607-610.

GOLDMAN, M.A. (1988). The chromatin domain as a unit of gene regulation. *BioEssays* **9**, 50-55.

GOLDMAN, M.A., HOLMQUIST, G.P., GRAY, M.C., CASTON, L.A. & NAG, A. (1984). Replication timing of gene and middle repetitive sequences. *Science* **224**, 686-692.

GOLDWAY, M., SHERMAN, A., ZENVIRTH, D., ARBEL, T. & SIMCHEN, G. (1993). A short chromosomal region with major roles in yeast chromosome III meiotic disjunction, recombination and double-strand breaks. *Genetics* **133**, 159-169.

GOLLIN, S.M., WRAY, W., HANKS, S.K., HITTELMAN, W.N. & RAO, P.N. (1984). The ultrastructural organisation of prematurely condensed chromosomes. *Journal of Cell Science Supplement* **1**, 203-221.

GOODRICH, J., PUANGSOMLEE, P., MARTIN, M., LONG, D., MEYEROWITZ, E.M. & COUPLAND, G. (1997). A *Polycomb*-group gene regulates homeotic gene expression in *Arabidopsis*. *Nature* **386**, 44-51.

GORMAN, M., FRANKE, A. & BAKER, B.S. (1995). Molecular characterisation of the *male-specific lethal-3* gene and investigations of the regulation of dosage compensation in *Drosophila*. *Development* **121**, 463-475.

GOSDEN, J.R., MITCHELL, A.R., BUCKLAND, R.A., CLAYTON, R.P. & EVANS, H.J. (1975). The location of four human satellite DNAs on the human chromosomes. *Experimental Cell Research* **92**, 148-158.

GOTTLEIB, S. & ESPOSITO, R.E. (1989). A new role for a yeast transcriptional silencer gene, SIR2, in regulation of recombination in ribosomal DNA. *Cell* **56**, 771-776.

GOTTA, M., LAROCHE, T., FORMENTON, A., MAILLET, L., SCHERTHAN, H. & GASSER, S.M. (1996). The clustering of telomeres and colocalisation with Rap1, Sir3 and Sir4 proteins in wild-type *Saccharomyces cerevisiae*. *The Journal of Cell Biology* **134**, 1349-1363.

GOTTA, M., STRAHL-BOLSINGER, S., RENAULD, H., LAROCHE, T., KENNEDY, B.K., GRUNSTEIN, M. & GASSER, S. (1997). Localisation of Sir2p: The nucleolus as a compartment for silent information regulators. *The EMBO Journal* **16**, 3243-3255.

GOTTSCHLING, D.E. (1992). Telomere-proximal DNA in *Saccharomyces cerevisiae* is refractory to methyltransferase activity *in vivo*. *Proceedings of the National Academy of Sciences U.S.A.* **89**, 4062-4065.

GOTTSCHLING, D.E., APARICIO, O.M., BILLINGTON, B.L. & ZAKIAN, V.A. (1990). Position effect at *S.cerevisiae* telomeres: Reversible repression of pol I transcription. *Cell* **63**, 751-762.

GOULD, A. (1997). Functions of mammalian *Polycomb* group and *trithorax* group related genes. *Current Opinion in Genetics and Development* **7**, 488-494.

GRANDE, M.A., VAN DER KRAAN, DE JONG, L. & VAN DRIEL, R. (1997). Nuclear distribution of transcription factors in relation to sites of transcription and RNA polymerase II. *Journal of Cell Science* **110**, 1781-1791.

GRANOK, H., LIEBOVITCH, B.A., SHAFFER, C.D. & ELGIN, S.C.R. (1995). Ga-ga over GAGA factor. *Current Biology* **5**, 238-241.

GREIG, G.M. & WILLARD, H.F. (1992). β-satellite DNA: Characterisation and localisation of two subfamilies from the distal and proximal short arms of the human acrocentric chromosomes. *Genomics* **12**, 573-580.

GROSS, D.S. & GARRARD, W.T. (1988). Nuclease hypersensitive sites in chromatin. *Annual Review of Biochemistry* **57**, 159-197.

GROSSCHEDL, R., GIESE, K. & PAGEL, J. (1994). HMG domain proteins: Architectural elements in the assembly of nucleoprotein structures. *Trends in Genetics* **10**, 94-100.

GROSVELD, F., VAN ASSENDELFT, G.B., GREAVES, D.R. & KOLIAS, G. (1987). Position-independent, high-level expression of the human β-globin gene in transgenic mice. *Cell* **51**, 975-985.

GRUNSTEIN, M. (1997). Histone acetylation in chromatin structure and transcription. *Nature* **389**, 349-352.

GRUNSTEIN, M., HECHT, A., FISHER-ADAMS, G., WAN, J., MANN, R.K., STRAHL-BOLSINGER, S., LAROCHE, T. & GASSER, S. (1995). The regulation of euchromatin and heterochromatin by histones in yeast. *Journal of Cell Science Supplement* **19**, 29-36.

GUACCI, V., KOSHLAND, D. & STRUNNIKOV, A. (1997). A direct link between sister chromatid cohesion and chromosome condensation revealed through the analysis of *MCD1* in *S.cerevisiae*. *Cell* **91**, 47-57.

GUAN, X., MELTZER, P.S. & TRANT, J.M. (1994). Rapid generation of whole chromosome painting probes (WCPs) by chromosome microdissection. *Genomics* **22**, 101-107.

GUNSTER, M.J, SATIJN, D.P.E., HAMER, K.M., DEN BLAAUWEN, J.L., DE BRUIJN, D., ALKEMA, M.J., VAN LOHUIZEN, M., VAN DRIEL, R. & OTTE, A.P. (1997). Identification and characterisation of interactions between the vertebrate *Polycomb*-group protein BMI1 and human homologues of polyhomeotic. *Molecular and Cellular Biology* **17**, 2326-2335.

GUO, X.W., TH'NG, J.P.H., SWANK, R.A., ANDERSON, H.J., TUDAN, C., BRADBURY, E.M. & ROBERGE, M. (1995). Chromosome condensation induced by fostriecin does not require $p34^{cdc2}$ kinase activity and histone H1 hyperphosphorylation, but is associated with enhanced histone H2A and H3 phosphorylation. *The EMBO Journal* **14**, 976-985.

HAAF, T. & SCHMID, M. (1991). Chromosome topology in mammalian interphase nuclei. *Experimental Cell Research* **192**, 325-332.

HAAF, T., WARBURTON, P.E. & WILLARD, H.F. (1992). Integration of human α-satellite DNA into simian chromosomes: Centromere protein binding and disruption of normal chromosome segregation. *Cell* **70**, 681-696.

HAAF, T. & WARD, D.C. (1996). Inhibition of RNA polymerase II transcription causes chromatin decondensation, loss of nucleolar structure, and dispersion of chromosomal domains. *Experimental Cell Research* **224**, 163-173.

HALMER, L. & GRUSS, C. (1996). Effects of cell cycle dependent histone H1 phosphorylation on chromatin structure and chromatin replication. *Nucleic Acids Research* **24**, 1420-1427.

HAMLIN, J.L. & DIJKWEL, P.A. (1995). On the nature of replication origins in higher eukaryotes. *Current Opinions in Genetics and Development* **5**, 153-161.

HAND, R. (1978). Eukaryotic DNA: Organisation of the genome for replication. *Cell* **15**, 317-325.

HANSEN, R.S., CANFIELD, T.K., FJELD, A.D. & GARTLER, S.M. (1996). Role of late replication timing in the silencing of X-linked genes. *Human molecular genetics* **5**, 1345-1353.

HARAUZ, G., BORLAND, L., BAHR, G.F., ZEITLER, E. & VAN HEEL, M. (1987). Three-dimensional reconstruction of a human metaphase chromosome from electron micrographs. *Chromosoma* **95**, 366-374.

HARLEY, C.B., FUTCHER, A.B. & GREIDER, C.W. (1990). Telomeres shorten during ageing of human fibroblasts. *Nature* **345**, 458-460.

HASSAN, A.B. & COOK, P.R. (1994). Does transcription by RNA polymerase play a direct role in the initiation of replication? *Journal of Cell Science* **107**, 1381-1387.

HASSAN, A.B., ERRINGTON, R.J., WHITE, N.S., JACKSON, D.A. & COOK, P.R. (1994). Replication and transcription sites are co-localised in human cells. *Journal of Cell Science* **107**, 425-434.

HATTON, K.S., DHAR, V., BROWN, E.H., IQBAL, M.A., STUART, S., DIDAMO, V.T. & SCHILDKRAUT, C.L. (1988). Replication program of active and inactive multigene families in mammalian cells. *Molecular and Cellular Biology* **8**, 2149-2158.

HE, D. & BRINKLEY, B.R. (1996). Structure and dynamic organisation of centromeres/ prekinetochores in the nucleus of mammalian cells. *Journal of Cell Science* **109**, 2693-2704.

HEBBES, T.R., THORNE, A.W. & CRANE-ROBINSON, C. (1988). A direct link between core histone acetylation and transcriptionally active chromatin. *The EMBO Journal* **7**, 1395-1402.

HEBBES, T.R., THORNE, A.W., CLAYTON, A.L. & CRANE-ROBINSON, C. (1992). Histone acetylation and globin gene switching. *Nucleic Acids Research* **20**, 1017-1022.

HEBBES, T.R., CLAYTON, A.L., THORNE, A.W. & CRANE-ROBINSON, C. (1994). Core histone hyperacetylation co-maps with generalised DNAseI sensitivity in the chicken β-globin chromosomal domain. *The EMBO Journal* **13**, 1823-1830.

HECHT, A., LAROCHE, T., STRAHL-BOLSINGER, S., GASSER, S.M. & GRUNSTEIN, M. (1995). Histone H3 and H4 N-termini interact with Sir3 and Sir4 proteins: A molecular model for the formation of heterochromatin in yeast. *Cell* **80**, 583-592.

HECK, M.M.S. (1997). Condensins, cohesins, and chromosome architecture: How to make and break a mitotic chromosome. *Cell* **91**, 5-8.

HECK, M.M.S. & EARNSHAW, W.C. (1986). Topoisomerase II: A specific marker for cell proliferation. *The Journal of Cell Biology* **103**, 2569-2581.

HECK, M.M.S. & EARNSHAW, W.C. (1989). *In vivo* phosphorylation of the 170-kDa form of eukaryotic DNA topoisomerase II. *The Journal of Biological Chemistry* **26**, 15161-15164.

HENDERSON, A.S., WARBURTON, D. & ATWOOD, K.C. (1972). Location of ribosomal DNA in the human chromosome complement. *Proceedings of the National Academy of Sciences U.S.A.* **69**, 3394-3398.

HENDZEL, M.J. & BAZETT-JONES, D.P. (1997). Fixation-dependent organisation of core histones following DNA fluorescent *in situ* hybridisation. *Chromosoma* **106**, 114-123.

HENDZEL, M.J., DELCUVE, G.P. & DAVIE, J.R. (1991). Histone deacetylase is a component of the internal nuclear matrix. *The Journal of Biological Chemistry* **266**, 21936-21942.

HENDZEL, M.J., SUN, J.-M., CHEN, H.Y., RATTNER, J.B. & DAVIE, J.R. (1994). Histone acetyltransferase is associated with the nuclear matrix. *The Journal of Biological Chemistry* **269**, 22894-22901.

HENDZEL, M.J., WEI, Y., MANCINI, M.A., VAN HOOSER, A., RANALLI, T., BRINKLEY, B.R., BAZETT-JONES, D.P. & ALLIS, C.D. (1997). Mitosis-specific phosphorylation of histone H3 initiates primarily within pericentromeric heterochromatin during G2 and spreads in an ordered fashion coincident with mitotic chromosome condensation. *Chromosoma* **106**, 348-360.

HENG, H.H.Q., SYPROPOULOS, B. & MOENS, P.B. (1997). FISH technology in chromosome and genome research. *BioEssays* **19**, 75-84.

HENIKOFF, S. (1990). Position-effect variegation after 60 years. *Trends in Genetics* **6**, 422-426.

HENIKOFF, S. (1996). Dosage-dependent modification of position-effect variegation in *Drosophila*. *BioEssays* **18**, 401-409.

HENIKOFF, S. (1997). Nuclear organisation and gene expression: Homologous pairing and long-range interactions. *Current Opinion in Cell Biology* **9**, 388-395.

HENIKOFF, S. & DREESEN, T.D. (1989). Trans-inactivation of the *Drosophila* brown gene: Evidence for transcriptional repression and somatic pairing dependence. *Proceedings of the National Academy of Sciences U.S.A.* **86**, 6704-6708.

HENS, L., BAUMANN, H., CREMER, T., SUTTER, A., CORNELIS, J.J. & CREMER, C. (1983). Immunocytochemical localisation of chromatin regions UV-microirradiated in S phase or anaphase. *Experimental Cell Research* **149**, 257-269.

HENS, L., KIRSCH-VOLDERS, M., VERSCHAEVE, L. & SUSANNE, C. (1982). Central localisation of the small and early replicating chromosomes of human diploid metaphase figures. *Human Genetics* **60**, 249-256.

HERNANDEZ-VERDUN, D. (1991). The nucleolus today. *Journal of Cell Science* **99**, 465-471.

HERNANDEZ-VERDUN, D. & GAUTIER, T. (1994). The chromosome periphery during mitosis. *BioEssays* **16**, 179-185.

HESLOP-HARRISON, J.S. & BENNETT, M.D. (1990). Nuclear architecture in plants. *Trends in Genetics* **6**, 401-405.

HIGASHIURA, M., SHIMIZU, Y., TANIMOTO, M., MORITA, T. & YAGURA, T. (1992). Immunolocalisation of Ku-proteins (p80/p70): Localisation of p70 to nucleoli and periphery of both interphase nuclei and metaphase chromosomes. *Experimental Cell Research* **201**, 444-451.

HILFIKER, A., HILFIKER-KLEINER, D., PANNUTI, A. & LUCCHESI, J.C. (1997). *mof*, a putative acetyl transferase gene related to Tip60 and MOZ human genes and to the SAS genes of yeast, is required for dosage compensation in *Drosophila*. *The EMBO Journal* **16**, 2054-2060.

HILL, R.J. & STOLLER, B.D. (1983). Dependence of Z-DNA antibody binding to polytene chromosomes on acid fixation and DNA torsional strain. *Nature* **305**, 338-340.

HILLIKER, A.J. & APPELS, R. (1982). Pleiotropic effects associated with the deletion of heterochromatin surrounding rDNA on the X chromosome of *Drosophila*. *Chromosoma* **86**, 469-490.

HILLIKER, A.J. & APPELS, R. (1989). The arrangement of interphase chromosomes: Structural and functional aspects. *Experimental Cell Research* **185**, 297-318.

HIRANO, T. & MITCHISON, T.J. (1993). Topoisomerase II does not play a scaffolding role in the organisation of mitotic chromosomes assembled in *Xenopus* egg extracts. *The Journal of Cell Biology* **120**, 601-612.

HIRANO, T. & MITCHISON, T.J. (1994). A heterodimeric coiled-coil protein required for mitotic chromosome condensation *in vitro*. *Cell* **79**, 449-458.

HIRANO, T. & MITCHISON, T.J. (1997). Condensins, chromosome condensation protein complexes containing XCAP-C, XCAP-E and a *Xenopus* homologue of the *Drosophila* Barren protein. *Cell* **89**, 511-521.

HIRANO, T., MITCHISON, T.J. & SWEDLOW, J.R. (1995). The SMC family: From chromosome condensation to dosage compensation. *Current Biology* **7**, 329-336.

HIRAOKA, Y., AGARD, D.A. & SEDAT, J.W. (1990). Temporal and spatial coordination of chromosome movement, spindle formation, and nuclear envelope breakdown during prometaphase in *Drosophila melanogaster* embryos. *The Journal of Cell Biology* **111**, 2815-2828.

HIZUME, M. (1992). Exact location of rRNA genes in *Vicia faba* chromosomes. *Cytologia* **57**, 471-475.

HOCK, R., CARL, M., LIEB, B., GEBAUER, D. & SCHEER, U. (1996). A monoclonal antibody against topoisomerase II labels the axial granules of *Pleurodeles* lampbrush chromosomes. *Chromosoma* **104**, 358-366.

HOFERS, C., BAUMANN, P., HUMMER, G., JOVIN, T.M. & ARDNT-JOVIN, D.J. (1993). The localisation of chromosome domains in human interphase nuclei. Three-dimensional distance determinations of fluorescence *in situ* hybridisation signals from confocal laser scanning microscopy. *Bioimaging* **1**, 96-106.

HOFFMANN, A., CHIANG, C.-M., OELGESCHLAGER, T., XIE, X., BURLEY, S.K., NAKATANI, Y. & ROEDER, R.G. (1996). A histone octamer-like structure within TFIID. *Nature* **380**, 356-359.

HOLLOWAY, S.L. (1995). Sister chromatid separation *in vivo* and *in vitro*. *Current Biology* **5**, 243-248.

HOLM, C. (1994). Coming undone: How to untangle a chromosome. *Cell* **77**, 955-957.

HOLM, C., GOTO, T., WANG, J.C. & BOSTEIN, D. (1985). DNA topoisomerase II is required at the time of mitosis in yeast. *Cell* **41**, 553-563.

HOLMBERG, M. & JONASSON, J. (1973). Preferential location of X-ray induced chromosome breakage in the R-bands of human chromosomes. *Hereditas* **74**, 57-68.

HOLMES, S.G., ROSE, A.B., STEUERLE, K., SAEZ, E., SAYEGH, S., LEE, Y.M. & BROACH, J.R. (1997). Hyperactivation of silencing proteins, Sir2p and Sir3p, causes chromosome loss. *Genetics* **145**, 605-614.

HOLMQUIST, G.P. (1987). Role of replication time in the control of tissue-specific gene expression. *American Journal of Human Genetics* **40**, 151-173.

HOLMQUIST, G.P. (1992). Chromosome bands, their chromatin flavours, and their functional features. *American Journal of Human Genetics* **51**, 17-37.

HOLMQUIST, G., GRAY, M., PORTER, T. & JORDAN, J. (1982). Characterisation of Giemsa dark- and light-band DNA. *Cell* **31**, 121-129.

HOROWITZ, R.A., AGARD, D.A., SEDAT, J.W. & WOODCOCK, C.L. (1994). The three-dimensional architecture of chromatin *in situ*: Electron tomography reveals fibres composed of a continuously variable zig-zag nucleosomal ribbon. *The Journal of Cell Biology* **125**, 1-10.

HOSODA, F., ARAI, Y., KITAMURA, E., INAZAWA, J., FUKUSHIMA, M., TOKINO, T., NAKAMURA, Y., JONES, C., KAKAZU, N., ABE, T. & OHKI, M. (1997). A complete *NotI* restriction map covering the entire length of the long arm of human chromosome 11. *Genes to Cells* **2**, 345-357.

HOUBEN, A., BELYAEV, N.D., LEACH, C.R. & TIMMIS, J.N. (1997). Differences of histone H4 acetylation and replication timing between A and B chromosomes of *Brachycome dichromosomatica*. *Chromosome Research* **5**, 233-237.

HOUBEN, A., BELYAEV, N.D., TURNER, B.M. & SCHUBERT, I. (1996). Differential immunostaining of plant chromosomes by antibodies recognising acetylated histone H4 variants. *Chromosome Research* **4**, 191-194.

HOWELL, W.M. & HSU, T.C. (1979). Chromosome core structure revealed by silver staining. *Chromosoma* **73**, 61-66.

HOWIE, J.B. & HEYLER, B.J. (1968). The immunology and pathology of NZB mice. *Advances in Immunology* **9**, 215-266.

HOZAK, P., HASSAN, A.B., JACKSON, D.A. & COOK, P.R. (1993). Visualisation of replication factories attached to a nucleoskeleton. *Cell* **73**, 361-373.

HOZAK, P., JACKSON, D.A. & COOK, P.R. (1994). Replication factories and nuclear bodies: The ultrastructural characterisation of replication sites during the cell cycle. *Journal of Cell Science* **107**, 2191-2202.

HOZAK, P. SASSEVILLE, A.M., RAYMOND, Y. & COOK, P.R. (1995). Lamin proteins form an internal nucleoskeleton as well as a peripheral lamina in human cells. *Journal of Cell Science* **108**, 635-644.

HUANG, H.-C. & COLE, R.D. (1984). The distribution of H1 histone is nonuniform in chromatin and correlates with different degrees of condensation. *The Journal of Biological Chemistry* **259**, 14237-14242.

HUANG, S. & SPECTOR, D.L. (1996). Intron-dependent recruitment of pre-mRNA splicing factors to sites of transcription. *The Journal of Cell Biology* **133**, 719-732.

HUMAN GENOME DATA BASE WEB SITE
http://gdbwww.gdb.org/gdbreports/CountGeneByChromosome.html

HUTCHISON, C.J. (1995). Local and global changes in the morphology and distribution of replication centres in rapidly expanding nuclei. *Chromosome Research* **3**, 16-26.

HUTCHISON, N. & WEINTRAUB, H. (1985). Localisation of DNAse I-Sensitive Sequences to Specific Regions of Interphase Nuclei. *Cell* **43**, 471-482.

HWU, H.R., ROBERTS, J.W., DAVIDSON, E.H. & BRITTEN, R.J. (1986). Insertion and/or deletion of many repeated DNA sequences in human and higher ape evolution. *Proceedings of the National Academy of Sciences U.S.A.* **83**, 3875-3879.

IAROVAIA, O., HANCOCK, R., LAGARKOVA, M., MIASSOD, R. & RAZIN, S.V. (1996). Mapping of genomic DNA loop organisation in a 500-kilobase region of the *Drosophila* X chromosome by the topoisomerase II-mediated DNA loop excision protocol. *Molecular and Cellular Biology* **16**, 302-308.

ICHIKAWA, H., HOSODA, F., ARAI, Y., SHIMIZU, K., OHIRA, M. & OHKI, M. (1993). A *NotI* restriction map of the entire long arm of chromosome 21. *Nature Genetics* **4**, 361-365.

IDEI, S., KONDO, K., TURNER, B.M. & FUKUI, K. (1996). Tomographic distribution of acetylated histone H4 in plant chromosomes, nuclei and nucleoli. *Chromosoma* **105**, 293-302.

IKEMURA, T. & WADA, K.-N. (1991). Evident diversity of codon usage patterns of human genes with respect to chromosome banding patterns and chromosome numbers: Relation between nucleotide sequence data and cytogenetic data. *Nucleic Acids Research* **19**, 4333-4339.

IKEMURA, T., WADA, K.-N. & AOTA, S.-I. (1990). Giant G+C% mosaic structures of the human genome found by arrangement of GenBank human DNA sequences according to genetic positions. *Genomics* **8**, 207-216.

ISHIDA, R., SATO, M., NARITA, T., USTUMI, K.R., NISHIMOTO, T., MORITA, T., NAGATA, ANDO, T. (1994). Inhibition of DNA topoisomerase II by ICRF-193 induces polyploidisation by uncoupling chromosome dynamics from other cell cycle events. *The Journal of Cell Biology* **126**, 1341-1351.

ISCN (1985). *An International System for Human Cytogenetic Nomenclature*. Ed. D.G. Harnden & H.P. Klinger. Basel: Karger.

IZAURRALDE, E. MIRKOVITCH, J. & LAEMMLI, U.K. (1988). Interaction of DNA with nuclear scaffolds *in vitro*. *Journal of Molecular Biology* **200**, 111-125.

JABLONKA, E., GOITEIN, R., MARCUS, M. & CEDAR, H. (1985). DNA hypomethylation causes an increase in DNAse-I sensitivity and an advance in the time of replication of the entire inactive X chromosome. *Chromosoma* **93**, 152-156.

JACK, R.S. & EGGERT, H. (1992). The elusive nuclear matrix. *European Journal of Biochemistry* **209**, 503-509.

JACKSON, D.A. (1990). The organisation of replication centres in higher eukaryotes. *BioEssays* **12**, 87-89.

JACKSON, D.A. (1991). Structure-function relationships in eukaryotic nuclei. *BioEssays* **13**, 1-10.

JACKSON, D.A., BARTLETT, J. & COOK, P.R. (1996). Sequences attaching loops of the nuclear and mitochondrial DNA to underlying structures in human cells: The role of transcription units. *Nucleic Acids Research* **24**, 1212-1219.

JACKSON, D.A. & COOK, P.R. (1985). Transcription occurs at the nucleoskeleton. *The EMBO Journal* **4**, 919-925.

JACKSON, D.A. & COOK, P.R. (1986). Replication occurs at the nucleoskeleton. *The EMBO Journal* **5**, 1403-1410.

JACKSON, D.A. & COOK, P.R. (1993). Transcriptionally active minichromosomes are attached to transiently in nuclei through transcription factors. *Journal of Cell Science* **105**, 1143-1150.

JACKSON, D.A., DICKINSON, P. & COOK, P.R. (1990). The size of chromatin loops in HeLa cells. *The EMBO Journal* **9**, 567-571.

JACKSON, D.A., MCCREADY, S.J. & COOK, P.R. (1981). RNA is synthesised at the nuclear cage. *Nature* **292**, 552-555.

JACKSON, D.A., MCCREADY, S.J. & COOK, P.R. (1984). Replication and transcription depend on attachment of DNA to the nuclear cage. *Journal of Cell Science Supplement* **1**, 59-79.

JACKSON, D.A., YUAN, J. & COOK, P.R. (1988). A gentle method for preparing cyto- and nucleo-skeletons and associated chromatin. *Journal of Cell Science* **90**, 365-378.

JARMAN, A.P. & HIGGS, D.R. (1988). Nuclear scaffold attachment sites in the human globin gene complexes. *The EMBO Journal* **7**, 3337-3344.

JELINEK, W.R. & SCHMID, C.W. (1982). Repetitive sequences in eukaryotic DNA and their expression. *Annual Review of Biochemistry* **51**, 813-844.

JENUWEIN, T., FORRESTER, W.C., FERNANDEZ-HERRERO, L.A., LAIBLE, G., DULL, M. & GROSSCHEDL, R. (1997). Extension of chromatin accessibility by nuclear matrix attachment regions. *Nature* **385**, 269-272.

JEPPESEN, P. (1997). Histone acetylation: A possible mechanism for the inheritance of cell memory at mitosis. *BioEssays* **19**, 67-74.

JEPPESEN, P., MITCHELL, A., TURNER, B. & PERRY, P. (1992). Antibodies to defined histone epitopes reveal variations in chromatin conformation and underacetylation of centric heterochromatin in human metaphase chromosomes. *Chromosoma* **101**, 322-332.

JEPPESEN, P. & TURNER, B.M. (1993). The inactive X chromosome in female mammals is distinguished by a lack of histone H4 acetylation, a cytogenetic marker for gene expression. *Cell* **74**, 281-289.

JESSBERGER, , R., RIWAR, B., BAECHTOLD, H. & AKHMEDOV, A.T. (1996). SMC proteins constitute two subunits of the mammalian recombination complex RC-1. *The EMBO Journal* **15**, 1062-1069.

JIMENEZ-GARCIA, L.F., ROTHBLUM, L.I., BUSCH, H. & OCHS, R.L. (1989). Nucleogenesis: Use of non-isotopic *in situ* hybridisation and immunocytochemistry to compare the localisation of rDNA and nucleolar proteins during mitosis. *Biology of the Cell* **65**, 239-246.

JOHN, J.M. & SURANI, M.A. (1996). Imprinted genes and regulation of gene expression by epigenetic inheritance. *Current Opinion in Cell Biology* **8**, 384-353.

JOST, J.-P. & HOFSTEENGE, J. (1992). The repressor MDBP-2 is a member of the histone H1 family that binds preferentially *in vitro* and *in vivo* to methylated nonspecific DNA sequences. *Proceedings of the National Academy of Science U.S.A.* **89**, 9499-9503.

JURKA, J. & MILOSAVLJEVIC, A. (1991). Reconstruction and analysis of human *Alu* genes. *Journal of molecular evolution* **32**, 105-121.

KALOS, M. & FOURNIER, R.E.K. (1995). Position-independent transgene expression mediated by boundary elements from the apolipoprotein B chromatin domain. *Molecular and Cellular Biology* **15**, 198-207.

KAMAKAKA, R.T. & THOMAS, J.O. (1990). Chromatin structure of transcriptionally competent and repressed genes. *The EMBO Journal* **9**, 3997-4006.

KANDA, N. (1973). A new differential technique for staining the heteropycnotic X chromosome in female mice. *Experimental Cell Research* **80**, 463-467.

KAPLAN, F.S., MURRAY, J., SYLVESTER, J.E., GONZALEZ, I.L., O'CONNOR, J.P., DOERING, J.L., MUENKE, M., EMANUEL, B.S. & ZASLOFF, M.A. (1993). The topographic organisation of repetitive DNA in the human nucleolus. *Genomics* **15**, 123-132.

KARPEN, G.H. (1994). Position-effect variegation and the new biology of heterochromatin. *Current Opinion in Genetics and Development* **4**, 281-291.

KARPEN, G.H., SCHAEFER, J.E. & LAIRD, C.D. (1988). A *Drosophila* rRNA gene located in euchromatin is active in transcription and nucleolus formation. *Genes and Development* **2**, 1745-1763.

KAS, E., IZAURRALDE, E. & LAEMMLI, U.K. (1989). Specific inhibition of DNA binding to nuclear scaffolds and histone H1 by distamycin. *Journal of Molecular Biology* **210**, 587-599.

KASS, S., CRAIG, N. & SOLLNER-WEBB, B. (1987). Primary processing of mammalian rRNA involves two adjacent cleavages and is not species specific. *American Society for Microbiology* **7**, 2891-2898.

KAUFMAN, P.D. & BOTCHAN, M.R. (1994). Assembly of nucleosomes: Do multiple assembly factors mean multiple mechanisms? *Current Opinion in Genetics and Development* **4**, 229-235.

KAYNE, P.S., KIM, U.J., HAN, M., MULLEN, J.R., YOSHIZAKI, F. & GRUNSTEIN, M. (1988). Extremely conserved histone H4 N terminus is dispensable for growth but essential for repressing the silent mating loci in yeast. *Cell* **55**, 27-39.

KELLEY, R.L. & KURODA, M.I. (1995). Equality for X chromosomes. *Science* **270**, 1607-1613.

KELLEY, R.L., SOLOVYEVA, I., LYMAN, L.M., RICHMAN, R., SOLOVYEV, V. & KURODA, M.I. (1995). Expression of Msl-2 causes assembly of dosage compensation regulators on the X chromosomes and female lethality in *Drosophila*. *Cell* **81**, 867-877.

KELLUM, R. & ALBERTS, B.M. (1995). Heterochromatin protein 1 is required for correct chromosome segregation in *Drosophila* embryos. *Journal of Cell Science* **108**, 1419-1431.

KELLUM, R., RAFF, J.W. & ALBERTS, B.M. (1995). Heterochromatin protein 1 distribution during development and during the cell cycle in *Drosophila* embryos. *Journal of Cell Science* **108**, 1407-1418.

KENNET, R., DENIS, K., TUNG, A.S. & KLINMAN, N.R. (1978). Hybrid plasmacytoma production: Fusions with adult spleen cells, monoclonal spleen fragments, neonatal spleen cells and human spleen cells. *Current Topics in Microbiology and Immunology* **81**, 77-90.

KEOHANE, A.M., O'NEILL, L.P., BELYAEV, N.D., LAVENDER, J.S. & TURNER, B.M. (1996). X-inactivation and histone H4 acetylation in embryonic stem cells. *Developmental Biology* **180**, 618-630.

KEREM, B., GOITEIN, R., DIAMOND, G., CEDAR, H. & MARCUS, M. (1984). Mapping of DNAse I sensitive regions on mitotic chromosomes. *Cell* **38**, 493-499.

KERREBROCK, A.W., MOORE, D.P., WU, J.S. & ORR-WEAVER, T.L. (1995). Mei-S332, a *Drosophila* protein required for sister-chromatid cohesion, can localise to meiotic centromere regions. *Cell* **83**, 247-256.

KESHET, I., LIEMAN-HURWITZ, J. & CEDAR, H. (1986). DNA methylation affects the formation of active chromatin. *Cell* **44**, 535-543.

KIEVITS, T., DEVILEE, P., WIEGANT, J., WAPENAAR, M.C., CORNELISSE, C.J., VAN OMMEN, G.J.B. & PEARSON, P.L. (1990). Direct non-radioactive *in situ* hybridisation of somatic cell hybrid DNA to human lymphocyte chromosomes. *Cytometry* **11**, 105-109.

KILL, I.R., BRIDGER, J.M., CAMPBELL, K.H.S., MALDONADO-CODINA, G. & HUTCHISON, C.J. (1991). The timing of the formation and usage of replicase clusters in S-phase nuclei of human diploid fibroblasts. *Journal of Cell Science* **100**, 869-876.

KIM, N.W., PIATYSZEK, M.A., PROWSE, K.R., HARLEY, C.B., WEST, M.D., HO, P.L.C., COVIELLO, G.M., WRIGHT, W.E., WEINRICH, S.L. & SHAY, J.W. (1994). Specific association of human telomerase activity with immortal cells and cancer. *Science* **266**, 2011-2015.

KIMURA, K. & HIRANO, T. (1997). ATP-dependent positive supercoiling of DNA by 13S condensin: A biochemical implication for chromosome condensation. *Cell* **90**, 625-634.

KING, V., KORN, R., KWOK, C., RAMKISSOON, Y., WUNERLE, V. & GOODFELLOW, P. (1995). One for a boy, two for a girl? *Current Biology* **5**, 37-39.

KINGSTON, R.E., BUNKER, C.A. & IMBALZANO, A.N. (1996). Repression and activation by multi-protein complexes that alter chromatin structure. *Genes and Development* **10**, 905-920.

KLAR, A.M.J., FOGEL, S. & MACLEOD, K. (1979). MAR1: A regulator of the HMa and HMα loci in *Saccharomyces cerevisiae*. *Genetics* **93**, 37-50.

KOHLER, G. & MILSTEIN, C. (1975). Continuous cultures of fused cells secreting antibody of predefined specificity. *Nature* **256**, 495-497.

KOI, M., SHIMIZU, M., MORITA, H., YAMADA, H. & OSHIMURA, M. (1989). Construction of mouse A9 clones containing a single human chromosome tagged with neomycin-resistance gene via microcell fusion. *Japanese Journal of Cancer Research* **80**, 413-418.

KOONIN, E.V., ZHOU, S. & LUCCHESI, J.C. (1995). The chromo superfamily: New members, duplication of the chromodomain and possible role in delivering transcription regulators to chromatin. *Nucleic Acids Research* **23**, 4229-4233.

KOMURA, J.-I., SHEARDOWN, S.A., BROCKDORFF, N., SINGER-SAM, J. & RIGGS, A.D. (1997). *In vivo* ultraviolet and dimethyl sulphate footprinting of the 5' region of the expressed and silent *Xist* alleles. *The Journal of Biological Chemistry* **262**, 10975-10980.

KORENBERG, J.R. & RYKOWSKI, M.C. (1988). Human genome organisation. *Alu*, LINEs and the molecular structure of metaphase chromosome bands. *Cell* **53**, 391-400.

KOSHLAND, D. & STRUNNIKOV, A. (1996). Mitotic chromosome condensation. *Annual Review of Cell and Developmental Biology* **12**, 305-333.

KRUH, J. (1982). Effects of sodium butyrate, a new pharmacological agent, on cells in culture. *Molecular and Cellular Biochemistry* **42**, 65-82.

KRYSTOSEK, A. & PUCK, T.T. (1990). The spatial distribution of exposed nuclear DNA in normal, cancer and reverse-transformed cells. *Proceedings of the National Academy of Sciences U.S.A.* **87**, 6560-6564.

KUANG, J., ASHORN, C.L., GONZALEZ-KUYVENHOVEN, M. & PENKALA, J.E. (1994). Cdc25 is one of the MPM-2 antigens involved in the activation of maturation-promoting factor. *Molecular Biology of the Cell*, **5** 135-145.

KUHN, E.M., THERMAN, E. & DENNISTON, C. (1985). Mitotic chiasmata, gene density, and oncogenes. *Human Genetics* **70**, 1-5.

KUO, M.-H., BROWNELL, J.E., SOBEL, R.E., RANALLI, T.A., COOK, R.G., EDMONDSON, D.G., ROTH, S.Y. & ALLIS, C.D. (1996). Transcription-linked acetylation by Gcn5p of histones H3 and H4 at specific lysines. *Nature* **383**, 269-272.

KURNIT, D.M., ROY, S., STEWART, G.D., SCHWEDOCK, J., NEVE, R.L., BRUNS, G.A.P., VAN KEUREN, M.L. & PATTERSON, D. (1986). The 724 family of DNA sequences is interspersed about the pericentric regions of human acrocentric chromosomes. *Cytogenetics and Cell Genetics* **43**, 109-116.

KURODA, M.I., KERNAN, M.J., KREBER, R., GANETZKY, B. & BAKER, B.S. (1991). The *maleless* protein associates with the X chromosome to regulate dosage compensation in *Drosophila*. *Cell* **66**, 935-947.

KUROIWA, T. (1971). Asynchronous condensation of chromosomes from early prophase to late prophase as revealed by electron microscopic autoradiography. *Experimental Cell Research* **69**, 97-105.

KURZ, A., LAMPEL, S., NICKOLENKO, J.E., BRADL, J., BENNER, A., ZIRBEL, R.K., CREMER, T. & LICHTER, P. (1996). Active and inactive genes localise preferentially in periphery of chromosome territories. *The Journal of Cell Biology* **135**, 1195-1205.

LAEMMLI, U.K., CHENG, S.M., ADOLPH, K.W., PAULSON, J.R., BROWN, J.A. & BAUMBACH, W.R. (1978). Metaphase chromosome structure: The role of non-histone proteins. *Cold Spring Harbour Symposia on Quantitative Biology* **XLII**, 351-360.

LAEMMLI, U.K., KAS, E., POLJAK, L. & ADACHI, Y. (1992). Scaffold-associated regions: *Cis*-acting determinants of chromatin structural loops and functional domains. *Current Opinion in Genetics and Development* **2**, 275-285.

LAMOND, A.I. & CARMO-FONSECA, M. (1993). The coiled body. *Trends in Cell Biology* **3**, 198-204.

LANGER-SAFER, P.R., LEVINE, M. & WARD, D.C. (1982). Immunological method for mapping genes on *Drosophila* polytene chromosomes. *Proceedings of the National Academy of Sciences U.S.A.* **79**, 4381-4385.

LANGST, G., BLANK, T.A., BECKER, P.B. & GRUMMT, I. (1997). RNA polymerase I transcription on nucleosomal templates: The transcription termination factor TTF-1 induces chromatin remodelling and relieves transcriptional repression. *The EMBO Journal* **16**, 760-768.

LAPEYRE, B., BOURBON, H. & AMALRIC, F. (1987). Nucleolin, the major nucleolar protein of growing eukaryotic cells: An unusual protein structure revealed by the nucleotide sequence. *Proceedings of the National Academy of Sciences U.S.A.* **84**, 1472-1476.

LARSEN, F., GUNDERSEN, G., LOPEZ,R. & PRYDZ, H. (1992). CpG-islands as gene markers in the human genome. *Genomics* **13**, 1095-1107.

LARSSON, S.H., CHARLIEU, J., MIGAGAWA, K., ENGLEKEMP, D., RASSOULZADEGAN, M., ROSS, A., CUZIN, F., VAN HEYNINGEN, V. & HASTIE, N. (1995). Subnuclear localisation of WT1 in splicing or transcription factor domains is regulated by alternative splicing. *Cell* **81**, 391-401.

LASALLE, J.M. & LALANDE, M. (1996). Homologous association of appositely imprinted chromosomal domains. *Science* **272**, 725-728.

LAURENT, B.C., TRIECH, I. & CARLSON, M. (1993). The yeast SNF2/SWI2 protein has DNA-stimulated ATPase activity required for transcriptional activation. *Genes and Development* **7**, 583-591.

LAURIE, D.A. & HULTEN, M.A. (1985). Further studies on chiasmata distribution and interference in the human male. *Annals of Human Genetics* **49**, 203-214.

LAWLIS, S.J., KEEZER, S.M., WU, J.-R. & GILBERT, D.M. (1996). Chromosome architecture can dictate site-specific initiation of DNA replication in *Xenopus* egg extracts. *The Journal of Cell Biology* **135**, 1207-1218.

LAWRENCE, J.B., CARTER, K.C. & XING, X. (1993). Probing functional organisation within the nucleus: Is genome structure integrated with RNA metabolism? *Cold Spring Harbour Symposia on Quantitative Biology* **LVIII**, 807-818.

LAWRENCE, J.B. & SINGER, R.H. (1991). Spatial organisation of nucleic acid sequences within cells. *Seminars in Cell Biology* **2**, 83-101.

LAWRENCE, J.B., SINGER, R.H. & MARSELLE, L.M. (1989). Highly localised tracks of specific transcripts within interphase nuclei visualised by *in situ* hybridisation. *Cell* **57**, 493-502.

LAWRENCE, J.B., SINGER, R.H. & MCNEIL, J.A. (1990). Interphase and metaphase resolution of different distances within the human dystrophin gene. *Science* **249**, 928-932.

LAWRENCE, J.B., VILLNAVE, C.A. & SINGER, R.H. (1988). Sensitive, high-resolution chromatin and chromosome mapping *in situ*: Presence and orientation of two closely integrated copies of EBV in a lymphoma line. *Cell* **52**, 51-61.

LEBLANC, B., READ, C. & MOSS, T. (1993). Recognition of the *Xenopus* ribosomal core promoter by the transcription factor xUBF involves multiple HMG box domains and leads to an xUBF interdomain interaction. *The EMBO Journal* **12**, 513-525.

LEE, D.Y., HAYES, J.J., PRUSS, D. WOLFFE, A.P. (1993). A positive role for histone acetylation in transcription factor access to nucleosomal DNA. *Cell* **72**, 73-84.

LEE, J.T., STRAUSS, W.M., DAUSMAN, J.A. & JAENISCH, R. (1996). A 450Kb transgene displays properties of the mammalian X-inactivation centre. *Cell* **86**, 83-94.

LEE, W., SHEW, J., HONG, F.D., SERY, T., DONOSO, L.A., YOUNG, L., BOOKSTEIN, R. & LEE, E.Y.P. (1987). The retinoblastoma susceptibility gene encodes a nuclear phosphoprotein associated with DNA binding activity. *Nature* **329**, 642-645.

LEFEBVRE, S., BURGLEN, L., REBOULLET, S., CLERMONT, O., BURLET, P., VIOLLET, L., BENICHOU, B., CRUAND, C., MILLASSEAU, P., ZEVIANI, M., LE PASLIER, D., FREZAL, J., COHEN, D., WEISSENBACH, J., MUNNICH, A. & MELKI, J. (1995). Identification and characterisation of a spinal muscular atrophy-determining gene. *Cell* **80**, 155-165.

LENFANT, F., MANN, R.K., THOMSEN, B., LING, X. & GRUNSTEIN, M. (1996). All four core histone N-termini contain sequences required for the repression of basal transcription in yeast. *The EMBO Journal* **15**, 3974-3985.

LENGAUER, C., ECKELT, A., WEITH, A., ENDLICH, N., PONELIES, N., LICHTER, P., GREULICH, K.O. & CREMER, T. (1991). Painting of defined chromosomal regions by *in situ* suppression hybridisation of libraries from laser-microdissected chromosomes. *Cytogenetics and Cell Genetics* **56**, 27-30.

LERNER, E.A., LERNER, M.R., JANEWAY, L.A. & STEITZ, J.A. (1981). Monoclonal antibodies to nucleic acid containing cellular constituents: Probes for molecular biology and autoimmune disease. *Proceedings of the National Academy of Sciences U.S.A.* **78**, 2737-2741.

LETOVSKY, J. & DYNAN, W.S. (1989). Measurement of the binding of transcription factor Sp1 to a single GC box recognition sequence. *Nucleic Acids Research* **17**, 2639-2653.

LEVINE, A., YEIVIN, A., BEN-ASHER, E., ALONI, Y. & RAZIN, A. (1993). Histone H1-mediated inhibition of transcription initiation of methylated templates *in vitro*. *The Journal of Biological Chemistry* **268**, 21754-21759.

LEVIS, R., HAZELRIGG, T., RUBIN, G.M. (1985). Effects of genominc position on the expression of transduced copies of the *white* gene in *Drosophila*. *Science* **229**, 558-561.

LEWIN, B. (1994). Genome size and genetic content. In *Genes V*. Oxford: University Press. pp657-676.

LEWIS, C.D. & LAEMMLI, U.K. (1982). Higher order metaphase chromosome structure: Evidence for metalloprotein interactions. *Cell* **17**, 849-858.

LEWIS, C.D., LEBOWSKI, J.S., DALY, A.K. & LAEMMLI, U.K. (1984). Interphase nuclear matrix and interphase scaffolding structures. *Journal of Cell Science Supplement* **1**, 103-122.

LEWIS, J.D., MEEHAN, R.R., HENZEL, W.J., MAURER-FOGY, I., JEPPESEN, P. & BIRD, A. (1992). Purification, sequence, and cellular localisation of a novel chromosomal protein that binds to methylated DNA. *Cell* **69**, 905-914.

LI, E., BESTOR, T.H. & JAENISCH, R. (1992). Targeted mutation of the DNA methyltransferase gene results in embryonic lethality. *Cell* **69**, 915-926.

LI, Y., STRAHLER, J.R. & DODGSON, J.B. (1997). Neither HMG-14a nor HMG-17 gene function is required for growth of chicken DT40 cells or maintenance of DNAseI-hypersensitive sites. *Nucleic Acids Research* **25**, 283-288.

LICHTER, P., CREMER, T., BORDEN, J., MANNUELIDIS, L. & WARD, D.C. (1988). Delineation of individual human chromosomes in metaphase and interphase cells by *in situ* suppression hybridisation using recombinant DNA libraries. *Human Genetics* **80**, 224-234.

LICHTER, P., LEDBETTER, S.A., LEDBETTER, D.H. & WARD, D.C. (1990). Fluorescence *in situ* hybridisation with *Alu* and L1 polymerase chain reaction probes for rapid characterisation of human chromosomes in hybrid cell lines. *Proceedings of the National Academy of Sciences U.S.A.* **87**, 6634-6638.

LIEB, J.D., CAPOWSKI, E.E., MENEELY, P. & MEYER, B.J. (1996). DPY-26, a link between dosage compensation and meiotic chromosome segregation in the nematode. *Science* **274**, 1732-1736.

LING, X., HARKNESS, T.A.A., SCHULTZ, M.C., FISHER-ADAMS, G. & GRUNSTEIN, M. (1996). Yeast histone H3 and H4 amino termini are important for nucleosome assembly *in vivo* and *in vitro*: Redundant and position-independent functions in assembly but not in gene regulation. *Genes and Development* **10**, 686-699.

LIU, J., SONG, K. & WOLFNER, M.F. (1995). Mutational analyses of *fs(1)Ya*, an essential, developmentally regulated, nuclear envelope protein in *Drosophila*. *Genetics* **141**, 1473-1481.

LIU, Q. & DREYFUSS, G. (1996). A novel nuclear structure containing the survival of motor neurons protein. *The EMBO Journal* **15**, 3555-3565.

LIU, Q., FISCHER, U., WANG, F. & DREYFUSS, G. (1997). The spinal muscular atrophy disease gene product, SMN, and its associated protein SIP1 are in a complex with spliceosomal snRNP proteins. *Cell* **90**, 1013-1021.

LOHE, A.R. & HILLIKER, A.J. (1995). Return of the H-word (heterochromatin). *Current Opinion in Genetics and Development* **5**, 746-755.

LOIDL, P. (1994). Histone acetylation: Facts and questions. *Chromosoma* **103**, 441-449.

LONG, E.O. & DAWID, I.B. (1980). Repeated genes in eukaryotes. *Annual review of Biochemistry* **49**, 727-764.

LOPEZ, J.M. & WOLFNER, M.F. (1997). The developmentally regulated *Drosophila* embryonic nuclear lamina protein "Young Arrest" (fs(1)Ya) is capable of associating with chromatin. *Journal of Cell Science* **110**, 643-651.

LORENTZ, A., OSTERMANN, K., FLECK, O. & SCHMIDT, H. (1994). Switching gene *swi6*, involved in repression of silent mating-type loci in fission yeast, encodes a homologue of chromatin-associated proteins from *Drosophila* and mammals. *Gene* **143**, 139-143.

LU, B.Y., BISHOP, C.P. & EISSENBERG, J.C. (1996). Developmental timing and tissue specificity of heterochromatin-mediated silencing. *The EMBO Journal* **15**, 1323-1332.

LU, M.J., DADD, C.A., MIZZEN, C.A., PERRY, C.A., MCLACHLAN, D.R., ANNUNZIATO, A.T. & ALLIS, C.D. (1994). Generation and characterisation of novel antibodies highly selective for phosphorylated linker histone H1 in *Tetrahymena* and HeLa cells. *Chromosoma* **103**, 111-121.

LU, M.J., MPOKE, S.S., DADD, C.A. & ALLIS, C.D. (1995). Phosphorylated and dephosphoryled linker histone H1 reside in distinct chromatin domains in *Tetrahymena* macronuclei. *Molecular Biology of the Cell* **6**, 1077-1087.

LUCCHESI, J.C. (1996). Dosage compensation in *Drosophila* and the "complex" world of transcriptional regulation. *BioEssays* **18**, 541-547.

LUDENA, P., SENTIS, C., DE CABO, S.F., VELAZQUEZ, M. & FERNANDEZ-PIQUERAS, J. (1991). Visualisation of R-bands in human metaphase chromosomes by the restriction endonuclease *MseI*. *Cytogenetics and Cell Genetics* **57**, 82-86.

LUDERUS, M.E.E., DE GRAAF, A., MATTIA, E., DEN BLAAUWEN, J.L., GRANDE, M.A., DE JONG, L. & VAN DRIEL, R. (1992). Binding of matrix attachment regions to lamin B_1. *Cell* **70**, 949-959.

LUDERUS, M.M.E., VAN STEENSEL, B., CHONG, L., SIBON, O.C.M., CREMERS, F.F.M. & DE LANGE, T. (1996). Structure, subnuclear distribution and nuclear matrix association of the mammalian telomeric complex. *The Journal of Cell Biology* **135**, 867-881.

LUGER, K., MADER, A.W., RICHMOND, R.K., SARGENT, D.F. & RICHMOND, T.J. (1997). Crystal structure of the nucleosome core particle at 2.8Å resolution. *Nature* **389**, 251-260.

LUSSER, A., BROSCH, G., LOIDL, A., HAAS, H. & LOIDL, P. (1997). Identification of maize histone deacetylase HD2 as an acidic nucleolar phosphoprotein. *Science* **277**, 88-91.

LYNDERSEN, B.K. & PETTIJOHN, D.E. (1980). Human-specific nuclear protein that associates with the polar region of the mitotic apparatus: Distribution in a human/hamster hybrid cell. *Cell* **22**, 489-499.

MACKAY, A.M., ECKLEY, D.M., CHUE, C. & EARNSHAW, W.C. (1993). Molecular analysis of the INCENPs (inner centromere proteins): Separate domains are required for association with microtubules during interphase and with the central spindle during anaphase. *The Journal of Cell Biology* **123**, 373-385.

MAGAUD, J.-P., RIMOKH, R., BROCHIER, J., LAFAGE, M & GERMAIN, D. (1985). Chromosomal R-banding with a monoclonal antidouble-stranded DNA antibody. *Human Genetics* **69**, 238-242.

MAHADEVAN, L.C., WILLIS, A.C. & BARRATT, M.J. (1991). Rapid histone H3 phosphorylation in response to growth factors, phorbol esters, okadaic acid, and protein synthesis inhibitors. *Cell* **65**, 775-783.

MAILLET, L., BOSCHERON, C., GOTTA, M., MARCAND, S., GILSON, E. & GASSER, S.M. (1996). Evidence for silencing compartments within the yeast nucleus: A role for telomere proximity and Sir protein concentration in silence-mediated repression. *Genes and Development* **10**, 1796-1811.

MANN, R.K. & GRUNSTEIN, M. (1992). Histone H3 N-terminal mutations allow hyperactivation of the yeast *GAL1* gene *in vivo*. *The EMBO Journal* **11**, 3297-3306.

MANUELIDIS, L. (1978). Chromosomal localisation of complex and simple repeated human cDNAs. *Chromosoma* **66**, 23-32.

MANUELIDIS, L. (1984). Different central nervous system cell types display distinct and non-random arrangements of satellite DNA sequences. *Proceedings of the National Academy of Science U.S.A.* **81**, 3123-3127.

MANUELIDIS, L. (1985a). Indications of centromere movement during interphase and differentiation. *Annals New York Academy of Science* **450**, 205-221.

MANUELIDIS, L. (1985b). Individual interphase chromosome domains revealed by *in situ* hybridisation. *Human Genetics* **71**, 288-293.

MANEULIDIS, L. (1990). A view of interphase chromosomes. *Science* **250**, 1533-1540.

MANUELIDIS, L. & BORDEN, J. (1988). Reproducible compartmentalisation of individual chromosome domains in human CNS cells revealed by *in situ* hybridisation and three-dimensional reconstruction. *Chromosoma* **96**, 397-410.

MANUELIDIS, L. & CHEN, T.L. (1990). A unified model of eukaryotic chromosomes. *Cytometry* **11**, 8-25.

MANUELIDIS, L. & WARD, D.C. (1984). Chromosomal and nuclear distribution of the *HindIII* 1.9Kb human DNA repeat segment. *Chromosoma* **91**, 28-38.

MARCAND, S., GASSER, S.M. & GILSON, E. (1996). Chromatin: A sticky silence. *Current Biology* **6**, 1222-1225.

MARCAND, S., GILSON, E. & SHORE, D. (1997). A protein-counting mechanism for telomere length regulation in yeast. *Science* **275**, 986-990.

MARSDEN, M.P.F. & LAEMMLI, U.K. (1979). Metaphase chromosome structure: Evidence for a radial loop model. *Cell* **17**, 849-858.

MARSHALL, I.C.B. & WILSON, K.L. (1997). Nuclear envelope assembly after mitosis. *Trends in Cell Biology* **7**, 69-74.

MARSHALL, W.F., FUNG, J.C. & SEDAT, J.W. (1997a). Deconstructing the nucleus: Global architecture from local interactions. *Current Opinion in Genetics and Development* **7**, 259-263.

MARSHALL, W.F., DERNBURG, A.F., HARMON, B., AGARD, D.A. & SEDAT, J.W. (1996). Specific interactions of chromatin with the nuclear envelope: Positional determination within the nucleus in *Drosophila melanogaster*. *Molecular Biology of the Cell* **7**, 825-842.

MARSHALL, W.F., STRAIGHT, A., MARKO, J.F., SWEDLOW, J., DERNBURG, A., BELMONT, A., MURRAY, A.W., AGARD, D.A. & SEDAT, J.W. (1997b). Interphase chromosomes undergo constrained diffusional motion in living cells.

MARTIENSSEN, R.A. & RICHARDS, E.J. (1995). DNA methylation in eukaryotes. *Current Opinion in Genetics and Development* **5**, 234-242.

MARTINEZ-BALBAS, M.A., DEY, A., RABINDRAN, S.K., OZATO, K. & WU, C. (1995). Displacement of sequence-specific transcription factors from mitotic chromatin. *Cell* **83**, 29-38.

MARTIN, L., CRIMAUDO, C. & GERACE, L. (1995). cDNA cloning and characterisation of lamina-associated polypeptide 1C (LAP1C), an integral protein of the inner nuclear membrane. *The Journal of Biological Chemistry* **270**, 8822-8828.

MATHOG, D., HOCHSTRASSER, M., GRUENBAUM, Y., SAUMWEBER, H. & SEDAT, J. (1984). Characteristic folding pattern of polytene chromosomes in *Drosophila* salivary gland nuclei. *Nature* **308**, 414-421.

MATSUI, S.-I., SEON, B.K. & SANDBERG, A.A. (1979). Disappearance of a structural chromatin protein A24 in mitosis: Implications for molecular basis of chromatin condensation. *Proceedings of the National Academy of Sciences U.S.A.* **76**, 6386-6390.

MCARTHUR, M. & THOMAS, J.O. (1996). A preference of histone H1 for methylated DNA. *The EMBO Journal* **15**, 1705-1714.

MCCALL, K. & BENDER, W. (1996). Probes for chromatin accessibility in the *Drosophila* bithorax complex respond differently to *Polycomb*-mediated repression. *The EMBO Journal* **15**, 569580.

MCCREADY, S.J., AKRIGG, A. & COOK, P.R. (1979). Electron-microscopy of intact nuclear DNA from human cells. *Journal of Cell Science* **39**, 53-62.

MCCREADY, S.J., GODWIN, J., MASON, D.W., BRAZELL, I.A. & COOK, P.R. (1980). DNA is replicated at the nuclear cage. *Journal of Cell Science* **46**, 365-386.

MCKAY, R.D.G. (1973). The mechanism of G and C banding in mammalian metaphase chromosomes. *Chromosoma* **44**, 1-14.

MCKNIGHT, G.S., HAGER, L. & PALMITER, R.D. (1980). Butyrate and related inhibitors of deacetylation block the induction of egg white genes by steroid hormones. *Cell* **22**, 469-477.

MCQUEEN, H.A., FANTES, J., CROSS, S.H., CLARK, V.H., ARCHIBALD, A.L. & BIRD, A.P. (1996). CpG-islands of chicken are concentrated on michrochromosomes. *Nature Genetics* **12**, 321-324.

MEGEE, P.C., MORGAN, B.A. & MITCHELL SMITH, M. (1995). Histone H4 and the maintenance of genome integrity. *Genes and Development* **9**, 1716-1727.

MEEHAN, R.R., LEWIS, J.D. & BIRD, A.P. (1992). Characterisation of MeCp2, a vertebrate DNA binding protein with affinity for methylated DNA. *Nucleic Acids Research* **20**, 5085-5092.

MEEHAN, R.R., LEWIS, J.D., MCKAY, S., KLEINER, E.L. & BIRD, A.P. (1989). Identification of a mammalian protein that binds specifically to DNA containing methylated CpGs. *Cell* **58**, 499-507.

MELLER, V.H., WU, K.H., ROMAN, G., KURODA, M.I. & DAVIS, R.L. (1997). *roX1* RNA paints the X chromosome of male *Drosophila* and is regulated by the dosage compensation system. *Cell* **88**, 445-457.

MENG, C. & BEREZNEY, R. (1991). Replication cluster domains persist throughout the cell cycle of mouse 3T3 cells. *The Journal of Cell Biology Meeting Abstracts* **115**, 95a.

MESSIER, P.-E., DROUIN, R. & RICHER, C.L. (1989). Electron microscopy of gold-labelled human and equine chromosomes. *The Journal of Histochemistry and Cytochemistry* **37**, 1443-1447.

MESSMER, S., FRANKE, A. & PARO, R. (1992). Analysis of the functional role of the *Polycomb* chromo domain in *Drosophila melanogaster*. *Genes and Development* **6**, 1241-1254.

MEYER, K.N., KJELDSEN, E., STRAUB, T., KNUDSEN, B.R., HICKINSON, I.D., KIKUCHI, A., KREIPE, H. & BOEGE, F. (1997). Cell cycle-coupled relocation of types I and II topoisomerases and modulation of catalytic enzyme activities. *The Journal of Cell Biology* **136**, 775-788.

MICHAELIS, C., CIOSK, R. & NASMYTH, K. (1997). Cohesins: Chromosomal proteins that prevent premature separation of sister chromatids. *Cell* **91**, 35-45.

MICHELI, G., LUZZATTO, A.R.C., CARRI, M.T., DE CAPOA, A. & PELLICCIA, F. (1993). Chromosome length and DNA loop size during early embryonic development of *Xenopus laevis*. *Chromosoma* **102**, 478-483.

MICHELOTTI, E.F., SANFORD, S. & LEVENS, D. (1997). Marking of active genes on mitotic chromosomes. *Nature* **388**, 895-899.

MIDGEON, B.R. (1994). X chromosome inactivation: Molecular mechanisms and genetic consequences. *Trends in Genetics* **10**, 230-235.

MIESFIELD, R., SOLLNER-WEBB, B., CROCE, C. & ARNHEIM., N. (1984). The absence of a human-specific ribosomal DNA transcription factor leads to nucleolar dominance in mouse>human hybrid cells. *Molecular and Cellular Biology* **4**, 1306-1312.

MIKLOS, G.L.G. & JOHN, B. (1979). Heterochromatin and satellite DNA in man: Properties and prospects. *American Journal of Human Genetics* **31**, 264-280.

MILLER, O.J., BREG, W.R., MUKHERJEE, B.B., GAMBLE, A.V.N. & CHRISTAKOS, A.C. (1963). Non-random distribution of chromosomes in metaphase figures from cultured human leucocytes. II The peripheral location of chromosomes 13, 17-18 and 21. *Cytogenetics* **2**, 152-167.

MILLER, O.J., MILLER, D.A., DEV, V.G., TANTRAVAHI, R. & CROCE, C.M. (1976). Expression of human and suppression of mouse nucleolus organiser activity in mouse-human somatic cell hybrids. *Proceedings of the National Academy of Sceinces U.S.A.* **73**, 4531-4535.

MILLER, O.J., SCHNEDL, W., ALLEN, J. & ERLANGER, B.F. (1974). 5-Methylcytosine localised in mammalian constitutive heterochromatin. *Nature* **251**, 636-637.

MILLER, O.L.Jr. & BAKKEN, A.H. (1972). Morphological studies of transcription. *Acta Endocrinology Supplement* **168**, 155-177.

MILOT, E., FRASER, P. & GROSVELD, F. (1996). Position effects and genetic disease. *Trends in Genetics* **12**, 123-126.

MIMORI, T., HARDIN, J.A. & STEITZ, J.A. (1986). Characterisation of the DNA-binding protein antigen Ku recognised by autoantibodies from patients with rheumatic disorders. *The Journal of Biological Chemistry* **261**, 2274-2278.

MIRKOVITCH, J., GASSER, S.M. & LAEMMLI, U.K. (1988). Scaffold attachment of DNA loops in metaphase chromosomes. *Journal of Molecular Biology* **200**, 101-109.

MIRKOVITCH, J., MIRAULT, M. & LAEMMLI, U.K. (1984). Organisation of the higher-order chromatin loop: Specific DNA attachment sites on the nuclear scaffold. *Cell* **39**, 223-232.

MISTELI, T., CACERES, J.F. & SPECTOR, D.L. (1997). The dynamics of pre-mRNA splicing factor in living cells. *Nature* **387**, 523-527.

MITCHELL, A.R., GOSDEN, J.R. & MILLER, D.A. (1985). A cloned sequence, p82H, of the alphoid repeated DNA family found at centromeres of all human chromosomes. *Chromosoma* **92**, 369-371.

MITELMAN, F., MERTENS, F. & JOHANSSON, B. (1997). A breakpoint map of recurrent chromosomal rearrangements in human neoplasia. *Nature Genetics* **15S**, 417-474.

MIZZEN, C.A., YANG, X.-J., KOKUBO, T., BROWNELL, J.E., BANNISTER, A.J., OWEN-HUGHS, T., WORKMAN, J., WANG, L., BERGER, S.L., KOUZARIDES, T., NAKATANI, Y. & ALLIS, C.D. (1996). The $TAF_{II}250$ subunit of TFIID has histone acetyltransferase activity. *Cell* **87**, 1261-1270.

MOROI, Y., PEEBLES, C., FRITZLER, M.J., STEIGERWALD, J. & TAN, E.M. (1980). Autoantibody to centromere (kinetochore) in scleroderma. *Proceedings of the National Academy of Sciences U.S.A.* **77**, 1627-1631.

MORTON, N.E. (1991). Parameters of the human genome. *Proceedings of the National Academy of Sciences U.S.A.* **88**, 7474-7476.

MOUCHIROUD, D., D'ONOFRIO, G., AISSANI, B., MACAYA, G., GAUTIER, C. & BERNARDI, G. (1991). The distribution of genes in the human genome. *Gene* **100**, 181-187.

MOYZIS, R.K., TORNEY, D.C., MEYNE, J., BUCKINGHAM, J.M., WU, J., BURKS, C., SIROTKIN, K.M. & GOAD,W.B. (1989). The distribution of interspersed repetitive DNA sequences in the human genome. *Genomics* **4**, 273-289.

MUELLER, R.D., YASUDA, H., HATCH, C.L., BONNER, W.M. & BRADBURY, E.M. (1985). Identification of ubiquitinated histones 2A and 2B in *Physarum polycephalum*. *The Journal of Biological Chemistry* **260**, 5147-5153.

MULLER, J. (1995). Transcriptional silencing by the *Polycomb* protein in *Drosophila* embryos. *The EMBO Journal* **14**, 1209-1220.

MULLER, J., GAUNT, S. & LAWRENCE, P.A. (1995). Function of the *Polycomb* protein is conserved in mice and flies. *Development* **121**, 2847-2852.

MURRAY, E.J. & GROSVELD, F. (1987). Site specific demethylation in the promoter of human γ-globin gene does not alleviate methylation mediated suppression. *The EMBO Journal* **6**, 2329-2335.

MUSIO, A., MARIANI, T., FREDIANI, C., SBRANA, I. & ASCOLI, C. (1994). Longitudinal patterns similar to G-banding in untreated human chromosomes: Evidence from atomic force microscopy. *Chromosoma* **103**, 225-229.

MUSTKOV, V.J., RUSSANOVA, V.R., DIMITROV, S.I. & PASHEV, I.G. (1996). Histones associated with non-nucleosomal rat ribosomal genes are acetylated while those bound to nucleosome-organised gene copies are not. *The Journal of Biological Chemistry* **271**, 11852-11857.

NACHMAN, M.W. & CHUCHILL, G.A. (1996). Heterogeneity in rates of recombination across the mouse genome. *Genetics* **142**, 537-548.

NAEGLE, R., FREEMAN, T., MCMORROW, L. & LEE, H.-Y. (1995). Precise spatial positioning of chromosomes during prometaphase: Evidence for chromosomal order. *Science* **270**, 1831-1835.

NAKAYASU, H. & BEREZNEY, R. (1989). Mapping replication sites in the eukaryotic cell nucleus. *The Journal of Cell Biology* **108**, 1-11.

NAN, X.F., CAMPOY, J. & BIRD, A. (1997). MeCP2 is a transcriptional repressor with abundant binding sites in genomic chromatin. *Cell* **88**, 471-481.

NAN, X., TATE, P., LI, E. & BIRD, A. (1996). DNA methylation specifies chromosomal localisation of MeCP2. *Molecular and Cellular Biology* **16**, 414-421.

NATSOULIS, G., THOMAS, W., ROGHMANN, M.-C., WINSTON, F. & BOEKE, J.D. (1989). *Ty1* transposition in *Saccharomyce cerevisiae* is non-random. *Genetics* **123**, 269-279.

NEITZEL, H. (1986). A routine method for the establishment of permanent growing lymphoblastoid cell lines. *Human Genetics* **73**, 320-326.

NELSON, D.L., LEDBETTER, S.A., CORBO, L., VICTORIA, M.F., RAMIREZ-SOLIS, R., WEBSTER, T.D., LEDBETTER, D.H. & CASKEY, C.T. (1989). *Alu* polymersae chain reaction: A method for rapid isolation of human-specific sequences from complex DNA sources. *Proceedings in the National Academy of Sciences U.S.A* **86**, 6686-6690.

NER, S.S. & TRAVERS, A.A. (1994). HMG-D, the *Drosophila melanogaster* homologue of HMG 1 protein, is associated with early embryonic chromatin in the absence of histone H1. *The EMBO Journal* **13**, 1817-1822.

NEUWALD, A.F. & LANDSMAN, D. (1997). GCN5-related histone *N*-acetyltransferases belong to a diverse superfamily that includes the yeast SPT10 protein. *Trends in Biological Sciences* **22**, 154-155.

NEWMEYER, D.D. & OHLSSON-WILHELM, B.M. (1985). Monoclonal antibody to a protein of the nucleus and mitotic spindle of mammalian cells. *Chromosoma* **92**, 297-303.

NICKEL, B.E., ALLIS, C.D. & DAVIE, J.R. (1989). Ubiquitinated histone H2B is a preferentially located in transcriptionally active chromatin. *Biochemistry* **28**, 958-963.

NICKOLOFF, J.A. (1992). Transcription enhances intrachromosomal homologous recombination in mammalian cells. *Molecular and Cellular Biology* **12**, 5311-5318.

NIKOLAEV, L.G., TSEVEGIYN, T., AKOPOV, S.B., ASHWORTH, L.K. & SVERDLOV, E.D. (1996). Construction of a chromosome specific library of human MARs and mapping of matrix attachment regions on human chromosome 19. *Nucleic Acids Research* **24**, 1330-1336.

NIMMO, E.R., CRANSTON, G. ALLSHIRE, R.C. (1994). Telomere-associated chromosome breakage in fission yeast results in variegated expression of adjacent genes. *The EMBO Journal* **13**, 3801-3811.

NOTARNICOLA, S.M., MCINTOSH, M.A. & WISE, K.S. (1991). A *Mycoplasma hyorhinis* protein with sequence similarities to nucleotide-binding enzyme. *Gene* **97**, 77-85.

O'BRIEN, S.J., SEUANEX, H.N. & WOMACK, J.E. (1988). Mammalian genome organisation: An evolutionary view. *Annual Review of Genetics* **22**, 323-351.

OCHS, R.L., LICSHWE, M.A., SPOHN, W.H. & BUSCH, H. (1985). Fibrillarin: A new protein of the nucleolus identified by autoimmune sera. *Biological Cell* **54**, 123-134.

OGRYZKO, V.V., SCHILTZ, R.L., RUSSANOVA, V., HOWARD, B.H. & NAKATANI, Y. (1996). The transcriptional coactivators p300 and CBP are histone acetyltransferases. *Cell* **87**, 953-959.

OHSUMI, K., KATAGIRI, C. & KISHIMOTO, T. (1993). Chromosome condensation in *Xenopus* mitotic extracts without histone H1. *Science* **262**, 2033-2035.

OKADA, T.A. & COMINGS, D.E. (1974). Mechanisms of chromosome banding: Similarity between G-bands of mitotic chromosomes and chromomeres of meiotic chromosomes. *Chromosoma* **48**, 65-71.

O'KEEFE, R.T., HENDERSON, S.C. &SPECTOR, D.L. (1992). Dynamic organisation of DNA replication in mammalian cell nuclei: Spatially and temporally-defined replication of chromosome-specific α-satellite DNA sequences. *The Journal of Cell Biology* **116**, 1095-1110.

O'NEILL, L.P. & TURNER, B.M. (1995). Histone H4 acetylation distinguishes coding regions of the human genome from heterochromatin in a differentiation-dependent but transcription-independent manner. *The EMBO Journal* **14**, 3946-3957.

ORLANDO, V. & PARO, R. (1995). Chromatin multi-protein complexes involved in the maintenance of transcription patterns. *Current Opinion in Genetics and Development* **5**, 174-179.

OWEN-HUGHES, T., UTLEY, R.T., COTE, J., PETERSON, C.L. & WORKMAN, J.L. (1996). Persistent site-specific remodelling of a nucleosome array by transient action of the SWI/SNF complex. *Science* **273**, 513-516.

PAK, D.T.S., PFLUMM, M., CHESNOKOV, I., HUANG, D.A., KELLUM, R., MARR, J., ROMANOWSKI, P. & BOTCHAN, M.R. (1997). Association of the origin recognition complex with heterochromatin and HP1 in higher eukaryotes. *Cell* **91**, 311-323.

PALLADINO, F., LAROCHE, T., GILSON, E., AXELROD, A., PILLUS, L.. & GASSER, S.M. (1993). SIR3 and SIR4 proteins are required for the positioning and integrity of yeast telomeres. *Cell* **75**, 543-555.

PALMER, M.J., MERGNER, V.A., RICHMAN, R., MANNING, J.E., KURODA, M.I. & LUCCHESI, J.C. (1993). The *male-specific-one* (*msl-1*) gene of *Drosophila melanogaster* encodes a novel protein that associates with the X chromosome in males. *Genetics* **134**, 545-557.

PANNING, B. & JAENISCH, R. (1996). DNA hypomethylation can activate *Xist* expression and silence X-linked genes. *Genes and Development* **10**, 1991-2002.

PANNING, B., DAUSMAN, J. & JAENISCH, R. (1997). X chromosome inactivation is mediated by *Xist* RNA stabilisation. *Cell* **90**, 907-916.

PARANJAPE, S.M., KRUMM, A. & KADONAGA, J.T. (1995). HMG17 is a chromatin-specific transcription coactivator that increases the efficiency of transcription initiation. *Genes and Development* **9**, 1978-1991.

PARK, P.C. & DE BONI, U. (1996). Transposition of DNAse hypersensitive chromatin to the nuclear periphery coincides temporally with nerve growth factor-induced up-regulation of gene expression in PC12 cells. *Proceedings of the National Academy of Sciences U.S.A.* **93**, 11646-11651.

PARO, R. (1993). Mechanisms of heritable gene repression during development of *Drosophila*. *Current Opinion in Cell Biology* **5**, 999-1005.

PARO, R. & HOGNESS, D.S. (1991). The *Polycomb* protein shares a homologous domain with a heterochromatin-associated protein of *Drosophila*. *Proceedings of the National Academy of Sciences U.S.A.* **88**, 263-267.

PARTHUN, M.R., WIDOM, J. & GOTTSCGLING, D.E. (1996). The major cytoplasmic histone acetyltransferase in yeast: Links to chromatin replication and histone metabolism. *Cell* **87**, 85-94.

PAULSON, J.R. (1989). Scaffold morphology in histone-depleted HeLa metaphase chromosomes. *Chromosoma* **97**, 289-295.

PAULSON, J.R. & LAEMMLI, U.K. (1977). The structure of histone-depleted metaphase chromosomes. *Cell* **12**, 817-828.

PAZIN, M.J. & KADONAGA, J.T. (1997). What's up and down with histone deacetylation and transcription? *Cell* **89**, 325-328.

PEARCE, J.J.H., SINGH, P.B. & GAUNT, S.J. (1992). The mouse has a *Polycomb*-like chromobox gene. *Development* **114**, 921-929.

PEARSE, A.G.E. (1968). *Histochemistry: Volume I.* London: J. & A. Churchill Ltd. pp70-86.

PELEGRI, F. & LEHMANN, R. (1994). A role of *Polycomb* group genes in the regulation of gap gene expression in *Drosophila*. *Genetics* **136**, 1341-1353.

PENNY, G.D., KAY, G.F., SHEARDOWN, S.A., RASTAN, S. & BROCKDORFF, N. (1996). Requirement for *Xist* in X chromosome inactivation. *Nature* **379**, 131-137.

PETERSON, C.L. (1994). The SMC family: Novel proteins for chromosome condensation? *Cell* **79**, 389-392.

PETERSON, C.L. (1996). Multiple SWItches to turn on chromatin? *Current Opinion in Genetics and Development* **6**, 171-175.

PETERSON, C.L. & TAMKUN, J.W. (1995). The SWI-SNF complex: A chromatin remodelling machine? *Trends in Biochemical Sciences* **20**, 143-146.

PETES, T.D. (1979). Yeast ribosomal DNA genes are located on chromosome XII. *Proceedings of the National Academy of Sciences U.S.A.* **76**, 410-414.

PETTERSSON, I., HINTERBERGER, M., MIMORI, T., GOTTLEIB, E. & STEITZ, J.A. (1984). The structure of mammalian small nuclear ribonucleoproteins. *The Journal of Biological Chemistry* **259**, 5907-5914.

PHI-VAN, L. & STRATLING, W.H. (1988). The matrix attachment regions of the chicken lysozyme gene co-map with the boundaries of the chromatin domain. *The EMBO Journal* **7**, 655-664.

PIEK, A.C.M., VAN DER VELDEN, H.M.W., RIJKEN, A.A.M., NEIS, J.M. & WANKA, F. (1985). Protein composition of the chromosomal scaffold and interphase nuclear matrix. *Chromosoma* **91**, 137-144.

PILIA, G., LITTLE, R.D., AISSANI, B., BERNARDI, G. & SCHLESSINGER, D. (1993). Isochores and CpG-islands in YAC contigs in human Xq26.1-qter. *Genomics* **17**, 456-462.

PINKEL, D., GRAY, J.W., TRASK, B., VAN DEN ENGH, G., FUSCOE, J. & VAN DEKKEN, H. (1986). Cytogenetic analysis by *in situ* hybridisation with fluorescently labelled nucleic acid probes. *Cold Spring Harbour Symposia on Quantitative Biology* **LI**, 151-157.

PINKEL, D., LANDEGENT, J., COLLINS, C., FUSCOE, J., SEGRAVES, R., LUCAS, J. & GRAY, J. (1988). Fluorescence *in situ* hybridisation with human chromosome-specific libraries: Detection of trisomy 21 and translocations of chromosome 4. *Proceedings of the National Academy of Sciences U.S.A.* **85**, 9138-9142.

PIRROTTA, V. (1995). Chromatin complexes regulating gene expression in *Drosophila*. *Current Opinion in Genetics and Development* **5**, 466-472.

PIRROTTA, V. (1997). Chromatin-silencing mechanisms in *Drosophila* maintain patterns of gene expression. *Trends in Genetics* **13**, 314-318.

PLATERO, J.S., HARTNETT, T. & EISSENBERG, J.C. (1995). Functional analysis of the chromo domain of HP1. *The EMBO Journal* **14**, 3977-3986.

PLUTA, A.F., MACKAY, A.M., AINSZTEIN, A.M., GOLDBERG, I.G. & EARNSHAW, W.C. (1995). The centromere: Hub of chromosomal activities. *Science* **270**, 1591-1594.

POPP, S., SCHOLL, H.P., LOOS, P., JAUCH, A. STELZER, E., CREMER, C. & CREMER, T. (1990). Distribution of chromosome 18 and X centric heterochromatin in the interphase nucleus of cultured human cells. *Experimental Cell Research* **189**, 1-12.

POSTNIKOV, Y.V., SHICK, V.V., BELYAVSKY, A.V., KHRAPKO, K.R., BRODOLIN, K.L., NIMOLSKAYA, T.A. & MIRZABEKOV, A.D. (1991). Distribution of high mobility group proteins 1/2, E and 14/17 and linker histones H1 and H5 on transcribed and non-transcribed regions of chicken erythrocyte chromatin. *Nucleic Acids Research* **19**, 717-725.

POVEY, S., SMITH, M., HAINES, J., KWIATKOWSKI, D., FOUNTAIN, J., BALE, A., ABBOTT, C., JACKSON, I., LAWRIE, M. & HULTEN, M. (1992). Report on the first international workshop on chromosome 9. *Annals of Human Genetics* **56**, 167-221.

PROSSER, J., FROMMER, M., PAUL, C. & VINCENT, P.C. (1986). Sequence relationships of three human satellite DNAs. *Journal of Molecular Biology* **187**, 145-155.

PRUSS, D., HAYES, J.J. & WOLFFE, A.P. (1995). Nucleosomal anatomy: Where are the histones? *BioEssays* **17**, 161-170.

PUVION-DUTILLEUL, F. & BESSE, S. (1994). Induction of complete segregation of cellular DNA and non-encapsulated viral genomes in herpes simplex virus type 1 infected HeLa cells as revealed by *in situ* hybridisation. *Chromosoma* **103**, 104-110.

PYRPASOPOULOU, A., MEIER, J., MAISON, C., SIMOS, G. & GEORGATOS, S.D. (1996). The lamin B receptor (LBR) provides essential chromatin docking sites at the nuclear envelope. *The EMBO Journal* **15**, 7108-7119.

RABL, C. (1885). Uber Zelltheilung. *Morphologisches Jahrbuch* **10**, 214-330.

RAE, P.M.M. & FRANKE, W.W. (1972). The interphase distribution of satellite DNA-containing heterochromatin in mouse nuclei. *Chromosoma* **39**, 443-456.

RAO, P.N., ZHAO, J., GANJU, R.K. & ASHORN, C.L. (1989). Monoclonal antibody against the centrosome. *Journal of Cell Science* **93**, 63-69.

RAPPOLD, G.A., CREMER, T., HAGER, H.D., DAVIES, K.E., MULLER, C.R. & YANG, T. (1984). Sex chromosome positions in human interphase nuclei as studied by *in situ* hybridisation with chromosome specific DNA probes. *Human Genetics* **67**, 317-325.

RASHEED, S., NELSON-REES, W.A., TOTH, E.M., ARNSYEIN, P., GARDNER, M.B. (1974). Characterisation of a newly derived human sarcoma cell line (HT-1080). *Cancer* **33**, 1027-1033.

RASTELLI, L., CHAN, C.S. & PIRROTTA, V. (1993). Related chromosome binding sites for *zeste*, suppressors of *zeste* and *Polycomb* group proteins in *Drosophila* and their dependence *Enhancer of zeste* function. *The EMBO Journal* **12**, 1513-1522.

RATTNER, J.B. (1992). Integrating chromosome structure with function. *Chromosoma* **101**, 259-264.

RATTNER, J.B., HENDEZEL, M.J., SOMMER FURBEE, C., MULLER, M.T. & BAZZET-JONES, D.P. (1996). Topoisomerase IIα is associated with the mammalian centromere in a cell cycle- and species-specific manner and is required for proper centromere/kinetochore structure. *The Journal of Cell Biology* **134**, 1097-1107.

RATTNER, J.B., KINGWELL, B.G. & FRITZLER, M.J. (1988). Detection of distinct structural domains within the primary constriction using autoantibodies. *Chromosoma* **96**, 360-367.

RATTNER, J.B. & LIN, C.C. (1985). Radial loops and helical coils coexist in metaphase chromosomes. *Cell* **42**, 291-296.

RAWLINS, D.J. & SHAW, P.J. (1991). Three-dimensional organisation of ribosomal DNA in interphase nuclei of *Pisum sativum* by *in situ* hybridisation and optical tomography. *Chromosoma* **99**, 143-151.

RAZIN, A. & SHEMER, R. (1995). DNA methylation in early development. *Human Molecular Genetics* **4**, 1751-1755.

RAZIN, S.V. & GROMOVA, I.I. (1995). The channels model of nuclear matrix structure. *BioEssays* **17**, 443-450.

RAZIN, S.V., HANCOCK, R., IAROVAIA, O., WESTERGAARD, O., GROMOVA, I. & GEORGIEV, G.P. (1993). Structural-functional organisation of chromosomal DNA domains. *Cold Spring Harbour Symposia on Quantitative Biology* **LVIII**, 25-35.

RAZIN, S.V., KEKELIDZE, M.G., LUKANIDIN, E.M., SCHERRER, K. & GEORGIEV, G.P. (1986). Replication origins are attached to the nuclear skeleton. *Nucleic Acids Research* **14**, 8189-8207.

REEVES, R. & NISSEN, M.S. (1990). The A.T-DNA-binding domain of mammalian high mobility group I chromosomal proteins. *The Journal of Biological Chemistry* **265**, 8573-8582.

REEVES, R. & WOLFFE, A.P. (1996). Substrate structure influences binding of the non-histone protein HMG-I(Y) to free and nucleosomal DNA. *Biochemistry* **35**, 5063-5074.

REIN, T., ZORBAS, H. & DEPAMPHILIS, M.L. (1997). Active mammalian replication origins are associated with a high-density cluster of ^{m}CpG dinucleotides. *Molecular and Cellular Biology* **17**, 416-426.

RENAULD, H., APARICIO, O.M., ZIERATH, P.D., BILLINGTON, B.L., CHHABLANI, S.K. & GOTTSCHLING, D.E. (1993). Silent domains are assembled continuously from the telomere and are defined by promoter distance and strength, and by SIR3 dosage. *Genes and Development* **7**, 1133-1145.

RICH, A., NORDHEIM, A. & WANG, A.H.-J. (1984). The chemistry and biology of left-handed Z-DNA. *Annual review of Biochemistry* **53**, 791-846.

RICHTER, L., BONE, J.R. & KURODA, M.I. (1996). RNA-dependent association of the *Drosophila* maleless protein with the male X chromosome. *Genes to Cells* **1**, 325-336.

RIGGS, A.D. & PFEIFER, G.P. (1992). X chromosome inactivation and cell memory. *Trends in Genetics* **8**, 169-174.

RIGGS, M.G., WHITTAKER, R.G., NEUMANN, J.R. & INGRAM, V.M. (1977). *n*-Butyrate causes histone modification in HeLa and Friend erythroleukaemia cells. *Nature* **268**, 462-464.

RINE, J. & HERSKOWITZ, I. (1987). Four genes responsible for a position effect on expression from HML and HMR in *Saccharomyces cerevisiae*. *Genetics* **116**, 9-22.

RINE, J., STRATHERN, J.N., HICKS, J.B. & HERSKOWTITZ, I. (1979). A suppressor of mating type locus mutations in *Saccharomyces cerevisiae*: Evidence for and identification of cryptic mating type loci. *Genetics* **93**, 877-901.

RIVIER, D.H. & RINE, J. (1992). Silencing: The establishment and inheritance of stable, repressed transcription states. *Current Opinion in Genetics and Development* **2**, 286-292.

ROBERTSON, G., GARRICK, D., WU, W., KEARNS, M. & MARTIN, D. (1995). Position-dependent variegation of globin expression in mice. *Proceedings of the National Academy of Sciences U.S.A.* **92**, 5371-5375.

ROBINETT, C.C., STRAIGHT, A., LI, G., WILLHELM, C., SUDLOW, G., MURRAY, A. & BELMONT, A.S. (1996). *In vivo* localisation of DNA sequences and visualisation of large-scale chromatin organisation using *Lac* operator/repressor recognition. *The Journal of Cell Biology* **135**, 1685-1700.

ROBINSON, S.I., SMALL, D., IZERDA, R., MCKNIGHT, G.S. & VOGELSTEIN, B. (1983). The association of transcriptionally active genes with the nuclear matrix of the chicken oviduct. *Nucleic Acids Research* **11**, 5113-5130.

ROCA, J. (1995). The mechanisms of DNA topoisomerases. *Trends in Biochemical Sciences* **20**, 156-160.

ROCCHI, M., DI CASTRO, M. & PRANTERA, G. (1979). Effects of DAPI on human leukocytes *in vitro*. *Cytogenetics and Cell Genetics* **23**, 250-254.

ROTH, S.Y. & ALLIS, C.D. (1992). Chromatin condensation: Does histone H1 dephosphorylation play a role? *Trends in Biochemical Sciences* **17**, 93-98.

ROTH, S.Y. & ALLIS, C.D. (1996). Histone acetylation and chromatin assembly: A single escort, multiple dances? *Cell* **87**, 5-8.

ROTHSTEIN, R. & GANGLOFF, S. (1995). Hyper-recombination and Bloom's Syndrome: Microbes again provide clues about cancer. *Genome Research* **5**, 421-426.

RUSSELL, L.B. & MONTGOMERY, C.S. (1970). Comparative studies on X-autosome translocations in the mouse. II. Inactivation of autosomal loci, segregation, and mapping of autosomal breakpoints in five T(X;1)S. *Genetics* **64**, 281-312.

SACCONE, S., DE SARIO, A., WEIGANT, J., RAAP, A.K., DELLA VALLE, G. & BERNARDI, G. (1993). Correlations between isochores and chromosomal bands in the human genome. *Proceedings in the National Academy of Sciences U.S.A.* **90**, 11929-11933.

SACHS, R.K., VAN DEN ENGH, G., TRASK, B. & HEARST, J.E. (1995). A random-walk/giant-loop model for interphase chromosomes. *Proceedings of the National Academy of Sciences U.S.A.* **92**, 2710-2714.

SAINZ, J., PEVNY, L., WU, Y., CANTOR, C.R. & SMITH, C.L. (1992). Distribution of interspersed repeats (*Alu* and *Kpn*) on *NotI* restriction fragments of human chromosome 21. *Proceedings of the National Academy of Sciences U.S.A.* **89**, 1080-1084.

SAITOH, N., GOLDBERG, I.G., WOOD, E.R. & EARNSHAW, W.C. (1994). ScII: An abundant chromosome scaffold protein is a member of a family of putative ATPases with an unusual predicted tertiary structure. *The Journal of Cell Biology* **127**, 303-318.

SATOIH, N., GOLDBERG, I. & EARNSHAW, W.C. (1995). The SMC proteins and the coming of age of the chromosome scaffold hypothesis. *BioEssays* **17**, 759-766.

SAITOH, Y. & LAEMMLI, U.K. (1994a). Metaphase chromosome structure: Bands arise from a differential folding path of the highly AT-rich scaffold. *Cell* **76**, 609-622.

SAITOH, Y. & LAEMMLI, U.K. (1994b). From the chromosomal loops and the scaffold to the classic bands of metaphase chromosomes. *Cold Spring Harbour Symposia on Quantitative Biology* **LVIII**, 755-765.

SAKA, Y., SUTANI, T., YAMASHITA, Y., SAITOH, S., TAKEUCHI, M., NAKASEKO, Y. & MITSUHIRO, Y. (1994). Fission yeast *cut3* and *cut14*, members of a ubiquitous protein family, are required for chromosome condensation and segregation in mitosis. *The EMBO Journal* **13**, 4938-4952.

SATIJN, D.P.E., GUNSTER, M.J., VAN DER VLAG, V., HAMER, K.M., SCHUL, W., ALKEMA, M.J., SAURIN, A.J., FREEMONT, P.S., VAN DRIEL, R. & OTTE, A.P. (1997). RING1 is associated with the *Polycomb* group protein complex and acts as a transcriptional repressor. *Molecular and Cellular Biology* **17**, 4105-4113.

SAUNDERS, W.S., CHUE, C., GOEBL, M., CRAIG, C., CLARK, R.F., POWERS, J.A., EISSENBERG, J.C., ELGIN, S.C.R., ROTHFIELD, N.F. & EARNSHAW, W.C. (1993). Molecular cloning of a human homologue of *Drosophila* heterochromatin protein HP1 using anti-centromere autoantibodies with anti-chromo specificity. *Journal of Cell Science* **104**, 573-582.

SAX, K. (1940). An analysis of X-ray induced chromosomal aberrations in *Tradescantia*. *Genetics* **25**, 41-68.

SCHARDIN, M., CREMER, T., HAGER, H.D. & LANG, M. (1985). Specific staining of human chromosomes in Chinese hamster X man hybrid cell lines demonstrates interphase chromosome territories. *Human Genetics* **71**, 281-287.

SCHEER, U. & WEISENBERGER, D. (1994). The nucleolus. *Current Opinion in Cell Biology* **6**, 354-359.

SCHERLY, D., BOELENS, W., VAN VENJOOIJ, W.J., DATHAN, N.A., HAMM, J. & MATTAJ, I.W. (1989). Identification of the RNA binding segment of human U1A protein and definition of its binding site on U1 snRNA. *The EMBO Journal* **8**, 4163-4170.

SCHERDIN, U., RHODES, K. & BREINDL, M. (1990). Transcriptionally active genome regions are preferred targets for retrovirus integration. *Journal of Virology* **64**, 907-912.

SCHMICKEL, R.D., GONZALIEZ, I.L. & ERICKSON, J.M. (1985). Nucleolus organising genes on chromosome 21: Recombination and non-disjunction. *Annals of the New York Academy of Sciences* **450**, 121-131.

SCHMID, M., ENDERLE, E., SCHINDLER, D. & SCHEMPP, W. (1989). Chromosome banding and DNA replication patterns in bird karyotypes. *Cytogenetics and Cell Genetics* **52**, 139-146.

SCHMID, M., HAAF, T. & GRUNERT, D. (1984). 5-Azacytidine-induced under-condensation in human chromosomes. *Human Genetics* **67**, 257-263.

SCHULER, G.D. *et al.* (1996). A gene map of the human genome. *Science* **274**, 540546.

SEABRIGHT, M. (1971). A rapid banding technique for human chromosomes. *The Lancet* **2**, 971-972.

SELKER, E.U. & STEVENS, J.N. (1985). DNA methylation at asymmetric sites is associated with numerous transition mutations. *Proceedings of the National Academy of Sciences U.S.A.* **82**, 8114-8118.

SENTIS, C., LUDENA, P. & FERNANDEZ-PIQUERAS, J. (1993). Non-uniform distribution of methylatable CCGG sequences on human chromosomes as shown by *in situ* methylation. *Chromosoma* **102**, 267-271.

SHAMU, C.E. & MURRAY, A. (1992). Sister chromatid separation in frog extracts requires DNA topoisomerase II activity during anaphase. *The Journal of Cell Biology* **117**, 921-934.

SHELBY, R.D., HAHN, K.M. & SULLIVAN, K.F. (1996). Dynamic elastic behaviour of α-satellite DNA domains visualised *in situ* in living human cells. *The Journal of Cell Biology* **135**, 545-557.

SHEN, X. & GOROVSKY, M.A. (1996). Linker histone H1 regulates specific gene expression but not global transcription *in vivo*. *Cell* **86**, 475-483.

SHEN, X., YU, L., WEIR, J.W. & GOROVSKY, M.A. (1995). Linker histone are not essential and affect chromatin condensation *in vivo*. *Cell* **82**, 47-56.

SHENKAR, R., SHEN, M. & ARNHEIM, N. (1991). DNase I-hypersensitive sites and transcription factor-binding motifs within the mouse Eβ meiotic recombination hot spot. *Molecular and Cellular Biology* **11**, 1813-1819.

SHERMAN, J.M. & PILLUS, L. (1997). An uncertain silence. *Trends in Genetics* **13**, 308-313.

SHEWCHUK, B.M. & HARDISON, R.C. (1997). CpG-islands from the α-globin gene cluster increase gene expression in an integration-dependent Manner. *Molecular and Cellular Biology* **17**, 5856-5866.

SHEILS, C., COUTELLE, C. & HUXLEY, C. (1997). Contiguous arrays of satellites 1, 3 and β form a 1.5Mb domain on chromosome 22p. *Genomics* **44**, 35-44.

SHUMACHER, A. & MAGNUSON, T. (1997). Murine *Polycomb*- and *trithorax*-group gene regulate homeotic pathways and beyond. *Trends in Genetics* **13**, 167-170.

SHYKIND, B.M., KIM, J. & SHARP, P.A. (1995). Activation of the TFIID-TFIIA complex with HMG-2. *Genes and Development* **9**, 1354-1365.

SILLAR, R. & YOUNG, B.D. (1981). A new method for the preparation of metaphase chromosomes for flow analysis. *The Journal of Histochemistry and Cytochemistry* **29**, 74-78.

SIMON, J. (1995). Locking in stable states of gene expression: Transcriptional control during *Drosophila* development. *Current Opinion in Cell Biology* **7**, 376-385.

SINGER, M.F. (1982). Highly repeated sequences in mammalian genomes. *International Review of Cytology* **76**, 67-112.

SINGER, R.H. & GREEN, M.R. (1997). Compartmentalisation of eukaryotic gene expression: Causes and effects. *Cell* **91**, 291-294.

SINGH, P.B., MILLER, J.R., PEARCE, J., KPTHARY, R., BURTON, R.D., PARO, R., JAMES, T.C. & GUANT, S.J. (1991). A sequence motif found in a *Drosophila* heterochromatin protein is conserved in animals and plants. *Nucleic Acids Research* **19**, 789-794.

SMITH, B.J., ROBERTSON, D., BIRBECK, S.C., GOODWIN, G.H. & JUHNS, E.W. (1978). Immunochemical studies of high mobility group non-histone chromatin proteins HMG 1 and HMG 2. *Experimental Cell Research* **115**, 420-423.

SMITH, J.S. & BOEKE, J.D. (1997). An unusual form of transcriptional silencing in yeast ribosomal DNA. *Genes and Development* **11**, 241-254.

SOBEL, R.E., COOK, R.G., PERRY, C.A., ANNUNZIATO, A.T. & ALLIS, C.D. (1995). Conservation of deposition-related acetylation sites in newly synthesised histones H3 and H4. *Proceedings of the National Academy of Sciences U.S.A.* **92**, 1237-1241.

SOLLNER-WEBB, B. & TOWER, J. (1986). Transcription of cloned eukaryotic ribosomal RNA genes. *Annual Review of Biochemistry* **55**, 801-830.

SOMSSICH, I., HAMEISTER, H. & WINKING, H. (1981). The pattern of early replicating bands in the chromosomes of the mouse. *Cytogenetics and Cell Genetics* **30**, 222-231.

SORIANO, P., MEUNIER-ROTIVAL, M. & BERNARDI, G. (1983). The distribution of interspersed repeats is non-uniform and conserved in the mouse and human genomes. *Proceedings of the National Academy of Sciences U.S.A.* **80**, 1816-1820.

SPANN, T.P., MOIR, R.D., GOLDMAN, A.E., STICK, R. & GOLDMAN, R.D. (1997). Disruption of nuclear lamin organisation alters the distribution of replication factors and inhibits DNA synthesis. *The Journal of Cell Biology* **136**, 1201-1212.

SPARVOLI, E., LEVI, M. & ROSSI, E. (1994). Replicon clusters may form stable complexes of chromatin and chromosomes. *Journal of Cell Science* **107**, 3097-3103.

SPECTOR, D.L. (1990). Higher order nuclear organisation: Three-dimensional distribution of small nuclear ribonucleoprotein particles. *Proceedings of the National Academy of Sciences U.S.A.* **87**, 147-151.

SPECTOR, D.L. (1993). Macromolecular domains within the cell nucleus. *Annual Review of Cell Biology* **9**, 265-315.

SPECTOR, D.L. & SMITH, H.C. (1986). Redistribution of U-snRNPs during mitosis. *Experimental Cell Research* **163**, 87-94.

STANCHEVA, I., LUCCHINI, R., KOLLER, T. & SOGO, J.M. (1997). Chromatin structure and methylation of rat rRNA genes studied by formaldehyde fixation and psoralen cross-linking. *Nucleic Acids Research* **25**, 1727-1735.

STEINBACH, O.C., WOLFFE, A.P. & RUPP, R.A.W. (1997). Somatic linker histones cause loss of mesodermal competence in *Xenopus*. *Nature* **389**, 395-400.

STRATMANN, R. & LEHNER, C.F. (1996). Separation of sister chromatids in mitosis requires the *Drosophila pimples* product, a protein degraded after the metaphase/anaphase transition. *Cell* **84**, 25-35.

STRAUSS, F. & VARSHAVSKY, A. (1984). A protein binds to a satellite DNA repeat at three specific sites that would be brought into mutual proximity by DNA folding in the nucleosome. *Cell* **37**, 889-901.

STREHL, S., LASALLE, J.M. & LALANDE, M. (1997). High-resolution analysis of DNA replication domain organisation across an R/G-band boundary. *Molecular and Cellular Biology* **17**, 6157-6166.

STRICK, R. & LAEMMLI, U.K. (1995). SARs are *cis* DNA elements of chromosome dynamics: Synthesis of a SAR repressor protein. *Cell* **83**, 1137-1148.

STRISSEL, P.L., ESPINOSA III, R., ROWLEY, J.D. & SWIFT, H. (1996). Scaffold attachment regions in centromere-associated DNA. *Chromosoma* **105**, 122-133.

STROUBOULIS, J. & WOLFFE, A.P. (1996). Functional compartmentalisation of the nucleus. *Journal of Cell Science* **109**, 1991-2000.

STRUNNIKOV, A.V., HOGAN, E. & KOSHLAND, D. (1995). SMC2, a *Saccharomyces cerevisiae* gene essential for chromosome segregation and condensation, defines a subgroup within the SMC family. *Genes and Development* **9**, 587-599.

STRUNNIKOV, A.V., LARIONOV, V.L. & KOSHLAND, D. (1993). SMC1: An essential yeast gene encoding a putative head-rod-tail protein is required for nuclear division and defines a new ubiquitous protein family. *The Journal of Cell Biology* **123**, 1635-1648.

STRUTT, H., CAVALLI, G. & PARO, R. (1997). Co-localisation of *Polycomb* protein and GAGA factor on regulatory elements responsible for the maintenance of homeotic gene expression. *The EMBO Journal* **16**, 3621-3632.

STRUTT, H. & PARO, R. (1997). The *Polycomb* group complex of *Drosophila melanogaster* has different compositions at different target genes. *Molecular and Cellular Biology* **17**, 6773-6783.

STRYER, L. (1981). *Biochemistry*. San Francisco: W.H. Freeman and Company. pp613-615.

STUURMAN, N., DE GRAAF, A., FLOORE, A., JOSSO, A., HUMBEL, B., DE JONG, L. & VAN DRIEL, R. (1992). A monoclonal antibody recognising nuclear matrix-associated nuclear bodies. *Journal of Cell Science* **101**, 773-784.

STUURMAN, N., MEIJNE, A.M.L., VAN DER POL, A.J., DE JONG, L., VAN DRIEL, R. & VAN RENSWOUDE, J. (1990). The nuclear matrix from cells of different origin. *The Journal of Biological Chemistry* **265**, 5460-5465.

SUDA, T., MISHIMA, Y., TAKAYANAGI, K., ASAKURA, H., ODANI, S. & KOMINAMI, R. (1996). A novel activity of HMG domains: Promotion of the triple-stranded complex formation between DNA containing $(GGA/TCC)_{11}$ and $d(GGA)_{11}$ oligonucleotides. *Nucleic Acids Research* **24**, 4733-4740.

SULLIVAN, B.A. (1995). Characterisation of chromosome structure and centromeric activity of Robertsonian translocations. PhD thesis, University of Baltimore.

SULLIVAN, B.A. & SCHWARTZ, S. (1995). Identification of centromeric antigens in dicentric Robertsonian translocations: CENP-C and CENP-E are necessary components of functional centromeres. *Human Molecular Genetics* **4**, 2189-2197.

SULLIVAN, K.F., HECHENBERGER, M. & MASRI, K. (1994). Human CENP-A contains a histone H3 related histone fold domain that is required for targeting to the centromere. *The Journal of Cell Biology* **127**, 581-592.

SUMNER, A.T. (1990). *Chromosome banding*. London: Unwin Hyman Ltd.

SUMNER, A.T. (1991). Scanning electron microscopy of mammalian chromosomes from prophase to telophase. *Chromosoma* **100**, 410-418.

SUMNER, A.T. (1996). The distribution of topoisomerase II on mammalian chromosomes. *Chromosome Research* **4**, 5-14.

SUMNER, A.T. & EVANS, H.J. (1971). New techniques for distinguishing between human chromosomes. *Nature New Biology* **232**, 31-32.

SUMNER, A.T., DE LA TORRE, J. & STUPPIA, L. (1993). The distribution of genes on chromosomes: A cytological approach. *Journal of Molecular Evolution* **37**, 117-122.

SUMNER, A.T., TAGGART, M.H., MEZZANOTTE, R. & FERRUCCI, L. (1990). Patterns of digestion of human chromosomes by restriction endonuclease demonstrated by *in situ* nick translation. *Histochemical Journal* **22**, 639-652.

SUN, J.-M., CHEN, H.Y. & DAVIE, J.R. (1994). Nuclear Factor 1 is a component of the nuclear matrix. *Journal of Cellular Biochemistry* **55**, 252-263.

SUN, J., WIADERKIEWICZ, R. & RUIZ-CARRILLO, A. (1989). Histone H5 in the control of DNA synthesis and cell proliferation. *Science* **245**, 68-71.

SUN, L., PAULSON, K.E., SCHMID, C.W., KADYK, L. & LEINWAND, L. (1984). Non-*Alu* family interspersed repeats in human DNA and their transcriptional activity. *Nucleic Acids Research* **12**, 2669-2690.

SUPAKAR, P.C., WEIST, D., ZHANG, D., INAMDAR, N., ZHANG, X.-Y., KHAN, R., EHRLICH, K.C. & EHRLICH, M. (1988). Methylated DNA-binding protein is present in various mammalian cell types. *Nucleic Acids Research* **16**, 8029-8044.

SURRALLES, J., JEPPESEN, P., MORRISON, H. & NATARAJAN, A.T. (1996). Analysis of loss of inactive X chromosomes in interphase cells. *American Journal of Human Genetics* **59**, 1091-1096.

SUSO PLATERO, J., HARTNETT, T. & EISENBERG, J.C. (1995). Functional analysis of the chromo domain of HP1. *The EMBO Journal* **14**, 3977-3986.

SUTANI, T. & YANAGIDA, M. (1997). DNA renaturation activity of the SMC complex implicated in chromosome condensation. *Nature* **388**, 798-801.

SWEDLOW, J.R. & HIRANO, T. (1996). Chromosome dynamics: Fuzzy sequences, specific attachments? *Current Biology* **6**, 544-547.

SWEDLOW, J.R., SEDAT, J.W., AGARD, D.A. (1993). Multiple chromosomal populations of topoisomerase II detected *in vivo* by time-lapse, three-dimensional wide-field microscopy. *Cell* **73**, 97-108.

SYKES, R.C., LIN, D., HWANG, S.J., FRAMSON, P.E. & CHINAULT, A.C. (1988). Yeast ARS function and nuclear matrix association coincide in a short sequence from the human HPRT locus. *Molecules, Genes and Genetics* **212** , 301-309.

TAAGEPERA, S., RAO, P.N., DRAKE, F.H. & GORBSKY, G.J. (1993). DNA topoisomerase IIα is the major chromosome protein recognised by the mitotic phosphoprotein antibody MPM-2. *Proceedings of the National Academy of Sciences U.S.A.* **90**, 8407-8411.

TAGARRO, I., GONZALEZ-AGUILERA, J.J. & FERNANDEZ-PERALTA, A.M. (1992). Induction of R-bands on human chromosomes by *TfiI* as the consequence of local differences in target richness. *Cytogenetics and Cell Genetics* **60**, 154-156.

TAKAGI, N., SUGAWARA, O., SASAKI, M. (1982). Regional and temporal changes in the pattern of X chromosome replication during the early post-implantation development of female mouse. *Chromosoma* **85**, 275-286.

TALASZ, H., HELLINGER, W., PUSCHENDORF, B. & LINDNER, H. (1996). *In vivo* phosphorylation of histone H1 variants during the cell cycle. *Biochemistry* **35**, 1761-1767.

TAN, E.M. (1982). Autoantibodies to nuclear antigens (ANA): Their immunobiology and medicine. *Advances in Immunology* **33**, 167-240.

TANIURA, H., GLASS, C. & GERACE, L. (1995). A chromatin binding site in the tail domain of nuclear lamins that interact with core histones. *The Journal of Cell Biology* **131**, 33-44.

TARTOF, K.D. & HENIKOFF, S. (1991). Trans-sensing effects from *Drosophila* to humans. *Cell* **65**, 201-203.

TATE, P. & BIRD, A.P. (1996). Effects of DNA methylation on DNA-binding proteins and gene expression. *Current Opinion in Genes and Development* **3**, 226-231.

TATE, P., SKARNES, W. & BIRD, A. (1996). The methyl-CpG binding protein MeCP2 is essential for embryonic development in the mouse. *Nature Genetics* **12**, 205-208.

TAUNTON, J., HASSIG, C.A. & SCHREIBER, S.L. (1996). A mammalian histone deacetylase related to the yeast transcriptional regulator Rpd3p. *Science* **272**, 408-411.

TAZI, J. & BIRD, A. (1990). Alternative chromatin structure at CpG-islands. *Cell* **60**, 909-920.

TELENIUS, H., PELMEAR, A.H., TUNNACLIFFE, A., CARTER, N.P., BEHMEL, A., FERGUSON-SMITH, M.A., NORDENSKJOLD, M., PFRAGNER, R. & PONDER, B.A.J. (1992). Cytogenetic analysis by chromosome painting using DOP-PCR amplified flow-sorted chromosomes. *Genes, Chromosomes and Cancer* **4**, 257-263.

THANOS, D., DU, W. & MANIATI, T. (1993). The high mobility group protein HMG I (Y) is an essential structural component of a virus-inducible enhancer complex. *Cold Spring Harbour Symposia on Quantitative Biology* **LVIII**, 73-81.

THOMA, F., KOLLER, TH. & KLUG, A. (1979). Involvement of histone H1 in the organisation of the nucleosome and of the salt-dependent superstructures of chromatin. *The Journal of Cell Biology* **83**, 407-427.

THOMPSON, J.S., HECHT, A. & GRUNSTEIN, M. (1993). *Cold Spring Harbour Symposia on Quantitative Biology* **LVIII**, 247-256.

THOMPSON, E.M., CHRISTIANS, E., STINNAKRE, M.-G. & RENARD, J.-P. (1994a). Scaffold attachment regions stimulate HSP70.1 expression in mouse pre-implantation embryos but not in differentiated tissues. *Molecular and Cellular Biology* **14**, 4694-4703.

THOMPSON, J.S., LING, X. & GRUNSTEIN, M. (1994b). Histone H3 amino terminus is required for telomeric and silent mating locus repression in yeast. *Nature* **369**, 245-247.

THON, G., COHEN, A. & KLAR, A.J. (1994). Three additional linkage groups that repress transcription and meiotic recombination in the mating-type region of *Schizosaccharomyces pombe* **138**, 29-38.

TOBEY, R.A., VALDEZ, J.G. & CRISSMAN, H.A. (1988). Synchronisation of human diploid fibroblasts at multiple stages of the cell cycle. *Experimental Cell Research* **179**, 400-416.

TOMILIN, N., SOLOVJEVA, L., KRUTILINA, R., CHAMBERLAND, C., HANCOCK, R. & VIG, B. (1995). Visualisation of elementary DNA replication units in human nuclei corresponding in size to DNA loop domains. *Chromosome Research* **3**, 32-40.

TOMMERUP, H., DOUSMANIS, A. & DE LANGE, T. (1994). Unusual chromatin in human telomeres. *Molecular and Cellular Biology* **14**, 5777-5785.

TRASK, B.J., ALLE, S., MASSA, H., FERTITTA, A., SACHS, R., VAN DEN ENGH, G. & WU, M. (1993). Studies of metaphase and interphase chromosomes using fluorescence *in situ* hybridisation. *Cold Spring Harbour Symposia on Quantitative Biology* **LVIII**, 767-775.

TRAVERS, A.A. (1994). DNA chaperones: A solution to a persistence problem? *Cell* **77**, 167-169.

TRENT, J.M., KANEKO, Y. & MITELMAN, F. (1989). Report of the committee on structural chromosome changes in neoplasia. *Cytogenetics and Cell Genetics* **51**, 533-562.

TRIESCHMANN, L., POSTNIKOV, Y.V., RICKER, A. & BUSTIN, M. (1995). Modular structure of chromosomal proteins HMG-14 and HMG-17: Definition of a transcriptional enhancement domain distinct from the nucleosomal binding domain. *Molecular and Cellular Biology* **15**, 6663-6669.

TSUKAMOTO, Y., KATO, J.-I. & IKEDA, H. (1997). Silencing factors participate in DNA repair and recombination in *Saccharomyces cerevisiae*. *Nature* **388**, 900-903.

TSUKIYAMA, T., BECKER, P.B. & WU, C. (1994). ATP-dependent nucleosome disruption at a heat-shock promoter mediated by binding of GAGA transcription factor. *Nature* **367**, 525-532.

TSUKIYAMA, T., DANIEL, C., TAMKUN, J. & WU, C. (1995). ISWI, a member of the SWI2/SNF2 ATPase family, encodes the 140 KDa subunit of the nucleosome remodelling factor. *Cell* **83**, 1021-1026.

TSUKIYAMA, T. & WU, C. (1995). Purification and properties of an ATP-dependent nucleosome remodelling factor. *Cell* **83**, 1011-1020.

TURNER, B.M. (1989). Acetylation and deacetylation of histone H4 continue through metaphase with depletion of more-acetylated isoforms and altered site usage. *Experimental Cell Research* **182**, 206-214.

TURNER, B.M. (1995). Histone H4, the cell cycle and a question of integrity. *BioEssays* **17**, 1013-1015.

TURNER, B.M., BIRLEY, A.J. & LAVENDER, J. (1992). Histone H4 isoforms acetylated at specific lysine residues define individual chromosomes and chromatin domains in *Drosophila* polytene nuclei. *Cell* **69**, 375-384.

TURNER, B.M. & FELLOWS, G. (1989). Specific antibodies reveal ordered and cell-cycle-related use of histone-H4 acetylation sites in mammalian cells. *European Journal of Biochemistry* **179**, 131-139.

TURNER, B.M., FRANCHI, L. & WALLACE, H. (1990). Islands of acetylated histone H4 in polytene chromosomes and their relationship to chromatin packaging and transcriptional activity. *Journal of Cell Science* **96**, 335-346.

TURNER, B.M. & O'NEILL, L.P. (1995). Histone acetylation in chromatin and chromosomes. *Seminars in Cell Biology* **6**, 229-236.

UEMURA, T., OHKURA, H., ADACHI, Y., MORINO, K., SHIOZAKI, K. & YANAGIDA, M. (1987). DNA topoisomerase II is required for condensation and separation of mitotic chromosomes in *S.pombe*. *Cell* **50**, 917-925.

UMESONO, K., HIRAOKA, Y., TODA, T. & YANAGIDA, M. (1983). Visualisation of chromosomes in mitotically arrested cells of the fission yeast *Schizosaccharomyces pombe*. *Current Genetics* **7**, 123-128.

URA, K., HAYES, J.J. & WOLFFE, A.P. (1995). A positive role for nucleosome mobility in the transcriptional activity of chromatin templates: Restriction by linker histones. *The EMBO Journal* **14**, 3752-3765.

URA, K., KURUMIZAKA, H., DIMITROV, S., ALMOUZNI, G. & WOLFFE, A.P. (1997). Histone acetylation: Influence on transcription, nucleosome mobility and positioning, and linker histone-dependent transcription repression. *The EMBO Journal* **16**, 2096-2107.

URA, K., NIGHTINGALE, K. & WOLFFE, A.P. (1996). Differential association of HMG1 and linker histones B4 and H1 with dinucleosomal DNA: Structural transactions and transcriptional repression. *The EMBO Journal* **15**, 4959-4969.

VAN DEN ENGH, G., SACHS, R. & TRASK, B.J. (1992). Estimating genomic distance from sequence location in cell nuclei by a random walk model. *Science* **257**, 1410-1412.

VANDRE, D.D., DAVIS, F.M., RAO, P.N. & BORISY, G.G. (1984). Phosphoproteins are components of mitotic microtubule organising centres. *Proceedings of the National Academy of Sciences U.S.A.* **81**, 4439-4443.

VANDRE, D.D., CENTONZE, V.E., PELOQUIN, J., TOMBES, R.M. & BORISY, G.G. (1991). Proteins of the mammalian mitotic spindle: Phosphorylation/dephosphorylation of MAP4 during mitosis. *Journal of Cell Science* **98**, 577-588.

VAN DRIEL, R., WANSINK, D.G., VAN STEENSEL, B., GRANDE, M.A., SCHUL, W. & DE JONG, L. (1995). Nuclear domains and the nuclear matrix. *International Review of Cytology* **162A**, 151-189.

VAN DYKE, D.L., WORSHAM, M.J., FISHER, L.J. & WEISS, L. (1986). The centromere index and relative length of human high-resolution G-banded chromosomes. *Human Genetics* **73**, 130-132.

VAN GENT, D.C., HIOM, K., PAULL, T.T. & GELLERT, M. (1997). Stimulation of V(D)J cleavage by high mobility group proteins. *The EMBO Journal* **16**, 2665-2670.

VAN HOLDE, K. & ZLATANOVA, J. (1995). Chromatin higher order structure: Chasing a mirage? *The Journal of Biological Chemistry* **270**, 8373-8376.

VAN LINT, C., EMILIANI, S. & VERDIN, E. (1996). The expression of a small fraction of cellular genes is changed in response to histone acetylation. *Gene Expression* **5**, 245-253.

VAN LOHUIZEN, M., FRASCH, M., WIENTJENS, E. & BERNS, A. (1991). Sequence similarity between the mammalian *bmi-1* proto-oncogene and the *Drosophila* regulatory genes *Psc* and *Su(z)2*. *Nature* **353**, 353-355.

VAN OMMEN, G.B., BREUNING, M.H. & RAAP, A.K. (1995). FISH in genome research and molecular diagnostics. *Current Opinion in Genetics and Development* **5**, 304-308.

VAN WIJEN, A.J., BIDWELL, J.P., FEY, E.G., PENMAN, S., LIAN, J.B., STEIN, J.L. & STEIN, G.S. (1993). Nuclear matrix association of multiple sequence-specific DNA binding activities related to SP-1, ATF, CCAAT, C/EBP, OCT-1 and AP-1. *Biochemistry* **32**, 8397-8402.

VAN STEENSEL, B. & DE LANGE, T. (1997). Control of telomere length by the human telomeric protein TRF1. *Nature* **385**, 740-743.

VARGA-WEISZ, P.D. WILM, M., BONTE, E., DUMAS, K., MANN, M. & BECKER, P.B. (1997). Chromatin-remodelling factor CHRAC contains the ATPases ISWI and topoisomerase II. *Nature* **388**, 598-602.

VASSILEV, A.P., RASMUSSEN, H.H., CHRISTENSEN, E.I., NIELSEN, S. & CELIS, J.E. (1995). The levels of ubiquitinated histone H2A are highly up-regulated in transformed human cells: Partial co-localisation of uH2A clusters and PCNA/cyclin foci in a fraction of cells in S-phase. *Journal of Cell Science* **108**, 1205-1215.

VEGA-SALAS, D.E. & SALAS, P.J.I. (1996). Cell cycle related behaviour of a chromosomal scaffold protein in MDCK epithelial cells. *Chromosoma* **104**, 321-331.

VERHEIJEN, R., KUIPERS, H.J.H., SCHLINGEMANN, R.O., BOEHMER, A.L.M., VAN DRIEL, R., BRAKENHOFF, G.J. & RAMAEKERS, F.C.S. (1989). Ki-67 detects a nuclear matrix-associated proliferation-related antigen. *Journal of Cell Science* **92**, 123-130.

VERREAULT, A., KAUFMAN, P.D., KOBAYASHI, R. & STILLMAN, B. (1996). Nucleosome assembly by a complex of CAF-1 and acetylated histones H3/H4. *Cell* **87**, 95-104.

VETTESE-DADEY, M., GRANT, P.A., HEBBES, T.R., CRANE-ROBINSON, C., ALLIS, C.D. & WORKMAN, J.L. (1996). Acetylation of histone H4 plays a primary role in enhancing transcription factor binding to nucleosomal DNA *in vitro*. *The EMBO Journal* **15**, 2508-2518.

VETTESE-DADEY, M., WALTER, P., CHEN, H., JUAN, L.-J. & WORKMAN, J.L. (1994). Role of the histone amino termini in facilitated binding of a transcription factor, GAL-AH, to nucleosome cores. *Molecular and Cellular Biology* **14**, 970-981.

VIDAL, M. & GABER, R.F. (1991). RPD3 encodes a second factor required to achieve maximum positive and negative transcription states in *Saccharomyces cerevisiae*. *Molecular and Cellular Biology* **11**, 6317-6327.

VIDALI, G., BOFFA, L.C., BRADBURY, E.M. & ALLFREY, V.G. (1978). Butyrate suppression of histone deacetylation leads to accumulation of multi-acetylated forms of histones H3 and H4 and increased DNase I sensitivity of the associated DNA sequences. *Proceedings of the National Academy of Sciences U.S.A.* **75**, 2239-2243.

VIEGAS-PEQUIGNOT, E., DERBIN, C., MALFOY, B., TAILLANDIER, E., LENG, M. & DUTRILLAUX, B. (1983). Z-DNA immunoreactivity in fixed metaphase chromosomes of primates. *Proceedings of the National Academy of Sciences U.S.A.* **80**, 5890-5894.

VIEGAS-PEQUIGNOT, E. & DUTRILLAUX, B. (1976). Segmentation of human chromosomes induced by 5-ACR (5-azacytidine). *Human Genetics* **34**, 247-254.

VILLARREAL, L.P. (1991). Relationship of eukaryotic DNA replication to committed gene expression: General theory for gene control. *Miocrobiological Review* **55**, 512-542.

VINDELOV, L.L., CHRISTENSEN, I.J. & NISSEN, N.I. (1983). A detergent-trypsin method for the preparation of nuclei for flow cytometry DNA analysis. *Cytometry* **3**, 323-327.

VOGEL, W., AUTENRIETH, M. & MEHNERT, K. (1989). Analysis of chromosome replication by a BrdU antibody technique. *Chromosoma* **98**, 335-341.

VOGELSTEIN, B., PARDOLL, D.M. & COFFEY, D.S. (1980). Supercoiled loops and eukaryotic DNA replication. *Cell* **22**, 79-85.

VOULLAIRE, L.E., SLATER, H.R., PETROVIC, V. & CHOO, K.H.A. (1993). A functional marker centromere with no detectable alpha-satellite, satellite III, or CENP-B protein: Activation of a latent centromere? *American Journal of Human Genetics* **52**, 1153-1163.

VOURC'H, C., TARUSCIO, D., BOYLE, A.L. & WARD, D.C. (1993). Cell cycle-dependent distribution of telomeres, centromeres, and chromosome-specific subsatellite domains in the interphase nucleus of mouse lymphocytes. *Experimental Cell Research* **205**, 142-151.

WACHTLER, F., HOPMAN, A.H.N., WIEGANT, J. & SCHWARZACHER, H.G. (1986). On the position of nucleolar organising regions (NORs) in interphase nuclei. *Experimental Cell Research* **167**, 227-240.

WADE, P.A., PRUSS, D. & WOLFFE, A.P. (1997). Histone acetylation: Chromatin in action. *Trends in Biochemical Sciences* **22**, 128-132.

WAKEFIELD, M.J., KEOHANE, A.M., TURNER, B.M. & MARSHALL GARVES, J.A. (1997). Histone underacetylation is an ancient component of mammalian X chromosome inactivation. *Proceedings of the National Academy of Sciences U.S.A.* **9**, 9665-9668.

WALLRATH, L.L. & ELGIN, S.C.R. (1995). Position effect variegation in *Drosophila* is associated with an altered chromatin structure. *Genes and Development* **9**, 1263-1277.

WANG, J., CAO, L.-G., WANG, Y.-L. & PEDERSON, T. (1991). Localisation of pre-messenger RNA at discrete nuclear sites. *Proceedings of the National Academy of Sciences U.S.A.* **88**, 7391-7395.

WANG, J.C. (1996). DNA topoisomerases. *Annual Review of Biochemistry* **65**, 635-692.

WANG, W., COTE, J., XUE, Y., ZHOU, S., KHAVARI, P.A., BIGGAR, S.R., MUCHARDT, C., KALPANA, G.V., GOFF, S.P., YANIV, M., WORKMAN, J.L. & CRABTREE, G.R. (1996). Purification and biochemical heterogeneity of the mammalian SWI-SNF complex. *The EMBO Journal* **15**, 5370-5382.

WANG, L., MIZZEN, C., YING, C., CANDAU, R., BARLEV, N., BROWNELL, J., ALLIS, C.D. & BERGER, S.L. (1997). Histone acetyltransferases activity is conserved between yeast and human GCN5 and is required for complementation of growth and transcriptional activation. *Molecular and Cellular Biology* **17**, 519-527.

WANSINK, D.G., SCHUL, W., VAN DER KRAAN, I., VAN STEENSEL, B., VAN DRIEL, R. & DE JONG, L. (1993). Fluorescent labelling of nascent RNA reveals transcription by RNA polymerase II in domains scattered throughout the nucleus. *The Journal of Cell Biology* **122**, 283-293.

WARBURTON, D., NAYLOR, A.F. & WARBURTON, F.E. (1973). Spatial relations of human chromosomes identified by quinacrine fluorescence at metaphase. *Humangenetik* **18**, 297-306.

WARBURTON, P.E. & EARNSHAW, W.C. (1997). Untangling the role of DNA topoisomerase II in mitotic chromosome structure and function. *BioEssays* **19**, 97-99.

WARNER, J.R. (1990). The nucleolus and ribosome formation. *Current Opinion in Cell Biology* **2**, 521-527.

WATCHLER, F., HOPMAN, A.H.N., WIEGANT, J. & SCHWARZACHER, H.G. (1986). On the position of the nucleolus organiser regions (NORs) in interphase nuclei. *Experimental Cell Research* **167**, 227-240.

WAYE, J.S. & WILLARD, H.F. (1989). Human β-satellite DNA: Genomic organisation and sequence definition of a class of highly repetitive tandem DNA. *Proceedings of the National Academy of Sciences U.S.A.* **86**, 6250-6254.

WEINER, A.M., DEININGER, P.L. & EFSTRATIADIS, A. (1986). Nonviral retroposons: Genes, pseudogenes, and transposable elements generated by the reverse flow of genetic information. *Annual Review of Biochemistry* **55**, 631-661.

WEINTRAUB, H. & GROUDINE, M. (1976). Chromosomal subunits in active genes have an altered conformation. *Science* **193**, 848-856.

WEIPOLTSHAMMER, K., SCHOFER, C., ALMEDER, M., SYLVESTER, J. & WACHTLER, F. (1996). Spatial distribution of sex chromosomes and ribosomal genes: A study on human lymphocytes and testicular cells. *Cytogenetics and Cell Genetics* **73**, 108-113.

WEIS, K., RAMBAUD, S., LAVAU, C., JANSEN, J., CARVALHO, T., CARMO-FONSECA, M., LAMOND, A. & DEJEAN, A. (1994). Retinoic acid regulates aberrant nuclear localisation of PML-RARα in acute promyelotic leukaemia cells. *Cell* **76**, 345-356.

WENG, A., ENGLER, P. & STORB, U. (1995). The bulk chromatin structure of a murine transgene does not vary with its transcriptional or DNA methylation status. *Molecular and Cellular Biology* **15**, 572-579.

WILLARD, H.F. (1991). Evolution of alpha satellite. *Current Opinion in Genetics and Development* **1**, 509-514.

WILSON, C.J., CHAO, D.M., IMBALZANO, A.N., SCHNITZLER, G.R., KINGSTON, R.E. & YOUNG, R.A. (1996). RNA polymerase II holoenzyme contains SWI/SNF regulators involved in chromatin remodelling. *Cell* **84**, 235-244.

WISCHNITZER, S. (1973). The submicroscopic morphology of the interphase nucleus. *International Review of Cytology* **34**, 1-48.

WITKOWSKI, J.A. (1986). Somatic cell hybrids: A fusion of biochemistry, cell biology and genetics. *Trends in Biological Sciences* **11**, 149-152.

WOLFE, K.H., SHARP, P.M. & LI, W.H. (1989). Mutation rates differ among regions of the mammalian genome. *Nature* **337**, 283-285.

WOLFFE, A.P. (1994a). Architectural transcription factors. *Science* **264**, 1100-1101.

WOLFFE, A.P. (1994b). The transcription of chromatin templates. *Current Opinion in Genetics and Development* **4**, 245-254.

WOLFFE, A.P. (1995a). Histone deviants. *Current Biology* **5**, 452-454.

WOLFFE, A.P. (1995b). *Chromatin.* London: Academic Press Limited.

WOLFFE, A.P., KHOCHBIN, S. & DIMITROV, S. (1997a). What do linker histones do? *BioEssays* **19**, 249-255.

WOLFFE, A.P., WONG, J. & PRUSS, D. (1997b). Activators and repressors: Making use of chromatin to regulate transcription. *Genes to Cell* **2**, 291-302.

WOLLENBERG, C., KIEFABER, M.P. & ZANG, K.D. (1982). Quantitative studies on the arrangement of human metaphase chromosomes. IX Arrangement of chromosomes with and without spindle apparatus. *Human Genetics* **62**, 310-315.

WOOD, K.W., SAKOWICZ, R., GOLDSTEIN, L.S.B. & CLEVELAND, D.W. (1997). CENP-E is a plus end-directed kinetochore motor required for metaphase chromosome alignment. *Cell* **91**, 357-366.

WOODCOCK, C.L., GRIGORYEV, S.A., HOROWITZ, R.A. & WHITAKER, N. (1993). A chromatin folding model that incorporates linker variability generates fibres resembling native structures. *Proceedings of the National Academy of Sciences U.S.A.* **90**, 9021-9025.

WORMAN, H.J., YUAN, J., BLOBEL, G. & SPYROS, G.D. (1988). A lamin B receptor in the nuclear envelope. *Proceedings of the National Academy of Sciences U.S.A.* **85**, 8531-8534.

WORTON, R.G., SUTHERLAND, J., SYLVESTER, J.E., WILLARD, H.F., BODRUG, S., DUBE, I., DUFF, C., KEAN, V., RAY, P.N. & SCHMICKEL, R.D. (1988). Human ribosomal RNA genes: Orientation of the tandem array and conservation of the 5' end. *Science* **239**, 64-68.

WU, J.-R. & GILBERT, D.M. (1996). A distinct G1 step required to specify the Chinese hamster DHFR replication origin. *Science* **271**, 1270-1272.

WU, T.-C. & LITCHEN, M. (1994). Meiosis-induced double-strand break sites determined by yeast chromatin structure. *Science* **263**, 515-518.

XIE, X., KOKUBO, T., COHEN, S.L., MIRZA, U.A., HOFFMANN, A., CHAIT, B.T., ROEDER, R.G., NAKATANI, Y. & BURLEY, S.K. (1996). Structural similarity between TAFs and the heterotetrameric core of the histone octamer. *Nature* **380**, 316-322.

XING, Y., JOHNSON, C.V., DOBNER, P.R. & LAWRENCE, J.B. (1993). Higher level organisation of individual gene transcription and RNA splicing. *Science* **259**, 1326-1330.

XING, Y., JOHNSON, C.V., MOEN, P.T., MCNEIL, J.A. & LAWRENCE, J.B. (1995). Nonrandom gene organisation: Structural arrangements of specific pre-mRNA transcription and splicing with SC-35 domains. *The Journal of Cell Biology* **131**, 1635-1647.

YANG, L., GUAN, T. & GERACE, L. (1997). Lamin-binding fragment of LAP2 inhibits increase in nuclear volume during the cell cycle and progression into S phase. *The Journal of Cell Biology* **139**, 1077-1087.

YANG, L., WOLD, M.S., LI, J.J. KELLY, T.J. & LIU, L.F. (1987). Roles of DNA topoisomerases in simian virus 40 DNA replication *in vitro*. *Proceedings of the National Academy of Sciences U.S.A.* **84**, 950-954.

YANG, W.M., INOUYE, C., ZENG, Y., BEARSS, D. & SETO, E. (1996a). Transcriptional repression by YY1 is mediated by interaction with a mammalian homologue of the yeast global regulator RPD3. *Proceedings of the National Academy of Sciences U.S.A.* **93**, 12845-12850.

YANG, X.-J., OGRYZKO, V.V., NISHIKAWA, J.-I., HOWARD, B.H. & NAKATANI, Y. (1996b). A p300/CBP-associated factor that competes with the adenoviral oncoprotein E1A. *Nature* **382**, 319-324.

YASUDA, Y. & MAUL, G.G. (1990). A nucleolar auto-antigen is part of a major chromosomal surface component. *Chromosoma* **99**, 152-160.

YE, Q. & WORMAN, H.J. (1994). Primary structure analysis and lamin B and DNA binding of human LBR, an integral protein of the nuclear envelope inner membrane. *The Journal of Biological Chemistry* **269**, 11306-11311.

YE, Q. & WORMAN, H.J. (1996). Interactions between an integral protein of the nuclear envelope inner membrane and human chromodomain proteins homologous to *Drosophila* HP1. *The Journal of Biological Chemistry* **271**, 14653-14656.

YE, Q. & WORMAN, H.J. (1997). Domain-specific interactions of human HP1-type chromodomain proteins and inner nuclear membrane protein LBR. *The Journal of Biological Chemistry* **272**, 14983-14989.

YEBRA, M.J. & BHARWAT, A.S. (1995). A cytosine methyltransferase converts 5-methylcytosine in DNA to thymine. *Biochemistry* **34**, 14752-14757.

YELTON, D.E., DIAMOND, B.A., KWAN, S.P. & SCHARFF, M.D. (1978). Fusion of mouse myeloma and spleen cells. *Current Topics in Microbiology and Immunology* **81**, 1-7.

YIE, J., LIANG, S., MERIKA, M. & THANOS, D. (1997). Intra- and intermolecular co-operative binding of High-Mobility-Group protein I(Y) to the beta-interferon promoter. *Molecular and Cellular Biology* **17**, 3649-3662.

YODER, J.A., WALSH, C.P. & BESTOR, T.H. (1997). Cytosine methylation and ecology of intragenomic parasites. *Trends in Genetics* **13**, 335-340.

YOKOTA, H., SINGER, M.J., VAN DEN ENGH, G.J. & TRASK, B.J. (1997). Regional differences in the compaction of chromatin in human G0/G1 interphase nuclei. *Chromosome Research* **5**, 157-166.

YOKOTA, H., VAN DEN ENGH, G.J., HEARST, J.E., SACHS, R.K. & TRASK,B.J. (1995). Evidence for the organisation of chromatin in megabase pair-sized loops arranged along a random walk path in the human G0/G1 interphase nucleus. *The Journal of Cell Biology* **130**, 1239-1249.

YOSHIDA, I., KASHIO, N. & TAKAGI, N. (1993). Cell fusion-induced quick change in replication time of inactive mouse X chromosome: An implication for the maintenance mechanism of late replication. *The EMBO Journal* **12**, 4397-4405.

YOSHIDA, M., HORINOUCHI, S. & BEPPU, T. (1995). Trichostatin A and trapoxin: Novel chemical probes for the role of histone acetylation in chromatin structure and function. *BioEssays* **17**, 423-430.

YOSHIDA, M., KIJIMA, M., AKITA, M. & BEPPU, T. (1990). Potent and specific inhibition of mammalian histone deacetylase both *in vivo* and *in vitro* by Trichostatin A. *The Journal of Biological Chemistry* **265**, 17174-17179.

YOSHIURA, K.-I., KUBOTA, T., SOEJIMA, H., TAMURA, T., IZUMIKAWA, Y., NIIKAWA, N. & JINNO, Y. (1994). A comparison of GC content and proportion of *Alu*/*Kpn*I-repetitive sequences in a single dark- and light-band region from a human chromosome. *Genomics* **20**, 243-248.

YUNIS, J.J. (1981). Mid-prophase human chromosomes. the attainment of 2000 bands. *Human Genetics* **56**, 293-298.

YUNIS, J.J., KUO, M.T. & SAUNDERS, G.F. (1977). Localisation of sequences specifying mRNA to light-staining G-bands of human chromosomes. *Chromosoma* 61, 335-344.

YUNIS, J.J. & TSAI, M.Y. (1978). Mapping of polysomal messenger RNA and heterogeneous nuclear RNA to the lightly staining G-bands of human chromosomes. *Cytogenetics and Cell Genetics* **22**, 364-367.

ZAKIAN, V.A. (1997). Life and cancer without telomerase. *Cell* **91**, 1-3.

ZAMB, T.J. & PETES, T.D. (1982). Analysis of the junction between ribosomal RNA genes and single-copy chromosomal sequences in yeast *Saccharomyces cerevisiae. Cell* **28**, 355-364.

ZAPPAVIGNA, V., FALCIOLA, L., CITTERICH, M.H., MAVILIO, F. & BIANCHI, M.E. (1996). HMG1 interacts with HOX proteins and enhances their DNA binding and transcriptional activation. *The EMBO Journal* **15**, 4981-4991.

ZENG, C., KIM, E., WARREN, S.L. & BERGET, S.M. (1997). Dynamic relocation of transcription and splicing factors dependent upon transcriptional activity. *The EMBO Journal* **16**, 1401-1412.

ZETKA, M.-C. & ROSE, A.-M. (1995). Mutant *rec-1* eliminates the meiotic pattern of crossing over in *Caenorhabditis elegans. Genetics* **141**, 1339-1349.

ZHANG, G., TANEJA, K.L., SINGER, R.H. & GREEN, M.R. (1994). Localisation of pre-mRNA splicing in mammalian nuclei. *Nature* **372**, 809-812.

ZHAO, K., KAS, E., GONZALEZ, E. & LAEMMLI, U.K. (1993). SAR-dependent mobilisation of histone H1 by HMG-I/Y *in vitro*: HMG-I/Y is enriched in H1-depleted chromatin. *The EMBO Journal* **12**, 3237-3247.

ZHOU, S., YANG, Y., SCOTT, M.J., PANNUTI, A., FEHR, K.C., EISEN, A., KOONIN, E.V., FOUTS, D.L., WRIGHTSMAN, R., MANNING, J.E. & LUCCHESI, J.C. (1995). Male-specific lethal-2, a dosage compensation gene of *Drosophila*, undergoes a sex-specific regulation and encodes a protein with a RING finger and a metallothionein-like cysteine cluster. *The EMBO Journal* **14**, 2884-2895.

ZINK, D., BORNFLETH, H., VISSER, A., CREMER, C. & CREMER, T. (1997). Interphase chromosome banding: Approaching the functional organisation of human chromosome territories. *Biophysical Journal* **72**, THAM6.

ZIRBEL, R.M., MATHIEU, U.R., KURZ, A., CREMER, T. & LICHTER, P. (1993). Evidence for a nuclear compartment of transcription and splicing located at chromosome domain boundaries. *Chromosome Research* **1**, 93-106.

ZORN, C., CREMER, C., CRMEMR, T. & ZIMMER, J. (1979). Unscheduled DNA synthesis after partial UV irradiation of the cell nucleus. *Experimental Cell Research* **124**, 111-119.

References added in proof:

BORSANI, G., TONLORENZI, R., SIMMLER, M.C., *et al.* (1991). Characterisation of a murine gene expressed from the inactive X chromosome. *Nature* **352**, 325-329.

BROCKDORFF, N., ASHWORTH, A., KAY, G.F., COOPER, P., SMITH, S., MCCABE, V.M., NORRIS, D.P., PENNY, G.D., PATEL, D. & RASTAN, S. (1991). Conservation of position and exclusive expression of mouse *Xist* from the inactive X chromosome. *Nature* **351**, 329-331.

BROWN, C.J., BALLABIO, A., RUPERT, J.L., LAFRENIERE, R.G., GROMPE, M., TONLORENZI, R. & WILLARD, H. (1991). A gene from the region of the human x-inactivation centre is expressed exclusively from the X chromosome. *Nature* **349**, 38-44.

RASTAN, S. (1994). X chromosome inactivation and the *Xist* gene. *Current Opinion in Genetics and Develpoment* **4**, 292-297.

SHEARDOWN, S.A., DUTHIE, S.M., JOHNSON, C.M., NEWALL, A.E.T., FORMSTONE, E.J., ARKELL, R.M., NESTEROVA, T.B., ALGHISI, G.-C., RASTAN, S. & BROCKDORFF, N. (1997). Stabilisation of *Xist* RNA mediates initiation of X chromosome inactivation. *Cell* **91**, 99-107.

SUGIMOTO, K., YAMADA, T., MURO, Y. & HIMENO, M. (1996). Human homologue of *Drosophila* heterochromatin-associated protein 1 (HP-1) is a DNA-binding protein which possesses a DNA-binding motif with a waek similarity to that of human centromere protein C (CENP-C). *Journal of Biochemistry* **120**, 153-159.